Nitro- and oxyaromatic compounds: environmental cycling and exposure

Dissertation

zur Erlangung des Grades

"Doktor

der Naturwissenschaften"

im Promotionsfach Chemie

am Fachbereich Chemie, Pharmazie und Geowissenschaften

der Johannes Gutenberg-Universität

in Mainz

Paul Crutzen Graduate School

Marco Wietzoreck

geb. in Frankfurt am Main

Mainz, den 17.01.2022

I hereby declare that I wrote the dissertation submitted without any unauthorized external assistance and used only sources acknowledged in the work. All textual passages which are appropriated verbatim or paraphrased from published and unpublished texts as well as all information obtained from oral sources are duly indicated and listed in accordance with bibliographical rules. In carrying out this research, I complied with the rules of standard scientific practice as formulated in the statutes of Johannes Gutenberg-University Mainz to insure standard scientific practice.

Mainz, 17th January 2022, Marco Wietzoreck

Abstract

Parent polycyclic aromatic hydrocarbons (PAHs), their nitrated (NPAHs) and oxygenated (OPAHs) derivatives are pollutants leading to adverse health effects due to their carcinogenicity, mutagenicity and oxidative stress potential. Many of these polycyclic aromatic compounds (PACs) are long-lived and undergo long-range atmospheric transport. PAHs have been studied and monitored in the environment since decades. In contrast, PAH derivatives are understudied despite comparable or even higher toxicity and bioaccessibility of some NPAHs and OPAHs than their parent PAHs. The air pollutants are formed during incomplete combustion processes of fossil fuels and biomass but can also be formed secondarily in the atmosphere by the reaction of parent PAHs with atmospheric oxidants. In order to understand the implication for human health, the occurrence and levels in the environment as well as the bioavailability and the negative health effects of the pollutants should be known. The concentrations of the pollutants are governed by their emission, photochemical formation, degradation and deposition, which is significantly influenced by, e.g. the gas-particle partitioning and the mass size distribution. This thesis advances the knowledge about the concentrations, cycling, fate in the atmospheric environment and adverse health effects of the PAH derivatives studying the following aspects:

1. Investigation of the occurrence and multi-annual variations of PACs in topsoil at a semi-urban and a background site in Central Europe: The concentration of PAH derivatives was higher in the soil at the semi-urban site compared to the background site, where we could find concentrations that are among the lowest ever reported. Five of 18 targeted NPAHs were found in the soil samples collected between 2006 and 2017. The highly toxic 1-nitropyrene and 6-nitrobenzo[a]pyrene were the most abundant NPAHs. In contrast to the NPAHs, the relative abundance of OPAHs was more equally distributed, with the highest contribution from 9-fluorenone. A correlation between high-molecular weight OPAHs and PAHs with the total organic carbon content (TOC) in soil was found. The high ratios of the PAH derivatives to their parent PAHs at the background site indicate that the deposited aerosols came from long-range transport. Although gas-particle partitioning was expected as one major factor influencing the concentrations in soil, more research is needed to understand the long-term trends in PAC concentrations.

2. Investigation of the occurrence, sources and cycling of PACs in the marine atmosphere of the Mediterranean Sea and around the Arabian Peninsula during a ship-borne campaign in summer of 2017: The regional differences in the concentrations during the AQABA (Air Quality and Climate Change in the Arabian Basin) ship-borne campaign, were pronounced. While the concentrations of the PACs in the Arabian Sea were among the lowest ever reported, the concentration in the Mediterranean Sea and the Arabian Gulf reached levels previously found at suburban sites. According to source apportionment investigations, ship emissions, continental pollution and residual oil combustion were the major sources of PACs in the marine atmosphere of that region. Another result of the study was that in addition to 2-nitrofluoranthene and 2-nitropyrene, several other PAH derivatives were formed by photochemical reactions, too.
3. Investigation of the oxidative potential (OP) causing oxidative stress on the cellular level of PACs and its predictability: The acellular OP of 39 PACs, abundant in ambient particulate matter, was measured for the first time for many air pollutants. Similar to earlier studies, 1,2-naphthoquinone, 1,4-naphthoquinone and 9,10-phenanthrenequinone exhibit the highest H_2O_2 formation and a high dithiothreitol (DTT) depletion rate. In contrast to most previous studies, it could be revealed that several 4-5 ring quinones obtain a high OP, too. 4,5-Pyrenequinone even showed the highest DTT depletion rate of all target compounds. Due to the combination of high concentration and high OP, 4,5-pyrenequinone contributes significantly to the OP of all 39 investigated PACs in the standard reference material (SRM) ‘urban dust’ (US NIST SRM 1649b). It was also demonstrated for the first time that NPAHs produce significant signals in the acellular OP assays. However, the NPAHs as well as some highly abundant OPAHs do not contribute significantly to the overall OP of PACs in SRM dust since their OP is negligible compared to the quinones with the highest OPs. Based the dataset including 39 PACs, the influence of different functional groups and the structure could be shown. The important finding of the study that the OP of PACs can be predicted by using the standard reduction potential or the energy level of the lowest unoccupied molecular orbital (LUMO) could be used for simple and rapid estimation of the OP, for evaluation of existing or new substances in the environment, and in models.

Zusammenfassung

Polyzyklische aromatische Kohlenwasserstoffe (PAKs), ihre nitrierten (NPAHs) und oxidierten (OPAHs) Derivate sind Schadstoffe, die aufgrund ihrer Kanzerogenität, Mutagenität und ihres Potenzials für oxidativen Stress gesundheitsschädlich sind. Viele dieser polyzyklischen aromatischen Verbindungen (PACs) sind langlebig und können in der Atmosphäre über weite Strecken transportiert und verteilt werden. PAKs in der Umwelt werden seit mehreren Jahrzehnten untersucht und überwacht. Im Gegensatz dazu sind die PAK-Derivate noch wenig erforscht, obwohl Toxizität und Bioverfügbarkeit einiger NPAHs und OPAHs vergleichbar oder sogar höher als die der Vorläufer sind. Die PAK-Derivate entstehen bei der unvollständigen Verbrennung von fossilen Brennstoffen und Biomasse, können aber auch sekundär in der Atmosphäre durch die Reaktion der PAKs mit Photooxidantien gebildet werden. Um die Auswirkungen der PACs auf die menschliche Gesundheit zu verstehen, ist umfangreiches Wissen über deren Vorkommen und Konzentrationen in der Umwelt, sowie deren Bioverfügbarkeit und gesundheitlichen Auswirkungen notwendig. Die Konzentration der Schadstoffe wird durch deren Emission, photochemische Bildung, Abbau, und Deposition bestimmt, was z. B. von der Gas-Partikel-Phasenverteilung und der Massengrößenverteilung maßgeblich beeinflusst wird. Diese Dissertation beinhaltet neue Erkenntnisse über die Konzentrationen, die Verteilung, den Verbleib in der atmosphärischen Umwelt und die gesundheitliche Relevanz der PAK-Derivate durch die Untersuchung folgender Schwerpunkte:

1. Untersuchung des Vorkommens und der mehrjährigen Schwankungen von PAKs in Oberböden an zwei Standorten in Mitteleuropa, einem vorstädtischen mit Industrie und einem ländlichen, der die mitteleuropäische Hintergrundbelastung abbildet: Die Konzentration von PAK-Derivaten im Boden des semi-städtischen Standorts war höher als am im Hintergrund, wo wir Konzentrationen fanden, die zu den niedrigsten gehören, die jemals berichtet wurden. In den zwischen 2006 und 2017 gesammelten Bodenproben wurden fünf von 18 untersuchten NPAKs gefunden. Die am häufigsten vorkommenden NPAHs waren die hochtoxischen Verbindungen 1-Nitropyren und 6-Nitrobenzo[a]pyren. Im Gegensatz zu den NPAHs, war die relative Häufigkeit der einzelnen OPAHs gleichmäßiger verteilt, wobei 9-Fluorenon den größten Anteil an der Summe aller OPAHs ausmachte. Es wurde eine Korrelation von OPAHs mit hohem Molekulargewicht sowie den

meisten PAKs mit dem gesamten organischen Kohlenstoff (TOC) im Boden festgestellt. Der hohe Anteil an PAK-Derivaten im Vergleich zu ihren Vorläufer-PAKs am Hintergrundstandort deutet darauf hin, dass ein Teil der abgelagerten Aerosole dem Ferntransport unterlagen. Obwohl gezeigt werden konnte, dass die Gas-Partikel-Phasenverteilung ein wichtiger Faktor ist, der die Konzentrationen im Boden beeinflusst, sind weitere Untersuchungen erforderlich, um langzeitlichen Trends der PAC-Konzentrationen im Boden vollständig zu verstehen.

2. Untersuchung des Vorkommens, der Quellen und der Verteilung von PACs in der marinen Atmosphäre über dem Mittelmeer und über den Meeren rund um die Arabische Halbinsel während einer Schiffskampagne im Sommer 2017: Die regionalen Unterschiede in den Konzentrationen während der AQABA (Air Quality and Climate Change in the Arabian Basin) Schiffskampagne waren deutlich ausgeprägt. Während die PAC-Konzentrationen im Arabischen Meer zu den niedrigsten jemals gemeldeten Werten gehörten, erreichten die Konzentrationen im Mittelmeer und im Arabischen Golf Werte, die eher typisch für vorstädtische Gebiete sind. Untersuchungen zur Herkunft der Schadstoffe ergaben, dass Schiffsemissionen, Schadstoffbelastung vom Festland und die Verbrennung von Rückstandsöl die Hauptquellen für PACs in der marinen Atmosphäre der untersuchten Region waren. Ein weiteres Resultat der Studie war, dass neben 2-Nitrofluoranthen und 2-Nitropyren auch mehrere weitere PAK-Derivate photochemisch gebildet wurden.
3. Untersuchung des Potenzials für oxidativen Stress auf der Zellebene (OP) von PACs und seiner Vorhersagbarkeit: Für viele der untersuchten 39 PACs, die bereits in der Atmosphäre nachgewiesen werden konnten, wurde zum ersten Mal das OP mit einem azellulären Test gemessen. Ähnlich wie in früheren Studien, wiesen 1,2-Naphthochinon, 1,4-Naphthochinon und 9,10-Phenanthrenchinon die höchste Konzentration an gebildetem H_2O_2 und eine hohe Dithiothreitol (DTT)-Abbaugeschwindigkeit auf. Im Gegensatz zu den meisten früheren Studien konnte jedoch gezeigt werden, dass auch mehrere 4-5-Ring-Chinone einen hohen OP erzielen. 4,5-Pyrenchinon besaß sogar die höchste DTT-Abbaurate von allen untersuchten Substanzen. Durch die Kombination aus hoher Konzentration und hohem OP trägt 4,5-Pyrenchinon einen signifikanten Anteil am OP aller 39 untersuchten PACs im Standardreferenzmaterial städtischer Luftstaub (US NIST SRM urbn dust, No. 1649b) bei. Außerdem wurde zum ersten Mal nachgewiesen, dass auch NPAHs signifikante Signale in den azellulären OP-Tests erzeugen. Diejenigen NPAHs

sowie einige der OPAHs, die zumeist in hohen Konzentration in der Luft nachgewiesen werden, tragen jedoch nicht wesentlich zum OP aller untersuchten PACs im Luftstaub bei, da ihr OP im Vergleich zu den vorgenannten Chinonen vernachlässigbar gering ist. Anhand des Datensatzes mit 39 PACs konnte der Einfluss verschiedener funktioneller Gruppen und ihrer Struktur aufgezeigt werden. Die wichtige Erkenntnis der Studie, dass man das OP der PACs mithilfe des Standardreduktionspotenzials oder des Energieniveaus des niedrigsten unbesetzten Molekülorbitals (LUMO) vorhersagen kann, könnte zu einer einfachen und schnellen Abschätzung des OP, zur Bewertung bereits vorhandener oder neuer Substanzen in der Umwelt, sowie in Modellen genutzt werden.

Contents

1 Introduction

1.1 Sources and formation

PAHs and several nitrated (NPAHs) and oxygenated PAHs (OPAHs) are formed during incomplete combustion of fossil fuels, biofuels and biomass (Baek et al., 1991; Walgraeve et al., 2010; Bandowe and Meusel, 2017). Accordingly, these substances are emitted e.g. by road, ship and air traffic, various industries, household stoves, smoking, wildfires, volcanic eruptions and waste incinerators (Baek et al., 1991; Mitra and Ray, 1995; Bamford et al., 2003; Watanabe and Noma, 2009; Layshock et al., 2010; IARC, 2012; Shen et al., 2013; Huang et al., 2014; Nalin et al., 2016; Zhuo et al., 2017; de Oliveira Galvão et al., 2018; Clergé et al., 2019; Zhao et al., 2020). Furthermore, few PAH derivatives were used as intermediates in the chemical industry or were commercially produced (Bausinger et al., 2007). Anthraquinones are used extensively as dyes in the textile industry (Li et al., 2019).

Besides these primary emissions, PAH derivatives can also be formed secondarily by the reaction of parent PAHs with atmospheric oxidants, mainly hydroxyl radicals (OH) and nitrate radicals (NO_3) as well as ozone (O_3) (Atkinson and Arey, 1994; Finlayson-Pitts & Pitts, 2000; Vione et al., 2004). During daytime, the OH radical is the main oxidant in the atmosphere. The formed intermediate of the reaction of a PAH with OH further reacts with molecular oxygen to hydroxyl and carbonyl PAHs or with NO_2 to NPAHs (Vione et al., 2004). During night, the NO_3 radical is the most abundant oxidant responsible for the oxidation of the PAHs, which can react to NPAHs or OPAHs (Atkinson and Arey, 1994). This homogeneous gas phase formation is the main pathway for the secondary formation of PAH derivatives. Furthermore, NPAHs and OPAHs can be formed by heterogeneous reaction of PAHs in particulate matter (PM) with atmospheric oxidants, mainly ozone (Letzel et al., 1999; Keyte et al., 2013; Jariyasopit et al., 2014). NPAHs and OPAHs can also be formed in other environmental compartments, such as in soil by microbiological formation (Cerniglia, 1992; Lundstedt et al., 2007; Haritash and Kaushik, 2009; Wilcke et al., 2014a) and in water (Vione et al., 2005).

It is known for a few PAH derivatives that they are predominantly emitted during primary emissions such as 1-nitropyrene (1-NPYR) or 3-nitrofluoranthene (3-NFLT), or predominantly formed secondarily in the atmosphere such as 2-nitropyrene (2-NPYR) or 2-nitrofluoranthene (2-NFLT) (Atkinson and Arey, 1994; Bezabeh et al., 2003; Reisen and Arey, 2005). Therefore, the

ratio of 2-NFLT/1-NPYR has been used to identify the major source of the PACs. A ratio <5 indicates combustion processes as the main source, while a ratio >5 suggests aerosols containing a high fraction of photochemically formed compounds (Bamford and Baker, 2003). Since 2-NFLT can be formed by reaction with the OH and the NO_3 radical, while 2-NPYR can only be formed with OH, the ratio of 2-NFLT/2-NPYR can be used to determine the main atmospheric oxidant involved in the formation of PAH derivatives from PAHs (Feilberg et al., 2001; Bamford and Baker, 2003). A ratio of 5-10 indicates that the NPAHs were formed by OH radical initiated reactions, while a ratio of > 100 suggests the dominant reaction of PAHs with NO_3 radicals.

However, the relative contribution of different source types is not known for most OPAHs and several NPAHs, although several studies tried to estimate the relative contributions (Eiguren-Fernandez et al., 2008; Kojima et al., 2010; Souza et al., 2014; Lin et al., 2015; 2016; Ma et al., 2016; Zhuo et al., 2017).

1.2 Occurrence and levels in the environment

Several PACs are ubiquitous in the environment. They have been detected at rural/background sites and even in very remote sites such as the Antarctic (Vincenti et al., 2001; Vikelsøe et al. 2002; Tsapakis and Stephanou, 2007; Bandowe and Wilcke, 2010; Brorström-Lundén et al., 2010; Minero et al., 2010; Scipioni et al., 2012; Bandowe et al., 2014a; Tang et al., 2014; Wilcke et al., 2014b; Nežiková et al., 2021) and in different environmental compartments, such as air, soil, water, sediment and biota (Murahasi et al., 2001; Kurihara et al., 2005; Watanabe et al., 2005; Holoubek et al., 2007; Walgraeve et al., 2010; Fujiwara et al., 2014; Bandowe and Meusel, 2017; Clergé et al., 2019; Idowu et al., 2020). However, data in remote marine environments as well as long-term measurements are lacking for most PACs, especially for NPAHs and OPAHs, although this data is needed to evaluate the exposure and the health effects, as well as to develop and evaluate global models.

As already mentioned, PAHs, in particular the 16 US EPA-prioritized PAHs (Keith, 2015) have already been studied quite extensively (Phillips, 1983; Baek et al., 1991; CARB, 1994; Ravindra et al., 2008; Abdel-Shafy and Mansour, 2016; Galmiche et al., 2021a). Nevertheless, the number of papers published per day dealing with PAHs continued to increase for decades (Cave et al., 2018). Galmiche et al. (2021a) summarized that the reported PAH concentrations in atmospheric PM in Europe and south-east Asia. Gonzales-Gaya et al. (2016) measured PAH concentrations over the oceans in a circumnavigation expedition onboard a research vessel. Different studies using

modelling of PAHs (Lammel et al., 2009; Galarneau et al., 2014; Octaviani et al., 2019; Kelly et al., 2021) show the regional and global distribution of PAHs varying by several orders of magnitude depending on the region.

The concentrations of individual OPAHs in PM range between few pg m^{-3} and few ng m^{-3} depending on the selected compound, site and season (Walgraeve et al., 2010). The concentrations of NPAHs usually are in the range of pg m^{-3} (Bandowe and Meusel, 2017; Galmiche et al., 2021a). It has been shown for most OPAHs and NPAHs that the concentrations in winter usually are higher than in summer due to higher emissions, slower degradation rates and other meteorological factors such as differences in atmospheric mixing in winter (Bandowe et al., 2014b; Alves et al., 2017; Bandowe and Meusel, 2017; Tomaz et al., 2017; Degrendele et al., 2021; Nežiková et al., 2021). In contrast, some studies showed the opposite, which can mainly be explained by enhanced photochemical formation of PAH derivatives in summer (Reisen and Arey, 2005).

The highest concentrations in air and soil have been measured close to sources, e.g. at industrial, traffic, urban and suburban sites (Bamford and Baker, 2003; Lundstedt et al. 2007; Bandowe et al. 2011; 2014b; Wei et al., 2012; Arp et al., 2014; Li et al., 2015; Pham et al., 2015; Alves et al., 2016; 2017; Tomaz et al., 2016; Cai et al., 2017). The concentration of PACs usually decreases with distance to sources (Bandowe et al., 2010; 2019; Wilcke et al., 2014b; Jariyasopit et al., 2016). Albinet et al. (2007) found a 3 to 13 times higher OPAH concentration at an urban site compared to a rural site. Similarly, Scipioni et al. (2012) measured concentrations of PAHs and NPAHs, which were around 10 times higher at the urban site compared to the remote site in Chile.

Most studies suggest that the OPAHs in the atmosphere are similarly or slightly less abundant (up to one order of magnitude) than the PAHs. The NPAH concentration in air is mostly between two and three orders of magnitude lower than the PAH concentration (Albinet et al., 2007; 2008; Wei et al., 2012; Lin et al., 2015; Tomaz et al., 2016; Alves et al., 2017; Bandowe and Meusel, 2017; Zhang et al., 2018; Nežiková et al., 2021). As shown by Walgraeve et al. (2010), the ratio of PAH derivatives and PAHs can vary substantially depending on site, season, selected compounds and selected PM size. Similarly, the ratio of NPAHs and OPAHs to PAHs in soil can vary depending on the site (Bandowe and Wilcke, 2010; Bandowe et al., 2019). The ratio of the sum of OPAHs to the sum of PAHs in soil if often comparable to the relative concentrations in air, with the OPAHs slightly less abundant than the PAHs (Brorström-Lunden et al., 2010; Wei et al., 2015, Cai et al., 2017; Bandowe et al., 2019). However, a lot higher ratio was observed by Bandowe et al. (2010)

at a former gasworks site. The NPAHs in soil were observed 1-3 orders of magnitude lower abundant than the PAHs (Brorström-Lunden et al., 2010; Wei et al., 2015, Cai et al., 2017).

1.3 Multiphase cycling

Due to their vapor pressure, PACs cycle between different environmental compartments, such as gas and particulate phase in air, soil, water and sediment. The vapor pressure of almost all PAHs and PAH derivatives is within the range of 10^{-2} to 10^{-6} Pa (US EPA, 2021). Thus, these semivolatile compounds, by definition with a boiling point of 240-260°C to 380-400°C (WHO, 1989), partition between gas phase and particulate phase of ambient aerosols (Bidleman, 1989). It was found that the lower the vapor pressure of a PAC, the higher its particulate mass fraction (theta, θ) (Albinet et al., 2008; Delgado-Saborit et al., 2013; Wei et al., 2015; Tomaz et al., 2016). θ of a specific compound depends on temperature, humidity, particle surface area and composition of the aerosol particle (Lohmann and Lammel, 2004; Shahpoury et al., 2016; Tomaz et al., 2016). However, the knowledge about the influence of the aerosol composition is still limited, especially for the PAH derivatives. Tomaz et al. (2016) suggested a dependency of organic matter and soot in the aerosol on the gas-particle partitioning of NPAHs and OPAHs. The detailed knowledge about gas-particle partitioning is crucial since it influences several processes, such as transport, atmospheric degradation and deposition (Bidleman, 1988; Lohmann and Lammel, 2004b; Lammel et al., 2009; Shahpoury et al., 2015) as well as the bioavailability (Pankow et al., 2001; Wei et al., 2008).

PACs can be degraded by homogeneous and heterogeneous reaction with atmospheric oxidants in the atmosphere. In the gas phase, the air pollutants are mainly degraded by OH and NO_3 radicals (Atkinson and Arey, 1994; Keyte et al., 2013). Some studies report the heterogeneous degradation of PACs (Miet et al., 2009; Zhang et al., 2011; Ringuet et al., 2012; Keyte et al., 2013; Jariyasopit et al., 2014). Especially NPAHs are prone to photodegradation (Fan et al., 1996). Feilberg et al. (1999) showed that photodegradation in the gas phase is the major pathway for the degradation of nitronaphthalenes. However, available degradation rates are still limited to several PAHs and only some PAH derivatives (Lammel et al., 2015).

In addition to degradation, PACs are removed from the atmosphere by deposition (Bidleman, 1988; Murahashi et al., 2001; Keyte et al., 2013; Shahpoury et al., 2015; Shahpoury et al., 2018). PACs in the gas phase can be deposited by wet scavenging, while PACs in the particulate phase are removed from the atmosphere by dry deposition and wet particle scavenging (Ligocki et al., 1985a; b; Cousins et al., 1999; Shahpoury et al., 2018). Since particles are deposited more efficiently than

substances in the gas phase, it is expected that PAH derivatives, having a higher particulate mass fraction, get faster removed from the atmosphere than their parent PAHs (Cousins et al., 1999; Shahpoury et al., 2015; 2018). However, some papers showed that the dry deposition velocity is higher for low-molecular weight PAHs since high-molecular weight PAHs are mainly distributed in the fine particulate fraction, while low-molecular weight PAHs can repartition to coarser particles, which are deposited more efficiently than small particles (Odabasi et al., 1999; Shannigrahi et al., 2005; Bozlaker et al., 2008). However, this depends on the studied site since repartitioning takes time and close to sources the higher particulate fraction of high-molecular weight PAHs plays the major role (Terzi and Samara, 2005). For most PAH derivatives, deposition fluxes are still largely unknown. The compounds get deposited to the ground, e.g. to surface waters, soil and vegetation (Baek et al. 1991; Horstmann and McLachlan, 1998; Bandowe & Meusel 2017). Bandowe and Meusel (2017) summarized that atmospheric deposition is the major source of NPAHs in urban surface waters and soils. The pollutants can accumulate in the sediment and in soil. However, depending on the concentrations in the different compartments, as well as on the temperature, PACs can also revolatilize from the surface back to the atmosphere (Cousins et al., 1999; Lammel et al., 2009; Degrendele et al., 2016; Lammel et al., 2018).

1.4 Health effects

PACs can enter the human body by dermal contact, e.g. with soil or smoke, by ingestion, e.g. via food, as well as by inhalation of polluted air (Ruby et al., 2016; Lao et al., 2018). However, this PhD project focused on the pathway of inhalation.

Inhalation of polluted air is a major health risk, leading to different adverse health effects, such as respiratory and cardiovascular diseases (Shiraiwa et al., 2017; Lelieveld et al., 2019; WHO, 2021). Lelieveld and colleagues (2020) estimated that global air pollution is attributable to an excess mortality rate of about 8.8 million people per year. PAHs and PAH derivatives are constituents of atmospheric PM. Several PACs are carcinogenic or possibly carcinogenic (IARC, 1983; 1989; 2012; Collins et al., 1998), mutagenic (Durant et al., 1996; Clergé et al., 2019), ecotoxic (El Alawi et al., 2002; Sverdrup et al., 2002a; b) and have endocrine disrupting potential (Lampi et al. 2006; Lundstedt et al. 2007; Nováková et al. 2020). Some OPAHs and NPAHs even show a higher toxicity than their parent PAHs and are direct-acting mutagens and carcinogens, while PAHs need metabolic activation (Durant et al., 1996; Collins et al., 1998; IARC, 2012; Misaki et al., 2016; Clergé et al., 2019). Nevertheless, PAH derivatives are studied by far not as extensively as the 16

EPA-prioritized PAHs. This research gap has already been emphasized by Andersson and Achten (2015) and Lammel (2015).

Until today, health effects of air pollution are mainly linked to the PM mass concentration. However, this ignores the different chemical composition of PM, which may lead to different health effects despite similar PM masses (Schaumann et al., 2004). As suggested by Borm et al. (2007), the oxidative potential (OP) has become a common alternative measure for the toxicity of PM (Yang et al., 2015; Daellenbach et al., 2020; Gao et al., 2020; Lelieveld et al., 2021) as it is one of the biological pathways that negatively impacts human health (Nel, 2005; Sies, 2017). A high OP of PM and constituents of PM leads to the production of an excess amount of reactive oxygen species (ROS) in the body. An excess of ROS can lead to oxidation of cells, tissues and biological molecules, such as proteins and DNA, resulting in oxidative stress including e.g. inflammation, DNA damage and cell injuries (Bolton et al., 2000; Penning, 2017; Sies, 2017).

In order to understand the cause for oxidative stress triggered by PM, particle size, area and the composition, as well as the OP of the individual constituents should be known (Nel, 2005). Several studies have investigated the importance of PM constituents on the OP, focusing mainly on metals and organics. Several studies found that transition metals and water-soluble organic compounds (WSOC) correlate with the OP (Chung et al., 2006; Biswas et al., 2009; Nawrot et al., 2009; Verma et al., 2009; 2011; 2015a; b; Shen and Anastasio, 2011; Charrier and Anastasio, 2012; Charrier et al., 2014; Saffari et al., 2014; Fang et al., 2016; 2019; Tuet et al., 2016; Calas et al., 2017a; Lyu et al., 2018; Pietrogrande et al., 2019; Bates et al., 2019; Gao et al., 2020). While transition metals, especially copper, contribute between 40 and 97 % to the OP, quinones account for 0 to 20 % (Shen and Anastasio, 2011; Charrier and Anastasio, 2012; Charrier et al., 2014; Verma et al., 2015a; b; Lyu et al., 2018). Studies suggest that the sensitivity to different PM constituents depends on the assay (Calas et al., 2017a; Bates et al., 2019; Pietrogrande et al., 2019). As it will be explained in Chapter 1.5, there are various cellular and acellular assays in use to measure the OP. In the majority of studies, the acellular dithiothreitol (DTT) depletion assay is applied (Biswas et al., 2009; Verma et al., 2009; 2011; 2015a; b; Charrier and Anastasio, 2012; Fang et al., 2015; 2016; 2019; Tuet et al., 2016; Calas et al., 2017a; Lyu et al., 2018; Pietrogrande et al., 2019; Bates et al., 2019; Gao et al., 2020). Almost all studies investigating the OP of individual PACs, as part of WSOCs, only consider a few selected quinones (Chung et al., 2006; Charrier and Anastasio, 2012; McWhinney et al., 2013; Charrier et al., 2014; Verma et al., 2015a; Visentin et al., 2016; Xiong et al., 2017;

Lyu et al., 2018; Wang et al., 2018). The same is true for a developed model for ROS generation of $PM_{2.5}$ (Lakey et al., 2016; Fang et al., 2019; Lelieveld et al., 2021). In addition, the gas phase pollutants are usually not considered in any of the studies but are expected to be relevant, too (Wei et al., 2018).Several studies show that atmospherically aged aerosols show a higher OP than fresh aerosols (Li et al., 2009; Verma et al., 2009; Rattanavaraha et al., 2011; Verma et al., 2015a). As shown by Lyu et al. (2018), a significant amount of the OP cannot be explained by metals and the typically measured quinones. During haze periods in China, the contribution of unidentified substances to the OP is even higher than during non-haze periods.

In contrast to quinones, to the best of our knowledge, there are no studies about the acellular OP of other OPAHs or NPAHs. In contrast, it was already shown in cellular assays that these PAH derivatives can produce ROS, too. Tuet et al. (2019) showed that 1-nitropyrene, 6-nitrochrysene, 9-fluorenone and 2-methylanthraquinone show a significant response in the used cellular OP test. The OP of 9-fluorenone in cells was also observed by Atsumi et al. (2004). Hansen and colleagues (2007) showed the ROS generation of 3-nitrobenzanthrone in human lung epithelial cells. In addition, several studies (Park and Park, 2009; Andersson et al., 2009; Shang et al., 2017 and Zhao et al., 2019) demonstrated the formation of ROS in cells induced by NPAHs. Chung et al. (2007) even found ROS formation of PAHs, which do not possess redox-active properties themselves (Cho et al., 2005). This was explained by the metabolic transformation from PAHs to quinones in living cells, e.g. by cytochrome P450 enzymes (Chung et al., 2007; Bolton et al., 2000).

1.5 Methodological background

The PACs in the particulate phase are sampled on filters, e.g. quartz fiber or Teflon filter, while gaseous PACs are often sampled on polyurethane foams (Pöhlker et al., 2021, Galmiche et al., 2021b). The compounds are extracted from the sampling media and the matrix, e.g. soil, filters, polyurethane foams, by Soxhlet, pressurized liquid, ultrasound assisted or microwave assisted extraction using different organic solvents (Galmiche et al., 2021b). Due to the matrix and the low relative concentrations in the environmental matrices, purification and concentration are needed. The clean-up is often performed by solid phase extraction (SPE) (Toledo et al., 2007; Bandowe and Meusel, 2017; Shahpoury et al., 2018; Galmiche et al., 2021b). The decision of the used solvents for elution of the target compounds from the absorbent phase can be used to fractionate the PACs depending on their polarity (Bodzek et al., 1993; Bandowe and Wilcke, 2010; Cochran et al., 2012). To determine the concentration in water, thawed snow samples or aqueous extracts,

liquid-liquid extraction or SPE is usually used (Galmiche et al., 2021a). Further separation of the compound is often necessary because of the high amount of chemically similar substances and the need to differentiate between isomers. This is mostly done by gas chromatography (GC) or liquid chromatography (LC) (Galmiche et al., 2021a). It is widely used for decades for volatile and semivolatile organic compounds (VOCs and SVOCs). The separation of compounds in GC is mainly due to the boiling point and supported by interaction with the stationary phase. For compounds which have a too high boiling point or are thermolabile, derivatisation (Cho et al., 2004; Delgado-Saborit et al., 2013; Sousa et al., 2015; Toriba et al., 2016) or LC (Mirivel et al., 2010; Garcia-Alonso et al., 2012; Fujiwara et al., 2014; Nyiri et al., 2016) could be a solution. The detection of PACs after separation by GC is usually done by mass spectrometry (Albinet et al., 2008; Wei et al., 2012; Alves et al., 2016; Shahpoury et al., 2018; Bandowe et al., 2019; Nežiková et al., 2021) or electron capture detectors (Vincenti et al., 1996; Castells et al., 2003; Priego-Capote et al., 2003), while fluorescence (Garcia-Alonso et al., 2012) detectors and mass spectrometers (Mirivel et al., 2010; Fujiwara et al., 2014; Nyiri et al., 2016) are mostly used after LC.

In order to measure the health effects of atmospheric particles, aqueous extracts of collected aerosol particles are prepared and investigated by different cellular and acellular assays. Most studies extract the filter samples by distilled water (Biswas et al., 2009; Nawrot et al., 2009; Verma et al., 2009; 2011; 2015a; b; Saffari et al., 2014; Fang et al., 2016; 2019; Tuet et al., 2016; de Jesus et al., 2018; Lyu et al., 2018). Some studies use a phosphate buffer (Shen and Anastasio, 2011; Charrier and Anastasio, 2012; Charrier et al., 2014) or organic solvent (Mudway et al., 2004). Tuet and colleagues (2016) used cell culture media for the extraction to measure cellular ROS production and Calas et al. (2017b) used Gamble solution with an additional lipid constituent for the extraction. In addition, the extraction procedure differed in additional parameters, such as the extraction technique, extraction time and extraction temperature. As extraction technique, vortexing (Mudway et al., 2004; Calas et al., 2017b; de Jesus et al., 2018), sonication (Biswas et al., 2009; Verma et al., 2015a; Fang et al., 2016; Tuet et al., 2016; Lyu et al., 2018) agitated/shaken (Verma et al., 2009; Shen and Anastasio, 2011; Fang et al., 2015) or combination of different techniques (Nawrot et al., 2009) are used. As extraction temperature can be differentiated between studies using room temperature (Verma et al., 2011; Saffari et al., 2014) and studies using 37 °C (Fang et al., 2015; Calas et al., 2017b) in order to better simulate physiologic conditions in the human body.

For the determination of the OP, as described in Chapter 1.4, there are different cellular and acellular assays (Hedayat et al., 2014; Hellack et al., 2017; Bates et al., 2019). In this PhD thesis, acellular OP assays were applied. One widely used OP assay is the dithiothreitol (DTT) depletion assay (Jiang et al., 2019). This assay measured the ability of compounds to oxidize the thiol groups of DTT while being reduced. DTT can be seen as a substitute for physiologically relevant reductants, such as NADPH (Kumaiga et al., 2002). The DTT concentration, which is decreasing with reaction time, can be quantified by measuring the absorbance of 2-nitro-5-thiobenzoic acid (TNB), the product of the reaction of DTT with 5,5'-ditiobis-2-nitrobenzoic acid (DTNB) (Jiang et al., 2019). Furthermore, there are several assays measuring the depletion of different antioxidants, such as ascorbic acid, uric acid and glutathione (GSH), either by using liquid-chromatography or spectrophotometry (Hellack et al., 2017). Furthermore, there are assays using fluorescence spectroscopy to measure the OP by the oxidation of different substrates like dichlorofluorescein (DCFH) and N-acetyl-3,7-dihydroxy-phenoxazine (Amplex red) or related structures to fluorescent products (Hellack et al., 2017) such as in the H_2O_2 assay (Tong et al., 2018). As another technique, focusing on radicals, electron paramagnetic resonance spectroscopy (EPR) can be used. As already mentioned in Chapter 1.4, the assays differ in their sensitivity for chemical species and can be specific or unspecific for various types of ROS (Hellack et al., 2017; Bates et al., 2019).

1.6 Research objectives

The aim of this PhD study was the investigation of the occurrence, cycling and fate in the environment of NPAHs and OPAHs as well as their uptake and health effects on humans. This basic research is needed to understand the importance of these air pollutants. The overall aim was divided into three key research objectives, which are illustrated in Figure 1 and summarized in the following:

1. Determine the concentrations, composition patterns and long-term variations of NPAHs and OPAHs in soil at a semi-urban and a background site in Czech Republic.
2. Determine the concentrations, the sources, the formation, the gas-particle partitioning and the mass size distributions of PAH derivatives in the marine boundary layer over the Mediterranean Sea and around the Arabian Peninsula.

3. Determine the OP and the resulting relevance of individual NPAHs and OPAHs and investigate the predictability of the OP values by molecular structure, reduction potential or the energy level of the lowest unoccupied molecular orbital (LUMO).

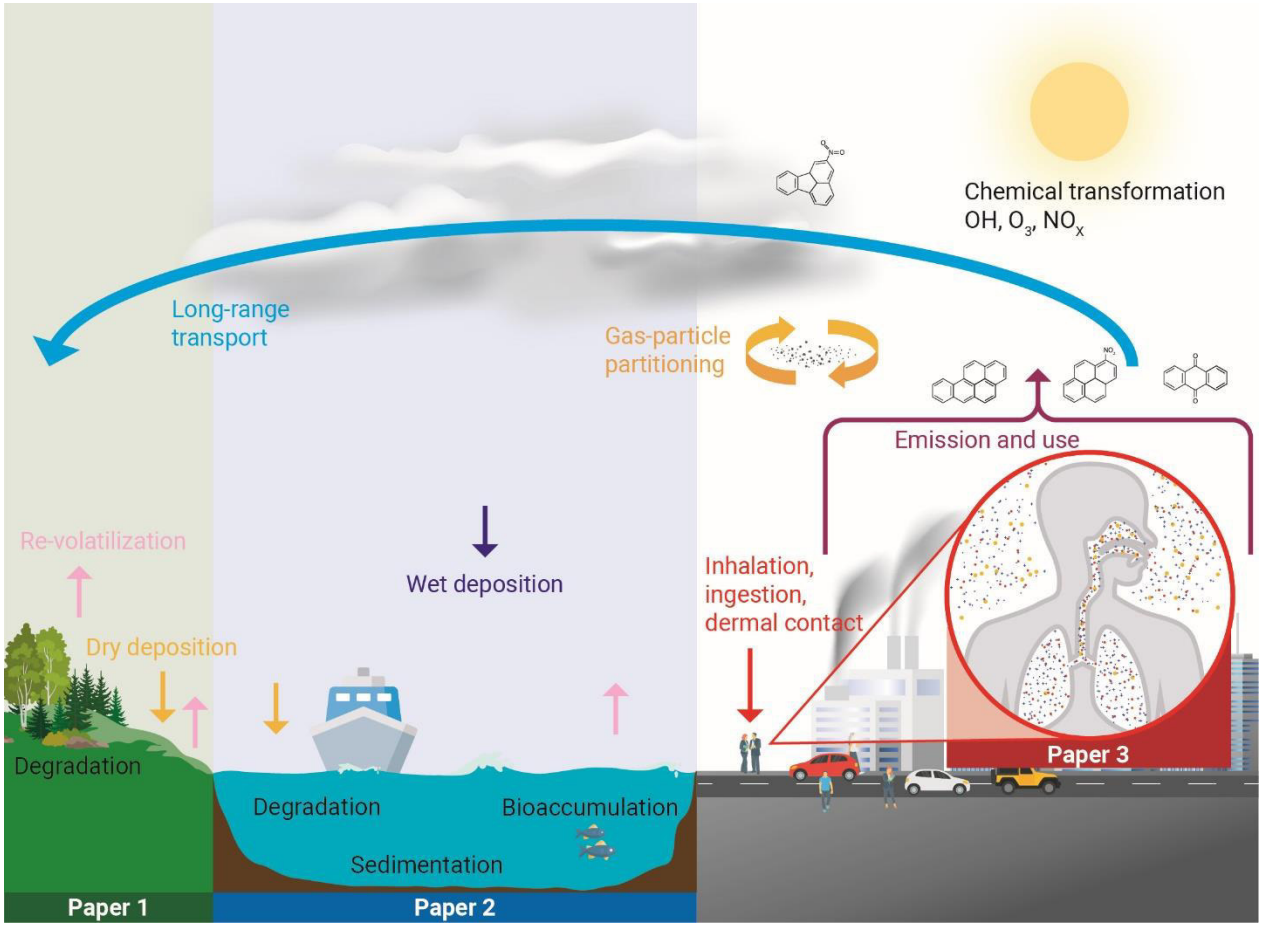

Figure 1. Visualization of the main topics of the PhD project. Paper 1: Nitro- and oxy-PAHs in soil; Paper 2: PACs in the marine atmosphere; Paper 3: Oxidative potential of PACs.

2 Results

2.1 Nitro- and oxy-PAHs in soil

This chapter has already been published as a research paper in the journal *Environmental Geochemistry and Health*. As the first author of this manuscript, I have done the sample preparation and purification of the samples in the trace analytical laboratory of the RECETOX, Faculty of Science, Masaryk University in Brno (Czech Republic), as well as the validation of this method in advance. Furthermore, I evaluated the data and was mainly responsible for the interpretation of the data. I wrote the first draft of the manuscript, created the figures, edited the manuscript based on feedback and exchange with the coauthors and played a primary role in the revision process.

Environ. Geochem. Health (2021) https://doi.org/10.1007/s10653-021-01066-y

Nitro- and oxy-PAHs in grassland soils from decade-long sampling in Central Europe

M. Wietzoreck[a], B. A. M. Bandowe[a], J. Hofman[b], J. Martiník[b], B. Nežiková[b], P. Kukučka[b], P. Přibylová[b], G. Lammel[a,b,*]

[a]Max Planck Institute for Chemistry, Multiphase Chemistry Dept., Mainz, Germany

[b]Masaryk University, Research Centre for Toxic Compounds in the Environment, Brno, Czech Republic

Environ Geochem Health
https://doi.org/10.1007/s10653-021-01066-y

ORIGINAL PAPER

Nitro- and oxy-PAHs in grassland soils from decade-long sampling in central Europe

M. Wietzoreck · B. A. M. Bandowe · J. Hofman · J. Martiník · B. Nežiková · P. Kukučka · P. Přibylová · G. Lammel

Received: 10 February 2021 / Accepted: 4 August 2021

Abstract Long-term exposure to polycyclic aromatic hydrocarbons (PAHs) and their nitrated (NPAHs) and oxygenated (OPAHs) derivatives can cause adverse health effects due to their carcinogenicity, mutagenicity and oxidative potential. The distribution of PAH derivatives in the terrestrial environment has hardly been studied, although several PAH derivatives are ubiquitous in air and long-lived in soil and water. We report the multi-annual variations in the concentrations of NPAHs, OPAHs and PAHs in soils sampled at a semi-urban (Mokrá, Czech Republic) and a regional background site (Košetice, Czech Republic) in central Europe. The concentrations of the Σ_{18}NPAHs and the Σ_{11+2}OPAHs and O-heterocycles were 0.31 ± 0.23 ng g^{-1} and 4.03 ± 3.03 ng g^{-1}, respectively, in Košetice, while slightly higher concentrations of 0.54 ± 0.45 ng g^{-1} and 5.91 ± 0.45 ng g^{-1}, respectively, were found in soil from Mokrá. Among the 5 NPAHs found in the soils, 1-nitropyrene and less so 6-nitrobenzo(a)pyrene were most abundant. The OPAHs were more evenly distributed. The ratios of the PAH derivatives to their parent PAHs in Košetice indicate that they were long-range transported to the background site. Our results show that several NPAHs and OPAHs are abundant in soil and that gas-particle partitioning is a major factor influencing the concentration of several semi-volatile NPAHs and OPAHs in the soils. Complete understanding of the long-term variations of NPAH and OPAH concentrations in soil is limited by the lack of kinetic data describing their formation and degradation.

Keywords Polycyclic aromatic compounds, soil pollution · Nitrated PAHs · Soil exposure · Background · Temporal variation

Introduction

The combustion of fossil fuels and biomass is the main source of polycyclic aromatic compounds (PACs) such as polycyclic aromatic hydrocarbons (PAHs) and their nitrated (NPAHs) and oxygenated (OPAHs) derivatives (Baek et al., 1991; Bandowe & Meusel, 2017; Walgraeve et al., 2010). Besides these pyrogenic sources, PACs in contaminated soils can originate from fossil material such as coal, crude oil,

Supplementary Information The online version contains supplementary material available at https://doi.org/10.1007/s10653-021-01066-y.

M. Wietzoreck · B. A. M. Bandowe · G. Lammel (✉)
Max Planck Institute for Chemistry, Multiphase Chemistry Dept, Mainz, Germany
e-mail: g.lammel@mpic.de

J. Hofman · J. Martiník · B. Nežiková · P. Kukučka · P. Přibylová · G. Lammel
Masaryk University, Research Centre for Toxic Compounds in the Environment, Brno, Czech Republic

Published online: 20 August 2021

petroleum, chemical waste, contaminated sewage sludge and water (Bandowe & Meusel, 2017; Bandowe et al., 2019; Vikelsøe et al., 2002). The O-heterocycle dibenzofuran could originate from the chemical industry (Nežiková et al., 2021). Another source for PAH derivatives in soils is their formation from the biodegradation and (photo)chemical oxidation of PAHs (Cerniglia, 1992; Finlayson-Pitts & Pitts, 2000; Keyte et al., 2013; Walgraeve et al., 2010). PACs in soil can enter the human body by inhalation, oral ingestion and dermal contact (Ruby et al., 2016) and can adversely affect humans as well as the ecosystem. Several PACs are carcinogenic (Collins et al., 1998; IARC, 2010, 2012) and mutagenic (Durant et al., 1996), cause oxidative stress (Bolton et al., 2000) and are endocrine-disrupting compounds (Lampi et al., 2006; Lundstedt et al., 2007; Nováková et al., 2020) and ecotoxic (Bandowe & Meusel, 2017; el Alawi et al., 2002; Sverdrup et al., 2002a, 2002b). Dibenzofuran causes effects in lung cells, contributes to oxidative stress and has estrogenic properties (Brinkmann et al., 2014; Duarte et al., 2011, 2012; Jaiswal et al., 2012), while 9-fluorenone is cytotoxic (Atsumi et al., 1998). However, these two substances were so far not found to be genotoxic or mutagenic (Leary et al., 1983; Matsumoto et al., 1988; Mortelmans et al., 1984; USEPA, 2020; Vasilieva et al., 1990). Even though several PAH derivatives can be even more toxic than the parent PAHs (Lampi et al., 2006; Lundstedt et al., 2007; WHO, 2003), the knowledge about the occurrence, cycling, fate, spatial, seasonal and long-term temporal trends of NPAHs, OPAHs and heterocyclic aromatics is limited (Lammel, 2015; Schlanges et al., 2008).

Significant portions of PACs emitted from various anthropogenic activities are transferred into soils by wet and dry deposition (Baek et al., 1991; Bandowe & Meusel, 2017) or by litter fall (Horstmann & McLachlan, 1998). Semi-volatile compounds, such as several PACs, can revolatilize from the soil to the atmosphere (Keyte et al., 2013; Lammel et al., 2009). Hence, soils are an important compartment and a major repository for the global cycling and large-scale chemodynamics of PACs (Lammel et al., 2009; Wild & Jones, 1995).

The concentration of a PAC in soil at every timepoint depends on its emission intensity, formation in air and soil, degradation in air, deposition, volatilization, transport, sequestration, sorption and desorption to soil matrix, degradation in soil (biotic and abiotic), bioaccumulation, plant-uptake, formation of non-extractable residues amongst others (Idowu et al., 2019; Semple et al., 2003; Wilcke, 2000). Several of these processes were not studied in detail yet. Few studies addressed NPAHs and OPAHs in precipitation (Kawamura & Kaplan, 1983), and in fresh snow (Shahpoury et al., 2018), but no relevant model-based estimates of deposition fluxes or velocities are available. The deposition velocity depends on gas-particle partitioning in the aerosol, i.e. pollutants sorbed to particles are more efficiently deposited than gaseous, and even more so if lipophilic (Bidleman, 1988; Shahpoury et al., 2015, 2018; Škrdlíková et al., 2011). Thus, PAH derivatives might be deposited faster than their parent PAHs due to their lower vapour pressure (Tomaz et al., 2016).

The concentrations of most PACs in air and soil mainly depend on their proximity to emission sources (Bandowe et al., 2010, 2019). The highest concentrations in air and soil are found at urban and industrial sites (Arp et al., 2014; Bandowe et al., 2010, 2011, 2014; Cai et al., 2017; Lundstedt et al., 2007; Pham et al., 2015; Watanabe et al., 2005). Since PACs can undergo long-range transport due to their long lifetime in air and their vapour pressure (Keyte et al., 2013; Wilcke et al., 2014a; Wilson et al., 2020), PACs are abundant in rural and remote sites too. Despite that, the literature of PACs in soil at remote places is still limited. Some studies determined the abundance of PAHs in remote soils (Fernández et al., 2003; Marquès et al., 2017; Wang et al., 2009; Wilcke & Amelung, 2000), but the only studies about NPAHs and OPAHs in background soil samples are from Scandinavia (Brorström-Lundén et al., 2010; Vikelsøe et al., 2002), South America (Bandowe & Wilcke, 2010; Wilcke et al., 2014a), China (Bandowe et al., 2019) and the USA (Obrist et al., 2015).

PACs can also be found in subsoils due to transport by leaching, bioturbation and colloid-assisted transport (Bandowe et al., 2010; Krauss et al., 2000; Wilcke, 2000). The higher water solubility and lower lipophilicity of OPAHs than their related PAHs might render them more mobile in soils than PAHs (Lundstedt et al., 2007). Some NPAHs are less water soluble and have higher sorption coefficients (K_{oc}) than their related parent PAHs, which might result in their diminished mobility in soil (Sun et al., 2017; WHO, 2003). Another major factor influencing the concentrations of PACs in soil is their formation and

degradation. The half-lives of PAHs until mineralization range between days and years (Cerniglia, 1992). The biological degradation of PAHs by bacteria and fungi can result in the formation of OPAHs (Cerniglia, 1992).

There is no long-term study of PAH derivatives in soil, unlike for parent PAHs. The long-term studies of PAHs in soil found an increase in PAH abundance from 1880 to 1986 in England (Jones et al., 1989a, 1989b) and in the 1970s in Japan (Honda et al., 2007) followed by a levelling off or even a decrease in concentration thereafter (Becker et al., 2006; Cui et al., 2020; Holoubek et al., 2007b; Honda et al., 2007). In contrast, Gubler et al. (2015) only found a decreasing trend for light PAHs in Swiss soils between 1985 and 2013, while the concentration of the heavier PAHs almost stayed constant.

The aim of our study was to determine the temporal variations in the concentrations and composition profiles of OPAHs, O-heterocycles, NPAHs and PAHs in grassland soils of a central European background and a semi-urban site both located in Czech Republic. By elucidating the difference between soil at semi-urban vs rural sites and between air and soil concentration, we aim to improve the understanding of the sources, occurrence and fate of PAH derivatives in soil. We include 3-nitrobenzanthrone, a highly mutagenic nitrated oxy-PAH (Enya et al., 1997; Lübcke-von Varel et al., 2012) and less studied but abundant OPAHs and O-heterocycles, i.e. benzanthrone and 6H-benzo(c)chromen-6-one. To the best of our knowledge, this is the first study determining a time series of PAH derivatives in soil.

Methods and materials

Sampling

We sampled soils at grassland sites in Košetice and Mokrá, in the Czech Republic. Košetice is a rural background site located 534 m above the sea level in the central Czech Republic (85 km from Prague). The site is also a station of the European Monitoring and Evaluation Programme (EMEP), the Global Atmosphere Watch programme (GAW) and other networks. The average annual temperature (1988–2017) is 8.1 °C, and the average annual precipitation is around 650 mm. Košetice location 1 (Košetice-1) is located at the observatory on open area covered by grass. Košetice location 2 (Košetice-2) is close (28 m) to the confluence of two brooks at an open meadow. The soil samples from Košetice locations 1 and 2 were taken in summer of each year from 2010 to 2017. In this study, the soil samples from the years 2010–2017 except for year 2011 were analysed.

Mokrá is a semi-urban site at the rim of an urban and an industrial area at an elevated altitude. The site is located 13 km east–north-east of the city centre of Brno. The Brno metropolitan area has a population of $\approx$500,000 inhabitants (Czech Statistical Office, 2019). Mokrá location 1 (Mokrá-1) (Hostěnice Čihálky) is near a small forest that is close (40 m) to the edge of a quarry of a cement works. It is an open area covered by uncultivated grass and few small bushes. Mokrá location 2 (Mokrá-2) (Velká Baba), 3.5 km south of sampling site 1, is close to the village Sivice with approximately 1000 inhabitants (Czech Statistical Office, 2019). The sampling site is on an open grassland with a small forest 30 m to the west. To the north-west (940 m), there is a cement factory.

The soil samples from seven archived soil samples within 2006–2015 from Mokrá-1 and Mokrá-2, sampled in spring (Sp), fall (F) or summer (S), were analysed. Detailed information about the sampling dates and locations can be found in the Online Resource (Supplementary Information, SI) in Table S1. A map including both sampling locations per site is shown in Fig. S1.

A detailed description of the sampling procedure has previously been reported (Holoubek et al., 2007b, 2009). At each sampling site, the soils were inspected and the top 10 cm of the surface soil within the A horizon was sampled using a stainless steel spade (after removing the vegetation layer). At all four locations, the soil evolutions seemed identical based on visual inspection. The soil samples were all characterized as Cambisol, except at Košetice-2, where it is fluvisol. Each location was represented by a mixture of ten sub-samples collected from an area of 25 $\times$ 25 m. The samples were transported to the laboratory, air-dried at room temperature, sieved (2 mm mesh) and stored in paper bags in a dark room at constant temperature and humidity.

Determination of soil properties

Several soil physico-chemical properties were determined on aliquots of each soil sample. The properties

were measured by standard operational procedures. These include total organic carbon (TOC) content (ISO 14235, 1998), total soil nitrogen (N_{tot}) (ISO 11261, 1995), soil pH_{KCl} and pH_{H2O} (ISO 10390, 2005). The basic soil properties can be found in the SI in Table S2.

Determination of PAHs, NPAHs and OPAHs in soils

The concentrations of PAHs were determined in aliquots of the soil samples directly after sampling as described by Holoubek et al., (2007a, 2009). In brief, the soils were extracted with dichloromethane (DCM) on a Soxhlet apparatus. The soil extracts were subsequently purified on silica gel columns. PAHs in the purified soils extracts were measured by gas chromatography-mass spectrometry (GC–MS). Except for the extraction solvent, the sample preparation and the analysis of the PAHs were done similarly between the first PAH measurement (called "original" concentration) and the remeasurement taking another aliquot of the archived soil samples in May 2018. Additionally to the PAH concentration, the OPAH and NPAHs content in the soil samples was analysed as described below.

Aliquots (5 g) of the soil samples were transferred into cellulose extraction thimbles (Whatman 603 33 × 100 mm 10,350,242 and Advantec N08433X37X94mm) and placed into a Soxhlet extractor (Büchi B-811, Flawil, Switzerland). The soils were spiked with 50 µL of a standard mixture of deuterated PAHs [naphthalene-D8, phenanthrene-D10 and perylene-D12 (Dr. Ehrenstorfer, Augsburg, Germany), each with a concentration of 6.6 µg mL^{-1} in toluene] and 50 µL of a standard mixture of deuterated NPAHs [1-nitronaphthalene-D7, 2-nitrofluorene-D9, 9-nitroanthracene-D9, 3-nitrofluoranthene-D9, 1-nitropyrene-D9, 6-nitrochrysene-D11 and 6-nitrobenzo(a)pyrene-D11 (Chiron, Trondheim, Norway)], each with a concentration of 0.4 µg mL^{-1} in toluene as surrogate standards for PAHs and NPAHs, respectively. In addition, 50 µL of a deuterated OPAH standard mixture [9-fluorenone-D8 and 9,10-anthraquinone-D8 (Chiron, Trondheim, Norway)], each with a concentration of 0.8 µg mL^{-1} in ethyl acetate (EA, MS Suprasolv, Merck, Darmstadt, Germany), was spiked to the soil samples (except for the first 11 samples) to serve as surrogate standards for the OPAHs. Each sample was then extracted with 150 mL of a DCM/acetone (2:1, v:v, Rotisolv GC Ultra Grade, Roth, Karlsruhe, Germany and Suprasolv, Merck, Darmstadt, Germany) mixture for 40 min, as previously done (Klánová et al., 2008). The soil extracts were concentrated (to 1–2 mL), quantitatively transferred to an amber vial and stored until clean-up by column chromatography.

Each column was packed with 0.5 g of dried Na_2SO_4 and 8 g of 10% deactivated silica (Sigma Aldrich, St. Louis, MO, USA). On the top, another layer of 0.5 g of Na_2SO_4 was added. The column was conditioned with 6 mL of DCM followed by 6 mL of EA. The soil extract was then transferred into the column and solvent allowed to drain off. The target compounds were then eluted with 24 mL of EA followed by 24 mL of DCM collecting the eluates in vials. During the entire purification process, the column was covered with aluminium foil to avoid photodegradation of target compounds. The purified extracts were transferred into glass tubes and concentrated in an evaporation system (Turbovap II, Biotage, Uppsala, Sweden) to approximately 0.3 mL and then transferred to a GC vial. The extracts were further concentrated to 200 µL using a gentle stream of N_2. This was followed by the addition of 50 µL nonane as a keeper, shaking and further evaporation to 50 µL. As the last step, 50 µL of a PCB121 solution (0.2 µg mL^{-1} in cyclohexane) and 50 µL of a p-terphenyl solution (4 µg mL^{-1} in toluene) were added as internal standards.

Polycyclic aromatic compounds (PACs) in the soil extracts were analysed by GC–MS in the Trace Analytical Laboratory of the research centre RECETOX at the Masaryk University in Brno, Czech Republic similar to Nežiková et al. (2021). The target compounds in this study were 27 PAHs, 17 NPAHs, 1 NOPAH, 11 OPAHs and 2 O-heterocycles. The 27 PAHs were naphthalene (NAP), acenaphthylene (ACY), acenaphthene (ACE), fluorene (FLN), phenanthrene (PHE), retene (RET), anthracene (ANT), fluoranthene (FLT), pyrene (PYR), benzo(a)anthracene (BAA), chrysene (CHR), benzo(b)fluoranthene (BBF), benzo(k)fluoranthene (BKF), benzo(a)pyrene (BAP, also called benzo(def)chrysene), indeno(1,2,3-cd)pyrene (INP), dibenz(ah)anthracene (DBA), benzo(ghi)perylene (BPE), benzo(b)fluorene (BBN), benzo(ghi)fluoranthene (BGF), cyclopenta(cd)pyrene (CCP),

triphenylene (TPH), benzo(j)fluoranthene (BJF), benzo(e)pyrene (BEP), perylene (PER), dibenz(ac)anthracene (DCA), anthanthrene (ATT), coronene (COR). The target NPAHs were 1-nitronaphthalene (1-NNAP), 2-nitronaphthalene (2-NNAP), 3-nitroacenaphthene (3-NACE), 5-nitroacenaphthene (5-NACE), 2-nitrofluorene (2-NFLN), 9-nitroanthracene (9-NANT), 9-nitrophenanthrene (9-NPHE), 3-nitrophenanthrene (3-NPHE), 2-nitrofluoranthene (2-NFLT), 3-nitrofluoranthene (3-NFLT), reported as sum (2- + 3-NFLT), 1-nitropyrene (1-NPYR), 7-nitrobenzo(a)anthracene (7-NBAA), 6-nitrochrysene (6-NCHR), 1,3-dinitropyrene (1,3-N_2PYR), 1,6-dinitropyrene (1,6-N_2PYR), 1,8-dinitropyrene (1,8-N_2PYR) and 6-nitrobenzo(a)pyrene (6-NBAP). In addition, the NOPAH 3-nitrobenzanthrone (3-NBAN) was another target compound. The OPAHs were 1,4-naphthoquinone (1,4-O_2NAP), naphthalene-1-aldehyde (1-(CHO)NAP), 9H-fluoren-9-one (9-OFLN), 9,10-anthraquinone (9,10-O_2ANT), 11H-benzo(a)fluoren-11-one (11-OBaFLN), 11H-benzo(b)fluoren-11-one (11-OBbFLN), benzanthrone (7H-benz(de)anthracene-7-one) (BAN), benz(a)anthracene-7,12-dione (7,12-O_2BAA), 5,12-naphthacenequinone (5,12-O_2NAC) and 6H-benzo(cd)pyren-6-one (6-OBPYR), while O-heterocycles were dibenzofuran (DBF) and 6H-benzo(c)chromen-6-one (6-OBCC, also called 6H-dibenzo(bd)pyran-6-one). All targeted compounds including their physico-chemical properties are shown in Table S3.

PAHs were measured on a GC (GC 7890A Agilent Technologies, Santa Clara, USA) using a 60 m × 0.25 mm × 0.25 μm Rxi-5Sil MS column (Restek, Bellefonte, USA). The instrument was coupled to a triple quadrupole mass spectrometer (MS 7000B, Agilent Technologies, Santa Clara, USA). The GC temperature programme started at 80 °C (hold for 1 min) followed by an increase by 15 °C min^{-1} to 180 °C and by 5 °C min^{-1} to 310 °C, which was held for 20 min. The injection volume was 1 μL in splitless mode at 280 °C. As carrier gas, helium with a flow rate of 1.5 mL min^{-1} was used. The transfer line and the ion source were set to 310 °C and 320 °C, respectively. Electron ionization (EI) in positive mode was applied as the ionization technique. Selected ion monitoring (SIM) mode was applied using one ion for quantification and one or two ions per compound for qualification. The retention times as well as the quantifying ions of the targeted PAHs are shown in Table S4. For the evaluation, the internal standard method was used, calculating the ratio of the internal standard p-terphenyl and the target compound.

All nitrated and oxygenated PAHs were analysed by GC–MS using atmospheric pressure chemical ionization (APCI) in negative mode on a 7890 GC (Agilent Technologies, Santa Clara, USA) coupled to a triple quadrupole MS Xevo TQ-S (Waters, Milford, USA). A 30 m × 0.25 mm × 0.25 μm Rxi-5Sil MS column (Restek, Bellefonte, USA) was used. One microlitre of the samples was injected splitless at 270 °C. Helium was used as the carrier gas at a constant flow of 1.5 mL min^{-1}. The oven temperature program was starting at 90 °C for 1 min followed by an increase of 40 °C min^{-1} to 180 °C and 5 °C min^{-1} to 320 °C (6 min hold). The target compounds were measured in the multiple reaction monitoring (MRM) mode. The MRM m/z ratios and the retention time of the targeted OPAHs and NPAHs are given in Table S5. The ratio of the target compound and the internal standard PCB121 was used to determine the target compound concentration.

Quality control

Details about the quality control such as the limits of quantification (LOQs), the recovery correction and the repeatability of the method can be found in the SI (Chapter S1). All reported values are blank corrected by using five method blanks (undergone whole procedure but without any soil). The NPAH concentrations are recovery-corrected since the variability of the recoveries of the deuterated NPAHs was relatively high. In contrast, the PAHs (except for the low molecular weight PAHs in three samples due to accidentally evaporation to almost dryness) and OPAHs are not recovery-corrected due to lower variability and higher values of the recoveries. The coefficient of variation of the deuterated PAHs and OPAHs was 15–33%, while it was 32–73% for the NPAHs.

The average recoveries of the deuterated PAHs (NAP-D8, PHE-D10 and PER-D12) in the samples and blanks were 37 ± 17%, 75 ± 12% and 102 ± 16%, respectively. The average recoveries of 9-OFLN-D8 and 9,10-O_2ANT-D9 in the samples and blanks were 101% ± 34% and 107% ± 33%, respectively. The average recoveries of 1-NNAP-D7, 2-NFLN-D9, 9-NANT-D9, 3-NFLT-D9, 1-NPYR-

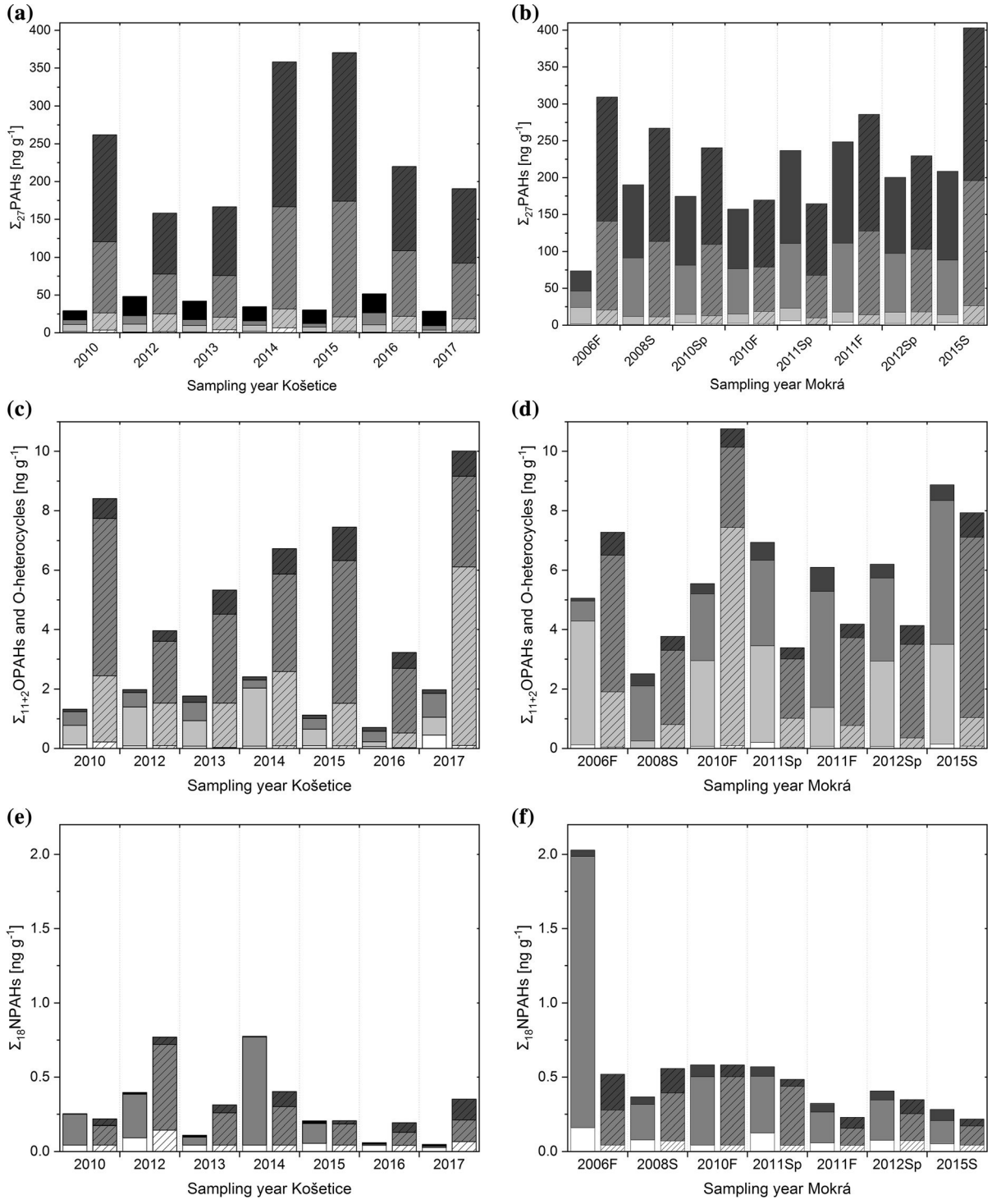
(a)
Σ_{27}PAHs [ng g^{-1}]
Sampling year Košetice
(b)
Σ_{27}PAHs [ng g^{-1}]
Sampling year Mokrá
(c)
Σ_{11+2}OPAHs and O-heterocycles [ng g^{-1}]
Sampling year Košetice
(d)
Σ_{11+2}OPAHs and O-heterocycles [ng g^{-1}]
Sampling year Mokrá
(e)
Σ_{18}NPAHs [ng g^{-1}]
Sampling year Košetice
(f)
Σ_{18}NPAHs [ng g^{-1}]
Sampling year Mokrá

◀ **Fig. 1** Concentration of **a**, **b** Σ_{27}PAHs split into 2-ring (white), 3-ring (light grey), 4-ring (grey) and 5–7-ring PAHs (dark grey), **a** at Košetice-1 (plain) and Košetice-2 (dashed); **b** at Mokrá-1 (plain) and Mokrá-2 (dashed); **c**, **d** Σ_{11+2}OPAHs and O-heterocycles split into 2-ring (white), 3-ring (light grey), 4-ring (grey) and 5-ring OPAHs (dark grey), **c** at Košetice-1 (plain) and Košetice-2 (dashed); **d** at Mokrá-1 (plain) and Mokrá-2 (dashed); **e**, **f** Σ_{18}NPAHs split into 2-ring NPAHs (white), 3-ring NPAHs (light grey), 4-ring NPAHs (grey) and 5-ring NPAHs (dark grey), **e** at Košetice-1 (plain) and Košetice-2 (dashed); **f** at Mokrá-1 (plain) and Mokrá-2 (dashed); (F, fall; Sp, spring; S, Summer). Concentrations normalized to TOC content shown in Fig. S4 in the SI

D9, 6-NCHR-D11 and 6-NBAP-D11 in the samples and blanks were 15 ± 10%, 78 ± 25%, 55 ± 34%, 41 ± 23%, 32 ± 24%, 31 ± 19% and 43 ± 47%, respectively. More details about the recoveries are given in the SI in Chapter S1.3. The instrumental LOQs (iLOQs) ranged between 0.020–0.107 ng g^{-1}, 0.001–0.026 ng g^{-1} (except 9,10-phenanthrenequinone with 2.844 ng g^{-1}) and 0.001–0.488 for the PAHs, OPAHs + O-heterocycles and NPAHs, respectively. The individual LOQs including the method LOQs (mLOQs) are shown in Table S7.

Results and discussion

PAHs

Comments on preservation of PAHs during storage

Polycyclic aromatic compounds (PACs) in sampled soils are subject to contamination from the laboratory environment and processes such as volatilization, degradation (microbial, thermal and photodegradation) and formation of non-extractable residues, which might alter their concentrations if the soils are not properly protected, pre-treated and stored under the right conditions. Air-drying and storage of the archived soil samples in closed paper bags in a dark room at ambient temperature and constant relative humidity are considered being adequate for the preservation of PAH components of soils and has been adopted in the preservation and archiving in other studies (Bandowe et al., 2014; Jones et al., 1989a, 1989b).

In order to verify that the composition of PACs in the soil has been preserved during the (between 3 and almost 12 years), we compared the concentrations of the $\sum_{16}$PAHs measured in this study ("archived samples") to the concentrations measured in the same samples before archiving ("original"). Based on the strong correlations (Košetice: Pearson correlation coefficient $r = 0.85$, $p < 0.01$; Mokrá, in brackets without 2 outliers: $r = 0.47$ (0.90), $p = 0.06$ (< 0.01)) between the concentrations determined before storage and after storage (archived samples), we conclude that the PAHs composition in soils has remained uncontaminated and stable (preserved) during long years of storage. More information can be found in the Online Resource (Supplementary Information, SI) (Chapter S2).

Concentration of PAH in soils

We found 26 PAHs in over 75% of the examined soil samples from Košetice and Mokrá, while CCP could only be quantified in one soil sample. The detection frequencies of the PAHs are shown in the SI, Fig. S3a. Except for CCP, the detection frequencies of PAHs were > 75% with higher MW PAHs even > 90%. Figure 1a, b illustrates the concentration of $\sum_{27}$PAHs, disaggregated for number of rings and examined years. The same plot but with the concentrations normalized to the total organic carbon (TOC) content (Table S2) is shown in Fig. S4. Figure S5 in the SI illustrates the location averaged concentrations shown as box plots. The concentrations of the sum of 16 EPA-prioritized PAHs ($\sum_{16}$PAHs) as well as the concentrations normalized to the TOC content are shown in the SI in Tables S9 and S10, and the concentrations of the individual PAHs in Table S11.

As summarized by Wilcke (2000), the soil properties influence the concentration and distribution of PAHs in soil. The basic soil properties can be found in the SI in Table S2. The locations mainly differ by the TOC content. The average TOC content is 1.9 ± 0.5%, 5.2 ± 0.7%, 3.7 ± 1.5% and 1.8 ± 0.6% at Košetice-1, Košetice-2, Mokrá-1 and Mokrá-2, respectively. The influence of the TOC content on the concentration of PAHs and PAH derivatives in soil will be described in the following as well as in "OPAHs and O-heterocycles" and "NPAHs" sections. In addition, Wilcke summarizes the influence of vegetation, land use and aggregate surface on the PAH concentration. However, these factors are not crucial for the comparison of the four locations in this study since these soil properties are

similar or at least comparable between the four locations.

The concentration of the $\sum_{27}$PAHs is 30 and 26% higher than the $\sum_{16}$PAHs in Košetice and Mokrá, respectively. Our study reveals that several PAHs, which are not included in the list of traditionally measured 16 EPA-PAHs, showed higher concentrations than some of the 16 EPA-PAHs in these central European background and semi-urban soils. Many of these PAHs could contribute significantly to the overall risk posed by organic pollutants in the soils and are of value for determining the sources of PAHs (Andersson & Achten, 2015; Dvorská et al., 2012; Richter-Brockmann & Achten, 2018). For example, we found BJF and ATT with known carcinogenicity and toxicity equivalence factors (TEFs) of 0.1, respectively, in all examined soil samples (Greim, 2008).

The mean concentrations of the Σ_{27}PAHs at the locations in Košetice and Mokrá are 142 ± 124 (29–370) ng g^{-1} and 223 ± 75 (74–403) ng g^{-1}, respectively. The PAH levels found are at the lower end of the range spanned by other rural sites in Europe and comparable with levels reported from background sites in Northern Europe (Table S12). When studying the spatial variation of the samples from this study, it has to be considered that the sampling years between the samples from Mokrá are not totally matching the sampling years from the Košetice soil. Nevertheless, we can conclude that the mean concentration of the Σ_{27}PAHs in Mokrá soils is statistically significantly higher than in Košetice soils ($p < 0.05$, Student's t-test). We assume that the significant difference between the PAH concentrations of both sites is caused by the higher influence of anthropogenic emission sources at Mokrá due to higher proximity to urban and industrial areas. The greater contribution of high molecular weight (MW) PAHs in near source locations, such as Mokrá in our study, compared to rural background sites was reported before (International POPs Elimination Project—IPEP, 2006; Nam et al., 2008).

The concentration of Σ_{27}PAHs at Mokrá-1 is lower, but not significantly ($p = 0.051$, Student's t-test), than at Mokrá-2, i.e. average: 186 ± 54 (range: 74–249) ng g^{-1} and 259 ± 78 (165–403) ng g^{-1}, respectively. The average concentration of Σ_{27}PAHs at Košetice-2 (247 ± 88 (158–370) ng g^{-1}) is in the same range as in both locations in Mokrá (Fig. S5a) but significantly higher ($p < 0.01$, Student's t-test) than at Košetice-1 (38 ± 9 (29–52) ng g^{-1}). The concentrations of PAHs in our studied soils significantly correlated ($\sum_{27}$-PAHs, $r = 0.39$, $p < 0.05$) with the TOC content, a finding which was also reported in earlier findings (Cai et al., 2017; Holoubek et al., 2009; Wilcke & Amelung, 2000). Our finding suggests that variations in organic matter levels might partly explain the spatial and temporal variations of the PAH levels in the sampled soils. Organic matter in soil is the main sorbent for PAHs and hence ultimately drives the amount of PAHs that are partitioned into soil from diffusely contaminated atmosphere (if the concentration of PAHs is in equilibrium with the concentration in soil; Wilcke & Amelung, 2000). Normalization of the PAH concentration with the soil organic carbon concentrations (Fig. S5d and Table S10), did not completely remove the differences in concentrations between the Mokrá and Košetice soils. We therefore conclude that variability of soil organic carbon cannot completely explain the observed temporal and spatial differences. The temporal variation is discussed in "Temporal variations of PACs in soil" section and in Chapter S3 in the SI considering soil samples since 1996.

OPAHs and O-heterocycles

Out of the targeted 11 oxygenated PAHs (OPAHs) and 2 O-heterocycles, 10 OPAHs and both O-heterocycles were found in soils of Košetice and Mokrá. Only 9,10-O_2PHE was not detected in any sample. This has to be interpreted considering the relatively high LOQ of 9,10-O_2PHE (see Table S7b in the SI). The detection frequencies of the PAH derivatives are shown in the SI, Fig. S3b. The detection frequencies of high MW OPAHs (≥ 4-ring OPAHs) were > 90%, while the lower MW OPAHs and O-heterocycles had a detection frequency of more than 75%, except for 6-OBCC (58%), 9,10-O_2ANT (23%) and 9,10-O_2PHE (0%). Regarding the low detection frequencies of 9,10-O_2ANT, the high and varying amount in the blanks leading to a high mLOQ of 9,10-O_2ANT has to be considered.

The concentrations of the sum of 11 OPAHs and the 2 O-heterocycles ($\sum_{11+2}$OPAHs and O-heterocycles) are shown in Fig. 1c, d. The TOC normalized

concentrations and the results of the individual compounds are given in Fig. S4 and in Tables S9, S10 and S13 in the SI.

The averaged concentration of the Σ_{11+2}OPAHs and O-heterocycles in Košetice (4.07 ± 3.08 ng g^{-1}) is lower ($p = 0.076$, Student's t-test) than in Mokrá (5.91 ± 2.30 ng g^{-1}). The TOC normalized concentrations are even significantly different ($p < 0.05$, Student's t-test) between the two sites (see Fig. S5b, e) showing that the difference is not caused by the influence of the soil TOC content. As mentioned in "Concentration of PAH in soils" section, it should be considered that spatial and temporal differences are conflated when comparing the average concentrations between both sites since the sampling years differ between soil samples from Košetice and Mokrá. The temporal variation (coefficient of variation) of the concentrations at each location is between 31 and 48%. Nevertheless, the higher OPAH burden at Mokrá is significant and might be caused by the higher proximity to emission sources showing the importance of primary emitted OPAHs on the soil pollution. The average concentration of the Σ_{11+2}OPAHs and O-heterocycles at Košetice-1 (1.61 ± 0.59 ng g^{-1}) is significantly lower ($p < 0.01$, Student's t-test) than the concentrations at Košetice-2, Mokrá-1 and Mokrá-2 (6.54 ± 2.48 ng g^{-1}, 5.89 ± 1.93 ng g^{-1} and 5.92 ± 2.79 ng g^{-1}). The difference of the concentrations between the two locations in Košetice can mainly be explained by the TOC content. The average TOC content of Košetice-1 is 1.9%, while it is 5.0% at Košetice-2. Instead of 600% when comparing the concentrations per mass of soil, the average TOC content normalized concentration at Košetice-2 is only 60% higher than at Košetice-1.

We found a correlation ($r = 0.55$, $p < 0.01$) of the high MW (4–5-ring) OPAHs and O-heterocycles with the TOC content in soil, but no significant correlation of the low MW (2–3-ring) OPAHs and O-heterocycles ($r = 0.13$, $p = 0.52$). The determined correlation combines temporal and spatial correlation. Wilcke et al. (2014a) found a correlation of the OPAHs to the TOC content at spatial scale. The lack of significant correlation between the TOC content and the concentrations of 2–3-ring OPAHs over the spatial and temporal scales covered by our soils might be due their higher mobility, degradability and formation in soil (Table S3, Wilcke et al., 2014b). At the site Košetice, the correlation of TOC with high MW OPAHs is 0.92 ($p < 0.01$), but the correlation was not statistically significant ($r = 0.38$, $p = 0.18$) in the Mokrá soils. The lack of correlation at Mokrá is because close to sources, spatial distribution of the OPAHs in soil will be more influenced by the intensity of input from primary sources and less influenced by the soil's spatial heterogeneity of soil property such as organic matter content. Apart from Wilcke et al. (2014a), Bandowe et al. (2014) also found a correlation of the soil organic carbon content with the concentration of several PAHs and OPAHs for spatial differences, whereas others (Bandowe et al., 2011; Cai et al., 2017; Sun et al., 2017) did not.

Apart from the TOC content, other characteristics of the locations may have influenced soil burdens. In contrast to Košetice-1 with no major influence other than OPAHs from the air by wet and dry deposition and from formation in soil, Košetice-2 is partly surrounded by trees at the confluence of two brooks resulting in a more diverse impact on the PAC levels. Soils in river valleys or flooded areas often contain higher amounts of PAHs due to the accumulation of river sediment with high organic matter (Wilcke, 2000).

Only few studies addressed OPAHs in soil at semi-urban and/or background sites (Table 1). Brorström-Lundén et al. (2010) measured 10 OPAHs in background and urban soil samples from Sweden. The concentrations of 9-OFLN, 9,10-O_2ANT, 7,12-O_2BAA and 6-OBPYR in the Swedish background soil samples were higher than in the soil samples from this study. However, specific information about the land use is not available, making a comparison more difficult since the PAC concentration is strongly influenced by land use and vegetation (Bandowe et al., 2019). One study with lower OPAH levels than in soil from Košetice and Mokrá is from grassland and scrubland soil samples in Argentina (Wilcke et al., 2014a). This can be explained by the overall low pollution of the investigated soil due to lower anthropogenic influence compared to samples from Europe. Slightly higher OPAH concentrations compared to this study were found in agricultural and remote forest soil samples (Obrist et al., 2015; Sun et al., 2017). Direct comparison is not possible due to pollution situation and land-use type. Bandowe and Wilcke (2010) measured OPAHs in rural tropical forest soil, Amazonia, Brazil. There, concentrations of 1-(CHO)NAP, 9-OFLN and 9,10-O_2ANT were over one order of

Table 1 OPAH concentration in surface soil (ng g^{-1}; sampling depth 10 cm) at different locations; ND = not determined; < x = smaller than LOQ but LOQ unknown

Location	Košetice, Czech Republic[c]	Mokrá, Czech Republic[c]	North of Manaus, Brazil[d]	Gardsjön, Sweden[a,e]	20 sites in Argentina[f]	Eastern China[b, g]	China plateau[h]	China temperate[h]	China subtropical[h]	China tropical[h]
Type of location	Background	Semi-urban	Background	Background	Remote	Agricultural	Rural			
Land use	Grassland	Grassland	Forest	Not specified	Grassland/ scrubland	Agricultural	Forest, agricultural, river shore, grassland			
Number of OPAHs	11	11	7	10	15	4	15	15	15	15
ΣOPAHs	4.1	5.9	6.6	112	0.1–125	9	123	76	147	70
1,4-O_2NAP	0.13	0.05	< 1	ND	< x	ND	0.5	0.5	1	0.5
1-(CHO)NAP	0.02	0.02	1.1	ND	< x	ND	0.7	0.8	1.9	0.6
9-OFLN	0.57	0.70	1.7	3.6	< x − 2.8	3.7	4.5	9.4	13.4	5.0
9,10-O_2ANT	0.32	0.85	2.1	13	< x − 8.6	7.1	4.8	12.2	26.2	3.6
9,10-O_2PHE	< 2.8	< 2.8	ND	ND	ND	ND	ND	ND	ND	ND
11-OBaFLN	0.52	0.94	ND	ND	< x − 5.2	ND	4.3	4.8	7.0	1.1
11-OBbFLN	0.56	0.92	ND	ND	ND	ND	ND	ND	ND	ND
BAN	0.27	0.40	ND	ND	< x − 16	6.1	51	12.6	33.4	17.5
7,12-O_2BAA	0.38	0.49	ND	28	< x − 20	2.9	39	9.4	19.6	5.9
5,12-O_2NAC	0.21	0.33	ND	ND	< x − 2.4	ND	4.5	3.2	6.2	6.9
6-OBPYR	0.43	0.53	ND	31	< x − 21	ND	9.6	9.1	15.1	12.6
DBF	0.37	0.37	ND	< 3	ND	ND	ND	ND	ND	ND
6-OBCC	0.28	0.29	ND	ND	ND	ND	ND	ND	ND	ND
TOC [g kg^{-1}]	37	28	41	ND	4–40	ND	39	19	19	21

[a]Sampling depth: upper 2–3 cm

[b]Sampling depth: 0–20 cm

[c]This study

[d]Bandowe and Wilcke (2010)

[e]Brorström-Lundén et al., (2010)

[f]Wilcke et al., (2014a)

[g]Sun et al., (2017)

[h]Bandowe et al., (2019)

magnitude higher than in Mokrá and Košetice, despite much lower PAH burden compared to our samples. However, these samples are not directly comparable because of differing land-use type (grassland vs forest, forest filter effect). Tropical regions might also exhibit higher formation rates of OPAHs from enhanced photochemical, thermal and microbial degradation of PAHs (higher in the inner tropics, and also in subtropical China; Bandowe et al., 2014, 2019). The soil temperature and higher microbial activity may explain more efficient formation of soil OPAH from soil PAH, and faster degradation of PAHs, hence, higher c_{OPAH}/c_{PAH} in warmer soils (Bandowe et al., 2014).

In this study, the O-heterocycle DBF was determined with a concentration of 0.2–0.5 ng g^{-1}. Brorström-Lundén et al. (2010) could not quantify DBF in Swedish background soil because it was lower than the LOQ. Since the LOQ was with 3 ng g^{-1} significantly higher than the examined concentrations in this study, a comparison is not possible for the background soil. However, the concentration of DBF in the least polluted urban soil sample, Göteborg, was slightly higher (0.94 ng g^{-1}).

Composition pattern of OPAHs

The composition patterns of OPAHs and O-heterocycles of each year and location can be found in Fig. 2. Figure S6b in the SI shows the location average composition patterns. 9-OFLN, 11-OBaFLN and 11-OBbFLN are the most abundant OPAHs. Some differences in the pattern might result from 9,10-O_2ANT, which has a low detection frequency and a relatively high LOQ (Table S7b). Concentrations $<$ LOQ of substance with a detection frequency $<$ 25% are replaced by 0 ng g^{-1}, substances detected more often by LOQ/2. Thus, the relative contribution of 9,10-O_2ANT to the total OPAHs can be relatively high if found $>$ LOQ but is not reflected if concentration was $<$ LOQ. At Košetice, DBF and 9-OFLN significantly contributed to the burden of OPAHs and O-heterocycles. The relative contribution of 9-OFLN and DBF to the ΣOPAHs and O-heterocycles was even higher in air samples (Nežiková et al., 2021) than in soil samples from Košetice (Figure S7b). Nežiková and colleagues explained the high relative concentrations of DBF by its high atmospheric lifetime compared to other PACs (Brubaker & Hites, 1998). In addition, we assume a slower deposition rate of DBF compared to other OPAHs or O-heterocycles since it is almost completely in the gas phase (Nežiková et al., 2021). Similar processes can be assumed for 9-OFLN. The estimated atmospheric lifetime of 9-OFLN is slightly shorter than of DBF, but longer than of all targeted 4-ring OPAHs (USEPA, 2019). Ding et al. (2019) even calculated an atmospheric lifetime of 9.7 days for 9-OFLN. DBF is found in coal tar as well

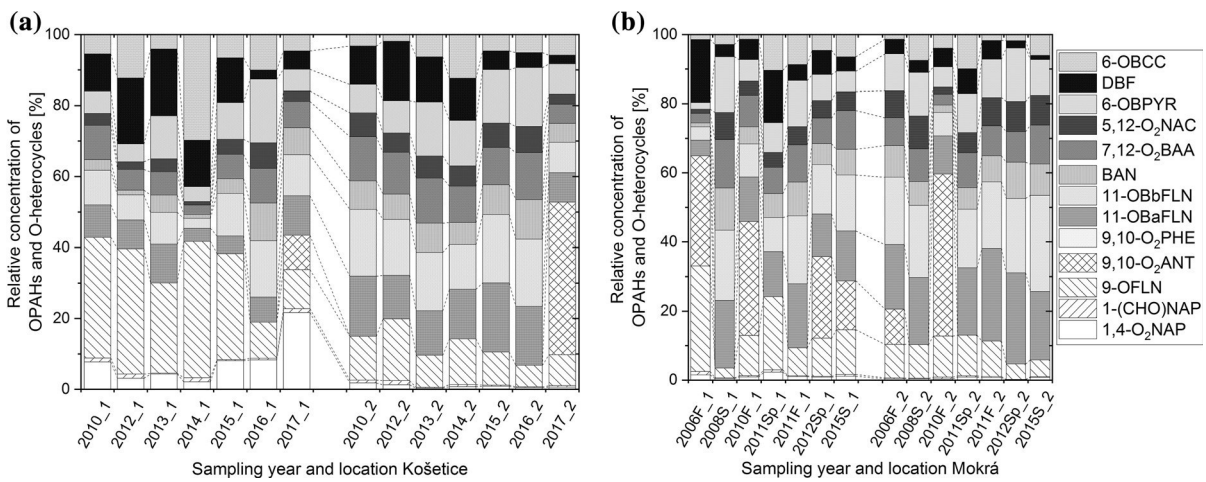

Fig. 2 Composition pattern of OPAHs and O-heterocycles **a** in Košetice **b** in Mokrá (F, fall; Sp, spring; S, summer). Absolute data available in Table S9. Values $<$ LOQ were replaced by LOQ/2 if the detection frequency was $>$ 25% (Fig. S3b), else replaced by 0 ng g^{-1}

as coal and wood tar creosotes. Furthermore, it is used in heat-transfer oils, as a carrier for dyeing and printing textiles, and as an antioxidant in plastics (PubChem, 2021a). 9-OFLN is used as an intermediate and as a reagent in the industry (PubChem, 2021b). Similar to other PACs, 9-OFLN and DBF are formed during the incomplete combustion of biomass and fossil fuels (PubChem, 2021a, 2021b). Since the dominance of 9-OFLN is widespread (see Table 1), we assume that the pollutant is not from a specific source but from combustion sources and secondary formation.

The samples from 2016 in Košetice at both locations and from 2008 at Mokrá-1 differ from the other samples at the same locations by their low concentrations of 9-OFLN and DBF. This is also the case for the 2–3-ring PAHs, as shown in the annual pattern of different ring size PAHs in Fig. S8 in the SI. The low contribution of the low MW OPAHs, especially 9-OFLN, strongly affects the absolute OPAH concentrations (Σ_{11+2}OPAHs and O-heterocycles) leading to the lowest values compared to the other years at each location (see Fig. 1). We hypothesize that this is caused by the weather conditions. Since it was shown before that the highest OPAH air concentrations are in the cold season due to heating (Nežiková et al., 2021), we focussed on the winter months December, January and February. It can be expected that the pollution from winter is still detected in the soil sampled in summer due to the high persistence of the targeted compounds in soil. Wild et al. (1991) determined a lifetime for PAHs of approximately 2 (NAP) to 9 years (BPE) in sewage sludge amended on soil. Kuśmierz et al. (2016) found slightly smaller half-lives, which still ranged 141–1165 d for 3-ring and 6-ring PAHs, respectively. Doick et al. (2005) found comparable values for BAP but smaller half-lives for FLT. According to Wild and Jones (1995), leaching is not a crucial factor for the loss of PAHs due to their low water solubility and high affinity to soil organic matter. Lundstedt et al. (2003) measured the percentage of residual soil pollutants after 29 days. While 90% of the initial concentration of 3-ring PAHs was degraded, 5–6 ring PAHs were not significantly degraded. Lundstedt et al. (2003) concluded that the OPAHs either degraded slower than the PAHs or that they get formed during storage since the residual amount of the OPAHs was generally higher than of the parent PAHs. Based on estimates (BioWin4 of EPI-Suite, USEPA, 2019; Table S3), the biodegradability of OPAHs is similar or slightly higher than of their parent PAHs. Obviously, more research is needed in this field.

The air temperature in winter 2015/2016 was the second highest in the studied period 2006–2017 (Table S14) resulting in a higher percentage of semi-volatile OPAHs in the gas phase. The higher share of OPAHs in the gas phase leads to a lower amount of deposited pollutants, since wet and dry deposition of gaseous substances is much less efficient than of substances in the particulate fraction (Bidleman, 1988; Shahpoury et al., 2015; Škrdlíková et al., 2011). Elevated concentrations in air of the examined OPAHs can be confirmed by data from Nežiková et al. (2021). They found significantly higher concentration of DBF in Košetice in winter 2015/2016 compared to the other years. In addition, the winter-to-summer ratio in 2016 was very high compared to 2015 and 2017 for DBF but also for almost all other OPAHs. The influence of the different gas-particle partitioning due to the temperature on the concentration in soil is only significant for compounds showing a high sensitivity of temperature on their particulate fraction. The deposition flux of low MW OPAHs such as 1-NAP(CHO) and 1,4-O_2NAP, as well as high MW OPAHs such as 11-OBaFLN, 11-OBbFLN, BAN, 7,12-O_2BAA and 5,12-O_2NAC will not change significantly with temperature since these compounds will stay in the gaseous phase (low MW OPAHs) or the particulate phase (high MW OPAHs), respectively (Lammel et al., 2020; Nežiková et al., 2021; Tomaz et al., 2016).

The lower than average precipitation in winter 2015/2016 (Table S14) can be another reason for the low amount of OPAHs in the soil samples from 2006. The amount and type of precipitation will have a significant influence for all OPAHs in the particulate fraction. High amounts of precipitation, especially of snow, an efficient scavenger of particulate matter (Shahpoury et al., 2018), lead to high OPAH concentrations in soil. The winter 2007/2008 was warmer and dryer than average (Table S14), which could be the reason for the low concentration of low MW OPAHs in soil from Mokrá in 2008. The opposite was found in 2006 and 2010. In these years, the absolute OPAH concentrations and the contributions of low MW PAHs and OPAHs are high. This can be explained by low temperatures and high precipitation in the

respective winters (Table S14), leading to a high amount of deposited particulate phase pollutants.

When comparing concentrations in air and soil, it has to be considered that the air concentration is composed of gas and particulate phase air pollutants, while the concentration in soil is mainly discriminating against the gas phase PACs, as dry deposition velocity of lipophilic trace gases is almost negligible (Atlas & Giam, 1988; Bidleman, 1988). It has to be considered that processes in air, especially the gas-particle partitioning can significantly influence the concentrations in soil due to atmospheric deposition. The substance pattern in air is preserved in soil if degradability in soil and runoff mass fluxes are much smaller than the deposition flux or if similar across substances provided that the deposition flux is similar for all substances. The Pearson correlation coefficient of the relative contribution of OPAHs in soil with air at Košetice-1 (2015–2017; Nežiková et al., 2021) was 0.15 ($p = 0.64$). The pattern mainly differed by the higher contribution of 9-OFLN and DBF in air (Fig. S7). Hence, ignoring the contributions of DBF and 9-OFLN, the correlation coefficient of the contributions between air and soil at Košetice-1 is 0.66 ($p < 0.05$). There is no indication for a particularly efficient degradation or leachability of DBF and 9-OFLN in soil (Table S3) that could explain the high difference. Thus, we hypothesize that the difference in contribution is caused by the gas-particle partitioning of these low MW OPAHs, which have a small particulate fraction, even in winter (particulate fraction of all seasons ≤ 0.01 and 0.04 ± 0.05 for DBF and 9-OFLN, respectively; Nežiková et al., 2021). Since the gaseous lipophilic pollutants are not efficiently deposited by wet and dry deposition (Bidleman, 1988; Shahpoury et al., 2015; Škrdlíková et al., 2011), their contribution in air is much higher than in soil. The same is found for the 3-ring PAHs FLN and PHE (Fig. S7). The particulate mass fractions of FLN and PHE range 0.06 ± 0.04 at Košetice (Degrendele et al., 2020; Lammel et al., 2010; Nežiková et al., 2021) and at rural sites and towns in the area of Mokrá (Landlová et al., 2014), similar to 9-OFLN and DBF.

OPAH/PAH ratios

Compared to findings of OPAHs in soil at other background/rural sites, the OPAH/PAH ratios at Mokrá and Košetice (Fig. S9) are among the lowest ever reported (Table S15). The contributing influences are difficult to reveal, as the ratios result from the combined influences of primary emission patterns, lifetimes in air and soil, and the efficiency of deposition and of conversion in air (along the transport from primary sources) and soil. Most of the related kinetic data are not available in literature yet. However, when comparing the soil ratios to the ratios in air at the same location (taken from Nežiková et al., 2021), the uncertainty of different primary emission patterns and of the formation and degradation in air can be ruled out. The air ratios are illustrated in Fig. S9b. The measured air concentration can be compared to the soil concentrations of the same period at Košetice-1 since the air was sampled at the very same location at the Košetice observatory. The high ratio of 1,4-O_2NAP and NAP in soil at Košetice-1 could be partly explained by a high ratio in air, possibly due to strong secondary formation of 1,4-O_2NAP by atmospheric oxidants (Lu et al., 2005). The higher ratio in soil compared to air could indicate formation of 1,4-O_2NAP in soil (Hadibarata et al., 2012). However, the difference is not significant due to the high variability of the ratio, which is mainly based on a low detection frequency in the air samples. The mobility and the biodegradability cannot be a cause for the higher ratio in soil compared to air since the mobility of NAP is lower than of 1,4-O_2NAP and their estimated biodegradabilities are almost similar (USEPA, 2019, see Table S3). However, the higher particulate fraction of 1,4-O_2NAP compared to NAP (Nežiková et al., 2021) could lead to a significantly higher percentage of deposited 1,4-O_2NAP compared to NAP. Furthermore, the ratio can also be influenced by the higher vapour pressure of NAP resulting in a higher revolatilization rate of NAP.

The higher particulate fraction of 9-OFLN compared to FLN might be a reason for the higher ratio of 9-OFLN/FLN in soil compared to air due to higher deposition flux of the particulate phase 9-OFLN. The mobility and biodegradability in soil can be neglected due to similar biodegradability and even higher mobility of 9-OFLN in soil (Table S3). Additionally, we hypothesize that the formation of 9-OFLN in soil from microbial transformation of FLN contributes to the higher ratio of 9-OFLN/FLN in soil compared to the ratio in air (George & Neufeld, 1989; Wilcke et al., 2014b). Since BBN was not measured by Nežiková et al. (2021) in air, the ratio 11-OBbFLN/BBN is not

available for air in Košetice. The lower ratio of 7,12-O_2BAA/BAA in soil compared to air cannot be caused by the difference in gas-particle partitioning, since the particulate mass fraction of 7,12-O_2BAA is higher (Nežiková et al., 2021), which would lead to higher ratios in soil. The lower ratio could indicate that the quinone is degraded faster and/or is more mobile in soil than the parent PAH, supported by the respective estimates of physico-chemical parameters (Table S3) and by degradability studies (Matscheko et al., 2002). Possibly, 7,12-O_2BAA is not or only with a low percentage formed in soil, because the bacteria mainly attack the bay region at the 1,2-position as well as the 8,9- and 10,11-position (Gibson et al., 1975; Jerina et al., 1984; Mahaffey et al., 1988; Schneider et al., 1996) to form dihydrodiols and aromatic acids. However, Moody et al. (2005) reported the formation of 7,12-O_2BAA from one bacterial strain along with several other degradation products. Wu et al. (2010) reported the formation of 7,12-O_2BAA in fungi from sediments and Cajthaml et al. (2006) by a ligninolytic fungus. We cannot draw conclusions from the 9,10-O_2ANT/ANT ratio since 9,10-O_2ANT was < LOQ in most soil samples, except 2017 at Košetice-1. Nevertheless, it is known from literature that, like 7,12-O_2BAA, another position than the 9- and 10-positions of ANT is preferably attacked by bacteria and in the metabolization from mammals to form dihydroxyanthracenes (Akhtar et al., 1975; Dean-Ross et al., 2001; Evans et al., 1965; Moody et al., 2001), while some fungi species form 9,10-O_2ANT from ANT (Cajthaml et al., 2002; Krivobok et al., 1998; Ye et al., 2011). The gas-particle partitioning would suggest a higher ratio in soil than in air, since the particulate fraction of the quinone is higher than of the parent PAH (Košetice 2015–2017; Nežiková et al., 2021). Indeed, 9,10-O_2ANT is degraded faster than ANT (Matscheko et al., 2002).

NPAHs

Out of the 17 targeted NPAHs and one NOPAH included into the group of NPAHs, 5 were found in soils from Košetice and Mokrá, respectively (Fig. S3c). However, it has to be considered that some low MW NPAHs could have been abundant but not detected due to the low recovery of the low MW NPAH 1-NNAP-D7 (see "Quality control" section and S.1.3). As shown in Fig. S3c, the three detected high MW NPAHs (≥ 4 ring NPAHs) had a detection frequency of > 85%, while the two detected low MW NPAHs had a detection frequency of 26% and 28%. For the results such as the sum of all NPAHs ($\sum_{18}$NPAHs), the concentrations < LOQ of substances with a detection frequency < 25% are replaced by 0 ng g^{-1}, substances detected more often by LOQ/2. The LOQs are found in Table S7 in the SI. The annual concentrations of $\sum_{18}$NPAHs and individual NPAHs are shown in Fig. 1e, f and S4 (normalized to soil TOC content) as well as Tables S9 (pg g^{-1}) and S10 (ng (g TOC)$^{-1}$), respectively.

Similar to the PAHs and OPAHs, lower NPAH levels are found in Košetice (0.31 ± 0.23 ng g^{-1}) than in Mokrá (0.54 ± 0.45 ng g^{-1}), though not significant (p = 0.11, Student's t-test). It should be considered that we are comparing the average of different sampling years between Košetice and Mokrá. The temporal variation (coefficient of variation) at the individual locations is between 36 and 97%.

When comparing the TOC normalized concentrations, the two sites are different, not significantly but close to significance (p = 0.054, Student's t-test) (see Fig. S5f). The concentration of $\sum_{18}$NPAHs at Košetice-1 is lower than at Košetice-2 (0.26 ± 0.26 ng g^{-1} vs 0.35 ± 0.20 ng g^{-1}, not significant: p = 0.49, Student's t-test) but higher when normalizing to the TOC content (13.7 ± 12.9 ng (g TOC)$^{-1}$ vs 6.5 ± 3.7 ng (g TOC)$^{-1}$, not significant: p = 0.19, Student's t-test). The highest concentration (0.65 ± 0.62 ng g^{-1}) was found at Mokrá-1. However, this is mainly caused by an exceptionally high NPAH concentration in one soil sample, from summer 2006. Without this value, the mean concentration of Σ_{18}NPAHs at Mokrá-1 is 0.42 ± 0.13 ng g^{-1}, similar ($p > 0.95$, Student's t-test) to the other location, Mokrá-2 (0.42 ± 0.15 ng g^{-1}).

We did not find significant correlations ($p < 0.05$) between the concentrations of the individual NPAHs or $\sum_{18}$NPAHs and the TOC content of the studied soils. Similar results were also reported by Cai et al. (2017) in their study. They explained that the lack of correlation between NPAH concentrations and TOC content in soils sampled over a wide spatial scale in China was due to the higher mobility of NPAHs and

OPAHs compared to PAHs (see log K_{ow} in Table S3). Our findings and their finding are however in contrast to the study of Sun et al. (2017), which reported significant correlations between the concentrations of NPAHs and the TOC content in soils.

A comparison to other studies is shown in Table S16. The average concentration of the Σ_{18}-NPAHs in soils from Košetice is similar to concentrations determined in urban soil from Basel, Switzerland, with 0.34 ng g^{-1} (Σ_8NPAHs, Niederer, 1998) and from Hanoi, Vietnam, with 0.32 ng g^{-1} (Σ_{10}NPAHs, Pham et al., 2015). The average concentration of Σ_{18}NPAHs at the semi-urban site Mokrá from this study (0.54 ng g^{-1}) was slightly higher than the above-mentioned concentrations. Soil from an urban site in Göteborg in Sweden, from the Yangtze River Delta in China and Ejby in Denmark showed similar concentrations with 0.54 ng g^{-1} (Σ_8NPAHs, Brorström-Lundén et al., 2010), 0.60 ng g^{-1} (Σ_{12}-NPAHs, Cai et al., 2017) and 0.50 ng g^{-1} (Σ_3NPAHs, Vikelsøe et al., 2002), respectively. All other sites showed a higher NPAH burden, although the number of examined NPAHs was generally lower. The studies including rural soils from China by Bandowe et al. (2019), from Gardsjön, a rural site in Sweden studied by Brorström-Lundén et al. (2010), and from the site Ejby in Denmark, investigated by Vikelsøe et al. (2002), are the only rural/background site in the literature reporting NPAH soil burden up to now.

Comparison to NPAHs' air concentration

Similar to the OPAHs, we compared the NPAH concentrations at Košetice in soil to the concentrations in air from the study of Nežiková et al. (2021). Only 4 of the 12 NPAHs detected in air were found in soil. This might mainly be limited by LOQs in soil due to low concentrations at the background and semi-urban sites based on the low air concentrations, but it should also be considered that degradation and leaching in soil may have caused dissipation of NPAHs. However, estimates of the soil adsorption coefficient, the biodegradability and the log K_{ow} (USEPA, 2019, Table S3) do not show an exceptionally high or low value to explain the disappearance of any particular NPAH detected in air but not in soil. A major difference between the detected NPAHs in air and soil is the relative abundance of 2 + 3-NFLT being higher in air than in soil and of 1-NPYR being higher in soil compared to the air, which will be explained in more detail in "Composition pattern of NPAHs" section.

Composition pattern of NPAHs

The NPAHs' composition patterns are shown in Fig. 3, temporally averaged in Fig. S6. The highest contribution between 50 and 66% is from 1-NPYR, followed by 6-NBAP (4–25%), which is very different

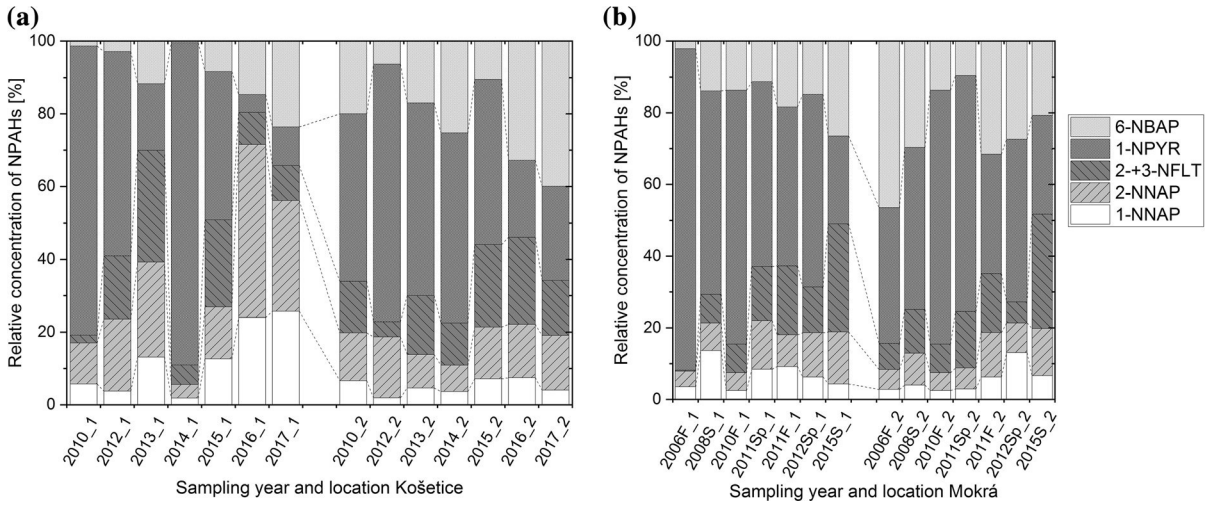

Fig. 3 Composition pattern of NPAHs **a** in Košetice **b** in Mokrá (F, fall; Sp, spring; S, summer); Absolute data in Table S9

from the NPAH pattern in air ($\approx$1% and $<$ 1%, respectively; Tomaz et al., 2016; Lammel et al., 2020; Nežiková et al., 2021) shown in Fig. S7c and probably explained by susceptibility to photolysis in air (see below, "NPAH/PAH ratios" section) in combination with slow degradation in soil (Table S3). As visible in Fig. 3, the contribution of 2- + 3-NFLT is in all samples between around 5–30%. In contrast, the contribution of 2- + 3-NFLT (relative to the sum of all NPAHs detected in both compartments) in air from Košetice measured by Nežiková et al. (2021) is 74% (Fig. S7c). Nežiková and colleagues showed that only 2-NFLT is abundant in air, while 3-NFLT could not be detected. Similarly, 2-NFLT is dominating the NFLT isomers in soil at the background and the semi-urban site. The separation of the two isomers was inadequate to quantify 2-NFLT and 3-NFLT separately but good enough to qualitatively report that 3-NFLT was either not detected or only detected as a small shoulder up to 5% of the peak area of the peak of 2-NFLT. This finding is in line with previous knowledge from air: 2-NFLT dominates NFLT isomers in ambient urban and even more so in rural and remote atmospheric environments (2-NFLT/(2-NFLT + 3-NFLT) $>$ 0.96), while 3-NFLT dominates NFLT isomers in exhaust of diesel engines only (Bamford et al., 2003; Schantz et al., 2005; Zimmermann et al., 2013; besides other).

In air samples, the ratio of the concentration of 2-NFLT to the concentration of 1-NPYR is often used as a diagnostic ratio for the relative importance of photochemical formation since 1-NPYR is known to be emitted primarily, while 2-NFLT is secondarily formed (Bandowe & Meusel, 2017). The ratio of 2- + 3-NFLT/1-NPYR (assuming 2- + 3-NFLT is approximately similar to 2-NFLT) in soil in this study ranging between 0.35 and 0.76 across the four locations is much lower than in air (23 at Košetice; Nežiková et al., 2021). Parameters that could influence this ratio in soil are deposition velocity, leachability and biodegradation or formation in soil. The deposition velocity hardly adds to the selectivity because of similarly high particulate mass fractions at Košetice (Nežiková et al., 2021) as well as at urban sites, also in the region (Lammel et al., 2020; Tomaz et al., 2016). The leachability depends on sorption and water solubility. As shown in Table S3, the calculated soil adsorption coefficient for both compounds is the same, while log K_{ow} of 1-NPYR is higher than of 2-NFLT (5.06 vs. 2.55 according to the KOWWIN model; USEPA, 2019). 2-NFLT is degraded faster than 1-NPYR (3.42 or days-weeks vs. 2.68 or weeks-months, respectively, according to BioWin 4; USEPA, 2019), leading to lower ratios in soil compared to the atmosphere. The indication of relative importance of primary emissions by this ratio from air is obviously not preserved in soil. However, the ratio is higher at the background site Košetice compared to the semi-urban site Mokrá (0.61 $\pm$ 0.58 vs. 0.36 $\pm$ 0.38).

NPAH/PAH ratios

The $\sum_{18}$NPAHs are found 2 to almost 3 orders of magnitude lower than the $\sum_{16}$PAHs. The temporal average ratios of NPAHs and the corresponding parent PAHs are illustrated in Fig. S10 in the SI. It can be hypothesized that the high concentration ratio of the sum of NPAHs to the sum of PAHs at the background site Košetice-1 is due to deposited long-range transported aerosols forming NPAHs in the atmosphere by reactions of parent PAHs with atmospheric oxidants. This is in line with the finding of a similar 2- + 3-NFLT/FLT concentration ratio between the soil at Košetice-1 and the air samples from Košetice with the secondarily formed 2-NFLT being dominant in both compartments (Nežiková et al., 2021) (Fig. S10b). The higher 1-NPYR/PYR concentration ratio in soil compared to air may be due to the higher persistence in soil compared to the corresponding PAH (lower biodegradability, by BIOWIN, USEPA, 2019; see Table S3) and shielding from photolysis, while the ratios 1-NNAP/NAP, 2-NNAP/NAP and, as already said, 2- + 3-NFLT/FLT in soil samples seem to be preserved from air. 3-NFLT and 1-NPYR are susceptible to photolysis in air due to a peri-H atom (Fan et al., 1995), which also applies to 6-NBAP (2 peri-H's), abundant in the soil samples, too (see above, "Composition pattern of NPAHs" section), while there are no peri-H atoms in 2-NNAP and 2-NFLT. Formation of NPAHs in soil is not indicated by the findings; degradability and sorption may vary considerably across NPAHs.

Temporal variations of PACs in soil

The results of the annual PAH, OPAH and NPAH concentrations, disaggregated for numbers of rings, are shown in Fig. 1 and Fig. S4 (normalized to TOC

content). The OPAH concentrations at the two locations in Mokrá follow a similar direction of the variation (except for fall 2010 and spring 2011) meaning, e.g. a decrease between fall 2006 to summer 2008 following by an increase between 2008 and fall 2010. However, this only shows the similar behaviour at both sites in Mokrá and not a trend between the years since at Mokrá we compare different seasons. Except for the samples from 2006, the NPAH concentrations at Mokrá-1 and Mokrá-2 also follow a similar direction of temporal variation but not the same as for the OPAHs. The NPAH concentration at Mokrá is smaller in summer 2015 compared to spring 2012 at both locations but for the OPAHs, the opposite is true for Mokrá-1 and Mokrá-2. The finding suggests that the soils from both locations at Mokrá receive the same varying primary pollution and that the transport processes influence the concentrations of the target compounds in these soils to a similar extent. The same is true for the NPAHs at the different locations in Košetice. Only in between 2016 and 2017, the behaviour at both locations is different meaning the NPAH concentration at Košetice-1 in 2017 is smaller than in 2016, while at Košetice-2 it is higher. In contrast, the OPAHs in Košetice do not follow a similar direction of the annual variation, except 2015–2017.

The concentrations of the Σ_{18}NPAHs at all examined locations decrease from older to contemporary samples (Fig. 1), significant for one out of four locations, i.e. Mokrá-2 ($p > 0.95$, Neumann test, Hecht, 2020). The compounds most contributing to the decrease are 1-NPYR and the 2-ring NPAHs. In contrast, the concentrations of 2- + 3-NFLT and 6-NBAP are mainly increasing.

An increasing trend (not significant; p = 0.91, Neumann trend test) is seen for Σ_{11+2}OPAHs and O-heterocycles at Mokrá-1 (Fig. 1). No such trend is seen for the Košetice and Mokrá-2 locations. The increasing OPAH concentration at Mokrá-1 is mainly driven by the 4–5-ring OPAHs. These are also slightly increasing at Mokrá-2 and Košetice-1. In contrast, it seems that the 3-rings DBF and 9-OFLN decrease from older to contemporary samples at all locations (significant for DBF at Košetice-2, $p > 0.95$; not significant at Košetice-1; p = 0.94, Neumann trend test). We hypothesize that the decrease might be related to increasing winter temperatures. Similar results were found for the PAHs. The 3-ring PAHs FLN and PHE are decreasing at all locations except for Mokrá-2 (significant for FLN at Košetice-1 and Košetice-2 and for PHE at Košetice-1, $p > 0.95$, Neumann trend test), while almost all other PAHs either stay the same or are increasing. In total, the concentration of Σ_{27}PAHs stayed constant at both locations in Košetice (Fig. 1a) in the studied period. At Mokrá, the PAH concentrations increase (not significant, Neumann trend test), although at Mokrá-2 this is strongly influenced by high levels in 2015 (Fig. 1b). Similar results were found for the concentration of Σ_{16}PAHs except for a slight, not significant decreasing trend at Košetice-1. Comparable results were determined when studying even longer time series of the same locations (Chapter S3 in the SI).

Nežiková et al. (2021) found a decreasing trend of several NPAHs and OPAHs in air in Košetice between 2015 and 2017 attributable to ongoing emission reductions of PAHs that are also effective for NPAHs and OPAHs. This could be one reason for the decreasing NPAH concentrations. Unfortunately, long-term measurements of PAHs, NPAHs and OPAHs in air at Mokrá to compare with are not available in the literature. Long-term studies for PACs in soil are so far only available for PAHs. Gubler et al. (2015) found similar results in Swiss soil samples between 1985 and 2013 as we found in the Czech soil samples, namely a decreasing trend for low MW PAHs and no or slightly increasing trend for the high MW PAHs. A decreasing trend of PAHs was examined for the period 1990–2009 in Scottish soil by Cui et al. (2020). Given the limited number of years sampled and the complex dependencies of the deposition, leaching, degradation and formation mass fluxes on climate parameters, the observed variabilities of the PAH derivatives in soil are not conclusive. Longer time series and deeper process understanding are needed.

Summary and conclusion

The concentrations of the PAH derivatives in soil at the central European background site Košetice are among the lowest ever reported. The average concentration in the studied period of the Σ_{18}NPAHs and the Σ_{11+2}OPAHs and O-heterocycles was 0.31 ± 0.23 ng g^{-1} and 4.07 ± 3.08 ng g^{-1}, respectively. At the semi-urban site Mokrá, the

concentrations were slightly higher (0.54 ± 0.45 ng g^{-1} and 5.91 ± 2.30 ng g^{-1}, respectively). Our results show that several NPAHs and OPAHs are abundant in soil at the background site. 1-NPYR and 6-NBAP, which are identified as highly toxic, were the most abundant NPAHs in soil. The findings suggest that 1-NPYR and 6-NBAP are more stable in soil than in air. Through eventual revolatilization, soil may turn into a secondary source of this and other NPAHs and OPAHs. The contributions of OPAHs were more equally distributed, showing the highest contributions from 9-OFLN, 11-OBaFLN and 11-OBbFLN. We found a correlation of the soil organic carbon content with the high MW OPAHs and PAHs, but not with the low MW OPAHs and PAHs, nor with the NPAHs. The temporal variation of the concentration of PACs in soil at Košetice and Mokrá significantly differed between substances. It could be noticed that the concentrations of dibenzofuran, 9-fluorenone and some 3-ring PAHs decreased, while it stayed constant or increased for higher MW PACs. In order to make more reliable statements about the temporal variation of the soil concentrations, longer time series and deeper understanding of the PAC chemodynamics in soil are needed.

Acknowledgements We thank Ondřej Sáňka (Masaryk University) for technical help and Roman Prokeš, Milan Sáňka and Ivan Holoubek (Masaryk University) for sampling. This research was supported by the Max Planck Society (MPG), the Czech Science Foundation (GACR #20-07117S), the Czech Ministry of Education, Youth and Sports (Projects ACTRIS-CZ #LM2018122, RI #CZ.02.1.01/0.0/0.0/16_013/0001315, RECETOX RI #LM2018121, CETOCOEN EXCELLENCE Teaming 2 #02.1.01/0.0/0.0/18_046/0015975), Českomoravský Cement a.s. (Projects SML 19,112,616,633, SML 19,112,616,634) and the European Union (Horizon2020 #857,560).

Funding Open Access funding by the Max Planck Society, enabled and organized by Projekt DEAL.

Availability of data and material All data are supplied in the SI or can be requested from the authors.

Declarations

Conflict of interest The authors have no conflicts of interest to declare that are relevant to the content of this article.

References

Akhtar, M. N., Boyd, D. R., Thomas, N. J., Koreeda, M., Gibson, D. T., Mahadevan, V., & Jerina, D. M. (1975). Absolute stereochemistry of the dihydroanthracene-cis- and -trans-,2-diols produced from anthracene by mammals and bacteria. *Journal of the Chemical Society, Perkin Transactions, 1*, 2506–2511.

Andersson, J. T., & Achten, C. (2015). Time to say goodbye to the 16 EPA PAHs? Toward an up-to-date use of PACs for environmental purposes. *Polycyclic Aromatic Compounds, 35*, 330–354.

Arp, H. P. H., Lundstedt, S., Josefsson, S., Cornelissen, G., Enell, A., Allard, A.-S., & Kleja, D. B. (2014). Native oxy-PAHs, N-PACs, and PAHs in historically contaminated soils from Sweden, Belgium, and France: Their soil-pore-water partitioning behavior, bioaccumulation in Enchytraeus crypticus, and bioavailability. *Environmental Science and Technology, 48*, 11187–11195.

Atlas, E., & Giam, C. S. (1988). Ambient concentration and precipitation scavenging of atmospheric organic pollutants. *Water, Air, and Soil Pollution, 38*, 19–36.

Atsumi, T., Murata, J., Kamiyanagi, I., Fujisawa, S., & Ueha, T. (1998). Cytotoxicity of photosensitizers camphorquinone and 9-fluorenone with visible light irradiation on a human submandibular-duct cell line in vitro. *Archives of Oral Biology, 43*, 73–81.

Baek, S. O., Field, R. A., Goldstone, M. E., Kirk, P. W., Lester, J. N., & Perry, R. (1991). A review of atmospheric polycyclic aromatic hydrocarbons: Sources, fate and behaviour. *Water, Air, and Soil Pollution, 60*, 279–300.

Bamford, H. A., Bezabeh, D. Z., Schantz, M. M., Wise, S. A., & Baker, J. E. (2003). Determination and comparison of nitrated-polycyclic aromatic hydrocarbons measured in air and diesel particulate reference materials. *Chemosphere, 50*, 575–587.

Bandowe, B. A. M., Shukurov, N., Kersten, M., & Wilcke, W. (2010). Polycyclic aromatic hydrocarbons (PAHs) and their oxygen-containing derivatives (OPAHs) in soils from the Angren industrial area, Uzbekistan. *Environmental Pollution, 158*, 2888–2899.

Bandowe, B. A. M., & Wilcke, W. (2010). Analysis of polycyclic aromatic hydrocarbons and their oxygen-containing derivatives and metabolites in soil. *Journal of Environmental Quality, 39*, 1349–1358.

Bandowe, B. A. M., Sobocka, J., & Wilcke, W. (2011). Oxygen-containing polycyclic aromatic hydrocarbons (OPAHs) in urban soils of Bratislava, Slovakia: Patterns, relation to PAHs and vertical distribution. *Environmental Pollution, 159*, 539–549.

Bandowe, B. A. M., Gómez, L. M., & Wilcke, W. (2014). Oxygenated polycyclic aromatic hydrocarbons and azaarenes in urban soils: A comparison of a tropical city (Bangkok) with two temperate cities (Bratislava and Gothenburg). *Chemosphere, 107*, 407–414.

Bandowe, B. A. M., & Meusel, H. (2017). Nitrated polycyclic aromatic hydrocarbons (nitro-PAHs) in the environment—a review. *Science of the Total Environment, 581–582*, 237–257.

Bandowe, B. A. M., Leimer, S., Meusel, H., Velescu, A., Dassen, S., Eisenhauer, N., Hoffmann, T., Oelmann, Y., & Wilcke, W. (2019). Plant diversity enhances the natural attenuation of polycyclic aromatic compounds (PAHs and oxygenated PAHs) in grassland soils. *Soil Biology and Biochemistry, 129*, 60–70.

Becker, S., Halsall, C. J., Tych, W., Hung, H., Attewell, S., Blanchard, P., Li, H., Fellin, P., Stern, G., Billeck, B., & Friesen, S. (2006). Resolving the long-term trends of polycyclic aromatic hydrocarbons in the Canadian Arctic atmosphere. *Environmental Science and Technology, 40*, 3217–3222.

Bidleman, T. F. (1988). Atmospheric processes Wet and dry deposition of organic compounds are controlled by their vapor-particle partitioning. *Environmental Science and Technology, 22*, 361–367.

Bolton, J. L., Trush, M. A., Penning, T. M., Dryhurst, G., & Monks, T. J. (2000). Role of quinones in Toxicology. *Chemical Research in Toxicology, 13*, 135–160.

Brinkmann, M., Maletz, S., Krauss, M., Bluhm, K., Schiwy, S., Kuckelkorn, J., Tiehm, A., Brack, W., & Hollert, H. (2014). Heterocyclic aromatic hydrocarbons show estrogenic activity upon metabolization in a recombinant transactivation assay. *Environmental Science and Technology, 48*, 5892–5901.

Brorström-Lundén, E., Remberger, M., Kaj, L., Hansson, K., Palm-Cousins, A., Andersson, H., Haglund, P., Ghebremeskel, M., & Schlabach, M. (2010). Results from the Swedish National Screening Programme 2008: Screening of unintentionally produced organic contaminants. *Swedish Environmental Research Institute (IVL) report B1944*, Göteborg, Sweden.

Brubaker, W. W., & Hites, R. A. (1998). OH reaction kinetics of polycyclic aromatic hydrocarbons andpolychlorinated dibenzo-p-dioxins and dibenzofurans. *The Journal of Physical Chemistry A, 102*, 915–921.

Cai, C. Y., Li, J. Y., Wu, D., Wang, X. L., Tsang, D. C. W., Li, X. D., Sun, J. T., Zhu, L. Z., Shen, H. Z., Tao, S., & Liu, W. X. (2017). Spatial distribution, emission source and health risk of parent PAHs and derivatives in surface soils from the Yangtze River Delta, eastern China. *Chemosphere, 178*, 301–308.

Cajthaml, T., Pacakova, V., & Sasek, V. (2002). Study of fungal degradation products of polycyclic aromatic hydrocarbons using gas chromatography with ion trap mass spectrometry detection. *Journal of Chromatography A, 974*, 213–222.

Cajthaml, T., Erbanova, P., Sasek, V., & Moeder, M. (2006). Breakdown products on metabolic pathway of degradation of benz[a]anthracene by a ligninolytic fungus. *Chemosphere, 64*, 560–564.

Cerniglia, C. E. (1992). Biodegradation of polycyclic aromatic hydrocarbons. *Biodegradation, 3*, 351–368.

Collins, J. F., Brown, J. P., Alexeeff, G. V., & Salmon, A. G. (1998). Potency equivalency factors for some polycyclic aromatic hydrocarbons and polycyclic aromatic hydrocarbon derivatives. *Regulatory Toxicology and Pharmacology, 28*, 45–54.

Cui, S., Zhang, Z., Fu, Q., Hough, R., Yates, K., & Osprey, M. (2020). Long-term spatial and temporal patterns of polycyclic aromatic hydrocarbons (PAHs) in Scottish soils over 20 years (1990–2009): A national picture. *Geoderma, 361*, 114135.

Czech Hydrometeorological Institute. (2006). Annual report 2006 (in Czech), *CHMI*, Prague.

Czech Statistical Office. (2019). Number of population in municipalities—population of municipalities. Publication Code: 130072-19.

Dean-Ross, D., Moody, J. D., Freeman, J. P., Doerge, D. R., & Cerniglia, C. E. (2001). Metabolism of anthracene by a Rhodococcus species. *FEMS Microbiology Letters, 204*, 205–211.

Degrendele, C., Fiedler, H., Kocan, A., Kukučka, P., Přibylová, P., Prokeš, R., Klánová, J., & Lammel, G. (2020). Multiyear levels of PCDD/Fs, dl-PCBs and PAHs in background air in central Europe and implications for deposition. *Chemosphere, 240*, 124852.

Ding, Z. Z., Yi, Y. Y., Zhang, Q. Z., & Zhuang, T. (2019). Theoretical investigation on atmospheric oxidation of fluorene initiated by OH radical. *Science of the Total Environment, 669*, 920–929.

Doick, K. J., Klingelmann, E., Burauel, P., Jones, K. C., & Semple, K. T. (2005). Long-term fate of polychlorinated biphenyls and polycyclic aromatic hydrocarbons in an agricultural soil. *Environmental Science & Technology, 39*, 3663–3670.

Duarte, F. V., Simoes, A. M., Teodoro, J. S., Rolo, A. P., & Palmeira, C. M. (2011). Exposure to dibenzofuran affects lung mitochondrial function in vitro. *Toxicology Mechanisms and Methods, 21*, 571–576.

Duarte, F. V., Teodoro, J. S., Rolo, A. P., & Palmeira, C. M. (2012). Exposure to dibenzofuran triggers autophagy in lung cells. *Toxicology Letters, 209*, 35–42.

Durant, J. L., Busby, W. F., Jr., Lafleur, A. L., Penman, B. W., & Crespi, C. L. (1996). Human cell mutagenicity of oxygenated, nitrated and unsubstituted polycyclic aromatic hydrocarbons associated with urban aerosols. *Mutation Research/genetic Toxicology, 371*, 123–157.

Dvorská, A., Komprdová, K., Lammel, G., Klánová, J., & Plachá, H. (2012). Polycyclic aromatic hydrocarbons in background air in central Europe - Seasonal levels and limitations for source apportionment. *Atmospheric Environment, 46*, 147–154.

el Alawi, Y. S., McConkey, B. J., Dixon, D. G., & Greenberg, B. M. (2002). Measurement of short and long-term toxicity of polycyclic aromatic hydrocarbons using luminescent bacteria. *Ecotoxicology and Environmental Safety, 51*, 12–21.

Enya, T., Suzuki, H., Watanabe, T., Hirayama, T., & Hisamatsu, Y. (1997). 3-Nitrobenzanthrone, a powerful bacterial mutagen and suspected human carcinogen found in diesel exhaust and airborne particulates. *Environmental Science and Technology, 31*, 2772–2776.

Evans, W. C., Fernley, H. N., & Griffiths, E. (1965). Oxidative metabolism of phenanthrene and anthracene by soil pseudomonads. *Biochemical Journal, 95*, 819–831.

Fan, Z., Chen, D., Birla, P., & Kamens, M. (1995). Modeling of nitro-polycyclic aromatic: Hydrocarbon formation and decay in the atmosphere. *Atmospheric Environment, 29*, 1171–1181.

Fernández, P., Carrera, G., Grimalt, J. O., Ventura, M., Camarero, L., Catalan, J., Nickus, U., Thies, H., & Psenner, R. (2003). Factors governing the atmospheric deposition of polycyclic aromatic hydrocarbons to remote areas. *Environmental Science and Technology, 37*, 3261–3267.

Finlayson-Pitts, B. J., & Pitts, J. N., Jr. (2000). *Chemistry of the upper and lower atmosphere* (p. 969). Academic Press.

George, E. J., & Neufeld, R. D. (1989). Degradation of fluorene in soil by fungus Phanerochaete chrysosporium. *Biotechnology and Bioengineering, 33*, 1306–1310.

Gibson, D. T., Mahadaven, V., Jerina, D. M., Yagi, H., & Yeh, H. J. C. (1975). Oxidation of the carcinogens benzo[a]-pyrene and benzo[a]anthracene to dihydrodiols by bacterium. *Science, 189*, 295–297.

Greim, H. (2008). Gesundheitsschädliche Arbeitsstoffe, Toxikologisch arbeitsmedizinische Begründungen von MAK-Werten und Einstufungen. Weinheim, Germany Wiley-VCH.

Gubler, A., Wachter, D., Blumb, F., & Buchelib, T. D. (2015). Remarkably constant PAH concentrations in Swiss soils over the last 30 years. *Environmental Science: Processes Impacts, 17*, 1816–1828.

Hadibarata, T., Yusoff, A. R. M., Aris, A., & Kristanti, R. A. (2012). Identification of naphthalene metabolism by white rot fungus Armillaria sp. F022. *Journal of Environmental Sciences, 24*, 728–732.

Hecht, T. (2020). *Elementare statistische Bewertung von Messdaten der analytischen Chemie mit Excel*. Springer.

Holoubek, I., Klánová, J., Jarkovský, J., & Kohoutek, J. (2007a). Trends in background levels of persistent organic pollutants at Kosetice observatory, Czech Republic, Part I: Ambient air and wet deposition 1996–2005. *Journal of Environmental Monitoring, 9*, 557–563.

Holoubek, I., Klánová, J., Jarkovský, J., Kubík, V., & Helešic, J. (2007b). Trends in background levels of persistent organic pollutants at Kosetice observatory, Czech Republic, Part II. Aquatic and terrestrial environments 1996–2005. *Journal of Environmental Monitoring, 9*, 564–571.

Holoubek, I., Dušek, L., Sáňka, M., Hofman, J., Čupra, P., Jarkovský, J., Zbíral, J., & Klánová, J. (2009). Soil burdens of persistent organic pollutants—their levels, fate and risk. Part I. Variation of concentration ranges according to different soil uses and locations. *Environmental Pollution, 157*, 3207–3217.

Horstmann, M., & McLachlan, M. S. (1998). Forests as filters of airborne organic pollutants: A model. *Environmental Science and Technology, 32*, 413–420.

Honda, K., Mizukami, M., Ueda, Y., Hamada, N., & Seike, N. (2007). Residue level of polycyclic aromatic hydrocarbons in Japanese paddy soils from 1959 to 2002. *Chemosphere, 68*, 1763–1771.

IARC. (2010). Some non-heterocyclic polycyclic aromatic hydrocarbons and some related exposures. *IARC Monographs on the Evaluation of Carcinogenic Risks to Humans, 92*, 1–852.

IARC. (2012). Diesel and gasoline engine exhausts and some nitroarenes. *IARC Monographs on the Evaluation of Carcinogenic Risks to Humans, 105*, 1–703.

Idowu, O., Semple, K. T., Ramadass, K., O'Connor, W., Hansbro, P., & Thavamani, P. (2019). Beyond the obvious: Environmental health implications of polar polycyclic aromatic hydrocarbons. *Environment International, 123*, 543–557.

International POPs Elimination Project—IPEP. (2006). Persistent organic pollutants in the Czech Republic—country situation report.

Jaiswal, P. K., Srivastava, S., Gupta, J., & Thakur, I. S. (2012). Dibenzofuran induces oxidative stress, disruption of transmitochondrial membrane potential and G1 arrest in human hepatoma cell line. *Toxicology Letters, 214*, 137–144.

Jerina, D. M., van Bladeren, P. F., Yagi, H., Gibson, D. T., Mahadeven, V., Neese, A. S., Koreeda, M., Sharma, N. D., & Boyd., D. . (1984). Synthesis and absolute configuration of cis-1-2-, 8-, 9- and 10,11-dihydrodiol metabolites of benz[a]anthracene formed by a strain of Beijerinckia. *Journal of Organic Chemistry, 49*, 1075–1082.

Jones, K. C., Stratford, J. A., Waterhouse, K. S., Furlong, E. T., Giger, W., Hites, R. A., Schaffner, C., & Johnston, A. E. (1989a). Increases in the polynuclear aromatic hydrocarbon content of an agricultural soil over the last Century. *Environmental Science and Technology, 23*, 95–101.

Jones, K. C., Stratford, J. A., Tidridge, P., Waterhouse, K. S., & Johnston, A. E. (1989b). Polynuclear aromatic hydrocarbons in an agricultural soil: Long-term changes in profile distribution. *Environmental Pollution, 56*, 337–351.

Kawamura, K., & Kaplan, I. R. (1983). Organic compounds in the rainwater of Los Angeles. *Environmental Science and Technology, 17*, 497–501.

Keyte, I. J., Harrison, R. M., & Lammel, G. (2013). Chemical reactivity and long-range transport potential of polycyclic aromatic hydrocarbons—a review. *Chemical Society Reviews, 42*, 9333–9391.

Klánová, J., Matykiewiczová, N., Máčka, Z., Prošek, P., Láska, K., & Klán, P. (2008). Persistent organic pollutants in soils and sediments from James Ross Island, Antarctica. *Environmental Pollution, 152*, 416–423.

Krauss, M., Wilcke, W., & Zech, W. (2000). Polycyclic aromatic hydrocarbons and polychlorinated biphenyls in forest soils: Depth distribution as indicator of different fate. *Environmental Pollution, 110*, 79–88.

Krivobok, S., Miriouchkine, E., Seiglemurandi, F., & Benoit-Guyod, J. L. (1998). Biodegradation of Anthracene by Soil Fungi. *Chemosphere, 31*, 523–530.

Kuśmierz, M., Oleszczuk, P., Kraska, P., Pałys, E., & Andruszczak, S. (2016). Persistence of polycyclic aromatic hydrocarbons (PAHs) in biochar-amended soil. *Chemosphere, 146*, 272–279.

Lammel, G. (2015). Polycyclic aromatic compounds in the atmosphere—a review identifying research needs. *Polycyclic Aromatic Compounds, 35*, 316–329.

Lammel, G., Sehili, A. M., Bond, T. C., Feichter, J., & Grassl, H. (2009). Gas/particle partitioning and global distribution of polycyclic aromatic hydrocarbons—a modelling approach. *Chemosphere, 76*, 98–106.

Lammel, G., Novák, J., Landlová, L., Dvorská, A., Klánová, J., Čupr, P., Kohoutek, J., Reimer, E., & Škrdlíková, L. (2010). Sources and distributions of polycyclic aromatic hydrocarbons and toxicity of polluted atmosphere aerosols. In F. Zereini & C. L. S. Wiseman (Eds.), *Urban airborne particulate matter: Origins, chemistry, fate and health impacts* (pp. 39–62). Springer.

Lammel, G., Kitanovski, Z., Kukučka, P., Novák, J., Arangio, A., Codling, G. P., Filippi, A., Hovorka, J., Kuta, J., Leoni, C., Příbylová, P., Prokeš, R., Sáňka, O., Shahpoury, P., Tong, H. J., & Wietzoreck, M. (2020). Levels, phase partitioning, mass size distributions and bioaccessibility of oxygenated and nitrated polycyclic aromatic hydrocarbons (OPAHs, NPAHs) in ambient air. *Environmental Science and Technology, 54*, 2615–2625.

Lampi, M. A., Gurska, J., McDonald, K. I. C., Xie, F. L., Huang, X. D., Dixon, D. G., & Greenberg, B. M. (2006). Photoinduced toxicity of polycyclic aromatic hydrocarbons to Daphnia magna: Ultraviolet-mediated effects and the toxicity of polycyclic aromatic hydrocarbon photoproducts. *Environmental Toxicology and Chemistry, 25*, 1079–1087.

Landlová, L., Čupr, P., Franců, J., Klánová, J., & Lammel, G. (2014). Composition and effects of inhalable size fractions of atmospheric aerosols in the polluted atmosphere. Part I. PAHs, PCBs and OCPs and the matrix chemical composition. *Environmental Science and Pollution Research, 21*, 6188–6204.

Leary, J. A., Lafleur, A., & L., Liber, H.L., Biemann, K. . (1983). Chemical and toxicologic characterization of fossil fuel combustion product phenalen-l-one. *Analytical Chemistry, 55*, 758–761.

Lu, R., Wu, J., Turco, R. P., Winer, A. M., Atkinson, R., Arey, J., Paulson, S. E., Lurmann, F. W., Miguel, A. H., & Eiguren-Fernandez, A. (2005). Naphthalene distributions and human exposure in Southern California. *Atmospheric Environment, 39*, 489–507.

Lübcke-von Varel, U., Bataineh, M., Lohrmann, S., Löffler, I., Schulze, T., Flückiger-Isler, S., et al. (2012). Identification and quantitative confirmation of dinitropyrenes and 3-nitrobenzanthrone as major mutagens in contaminated sediments. *Environment International, 44*, 31–39.

Lundstedt, S., Haglund, P., & Öberg, L. (2003). Degradation and formation of polycyclic aromatic compounds during bioslurry treatment of an acid aged gasworks soil. *Environmental Toxicology and Chemistry, 22*, 1413–1420.

Lundstedt, S., White, P. A., Lemieux, C. L., Lynes, K. D., Lambert, L. B., Öberg, L., et al. (2007). Sources, fate, and toxic hazards of oxygenated polycyclic aromatic hydrocarbons (PAHs) at PAH-contaminated sites. *Ambio, 36*, 475–485.

Mahaffey, W. R., Gibson, D. T., & Cerniglia, C. E. (1988). Bacterial oxidation of chemical carcinogens: Formation of polycyclic aromatic acids from benz[a]anthracene. *Applied and Environmental Microbiology, 54*, 2415–2423.

Marquès, M., Sierra, J., Drotikova, T., Mari, M., Nadal, M., & Domingo, J. (2017). Concentrations of polycyclic aromatic hydrocarbons and trace elements in Arctic soils: A case-study in Svalbard. *Environmental Research, 159*, 202–211.

Matscheko, N., Lundstedt, S., Svensson, L., Harju, M., & Tysklind, M. (2002). Accumulation and elimination of 16 polycyclic aromatic compounds in the earthworm (Eisenia fetida). *Environmental Toxicology and Chemistry, 21*, 1724–1729.

Matsumoto, M., Ando, M., & Ohta, Y. (1988). Mutagenicity of monochlorodibenzofurans detected in the environment. *Toxicology Letters, 40*, 21–28.

Moody, J. D., Freeman, J. P., Doerge, D. R., & Cerniglia, C. E. (2001). Degradation of phenanthrene and anthracene by cell suspensions of Mycobacterium sp. Strain PYR-1. *Applied and Environmental Microbiology, 67*, 1476–1483.

Moody, J. D., Freeman, J. P., & Cerniglia, C. E. (2005). Degradation of benz[a]anthracene by Mycobacterium vanbaalenii strain PYR-1. *Biodegradation, 16*, 513–526.

Mortelmans, K., Haworth, S., Speck, W., & Zeiger, E. (1984). Mutagenicity testing of agent orange components and related chemicals. *Toxicology and Applied Pharmacology, 75*, 137–146.

Nam, J. J., Thomas, G. O., Jaward, F. M., Steinnes, E., Gustafsson, O., & Jones, K. C. (2008). PAHs in background soils from Western Europe: Influence of atmospheric deposition and soil organic matter. *Chemosphere, 70*, 1596–1602.

Nežiková, B., Degrendele, C., Bandowe, B.A.M., Holubová Šmejkalová, A., Kukučka, P., Martiník, J., Prokeš, R., Přibylová, P., Klánová, J., & Lammel, G. (2021). Atmospheric concentrations of nitrated and oxygenated polycyclic aromatic hydrocarbons and oxygen heterocycles are declining in Central Europe. *Chemosphere, 269*,128738.

Niederer, M. (1998). Determination of polycyclic aromatic hydrocarbons and substitutes (nitro-, oxy-PAHs) in urban soil and airborne particulate by GCMS and NCI-MS/MS. *Environmental Science and Pollution Research, 5*, 209–216.

Nováková, Z., Novák, J., Kitanovski, Z., Kukučka, P., Smutá, M., Wietzoreck, M., Lammel, G., & Hilscherová, K. (2020). Toxic potentials of particulate and gaseous air pollutant mixtures and the role of PAHs and their derivatives. *Environment International, 139*, 105634.

Obrist, D., Zielinska, B., & Perlinger, J. A. (2015). Accumulation of polycyclic aromatic hydrocarbons (PAHs) and oxygenated PAHs (OPAHs) in organic and mineral soil horizons from four U.S. remote forests. *Chemosphere, 134*, 98–105.

Pham, C. T., Tang, N., & Toriba, A. (2015). Polycyclic aromatic hydrocarbons and nitropolycyclic aromatic hydrocarbons in atmospheric particles and soil at a traffic site in Hanoi, Vietnam. *Polycyclic Aromatic Compounds, 35*, 353–371.

PubChem. (2021a). Dibenzofuran. US national library for medicine. National Center for Biotechnology Information, Bethesda, USA. https://pubchem.ncbi.nlm.nih.gov/. Accessed 06 June 2021.

PubChem. (2021b). 9-Fluorenone. US national library for medicine. National Center for Biotechnology Information, Bethesda, USA. https://pubchem.ncbi.nlm.nih.gov/. Accessed 06 June 2021.

Richter-Brockmann, S., & Achten, C. (2018). Analysis and toxicity of 59 PAH in petrogenic and pyrogenic

environmental samples including dibenzopyrenes, 7H-benzo[c]fluorene, 5-methylchrysene and 1-methylpyrene. *Chemosphere, 200*, 495–503.

Ruby, M. V., Lowney, Y. W., Bunge, A. L., Roberts, S. M., Gomez-Eyles, J. L., Ghosh, U., Kissel, J. C., Tomlinson, P., & Menzie, C. (2016). Oral bioavailability, bioaccessibility, and dermal absorption of PAHs from soil—state of the science. *Environmental Science and Technology, 50*, 2151–2164.

Schantz, M., Wise, S.A., & Lewtas, J. (2005). Intercomparison Program for Organic Speciation in PM2.5 Air Particulate Matter: Description and Results for Trials I and II; Materials: Air Particulate Extract I, Air Particulate I and PM2.5 Interim RM, NIST Interagency/Internal Report (NISTIR) Vol. 7229.

Schlanges, I., Meyer, D., Palm, W. U., & Ruck, W. (2008). Identification, quantification and distribution of PAC-metabolites, heterocyclic PAC and substituted PAC in groundwater samples of tar-contaminated sites from Germany. *Polycyclic Aromatic Compounds, 28*, 320–328.

Schneider, J., Grosser, R., Jayasimhulu, K., Xue, W., & Warshawsky, D. (1996). Degradation of pyrene, benz[a]anthracene, and benzo[a]pyrene by Mycobacterium sp. RJGII-135, isolated from a former coal gasification site. *Applied and Environmental Microbiology, 62*, 13–19.

Semple, K. T., Morriss, A. W. J., & Paton, G. I. (2003). Bioavailability of hydrophobic organic contaminants in soils: Fundamental concepts and techniques for analysis. *European Journal of Soil Science, 54*, 809–818.

Shahpoury, P., Lammel, G., Holubová Šmejkalová, A., Klánová, J., Přibylová, P., & Váňa, M. (2015). Polycyclic aromatic hydrocarbons, polychlorinated biphenyls, and chlorinated pesticides in background air in central Europe—investigating parameters affecting wet scavenging of polycyclic aromatic hydrocarbons. *Atmospheric Chemistry and Physics, 15*, 1795–1805.

Shahpoury, P., Kitanovski, Z., & Lammel, G. (2018). Snow scavenging and phase partitioning of nitrated and oxygenated aromatic hydrocarbons in polluted and remote environments in central Europe and the European Arctic. *Atmospheric Chemistry and Physics, 18*, 13495–13510.

Škrdlíková, L., Landlová, L., Klánová, J., & Lammel, G. (2011). Wet deposition and scavenging efficiency of gaseous and particulate phase polycyclic aromatic compounds at a central European suburban site. *Atmospheric Environment, 45*, 4305–4312.

Sun, Z., Zhu, Y., Zhuo, S. J., Liu, W. P., Zeng, E. Y., Wang, X. L., Xing, B. S., & Tao, S. (2017). Occurrence of nitro- and oxy-PAHs in agricultural soils in eastern China and excess lifetime cancer risks from human exposure through soil ingestion. *Environment International, 108*, 261–270.

Sverdrup, L. E., Ekelund, F., Krogh, P. H., Nielsen, T., & Johnsen, K. (2002a). Soil microbial toxicity of eight polycyclic aromatic compounds: Effects on nitrification, the genetic diversity of bacteria, and the total number of protozoans. *Environmental Toxicology and Chemistry, 21*, 1644–1650.

Sverdrup, L. E., Krogh, P. H., Nielsen, T., & Stenersen, J. (2002b). Relative sensitivity of three terrestrial invertebrate tests to polycyclic aromatic compounds. *Environmental Toxicology and Chemistry, 21*, 1927–1933.

Tomaz, S., Shahpoury, P., Jaffrezo, J.-L., Lammel, G., Perraudi, E., Villenave, E., & Albinet, A. (2016). One-year study of polycyclic aromatic compounds at an urban site in Grenoble (France): Seasonal variations, gas/particle partitioning and cancer risk estimation. *Science of the Total Environment, 565*, 1071–1083.

USEPA. (2019). Estimation Programs Interface Suite™ for Microsoft® Windows, v 4.11. United States Environmental Protection Agency, Washington, DC, USA.

USEPA. (2020). U.S. Environmental Protection Agency's Integrated Risk Information System (IRIS). Summary on Dibenzofuran (132-64-9). https://www.epa.gov/iris/.

Vasilieva, S., Tanirbergenov, T., Abilev, S., Migachev, G., & Huttunen, M. T. (1990). A comparative study of mutagenic and SOS-inducing activity of biphenyls, phenanthrenequinones and fluorenones. *Mutation Research, 244*, 321–329.

Vikelsøe, J., Thomsen, M., Carlsen, L., & Johansen, E. (2002). Persistent organic pollutants in soil, sludge and sediment. A multianalytical field study of selected organic chlorinated and brominated compounds. National Environmental Research Institute, Denmark. NERI Technical Report No. 402, 100 pp. http://technical-reports.dmu.dk.

Walgraeve, C., Demeestere, K., Dewulf, J., Zimmermann, R., & Van Langenhove, H. (2010). Oxygenated polycyclic aromatic hydrocarbons in atmospheric particulate matter: Molecular characterization and occurrence. *Atmospheric Environment, 44*, 1831–1846.

Wang, Z., Ma, X., Na, G., Lin, Z., Ding, Q., & Yao, Z. (2009). Correlations between physicochemical properties of PAHs and their distribution in soil, moss and reindeer dung at Ny-Ålesund of the Arctic. *Environmental Pollution, 157*, 3132–3136.

Watanabe, T., Ohe, T., & Hirayama, T. (2005). Occurrence and origin of mutagenicity in soil and water environment. *Environmental Sciences, 12*, 325–346.

WHO. (2003). Selected nitro- and nitrooxy-polycyclic aromatic hydrocarbons. World Health Organization, Environmental health criteria 229. I. International Programme for Chemical Safety II. Series.

Wilcke, W. (2000). Synopsis polycyclic aromatic hydrocarbons (PAHs) in soil—a review. *Journal of Plant Nutrition and Soil Science, 163*, 229–248.

Wilcke, W., & Amelung, W. (2000). Persistent organic pollutants (POPs) in native grassland soils along a climosequence in North America. *Soil Science Society of America Journal, 64*, 2140–2148.

Wilcke, W., Bandowe, B. A. M., Gomez Lueso, M., Ruppenthal, M., del Valle, H., & Oelmann, Y. (2014a). Polycyclic aromatic hydrocarbons (PAHs) and their polar derivatives (oxygenated PAHs, azaarenes) in soils along a climosequence in Argentina. *Science of the Total Environment, 473–474*, 317–325.

Wilcke, W., Kiesewetter, M., & Bandowe, B. A. M. (2014b). Microbial formation and degradation of oxygen-containing polycyclic aromatic hydrocarbons (OPAHs) in soil during short-term incubation. *Environmental Pollution, 184*, 385–390.

Wild, S. R., Berrow, M. L., & Jones, K. C. (1991). The Persistence of Polynuelear Aromatic Hydrocarbons (PAHs) in

sewage sludge amended agricultural soils. *Environmental Pollution, 72*, 141–157.

Wild, S. R., & Jones, K. C. (1995). Polynuclear aromatic hydrocarbons in the United Kingdom environment: A preliminary source inventory and budget. *Environmental Pollution, 88*, 91–108.

Wilson, J., Octaviani, M., Bandowe, B. A. M., Wietzoreck, M., Zetzsch, C., Pöschl, U., Berkemeier, T., & Lammel, G. (2020). Modeling the formation, degradation and spatiotemporal distribution of 2–1 nitrofluoranthene and 2-nitropyrene in the global atmosphere. *Environmental Science and Technology, 54*, 14224–14234.

Wu, Y.-R., Luo, Z.-H., & Vrijmoed, L. L. P. (2010). Biodegradation of anthracene and benz[a]anthracene by two Fusarium solani strains isolated from mangrove sediments. *Bioresource Technology, 101*, 9666–9672.

Ye, J.-S., Yin, H., Qiang, J., Peng, J., Qin, H.-M., Zhang, N., & He, B.-Y. (2011). Biodegradation of anthracene by Aspergillus fumigatus. *Journal of Hazardous Materials, 185*, 174–181.

Zimmermann, K., Jariyasopit, N., Massey Simonich, S. L., Tao, S., Atkinson, R., & Arey, J. (2013). Formation of nitro-PAHs from the heterogeneous reaction of ambient particle-bound PAHs with N2O5/NO3/NO2. *Environmental Science and Technology, 47*, 8434–8442.

Supplementary Information

Nitro- and oxy-PAHs in grassland soils from decade-long sampling in central Europe

M. Wietzoreck[a], B.A.M. Bandowe[a], J. Hofman[b], J. Martiník[b], B. Nežiková[b], P. Kukučka[b], P. Přibylová [b], G. Lammel[a,b]

[a]Max Planck Institute for Chemistry, Multiphase Chemistry Dept., Mainz, Germany

[b]Masaryk University, Research Centre for Toxic Compounds in the Environment, Brno, Czech Republic

Contents

List of Tables

Table S3 Physico-chemical properties & degradation rates of a) PAHs, b) OPAHs and O-heterocycles, c) NPAHs; $k_{biodeg.1}$: > 0.50: Likely to biodegrade rapidly, < 0.50: Not likely to

List of Figures

4

S1 Quality control

S1.1 Method validation

The method was validated by a spike and recovery experiment. We performed the spiking experiments with top 10 cm surface soil within the A horizon after removing the vegetation layer collected at a grassland site in Mainz, Germany. The dried and sieved soil was spiked with 10 µL of a target analyte mix (1.5 ng μL^{-1}) directly onto 5 g portions of the soil (n =4) resulting in 15 ng of each target compound in the soil. The PACs were then determined in the spiked (n =2) and unspiked (n =2) soils as described below.

The extraction was done by Soxhlet (5 g of soil in extraction thimble) with 200 mL DCM/acetone (2:1, v:v) for 40 min (Soxhlet: Büchi B-811, Flawil, Switzerland). The purification was done by solid phase extraction using SiOH cartridges (6 mL, 2000 mg, Chromabond) eluting the target substances by ethyl acetate and dichloromethane. In addition, we re-extracted the soil samples with 200 mL DCM by Soxhlet extraction in order to check whether a re-extraction reveals a significant additional amount of substances making an improvement of the extraction efficiency necessary. The amount of target compounds from the second extraction of the soil was insignificant indicating that a the first extraction with DCM/acetone (2:1 v/v) was sufficient to recover the spiked PACs.

In order to calculate the recoveries, we subtracted the average amount of the duplicate measurement of the spiked samples by the average amount of the duplicate measurement of the unspiked sample and divided it by the expected amount of spiked substance of 15 ng. **Table S6** shows the recoveries of the target compounds. The recoveries were 132 ± 41 (61-171) % and 108 ± 17 (81-152) % for OPAHs and NPAHs, respectively. However, it has to be considered that these results are the upper limits of the recoveries since in real soil samples the substances can undergo stronger binding to the soil matrix than in the 30 min after spiking the soil in the recovery experiment.

S1.2 Limit of quantification and blank correction

For the evaluation of the results, we used two different limits of quantification (LOQs) i.e., first, the instrumental LOQ, iLOQ, based on the GC-MS analysis, and, secondly, the method LOQ, mLOQ. For NOPAHs, the iLOQ is calculated on the signal to noise ratio (S/N) for a specific compound and specific sample as the concentration which corresponds to S/N = 10:1. For PAHs, the iLOQ is calculated by extrapolation of S/N = 10:1 to the corresponding concentration, based

on calibration standards. The LOQs can be found in **Table S7**. We measured five method blanks (same sample preparation but without any soil) and calculated the mLOQ by calculating the mean concentration of a compound from the blanks μ_{mb} plus the standard deviation σ_{mb} of the blanks:

$mLOQ = \mu_{mb} + \sigma_{mb}$

The average amounts of the target compounds in the method blanks, μ_{mb}, were also used for blank correction. The final concentration C_i was calculated as follows:

a) If a value was higher than the LOQ, the raw concentration of a compound c_i was subtracted by the mean of the method blanks μ_{mb}
   $C_i = c_i - \mu_{mb}$
b) If a value was lower than the LOQ (using the maximum of iLOQ and mLOQ), we used the half of the value of LOQ subtracted by the mean of the method blanks μ_{mb}:
   $C_i = (\max(iLOQ, mLOQ) - \mu_{mb})/2$
   In case that the total detection frequency of a compound in all samples was lower than 25 %, a concentration of 0 was used for further calculations such as $\sum_{18}$ NPAHs

S1.3 Recoveries

The average recoveries (compared to the target amount) of 1-NNAP-D7, 2-NFLN-D9, 9-NANT-D9, 3-NFLT-D9, 1-NPYR-D9, 6-NCHR-D11 and 6-NBAP-D11 in the samples and blanks were 15 ± 10 %, 78 ± 25 %, 55 ± 34 %, 41 ± 23 %, 32 ± 24 %, 31 ± 19 % and 43 ± 47 %, respectively. Due to the high variability of the recoveries (CoV of 32-73 %) and the relatively low recoveries, the NPAH data was recovery corrected. The amounts of NPAHs detected in the samples were recovery corrected using the recoveries of their respective surrogate standards. Each compound was corrected with the corresponding deuterated NPAH. The amounts of 1-NNAP and 2-NNAP were corrected by the recovery of 1-NNAP-D7; 2-NFLT and 3-NFLT with 3-NFLT-D9; 1-NPYR with 1-NPYR-D9 and 6-NBAP with 6-NBAP-D11. For all other investigated NPAHs, the recovery correction was not needed since none of them was measured in concentrations higher than the LOQ.

The average recoveries (compared to the target amount) of NAP-D8, PHE-D10 and PER-D12 in the samples and blanks were 37 ± 17 %, 75 ± 12 % and 102 ± 16 %, respectively. The recovery correction was applied only for the samples, namely Kos_2010Sp_1b, Kos_2015_1b and

Mok_2012_2a, with a recovery of less than 10 % for NAP-D8 due to evaporation of the extract to almost dryness. NAP and BPH were corrected by NAP-D8; ACY, ACE, FLN by the average of the recoveries of NAP-D8 and PHE-D10 and PHE by PHE-D10. The concentrations of the compounds were corrected by the average recovery of their surrogates in all samples.

The average recoveries (compared to the target amount) of 9-OFLN-D8 and 9,10-O_2ANT-D9 in the samples and blanks were 101 % ± 34 % and 107 % ± 33 %.

The results of the PAHs and OPAHs were not recovery corrected since their recovery was acceptable and the variability of the recovery of the deuterated compounds was low (CoV of 15-33 %). The variability of the relative recoveries was smaller than the variability of the compound concentrations of the repeated measurements (shown in **Table S8**).

S1.4 Repeatability

A number (n = 11) of the soil samples were measured in duplicate or triplicate to determine the reproducibility of the method. The intra-sample coefficient of variation (CoV) for the 11 samples averaged 15±12 % (range: 2-40 %) for the $\sum_{16}$PAHs. The CoVs of the individual PAHs can be seen in **Table S8a**.

Typical CoVs for the reproducibility of PAHs in soil (from round robin tests) are 15-20 % for concentrations of 40-100 mg kg^{-1}. For each individual PAH, CoV is 30-40 % for concentrations of 2-15 mg/kg and 40-60 % for concentrations <2 mg kg^{-1} (UBA 2003). Since their evaluation shows that the CoV increases with decreasing concentrations, and the concentrations of the analysed soils are around three orders of magnitude lower than the concentrations in the study, the CoV for the reproducibility for PAHs could easily be 20-30 % for the same method and 20-40 % or more for a different sample preparation method. In comparison of the two measurements, only 6 out of 30 (i.e., 20 %) of our analysed samples show CoV >40 % and only 4 samples (13 %) show CoV >50 %.

The intra-sample CoV of the Σ_{11}OPAHs + 2 O-heterocycles is 22 ± 17 % (5-60 %). As shown in **Table S8b**, the CoV of the individual OPAHs ranged from 21 % by 5,12-O_2NAC to 48 % by 9-OFLN. The intra-sample CoV of the Σ_{18}NPAHs (**Table S8c)** (in fact quantified only 6) is 27 ± 25 % (0.7-71 %). The CoV is not very different for the individual NPAHs. It is the lowest for 2-NFLT

with 26 % followed by 6-NBAP and 2-NNAP with 28 and 31 %, respectively. 1-NNAP, 3-NFLT and 1-NPYR showed only a slightly higher CoV with 38 %, 34 % and 36 %, respectively.

S2 Comparison of remeasured to original PAH results

The concentrations of 16 US-EPA PAHs measured in this study ("archived samples") are similar to the previous measurements ("original") of the same samples (**Fig. S2**), except for two soil samples from Mokrá (Mokrá_2010F_1 and Mokrá_2006F_2), which are outliers ($P<0.01$, Grubbs' test). The PAH concentrations of the re-measurement of these two samples are shifted to a significantly lower concentration. The relative differences between both measurements $((c_{archived\ sample} - c_{original})\ (c_{archived\ sample} + c_{original})^{-1})$ are -94 ± 54 % and -91 ± 57 % for Mokrá_2010F_1 and Mokrá_2006F_2, respectively. Possible reasons for the significant differences in the concentrations of these two samples are soil heterogeneity at a small spatial scale (< 10 m) and/or reduced extractability (MacLeod & Semple 2003).

The correlation coefficient between the concentration of the original and the archived samples is 0.47 ($p = 0.06$), while it is 0.90 without the two outliers ($p <0.01$). The site-specific correlation coefficients are 0.83 ($p<0.05$) for Mokrá-1 and 0.89 ($p<0.05$) for Mokrá-2 without the two outliers (0.07 and 0.56 ($p = 0.87$ and $p = 0.15$) for all samples of Mokrá-1 and Mokrá-2, respectively). The correlation coefficients for the two PAH measurements of soil from Košetice are 0.12 and 0.41 ($p = 0.80$ and $p = 0.36$) for locations 1 and 2, respectively. Without sample Košetice_2015_2, for which a large difference between both measurements is found, the correlation coefficient is 0.82 ($p<0.05$). However, this is not an outlier (Grubbs test). The small correlation coefficient for Košetice-1 might be explained by a higher uncertainty of the concentrations close to the limit of quantification.

The difference between the concentration of the archived and the original measurement for each individual sample compared to the average of both measurements shows that the results from the archived samples is on average 7 ± 21 % higher than the original data. However, this is slightly biased by the two samples from Mokrá (Mokrá_2010F_1 and Mokrá_2006F_2) with comparably high PAH concentrations in the original measurement. Excluding these two samples, the re-measured concentrations are 11 ± 17 % higher than the original data. Although this is lower than the variability of the concentration of the Σ_{16}PAHs from the repeatability experiments of 11 soil samples, which is 14.7 %, we try to reveal the cause for this deviation. Possible reasons for the

differences are (a) the extractability of PAHs in soil has increased during sample storage or (b) sample contamination during storage or (c) difference in sample preparation or (d) soil heterogeneity. The soil samples were air-dried before the first analysis and stored under controlled conditions. Hence, it is unlikely that air contamination during sample storage caused the observed differences. Explanation (a) can be rejected, because there was no trend between concentration differences and storage time. Furthermore, MacLeod et al. (2003) found that the non-extractable fraction tends to increase with storing time, rather than decrease. Reason (b) is very unlikely since Cousins et al. (1997) found that contaminations during air-drying mainly affect the lower MW PAHs. In this work, the difference between the original PAH concentration and the PAH concentration of the remeasured archived samples were mainly due to the higher MW PAHs. Therefore, we conclude that this could not be due to air contamination during storage. We suggest that (c), the difference in sample preparation might have caused the observed differences. For the higher recovery of the OPAHs, a slightly more polar extraction solvent mixture was used compared to the original PAH measurement. Hollender et al. (2002) and Lau et al. (2010) found that slightly polar solvents can increase the extractable amount of PAHs in soil with a low degree of pollution, since it can break up soil aggregates. In addition, (d) soil heterogeneity, might play an important role for the observed differences, too. However, this relatively small difference between both measurements should not be overstated, since the uncertainties in determining representative pollutant concentrations in soil samples are generally higher than in other environmental matrices, such as water or air. This could also be seen from the repeatability results of our samples, which are shown as quality control data (**Table S8**). The variation between different measurements of the same sample can be significant for soil samples (UBA 2003). In summary, the PAHs in the archived soil samples were not prone to degradation or any other strong modification. The concentrations of the re-measured compounds are comparable to the original results determined shortly after sampling.

S3 PAHs multiannual variation

The annual PAH concentrations of the samples from this study are shown in **Table S11**. In order to reveal time-related trends, we looked at even longer time series. An overview of the PAH concentrations in soil from Košetice and Mokrá from the very same locations from different periods in the past can be found in **Table S17**. Compared to the data from 1996 to 2007 from the same

locations in Košetice reported by Holoubek et al. (2007), the concentration of the $\sum_{16}$PAHs in the more recently sampled soils (2010-2017) from Košetice-1 is significantly ($p<0.0001$, Student's t-test) lower, by 63 %. The levels at Košetice-2 are 12% lower in the more recent period (2009-2017) compared to 1996-2007. The trend between 1996 and 2017 is not significant at Košetice-2 according to the trend test from Neumann (Hecht 2020). In contrast, there is a significant decreasing trend for the Σ_{16}PAHs at Košetice-1 ($p<0.01$, trend test by Neumann), which was already observed 1996-2007 at several locations, including Košetice-1 (Holoubek et al. 2007). A probable explanation for the difference can be given when looking at the sampling locations in detail. Košetice-1 is at the EMEP station on grassland with no influence other than PAHs from the air by wet and dry deposition. Since the concentration of PAHs in air has decreased during the study period (2010-17) at the regional background site Košetice, weakly but significantly (Kalina et al. 2017; Lhotka et al. 2019; Degrendele et al. 2020), the concentrations in soil might also decrease with a time lag. A decreasing trend for both air and soil had been found at the site for the years 1996-2005 (Holoubek et al. 2007), a faster decrease than later, though. Furthermore, a decrease was also examined for other matrices studied at the site i.e., water, rainwater, and mosses (Prokeš et al. 2019). In contrast, Košetice-2 (location 8 in Holoubek et al. 2007) is on grassland, partly surrounded by trees at the confluence of two brooks resulting in a more diverse impact on the PAH levels. There is first the higher TOC content in this soil and second the possible influence of PAHs from the river water to the examined soil samples in addition to the PAHs from the air. Different TOC content in soil can affect the trend of the pollutant concentration, since it could affect leachability, revolatilisation as well as biodegradability due to stronger interaction between the pollutant and the soil matrix (Wilcke, 2000).

At Mokrá-1, the concentrations of $\sum_{16}$PAHs in the period 1998-2005 are significantly different to 2006-2015. The more recent PAH concentration is 66 % higher than the old one. The trend test by Neumann does not reveal a significant trend, because of an exceptionally high value in April 2001. Excluding this value as an outlier ($p<0.01$, Grubbs test), a significant increasing trend is found ($p<0.05$, Neumann trend test). To determine the exact reason, decade-long monitoring of air, deposition and soil samples would be needed. We hypothesize that the trend is caused by a slight change of the sampling site by around 80-100 m in 2007. Even minor changes in the sampling location can have a great impact on the results. This hypothesis is supported in our case by a significant difference in PAH concentrations before and after changing the location ($p<0.06$,

Student's t-test). Looking at the specific locations individually, there is a significant ($p<0.05$, Neumann test) decreasing trend for the period 1998-2006 and no trend for the period 2007-2015.

There is no significant trend regarding the concentration of the $\sum_{16}$PAHs at Mokrá-2. The $\sum_{16}$PAHs of this study, 2006-2015, is 6 % higher than the data found for 1998-2005. However, this difference is not significant, but within the variability (CoV = 65 %). Accordingly, the slight change of the sampling position in 2009 did not result in a significant change of the PAH concentration ($p<0.22$, Student's t-test), but reflects the variability.

11

Tables and Figures

Table S1 Information about soil sampling sites and dates

Site	Location #	Sampling date	Season	Sample abbreviation	Detail location	Latitude (WGS84)	Longitude (WGS84)	Altitude [m]
Košetice	1	31.08.2010	Summer	Kos_2010_1[b]	EMEP station, observatory	49.57345	15.08041	534
		04.09.2012	Summer	Kos_2012_1				
		28.08.2013	Summer	Kos_2013_1				
		25.08.2014	Summer	Kos_2014_1				
		07.09.2015	Summer	Kos_2015_1[b]				
		22.08.2016	Summer	Kos_2016_1				
		22.08.2017	Summer	Kos_2017_1[b]				
	2	31.08.2010	Summer	Kos_2010_2[b]	Confluence - meadow	49.571724	15.091728	489
		04.09.2012	Summer	Kos_2012_2				
		28.08.2013	Summer	Kos_2013_2				
		25.08.2014	Summer	Kos_2014_2				
		08.09.2015	Summer	Kos_2015_2				
		23.08.2016	Summer	Kos_2016_2				
		22.08.2017	Summer	Kos_2017_2[b]				
Mokrá	1	15.11.2006	Fall	Mok_2006F_1	Hostěnice Čihálky	49.234939	16.77169	427
		12.09.2008	Summer/ Fall	Mok_2008S_1	Hostěnice Čihálky 2	49.235283	16.770733	427
		21.04.2010	Spring	Mok_2010Sp_1				
		01.10.2010	Fall	Mok_2010F_1				
		21.04.2011	Spring	Mok_2011Sp_1				
		01.10.2011	Fall	Mok_2011F_1[a]				
		25.04.2012	Spring	Mok_2012Sp_1[b]				
		11.06.2015	Summer	Mok_2015S_1[b]				
	2	15.11.2006	Fall	Mok_2006F_2[b]	Velká Baba	49.211188	16.784422	375
		12.09.2008	Summer/ Fall	Mok_2008S_2[b]				
		21.04.2010	Spring	Mok_2010Sp_2	Velká Baba 2	49.211117	16.784400	375
		01.10.2010	Fall	Mok_2010F_2				
		21.04.2011	Spring	Mok_2011Sp_2				
		01.10.2011	Fall	Mok_2011F_2				
		25.04.2012	Spring	Mok_2012Sp_2				
		11.06.2015	Summer	Mok_2015S_2[a]				

[a]measured in duplicate [b]measured in triplicate

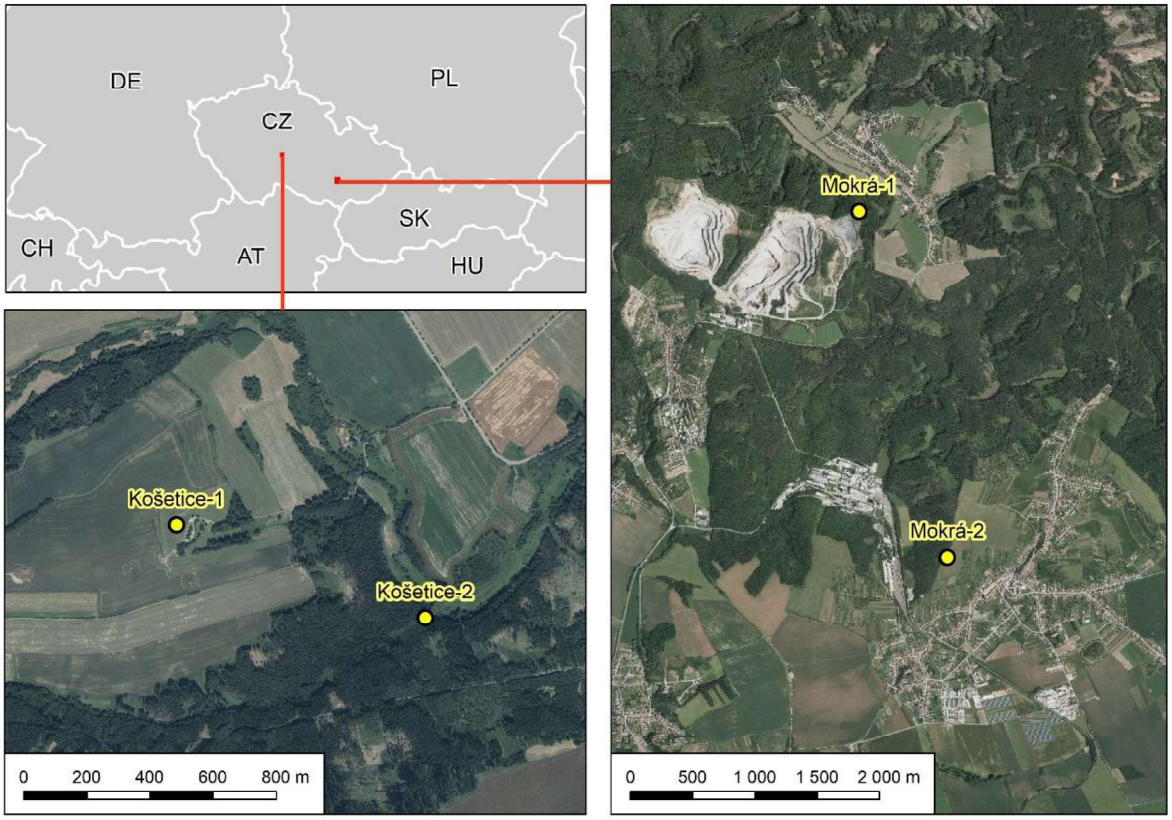

Fig. S1 Sampling locations Košetice-1, Košetice-2, Mokrá-1 and Mokrá-2 (Satellite image taken from CENIA, Czech Environmental Information Agency, Software used: ArcGIS 9.6, ESRI, Redlands, USA)

Table S2 Basic soil parameters of the analysed soil samples, n.d. = not determined

Site	Location #	Date of collection	Land use	Horizon	Depth [cm]	Texture	Soil type	Description of vegetation	Total organic carbon (TOC) [%]	pH (H_2O)	pH (KCl)	Total N [%]	C/N	Phys. clay (≤ 2 µm) [%]	Clay (≤ 10 µm) [%]	Dust (10-50 µm) [%]	Powdered sand (50-100 µm) [%]	Sand (100-2000 µm) [%]	$CaCO_3$ [%]
Košetice	1	31.08.2010	Grassland	A	0-10	Loam	Cambisol	Grass	1.29	n.d.	n.d.	n.d.	n.d.	n.d.	n.d.	n.d.	n.d.	n.d.	n.d.
		04.09.2012		A					n.d.	n.d.	n.d.	n.d.	n.d.	n.d.	n.d.	n.d.	n.d.	n.d.	n.d.
		28.08.2013		A					n.d.	n.d.	n.d.	n.d.	n.d.	n.d.	n.d.	n.d.	n.d.	n.d.	n.d.
		25.08.2014		A					n.d.	n.d.	n.d.	n.d.	n.d.	n.d.	n.d.	n.d.	n.d.	n.d.	n.d.
		07.09.2015		A					2.20	n.d.	n.d.	n.d.	n.d.	n.d.	n.d.	n.d.	n.d.	n.d.	n.d.
		22.08.2016		A					2.20	n.d.	n.d.	n.d.	n.d.	n.d.	n.d.	n.d.	n.d.	n.d.	n.d.
		22.08.2017		A					2.48	n.d.	n.d.	n.d.	n.d.	n.d.	n.d.	n.d.	n.d.	n.d.	n.d.
	2	31.08.2010	Grassland	A	0-10	Loam	Fluvisol	Grass	5.70	n.d.	n.d.	n.d.	n.d.	n.d.	n.d.	n.d.	n.d.	n.d.	n.d.
		04.09.2012		A					n.d.	n.d.	n.d.	n.d.	n.d.	n.d.	n.d.	n.d.	n.d.	n.d.	n.d.
		28.08.2013		A					n.d.	n.d.	n.d.	n.d.	n.d.	n.d.	n.d.	n.d.	n.d.	n.d.	n.d.
		25.08.2014		A					n.d.	n.d.	n.d.	n.d.	n.d.	n.d.	n.d.	n.d.	n.d.	n.d.	n.d.
		08.09.2015		A					5.94	n.d.	n.d.	n.d.	n.d.	n.d.	n.d.	n.d.	n.d.	n.d.	n.d.
		23.08.2016		A					4.81	n.d.	n.d.	n.d.	n.d.	n.d.	n.d.	n.d.	n.d.	n.d.	n.d.
		22.08.2017		A					5.23	n.d.	n.d.	n.d.	n.d.	n.d.	n.d.	n.d.	n.d.	n.d.	n.d.
Mokrá	1	15.11.2006	Grassland	A	0-10	sandy loam	Cambisol	Low growth of grass, shrubs, deciduous trees (approx. 10 years)	1.89	n.d.	n.d.	n.d.	n.d.	n.d.	n.d.	n.d.	n.d.	n.d.	n.d.
		12.09.2008		A					3.19	6.04	5.08	n.d.	n.d.	n.d.	n.d.	n.d.	n.d.	n.d.	n.d.
		21.04.2010		A					n.d.	n.d.	n.d.	n.d.	n.d.	n.d.	n.d.	n.d.	n.d.	n.d.	n.d.
		01.10.2010		A					3.25	5.74	4.90	0.27	12.04	7.28	32.33	16.73	7.23	43.70	0.10
		21.04.2011		A					1.85	n.d.	n.d.	n.d.	n.d.	n.d.	n.d.	n.d.	n.d.	n.d.	n.d.
		01.10.2011		A					4.83	6.46	5.76	0.38	14.89	1.48	24.00	12.80	13.00	50.10	0.15
		25.04.2012		A					5.05	n.d.	n.d.	n.d.	n.d.	n.d.	n.d.	n.d.	n.d.	n.d.	n.d.
		11.06.2015		A					6.52	6.58	6.28	n.d.	n.d.	n.d.	n.d.	n.d.	n.d.	n.d.	n.d.

Site	Location #	Date of collection	Land use	Horizon	Depth [cm]	Texture	Soil type	Description of vegetation	Total organic carbon (TOC) [%]	pH (H_2O)	pH (KCl)	Total N [%]	C/N	Phys. clay (≤ 2 µm) [%]	Clay (≤ 10 µm) [%]	Dust (10-50 µm) [%]	Powdered sand (50-100 µm) [%]	Sand (100-2000 µm) [%]	$CaCO_3$ [%]
Mokrá	2	15.11.2006	Arable land	A	0-10	sandy loam	Cambisol	alternation of cultures	1.78	n.d.	n.d.	n.d.	n.d.	n.d.	n.d.	n.d.	n.d.	n.d.	n.d.
		12.09.2008		A					1.97	6.94	6.30	0.21	9.37	5.00	17.70	13.30	9.60	59.40	0.13
		21.04.2010	Grass-land	A				Grass	1.38	n.d.	n.d.	n.d.	n.d.	n.d.	n.d.	n.d.	n.d.	n.d.	n.d.
		01.10.2010		A					1.23	6.52	5.97	0.20	6.14	4.56	24.27	8.60	10.97	56.17	0.10
		21.04.2011		A					1.61	n.d.	n.d.	n.d.	n.d.	n.d.	n.d.	n.d.	n.d.	n.d.	n.d.
		01.10.2011		A					1.73	6.85	6.17	0.21	11.62	0.57	13.90	11.90	12.90	61.30	0.05
		25.04.2012		A					1.81	n.d.	n.d.	n.d.	n.d.	n.d.	n.d.	n.d.	n.d.	n.d.	n.d.
		11.06.2015		A					3.33	n.d.	n.d.	n.d.	n.d.	n.d.	n.d.	n.d.	n.d.	n.d.	n.d.

Table S3 Physico-chemical properties and degradation rates of a) PAHs, b) OPAHs and O-heterocycles, c) NPAHs; $k_{biodeg.1}$: > 0.50: Likely to biodegrade rapidly, < 0.50: Not likely to biodegrade rapidly, $k_{biodeg.2}$: >4.75 – 5: Hours, >4.25 - 4.75: Hours – days, >3.75 - 4.25: Days, >3.25 - 3.75: Days – weeks, >2.75 - 3.25: Weeks, >2.25 - 2.75: Weeks – months, >1.75 - 2.25: Months, <1.75: Longer "recalcitrant"; MW = molecular weight, n.d. = not determined

a)

Compound	Acronym	CAS #	MW [g mol^{-1}]	# of rings	Phase state [a,b]	log K_{ow}	$k_{biodeg.1}$ [c]	$k_{biodeg.2}$ [d]	log K_{oc}
Naphthalene	NAP	91-20-3	128.18	2	g	3.30	1.0057	3.3200	2.96
Acenaphthylene	ACY	208-96-8	152.20	3	g	3.94	0.6751	3.6282	3.70
Acenaphthene	ACE	83-32-9	154.20	3	g	3.92	0.7835	3.4882	3.59
Fluorene	FLN	86-73-7	166.23	3	g	4.18	0.7231	3.5394	3.70
Phenanthrene	PHE	85-01-8	178.24	3	g	4.46	0.9819	3.2478	4.35
Anthracene	ANT	120-12-7	178.24	3	g	4.45	0.9819	3.2478	4.31
Fluoranthene	FLT	206-44-0	202.26	4	g	5.16	-0.0060	2.8537	4.80
Pyrene	PYR	129-00-0	202.26	4	g	4.88	-0.0060	2.8537	4.90
Retene	RET	483-65-8	234.34	3	p	6.35	0.7453	3.3726	5.117
Benzo(b)fluorene	BBN	243-17-4	216.28	4	n.d.	5.77	0.6992	3.4672	4.987
Benzo(ghi)fluoranthene	BGF	203-12-3	226.28	5	n.d.	5.52	-0.0175	2.8190	5.256
Cyclopenta(cd)pyrene	CCP	27208-37-3	226.28	5	n.d.	5.70	-0.0175	2.8190	5.248
Benzo(a)anthracene	BAA	56-55-3	228.30	4	p	5.76	-0.0184	2.8161	5.248
Triphenylene	TPH	217-59-4	228.30	4	n.d.	5.49	-0.0184	2.8161	5.265
Chrysene	CHR	218-01-9	228.30	4	g	5.81	-0.0184	2.8161	5.256
Benzo(b)fluoranthene	BBF	205-99-2	252.32	5	p	5.78	-0.0299	2.7815	5.778
Benzo(j)fluoranthene	BJF	205-82-3	252.32	5	p	6.11	-0.0299	2.7815	5.778
Benzo(k)fluoranthene	BKF	207-08-9	252.32	5	p	6.11	-0.0299	2.7815	5.778
Benzo(e)pyrene	BEP	192-97-2	252.32	5	p	6.44	-0.0299	2.7815	5.778
Benzo(a)pyrene	BAP	50-32-8	252.32	5	p	6.13	-0.0299	2.7815	5.769
Perylene	PER	198-55-0	252.32	5	n.d.	6.25	-0.0299	2.7815	5.778
Indeno(123-cd)pyrene	INP	193-39-5	276.34	6	p	6.70	-0.0413	2.7468	6.290
Dibenz(ah)anthracene	DBA	53-70-3	278.36	5	p	6.54	-0.0423	2.7439	6.281
Dibenz(ac)anthracene	DCA	215-58-7	278.36	5	p	6.41	-0.0423	2.7439	6.290
Benzo(ghi)perylene	BPE	191-24-2	276.34	6	p	6.63	-0.0413	2.7468	6.290

Compound	Acronym	CAS #	MW [g mol^{-1}]	# of rings	Phase state [a,b]	log K_{ow}	$k_{biodeg.1}$ [c]	$k_{biodeg.2}$ [d]	log K_{oc}
Anthanthrene	ATT	191-26-4	276.34	6	n.d.	7.04	-0.0413	2.7468	6.281
Coronene	COR	191-07-1	300.36	7	p	7.64	-0.0527	2.7121	6.803

[a]if seasonal average of particulate fraction <0.5: g (gas phase), if >0.5: p (particulate phase), [b]Data from Nežiková et al. (2021) and Tomaz et al. (2016), [c]linear, estimate fast degradation, BioWin1 of USEPA 2019, [c](primary, estimate), BioWin4 of USEPA 2019

b)

Compound	Acronym	CAS #	MW [g mol^{-1}]	# of rings	Phase state [a,b]	log K_{ow}	$k_{biodeg.1}$ [c]	$k_{biodeg.2}$ [d]	log K_{oc}
1,4-Naphthoquinone	1,4-O_2NAP	130-15-4	158.16	2	g	1.71	0.6859	3.3200	2.657
Naphthalene-1-aldehyde	1-(CHO)NAP	66-77-3	156.19	2	g	2.89	0.9578	3.8190	2.079
Dibenzofuran	DBF	132-64-9	168.19	3	g	4.12	0.6675	3.6051	3.962
9-Fluorenone	9-OFLN	486-25-9	180.21	3	g	3.58	0.6686	3.5655	3.056
6H-Benzo(c)chromen-6-one	6-OBCC	2005-10-9	196.21	3	g	1.99	0.8283	3.7936	3.140
9,10-Anthraquinone	9,10-O_2ANT	84-65-1	208.22	3	g	3.39	0.6621	3.5029	3.700
9,10-Phenanthroquinone	9,10-O_2PHE	84-11-7	208.22	3	p	2.52	0.6484	3.5473	1.450
11H-Benzo(a)fluoren-11-one	11-OBaFLN	479-79-8	230.27	4	p	4.73	0.6448	3.4933	4.090
11H-Benzo(b)fluoren-11-one	11-OBbFLN	3074-03-1	230.27	4	p	4.73	0.6448	3.4933	4.081
Benzanthrone	BAN	82-05-3	230.27	4	p	4.81	0.6448	3.4933	4.090
Benz(a)anthracene-7,12-dione	7,12-O_2BAA	2498-66-0	258.27	4	p	4.61	0.6382	3.4307	4.734
5,12-Naphthacenequinone	5,12-O_2NAC	1090-13-7	258.27	4	p	4.52	0.6382	3.4307	4.725
6H-Benzo(cd)pyren-6-one	6-OBPYR	3074-00-8	254.28	5	p	5.31	-0.0240	2.7564	4.602

[a]if seasonal average of particulate fraction <0.5: g (gas phase), if >0.5: p (particulate phase), [b]Data from Nežiková et al. (2021) and Tomaz et al. (2016), [c]linear, estimate fast degradation, BioWin1 of USEPA 2019, [c](primary, estimate), BioWin4 of USEPA 2019

c)

Compound	Acronym	CAS #	MW [g mol^{-1}]	# of rings	Phase state [1,2]	log K_{ow}	$k_{biodeg.1}$ [3]	$k_{biodeg.2}$ [4]	log K_{oc}
1-Nitronaphthalene	1-NNAP	86-57-7	173.17	2	g	3.19	0.3601	3.4895	3.389
2-Nitronaphthalene	2-NNAP	581-89-5	173.17	2	g	3.24	0.3601	3.4895	3.380
3-Nitroacenaphthene	3-NACE	3807-77-0	199.21	3	g	3.97	0.4570	3.3149	3.901
5-Nitroacenaphthene	5-NACE	602-87-9	199.21	3	g	3.85	0.4570	3.3149	3.901
2-Nitrofluorene	2-NFLN	607-57-8	211.22	3	g	3.37	0.3966	3.3661	4.153
9-Nitroanthracene	9-NANT	602-60-8	223.23	3	g	4.78	0.3362	3.4173	4.423
9-Nitrophenanthrene	9-NPHE	954-46-1	223.23	3	g	4.16	0.3362	3.4173	4.423
3-Nitrophenanthrene	3-NPHE	17024-19-0	223.23	3	g	4.16	0.3362	3.4173	4.414
2-Nitrofluoranthene	2-NFLT	13177-29-2	247.26	4	p	4.29	0.6835	3.4196	4.935
3-Nitrofluoranthene	3-NFLT	892-21-7	247.26	4	p	4.75	-0.3325	2.6804	4.944
1-Nitropyrene	1-NPYR	5522-43-0	247.26	4	p	5.06	-0.3325	2.6804	4.935
7-Nitrobenzo(a)anthracene	7-NBAA	20268-51-3	273.29	4	p	5.34	-0.3449	2.6428	5.456
6-Nitrochrysene	6-NCHR	7496-02-8	273.29	4	p	5.34	-0.3449	2.6428	5.456
1,3-Dinitropyrene	1,3-N_2PYR	75321-20-9	292.25	4	p	4.57	-0.6590	2.5071	5.135
1,6-Dinitropyrene	1,6-N_2PYR	42397-64-8	292.25	4	p	4.57	-0.6590	2.5071	5.135
1,8-Dinitropyrene	1,8-N_2PYR	42397-65-9	292.25	4	p	4.57	-0.6590	2.5071	5.135
3-Nitrobenzanthrone	3-NBAN	17117-34-9	275.27	4	n.d.	4.54	0.3183	3.3200	4.290
6-Nitrobenzo(a)pyrene	6-NBAP	63041-90-7	297.32	5	p	5.93	-0.3563	2.6082	5.978

[a]if seasonal average of particulate fraction <0.5: g (gas phase), if >0.5: p (particulate phase), [b]Data from Nežiková et al. (2021) and Tomaz et al. (2016), [c]linear, estimate fast degradation, BioWin1 of USEPA 2019, [c](primary, estimate), BioWin4 of USEPA 2019

Table S4 SIM masses and retention times of PAHs in GC-MS analysis

Substance	Acronym	SIM [m/z]	Retention time [min]
Naphthalene	NAP	128.0	9.167
Acenaphthylene	ACY	152.0	12.207
Acenaphthene	ACE	154.0	12.613
Fluorene	FLN	166.0	13.952
Phenanthrene	PHE	178.0	16.987
Anthracene	ANT	178.0	17.170
Fluoranthene	FLT	202.0	21.628
Pyrene	PYR	202.0	22.574
Retene	RET	219.0	23.950
Benzo(b)fluorene	BBN	216.0	24.369
Benzo(ghi])fluoranthene	BGF	226.0	27.047
Cyclopenta(cd)pyrene	CCP	228.0	27.953
Benzo(a)anthracene	BAA	226.0	28.056
Triphenylene	TPH	228.0	28.056
Chrysene	CHR	228.0	28.105
Benzo(b)fluoranthene	BBF	252.0	32.634
Benzo(j)fluoranthene	BJF	252.0	32.674
Benzo(k)fluoranthene	BKF	252.0	32.742
Benzo(e)pyrene	BEP	252.0	33.733
Benzo(a)pyrene (also called benzo(def)chrysene)	BAP	252.0	33.931
Perylene	PER	252.0	34.265
Indeno(123-cd)pyrene	INP	276.0	38.602
Dibenz(ah)anthracene	DBA	278.0	38.710
Dibenz(ac)anthracene	DCA	278.0	38.710
Benzo(ghi)perylene	BPE	276.0	39.848
Anthanthrene	ATT	276.0	40.510
Coronene	COR	300.0	49.473

Table S5 MRM masses and retention times of NOPAHs in GC-MS

Substance	Acronym	Group	Target ions [m/z]	Qualifier ions [m/z]	Reten-tion time [min]
1,4-Naphthoquinone	1,4-O2NAP	OPAH	158 > 102	159 > 103	4.06
Dibenzofuran	DBF	O-heterocycle	168 > 139	169 > 140	5.29
Naphthalene-1-aldehyde	1-(CHO)NAP	OPAH	156 > 128	157 > 128	5.33
1-Nitronaphthalene	1-NNAP	NPAH	174 > 127	173 > 145	6.01
2-Nitronaphthalene	2-NNAP	NPAH	173 > 127	174 > 127	6.37
9-Fluorenone	9-OFLN	OPAH	180 > 152	181 > 153	7.25
6H-Benzo[c]chromen-6-one (also called 6H-dibenzo(bd)pyran-6-one)	6-OBCC	O-heterocycle	196 > 139	197 > 140	9.5
3-Nitroacenaphthene	3-NACE	NPAH	199 > 152	200 > 153	9.81
9,10-Anthraquinone	9,10-O2ANT	OPAH	208 > 152	209 > 153	9.9
9,10-Phenanthrenequinone	9,10-O2PHE	OPAH	180 > 152	209 > 153	10.01
5-Nitroacenaphthene	5-NACE	NPAH	199 > 169	199 > 152	10.34
2-Nitrofluorene	2-NFLN	NPAH	211 > 164	212 > 195	11.69
9-Nitroanthracene	9-NANT	NPAH	223 > 193	223 > 178	12.06
9-Nitrophenanthrene	9-NPHE	NPAH	223 > 167	223 > 178	13.11
3-Nitrophenanthrene	3-NPHE	NPAH	223 > 176	223 > 193	13.82
Benzo[a]fluoren-11-one	11-OBaFLN	OPAH	230 > 202	231 > 203	15.19
Benzo[b]fluoren-11-one	11-OBbFLN	OPAH	230 > 202	231 > 203	16.09
Benzanthrone (also called 7H-Benz(de) anthracene-7-one)	BAN	OPAH	230 > 202	231 > 203	17.28
2-Nitrofluoranthene + 3-nitrofluoranthene	2-+3-NFLT	NPAH	247 > 201	248 > 202	18.18
Benz[a]anthracene-7,12-dione	7,12-O2BAA	OPAH	258 > 202	259 > 203	18.6
1-Nitropyrene	1-NPYR	NPAH	247 > 217	247 > 201	18.77
5,12-Naphthacenequinone	5,12-O2NAC	OPAH	258 > 202	259 > 203	19.77
7-Nitrobenzo[a]anthracene	7-NBAA	NPAH	273 > 215	274 > 257	21.44
6H-Benzo[c,d]pyren-6-one	6-OBPYR	OPAH	254 > 226	255 > 227	22.12
6-Nitrochrysene	6-NCHR	NPAH	273 > 215	274 > 226	22.65
1.3-Dinitropyrene	1,3-N2PYR	NPAH	292 > 188	292 > 176	23.65
1.6-Dinitropyrene	1,6-N2PYR	NPAH	292 > 176	292 > 232	24.4
3-Nitrobenzanthrone	3-NBAN	NOPAH	245 >217	246 > 218	24.77
1.8-Dinitropyrene	1,8-N2PYR	NPAH	292 > 176	292 > 232	24.93
6-Nitrobenzo[a]pyrene	6-NBAP	NPAH	297 > 239	297 > 224	26.81

Table S6 Recoveries of target compounds from duplicate measurements

Substance	Recovery [%]
1-NNAP	99
2-NNAP	127
9-OFLN	61
9,10-O2ANT	171
5-NACE	121
2-NFLN	113
9-NANT	106
9-NPHE	113
3-NPHE	105
11-OBaFLN	162
11-OBbFLN	154
BAN	113
2-NFLT	101
3-NFLT	94
7,12-O2BAA	128
1-NPYR	94
7-NBAA	109
6-NCHR	97
3-NBAN	86
1,3-N2PYR	81
1,6-N2PYR	123
1,8-N2PYR	152
6-NBAP	111

Table S7 Limits of quantification (LOQs) of a) PAHs b) OPAHs and O-heterocycles and c) NPAHs in ng g^{-1} (mLOQ: method LOQ; iLOQ: instrumental LOQ; STD: Standard deviation)

a)

Compound	mLOQ first 10 samples with blanks 1-2[a]	mLOQ samples all other samples with blanks 3-5	iLOQ	LOQ (max of iLOQ & mLOQ) first 10 samples with blanks 1-2[a]	LOQ (max of iLOQ & mLOQ) samples all other samples with blanks 3-5
Naphthalene	0.648	0.594	0.033	0.648	0.594
Acenaphthylene	0.000	0.000	0.023	0.023	0.023
Acenaphthene	0.000	0.000	0.027	0.027	0.027
Fluorene	0.684	0.438	0.020	0.684	0.438
Phenanthrene	5.241	4.288	0.025	5.241	4.288
Anthracene	0.015	0.520	0.030	0.030	0.520
Fluoranthene	3.014	4.695	0.029	3.014	4.695
Pyrene	0.756	3.680	0.031	0.756	3.680
Retene	0.034	14.425	0.068	0.068	14.425
Benzo(b)fluorene	0.000	0.000	0.081	0.081	0.081
Benzo(ghi)fluoranthene	0.010	0.607	0.021	0.021	0.607
Cyclopenta(cd)pyrene	0.000	0.000	0.030	0.030	0.030
Benzo(a)anthracene	0.015	0.943	0.029	0.029	0.943
Triphenylene	0.447	0.800	0.024	0.447	0.800
Chrysene	0.205	1.167	0.028	0.205	1.167
Benzo(b)fluoranthene	0.033	0.286	0.066	0.066	0.286
Benzo(j)fluoranthene	0.034	0.217	0.068	0.068	0.217
Benzo(k)fluoranthene	0.039	0.119	0.078	0.078	0.119
Benzo(e)pyrene	0.000	0.000	0.069	0.069	0.069
Benzo(a)pyrene	0.000	0.000	0.107	0.107	0.107
Perylene	0.000	0.000	0.090	0.090	0.090
Indeno(123-cd)pyrene	0.000	0.000	0.061	0.061	0.061
Dibenz(ah)anthracene	0.000	0.000	0.049	0.049	0.049
Dibenz(ac)anthracene	0.000	0.000	0.049	0.049	0.049
Benzo(ghi)perylene	0.000	0.000	0.051	0.051	0.051
Anthanthrene	0.202	1.172	0.058	0.202	1.172
Coronene	0.000	0.000	0.084	0.084	0.084

[a]First 10 samples: Kos_2010_1a,, Kos_2017_1a, Kos_2017_8a, Mokra_2015_5a, Mokra_2010Sp_2a, Mokra_2015_2a, Mokra_2010Sp_5a, Kos_2010_8a, Kos_2017_1b, Mokra_2015_2b

b)

Compound	mLOQ sample #1-4 with blanks 1-2[b]	mLOQ samples >#4 with blanks 3-5	iLOQ (average of sample-specific iLOQ)	STD of iLOQ	LOQ (max of iLOQ & mLOQ) sample #1-4 with blanks 1-2[b]	LOQ (max of iLOQ & mLOQ) samples >#4 with blanks 3-5
1,4-Naphthoquinone	0.17	0.04	0.016	0.01	0.17	0.04
Naphthalene-1-aldehyde	0.10	0.02	0.005	0.00	0.10	0.02
Dibenzofuran	0.35	0.12	0.001	0.00	0.35	0.12
9-Fluorenone	1.16	0.51	0.003	0.00	1.16	0.51
6H-Benzo(c)chromen-6-one	0.21	0.32	0.009	0.01	0.21	0.32
9,10-Anthraquinone	1.63	4.67	0.012	0.01	1.63	4.67
9,10-Phenanthroquinone	0.00	0.00	2.844	1.99	2.84	2.84
11H-Benzo(a)fluoren-11-one	0.10	0.16	0.026	0.05	0.10	0.16
11H-Benzo(b)fluoren-11-one	0.06	0.05	0.022	0.05	0.06	0.05
Benzanthrone	0.05	0.13	0.020	0.04	0.05	0.13
Benz(a)anthracene-7,12-dione	0.06	0.03	0.021	0.05	0.06	0.03
5,12-Naphthacenequinone	0.00	0.00	0.015	0.03	0.01	0.01
6H-Benzo(cd)pyren-6-one	0.01	0.02	0.012	0.03	0.01	0.02

[b]First 4 samples: Kos_2010_8a, Kos_2017_1b, Mokra_2015_2b, Kos_2017_1c

c)

Compound	mLOQ sample #1-4 with blanks 1-2[b]	mLOQ samples >#4 with blanks 3-5	iLOQ (average of sample-specific iLOQ)	STD of iLOQ	LOQ (max of iLOQ & mLOQ) sample #1-4 with blanks 1-2[b]	LOQ (max of iLOQ & mLOQ) samples >#4 with blanks 3-5
1-Nitronaphthalene	0.072	0.104	0.009	0.005	0.072	0.104
2-Nitronaphthalene	0.055	0.091	0.004	0.003	0.055	0.091
3-Nitroacenaphthene	0.000	0.000	0.178	0.127	0.178	0.178
5-Nitroacenaphthene	0.000	0.000	0.010	0.006	0.010	0.010
2-Nitrofluorene	0.000	0.000	0.002	0.001	0.002	0.002
9-Nitroanthracene	0.000	0.000	0.049	0.023	0.049	0.049
9-Nitrophenanthrene	0.000	0.000	0.041	0.017	0.041	0.041
3-Nitrophenanthrene	0.000	0.000	0.015	0.007	0.015	0.015
2-+3-Nitrofluoranthene	0.012	0.026	0.003	0.002	0.012	0.026
1-Nitropyrene	0.011	0.018	0.004	0.003	0.011	0.018
7-Nitrobenzo(a)anthracene	0.000	0.000	0.009	0.025	0.009	0.009
6-Nitrochrysene	0.000	0.000	0.007	0.018	0.007	0.007
1,3-Dinitropyrene	0.000	0.000	0.001	0.001	0.001	0.001
1,6-Dinitropyrene	0.000	0.000	0.003	0.002	0.003	0.003
1,8-Dinitropyrene	0.000	0.000	0.003	0.002	0.003	0.003
3-Nitrobenzanthrone	0.000	0.000	0.488	0.495	0.488	0.488
6-Nitrobenzo(a)pyrene	0.017	0.011	0.007	0.009	0.017	0.011

[b]First 4 samples: Kos_2010_8a, Kos_2017_1b, Mokra_2015_2b, Kos_2017_1c

Table S8 Repeatability (CoVs) of individual PACs, a) PAHs, b) OPAHs and O-heterocycles and c) NPAHs, of the 11 samples measured in duplicate or triplicate (STD: Standard deviation)

a)

Compound	Average of CoV [%]	STD of CoV [%]	Compound	Average of CoV [%]	STD of CoV [%]
Naphthalene	33	23	**Benzo(b)fluoranthene**	12	9
Acenaphthylene	15	18	**Benzo(j)fluoranthene**	19	11
Acenaphthene	21	31	**Benzo(k)fluoranthene**	12	9
Fluorene	41	40	**Benzo(e)pyrene**	14	12
Phenanthrene	31	34	**Benzo(a)pyrene**	14	10
Anthracene	35	40	**Perylene**	16	12
Fluoranthene	36	40	**Indeno(123-cd)pyrene**	12	11
Pyrene	32	30	**Dibenz(ah)anthracene**	12	10
Retene	33	21	**Dibenz(ac)anthracene**	16	8
Benzo(b)fluorene	27	35	**Benzo(ghi)perylene**	15	10
Benzo(ghi)fluoranthene	20	21	**Anthanthrene**	28	28
Cyclopenta(cd)pyrene	-	-	**Coronene**	20	15
Benzo(a)anthracene	26	20	**Σ_{16}US-EPA PAHs**	15	12
Triphenylene	22	22	**Σ_{27}PAHs**	15	12
Chrysene	21	18			

b)

Compound	Average of CoV [%]	STD of CoV [%]
1,4-Naphthoquinone	37	32
Naphthalene-1-aldehyde	35	27
Dibenzofuran	27	19
9-Fluorenone	48	43
6H-Benzo(c)chromen-6-one	38	34
9,10-Anthraquinone	135[a]	52
9,10-Phenanthroquinone	-	-
11H-Benzo(a)fluoren-11-one	31	24
11H-Benzo(b)fluoren-11-one	30	25
Benzanthrone	39	20
Benz(a)anthracene-7,12-dione	27	21
5,12-Naphthacenequinone	21	16
6H-Benzo(cd)pyren-6-one	24	14
Σ13OPAHs (11 OPAHs+2 O-heterocycles)	22	17
Σ11OPAHs	23	19

[a]High value since often close to LOQ, which is relatively high, and if <LOQ calculated with 0 ng g^{-1} since detection frequency is <25 %.

c)

Compound	Average of CoV [%]	STD of CoV [%]
1-Nitronaphthalene	31	31
2-Nitronaphthalene	38	45
2-+3-Nitrofluoranthene	26	22
1-Nitropyrene	36	34
6-Nitrobenzo(a)pyrene	28	23
Σ6NPAHs	27	25

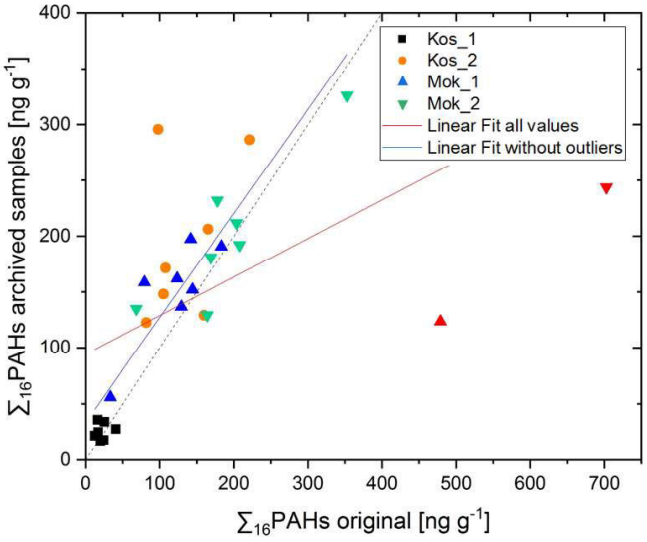

Fig. S2 $\sum_{16}$PAHs concentration from measurement done temporarily close to the sampling date, $c_{original}$, compared to $\sum_{16}$PAHs concentration from re-measurement, $c_{archived\ sample}$, of the archived soil samples. Linear fit with all values (red fit line with equation $c_{archived\ sample} = 0.35\ c_{original} + 94.25$; $R = 0.58$, $p<0.05$) and linear fit without two outlier values from Mokrá-1 and Mokrá-2 (marked in red) (blue fit line with equation $c_{archived\ sample} = 0.93\ c_{original} + 33.77$; $R = 0.86$, $p<0.05$)

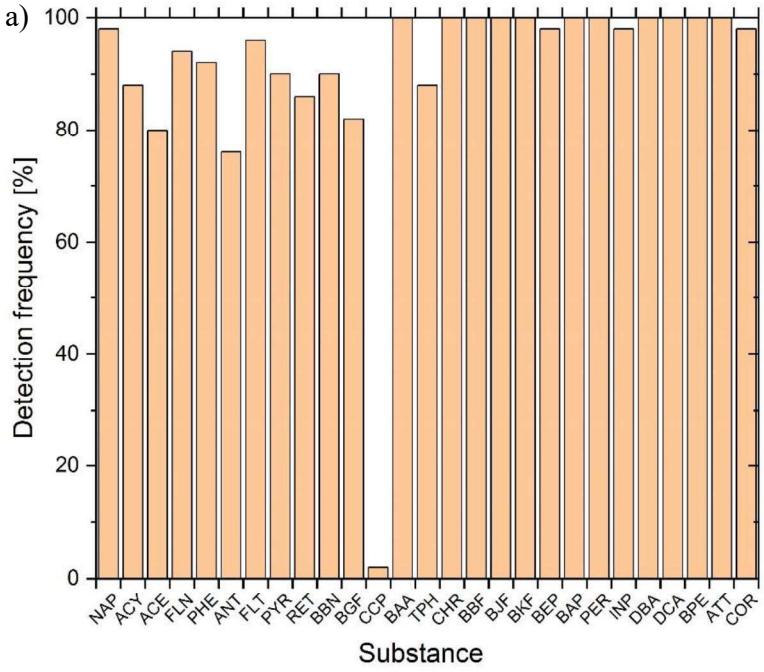

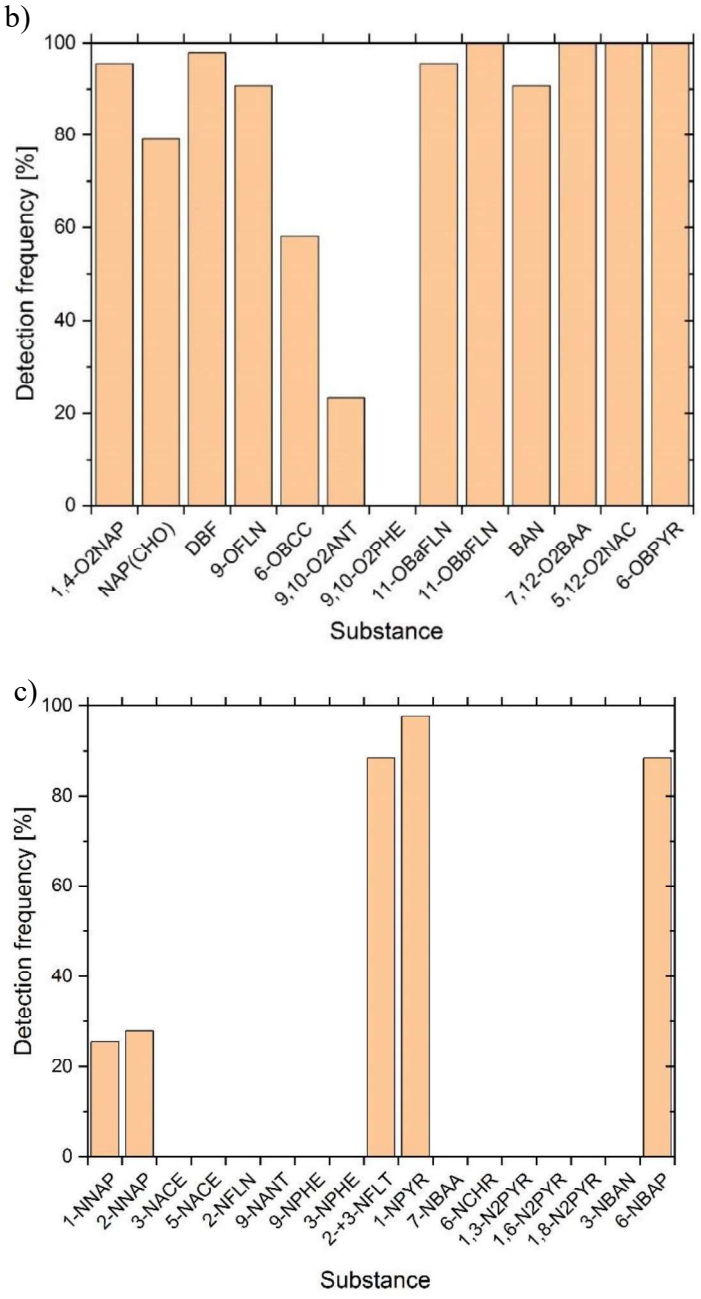

Fig. S3 Detection frequency of a) PAHs, b) OPAHs and O-heterocycles and c) NPAHs using the sum of the average of blanks and 1 × standard deviation of blanks as LOQ

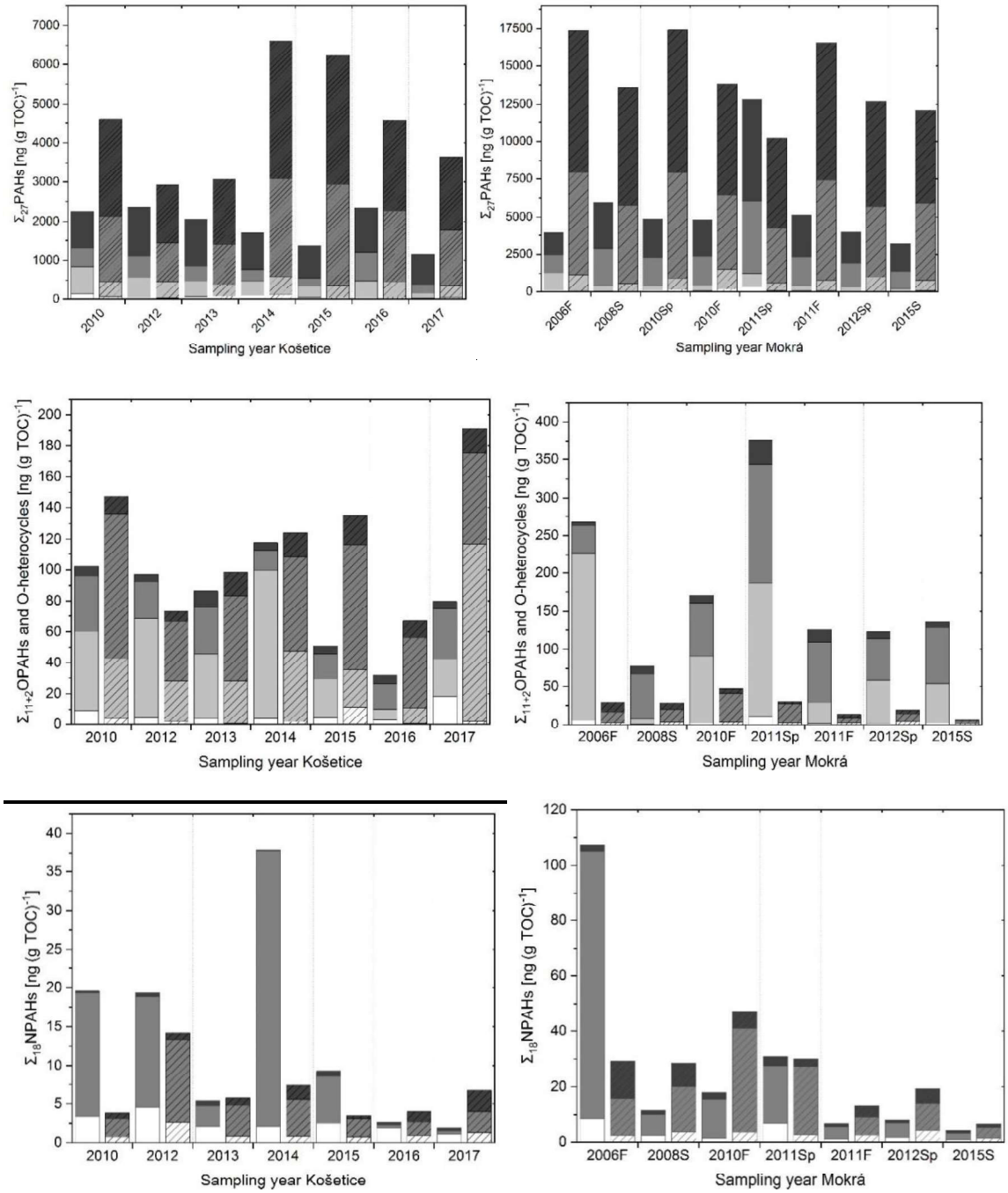

Fig. S4 Concentration normalized for TOC content in ng (g TOC)$^{-1}$ of A & B: Σ_{27}PAHs split into 2-ring (white), 3-ring (light grey), 4-ring (grey) and 5-7-ring PAHs (dark grey), A: at Košetice-1 (plain) and Košetice-2 (dashed); B: at Mokrá-1 (plain) and Mokrá-2 (dashed); C & D: Σ_{11+2}OPAHs and O-heterocycles split into 2-ring (white), 3-ring (light grey), 4-ring (grey) and 5-ring OPAHs (dark grey), C: at Košetice-1 (plain) and Košetice-2 (dashed); D: at Mokrá-1 (plain) and Mokrá-2 (dashed); E & F: Σ_{18}NPAHs split into 2-ring NPAHs (white), 3-ring NPAHs (light grey), 4-ring NPAHs (grey) and 5-ring NPAHs (dark grey), E: at Košetice-1 (plain) and Košetice-2 (dashed); F: at Mokrá-1 (plain) and Mokrá-2 (dashed); (F: Fall; Sp: Spring; S: Summer).

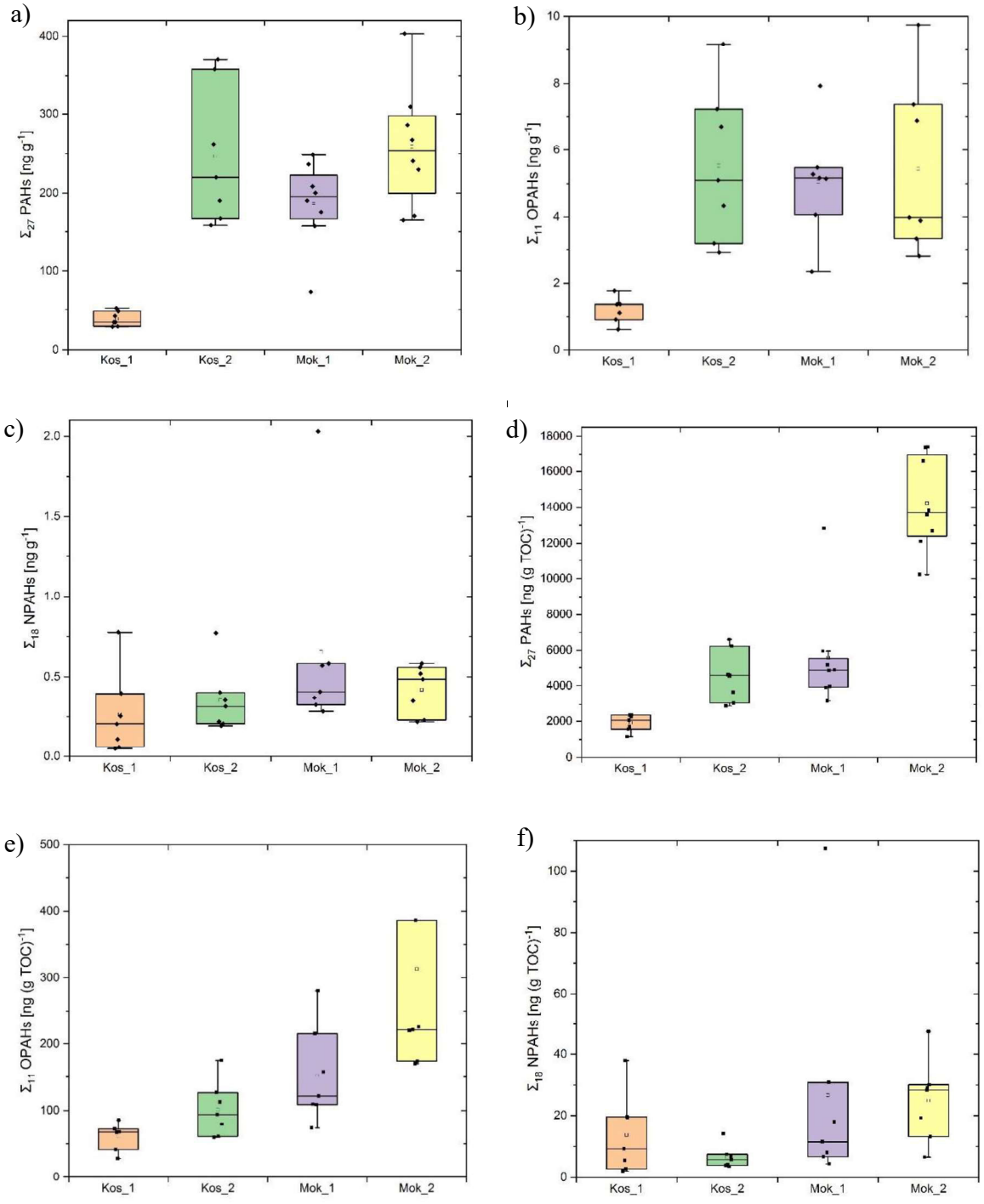

Fig. S5 Box-and-whisker-plot of location average concentrations of Σ27PAHs (a and d), Σ_{11}OPAHs (b and e) and Σ_{18}NPAHs (c and f) in ng g^{-1} (a-c) and normalized for TOC content in ng (g TOC)$^{-1}$ (d-f) (empty square: Mean value; Filled squares: Measurement points; Filled box with extra borders: Interquartile range (IQR) bound by the 75th and 25th percentile and range of 1.5 IQR; Horizontal line: Median)

Table S9 Concentration of a) Σ_{11}OPAHs, Σ_2O-heterocycles, Σ_{16}PAHs, Σ_{27}PAHs in ng g^{-1} and b) $\sum_{18}$NPAHs and individual NPAHs in pg g^{-1} (F: Fall; Sp: Spring; S: Summer). Values <LOQ were replaced by LOQ/2 if the detection frequency was >25 % (**Fig. S3**), else replaced by 0 ng g^{-1}

a)

Location	Year & season	Σ_{11}OPAHs	Σ_2O-heterocycles	Σ_{16}PAHs	Σ_{27}PAHs
Košetice-1	2010	1.11	0.21	22	29
	2012	1.37	0.61	36	48
	2013	1.36	0.40	28	42
	2014	1.37	1.03	25	35
	2015	0.91	0.22	18	34
	2016	0.62	0.09	34	52
	2017	1.78	0.19	17	29
Košetice-2	2010	7.22	1.18	206	262
	2012	3.22	0.74	122	158
	2013	4.32	1.01	129	167
	2014	5.10	1.63	286	358
	2015	6.70	0.74	296	370
	2016	2.92	0.30	171	220
	2017	9.18	0.83	148	191
Mokrá-1	2006F	4.06	1.00	56	74
	2008S	2.35	0.16	152	190
	2010Sp	-	-	137	175
	2010F	5.15	0.40	123	157
	2011Sp	5.17	1.77	191	237
	2011F	5.28	0.81	197	249
	2012Sp	5.48	0.72	159	200
	2015S	7.93	0.94	162	209
Mokrá-2	2006F	6.88	0.41	244	309
	2008S	3.36	0.41	212	267
	2010Sp	-	-	192	241
	2010F	9.75	1.01	135	170
	2011Sp	2.81	0.58	129	165
	2011F	3.89	0.30	232	286
	2012Sp	3.98	0.16	181	230
	2015S	7.36	0.58	326	403

b)

Location	Year	Σ_{18}NPAHs	1-NNAP	2-NNAP	2-+3-NFLT	1-NPYR	6-NBAP
Košetice-1	2010	255.1	14.5	28.7	5.3	201.2	3.5
	2012	403.5	14.9	78.4	68.8	222.5	11.5
	2013	112.9	14.5	28.7	33.8	20.1	12.9
	2014	779.3	14.5	28.8	41.5	686.4	3.5
	2015	209.8	25.9	29.1	49.1	83.4	17.1
	2016	59.6	14.1	28.0	5.2	2.9	8.7
	2017	48.8	12.4	14.7	4.6	5.1	11.4
Košetice-2	2010	220.1	14.5	28.7	30.8	100.7	43.7
	2012	773.6	14.7	129.2	31.8	544.9	49.4
	2013	318.1	14.5	28.8	50.5	165.6	53.1
	2014	414.4	14.7	29.2	46.9	210.2	101.8
	2015	210.9	14.8	29.3	46.7	93.5	21.6
	2016	193.3	14.3	28.4	46.0	40.7	63.2
	2017	355.2	14.3	52.9	53.2	90.9	140.4
Mokrá-1	2006F	2031.4	71.6	89.2	5.3	1820.7	43.2
	2008S	372.3	50.4	28.2	29.2	208.8	51.0
	2010F	583.0	14.6	28.9	46.5	412.6	79.7
	2011Sp	577.4	48.1	77.4	86.3	293.9	64.5
	2011F	326.0	29.8	28.6	62.1	143.5	59.4
	2012Sp	409.3	25.6	50.3	51.7	218.7	60.6
	2015S	288.9	12.3	41.0	85.1	69.0	74.8
Mokrá-2	2006F	523.9	14.6	28.9	37.6	197.1	241.3
	2008S	563.2	22.4	49.9	68.1	252.7	165.8
	2010F	583.0	14.6	28.9	46.5	412.6	79.7
	2011Sp	489.0	14.3	28.4	76.0	319.6	46.4
	2011F	229.2	14.3	28.4	37.4	76.2	72.1
	2012Sp	348.4	45.5	28.9	20.2	158.0	95.3
	2015S	229.1	14.5	28.7	69.5	60.0	45.1

Table S10 Same as Table S9 but normalized for soil TOC content in ng (g TOC)$^{-1}$

a)

Location	Year & season	Σ_{11}OPAHs	Σ_{2}O-heterocycles	Σ_{16}PAHs	Σ_{27}PAHs
Košetice-1	2010	86.0	16.3	1704	2262
	2012	67.2	29.9	1764	2360
	2013	66.7	19.8	1361	2059
	2014	67.2	50.5	1228	1689
	2015	41.3	9.8	826	1560
	2016	28.0	4.0	1553	2351
	2017	71.9	7.8	671	1153
Košetice-2	2010	126.8	20.8	3620	4597
	2012	59.5	13.6	2258	2917
	2013	79.6	18.7	2380	3073
	2014	94.1	30.0	5284	6609
	2015	112.8	12.5	4979	6235
	2016	60.7	6.3	3562	4574
	2017	175.5	15.8	2832	3643
Mokrá-1	2006F	215.0	52.7	2959	3902
	2008S	73.5	5.1	4765	5967
	2010Sp	-	-	3808	4868
	2010F	158.3	12.4	3796	4837
	2011Sp	280.4	95.9	10337	12828
	2011F	109.3	16.8	4080	5142
	2012Sp	108.6	14.2	3140	3968
	2015S	121.6	14.5	2483	3199
Mokrá-2	2006F	386.2	23.0	13692	17385
	2008S	170.7	21.1	10771	13585
	2010Sp	-	-	13891	17411
	2010F	794.3	82.5	10976	13818
	2011Sp	174.4	36.0	8022	10220
	2011F	225.2	17.4	13440	16576
	2012Sp	219.6	8.9	9994	12693
	2015S	220.9	17.3	9794	12107

b)

Location	Year & season	Σ_{18} NPAHs	1-NNAP	2-NNAP	2-+3-NFLT	1-NPYR	6-NBAP
Košetice-1	2010	19.74	1.12	2.22	0.41	15.57	0.27
	2012	19.75	0.73	3.84	3.37	10.89	0.56
	2013	5.52	0.71	1.40	1.65	0.99	0.63
	2014	38.15	0.71	1.41	2.03	33.60	0.17
	2015	9.54	1.18	1.32	2.23	3.79	0.78
	2016	2.71	0.64	1.27	0.24	0.13	0.39
	2017	1.97	0.50	0.59	0.19	0.21	0.46
Košetice-2	2010	3.86	0.25	0.50	0.54	1.77	0.77
	2012	14.27	0.27	2.38	0.59	10.05	0.91
	2013	5.87	0.27	0.53	0.93	3.05	0.98
	2014	7.65	0.27	0.54	0.87	3.88	1.88
	2015	3.55	0.25	0.49	0.79	1.57	0.36
	2016	4.02	0.30	0.59	0.96	0.85	1.31
	2017	6.79	0.27	1.01	1.02	1.74	2.68
Mokrá-1	2006F	107.48	3.79	4.72	0.28	96.33	2.29
	2008S	11.67	1.58	0.88	0.91	6.54	1.60
	2010F	17.93	0.45	0.89	1.43	12.69	2.45
	2011Sp	31.29	2.61	4.19	4.68	15.92	3.50
	2011F	6.74	0.62	0.59	1.28	2.97	1.23
	2012Sp	8.11	0.51	1.00	1.02	4.33	1.20
	2015S	4.43	0.19	0.63	1.31	1.06	1.15
Mokrá-2	2006F	29.43	0.82	1.62	2.11	11.07	13.56
	2008S	28.63	1.14	2.54	3.46	12.85	8.43
	2010F	47.50	1.19	2.35	3.79	33.61	6.49
	2011Sp	30.37	0.89	1.76	4.72	19.85	2.88
	2011F	13.28	0.83	1.65	2.17	4.42	4.18
	2012Sp	19.25	2.51	1.60	1.11	8.73	5.27
	2015S	6.88	0.43	0.86	2.09	1.80	1.35

Table S11 Concentrations of PAHs in soil samples from a) Košetice-1, b) Košetice-2, c) Mokrá-1 and d) Mokrá-2 in ng g^{-1} (F:Fall; Sp:Spring; S:Summer; STD: Standard deviation)

a)

Compound	2010	2012	2013	2014	2015	2016	2017	Mean	STD	Median
NAP	1.70	0.99	1.36	1.80	1.03	0.83	0.55	**1.18**	0.46	1.03
ACY	0.01	0.20	0.19	0.22	0.21	0.17	0.01	**0.15**	0.09	0.19
ACE	0.01	0.11	0.13	0.14	0.01	0.01	0.05	**0.07**	0.06	0.05
FLN	0.53	0.79	0.86	0.82	0.67	0.21	0.21	**0.59**	0.28	0.67
PHE	7.07	6.50	3.36	4.98	1.48	2.21	0.82	**3.77**	2.46	3.36
ANT	0.11	0.16	0.16	0.16	0.16	0.41	0.08	**0.18**	0.11	0.16
FLT	2.12	3.82	2.38	2.65	1.51	5.49	1.81	**2.82**	1.39	2.38
PYR	1.78	2.37	1.74	0.55	0.90	5.19	1.42	**1.99**	1.53	1.74
RET	1.42	2.69	3.54	1.75	3.94	6.69	1.85	**3.13**	1.83	2.69
BBN	0.32	0.52	0.40	0.44	0.15	0.04	0.35	**0.32**	0.17	0.35
BGF	0.21	0.14	0.14	0.14	0.14	0.62	0.22	**0.23**	0.17	0.14
CCP	<0.03	<0.03	<0.03	<0.03	<0.03	<0.03	0.15	**0.02**	0.05	<0.03
BAA	0.71	1.84	1.47	0.96	0.97	2.40	0.89	**1.32**	0.61	0.97
TPH	0.27	0.42	0.28	0.12	0.12	0.52	0.24	**0.28**	0.15	0.27
CHR	0.77	2.00	1.48	1.06	1.03	2.24	1.05	**1.38**	0.56	1.06
BBF	1.89	4.49	3.72	3.36	2.81	4.38	2.55	**3.31**	0.96	3.36
BJF	0.90	1.78	1.29	0.82	0.85	1.38	1.41	**1.20**	0.36	1.29
BKF	0.67	1.45	1.20	0.91	0.89	1.39	0.80	**1.04**	0.30	0.91
BEP	1.87	3.81	4.32	2.78	3.74	4.17	3.36	**3.44**	0.86	3.74
BAP	1.61	3.47	2.88	2.30	2.02	3.38	1.82	**2.50**	0.75	2.30
PER	0.35	0.75	0.67	0.62	0.44	0.78	0.41	**0.57**	0.17	0.62
INP	1.36	2.86	2.79	2.20	1.73	2.49	1.63	**2.15**	0.59	2.20
DBA	0.37	0.90	0.83	0.89	0.72	0.99	1.09	**0.83**	0.23	0.89
DCA	0.30	0.69	0.63	0.62	0.56	0.68	0.79	**0.61**	0.15	0.63
BPE	1.31	4.07	3.24	2.08	2.04	2.38	1.86	**2.43**	0.93	2.08
ATT	1.18	0.76	2.33	1.60	1.75	2.29	2.54	**1.78**	0.66	1.75
COR	0.38	0.62	0.67	0.52	0.36	0.39	0.63	**0.51**	0.13	0.52
$\sum_{16}$ PAHs	**22.02**	**36.03**	**27.80**	**25.09**	**18.18**	**34.16**	**16.64**	**25.70**	7.48	25.09

b)

Compound	2010	2012	2013	2014	2015	2016	2017	Mean	STD	Median
NAP	3.49	1.51	3.91	6.67	2.02	2.48	2.12	**3.17**	1.76	2.48
ACY	0.62	0.51	0.50	0.94	0.87	0.63	0.56	**0.66**	0.18	0.62
ACE	0.54	0.21	0.38	0.59	0.50	0.47	0.34	**0.43**	0.13	0.47
FLN	1.40	1.84	1.79	2.04	1.15	0.69	0.90	**1.40**	0.51	1.40
PHE	14.68	13.40	7.88	15.13	10.56	7.99	7.86	**11.07**	3.29	10.56
ANT	1.35	0.61	0.50	1.65	1.86	1.42	1.07	**1.21**	0.51	1.35
FLT	32.18	20.42	18.57	45.72	50.86	30.63	26.11	**32.07**	12.21	30.63
PYR	26.90	13.62	14.56	36.11	40.60	24.50	19.25	**25.08**	10.34	24.50
RET	4.34	6.84	5.57	4.56	3.98	8.22	5.71	**5.60**	1.51	5.57
BBN	3.01	1.50	2.06	4.53	5.30	3.15	2.48	**3.15**	1.35	3.01
BGF	2.76	1.61	1.61	3.74	4.35	2.67	2.39	**2.73**	1.02	2.67
CCP	<0.03	<0.03	<0.03	<0.03	<0.03	<0.03	<0.03	**<0.03**	0.00	<0.03
BAA	14.03	7.02	8.20	21.34	25.04	11.99	10.81	**14.06**	6.74	11.99
TPH	3.60	2.28	2.37	5.73	5.79	3.92	3.06	**3.82**	1.45	3.60
CHR	14.29	7.93	9.42	21.58	25.33	12.49	11.80	**14.69**	6.42	12.49
BBF	28.74	17.05	20.05	43.58	43.63	24.57	22.84	**28.64**	10.85	24.57
BJF	9.55	4.81	5.38	15.37	15.60	8.74	6.83	**9.47**	4.44	8.74
BKF	9.39	5.11	6.11	13.00	14.26	7.68	6.78	**8.90**	3.51	7.68
BEP	14.04	9.12	9.77	17.79	19.36	10.91	11.39	**13.20**	4.01	11.39
BAP	21.39	10.61	13.05	28.10	32.00	17.07	13.42	**19.38**	8.14	17.07
PER	5.14	2.47	3.35	7.14	7.50	4.31	3.13	**4.72**	1.97	4.31
INP	18.75	10.98	11.83	25.82	24.49	14.62	12.08	**16.94**	6.19	14.62
DBA	2.66	1.72	2.00	3.83	4.03	2.82	2.50	**2.80**	0.86	2.66
DCA	2.28	1.50	1.36	3.02	3.38	1.78	1.90	**2.17**	0.77	1.90
BPE	15.85	9.86	10.24	20.27	18.58	11.25	9.67	**13.67**	4.48	11.25
ATT	4.26	1.89	2.36	3.27	4.49	2.22	2.65	**3.02**	1.02	2.65
COR	6.65	3.67	3.72	6.63	4.83	2.79	2.87	**4.45**	1.64	3.72
$\sum_{16}$ PAHs	**206.27**	**122.40**	**129.00**	**286.38**	**295.78**	**171.31**	**148.09**	**194.18**	71.90	171.31

36

c)

Compound	2006F	2008S	2010Sp	2010F	2011Sp	2011F	2012Sp	2015S	Mean	STD	Median
NAP	1.57	0.90	3.05	2.53	5.98	3.78	2.30	3.32	**2.93**	1.55	2.79
ACY	0.26	0.34	0.50	0.38	0.74	0.60	0.53	0.55	**0.49**	0.15	0.51
ACE	0.01	0.50	0.46	0.40	0.70	0.50	0.40	0.44	**0.43**	0.19	0.45
FLN	0.94	0.41	0.61	0.65	1.16	0.71	0.75	0.68	**0.74**	0.23	0.69
PHE	13.87	5.52	7.13	7.03	11.26	8.59	7.64	6.10	**8.39**	2.82	7.38
ANT	0.45	1.21	0.81	0.57	1.30	1.39	0.94	1.10	**0.97**	0.34	1.02
FLT	10.55	28.04	23.95	22.92	29.82	30.38	27.59	24.74	**24.75**	6.35	26.16
PYR	6.19	23.16	19.33	17.20	23.23	25.49	22.85	20.61	**19.76**	6.07	21.73
RET	6.80	2.72	1.97	3.45	1.87	2.18	4.87	1.93	**3.22**	1.77	2.45
BBN	0.04	3.05	1.82	1.95	2.84	2.78	2.57	2.26	**2.16**	0.96	2.41
BGF	0.71	2.24	2.11	1.65	2.68	3.39	2.44	2.46	**2.21**	0.78	2.34
CCP	<0.03	<0.03	<0.03	<0.03	<0.03	<0.03	<0.03	<0.03	**<0.03**	0.00	<0.03
BAA	2.06	11.36	8.74	8.11	13.85	14.73	11.67	10.30	**10.10**	3.96	10.83
TPH	0.68	2.78	2.99	2.53	3.77	3.93	3.17	3.58	**2.93**	1.03	3.08
CHR	2.68	11.30	9.89	8.73	14.37	16.12	12.11	12.57	**10.97**	4.09	11.71
BBF	5.64	21.70	20.59	18.38	29.42	31.30	24.43	25.45	**22.11**	7.95	23.06
BJF	2.03	6.52	5.69	6.19	9.23	11.58	7.97	9.31	**7.31**	2.90	7.24
BKF	1.66	6.89	6.17	5.43	9.14	9.80	7.49	7.93	**6.81**	2.53	7.19
BEP	3.76	11.72	10.90	9.73	13.52	15.60	11.47	13.17	**11.23**	3.52	11.59
BAP	3.86	16.73	12.85	11.78	20.25	23.23	16.62	18.09	**15.43**	5.95	16.67
PER	0.73	3.56	2.49	2.41	4.27	4.51	3.47	3.55	**3.13**	1.22	3.51
INP	2.99	11.95	10.95	9.34	15.75	15.98	11.75	14.15	**11.61**	4.19	11.85
DBA	0.62	2.02	1.69	2.23	2.47	2.96	2.37	3.35	**2.22**	0.83	2.30
DCA	0.48	1.32	1.84	1.43	2.64	2.29	1.89	2.09	**1.75**	0.67	1.86
BPE	2.55	9.97	9.93	7.75	11.32	11.71	9.15	12.53	**9.36**	3.14	9.95
ATT	1.64	2.56	5.77	3.06	2.32	2.64	2.13	4.40	**3.07**	1.36	2.60
COR	0.95	1.86	2.46	1.43	2.82	2.44	1.80	3.95	**2.21**	0.93	2.15
$\sum_{16}$ PAHs	**55.92**	**152.00**	**136.65**	**123.42**	**190.77**	**197.26**	**158.57**	**161.90**	**147.06**	44.37	155.28

37

d)

Compound	2006F	2008S	2010Sp	2010F	2011Sp	2011F	2012Sp	2015S	Mean	STD	Median
NAP	1.02	1.00	1.97	2.15	1.08	1.29	0.09	2.16	**1.35**	0.72	1.19
ACY	0.96	0.56	0.71	0.64	0.59	0.66	3.54	0.78	**1.05**	1.01	0.68
ACE	0.32	0.24	0.30	0.24	0.24	0.39	0.56	0.91	**0.40**	0.23	0.31
FLN	0.63	0.39	0.39	1.16	0.41	0.69	2.63	1.24	**0.94**	0.76	0.66
PHE	10.86	5.83	6.32	10.55	5.36	8.05	7.22	16.54	**8.84**	3.73	7.63
ANT	1.62	1.32	1.58	0.78	0.65	1.67	1.10	3.30	**1.50**	0.82	1.45
FLT	38.24	28.68	30.07	20.04	16.86	31.52	24.97	56.36	**30.84**	12.29	29.38
PYR	32.42	25.86	25.90	14.32	14.57	29.28	21.95	46.99	**26.41**	10.52	25.88
RET	5.00	1.85	1.36	2.97	1.32	1.08	2.79	1.41	**2.22**	1.33	1.63
BBN	4.38	3.38	3.16	2.02	2.05	3.72	2.74	5.40	**3.36**	1.15	3.27
BGF	3.64	3.04	2.72	1.97	1.82	3.20	2.98	4.35	**2.97**	0.83	3.01
CCP	<0.03	<0.03	<0.03	<0.03	<0.03	<0.03	<0.03	<0.03	**<0.03**	0.00	<0.03
BAA	20.50	21.60	18.25	10.88	11.52	24.05	16.04	28.61	**18.93**	6.07	19.37
TPH	4.87	4.27	4.17	2.76	2.74	4.54	3.75	6.04	**4.14**	1.09	4.22
CHR	19.87	18.50	15.35	10.25	10.17	20.75	15.53	25.99	**17.05**	5.38	17.01
BBF	36.71	33.57	26.70	19.53	22.13	37.36	26.23	43.87	**30.76**	8.42	30.14
BJF	12.09	11.06	9.61	5.32	6.43	10.08	9.31	14.05	**9.74**	2.84	9.85
BKF	12.18	11.03	8.99	6.08	6.79	11.23	8.51	14.58	**9.93**	2.86	10.01
BEP	20.20	17.27	15.71	11.16	12.40	17.51	14.76	21.71	**16.34**	3.61	16.49
BAP	30.64	27.82	22.76	15.45	17.05	28.36	22.80	35.33	**25.03**	6.78	25.31
PER	7.00	6.12	4.85	3.36	3.74	6.40	5.15	7.97	**5.58**	1.59	5.64
INP	19.39	18.07	15.89	11.56	11.32	18.17	15.19	23.15	**16.59**	3.98	16.98
DBA	2.78	2.66	2.25	1.73	1.51	3.25	2.67	4.62	**2.68**	0.97	2.66
DCA	2.31	2.39	1.92	1.48	1.56	2.15	1.62	3.65	**2.14**	0.70	2.04
BPE	15.58	14.75	14.58	9.34	8.94	15.17	11.89	21.70	**13.99**	4.07	14.66
ATT	3.96	3.63	2.19	2.20	1.86	3.08	3.72	7.34	**3.50**	1.74	3.35
COR	2.27	2.35	2.97	1.63	1.47	2.35	2.03	5.10	**2.52**	1.14	2.31
∑16 PAHs	243.72	211.88	192.00	134.72	129.19	231.88	180.90	326.14	**206.30**	63.66	201.94

38

Table S12 PAH concentration in surface soil (sampling depth 10 cm)

Location	Type of site	Land use	Collection year	PAH concentration [ng g^{-1}]	Mean	PAHs	Reference
Košetice	Background	Grassland	2010-2017 (except 2011)	17-296	110	Σ16 EPA	This study
Mokrá	Semi-urban	Grassland	2006-2015	56-326	177	Σ16 EPA	This study
Košetice	Background	Different	1996-2005	41-5,600	600	Σ16 EPA	Holoubek et al. 2007
Central and Eastern Europe	Background, rural, urban, industrial	Not specified	2005-2006	68–58,384	n.d.	Σ16 EPA	Holoubek et al. 2007
Scotland[a]	Urban and rural	Different	2007-2009	34-12,560	1466	Σ16 EPA	Rhind et al. 2013
France[b]	Industrial, urban, suburban, remote	Not specified	2000	450-5,650	2510	Σ14	Motelay-Massei et al. 2004
	Remote		2000	450-940	n.d.	Σ14	
UK (England, Northern Ireland, Scotland, Wales)[a]	Rural heritage	Not specified	2001-2002	25-9,230	270	Σ22	Environmental Agency 2007
	Rural			43-167,502	2244	Σ22	
	Urban			92-551,000	14200	Σ22	
Estonia	Urban, rural	Not specified	1996	11-153,000	n.d.	Σ12	Trapido 1999
	Rural		1996	11-2240	≈100	Σ12	
Norway[a]	Background/remote	Grassland	1998	8.6-1050	63	Σ15	Nam et al. 2008
UK[a]			1998	56-11,200	700	Σ15	
Europe	Rural	Not specified	Not specified	Median: 300-400	n.d.	Σ16	UNEP 2003
Temperate latitudes	Remote	Grassland	1994	63-321	142	Σ20	Wilcke & Amelung 2000
Czech Republic	Mainly rural	Arable[c]	1992-2007	140-2,436	847	Σ16	Holoubek et al. 2009
		Grassland	Not specified	123-15,284	2511	Σ16	
		Forest-highland		149–1,435	539	Σ16	
Czech Republic	Different	Arable	1997-2009	538-933	n.d.	Σ16	National Centre for Toxic Compounds 2017
		Grassland	1997-2009	594 – 1,235	n.d.	Σ16	
	Protected area	Non-forest, not distorted	1997-2009	101 – 303	n.d.	Σ16	

[a]Sampling depth: 0-5 cm [b]Sampling depth: 3-10 cm [c]Sampling depth: 0-25 cm

Table S13 Concentrations of OPAHs and O-heterocycles in soil samples from a) Košetice-1, b) Košetice-2, c) Mokrá-1 and d) Mokrá-2 in ng g^{-1} (F: Fall; Sp: Spring; S:Summer; STD: Standard deviation). Values <LOQ were replaced by LOQ/2 if the detection frequency was >25 % (Fig. S3), else replaced by 0 ng g^{-1}

a)

Compound	2010	2012	2013	2014	2015	2016	2017	Mean	STD	Median
1,4-O_2NAP	0.10	0.06	0.08	0.05	0.09	0.06	0.43	**0.12**	0.14	0.08
1-(CHO)NAP	0.015	0.024	0.003	0.028	0.003	0.003	0.022	**0.014**	0.011	0.015
DBF	0.14	0.37	0.33	0.32	0.14	0.02	0.10	**0.20**	0.13	0.14
9-OFLN	0.45	0.70	0.45	0.92	0.34	0.07	0.22	**0.45**	0.29	0.45
6-OBCC	0.07	0.24	0.07	0.72	0.07	0.07	0.09	**0.19**	0.24	0.07
9,10-O_2ANT	<4.7	<4.7	<4.7	<4.7	<4.7	<4.7	0.19	**0.03**	0.07	0.19
9,10-O_2PHE	<2.8	<2.8	<2.8	<2.8	<2.8	<2.8	<2.8	<2.8	0.00	<2.8
11-OBaFLN	0.12	0.16	0.19	0.09	0.06	0.05	0.22	**0.13**	0.07	0.12
11-OBbFLN	0.13	0.14	0.16	0.07	0.13	0.11	0.23	**0.14**	0.05	0.13
BAN	0.04	0.03	0.09	0.03	0.05	0.08	0.15	**0.06**	0.04	0.05
7,12-O_2BAA	0.13	0.12	0.12	0.06	0.08	0.07	0.15	**0.10**	0.03	0.12
5,12-O_2NAC	0.04	0.04	0.06	0.02	0.05	0.05	0.06	**0.05**	0.01	0.05
6-OBPYR	0.08	0.10	0.21	0.10	0.12	0.13	0.12	**0.12**	0.04	0.12
Σ_{13}OPAHs and O-heterocycles	1.32	1.98	1.77	2.40	1.12	0.71	1.98	**1.61**	0.59	1.77
Σ_{11}OPAHs	1.11	1.37	1.36	1.37	0.91	0.62	1.78	**1.22**	0.38	1.36

b)

Compound	2010	2012	2013	2014	2015	2016	2017	Mean	STD	Median
1,4-O_2NAP	0.15	0.05	0.02	0.05	0.07	0.02	0.06	**0.06**	0.04	0.05
1-(CHO)NAP	0.069	0.046	0.011	0.038	0.023	0.007	0.041	**0.033**	0.021	0.038
DBF	0.91	0.66	0.68	0.80	0.39	0.14	0.24	**0.55**	0.29	0.66
9-OFLN	1.04	0.69	0.48	0.87	0.69	0.20	0.88	**0.69**	0.28	0.69
6-OBCC	0.27	0.07	0.34	0.83	0.35	0.17	0.59	**0.37**	0.26	0.34
9,10-O_2ANT	<4.7	<4.7	<4.7	<4.7	<4.7	<4.7	4.30	**0.61**	1.63	0.00
9,10-O_2PHE	<2.8	<2.8	<2.8	<2.8	<2.8	<2.8	<2.8	<2.8	0.00	<2.8
11-OBaFLN	1.42	0.49	0.67	0.95	1.45	0.54	0.83	**0.91**	0.40	0.83
11-OBbFLN	1.58	0.62	0.88	0.84	1.43	0.61	0.86	**0.98**	0.38	0.86
BAN	0.67	0.28	0.44	0.42	0.62	0.36	0.53	**0.47**	0.14	0.44
7,12-O_2BAA	1.05	0.47	0.67	0.69	0.78	0.43	0.54	**0.66**	0.21	0.67
5,12-O_2NAC	0.57	0.22	0.33	0.38	0.51	0.24	0.29	**0.36**	0.13	0.33
6-OBPYR	0.67	0.36	0.81	0.86	1.12	0.53	0.85	**0.74**	0.25	0.81
Σ_{13}OPAHs and O-heterocycles	8.41	3.96	5.33	6.73	7.44	3.22	10.01	**6.44**	2.43	6.73
Σ_{11}OPAHs	7.22	3.22	4.32	5.10	6.70	2.92	9.18	**5.52**	2.29	5.10

c)

Compound	2006F	2008S	2010F	2011Sp	2011F	2012Sp	2015S	Mean	STD	Median
1,4-O_2NAP	0.08	0.01	0.05	0.16	0.06	0.05	0.10	**0.07**	0.05	0.06
1-(CHO)NAP	0.049	0.003	0.023	0.045	0.011	0.014	0.048	**0.028**	0.019	0.023
DBF	0.92	0.09	0.33	1.05	0.28	0.44	0.37	**0.50**	0.35	0.37
9-OFLN	1.55	0.07	0.65	1.48	0.50	0.69	1.15	**0.87**	0.54	0.69
6-OBCC	0.07	0.07	0.07	0.72	0.53	0.28	0.57	**0.33**	0.27	0.28
9,10-O_2ANT	1.61	<4.7	1.83	<4.7	<4.7	1.46	1.26	**0.88**	0.84	1.26
9,10-O_2PHE	<2.8	<2.8	<2.8	<2.8	<2.8	<2.8	<2.8	<2.8	0.00	<2.8
11-OBaFLN	0.23	0.49	0.71	0.90	1.13	0.76	1.27	**0.79**	0.36	0.76
11-OBbFLN	0.19	0.51	0.53	0.68	1.19	0.89	1.44	**0.78**	0.43	0.68
BAN	0.06	0.31	0.27	0.48	0.60	0.37	0.66	**0.39**	0.21	0.37
7,12-O_2BAA	0.14	0.35	0.50	0.53	0.66	0.46	1.00	**0.52**	0.27	0.50
5,12-O_2NAC	0.06	0.20	0.23	0.30	0.32	0.31	0.48	**0.27**	0.13	0.30
6-OBPYR	0.10	0.40	0.34	0.60	0.81	0.46	0.52	**0.46**	0.22	0.46
Σ_{13}OPAHs and O-heterocycles	5.06	2.51	5.55	6.94	6.10	6.20	8.87	**5.89**	1.93	6.10
Σ_{11}OPAHs	4.06	2.35	5.15	5.17	5.28	5.48	7.93	**5.06**	1.67	5.17

d)

Compound	2006F	2008S	2010F	2011Sp	2011F	2012Sp	2015S	Mean	STD	Median
1,4-O_2NAP	0.028	0.016	0.034	0.028	0.032	0.005	0.062	**0.030**	0.018	0.028
1-(CHO)NAP	0.019	0.003	0.058	0.014	0.009	0.003	0.015	**0.017**	0.019	0.014
DBF	0.31	0.13	0.59	0.24	0.23	0.09	0.09	**0.24**	0.17	0.23
9-OFLN	0.71	0.37	1.28	0.40	0.43	0.18	0.39	**0.54**	0.36	0.40
6-OBCC	0.10	0.28	0.42	0.34	0.07	0.07	0.48	**0.25**	0.17	0.28
9,10-O_2ANT	0.75	<4.7	5.05	<4.7	<4.7	<4.7	<4.7	**0.83**	1.88	0.00
9,10-O_2PHE	<2.8	<2.8	<2.8	<2.8	<2.8	<2.8	<2.8	<2.8	0.00	<2.8
11-OBaFLN	1.36	0.73	1.18	0.66	1.13	1.09	1.57	**1.10**	0.32	1.13
11-OBbFLN	1.42	0.79	0.73	0.57	0.80	0.89	2.20	**1.06**	0.57	0.80
BAN	0.67	0.26	0.23	0.21	0.31	0.43	0.72	**0.41**	0.21	0.31
7,12-O_2BAA	0.59	0.36	0.34	0.34	0.36	0.37	0.89	**0.46**	0.21	0.36
5,12-O_2NAC	0.57	0.36	0.22	0.20	0.34	0.36	0.69	**0.39**	0.18	0.36
6-OBPYR	0.78	0.47	0.62	0.38	0.46	0.64	0.82	**0.60**	0.16	0.62
Σ_{13}OPAHs and O-heterocycles	7.28	3.77	10.76	3.39	4.19	4.14	7.93	**5.92**	2.79	4.19
Σ_{11}OPAHs	6.88	3.36	9.75	2.81	3.89	3.98	7.36	**5.43**	2.59	3.98

a)

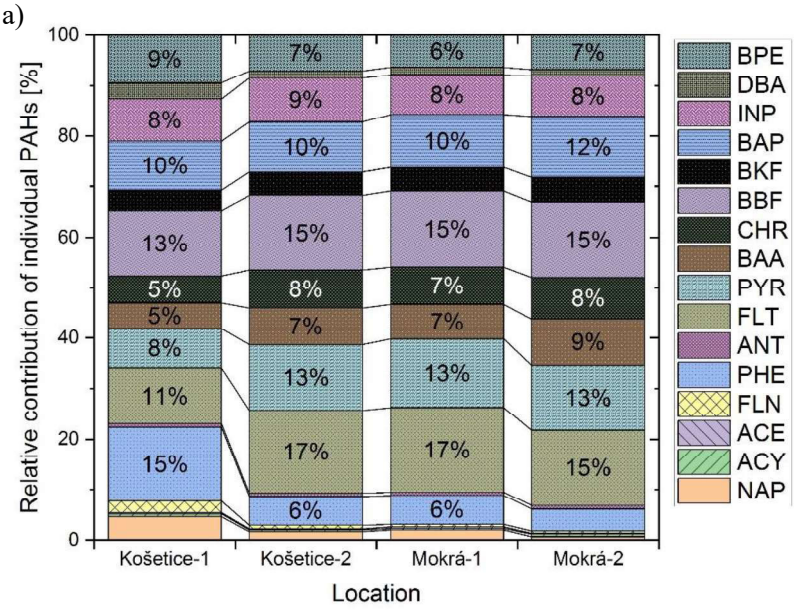

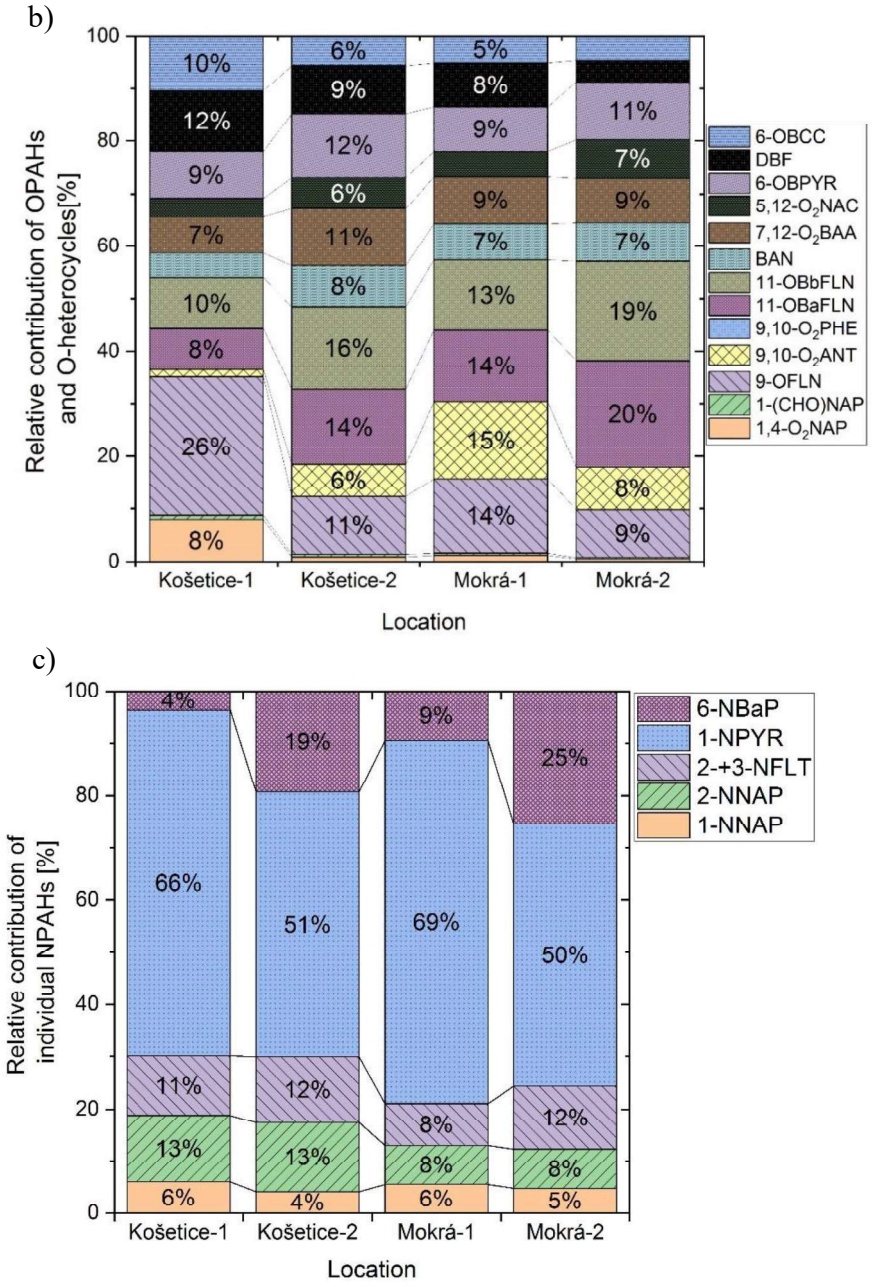

Fig. S6 Location average of relative concentrations of a) 16 PAHs, b) 11 OPAHs and 2 O-heterocycles and c) 18 NPAHs in soil from Košetice and Mokrá (average of all examined years)

a)

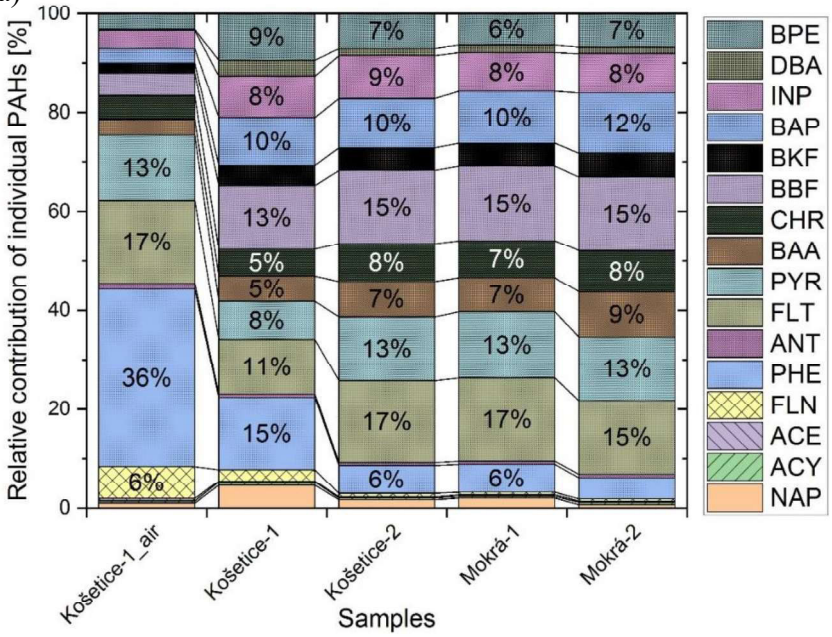
Relative contribution of individual PAHs [%]
Samples
Košetice-1_air
Košetice-1
Košetice-2
Mokrá-1
Mokrá-2
BPE
DBA
INP
BAP
BKF
BBF
CHR
BAA
PYR
FLT
ANT
PHE
FLN
ACE
ACY
NAP

b)

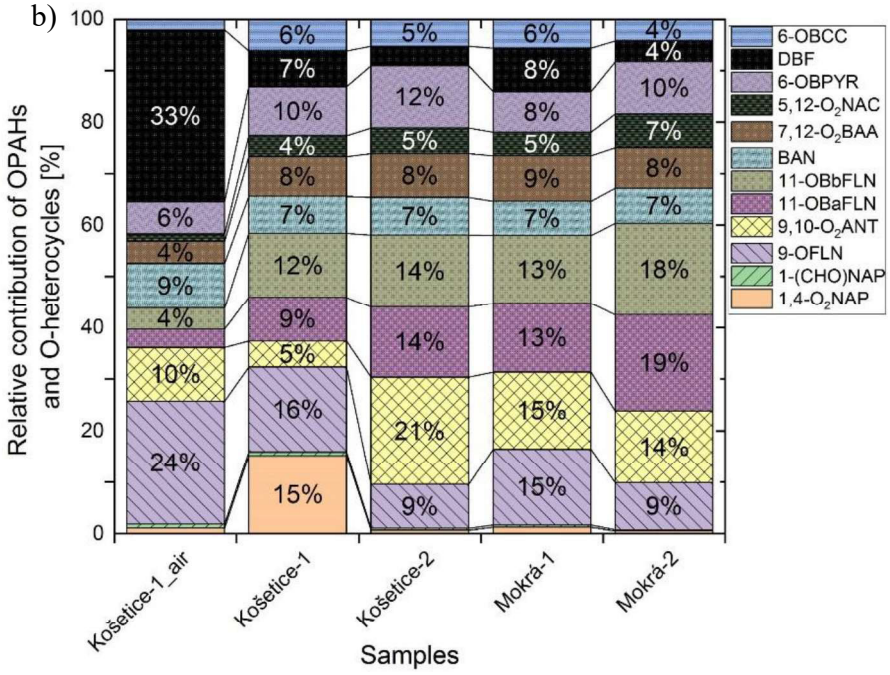
Relative contribution of OPAHs and O-heterocycles [%]
Samples
Košetice-1_air
Košetice-1
Košetice-2
Mokrá-1
Mokrá-2
6-OBCC
DBF
6-OBPYR
5,12-O2NAC
7,12-O2BAA
BAN
11-OBbFLN
11-OBaFLN
9,10-O2ANT
9-OFLN
1-(CHO)NAP
1,4-O2NAP

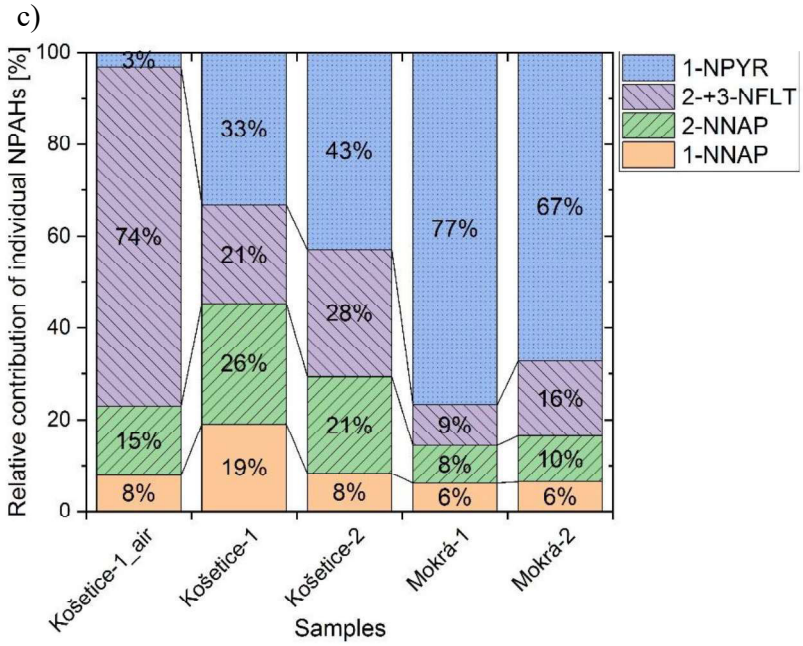

Fig. S7 Location average of relative contribution of a) 16 PAHs, b) 11 OPAHs and 2 O-heterocycles and c) 18 NPAHs in air at Košetice (taken from Nežiková et al. 2021) and in soil. The relative contributions in soil and air from Košetice show the average of the years 2015-2017, the mean of all examined years is shown for the locations in Mokrá

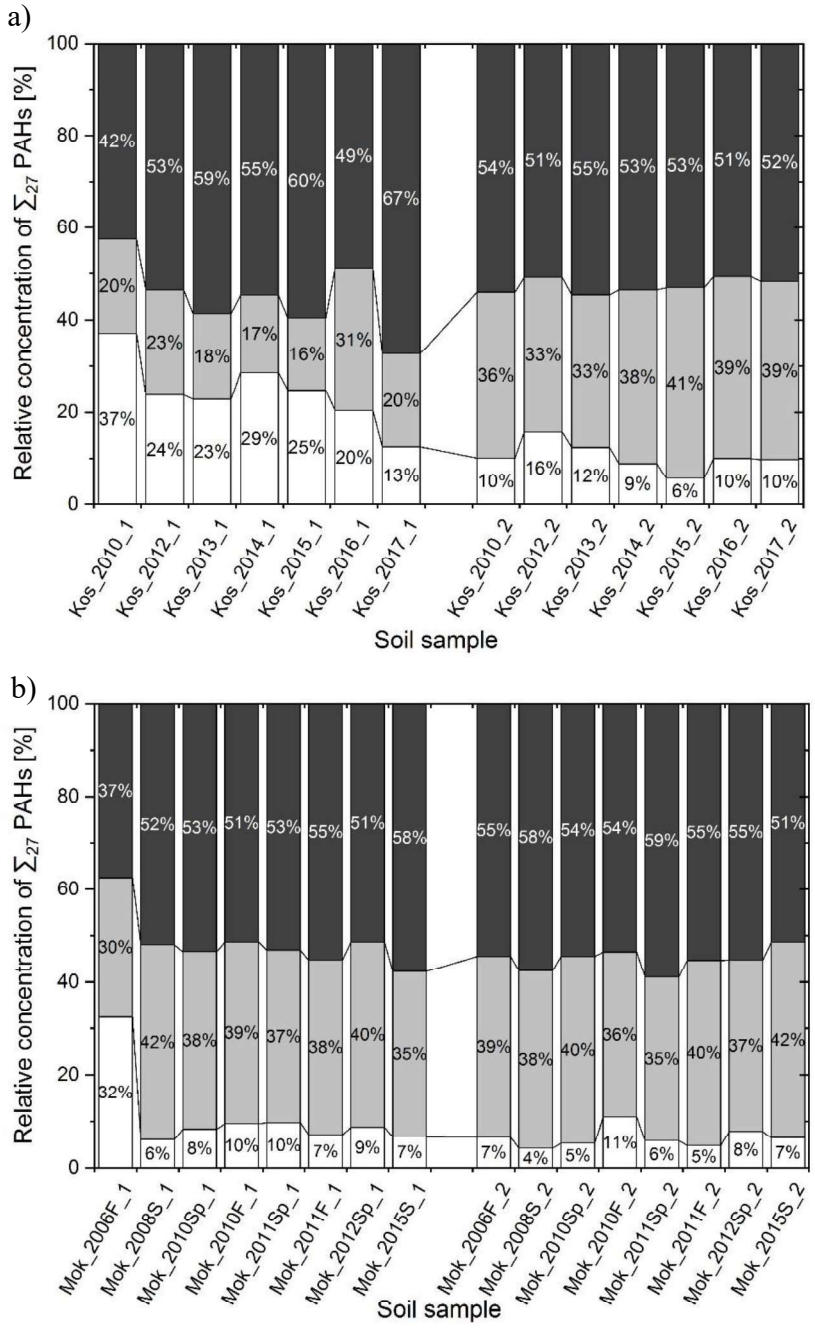

Fig. S8 Relative concentrations of different ring size PAHs to the $\sum_{27}$PAHs a) in Košetice and b) in Mokrá, split into 2-3-ring PAHs (white), 4 ring PAHs (light grey) and 5-7-ring PAHs (dark grey)

Table S14 Temperature and precipitation compared to average in Košetice and Mokrá (Czech Hydrometeorological Institute 2005-2017)

Site	Year	Deviation of average temperature (1981-2010) in winter (Dec/Jan/Feb) [°C]	Precipitation amount as % of the long-term normal (1981-2010) in winter (Dec/Jan/Feb)
Košetice	2010	-1.1	108.7
	2012	0.0	121.3
	2013	0.0	139.7
	2014	2.6	46.7
	2015	2.3	77.3
	2016	3.3	85.3
	2017	-0.9	69.3
Mokrá	2006	-2.0	139.3
	2008	2.0	58.7
	2010	-1.1	149.0
	2011	-1.1	63.7
	2012	0.0	84.3
	2015	2.3	83.7

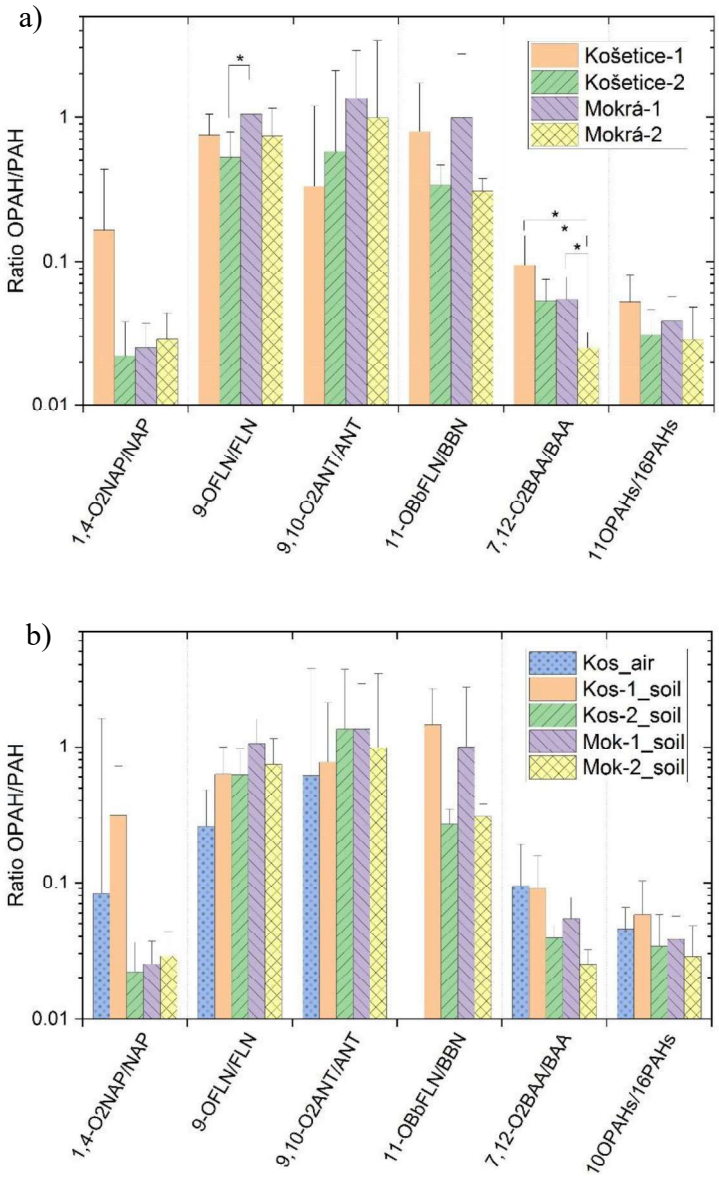

Fig. S9 Average ratio of OPAHs and corresponding parent PAHs in soil from Košetice and Mokrá a) of all examined years and b) of 2015-2017 at Košetice-1 and -2, of air data from 2015-2017 at Košetice (data from Nežiková et al. 2021) and for all examined years from Mokrá soil. Since BBN was not measured by Nežiková et al., the ratio 11-OBbFLN/BBN is not available for air in Košetice. "*" shows the significance with $p<0.05$ (Student's t-test). In b), only the significance between Košetice-1 air and soil was tested but difficult to achieve with only 3 soil samples between 2015-2017. Error bars show the standard deviation of the ratio from different years. Lower limit value for the ratio 9,10-O_2ANT/ANT since detection frequency of 9,10-O_2ANT was <25 % (23 %). For calculation: Values <LOQ were replaced by LOQ/2 if the detection frequency was >25 % (**Fig. S3**), else replaced by 0 ng g^{-1}. "*" shows the significance with $p<0.05$ (Student's t-test) in diagram a).

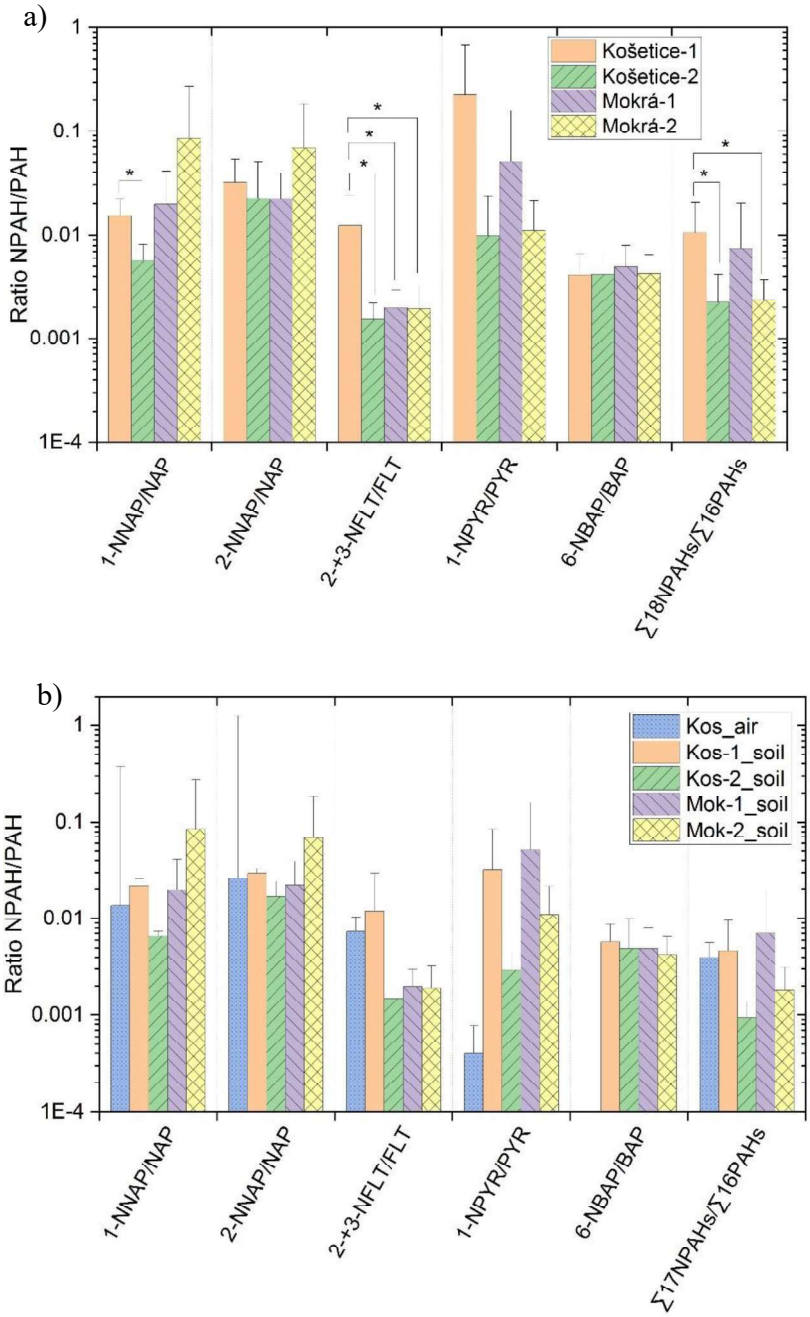

Fig. S10 Ratio of NPAHs and corresponding parent-PAHs in soil from Košetice and Mokrá a) of all examined years and b) of 2015-2017 at Košetice-1 and Košetice-2, of the air data from 2015-2017 at Košetice (data from Nežiková et al. 2021) and for all examined years from Mokrá soil. Since 6-NBAP was not measured by Nežiková et al., the ratio 6-NBAP/BAP is not available for air in Košetice. Ratios of 1-NNAP/NAP and 2-NNAP/NAP are upper limits, since NNAP values <LOQ were replaced by LOQ/2 (detection frequency >25% i.e., ≈30 %). "*" shows the significance with $p<0.05$ (Student's t-test) in diagram a).

Table S15 OPAH/PAH ratios in soil at different locations; n.d.: not determined

Location	**Košetice, Czech Republic**	**Mokrá, Czech Republic**	**Manaus, Brazil**	**Mainz, Germany**	**Berlin, Germany**	**Gardsjön, Sweden**	**Gothenburg, Sweden**	**Argentina**	**China**	**Bratislava, Slovakia**	**Bangkok, Thailand**	**Yangtze River Delta, China**	**Xi'an, China**	**Uzbekistan**
Type of location	Back-ground	Semi-urban	Back-ground	Urban	Contami nated	Back-ground	Urban	Remote	Mixed agri-cultural	Urban	Urban	Industrial, agricul-tural	Sub-urban	Indus-trial semi-arid
Reference	This study		Bandowe& Wilcke 2010			Brorström-Lundén et al. 2010		Wilcke et al. 2014	Sun et al. 2017	Bando-we et al. 2011	Bando-we et al. 2014	Cai et al. 2017	Wei et al. 2015	Bando we et al. 2010
Soil sampling depth [cm]	0-10	0-10	0-10	0-10	0-10	Not specified		Topsoil (ca. 0-10 or 20)	0-20	topsoil	0-5 & 5-10	surface	0-5	0-10 & 10-20
TOC [g kg^{-1}]	37	28	41	46	18	n.d.	n.d.	4-40	n.d.	5.6-53	4-52	n.d.	7.92	2-23
Average temp. [°C]	9.1	8.7	27.4	11	13.1	6.5	7.6	11.4-18	15-18	6.7	28.1	16	14.8	16
Mean annual precipitation [mm]	650	461	2145	334	570	1137	772	185-1100	500	649	1430	730-1526	528	320-550
1,4-O_2NAP/NAP	0.04	0.02	<0.06	<0.04	8.67	n.d.	n.d.	n.d.	n.d.	0.02	0.75	n.d.	0.13	0.01
9-OFLN/FLN	0.58	0.79	2.43	4.97	5089	1.80	0.72	70.5	0.4	5.58	12.20	1.32	4.44	31.00
9,10-O_2ANT/ANT	0.45[a]	1.17[a]	>8.4	6.30	11177	13.00	3.04	2.71-30.0	2.6	1.38	7.00	3.50	0.50	29.00
11-OBbFLN/BBN	0.32	0.33	n.d.	n.d.	n.d.	n.d.	n.d.	n.d.	n.d.	n.d.	n.d.	n.d.	n.d.	n.d.
7,12-O_2BAA/BAA	0.05	0.03	n.d.	n.d.	n.d.	2.33	0.28	30.3	0.14	0.54	1.90	0.15	0.99	n.d.

[a]Lower limit value since detection frequency of 9,10-O_2ANT only 23 %. For calculation: Values <LOQ were replaced by LOQ/2 if the detection frequency was >25 % (**Fig. S3**), else replaced by 0 ng g^{-1}

Table S16 NPAH concentration in surface soil (ng g^{-1}) at different locations; n.d. = not determined; <x = smaller than not reported limit

Location	Košetice, Czech Republic	Mokrá, Czech Republic	Gardsjön, Sweden	Gothenburg, Sweden	Ejby, Denmark	Yangtze River Delta, China	Basel, Switzerland	Hanoi, Vietnam	China plateau	China temperate	China temperate	China subtropical	China tropical
Type of location	Back-ground	Semi-urban	Back-ground	Urban	Back-ground	Urban	Urban	Urban, traffic	rural	urban	rural	rural	rural
Type of soil	Grassland		Not specified		Grass-land with cattle grazing	Not speci-fied	Parks & play-grounds	Not speci-fied	Forest, agricultural, river shore, grassland				
Reference	This study		Brorström-Lundén et al. 2010		Vikelsøe at al. 2002	Cai et al. 2017	Niederer 1998	Pham et al. 2015	Bandowe et al. 2019				
Soil sampling depth [cm]	0-10	0-10	upper 2-3	upper 2-3	0-50	0-10	0-5	0–5, 5–10 & 15–20	0-5	0-5	0-5	0-5	0-5
TOC [g kg^{-1}]	37	28	n.d.	n.d.	n.d.	n.d.	n.d.	n.d.	39	14	19	19	21
Number of NPAHs	18	18	8	8	3	12	8	10	n.d.	n.d.	n.d.	n.d.	n.d.
Sum of NPAHs [ng g^{-1}]	0.31	0.54	5.83	1.35	0.5	0.60	0.34	0.3	n.d.	n.d.	n.d.	n.d.	n.d.
1-NNAP	0.015	0.028	n.d.	n.d.	0.1	0.4	<0.03	n.d.	0.1	0.8	0.2	0.2	0.1
2-NNAP	0.040	0.040	n.d.	n.d.	<x	1.2	<0.03	n.d.	n.d.	n.d.	n.d.	n.d.	n.d.
3-NACE	<0.178	<0.178	n.d.	n.d.	n.d.	n.d.	n.d.	n.d.	n.d.	n.d.	n.d.	n.d.	n.d.
5-NACE	<0.010	<0.010	n.d.	n.d.	n.d.	<x	0.03	n.d.	0.1	0.3	0.4	0.2	0.2
2-NFLN	<0.002	<0.002	n.d.	n.d.	0.4	<x	0.07	n.d.	0.1	0.1	0.2	0.1	0.1
9-NANT	<0.049	<0.049	0.55	0.13	n.d.	<x	n.d.	0.0	0.1	0.2	0.2	0.1	0.1

Location	Košetice, Czech Republic	Mokrá, Czech Republic	Gardsjön, Sweden	Gothenburg, Sweden	Ejby, Denmark	Yangtze River Delta, China	Basel, Switzerland	Hanoi, Vietnam	China plateau	China temperate	China temperate	China subtropical	China tropical
9-NPHE	<0.041	<0.041	n.d.	n.d.	n.d.	<x	n.d.	n.d.	0.1	0.4	0.4	0.3	0.2
3-NPHE	<0.015	<0.015	n.d.	n.d.	n.d.	<x	n.d.	n.d.	n.d.	n.d.	n.d.	n.d.	n.d.
2+3-NFLT	0.037	0.052	1.7	0.50	n.d.	n.d.	0.03	n.d.	0.6	2.1	3.9	1.8	1.3
1-NPYR	0.176	0.332	3.2	0.31	n.d.	1.6	0.15	0.0	0.3	0.6	2	1.3	1.2
7-NBAA	<0.009	<0.009	<0.04	<0.02	n.d.	<x	n.d.	0.02	n.d.	n.d.	n.d.	n.d.	n.d.
6-NCHR	<0.007	<0.007	n.d.	n.d.	n.d.	<x	<0.03	0.113	0.7	0.5	0.5	0.8	2.4
1,3-N_2PYR	<0.001	<0.001	<0.1	<0.06	n.d.	n.d.	n.d.	0.0007	n.d.	n.d.	n.d.	n.d.	n.d.
1,6-N_2PYR	<0.003	<0.003	<0.1	<0.06	n.d.	n.d.	n.d.	0.0045	n.d.	n.d.	n.d.	n.d.	n.d.
1,8-N_2PYR	<0.003	<0.003	n.d.	n.d.	n.d.	n.d.	n.d.	0.007	n.d.	n.d.	n.d.	n.d.	n.d.
6-NBaP	0.039	0.084	n.d.	n.d.	n.d.	<x	n.d.	0.027	n.d.	n.d.	n.d.	n.d.	n.d.
3-NBAN	<0.488	<0.488	<0.2	<0.05	n.d.	n.d.	n.d.	n.d.	n.d.	n.d.	n.d.	n.d.	n.d.

Table S17 Sum of 16 EPA-prioritized PAHs, Σ_{16}PAH, in soil at Košetice and Mokrá in ng g^{-1} (STD: Standard deviation)

Site/Location	Year	Mean	STD	Median	Min	Max	Reference
Mokrá-1 & 2	2006-2015[b]	177	42	171	56	326	This study
Mokrá-1	2006-2015[b]	147	44	155	56	197	This study
Mokrá-2	2006-2015[b]	206	64	202	129	326	This study
Mokrá-1	1998-2005	89	75	61	27	382	Hofman, RECETOX, unpublished
Mokrá-2	1998-2005	194	121	148	96	593	Hofman, RECETOX, unpublished
Košetice-1 & 2	2010-2017[a]	110	100	79	16	295	This study
Košetice-1	2010-2017[a]	26	7	25	16	36	This study
Košetice-2	2010-2017[a]	194	72	171	122	295	This study
Košetice-1	1996-2007	72	25	66	41	116	Holoubek et al. 2007 + Prokeš et al. 2019
Košetice-2	1996-2007	146	56	137	80	256	Holoubek et al. 2007 + Prokeš et al. 2019
Košetice: 9 sites including 1 & 2	1996-2005	600		280	41	5400	Holoubek et al. 2007

[a]except 2011 [b]except 2007, 2009, 2013, 2014

References

Bandowe, B.A.M., Shukurov, N., Kersten, M., Wilcke, W. (2010). Polycyclic aromatic hydrocarbons (PAHs) and their oxygen-containing derivatives (OPAHs) in soils from the Angren industrial area, Uzbekistan. *Environmental Pollution*, 158, 2888–2899

Bandowe, B.A.M. & Wilcke W. (2010). Analysis of polycyclic aromatic hydrocarbons and their oxygen-containing derivatives and metabolites in soil. *Journal of Environmental Quality*, 39, 1349-1358

Bandowe, B.A.M., Sobocka J., Wilcke W. (2011). Oxygen-containing polycyclic aromatic hydrocarbons (OPAHs) in urban soils of Bratislava, Slovakia: patterns, relation to PAHs and vertical distribution. *Environmental Pollution,* 159, 539–549

Bandowe, B.A.M., Gómez Lueso M., Wilcke W. (2014). Oxygenated polycyclic aromatic hydrocarbons and azaarenes in urban soils: A comparison of a tropical city (Bangkok) with two temperate cities (Bratislava and Gothenburg). *Chemosphere,* 107, 407-414

Bandowe, B.A.M., Leimer, S., Meusel, H., Velescu, A., Dassen, S., Eisenhauer, N., Hoffmann, T., Oelmann, Y., Wilcke, W. (2019). Plant diversity enhances the natural attenuation of polycyclic aromatic compounds (PAHs and oxygenated PAHs) in grassland soils. *Soil Biology and Biochemistry,* 129, 60–70

Brorström-Lundén, E., Remberger, M., Kaj, L., Hansson, K., Palm-Cousins, A., Andersson, H., Haglund, P., Ghebremeskel, M., Schlabach, M. (2010). Results from the Swedish National Screening Programme 2008: screening of unintentionally produced organic contaminants. *Swedish Environmental Research Institute (IVL) report B1944*, Göteborg, Sweden

Cai, C.Y., Li, J.Y., Wu, D., Wang, X.L., Tsang, D.C.W., Li, X.D., Sun, J.T., Zhu, L.Z.,Shen, H.Z., Tao, S., Liu, W.X. (2017). Spatial distribution, emission source and health risk of parent PAHs and derivatives in surface soils from the Yangtze River Delta, eastern China. *Chemosphere,* 178, 301-308Cousins, I.T., Kreibich, H., Hudson, L.E., Lead, W.A., Jones, K.C. (1997). PAHs in soils: contemporary UK data and evidence for potential contamination problems caused by exposure of samples to laboratory air. *The Science of the Total Environment*, 203, 141-156

Czech Hydrometeorological Institute (2005-2017), https://www.chmi.cz/historicka-data/pocasi/uzemni-teploty?l=en#

Degrendele C., Fiedler H., Kocan A., Kukučka P., Přibylová P., Prokeš R., Klánová J., Lammel G. (2020). Multiyear levels of PCDD/Fs, dl-PCBs and PAHs in background air in central Europe and implications for deposition. *Chemosphere*, 240, 124852

Hollender, J., Koch, B., Lutermann, C, Dott, W. (2002). Efficiency of different methods and solvents for the extraction of polycyclic aromatic hydrocarbons from soils. *International Journal of Environmental Analytical Chemistry*, 83, 21–32

Holoubek, I., Klánová, J., Jarkovský, J., Kubík, V., Helešic, J. (2007). Trends in background levels of persistent organic pollutants at Košetice observatory, Czech Republic. Part II. Aquatic and terrestrial environments 1996–2005. *Journal of Environmental Monitoring,* 9, 564–571

Holoubek, I., Dušek, L., Sáňka, M., Hofman, J., Čupra, P., Jarkovský, J., Zbíral, J., Klánová, J. (2009). Soil burdens of persistent organic pollutants – Their levels, fate and risk. Part I. Variation of concentration ranges according to different soil uses and locations. *Environmental Pollution*, 157, 3207–3217

Kalina, J., Scheringer, M., Borůvková, J., Kukučka, P., Přibylová, P., Bohlin-Nizzetto, P., Klánova, J. (2017). Passive air samplers as a tool for assessing long-term trends in atmospheric concentrations of semivolatile organic compounds, *Environmental Science and Technology*, 51, 7047-7054

Lau, E.V., Gan, S., Ng, H.K. (2010). Extraction techniques for polycyclic aromatic hydrocarbons in soils. *International journal of analytical chemistry*, 2010, 1-9

Lhotka, R., Pokorná, P., Zíková, N.L. (2019). Long-term trends in PAH concentrations and sources at rural background site in Central Europe. *Atmosphere,* 10, 687

MacLeod, C.J.A. & Semple, K.T., 2003. Sequential extraction of low concentrations of pyrene and formation of non-extractable residues in sterile and non-sterile soils. *Soil Biology & Biochemistry*, 35, 1443–1450

Motelay-Massei, A., Ollivon, D., Garban, B., Teil, M.J., Blanchard, M., Chevreuil, M.,2004. Distribution and spatial trends of PAHs and PCBs in soils in the Seine River basin, France. *Chemosphere,* 55, 555-565

Nam, J.J., Thomas, G.O., Jaward, F.M., Steinnes, E., Gustafsson, O., Jones, K.C. (2008). PAHs in background soils from Western Europe: influence of atmospheric deposition and soil organic matter. *Chemosphere,* 70, 1596-1602

National Centre for Toxic Compounds (2017). Czech Republic updated national implementation plan for the Stockholm Convention on persistent organic pollutants in the period 2012 – 2017.

Nežiková, B., Degrendele, C., Bandowe, B.A.M., Holubová Šmejkalová, A., Kukučka, P., Martiník, J., Prokeš, R., Přibylová, P., Klánová, J., Lammel, G. (2021). Atmospheric concentrations of nitrated and oxygenated polycyclic aromatic hydrocarbons and oxygen heterocycles are declining in Central Europe, *Chemosphere*, 269, 128738

Niederer, M. (1998). Determination of polycyclic aromatic hydrocarbons and substitutes (nitro-, oxy-PAHs) in urban soil and airborne particulate by GCMS and NCI-MS/MS. *Environmental Science and Pollution Research,* 5, 209-216

Pham, C.T., Tang, N., Toriba, A. (2015). Polycyclic aromatic hydrocarbons and nitropolycyclic aromatic hydrocarbons in atmospheric particles and soil at a traffic site in Hanoi, Vietnam. *Polycyclic Aromatic Compounds*, 35, 353-371

Prokeš, R., Příbylová, P., Borůvková, J., Audy, O., Martiník, J., Vinkler, J., Klánová, J., Holoubek, I. (2019). 30 years of integrated POPs monitoring at National Atmospheric Observatory Kosetice, Ovzduší – 14th Czech-Slovak Meeting on Air Pollution, Brno, Czech Republic, 16.-17.4.2019 (published as: Ovzduší 2019 Program a Sborník Konference, Report Masaryk University, ISBN 978-80-210-6203-0, Brno, Czech Republic, pp. 36-37)

Rhind, S.M., Kyle, C.E., Kerr, C., Osprey, M., Zhang, Z.L., Duff, E.I., Lilly, A., Nolan, A., Hudson, G., Towers, W., Bell, J., Coull, M., McKenzie, C. (2013). Concentrations and geographic distribution of selected organic pollutants in Scottish surface soils. *Environmental Pollution,* 182, 15–27

Sun Z., Zhu Y., Zhuo S.J., Liu W.P., Zeng E.Y., Wang X.L., Xing B.S., Tao S. (2017). Occurrence of nitro- and oxy-PAHs in agricultural soils in eastern China and excess lifetime cancer risks from human exposure through soil ingestion. *Environment International*, 108, 261-270

Tomaz, S., Shahpoury, P., Jaffrezo, J.L., Lammel, G., Perraudin, E., Villenave, E., Albinet, A. (2016). One-year study of polycyclic aromatic compounds at an urban site in Grenoble (France): Seasonal variations, gas/particle partitioning and cancer risk estimation. *Science of the Total Environment*, 565, 1071–1083

UBA (2003). Überprüfung von Methoden des Anhanges 1 der Bundesbodenschutz- und Altlastenverordnung (BBodSchV) zur Beurteilung der Bodenqualität. *Umweltbundesamt report* #FB 000397 20174240 (*Texte* 37/03), Federal Environment Agency, Dessau, Germany

UNEP (2003). Global Report 2003 Regionally based assessment of POPs

USEPA (2007), Environment Agency, UKSHS Report No. 9 PAHs soil

USEPA (2019). Estimation Programs Interface Suite™ for Microsoft® Windows, v 4.11. United States Environmental Protection Agency, Washington, USA

Trapido, M. (1999). Polycyclic aromatic hydrocarbons in Estonian soil: contamination and profiles. *Environmental Pollution*, 105, 67-74

Vikelsøe, J., Thomsen, M., Carlsen, L., Johansen, E. (2002). Persistent organic pollutants in soil, sludge and sediment. A multianalytical field study of selected organic chlorinated and brominated compounds. National Environmental Research Institute, Denmark. *NERI Technical Report* No. 402, 100 pp. URL: http://technical-reports.dmu.dk

Wei, C., Bandowe, B.A.M., Han, Y., Cao, J., Zhan, C., Wilcke, W. (2015). Polycyclic aromatic hydrocarbons (PAHs) and their derivatives (alkyl-PAHs, oxygenated-PAHs, nitrated-PAHs and azaarenes) in urban road dusts from Xi'an, Central China. *Chemosphere,* 134, 512–520

Wilcke, W. (2000). Synopsis polycyclic aromatic hydrocarbons (PAHs) in soil - a review. *Journal of Plant Nutrition and Soil Science*, 163, 229-248

Wilcke, W., Amelung, W. (2000). Persistent organic pollutants (POPs) in native grassland soils along a climosequence in North America. *Soil Science Society of America Journal*, 64, 2140–2148

Wilcke, W., Bandowe, B.A.M., Gomez Lueso, M., Ruppenthal, M. del Valle, H. Oelmann, Y. (2014a). Polycyclic aromatic hydrocarbons (PAHs) and their polar derivatives (oxygenated PAHs, azaarenes) in soils along a climosequence in Argentina. *Science of the Total Environment,* 473–474, 317–325

2.2 PACs in the marine atmosphere

This chapter has been submitted to the journal *Atmospheric Chemistry and Physics*. As the first author of this manuscript, I evaluated the data and was mainly responsible for the interpretation of the data. I wrote the first draft of the manuscript, created the figures, organized the contributions from the coauthors and edited the manuscript based on feedback and exchange with the coauthors.

Atmos. Chem. Phys. Discuss., submitted (2022)

Polycyclic aromatic hydrocarbons (PAHs) and their alkylated-, nitro- and oxy-derivatives in the atmosphere over the Mediterranean and Middle East seas

M. Wietzoreck[1], M. Kyprianou[2], B. A. M. Bandowe[1], S. Celik[3], J. N. Crowley[4], F. Drewnick[3], P. Eger[4], N. Friedrich[4], M. Iakovides[2], P. Kukučka[5], J. Kuta[5], B. Nežiková[5], P. Pokorná[6], P. Přibylová[5], R. Prokeš[5,7], R. Rohloff[4], I. Tadic[4], S. Tauer[4], J. Wilson[1], H. Harder[4], J. Lelieveld[2,4], U. Pöschl[1], E. G. Stephanou[2,8], G. Lammel[1,5*]

[1]Multiphase Chemistry Department, Max Planck Institute for Chemistry, Mainz, 55128, Germany

[2]Climate and Atmosphere Research Centre, Cyprus Institute, Nicosia, 2121, Cyprus

[3]Particle Chemistry Department, Max Planck Institute for Chemistry, Mainz, 55128, Germany

[4]Atmospheric Chemistry Department, Max Planck Institute for Chemistry, Mainz, 55128, Germany

[5]RECETOX, Faculty of Science, Masaryk University, Brno, 625 00, Czech Republic

[6]Department of Aerosol Chemistry and Physics, Institute of Chemical Process Fundamentals of the CAS, Prague, 165 02, Czech Republic

[7]The Czech Academy of Sciences, Global Change Research Institute, Brno, 603 00, Czech Republic

[8]Department of Chemistry, University of Crete, Heraklion, 70013, Greece

Polycyclic aromatic hydrocarbons (PAHs) and their alkylated-, nitro- and oxy-derivatives in the atmosphere over the Mediterranean and Middle East seas

Marco Wietzoreck[1], Marios Kyprianou[2], Benjamin A. Musa Bandowe[1], Siddika Celik[3], John N. Crowley[4], Frank Drewnick[3], Philipp Eger[4], Nils Friedrich[4], Minas Iakovides[2], Petr Kukučka[5], Jan Kuta[5], Barbora Nežiková[5], Petra Pokorná[6], Petra Přibylová[5], Roman Prokeš[5,7], Roland Rohloff[4], Ivan Tadic[4], Sebastian Tauer[4], Jake Wilson[1], Hartwig Harder[4], Jos Lelieveld[2,4], Ulrich Pöschl[1], Euripides G. Stephanou[2,8], Gerhard Lammel[1,5]

[1]Multiphase Chemistry Department, Max Planck Institute for Chemistry, Mainz, 55128, Germany
[2]Climate and Atmosphere Research Centre, Cyprus Institute, Nicosia, 2121, Cyprus
[3]Particle Chemistry Department, Max Planck Institute for Chemistry, Mainz, 55128, Germany
[4]Atmospheric Chemistry Department, Max Planck Institute for Chemistry, Mainz, 55128, Germany
[5]RECETOX, Faculty of Science, Masaryk University, Brno, 625 00, Czech Republic
[6]Department of Aerosol Chemistry and Physics, Institute of Chemical Process Fundamentals of the CAS, Prague, 165 02, Czech Republic
[7]The Czech Academy of Sciences, Global Change Research Institute, Brno, 603 00, Czech Republic
[8]Department of Chemistry, University of Crete, Heraklion, 70013, Greece

Correspondence to: Gerhard Lammel (g.lammel@mpic.de)

Abstract. Polycyclic aromatic hydrocarbons (PAHs), their alkylated (RPAHs), nitrated (NPAHs) and oxygenated (OPAHs) derivatives are air pollutants. Many of these substances are long-lived, can undergo long-range atmospheric transport and adversely affect human health upon exposure. However, the occurrence and fate of these air pollutants has hardly been studied in the marine atmosphere. In this study, we report the atmospheric concentrations over the Mediterranean Sea, the Red Sea, the Arabian Sea, the Gulf of Oman and the Arabian Gulf, determined during the AQABA (Air Quality and Climate Change in the Arabian Basin) project, a comprehensive ship-borne campaign in summer 2017. The average concentrations of $\sum_{27}$PAHs, $\sum_{19}$RPAHs, $\sum_{11}$OPAHs and $\sum_{17}$NPAHs, in the gas and particulate phase, were 2.85 ± 3.35 ng m^{-3}, 0.83 ± 0.87 ng m^{-3}, 0.24 ± 0.25 ng m^{-3} and 4.34 ± 7.37 pg m^{-3}, respectively. The Arabian Sea region was the cleanest for all substance classes, with concentrations among the lowest ever reported. Over the Mediterranean Sea, we found the highest average burden of $\sum_{26}$PAHs and $\sum_{11}$OPAHs, while the $\sum_{17}$NPAHs were most abundant over the Arabian Gulf (known also as Persian Gulf). 1,4-Naphthoquinone (1,4-O_2NAP) followed by 9-fluorenone and 9,10-anthraquinone were the most abundant studied OPAHs in most samples. The NPAH composition pattern varied significantly across the regions, with 2-nitronaphthalene (2-NNAP) being the most abundant NPAH. According to source apportionment investigations, the main sources of PAH derivatives in the region were ship exhaust emissions, residual oil combustion and continental pollution. All OPAHs and NPAHs except 2-NFLT, which were frequently detected during the campaign, showed elevated concentrations in fresh shipping emissions. In contrast, 2-nitrofluoranthene (2-NFLT) and 2-nitropyrene (2-NPYR) were highly abundant in aged

shipping emissions due to secondary formation. Apart from 2-NFLT and 2-NPYR, also benz(a)anthracene-7,12-dione and 1,4-O_2NAP had significant photochemical sources. Another finding was that the highest concentrations of PAHs, OPAHs and NPAHs were found in the sub-micrometre fraction of particulate matter (PM_1).

1 Introduction

Air pollution contributes to the global burden of respiratory and cardiovascular diseases (Shiraiwa et al., 2017; Lelieveld et al., 2019). The Red Sea and especially the Arabian Gulf region are prone to major risks by air particulate matter (PM) and gas phase pollutants due to the hot and arid climate leading to high dust concentrations and photochemical activity (Lelieveld et al., 2009). In combination with high anthropogenic emissions from highly populated cities, intense marine traffic due to major trade routes (Johansson et al., 2017) and a strong petrochemical industry, air pollution can be significant in these regions (Lelieveld et al., 2015).

One major class of air pollutants are polycyclic aromatic hydrocarbons (PAHs) and their alkylated (RPAHs), nitrated (NPAHs) and oxygenated (OPAHs) derivatives. Several of these substances are classified as carcinogenic or possibly carcinogenic (IARC, 1983, 1989, 2018; OEHHA, 2021). Moreover, many polycyclic aromatic compounds (PACs) show strong mutagenic (Durant et al., 1996; Clergé et al., 2019) and ecotoxic effects (el Alawi et al., 2002; Sverdrup et al., 2002a, b). Quinones, a major subgroup of OPAHs, have received more attention in recent years due to their potential to contribute to oxidative stress on cell level (Bolton et al., 2000; Walgraeve et al., 2010; Xiong et al., 2017; Lyu et al., 2018). Although some PAH derivatives show even higher toxicity than their parent PAHs (Durant et al., 1996; Collins et al., 1998; Turcotte et al., 2011; IARC, 2018; Lee et al., 2017; Clergé et al., 2019), their atmospheric concentrations, their cycling and fate are not well studied. Alkylated 3-ring-PAHs are more persistent, bioaccumulative, and toxic than the parent 3-ring-PAHs, which have been identified within Europe (ECHA, 2021) as substances with persistent, bioaccumulative, and/or toxic properties (PBT). According to Wassenaar and Verbruggen (2021) alkylated 3-ring-PAHs could also be considered as PBT.

PAHs, OPAHs, NPAHs and RPAHs are formed by incomplete combustion of fossil fuels, biomass and waste (Baek et al., 1991; Lee et al., 2003; Walgraeve et al., 2010; Bandowe and Meusel, 2017). Apart from these pyrogenic sources, PAHs, especially low-molecular-weight PAHs and RPAHs, and some PAH derivatives can originate from petrogenic sources and spills of petroleum hydrocarbons (Andersson and Achten, 2015; Zhao et al., 2015; Abbas et al., 2018). In addition to these so-called primary emissions, NPAHs and OPAHs can also be formed by secondary formation by reactions of PAHs with atmospheric oxidants (Finlayson-Pitts and Pitts, 1999; Keyte et al., 2013). For most PAH derivatives, the contribution from secondary formation is not known. It was shown that 2-nitrofluoranthene (2-NFLT) is formed in gas phase reactions and was not found in direct emissions, while the opposite was reported for 1-nitropyrene (1-NPYR) (Arey et al., 1986; Bamford and Baker, 2003). Therefore, the ratio 2-NFLT/1-NPYR can be used as an indicator for the relative contributions of secondary formation reactions in the gas phase compared to primary emitted compounds (Bamford and Baker, 2003).

The concentration of PAHs in ambient air as well as other environmental compartments has been studied quite extensively in the last decades (Baek et al., 1991; Srogi, 2007; Ravindra et al., 2008), especially for the 16 USEPA-prioritized PAHs (Keith, 2015). However, our knowledge about the distribution of PAH derivatives is still limited (Andersson and Achten, 2015; Lammel, 2015; Bandowe and Meusel, 2017; Iakovides et al., 2021). There are several studies reporting atmospheric concentrations of OPAHs and NPAHs in the particulate and the gas phase at urban and semi-urban sites (Bamford and Baker, 2003; Garcia et al., 2014; Li et al., 2015; Tomaz et al., 2016; Alves et al., 2017; Kitanovski et al., 2020). Rural/continental background and remote continental sites were investigated in a small number of studies, indicating that several NPAHs and OPAHs are ubiquitous (Ciccioli et al., 1996; Tsapakis and Stephanou, 2007; Brorström-Lundén et al., 2010; Scipioni et al., 2012; Tang et al., 2014; Nežiková et al., 2021). Their detection in the Antarctic (Vincenti et al., 2001; Minero et al., 2010) confirms the long-range transport potential (Keyte et al., 2013). This is supported by global modelling studies of NPAHs (Wilson et al., 2020; Kelly et al., 2021). However, fewer studies have determined the pollutant concentrations in the marine environment, in polluted sea regions or in marine background air. Tsapakis and Stephanou (2007) and Lammel et al. (2017) measured NPAHs and OPAHs at an eastern Mediterranean marine background location, while Zhang et al. (2018) sampled air on Tuoji Island in the Yellow Sea. To the best of our knowledge, there is no study measuring NPAHs and OPAHs over the open ocean. The knowledge about the sources of pollution and the atmospheric fate processes such as gas-particle partitioning, photochemical degradation and deposition in the marine environment is crucial for understanding the distribution and fate of these pollutants, although very little is known (Keyte et al., 2013). In addition, these processes in marine air are crucial for modelling the distribution of these substances and the concentrations are needed for the validation of modelling results (Wilson et al., 2020).

The objective of this study was to determine the concentrations in the gas and particulate phase of the PAHs, RPAHs, NPAHs and OPAHs in the Mediterranean Sea and around the Arabian Peninsula including the Red Sea, Arabian Sea and the Arabian Gulf region. We aimed to study the gas-particle partitioning and the mass size distributions of PACs in the atmosphere of a hot marine environment. Furthermore, we provide information about the sources of air pollution in these regions.

2 Methods

2.1 The AQABA ship campaign

The Air Quality and Climate in the Arabian Basin (AQABA) campaign took place in summer 2017 from the 25 June until the 01 September 2017, sailing on a research vessel (*Kommandor Iona*) from Toulon, France, to Kuwait City, Kuwait, and back, with a 2-day stop in Jeddah, Saudi Arabia (first leg) and a 5-day stop in Kuwait. The sampling was performed only during cruise and outside the 12 nautical miles zones of the countries in the Mediterranean Sea (MS), Suez Canal, Red Sea (RS), Arabian Sea (AS, in the northern Indian Ocean), Gulf of Oman (OG) and the Arabian Gulf (AG, also known as the Persian Gulf). For the evaluation, the Red Sea is split into northern Red Sea (NRS) and southern Red Sea (SRS). The Suez

Canal is included into the northern Red Sea region; the Gulf of Aden is part of the Arabian Sea. The sampling regions and sampling cruises are shown in Fig. S1 in the Supplement.

2.2 Sampling

2.2.1 Air sampling for analysis of PAHs, OPAHs and NPAHs

The air pollutants were sampled separately in gas and particulate phases in polyurethane foams (PUFs, Molintan a.s., Břeclav, Czech Republic) and on quartz microfibre filters (QFFs, QMA type, Whatman, Sheffield, United Kingdom), respectively, by active air sampling on the observation deck (in the front part of the vessel, around 7.7 m a.s.l. and 55 m away from the stack). The aerosol was sampled as PM_{10} (all particles with an aerodynamic equivalent diameter of <10 µm) by a Digitel sampler (DH77, Hegnau, Switzerland). Additionally, PM was collected size-segregated with 6 size fractions (5 stages + backup filter) within PM_{10} ($PM_{<0.49µm}$ (backup filter), $PM_{0.49\text{-}0.95µm}$, $PM_{0.95\text{-}1.5µm}$, $PM_{1.5\text{-}3µm}$, $PM_{3\text{-}7µm}$ and $PM_{7\text{-}10µm}$) using a high-volume sampler (Baghirra HV 100-P, Prague, Czech Republic) equipped with a cascade impactor inlet (TE-235, Tisch Environmental, Inc., Cleves, USA). All filters were pre-baked at 300 °C for 12 h and the PUFs were pre-cleaned (8 h Soxhlet extraction in acetone and 8 h in dichloromethane (DCM)) before wrapping them into two layers of aluminium foil, placing into zip-lock polyethylene bags and keeping them frozen at -20 °C prior to deployment. After exposure, the samples were wrapped in aluminium foil and kept in polyethylene zip-lock bags at -20 °C during storage. During the whole cruise, 62 air samples (gas and particulate phase) and 30 size-resolved PM samples were collected together with 6 field blanks. Detailed sampling information is provided in Supplement Fig. S1 and in Table S1.

2.2.1 Air sampling for analysis of PAHs and RPAHs

45 air (gas and particulate phase) samples for the determination of PAHs and alkylated PAHs were collected on the monkey deck of the research vessel (around 4 m higher and 5 m less far away from the stack compared to the samplers for PAHs, OPAHs and NPAHs) during the campaign, using a high-volume air sampler (GMWL-2000H; General Metal Works, Cleves, USA). In contrast to the Digitel high volume sampler, total suspended particles (TSP) instead of PM_{10} were collected. The sampling duration varied from 6 to 24 h and the total volume of each air sample ranged from 318 to 1428 m^3 (Table S1 in the Supplement). Pre-combusted QFFs (3 h at 420 °C) and pre-extracted PUF plugs (8.0 x 7.5 cm, Ziemer, Langerwehe, Germany) were used for the collection of particulate and gaseous phases, respectively. TSP mass was gravimetrically determined. Filters were pre- and post-sampling weighed on a microbalance (KERN GmbH, Balingen, Germany; 1.0^{-5} g readability) at constant temperature (21±2 °C) and relative humidity (45±10%) conditions.

2.3 Sample preparation and analysis

2.3.1 PAHs, OPAHs and NPAHs

PUFs and QFFs were extracted using automated Soxhlet extraction (40 minutes Soxhlet extraction followed by 20 minutes of solvent rinsing) with DCM in a B-811 extraction unit (Büchi, Flawil, Switzerland). Prior to extraction, the samples were spiked with deuterated nitro-PAHs (1-nitronaphthalene-d7, 2-nitrofluorene-d9, 9-nitroanthracene-d9, 3-nitrofluoranthene-d9, 1-nitropyrene-d9, 6-nitrochrysene-d11, 6-nitrobenzo[a]pyrene-d11) and deuterated PAHs (d8-naphthalene, d10-phenanthrene, d12-perylene) as surrogate standards.

The extract was cleaned up using a silica column (5 g of silica, 0.063–0.200 mm, activated at 150 °C for 12 hours, 10% deactivated with water) and 1 g Na_2SO_4. The sample was loaded onto the column and the target substances were eluted by 5 mL *n*-hexane, followed by 50 mL DCM. The volume of the eluate was then reduced by a stream of nitrogen in a TurboVap II (Caliper LifeSciences, Mountain View, USA) concentrator unit and transferred into a GC vial, spiked with p-terphenyl and PCB 121 (syringe standards), and the final volume in the vial was adjusted to 200 µL.

Polycyclic aromatic compounds (PACs) in the sample extracts were analysed at the Trace Analytical Laboratory of the research centre RECETOX at the Masaryk University in Brno, Czech Republic, similar to the method described by Nežiková et al. (2021). The target compounds in this analysis were 26 PAHs, 1S-heterocycle, 1 RPAH, 17 NPAHs and 11 OPAHs. All target PAHs, OPAHs and NPAHs including their acronyms are shown in Table 1. The physico-chemical properties of all targeted compounds are shown in Table S2.

The analysis of PAHs was performed by gas chromatography (GC, 7890A, Agilent, Santa Clara, USA) equipped with a 60 m x 0.25 mm x 0.25 µm Rxi-5Sil MS column (Restek, Bellefonte, USA) coupled to a mass spectrometer (MS, 7000B triple quadrupole, Agilent, Santa Clara, USA). 1 µL of sample was injected splitless at 280 °C with He as carrier gas at a constant flow rate of 1.5 mL min^{-1}. The GC program was as follows: 80 °C (1 min hold), then heated at a rate of 15 °C min^{-1} to 180 °C, followed by 5 °C min^{-1} to 310 °C (20 min hold). The MS was operated in positive electron ionization (EI+) mode with selected ion monitoring (SIM). The SIM m/z ratios and the retention times of the targeted PAHs are shown in Table S3a.

NPAHs and OPAHs were analysed by GC atmospheric pressure chemical ionization tandem mass spectrometry (GC-APCI-MS/MS) on a Waters Xevo TQ-S MS (Waters, Mildford, USA) coupled to a GC (GC 7890, Agilent, Santa Clara, USA). The MS was operated under dry source conditions in multiple reactions monitoring (MRM) mode. The GC was fitted with a 30 m x 0.25 mm × 0.25 µm Rxi-5Sil MS column (Restek, Bellefonte, USA). The injection of 1 µL of the sample was splitless at 270 °C. He was used as carrier gas at a constant flow rate of 1.5 mL min^{-1}. The oven temperature program was as follows: 90 °C (1 min hold), then heated at a rate of 40 °C min^{-1} to 180 °C, followed by 5 °C min^{-1} to 320 °C (6 min hold). The MRM m/z ratios and the retention times of the targeted OPAHs and NPAHs are given in Table S3b.

155 **2.3.2 RPAHs**

For alkylated PAHs, particulate and gas-phase samples were extracted and cleaned-up separately following a procedure described in detail elsewhere (Iakovides et al., 2021). Each fraction was reduced to approximately 0.3 mL by rotary evaporation, transferred to 1.1 mL GC vials and further evaporated almost to dryness under a gentle stream of nitrogen at -10 °C to minimize evaporation losses. Prior to GC/MS analysis, a known amount of internal standard mixture (4-20 ng of
160 anthracene-d_{10} in iso-octane) was added in each GC vial to assess the analyte recovery in the collected samples. The sample extracts were analysed at the Cyprus Institute (Cyprus). The target compounds in this analysis were phenanthrene (PHE) and 18 RPAHs, which are shown in Table 1.

The analysis was carried out on a GC (7890N GC, Agilent, Santa Clara, USA) equipped with a deactivated fused silica guard column (5 m, Agilent, Santa Clara, USA) followed by a 30 m × 0.25 mm × 0.25 μm fused silica column (DB-5MS, J&W,
165 Santa Clara, USA). The GC was coupled to a mass selective detector (5977B Inert MSD, Agilent, Santa Clara, USA) operating in EI mode. Either 1 or 2 μL of the final extract were injected into the column using a cool-on-column inlet (80 °C constant temperature) with a column flow rate of 1.0 mL/min. The GC oven program was modified to 80 °C initial temperature, hold for 1 min, heated at a rate of 21 °C min^{-1} to 150 °C, 5 °C min^{-1} to 300 °C and finally hold for 20 min (54 min total run time). The transfer line was kept at 300 °C, while the MS quadrupole and ion source temperature were held at
170 150 and 230 °C, respectively. Molecular ions used for the identification are shown in Table S3c.

Table 1: Target compounds and their acronyms.

Compound	Acronym	Compound	Acronym
Polycyclic aromatic hydrocarbons:	**PAHs**	1,3-/2,10-/3,9-/3,10- Dimethylphenanthrene	1,3-/2,10-/3,9-/1,10-M_2PHE
Naphthalene	NAP	1,6-/2,9- Dimethylphenanthrene	1,6-/2,9-M_2PHE
Acenaphthylene	ACY	1,7-Dimethylphenanthrene	1,7-M_2PHE
Acenaphthene	ACE	2,3-Dimethylphenanthrene	2,3-M_2PHE
Fluorene	FLN	1,9-/4,9- Dimethylphenanthrene	1,9-/4,9-M_2PHE
Phenanthrene	PHE	1,8-Dimethylphenanthrene	1,8-M_2PHE
Anthracene	ANT	Retene (1-methyl-7-isopropylphenanthrene)	RET
Fluoranthene	FLT	**Oxygenated PAHs:**	**OPAHs**
Pyrene	PYR	1,4-Naphthoquinone	1,4-O_2NAP
Benzo(b)fluorene	BBN	Naphthalene-1-aldehyde	1-(CHO)NAP
Benzo(ghi)fluoranthene	BGF	9-Fluorenone	9-OFLN
Cyclopenta(cd)pyrene	CCP	9,10-Anthraquinone	9,10-O_2ANT
Benzo(a)anthracene	BAA	1,4-Anthraquinone	1,4-O_2ANT
Triphenylene	TPH	9,10-Phenanthrenequinone	9,10-O_2PHE
Chrysene	CHR	11H-Benzo(a)fluoren-11-one	11-OBaFLN
Benzo(b)fluoranthene	BBF	11H-Benzo(b)fluoren-11-one	11-OBbFLN
Benzo(j)fluoranthene	BJF	Benzanthrone (7H-benz(de)anthracene-7-one)	BAN
Benzo(k)fluoranthene	BKF	Benz(a)anthracene-7,12-dione	7,12-O_2BAA
Benzo(e)pyrene	BEP	5,12-Naphthacenequinone	5,12-O_2NAC
Benzo(a)pyrene (benzo(def)chrysene)	BAP	**Nitrated PAHs:**	**NPAHs**
Perylene	PER	1-Nitronaphthalene	1-NNAP
Indeno(123-cd)pyrene	INP	2-Nitronaphthalene	2-NNAP
Dibenz(ah)anthracene	DBA	3-Nitroacenaphthene	3-NACE
Dibenz(ac)anthracene	DCA	5-Nitroacenaphthene	5-NACE
Benzo(ghi)perylene	BPE	2-Nitrofluorene	2-NFLN
Anthanthrene	ATT	9-Nitroanthracene	9-NANT
Coronene	COR	9-Nitrophenanthrene	9-NPHE
Benzonaphthothiophene	BNT	3-Nitrophenanthrene	3-NPHE
Alkylated PAHs:	**RPAHs**	2-Nitrofluoranthene	2-NFLT
1-Methylphenanthrene	1-MPHE	1-Nitropyrene	1-NPYR
2-Methylphenanthrene	2-MPHE	2-Nitropyrene	2-NPYR
3-Methylphenanthrene	3-MPHE	7-Nitrobenzo(a)anthracene	7-NBAA
4-Methylphenanthrene	4-MPHE	6-Nitrochrysene	6-NCHR
3,6-Dimethylphenanthrene	3,6-M_2PHE	1,3-Dinitropyrene	1,3-N_2PYR
2,6-Dimethylphenanthrene	2,6-M_2PHE	1,6-Dinitropyrene	1,6-N_2PYR
2,7-Dimethylphenanthrene	2,7-M_2PHE	1,8-Dinitropyrene	1,8-N_2PYR
		6-Nitrobenzo(a)pyrene	6-NBAP

2.4 Supporting parameters

175 Further description of analytical methods and other supporting parameters such as meteorological data, PM_{10} mass and concentrations of transition metals, elemental carbon (EC) and organic carbon (OC) can be found in the Supplement. The methods and the resulting data of other additional supporting parameters during the AQABA campaign used in this paper are reported in the following studies: a) The ship exhaust filter, black carbon (BC) and surface PAH concentrations as well as

bypassing ships, potentially influencing the sampled air, in Celik et al. (2020), b) O_3, nitrogen oxides (NO_x, i.e. NO+NO_2) and OH radicals in Tadic et al. (2020), c) O_3, NO_2 and SO_2 in Eger et al. (2019) and d) NO_x and NO_y (i.e. NO_x+organic and inorganic oxides of nitrogen) in Friedrich et al. (2021). Measurements of OH radicals were done using the *H*ydr*O*xyl *R*adical measurement *U*nit based in fluorescence *S*pectroscopy (HORUS) instrument (Martinez et al., 2010; Hens et al., 2014), with the *I*nlet *P*re-*I*njector (IPI) modification (Novelli, et al., 2014). The measurement of the actinic flux was done by a spectral radiometer as described in Meusel et al. (2016). The measurement of polychlorinated biphenyls (PCBs), hexachlorocyclohexanes (HCHs), dichlorodiphenyl-trichloroethane and isomers (DDX), other organochlorine pesticides (drins) was done similar to Lammel et al. (2016).

2.5 Aerosol source apportionment

Positive Matrix Factorization (EPA PMF 5.0) was applied to the PM_{10} chemical composition using the concentrations of OC, EC, BC and metals in both PMF groups and the sum of PCBs, HCHs, DDX, drins, PAHs, NPAHs and OPAHs only in group 1 and selected individual PAHs, OPAHs and NPAHs in group 2 to obtain source profiles and their contributions. All Digitel high-volume samples were considered in the PMF runs including those with contamination from the ship's stack. The data matrix was prepared in compliance with the procedure described by Polissar et al. (1998). The final matrices had 62 samples with 26 and 30 species in group 1 and 2, respectively.

To estimate the optimal number of sources, the PMF model was run several times with different model settings and 3 to 7 factors tested. The Q values (Q_{true}, Q_{robust} and $Q_{expected/theoretical}$), the resulting source profiles, and the scaled residuals were examined. The optimum number of factors was chosen based on an adequate fit of the model to the data, as shown by the scaled residual histograms and physically interpretable results. The most stable solutions were found for 5 factors by extra modelling uncertainties of 26 % and 19 % for group 1 and group 2, respectively. All runs converged, the scale residuals were normally distributed and no swaps were observed with the displacement error analysis, indicating that there was limited rotational ambiguity (Table S9).

2.6 Air mass origin

Residence time distributions of air mass histories, 10 days backward in time, were studied using the FLEXPART Lagrangian particle dispersion model, with ECMWF meteorological data (0.5°×0.5°, 3-hourly; Seibert and Frank, 2004; Stohl et al., 2005). The output is a measure of the time the computational particles (fictive air parcels) resided in grid cells. Per 24 h sampling time, 100000 particles were released at a height of 100 m a.s.l..

2.7 Quality control

More information about the analytical quality assurance such as the filtering of the samples against contamination by the own ship exhaust, the quality control of the analysis of the PAH derivatives (recoveries, blank correction, detection frequencies, limits of quantifications (LOQs)) and a summary of PMF diagnostics is given in the Supplement (Chapter S1.5).

3 Results and discussion

3.1 Occurrence of PAHs and PAH derivatives

The average total (sum of gaseous and particulate phase) concentrations of the pollutants in the different sea regions are shown in Fig. 1. The average total concentrations (range in brackets) of the sum of one pollutant class from all high-volume air samples of the $\sum_{16}$PAHs, $\sum_{27}$PAHs (including the S-heterocycle BNT), $\sum_{19}$RPAHs (range without RET), $\sum_{11}$OPAHs and $\sum_{17}$NPAHs were 2.92 ± 3.34 (0.14-17.28) ng m^{-3}, 2.99 ± 3.35 (0.15-17.34) ng m^{-3}, 0.85 ± 0.87 (0.19-3.41) ng m^{-3}, 0.24 ± 0.25 (0.04-1.42) ng m^{-3} and 4.34 ± 7.37 (0.69-46.50) pg m^{-3}, respectively. All the data is filtered for contamination with the stack of our research vessel (details given in S1.5.1 in the Supplement). The detection frequencies of the compounds in the high-volume samples are shown in Fig. S1. All targeted PAHs, RPAHs and OPAHs were detected at least in one sample. From the 17 targeted NPAHs, 7 were detected in at least one high-volume sample. All total concentrations of the individual compounds and individual samples can be found in the Supplement, Tables S10-S14. Individual phases' concentrations are presented and discussed in a separate communication.

The spatial distribution of the concentrations of the different substance classes in both legs is shown in Fig. 2. The plot only shows the average concentration of each sampling stretch, which could also be impacted by individual local plumes at distinct times and locations. As visible in Figs. 1 and 2, the cleanest region, with the lowest concentration of all substance classes, was the Arabian Sea in the Indian Ocean. The average air concentrations (in brackets upper and lower estimate when using LOQ instead of LOQ/2 and 0 instead of LOQ/2, respectively) over the Arabian Sea were 0.59 (0.57-0.61) ng m^{-3}, 0.59 (no significant difference) ng m^{-3}, 47.8 (24.1-71.4) pg m^{-3} and 0.89 (0.29-1.49) pg m^{-3} for the $\sum_{27}$PAHs, $\sum_{19}$RPAHs, $\sum_{11}$OPAHs and $\sum_{17}$NPAHs, respectively. These concentrations are among the lowest ever reported levels of the PAHs and PAH derivatives. The air masses originated from the Indian Ocean and from parts of Somalia with no significant sources of PAHs or PAH derivatives (Fig. S3d). Similarly, findings from the same campaign for other air pollutants showed the lowest concentration over the Arabian Sea (Bourtsoukidis et al., 2019; Eger et al., 2019; Pfannerstill et al., 2019; Tadic et al., 2020; Wang et al., 2020). As shown in Fig. 2 a), c) and e), several samples in the Arabian Sea are missing in the first leg due to rejection as possibly contaminated by the stack of our research vessel *Kommandor Iona* (detailed overview of rejected samples and method description in Table S4 and Chapter S1.5.1, respectively). The Mediterranean Sea showed the highest average concentration of the $\sum_{27}$PAHs and $\sum_{11}$OPAHs, i.e. 4.40 ng m^{-3} and 0.37 ng m^{-3}, respectively. As illustrated in Fig. 2, the pollutant concentration over the Mediterranean Sea during the first leg differed from that of the second leg. The concentration of the $\sum_{27}$PAHs during the first leg (2.20 ng m^{-3}) was significantly lower ($p<0.05$, Student's t-test) than during the second leg (5.18 ng m^{-3}). The difference was also significant ($p<0.05$, Student's t-test) for the $\sum_{11}$OPAHs. The air mass histories (Fig. S2 and S3a) reveal that the difference is related to the different origin of the air masses. During the first leg, the sampled air predominantly originated from northern Africa and the western Mediterranean Sea, while during the second leg, the prevailing air masses came from north, transporting polluted air from large parts of Europe, including coastal areas and islands as also reported by Tadic et al. (2020). The northerly wind is a typical large-scale circulation pattern in summer

over the Mediterranean Sea (Lelieveld et al., 2002). The highest concentrations of the PAH derivatives throughout the entire cruise were found in sample D58 in the Mediterranean Sea close to Sicily. The concentrations of $\sum_{11}$OPAHs and $\sum_{17}$NPAHs were 1.42 ng m^{-3} and 46.5 pg m^{-3}, respectively. Sample D54, sampled 400 km south-east of Sicily, showed the highest concentration of the $\sum_{27}$PAHs, especially of the low-molecular-weight PAHs (2-3-ring PAHs). These samples will be evaluated in more detail in Sect. 3.3.4.

The concentration of the $\sum_{17}$NPAHs was similar during both legs in the Mediterranean Sea. On the one hand, 2-NFLT and 2-NPYR were more abundant during the first leg, possibly due to higher secondary formation in aged air (Atkinson and Arey, 1994; Arey et al., 1986) On the other hand, the primarily emitted 1-NPYR (Atkinson and Arey, 1994) as well as 2-NNAP (having primary and secondary sources, Zhuo et al., 2017; Atkinson and Arey, 1994) had a higher concentration during the second leg. In contrast to the PAHs and OPAHs, the concentration of the $\sum_{19}$RPAHs in the air over the Mediterranean Sea was higher (not significant, p=0.14, Student's t-test) and not lower during the first leg compared to the second leg. The different result for the RPAHs can firstly be explained by the different sampling intervals of the air sampler for the RPAHs (see Table S1). The RPAHs were not collected at the end of the campaign close to Sicily and Sardinia, where a high burden of PACs was measured. Second, north of Egypt in the Mediterranean Sea, close to the Suez Canal during the first leg, high concentrations of the MPHEs and M_2PHEs were found, possibly due to intense marine traffic concentrating or even queueing before entering into the Suez Canal.

The average concentration of the $\sum_{17}$NPAHs over the Mediterranean Sea was 5.23 pg m^{-3}, which was slightly higher than the average concentration over the northern Red Sea (4.52 pg m^{-3}) and the Gulf of Oman (4.37 pg m^{-3}) but slightly lower than the average concentration over the Arabian Gulf (6.65 pg m^{-3}). The concentration of the $\sum_{19}$RPAHs over the Mediterranean Sea (0.81 ng m^{-3}) was similar to the Gulf of Oman (0.83 ng m^{-3}) and lower than over the Arabian Gulf (1.12 ng m^{-3}), too. Similar to the NPAHs and RPAHs, most other air pollutants (e.g. non-methane hydrocarbons, carbonyl compounds, NO_x, NO_z, O_3, SO_2) measured during the AQABA campaign showed the highest concentration in the Arabian Gulf (Bourtsoukidis et al., 2019; Eger et al., 2019; Pfannerstill et al., 2019; Tadic et al., 2020; Wang et al., 2020; Friedrich et al., 2021).

The concentration of the $\sum_{17}$NPAHs over the southern Red Sea was 1.68 pg m^{-3}. Similar as for the $\sum_{17}$NPAHs, the southern Red Sea was the region with the second lowest concentrations of the $\sum_{27}$PAHs and the $\sum_{11}$OPAHs (0.94 ng m^{-3} and 88.3 pg m^{-3}, respectively). The pollutant burden was low since the air was predominantly coming from eastern Africa, mainly from Sudan, Eritrea and western and southern parts of Egypt (Fig. S3c), areas with low population and industrial emitter densities. Air over the northern Red Sea, including the Suez Canal, is more polluted owing to the dense shipping traffic in the canal (Bourtsoukidis et al., 2019), the vicinity of the megacity Cairo and the densely populated and urbanised Nile Delta. The total concentration of the $\sum_{19}$RPAHs over the northern Red Sea was 0.93 ng m^{-3}. The highest concentration was measured in air close to Jeddah, which was almost one order of magnitude higher polluted than the other samples.

As shown in Fig. 1, the Gulf of Oman and the Arabian Gulf were similarly polluted as the northern Red Sea. The concentrations of the $\sum_{27}$PAHs and the $\sum_{11}$OPAHs were higher (but not significantly according to Student's t-test) in the Arabian Gulf (2.8 ng m^{-3} and 181 pg m^{-3}, respectively) compared to the Gulf of Oman (2.0 ng m^{-3} and 161 pg m^{-3},

respectively). The air masses sampled in the Gulf of Oman were mainly transported from Oman, United Arab Emirates, Iran and the Arabian Sea (Fig S3e). The predominant wind direction in the Arabian Gulf during the first leg was northwest transporting air from Qatar, Bahrain, Kuwait and Iraq (Fig S3f, 28-30 July 2017), while during the second leg, the wind changed to northeast, increasing the contribution of air advected from Iran (Fig. S3f, 4-6 August 2017). A significantly higher ($p<0.05$, Student's t-test) concentration of the $\sum_{27}$PAHs prevailed during advection from northeast (second leg, 3.53 ng m^{-3}) than from northwest (first leg, 1.69 ng m^{-3}).

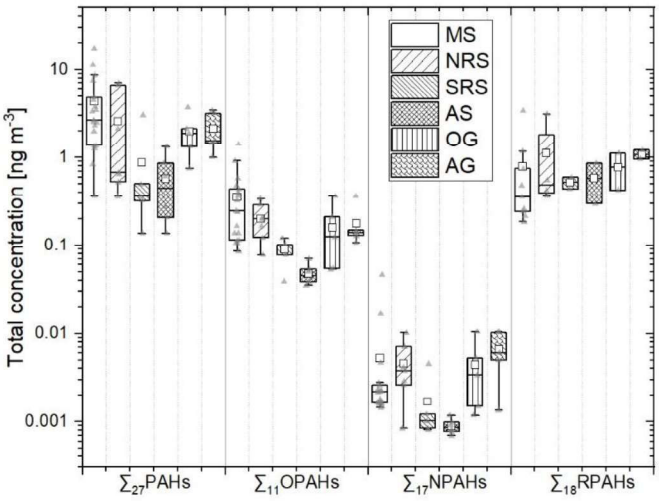

Figure 1: Total concentration (gas + particulate phase) of PAC groups across sea regions (MS: Mediterranean Sea; NRS: northern Red Sea; SRS: southern Red Sea; AS: Arabian Sea; OG: Gulf of Oman; AG: Arabian Gulf; Empty square: mean value; Grey triangles: Measurement points (difficult to see within the boxed); Box with additional borders: interquartile range (IQR) bound by the 75th and 25th percentile and range of 1.5 IQR; Horizontal line: Median).

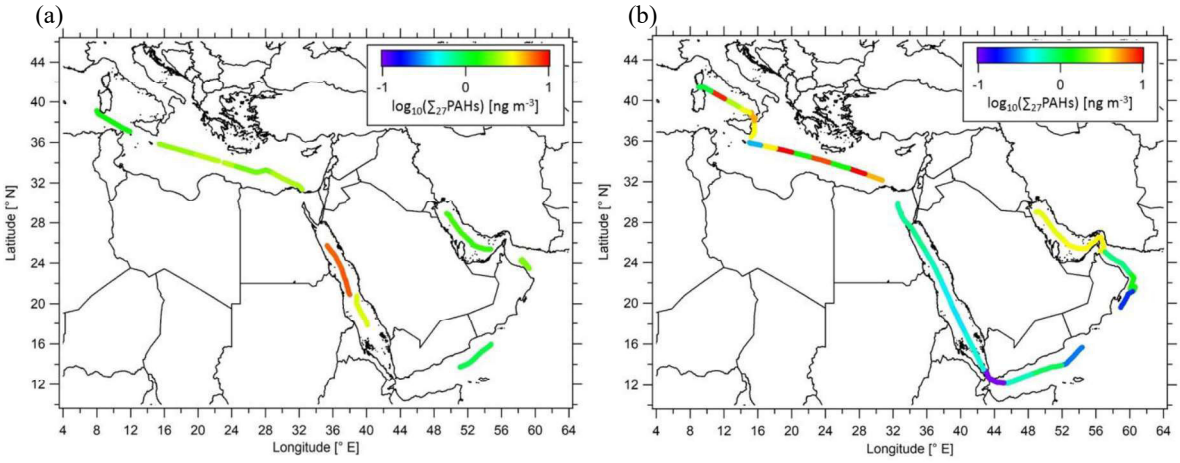

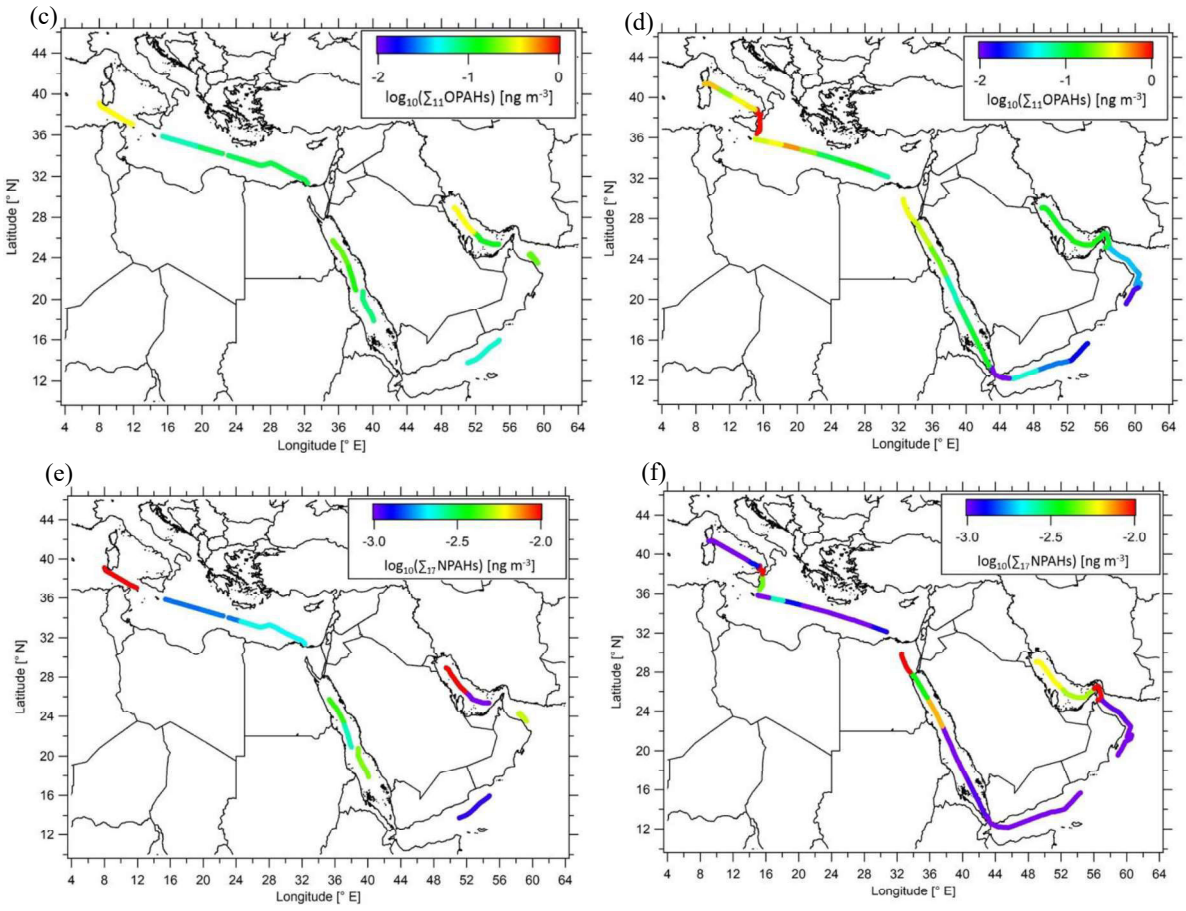

Figure 2: Total concentration (logarithmic scale) of $\sum_{27}$PAHs, in (a) and (b), $\sum_{11}$OPAHs in (c) and (d) and $\sum_{17}$NPAHs in (e) and (f) during the first leg in (a), (c), (e) and the second leg in (b), (d), (f). Spatial resolution of data limited to sampling stretches (see Fig. S1).

The concentrations of the PAH derivatives in a few samples in the remote sea regions were among the lowest ever reported, while other samples reached concentration levels previously found at suburban sites. The samples from near Sicily and Sardinia in the Mediterranean Sea, near the Suez Canal and over the Gulfs showed a total concentration of 0.1-1.4 ng m^{-3} and 1.2-47 pg m^{-3} for the $\sum_{11}$OPAHs and $\sum_{17}$NPAHs, respectively. The concentrations of the individual substances are similar to air samples from a rural and an urban site in Chile (Scipioni et al., 2012), a rural site in France (Albinet et al., 2007), a suburban site in the USA (Bamford and Baker, 2003) and a background site in the Czech Republic (Nežiková et al., 2021). NPAHs and OPAHs have rarely been examined in the marine environment. A study by Lammel et al. (2017) investigated the 3–4-ring NPAHs in the eastern Mediterranean under the influence of long-range transport from central and eastern Europe in summer 2012. The concentration of the $\sum_{11}$3–4-ring NPAHs (23.7 pg m^{-3}) was one order of magnitude higher than the concentration of the sum of the same NPAHs in the Mediterranean Sea in our study (2.75 pg m^{-3}). The concentration of the

samples with the lowest urban influence, found by Lammel and colleagues, were closer to our observed concentrations. In contrast to the NPAHs, the concentration of the $\sum_6$4-ring PAHs was in the same order of magnitude. Lammel and colleagues found 426 pg m^{-3} as average of all samples and 284 pg m^{-3} as average of the samples with the lowest urban influence, while we determined a concentration of 366 pg m^{-3} for the sum of the same PAHs. From the same study, Lammel et al. measured 1-NPYR, 2-NFLT and 2-NPYR in marine background air being 0.21, 1.68 and 0.92 pg m^{-3}, whereas respective concentrations were 0.42, 0.93 and 0.069 pg m^{-3} in air over the whole transect of the Mediterranean Sea of our campaign. The lower levels of secondarily formed 2-NFLT and 2-NPYR can be explained by significant long-range transport from NO_x poor areas, notably northern Africa during the first leg. One decade earlier, in the eastern Mediterranean Sea in summer 2001, Tsapakis and Stephanou (2007) report approximately one order of magnitude higher values, i.e. 29 and 21 pg m^{-3} for 2-NFLT and 2-NPYR, respectively. Furthermore, they determined 9,10-O_2ANT and 9-OFLN (34.2 and 46.3 pg m^{-3}, respectively), which was in the same range as our measurements in the Mediterranean Sea with 95.4 and 36.2 pg m^{-3}, respectively.

The concentrations of NPAHs (40, 90 and 60 pg m^{-3} for 1-NPYR, 2-NFLT and 2-NPYR, respectively) in source regions of the Mediterranean such as Athens (Marino et al., 2000) were approximately three orders of magnitude higher than those in our study over the Mediterranean Sea. This urban to marine background gradient is a lot smaller for the OPAHs compared to the NPAHs. In summer 2013, Alves et al. (2017) found at a suburban site in Athens an air concentration of 9, 28 and 242 pg m^{-3} for 9,10-O_2ANT, 9-OFLN and BAN, respectively. This is one order of magnitude lower for 9,10-O_2ANT, the same magnitude for 9-OFLN and one order of magnitude higher for BAN compared to our results in the Mediterranean Sea. This suggests longer lifetimes or higher formation rates of OPAHs than NPAHs.

Harrison et al. (2016) measured PAHs and its derivatives at three sites along the east coast of the Red Sea, in a plume of a major point source (petrochemical complex). 9,10-O_2ANT had a concentration between 3.15 and 4.02 ng m^{-3}, which is two orders of magnitude higher than in the particulate phase of samples over the northern Red Sea in our study. The concentration of 5,12-O_2NAC was between one and two orders of magnitude higher, while the difference was smaller for 7,12-O_2BAA. The difference of the individual NPAHs concentrations between the measurements at the coast from Harrison et al. and our measurements offshore is even more pronounced. The concentrations of 2-NNAP, 2-NFLT, 1-NPYR, 2-NPYR and 7-NBAA were over three orders of magnitude higher in the plume measured by Harrison and colleagues. In contrast, the PAH concentration was almost similar (for low-molecular-weight PAHs) or only one order of magnitude higher (for high-molecular-weight PAHs, i.e. 5-7-ring PAHs) onshore. This, again, points to short atmospheric lifetimes of NPAHs. The OH reaction rate coefficients of PAHs and NPAHs are similar (Table S2, US EPA, 2019), but NPAHs are more prone to photolysis (Fan et al., 1996; Keyte et al., 2013; Wilson et al., 2020). This is furthermore supported by findings that the NPAH/PAH ratios in mid-latitudes are higher in winter than in summer, obviously since the photochemical sink of NPAHs in summer overcompensates the higher formation potential as a source of NPAHs (Nežiková et al., 2021). Nassar et al. (2011) measured PAHs and two NPAHs in the area of Greater Cairo. The concentration of 1-NPYR in the study was around one order of magnitude higher than that in the air measured on the ship over the Suez Canal. In contrast, the concentration of

the low-molecular-weight PAHs was in the same range, while the concentrations of high-molecular-weight PAHs offshore were one or more orders of magnitude lower.

Few studies report MPHE and M_2PHE in the coastal marine atmosphere, the open sea, background and urban sites. Tsapakis and Stephanou (2005) analysed atmospheric samples collected offshore over the eastern Mediterranean Sea and at a background station in north-eastern Crete (Greece) and reported total (gas and particulate phase) concentrations for ∑MPHE of 13.6 ng m^{-3} and for ∑M_2PHE of 6.5 ng m^{-3}, respectively. Mandalakis et al. (2002) reported gas and particulate phase concentrations of 6.07 ng m^{-3} and 3.17 ng m^{-3} for ∑MPHE and ∑M_2PHE, respectively, in the Saronikos Gulf, which is impacted by busy marine traffic and the shipyard industry along the coast (Valavanidis et al., 2008). In the same study, corresponding concentrations of 6.95 ng m^{-3} for ∑MPHE and of 4.17 ng m^{-3} for ∑M_2PHE were reported for the urban atmosphere of Athens, and respectively 0.52 ng m^{-3} and 0.34 ng m^{-3} for the background urban agglomeration. The concentrations in our study were comparably to the background concentrations, i.e. 0.51 ng m^{-3} and 0.33 ng m^{-3} for ∑MPHE and ∑M_2PHE, respectively.

The results of the ∑MPHE in the gas phase (0.47 ng m^{-3}) in our study are also comparable to concentrations over the south-eastern Mediterranean Sea and the Aegean Sea measured by Castro-Jiménez et al. (2012), i.e. 0.58 ng m^{-3} and 0.61 ng m^{-3}, respectively, but lower than over the western Mediterranean Sea, the Ionian Sea and the Black Sea. On an Atlantic Ocean transect from the Netherlands to South Africa, concentrations of 1-MPHE as low as 0.022 ng m^{-3} were reported, compared to 0.45 ng m^{-3} for samples taken closer to Europe and western Africa (Jaward et al., 2004). In our study 1-MPHE ranged between 0.026 and 0.49 ng m^{-3}.

3.2 Composition patterns

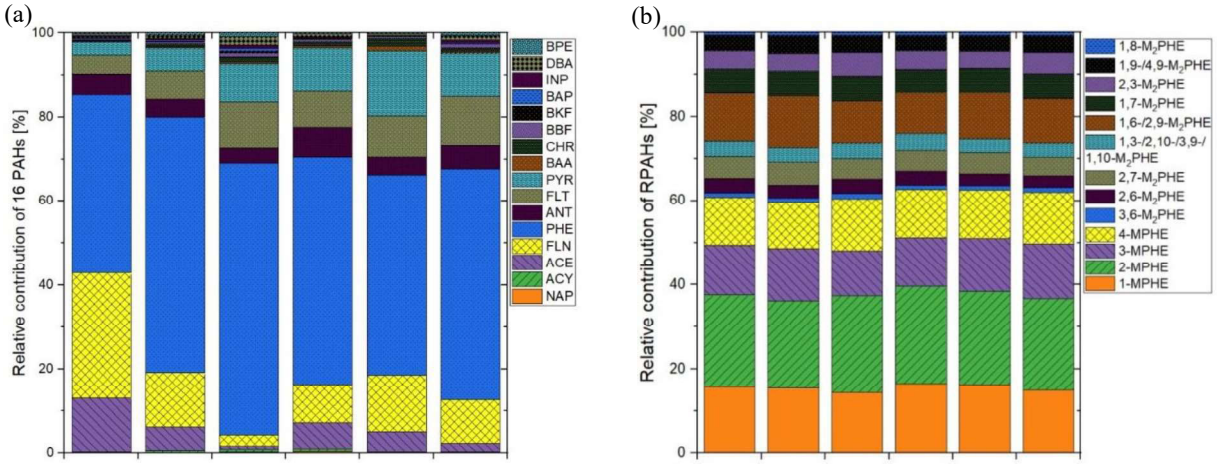

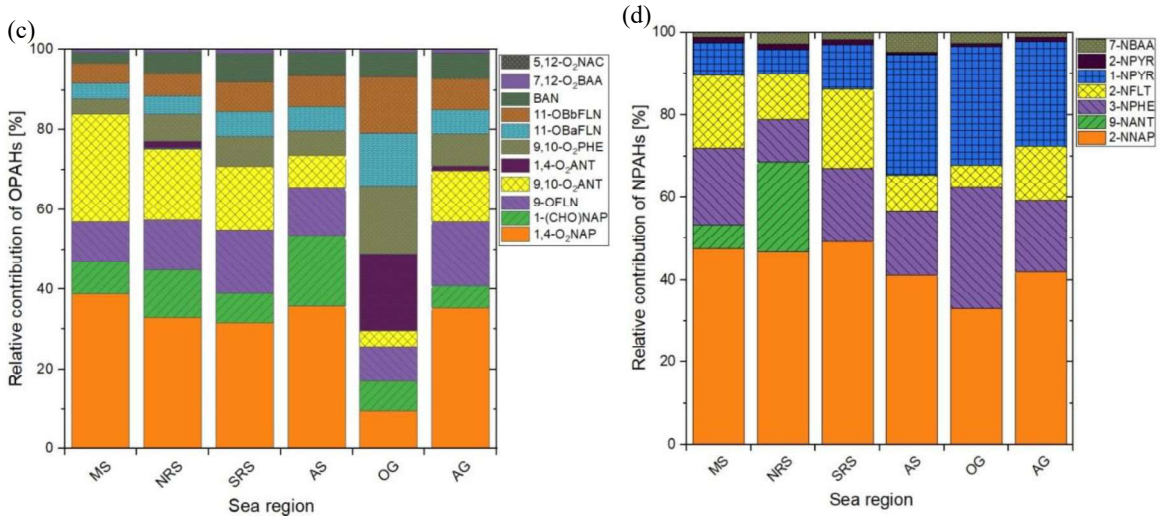

360 **Figure 3: Relative amount of (a) 16 EPA-PAHs, (b) RPAHs, (c) OPAHs, (d) NPAHs across sea regions (MS: Mediterranean Sea; NRS: northern Red Sea; SRS: southern Red Sea; AS: Arabian Sea; OG: Gulf of Oman; AG: Arabian Gulf). Full names of the substances are given in Sects. 2.3.1, 2.3.2 and Tables 1 and S2.**

3.2.1 PAHs

The substance patterns of PAHs in the six different sea regions are shown in Fig. 3a. PHE was by far the most abundant
365 PAH in all regions (average contribution of 49 %), followed by FLN, ACE, FLT and PYR with average contributions of 24 %, 10 %, 6 % and 5 %, respectively. It can be noted that the PAH composition patterns were similar in all regions. However, the patterns of the Mediterranean Sea and the southern Red Sea differed from the other regions. The contribution of PHE in the southern Red Sea was higher than the average, while it was lower than the average in the Mediterranean Sea. The opposite could be observed for FLN. The different pattern in the Mediterranean Sea was mainly caused by the samples from
370 the second leg with high influence of aerosols from Europe.

3.2.2 RPAHs

The distribution pattern of RPAHs among the campaign regions is presented in Fig. 3b. The RPAHs did not show significant regional differences in the composition pattern. 2-MPHE, 1-MPHE and 3-MPHE were the most abundant alkylated PAH species throughout the campaign, making up 22 %, 16 % and 12 % of the total RPAHs measured. Among the M_2PHEs, 1,6-
375 and 2,9-M_2PHE were the most abundant compounds.

3.2.3 OPAHs

As shown in Fig. 3c, the regional differences between the OPAH composition patterns are more pronounced than the regional average PAH and RPAH patterns. 1,4-O_2NAP, 9,10-O_2ANT and 9-OFLN were the most abundant OPAHs, with an average contribution of 35 %, 22 % and 11 %, respectively. The high share of 9,10-O_2ANT and 9-OFLN was also found at

several continental sites (Albinet et al., 2007; 2008; Li et al., 2015; Wei et al., 2015; Drotikova et al., 2020; Lammel et al., 2020; Jariyasopit et al., 2021; Nežiková et al., 2021). In several of these papers, 1,4-O_2NAP was not measured. Nežiková et al. (2021) and Jariyasopit et al. (2021) only found small relative amounts of 1,4-O_2NAP at the continental background site Košetice and in the Athabasca oil sands region in Canada, respectively. In contrast, Wei et al. (2015) and Lammel et al. (2020) found relatively high contributions to the total amount of OPAHs at urban sites in China and in the Czech Republic, respectively. Bandowe et al. (2014) observed higher concentrations of 1,4-O_2NAP in summer in $PM_{2.5}$ compared to the cold season, although the partitioning of the compound will be shifted to the gas phase in summer. This would lead to lower concentrations in summer since the degradation rates of most PACs are expected to be higher in the gas phase (Feilberg et al., 1999; Keyte et al., 2013). They hypothesized that 1,4-O_2NAP is significantly formed by secondary formation, as also shown by Kautzman et al. (2010) and Keyte et al. (2013). This can be supported by the low winter to summer ratio of 1,4-O_2NAP despite higher emissions in winter at Košetice (Nežiková et al., 2021). High secondary formation in plumes especially in the Mediterranean Sea and the Arabian Gulf (as explained in Sect. 3.3.4), as well as low reaction rates for the degradation of 1,4-O_2NAP compared to all other OPAHs (Table S2, Atkinson et al., 1989) might explain the high relative contribution of this quinone in our study. Except for the samples from the Gulf of Oman, 1,4-O_2NAP always had the highest contribution of 25-40 %. This quinone is frequently reported having a high ability to produce reactive oxygen species (Charrier and Anastasio, 2012; Verma et al., 2015).

In the Gulf of Oman, the contribution from high-molecular-weight OPAHs (4-ring OPAHs) was higher compared to the other regions. The composition pattern of the samples from the Arabian Sea differed from the other samples because of a lower share of 9,10-O_2ANT and a higher share of 1-(CHO)NAP. The same was true for the samples of the first leg in the Mediterranean Sea (see Table S16). 1-(CHO)NAP has been reported prominent among OPAHs from urban and other polluted sites, but not generally (Albinet et al., 2007; 2008 (partly); Wei et al., 2015; Tomaz et al., 2016; Lammel et al., 2020 (in Kladno)).

3.2.4 NPAHs

Similar to the OPAHs, the regional differences in the NPAH composition pattern are more pronounced than the PAH and RPAH patterns. As illustrated in Fig. 3d, the most abundant NPAHs were 2-NNAP, 3-NPHE, 2-NFLT and 1-NPYR, with an average contribution of 45 %, 18 %, 15 % and 12 %, respectively. The contribution of 2-NNAP ranged between one third and half in all regions. However, it was not detected above LOQ in the gas phase of samples from the Arabian Sea. Due to the total detection frequency of >30 %, the values were replaced by LOQ/2 what could lead to an overestimation in this case. A large fractional contribution of NNAPs, 3-NPHE and 2-NFLT was also found by Lammel et al. (2017) in the eastern Mediterranean Sea. At the continental site in the study from Lammel et al., as well as in other previous studies at continental sites, 2-NFLT, 9-NANT and 1-NNAP were the most abundant NPAHs (Bamford and Baker et al., 2003; Albinet et al., 2007; 2008; Tomaz et al., 2016; Drotikova et al., 2020; Lammel et al., 2020; Nežiková et al., 2021). In our study, 9-NANT had a significant contribution only in the northern Red Sea. We found only a few samples with 9-NANT >LOQ (LOQs in Table

S6c). The reason for the low contribution during the entire campaign might be the relatively high LOQ compared to other NPAHs (Table S6c) or that 9-NANT is prone to photolysis, which could have been high in this campaign because of high solar irradiation. The significance of photodegradation of 9-NANT is also supported by lower contributions in summer compared to the cold season, as found by Tomaz et al. (2016) and Nežiková et al. (2021). However, it can also be caused by seasonal variation in the emission sources or a higher degradation rate in the gas phase based on the significantly lower particulate fraction in summer (Tomaz et al., 2016; Nežiková et al., 2021). The same might be true for 1-NNAP. In contrast to our campaign, several other studies found significant amounts of 1-NNAP in air samples at mid-latitude but continental sites (Bamford and Baker et al., 2003; Albinet et al., 2007; 2008; Tomaz et al., 2016; Drotikova et al., 2020, Lammel et al., 2020; Nežiková et al., 2021). The low contribution of 1-NNAP in air over the Mediterranean and around the Arabian Peninsula could also be due to the relatively high LOQ in PUFs (Table S6c) or the photodegradation of 1-NNAP, which is faster than of 2-NNAP, as described by Feilberg et al. (1999). We hypothesize that the comparably low rate constants for the photodegradation as well as for the reaction with OH (Table S2, US EPA, 2019) are one reason for the high relative contribution of 2-NNAP. 2-NNAP is frequently detected in continental sites but mostly with lower relative contributions than 1-NNAP, 9-NANT and 2-NFLT (Bamford and Baker et al., 2003; Albinet et al., 2007; 2008; Tomaz et al., 2016; Drotikova et al., 2020, Lammel et al., 2020; Nežiková et al., 2021). Only at a remote site in Chile, 2-NNAP was also found to have a very high relative contribution, which was explained by direct emissions or transport assuming a long atmospheric lifetime (Scipioni et al., 2012). The resistance to photochemical degradation can also be supported by the finding from Nežiková et al. (2021) that the relative contribution of 2-NNAP is higher in summer than in winter. However, this can also be due to different emission sources or stronger secondary formation in summer (Zhuo et al., 2017).

The fractional contribution of 1-NPYR is high in the Gulf of Oman and the Arabian Gulf. This can be explained by a significant amount of 1-NPYR in the exhaust of fossil fuel combustion (IARC, 2018; Zhao et al., 2015) and its high abundance near petrochemical industries (Caumo et al., 2018). It is used as a marker for primary emissions since it does not have significant secondary sources (Arey et al., 1986). The relatively short estimated lifetime of 1-NPYR in air due to photodegradation (Feilberg and Nielsen, 2000) and the small reaction rate with OH (Table S2, US EPA, 2019) could explain its low contribution in the Mediterranean Sea, since we sampled relatively aged air samples in that region. The relatively high contribution of 1-NPYR in the Arabian Sea might be due to bypassing ships (Table S18) as we found 1-NPYR highly abundant in the ship exhaust (Sect. 3.3.1). The high contribution of 1-NPYR in samples D40-42, in or close to the Gulf of Aden, is possibly due to pollution from coastal cities in the northeastern province of Somalia. The continental influence of these samples is also shown in the results of the PMF analysis (Fig. 4b). The large contribution of long-range transported aerosols in the Mediterranean Sea is also illustrated by the high contribution of 2-NFLT, which is formed in secondary processes (Arey et al., 1986). The contribution of 2-NFLT is also high in the southern Red Sea and the Arabian Sea, two regions with minor influence of primary emissions but higher fraction of long-range transported aerosols. 3-NPHE, which has primary and secondary sources (Atkinson and Arey, 1994; Heeb et al., 2008; Ringuet et al., 2012a), has an almost similar contribution in all regions. This could be explained by various different sources or a long mean atmospheric lifetime.

3.3 Source apportionment

3.3.1 Sources of PAH derivatives by PMF

As shown in Figs. 4 and S4 as well as described in the Supplement (Chapter S2.4.1), the PMF analysis, revealed five different source factors, namely fresh and aged shipping emissions, continental emissions, residual oil combustion and desert dust.

The PAHs, NPAHs and OPAHs in the air over the Mediterranean Sea and in the seas around the Arabian Peninsula are believed to originate primarily from fresh and aged shipping emissions. Fresh shipping emissions, mainly from the ship stack of our research vessel *Kommandor Iona*, were predominantly apparent during the first leg due to the prevailing wind direction. Aged shipping emissions contributed to air pollution mainly in regions with congested marine routes such as the Suez Canal (4 July 2017 and 20-23 August 2017), the Bab al-Mandab Strait near Djibouti (16-17 July 2017) and the Strait of Hormuz, especially near Fujairah (26-28 July 2017 and 5-6 August 2017). The amount of bypassing ships, potentially influencing the sampled air, based on the data from Celik et al. (2020), is given in Table S18.

Another important source of PAH derivatives were continental emissions. Based on the distribution of residence times of air masses during these sampling times, we could conclude that these emissions mainly came from Europe (especially received in the Mediterranean Sea, but also in the Arabian Gulf), countries around the Arabian Gulf (mainly received there) and Egypt (mainly received in the northern Red Sea). Furthermore, the PACs originated from residual oil combustion. High factor contributions (Figs. 4b and S4b) in the period between 24 July and 6 August 2017 were linked to the samples collected in the Gulf of Oman and the Arabian Gulf and influenced by the emissions in the coastal areas and offshore (Fig. S3e and f) as also reported by Bourtsoukidis et al. (2019), Eger et al. (2019), Pfannerstill et al. (2019) and Wang et al. (2020). The source factor identified with minimum contributions of NPAH and OPAHs was desert dust. The finding of PAH derivatives in the factor desert dust could be explained by mixing of dust with other emissions sources such as continental pollution or shipping emissions. The concentration of the factor desert dust peaked primarily during a period of Sahara dust outbreaks (from 13-18 July 2017), while samples were collected over the Red Sea and over the western part of the Gulf of Aden (Fig. S3c and d, see also Eger et al. (2019)). Dust emitted on the Arabian Peninsula is evident during the sail in the Gulf of Oman and the Arabian Gulf (24 July and 6 August 2017, Fig. S3d and e) but mixed with several other sources.

The contribution of the individual OPAHs and NPAHs can be seen in PMF group 2 in Figs. 4 and 5, showing the relative contributions of each factor to the concentration of each substance. All PACs targeted in the PMF run (group 2) had a significant contribution from fresh shipping emissions as their source. Moreover, by comparing several samples with a significant influence of the exhaust from the own stack (samples D16; 17; 20; 22; 23; 28; 37; 38; see Table S4 and Fig. S4) to the stack filtered regional average concentrations, we could show that almost all detected PAHs, NPAHs and OPAHs were elevated in the samples with fresh shipping emissions (Table S17). 1-NPYR showed the highest ratio of contaminated to filtered samples among the NPAHs, while 11-OBaFLN and 1-(CHO)NAP had the highest ratio among the OPAHs. All targeted OPAHs showed a ratio higher than 1. For the NPAHs, only 2-NFLT was not elevated except for a ratio of 5 in the

Arabian Sea. 2-NFLT had been reported to be present in diesel particulate matter (Bamford et al., 2003; Zimmermann et al., 2012). However, this was explained by the gas phase formation of 2-NFLT after emission during sample collection. Surprisingly, the concentration of 2-NPYR was significantly elevated in the fresh shipping emissions. This is unexpected, as 2-NPYR was reported absent in diesel exhaust (Bamford et al., 2003) and believed to be formed through secondary formation only (Finlayson-Pitts and Pitts, 1999; Wilson et al., 2020). Zhao et al. (2019; 2020) found significant amounts of 2-NPYR in ship exhaust gas depending on the fuel type and the engine loading. They report high emissions of this compound, especially with heavy fuel oil use and mainly under low engine speeds. The abundance of 2-NPYR was explained by secondary formation due to higher NO_x emissions and higher residence times during these conditions. The results from Zhao et al. (2019; 2020) and from our study suggest a very high formation rate of 2-NPYR. According to Keyte et al. (2013) and Wilson et al. (2020), the reaction rate constant of PYR with OH is five times higher for 2-NPYR compared to 2-NFLT but the yield of 2-NPYR is lower.

The large contribution of aged shipping emissions to the concentration of 2-NFLT and 2-NPYR (Fig. 5) illustrates the importance of secondary formation of these two NPAHs. In contrast, 1-NPYR is not abundant in the aged shipping emissions showing that there is no significant secondary formation. It has been reported that 1-NPYR arises solely from primary emissions (Bezabeh et al., 2003; Reisen and Arey, 2005). The contribution of aged shipping emissions to the occurrence of 3-NPHE could either be explained by the higher atmospheric half-life of 79 h compared to 2-NFLT, 1-NPYR and 2-NPYR (Table S2, US EPA, 2019) or by secondary formation as previously suggested (Tomaz et al., 2017). All detected OPAHs were abundant in the aged shipping emissions. Their abundance points to a long lifetime or formation in the atmosphere. The relative contributions of 11-OBaFLN, BAN and 7,12-O_2BAA were relatively small (Fig. 5). For 5,12-O_2NAC and 1,4-O_2NAP, the contribution of aged shipping emissions was higher. It was previously reported that from the measured OPAHs, 1,4-O_2NAP, 1-(CHO)NAP, 9-OFLN, 9,10-O_2ANT, 1,4-O_2ANT, 9,10-O_2PHE, 11-OBaFLN and 7,12-O_2BAA can be formed from the reaction of parent-PAHs with oxidants (Helmig and Harger, 1994; Perraudin et al., 2007; Wang et al., 2007; Gao et al., 2009; Ringuet et al., 2012a; Keyte et al., 2013; Dang et al., 2015). Based on the previous findings from literature and the results of the PM factor “aged shipping emissions”, a contribution from secondary formation to the burden of 1,4-O_2NAP and 7,12-O_2BAA is likely, in addition to the known secondarily formed substances 2-NPYR and 2-NFLT. Since BAN and 11-OBaFLN have not been found as secondary formation products but highly abundant in primary emissions (Albinet et al., 2007; Ringuet et al., 2012a; Clergé et al., 2019), we hypothesize that their contribution to aged shipping emissions is only due to their atmospheric lifetime. Since the primary emitted 1-NPYR is not abundant in aged shipping emissions, it shows that BAN and 11-OBaFLN have a higher atmospheric lifetime than 1-NPYR. Since the estimated lifetime due to oxidation by OH is higher for 1-NPYR than for the two OPAHs (Table S2, US EPA, 2019), degradation of 1-NPYR is expected to be governed by photodegradation (Feilberg and Nielsen) as already mentioned in Sect. 3.2.4. Since there is not much data in the literature about 5,12-O_2NAC, it’s abundance in aged shipping emissions can either be due to high atmospheric lifetime or secondary formation.

1-NPYR and 3-NPHE seem to be good tracers for oil combustion, hence the correlation with emissions from the petrochemical industry in the Gulf of Oman and the Arabian Gulf. 1-NPYR and 3-NPHE are known to be emitted during combustion of oil (Streibel et al., 2017). In addition, all OPAHs included into the PMF, except for 1,4-O_2NAP, originated directly or secondarily from residual oil combustion.

Except for 11-OBaFLN, all considered PAHs, OPAHs and NPAHs are partly from continental pollution (Fig. 4a). The abundance of these air pollutants in continental pollution, including 11-OBaFLN, has been shown in many studies (Bamford and Baker, 2003; Albinet et al., 2007; 2008; Wei et al., 2015; Tomaz et al., 2016; Drotikova et al., 2020; Lammel et al., 2020; Nežiková et al., 2021). The missing contribution of continental pollution to the concentration of 11-OBaFLN might be because of its comparably low atmospheric half-life due to degradation by OH (Table S2, US EPA, 2019). Continental pollution was highly abundant in the Mediterranean Sea (Fig. 4b), where we found the highest concentrations of the OH radical of the entire AQABA campaign. 1,4-O_2NAP has a comparably high contribution of approx. 50 % by this factor. As explained in Sect. 3.2.3, this might be explained by high relative concentrations at the source, high atmospheric lifetime and secondary formation during the transport of the air to the sampler. In contrast, 1,4-O_2NAP seems to be significantly less abundant in pollution from the combustion of residual oil (Fig. 4a) and marine diesel (Table S17). However, more research is needed to evaluate this aspect in more detail. All PACs are abundant in desert dust, except for BAP and 2-NPYR. The presence of PAHs and PAH derivatives, especially 1-NPYR and 1,4-O_2NAP in the factor desert dust (Fig. 4a) may indicate co-emissions of dust and PACs in the region (e.g. close to onshore industries).

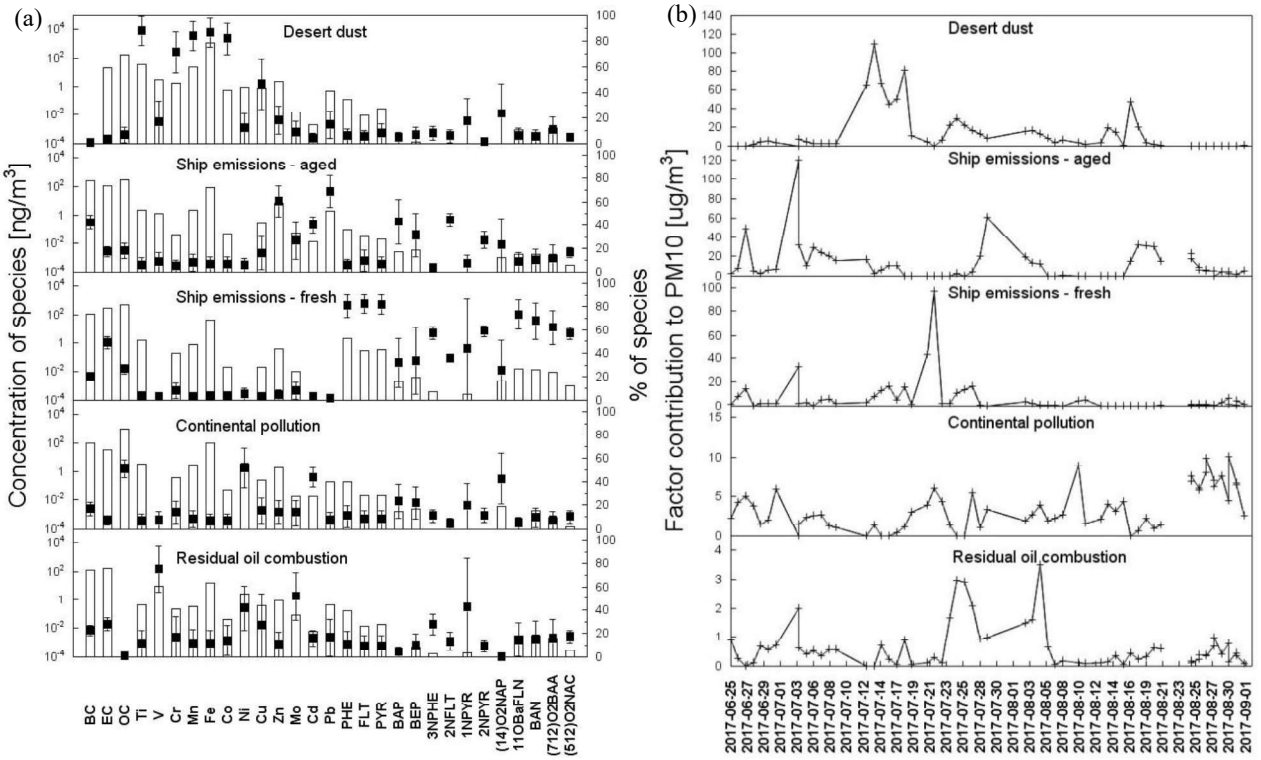

530

Figure 4: PMF group 2: (a) Factor profiles (Bars: Concentration of the species, black squares: Percentage of the species explained, box: Displacement (DISP) average, whiskers: DISP max and DISP min) and (b) time series of factor contributions to sample composition.

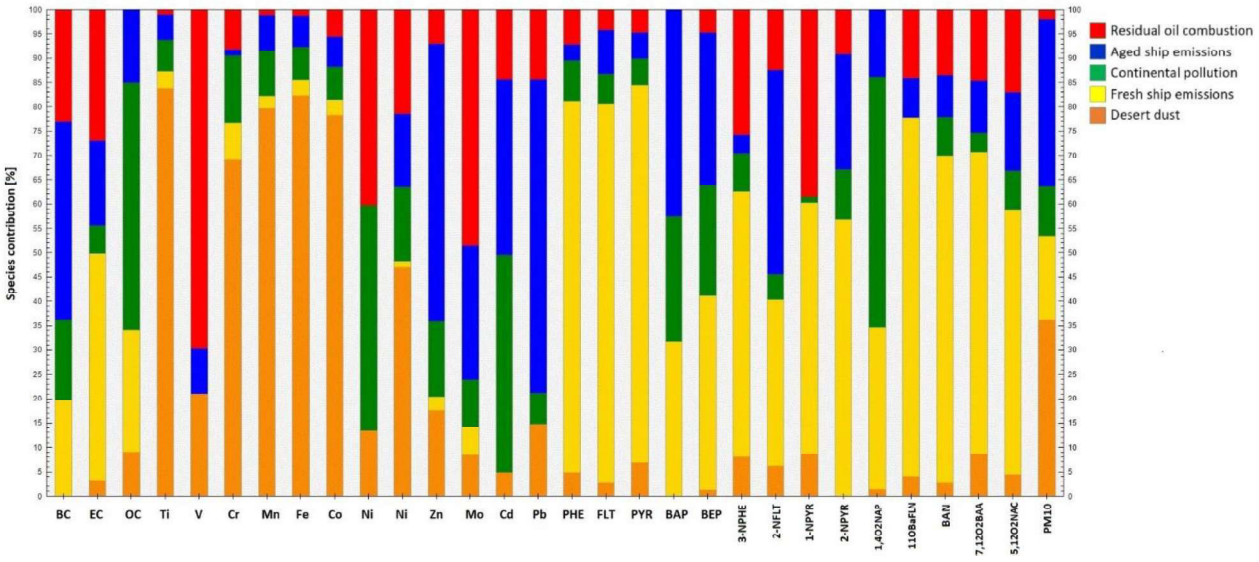

535 **Figure 5: Relative contribution of the five factors resolved by PMF to the concentration of each substance in PMF group 2.**

3.3.2 Source attribution by PAHs and alkylated PAHs

The ratio of the particulate concentration of BAP to BAP+BEP is often used as a marker for the ageing of atmospheric particles since photodegradation of BAP is faster than of BEP (Tobiszewski and Namieśnik, 2012). A concentration ratio BAP/(BAP+BEP) of less than 0.5 indicates photochemically aged aerosols. The ratio was <0.5 in all regions and ≈0.5 in the Arabian Sea (see Fig. S5). The somewhat elevated ratio in the Arabian Sea might be caused by local ship plumes (for number of encounters see Table S18; identification based on Celik et al. (2020)) and other offshore emissions, which contributed to the mostly long-range transported and aged air pollution in the region. This is also supported by Bourtsoukidis et al. (2019) studying non-methane hydrocarbons during the AQABA campaign.

The relatively low ratios in all other regions might be explained by the low amount of primary sources of air pollutants on sea except for ship traffic and some emissions from the offshore oil and gas industry. Thus, the pollution from urban and industrial areas, which are located mostly on the coast, is already slightly aged when reaching the sampler on the ship depending on the proximity to the emission sources. This could also be the explanation why the second-highest regional average values were found in the southern and the northern Red Sea receiving the emissions from the nearby coast as well as from the intense ship traffic in the region. The lowest regional average BAP/(BAP+BEP) values were detected in the Gulf of Oman and the Arabian Gulf. Air mass histories of sample D33 showed that a significant amount of aerosols came from less populated areas of Iran with a low amount of primary emissions (Fig. S3f, Wang et al., 2020). The results in the Mediterranean Sea can be divided into the first leg with a lower BAP/(BAP+BEP) ratio due to the prevalent westerly winds bringing aged air from Africa and from the sea and the second leg with higher ratios due to pollution from close European coastal areas and islands. The samples D58 and D49-52, close to Sicily and the Greek islands, respectively, showed the highest BAP/(BAP+BEP) ratios.

The ratio of ΣMPHE/PHE <1 indicates pyrogenic origin of PAHs for most days in the Red Sea, while a ratio of ΣMPHE/PHE >1 indicates petrogenic origin, i.e. from unburned fuel (Gogou et al., 1996), which occurred during the period from the 8-9 July 2017 in the northern Red Sea. Findings by Bourtsoukidis et al. (2020) could tentatively provide an explanation for the high ratio of ΣMPHE/PHE observed, namely degassing from the Red Sea Deep water.

The ratio of the sum of the four MPHE homologues to PHE (ΣMPHE/PHE) and the ratio 1,7-M2PHE /(1,7-M2PHE + 2,6-M2PHE) are given in Table S14. The distribution patterns and the concentration ratio 1,7-M_2PHE/(1,7-M_2PHE + 2,6-M_2PHE) may be interpreted by considering the emission sources of these compounds. Bläsing et al. (2016) characterised and compared patterns of alkylated PAHs in gaseous and particulate emissions from road traffic (diesel), domestic heating, inland navigation vessels (INVs) and ocean-going vessels (OGVs). The ratio of 1,7-M_2PHE/(1,7-M_2PHE + 2,6-M_2PHE) was used to distinguish the above-mentioned emissions. Thus, the ratio of 1,7-M_2PHE/(1,7-M_2PHE + 2,6-M_2PHE) for INVs (0.37–0.62) is comparable with that from road traffic and domestic heating. In comparison, 1,7-M_2PHE/(1,7-M_2PHE + 2,6-M_2PHE) for marine oil combustion (as used for OGVs) was 0.68 (Budzinski et al., 1995). In the present study, the calculated average ratios were 0.63 (first leg) and 0.66 (second leg) for the Mediterranean, 0.64 and 0.62 for the Red Sea, 0.66 and 0.71

for the Oman Gulf, 0.73 and 0.67 for the Arabian Gulf, respectively, and 0.61 (second leg) for the Arabian Sea. The calculated values for 1,7-M_2PHE/(1,7-M_2PHE + 2,6-M_2PHE) in the present study are within the range, 0.60-0.70, proposed by Bläsing et al. (2016) as an indicator for the emissions of OGVs.

3.3.3 Source attribution by NPAHs and OPAHs

Similar to the ratio of BAP/(BAP+BEP), the ratio of 2-NFLT/1-NPYR can indicate the photochemical age of aerosols. A ratio <5 shows the predominance of combustion sources, while a higher ratio indicates photochemically aged aerosols (Ciccioli et al., 1996). As illustrated in Fig. 6a, the highest regional average ratio of 2-NFLT/1-NPYR but also with the highest absolute and relative standard deviation was found over the Mediterranean Sea, followed by the southern and the northern Red Sea. However, the ratio was in only two samples (D1 and D58, collected over the Mediterranean Sea) higher than 5. In contrast, the ratio of BAP to BEP suggests aged aerosols in several samples as explained in Sect. 3.2.2.

The reason for the low incidence of high ratios could be that the concentrations of atmospheric oxidants OH and NO_3 radicals as well as NO_2 in some sea regions during the campaign were low (Bourtsoukidis et al., 2019; Tadic et al., 2020; Friedrich et al., 2021). The difference might be caused by different oxidants being responsible for degradation of BAP and formation of 2-NFLT. BAP, which is predominantly in the particulate phase, is mainly degraded by heterogeneous reaction with ozone (Shiraiwa et al., 2009), while 2-NFLT is mainly formed by homogeneous reaction of FLT with OH or NO_3 (Atkinson and Arey, 1994; Reisen and Arey, 2005) and subsequent reaction with NO_2. Ozone concentrations varied between 20 ppbv (in the Arabian Sea) and 150 ppbv (in the Arabian Gulf), while the variation of NO_x was higher (from 50 pptv in Arabian Sea to more than 10 ppbv in the northern Red Sea and the Arabian Gulf) (Tadic et al., 2020; Friedrich et al., 2021). The highest NO_x mixing ratios were found in the Northern Red Sea and the Gulf region, especially close to the Suez Canal, Kuwait and Fujairah (Tadic et al., 2020; Friedrich et al., 2021). NO_2 concentrations are generally significantly smaller in the marine environment than on land, as shown by satellite data (Roşu et al., 2019) due to the short lifetime (Schaub et al., 2007; Shah et al., 2020) and missing sources for NO_x on sea except for ship traffic and the offshore oil and gas industry. Friedrich et al. (2021) calculated NO_2 lifetimes of less than 6h during the AQABA campaign, which means that land-based NO_x emissions will be degraded before reaching the sampler for several samples, especially in parts of the Mediterranean Sea. Missing primary sources and high degradation due to high OH radical concentrations explain the low NO_x mixing ratios over the Mediterranean Sea (Friedrich et al., 2021). However, NO_2 is crucial for the formation of 2-NFLT competing with O_2 to either form NPAHs or OPAHs, respectively (Kamens et al., 1994; Finlayson-Pitts and Pitts, 1999; Atkinson and Arey, 2007).

The average 2-NFLT/1-NPYR ratio in air sampled over the Mediterranean Sea was significantly higher ($p<0.05$, Student's t-test) than in the air from Arabian Sea and the Gulf of Oman, respectively. Similarly, the ratio over the northern Red Sea was significantly higher ($p<0.05$, Student's t-test) than over both Gulf regions. In polluted air near the coast (e.g. as found in the Red Sea and at the beginning and the end of the campaign in the Mediterranean Sea) and in plumes (in samples D1, D30, D48 and D58), the 2-NFLT/1-NPYR ratio was high. These samples explain the high average 2-NFLT/1-NPYR ratio in the

Mediterranean Sea and the northern Red Sea. The ratio can rise during transport of the pollutants. However, the formation of 2-NFLT slows down or stops probably due to low concentrations of the parent-PAH (FLT), the atmospheric oxidants OH and NO_3 or NO_2 since formation of 2-NFLT depends on these reactants (Wilson et al., 2020). This was also shown by Lammel et al. (2017), who found much larger yields of 2-NFLT and 2-NPYR in the marine background with urban influence compared to the marine background without significant pollution sources.

In contrast to the regions with polluted air, a low ratio was observed in air over the Arabian Sea and in the parts of the Mediterranean Sea far from the coast. Due to these samples with low 2-NFLT/1-NPYR ratios in the Mediterranean Sea, the standard deviation of the regional average ratio is the highest among all sea regions. The average ratio in the Arabian Sea was only 0.36 (taking LOQ/2 values of 1-NPYR into account). This points to primary sources (as indicated in Sect. 3.3.2) and/or very low NO_2 concentrations in the sampled air masses, as shown by Friedrich et al. (2021). When secondary formation far away from sources is not significant anymore, the differences in characteristic time for chemical (which is primarily photolysis) and physical sinks (which is primarily particle deposition) determine the ratio 2-NFLT/1-NPYR. One influencing factor might be the difference in deposition velocity of the two compounds due to the different particulate fractions, which is lower for 2-NFLT (not shown, gas-particle partitioning is studied in a separate paper). A lower particulate mass fraction of 2-NFLT might lead to a slower deposition of this compound compared to 1-NPYR, which would lead to higher ratios. In contrast, a lower ratio would be the result of the faster degradation of 2-NFLT by OH and ozone compared to the degradation of 1-NPYR (Table S2, USEPA, 2019). In contrast, 1-NPYR is probably more prone to photodegradation, although the photodegradation rates strongly depend on the aerosol composition (Feilberg and Nielsen, 2000). The removal and degradation rates are reported to be approximately similar (Kamens et al., 1994; Fan et al., 1996; Feilberg and Nielsen, 2000; Albinet et al., 2008). However, this may not be the case in this study due to exceptionally low particulate mass fractions of the PACs due to the high temperature and the low EC and OC concentrations in the aerosols (Table S15). If degradation of 2-NFLT plays a larger role in the investigated regions, the ratio of 2-NFLT/1-NPYR would decrease with time, when there is no formation of 2-NFLT. This might be another explanation for the low 2-NFLT/1-NPYR ratios in some sea regions. However, more research is needed on the exact kinetics influencing the ratio, especially the photolysis rate coefficients. At continental sites, the ratio of 2-NFLT/1-NPYR mostly increases with distance to the emission source due to the significant formation of 2-NFLT (Ciccioli et al., 1996; Nežiková et al., 2021).

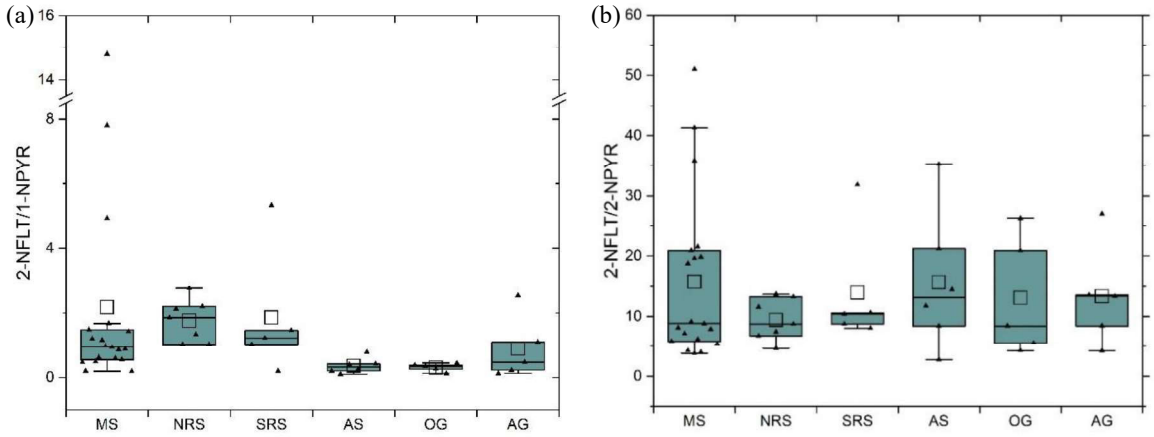

Figure 6: Box-Whisker plot of the ratios (a) 2-NFLT/1-NPYR and (b)2-NFLT/2-NPYR across sea regions (MS: Mediterranean Sea; NRS: northern Red Sea; SRS: southern Red Sea; AS: Arabian Sea; OG: Gulf of Oman; AG: Arabian Gulf; Empty square: mean value; Filled, grey triangles: Measurement points; Box with additional borders: interquartile range (IQR) bound by the 75th and 25th percentile and range of 1.5 IQR; Horizontal line: Median).

Since 2-NPYR is almost entirely formed by the reaction of PYR with OH radicals during daytime, while 2-NFLT can be formed by daytime reaction with OH as well as by nighttime reaction with NO_3, the ratio of 2-NFLT/2-NPYR can reveal the predominant formation pathway of NPAHs (Feilberg et al., 2001; Bamford and Baker, 2003). The main formation pathway during the campaign was the OH radical initiated formation, since the average concentration ratio of 2-NFLT/2-NPYR was 15.1 ± 11.6. This is close to a ratio of 5-10, suggesting the predominant formation of NPAHs by OH radicals and far from a ratio of >100, which would indicate reactions mainly involving the NO_3 radical. This result is similar to the findings by Tang et al. (2014) at a remote site on a Japanese peninsula. Lammel et al. (2017) determined even lower 2-NFLT/2-NPYR ratios in the eastern Mediterranean Sea, also pointing to a predominant NPAH formation by hydroxyl radicals.

As illustrated in Fig. 6b, the lowest average ratio (9.5) was found in the northern Red Sea, while the ratio of 15.8 (first leg: 22.3; second leg: 13.4) in the Mediterranean Sea was the highest regional average value. The high value in the Mediterranean Sea during the first leg was due to two exceptionally high values in samples D1 and D5. The formation of these NPAHs will be largely determined by the accumulated nighttime NO_2 and the actinic flux during the day, the air mass had been exposed to prior sampling. For example, samples D52 and D56 had relatively high ratios since the aerosols have picked up NO_x emissions from the urban areas of Athens and Istanbul (D52) or Rome and Naples (D56) in a previous night, which can be converted to the NO_3 radical by the reaction with ozone. Whereas the samples D50 and D54, which had not picked up NO_x emissions from particular source areas within ≈48h, did not show a high 2-NFLT/2-NPYR ratio.

3.3.4 PAHs and derivatives in photochemically aged pollution

A high ratio of the secondarily formed PAH derivatives 2-NPYR and 2-NFLT (Arey et al., 1986; Bamford and Baker, 2003; Reisen and Arey, 2005) to their parent PAHs indicates long-range transported aerosols with a significant concentration of the

atmospheric oxidants OH and NO_3 as well as NO_2. Similar to the ratio of 2-NFLT/1-NPYR, the highest ratios were observed in air over the Mediterranean Sea (especially during the first leg in aged aerosols). We determined the highest ratios in sample D1 at the beginning of the campaign close to Sardinia and Sicily. Another high ratio was found in sample D30 in the Arabian Gulf. As already revealed by Wang et al. (2020), photochemically aged air reached the ship from the first night of the first leg in the Arabian Gulf (28 July 2017 16:00 UTC) until the 30 July 2017 at 00:00 UTC (see air mass histories in Fig. 7a), as evidenced by high mixing ratios of some carbonyl compounds such as acetone. After that, the air was dominated by fresh emissions, while approaching Kuwait. According to the distribution of residence times of air masses, the air arrived from northwest with influence of several oil fields and refineries in that region (Fig. 7b and S3f; Bourtsoukidis et al., 2019; Pfannerstill et al., 2019; Wang et al., 2020). Thus, the samples from the first leg in the Arabian Gulf were affected by fresh emissions as well as photochemically aged air. Apart from 2-NFLT/FLT and 2-NPYR/PYR, several other PAH derivatives to parent-PAH concentration ratios (e.g. 1,4-O_2NAP/NAP, 9-OFLN/FLN and 9,10-O_2ANT/ANT) were also elevated in sample D30, showing the high contribution of photochemically aged air. In addition, the results indicate that these PAH derivatives are secondarily formed or significantly slower degraded and deposited than their parent PAH.

Another sample with a high ratio of secondarily formed NPAHs is sample D48 in the northern Red Sea nearby the Suez Canal. Similar to the first night in the Arabian Gulf, Wang et al. (2020) determined a high OH exposure during the first night in the Gulf of Suez (from the 22-23 August 2017) accompanied by a high mixing ratio of acetone. The finding that aerosols sampled between the 22 and 23 August 2017 (D48) were atmospherically aged, is supported the high PAH derivative/parent PAH ratios (e.g. of 2-NFLT/FLT, 2-NPYR/PYR, 7-NBAA/BAA, 1,4-O_2NAP/NAP and 9,10-O_2ANT/ANT). The enhanced formation of NPAHs and OPAHs from atmospheric reactions in this area commensurate with high concentrations of NO_2, and comparably high production rates of the NO_3 radical in this sea region, as reported by Eger et al. (2019). In addition, sample D48 is also affected by primary emissions, e.g., from oil refineries and shipping emissions (Bourtsoukidis et al., 2019). This is supported by the PMF, suggesting aged shipping emissions as well as continental pollution as the major sources.

Generally, low and high NPAH/PAH and OPAH/PAH ratios coincided with NO_x and radical availabilities. The highest concentrations of PAHs (D54) as well as of NPAHs and OPAHs (D58) were found in air masses carrying continental pollution, sampled in the Mediterranean Sea (from south-east Europe, covering major urban areas including Thessaloniki and Istanbul as well as from Sicily, Corsica, Sardinia and parts of continental Italy, respectively; Figs. 7c and d). While night-time sample D54 corresponded to low NO_x and low OH and NO_3 radical concentrations, 24 h sample D58 corresponded to high OH and NO_x concentrations (Tadic et al., 2020; Friedrich et al., 2021).

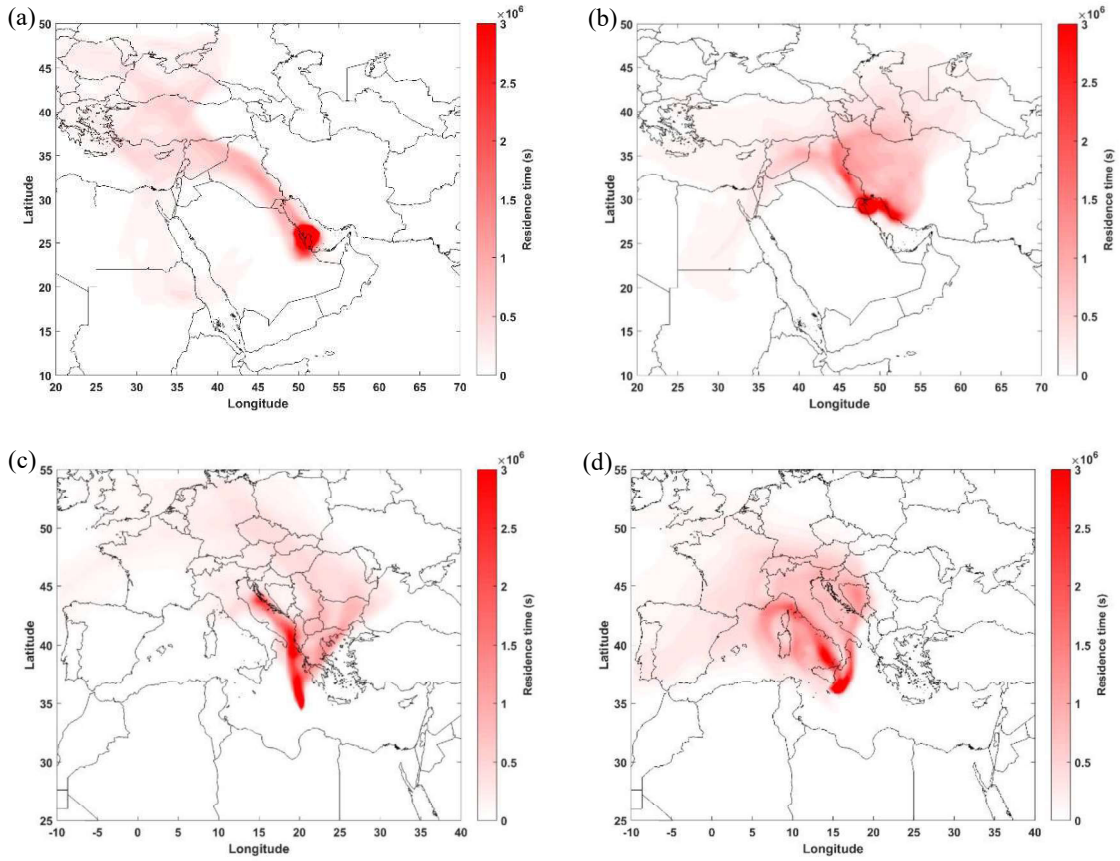

Figure 7: Distribution of residence times of air masses received in the Arabian Gulf: (a) D30 (29-30 July 2017), (b) D31 (3-4 August 2017) and the Mediterranean Sea: (c) D54-55 (27-28 August 2017), (d) D58 (29-30 August 2017) using FLEXPART Lagrangian particle dispersion model samples.

3.3.5 Significance of OPAHs and NPAHs photochemical sources

We found a significant positive correlation of 7,12-O_2BAA with the ratio of 2-NFLT/1-NPYR ($r=0.83$, $p<0.05$), which is typically used as an indicator for the contribution of PAH derivatives formed from oxidative reactions. Several laboratory studies have shown that 7,12-O_2BAA is formed from the heterogeneous reaction of BAA with O_3 alone and also with the combination of O_3 and NO_2 (Gao et al., 2009; Ringuet et al., 2012a, b). The formation of 7,12-O_2BAA from the photochemical reaction of BAA has also been reported (Jang and McDow, 1997; Shen et al., 2007). In our current study, the quinone weakly, not significantly correlated with ozone ($r=0.25$, $p=0.11$), the OH concentration ($r=0.29$, $p=0.11$) and the actinic flux ($r=0.23$, $p=0.14$). The weak correlation of the ratio of 7,12-O_2BAA and the parent-PAH BAA with the actinic flux ($r=0.28$, $p=0.07$) was the strongest correlation among all PAH derivative/PAH ratios. However, the secondary formation of 7,12-O_2BAA is expected to be only a part of the total burden of this quinone. We also found correlations with primary

pollutants, suggesting primary emissions. Similarly, Lin et al. (2015) reported that around 30 % of 7,12-O_2BAA in atmospheric PM sampled in Beijing was secondarily formed.

Lin and colleagues (2015) also found significant secondary formation of 3-NPHE and 7-NBAA. Tomaz et al. (2017) even suggested 3-NPHE to be used as a marker for secondary formation from PHE. However, 3-NPHE is not or only to trace amounts formed by homogeneous reactions with OH or NO_3 (Atkinson and Arey, 1994; Helmig and Harger, 1994; Lee and Lane, 2010). Though, Ringuet et al. (2012a) reported the formation of 3-NPHE and 7-NBAA by heterogeneous formation with atmospheric oxidants. Liu et al. (2019) found a correlation between 2-NFLT and 7-NBAA. We observed a significant correlation of the ratio 2-NFLT/1-NPYR with 3-NPHE ($r=0.44$, $p<0.05$) but not with 7-NBAA ($r=0.01$, $p=0.91$). 7-NBAA was positively correlated with the concentration of the NO_3 radical and NO_2 ($r=0.60$, $p<0.05$ and $r=0.67$, $p<0.05$, respectively), but not with the OH radical. 3-NPHE showed a weak correlation with NO_2 ($r=0.28$, $p=0.1$) and the actinic flux (0.25, $p=0.11$). Based on the high emission factors of 3-NPHE and 7-NBAA in diesel combustion (Heeb et al., 2008; Zhao et al., 2019), we expect primary pollution as the major source of these compounds and only a minor contribution from secondary formation. This is supported by Zhuo et al. (2017), who report a contribution from secondary formation of only 3-10 % to the total concentration of 3-NPHE in the city Nanjing in eastern China.

The secondary formation of 2-NNAP and 1,4-O_2NAP has already been determined earlier (Atkinson and Arey, 1994; Kautzman et al., 2010; Keyte et al., 2013) and was suggested by source attribution (Zhuo et al., 2017). 2-NNAP correlated with the ratio 2-NFLT/1-NPYR ($r=0.46$, $p<0.01$), while 1,4-O_2NAP only showed a weak correlation with the ratio ($r=0.29$, $p=0.06$). 2-NNAP correlated with NO_2 ($r=0.38$, $p<0.05$). 1,4-O_2NAP showed a weak positive correlation with O_3 ($r=0.22$, $p=0.14$). Both compounds are highly abundant in primary emissions, as already mentioned. Thus, 2-NNAP and 1,4-O_2NAP might have contributions from primary and secondary formation depending on the region.

From the literature, it is known that 9-OFLN and 9,10-O_2ANT can be formed in the atmosphere, mainly through the reaction of their parent PAH with O_3 and OH (Helmig and Harger, 1994; Perraudin et al., 2007; Wang et al., 2007; Keyte et al., 2013). In addition, source analysis of polluted air in the Chinese megacity Nanjing showed a significant contribution of secondarily formed 9-OFLN and 9,10-O_2ANT to the total concentration (Zhuo et al., 2017). In our dataset, we could find a positive correlation of these two OPAHs (significant only for 9-OFLN) with the concentration of O_3 ($r=0.42$, $p<0.01$ and $r=0.27$, $p=0.08$, respectively). Furthermore, 9-OFLN showed a significant positive correlation with the ratio 2-NFLT/1-NPYR ($r=0.33$, $p<0.05$), while 9,10-O_2ANT only showed a weak correlation ($r=0.22$, $p=0.15$). Based on the results from the PMF and other literature, we expect primary emissions as the major source of both OPAHs with a small contribution of secondary formation to the concentration of 9-OFLN and 9,10-O_2ANT.

1-(CHO)NAP was already reported to be secondarily formed by ozonolysis from ACY, 1-methylnaphthalene and possibly other precursors within hours (Dang et al., 2015). It is significantly correlating with the ratio of 2-NFLT/1-NPYR ($r=0.42$, $p<0.05$) and shows a very weak, not significant correlation with ozone ($r=0.11$, $p=0.47$). 5,12-O_2NAC showed a very weak correlation with ozone ($r=0.18$, $p=0.25$). However, we are not aware of any study showing secondary formation of this quinone. In contrast, 11-OBbFLN can be formed by the reaction of the parent PAH with ozone (Ringuet et al., 2012a).

However, we did not find any correlation. Thus, there is no clear indication for significant secondary formation of 11-OBaFLN, 11-BbOFLN and BAN, based on the correlation analysis.

In conclusion, our observations indicate photochemical sources to significantly have influenced 2-NFLT, 2-NPYR, 1,4-O_2NAP and 7,12-O_2BAA levels, while this was not the case for 1-NPYR, 11-OBaFLN, 11-BbOFLN and BAN. Indications for secondary formation but possibly only minor were found for 2-NNAP, 3-NPHE, 7-NBAA, 9-OFLN, 1-(CHO)NAP and 9,10-O_2ANT.

3.4 Mass size distributions

The highest concentrations of PAHs, OPAHs and NPAHs are found in the sub-micrometre fraction of particulate matter, PM_1. Fig. 8 shows the campaign average mass size distributions of the PAHs and PAH derivatives. The mass size distributions of PAHs, NPAHs and OPAHs are mainly unimodal given the coarse size resolution of the impactor with 6 size ranges within PM_{10}. The maximum was found in particles with an aerodynamic diameter <0.49 µm. For the sum of PAHs, four samples showed an apparently unimodal distribution with a maximum at a particle diameter of 0.49–0.95 µm in the accumulation mode instead of the lowest particle size. In addition, three samples (two in the Arabian Gulf and one in the Arabian Sea) showed a bimodal distribution with maxima in particles with an aerodynamic diameter <0.49 µm and of 0.95–1.5 µm. For the sum of NPAHs, only one sample (in the Mediterranean Sea) showed an apparently unimodal distribution with a maximum in another aerodynamic particle diameter range than <0.49 µm (0.49–0.95 µm). Since we did not resolve the <0.49 µm size fraction, more modes in the sub-micrometre fraction, as found by di Filippo et al. (2010) cannot be excluded.

The ratio between the concentrations in particles <0.49 µm compared to the concentrations in coarse mode PM particles is greater for high-molecular-weight PACs compared to low-molecular-weight PACs and higher for PAH derivatives compared to the parent-PAHs. This can be explained by the lower vapour pressure of PAH derivatives and high-molecular-weight PAHs compared to the parent-PAHs and low-molecular-weight PAHs. Compounds with lower vapour pressure are less subject to redistribution across particles sizes during transport (Degrendele et al., 2014). The process of redistribution is more effective that the pollutants reach higher particle size fractions than the process of coagulation of particles to form larger particles, which would transfer low vapour pressure PACs to bigger particle size fractions. The dependency of the vapour pressure on the mass median diameter was only found for PAHs and was not significant. This can partly be explained by limited explanatory power of the mass median diameter in this study due to low concentrations of e.g. the 3-ring PAHs and some NPAHs, leading to no detectable amount in coarse mode particles. The NPAHs generally had a low concentration in our study and the low-molecular-weight PAHs were not abundant in PM since these substances are preferable in the gas phase. The campaign average mass median diameters of the target compounds are shown in the Supplement Table S19.

Since the process of redistribution depends on time, a shift of the mass median diameter to larger particles sizes is found for aged aerosols (see exemplary Fig. S6). For instance, Lammel et al. (2017) found two maxima for the 4-ring PAHs at a marine background site (same cascade impactor as the one used in this study). The second maximum was explained by aged

aerosols at the marine site. The samples showing a maximum of the sum of PAHs at higher particle diameters in our study can also be attributed to aged aerosols (aged samples C6 and C7 in Arabian Gulf; C27, C28 in Mediterranean Sea without close primary emission sources; C22 in very clean air over the Arabian Sea, C24 in southern Red Sea possibly because of Saharan dust).

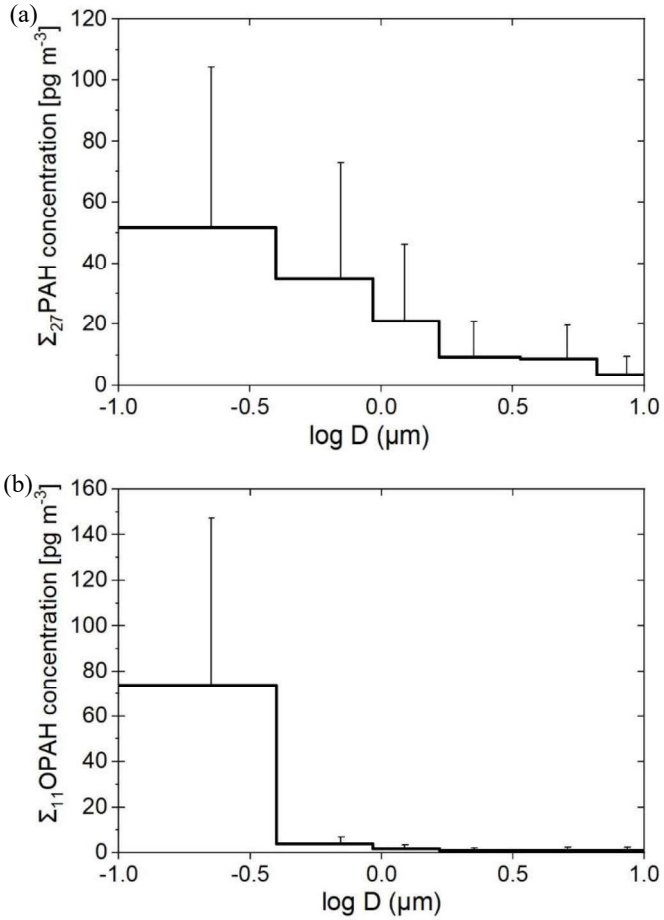

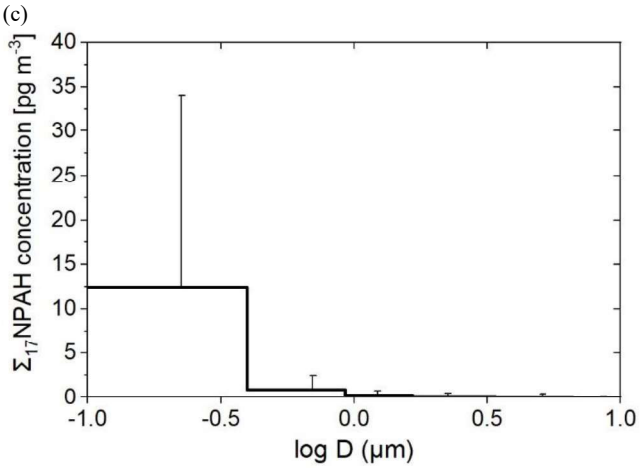

Figure 8: Campaign average mass size distributions of (a) $\sum_{27}$PAHs, (b) $\sum_{11}$OPAHs and (c) $\sum_{17}$NPAHs during the campaign; including standard deviation as error bars.

4 Conclusions

For the first time, PAHs and their derivatives were measured in the marine environment around the entire Arabian Peninsula in a comprehensive ship campaign. The atmospheric average concentrations of $\sum_{27}$PAHs, $\sum_{19}$RPAHs, $\sum_{11}$OPAHs and $\sum_{17}$NPAHs in the gas and particulate phase were 2.85 ± 3.35 ng m^{-3}, 0.83 ± 0.87 ng m^{-3}, 0.24 ± 0.25 ng m^{-3} and 4.34 ± 7.37 pg m^{-3}, respectively. The lowest burden of all targeted pollutant classes was observed in the Arabian Sea with concentrations among the lowest ever reported, followed by the southern Red Sea. The highest average concentrations of the PAHs and the OPAHs were detected in the Mediterranean Sea, while the NPAHs were most abundant in the Arabian Gulf. It was observed that the regional differences in the composition patterns of the NPAHs and OPAHs were more pronounced than those of the PAHs and RPAHs. 1,4-O_2NAP, 9-OFLN and 9,10-O_2ANT were the most abundant OPAHs. The NPAH composition pattern was dominated by a high contribution of 2-NNAP, followed by 1-NPYR, which was highly abundant in the Gulf region. Photochemical formation of 2-NFLT, 2-NPYR, 2-NNAP, 3-NPHE, 7-NBAA, 1,4-O_2NAP, 1-(CHO)NAP, 9-OFLN, 9,10-O_2ANT and 7,12-O_2BAA was indicated, while for 1-NPYR, 11-OBaFLN, 11-OBbFLN and BAN secondary sources were not significant.

Source apportionment showed that the PAHs and their nitrated and oxygenated derivatives mainly originated from fresh and aged shipping emissions. All OPAHs and NPAHs except 2-NFLT, which were frequently detected during the campaign, showed elevated concentrations in fresh shipping emissions. 1-NPYR among the NPAHs and 11-OBaFLN and 1-(CHO)NAP among the OPAHs showed the highest relative increase in their concentration. In contrast, 2-NFLT and 2-NPYR were highly abundant in aged shipping emissions due to secondary formation. 1-NPYR, 3-NPHE and several OPAHs had a significant contribution from residual oil combustion. PAH derivatives were clearly enriched in long-range transported plumes from polluted regions in Egypt, the Arabian Gulf, and southern and eastern Europe. Throughout the campaign, the

highest concentrations of PAHs, OPAHs and NPAHs were found in the sub-micrometre fraction of particulate matter (PM_1). Due to redistribution, the mass median diameter was shifted to higher values in long-range transported aerosols.

Data availability. The data used in this study are archived and distributed through the KEEPER service of the Max Planck Digital Library (https://keeper.mpdl.mpg.de, last access: 12 December 2021) and have been available from August 2019 to all scientists agreeing to the AQABA protocol.

Supplement. The supplement related to this article is available online at:

Author contributions. MW evaluated the data and wrote the manuscript. GL supervised this study. MI and RP did the sampling. MK, MI and ES provided the data about alkylated PAHs and wrote this part. PPo performed the PMF and wrote the part. BN created the FLEXPART Lagrangian particle dispersion model results. JK provided the data about metals. PK and PPr performed the PAH, NPAH and OPAH sample preparation and analysis. IT created GPS plots and provided NO_x and O_3 data. NF, PE and JNC contributed measurements of NO_2, NO_X, NO_y O_3 and SO_2. RR and ST provided OH radical data. JW was involved in the discussion about the sources. The stack filter and information about bypassing ships as well as BC and surface PAH concentrations were provided by FD and SC. HH took responsibility for the scientific coordination of the field campaign on board the research vessel. JL designed the AQABA campaign. GL designed this study, supported by ES and UP. All authors contributed to data interpretation and manuscript revision and approved the submitted version.

Competing interests. The authors declare that they have no conflict of interest.

Acknowledgements. We thank Hays Ships Ltd, Captain Pavel Kirzner and the *Kommandor Iona's* ship crew for the great support. We would like to thank Marcel Dorf and Claus Koeppel for the organization of the campaign, Hartwig Harder for the management on board, and all other participants and supporters of the campaign. We thank Benedikt Steil for processing meteorological data and Jan Schuladen for the data about the actinic flux. We also thank Abdulaziz al Senafi (Kuwait Inst. of Scientific Research). In addition, we thank Ondrej Sanka for the assistance in the plotting of sampling stretches. This research was supported by the Max Planck Society and by the Czech Ministry of Education, Youth and Sports - Research Infrastructure RECETOX RI (No LM2018121 and CZ.02.1.01/0.0/0.0/16_013/0001761), the project CETOCOEN EXCELLENCE (No CZ.02.1.01/0.0/0.0/17_043/0009632) and the Czech Science Foundation (GACR #20-07117S). This project was supported from the European Union's Horizon 2020 research and innovation programme under grant agreement No 857560. This publication reflects only the author's view and the European Commission is not responsible for any use that may be made of the information it contains.

Financial support. The article processing charges for this open-access publication were covered by the Max Planck Society.

Review statement.

References

Abbas, I., Badran, G., Verdin, A., Ledoux, F., Roumie, M., and Courcot, D.: Polycyclic aromatic hydrocarbon derivatives in airborne particulate matter: sources, analysis and toxicity, Environ. Chem. Lett., 16, 439–475, https://doi.org/10.1007/s10311-0170697-0, 2018.

Albinet, A., Leoz-Garziandia, E., Budzinski, H., and Villenave, E.: Polycyclic aromatic hydrocarbons (PAHs), nitrated PAHs and oxygenated PAHs in ambient air of the Marseilles area (south of France): concentrations and sources, Sci. Total Environ., 384, 280–292, http://dx.doi.org/10.1016/j.scitotenv.2007.04.028, 2007.

Albinet, A., Leoz-Garziandia, E., Budzinski, H., Villenave, E., and Jaffrezo, J. L.: Nitrated and oxygenated derivatives of polycyclic aromatic hydrocarbons in the ambient air of two French alpine valleys. Part 1: concentrations, sources and gas/particle partitioning, Atmos. Environ., 42, 43-54. https://doi.org/10.1016/j.atmosenv.2007.10.009, 2008.

Alves, C. A., Vicente, A. M., Custódio, D., Cerqueira, M., Nunes, T., Pio, C., Lucarelli, F., Calzolai, G., Nava, S., Diapouli, E., Eleftheriadis, K., Querol, X., and Bandowe, B. A. M.: Polycyclic aromatic hydrocarbons and their derivatives (nitro-PAHs, oxygenated PAHs, and azaarenes) in $PM_{2.5}$ from southern European cities, Sci. Total Environ., 595, 494–504, http://dx.doi.org/10.1016/j.scitotenv.2017.03.256, 2017.

Andersson, J. T. and Achten, C.: Time to say goodbye to the 16 EPA PAHs? Toward an up-to-date use of PACs for environmental purposes, Polycyclic Aromat. Compd., 35, 330-354, https://doi.org/10.1080/10406638.2014.991042, 2015.

Arey, J., Zielinska, B., Atkinson, R., Winer, A. M., Ramdahl, T., and Pitts, J. N.: The formation of nitro-PAH from gas-phase reactions of fluoranthene and pyrene with the OH radical in the presence of NO_x, Atmos. Environ., 20, 2339–2345, https://doi.org/10.1016/0004-6981(86)90064-8, 1986.

Atkinson, R. and Arey, J.: Atmospheric chemistry of gas-phase polycyclic aromatic hydrocarbons: formation of atmospheric mutagens, Environ. Health Perspect., 102, 117–126, https://doi.org/10.1289/ehp.94102s4117, 1994.

Atkinson, R. and Arey, J.: Mechanisms of the gas-phase reactions of aromatic hydrocarbons and PAHs with OH and NO3 radicals, Polycyclic Aromat. Compd., 27, 15–40, https://doi.org/10.1080/10406630601134243, 2007.

Atkinson, R., Aschmann, S. M., Arey, J., Zielinska, B., and Schuetzle, D.: Gas-phase atmospheric chemistry of 1-Nitronaphthalene and 2-Nitronaphthalene and 1,4-Naphthoquinone, Atmos. Environ., 23, 2679–2690, https://doi.org/10.1016/0004-6981(89)90548-9, 1989.

Bamford, H. A. and Baker, J. E.: Nitro-polycyclic aromatic hydrocarbon concentrations and sources in urban and suburban atmospheres of the mid-Atlantic region, Atmos. Environ., 37, 2077-2091, https://doi.org/10.1016/S1352-2310(03)00102-X, 2003.

Bamford, H. A., Bezabeh, D. Z., Schantz, M. M., Wise, S. A., and Baker, J. E.: Determination and comparison of nitrated-polycyclic aromatic hydrocarbons measured in air and diesel particulate reference materials, Chemosphere, 50, 575-587, https://doi.org/10.1016/S0045-6535(02)00667-7, 2003.

Bandowe, B. A. M., Meusel, H., Huang, R.-J., Ho, K., Cao, J., Hoffmann, T., and Wilcke, W.: $PM_{2.5}$-bound oxygenated PAHs, nitro-PAHs and parent-PAHs from the atmosphere of a Chinese megacity: seasonal variation, sources and cancer risk assessment, Sci. Total Environ., 473–474, 77–87, http://dx.doi.org/10.1016/j.scitotenv.2013.11.108, 2014.

Bandowe, B. A. M. and Meusel, H.: Nitrated polycyclic aromatic hydrocarbons (nitro-PAHs) in the environment – A review, Sci. Total Environ., 581–582, 237–257, https://doi.org/10.1016/j.scitotenv.2016.12.115, 2017.

Baek, S. O., Field, R. A., Goldstone, M. E., Kirk, P. W., Lester, J. N., and Perry, R.: A review of atmospheric polycyclic aromatic hydrocarbons: Sources, fate and behaviour, Water Air Soil Pollut., 60, 279–300, https://doi.org/10.1007/BF00282628, 1991.

Bezabeh, D. Z., Bamford, H. A., Schantz, M. M., and Wise, S. A.: Determination of nitrated polycyclic aromatic hydrocarbons in diesel particulate-related standard reference materials by using gas chromatography/mass

spectrometry with negative ion chemical ionization, Anal. Bioanal. Chem., 375, 381–388, https://doi.org/10.1007/s00216-002-1698-8, 2003.

Bläsing, M., Kistler, M., and Lehndorff, E.: Emission fingerprint of inland navigation vessels compared with road traffic, domestic heating and ocean-going vessels, Org. Geochem., 99, 1–9, https://doi.org/10.1016/j.orggeochem.2016.05.009, 2016.

Brorström-Lundén, E., Remberger, M., Kaj, L., Hansson, K., Palm Cousins, A., Andersson, H., Haglund, P., Ghebremeskel, M., and Schlabach, M.: Results from the Swedish national screening programme 2008: Screening of unintentionally produced organic contaminants, report B1944, Swedish Environmental Research Institute (IVL), Gothenburg, Sweden, 2010.

Bolton, J. L., Trush, M. A., Penning, T.M., Dryhurst, G., and Monks, T. J.: Role of quinones in toxicology, Chem. Res. Toxicol., 13, 135-160, https://doi.org/10.1021/tx9902082, 2000.

Bourtsoukidis, E., Ernle, L., Crowley, J. N., Lelieveld, J., Paris, J.-D., Pozzer, A., Walter, D., and Williams, J.: Nonmethane hydrocarbon (C2–C8) sources and sinks around the Arabian Peninsula, Atmos. Chem. Phys., 19, 7209–7232, https://doi.org/10.5194/acp-19-7209-2019, 2019.

Bourtsoukidis, E., Pozzer, A., Sattler, T., Matthaios, V. N., Ernle, L., Edtbauer, A., Fischer, H., Könemann, T., Osipov, S., Paris, J.-D., Pfannerstill, E. Y., Stönner, C., Tadic, I., Walter, D., Wang, N., Lelieveld, J., and Williams, J.: The Red Sea Deep Water is a potent source of atmospheric ethane and propane, Nat. Commun., 11, 447, https://doi.org/10.1038/s41467-020-14375-0, 2020.

Budzinski, H., Garrigues, P., Connan, J., Devillers, J., Domine, D., Radke, M., and Oudins, J. L.: Alkylated phenanthrene distributions as maturity and origin indicators in crude oils and rock extracts, Geochim. Cosmochim. Acta, 59, 2043–2056, https://doi.org/10.1016/0016-7037(95)00125-5, 1995.

Castro-Jiménez, J., Berrojalbiz, N., Wollgast, J., and Dachs, J.: Polycyclic aromatic hydrocarbons (PAHs) in the Mediterranean Sea: Atmospheric occurrence, deposition and decoupling with settling fluxes in the water column, Environ. Pollut., 166, 40-47, https://doi.org/10.1016/j.envpol.2012.03.003, 2012.

Caumo, S., Vicente, A., Custodio, D., Alves, C., and Vasconcellos, P.: Organic compounds in particulate and gaseous phase collected in the neighbourhood of an industrial complex in Sao Paulo (Brazil), Air Qual. Atmos. Hlth., 11, 271–283, https://doi.org/10.1007/s11869-017-0531-7, 2018.

Celik, S., Drewnick, F., Fachinger, F., Brooks, J., Darbyshire, E., Coe, H., Paris, J.-D., Eger, P. G., Schuladen, J., Tadic, I., Friedrich, N., Dienhart, D., Hottmann, B., Fischer, H., Crowley, J. N., Harder, H., and Borrmann, S.: Influence of vessel characteristics and atmospheric processes on the gas and particle phase of ship emission plumes: in situ measurements in the Mediterranean Sea and around the Arabian Peninsula, Atmos. Chem. Phys., 20, 4713–4734, https://doi.org/10.5194/acp-20-4713-2020, 2020.

Ciccioli, P., Cecinato, A., Brancaleoni, E., Frattoni, M., Zacchei, P., Miguel, A. H., and Vasconcellos, P. D.: Formation and transport of 2-nitrofluoranthene and 2-nitropyrene of photochemical origin in the troposphere, J. Geophys. Res.-Atmos., 101, 19567–19581., https://doi.org/10.1029/95JD02118, 1996.

Charrier, J.G., and Anastasio, C.: On dithiothreitol (DTT) as a measure of oxidative potential for ambient particles: evidence for the importance of soluble transition metals, Atmos. Chem. Phys., 12, 11317–11350, https://doi.org/10.5194/acpd-12-11317-2012, 2012.

Clergé, A., Le Goff, J., Lopez, C., Ledauphin, J., and Delépée, R.: Oxy-PAHs: occurrence in the environment and potential genotoxic/mutagenic risk assessment for human health, Crit. Rev. Toxicol., 49, 302–328, https://doi.org/10.1080/10408444.2019.1605333, 2019.

Collins, J. F., Brown, J. P., Alexeeff, G. V., and Salmon, A. G.: Potency equivalency factors for some polycyclic aromatic hydrocarbons and polycyclic aromatic hydrocarbon derivatives, Regul. Toxicol. Pharm., 28, 45–54, https://doi.org/10.1006/rtph.1998.1235, 1998.

Dang, J., Shi, X., Zhang, Q., Hu, J., Wang, W.: Mechanism and thermal rate constant for the gas-phase ozonolysis of acenaphthylene in the atmosphere, Sci. Tot. Environ., 514, 344-350, https://doi.org/10.1016/j.scitotenv.2014.12.009, 2015.

Degrendele, C., Okonski, K., Melymuk, L., Landlová, L., Kukučka, P., Čupr, P., and Klánová, J.: Size specific distribution of the atmospheric particulate PCDD/Fs, dl-PCBs and PAHs on a seasonal scale: Implications for cancer risks from inhalation, Atmos. Environ., 98, 410–416, https://doi.org/10.1016/j.atmosenv.2014.09.001, 2014.

Di Filippo, P., Riccardi, C., Pomata, D., and Buiarelli, F.: Concentrations of PAHs, and nitro- and methyl-derivatives associated with a size segregated urban aerosol, Atmos. Environ., 44, 2742-2749, https://doi.org/10.1016/j.atmosenv.2010.04.035, 2010.

Drotikova, T., Ali, A. M., Halse, A. K., Reinardy, H. C., and Kallenborn, R.: Polycyclic aromatic hydrocarbons (PAHs), oxy-and nitro-PAHs in ambient air of Arctic town Longyearbyen, Svalbard, Atmos. Chem. Phys., 20, 9997–10014, https://doi.org/10.5194/acp-20-9997-2020, 2020.

Durant, J. L., Busby Jr., W. F., Lafleur, A. L., Penman, B. W., and Crespi, C. L.: Human cell mutagenicity of oxygenated, nitrated and unsubstituted polycyclic aromatic hydrocarbons associated with urban aerosols, Mutat. Res., 371, 123–157, https://doi.org/10.1016/S0165-1218(96)90103-2, 1996.

ECHA - European Chemicals Agency: Grouping speeds up regulatory action - integrated regulatory strategy annual report 2020, https://doi.org/10.2823/092964, 2021.

Eger, P. G., Friedrich, N., Schuladen, J., Shenolikar, J., Fischer, H., Tadic, I., Harder, H., Martinez, M., Rohloff, R., Tauer, S., Drewnick, F., Fachinger, F., Brooks, J., Darbyshire, E., Sciare, J., Pikridas, M., Lelieveld, J., and Crowley, J. N.: Shipborne measurements of $ClNO_2$ in the Mediterranean Sea and around the Arabian Peninsula during summer, Atmos. Chem. Phys., 19, 12121–12140, https://doi.org/10.5194/acp-19-12121-2019, 2019.

El Alawi, Y. S., McConkey, B. J., Dixon, D. G., and Greenberg, B. M.: Measurement of short and long-term toxicity of polycyclic aromatic hydrocarbons using luminescent bacteria, Ecotoxicol. Environ. Saf., 51, 12–21, https://doi.org/10.1006/eesa.2001.2108, 2002.

Fan, Z. H., Kamens, R. M., Hu, J. X., Zhang, J.B., and McDow, S.: Photostability of nitropolycyclic aromatic hydrocarbons on combustion soot particles in sunlight, Environ. Sci. Technol. 30, 1358-1364, https://doi.org/10.1016/1352-2310(94)00347-N, 1996.

Feilberg, A. and Nielsen, T.: Effect of aerosol chemical composition on the photodegradation of nitro-polycyclic aromatic hydrocarbons, Environ. Sci. Technol., 34, 789–97, https://doi.org/10.1021/es990566r, 2000.

Feilberg, A., Kamens, R. M., Strommen, M. R., and Nielsen, T.: Modeling the formation, decay, and partitioning of semivolatile nitro-polycyclic aromatic hydrocarbons (nitronaphthalenes) in the atmosphere, Atmos. Environ., 33, 1231-1243, https://doi.org/10.1016/S1352-2310(98)00275-1, 1999.

Feilberg, A., Poulsen, M. W. B., Nielsen, T., and Skov, H.: Occurrence and sources of particulate nitro-polycyclic aromatic hydrocarbons in ambient air in Denmark, Atmos. Environ., 35, 353–366, https://doi.org/10.1016/S1352-2310(00)00142-4, 2001.

Finlayson-Pitts, B. J. and Pitts Jr, J. N.: Chemistry of the upper and lower atmosphere, 1st edition, Academic Press, New York, United States, 1999.

Friedrich, N., Eger, P., Shenolikar, J., Sobanski, N., Schuladen, J., Dienhart, D., Hottmann, B., Tadic, I., Fischer, H., Martinez, M., Rohloff, R., Tauer, S., Harder, H., Pfannerstill, E. Y., Wang, N., Williams, J., Brooks, J., Drewnick, F., Su, H., Li, G., Cheng, Y., Lelieveld, J., and Crowley, J. N.: Reactive nitrogen around the Arabian Peninsula and in the Mediterranean Sea during the 2017 AQABA ship campaign, Atmos. Chem. Phys., 21, 7473–7498, https://doi.org/10.5194/acp-21-7473-2021, 2021.

Gao, S., Zhang, Y., Meng, J., and Shu, J.: Online investigations on ozonation products of pyrene and benz[a]anthracene particles with a vacuum ultraviolet photoionization aerosol time-of-flight mass spectrometer, Atmos. Environ., 43, 3319–25, https://doi.org/10.1016/j.atmosenv.2009.04.021, 2009.

Garcia, K. O., Teixeira, E. C., Agudelo-Castañeda, D. M., Braga, M., Alabarse, P. G., Wiegand, F., Kautzmann, R. M., and Silva, L. F. O.: Assessment of nitro-polycyclic aromatic hydrocarbons in PM_1 near an area of heavy-duty traffic, Sci. Total Environ., 479–480, 57–65, https://doi.org/10.1016/j.scitotenv.2014.01.126, 2014.

Gogou, A., Stratigakis, N., Kanakidou, M. and Stephanou, E. G.: Organic aerosols in Eastern Mediterranean: components source reconciliation by using molecular markers and atmospheric back trajectories, Org. Geochem., 25, 79-96, https://doi.org/10.1016/S0146-6380(96)00105-2, 1996.

Harrison, R. M., Alam, M. S., Dang, J., Ismail, I. M., Basahi, J., Alghamdi, M. A., Hassan, I. A, and Khoder, M.: Relationship of polycyclic aromatic hydrocarbons with oxy(quinone) and nitro derivatives during air mass transport, Sci. Total Environ., 572, 1175-118, https://doi.org/10.1016/j.scitotenv.2016.08.030, 2016.

Heeb, N.V., Schmid, P., Kohler, M., Gujer, E., Zennegg, M., Wenger, D., Wichser, A., Ulrich, A., Gfeller, U., Honegger, P., Zeyer, K., Emmenegger, L., Petermann, J.L.,Czerwinski, J., Mosimann, T., Kasper, M., and Mayer, A.: Secondary

effects of catalytic diesel particulate filters: Conversion of PAHs versus formation of nitro-PAHs, Environ. Sci. Technol. 42, 3773–3779, https://doi.org/10.1021/es7026949, 2008.

Helmig, D. and Harger, W. P.: OH radical-initiated gas-phase reaction-products of phenanthrene, Sci. Total Environ., 148, 11-21, https://doi.org/10.1016/0048-9697(94)90368-9, 1994.

Hens, K., Novelli, A., Martinez, M., Auld, J., Axinte, R., Bohn, B., Fischer, H., Keronen, P., Kubistin, D., Nölscher, A. C., Oswald, R., Paasonen, P., Petäjä, T., Regelin, E., Sander, R., Sinha, V., Sipilä, M., Taraborrelli, D., Tatum Ernest, C., Williams, J., Lelieveld, J., and Harder, H.: Observation and modelling of HO_x radicals in a boreal forest, Atmos. Chem. Phys., 14, 8723–8747, https://doi.org/10.5194/acp-14-8723-2014, 2014.

Iakovides, M., Apostolaki, M., and Stephanou, E. G.: PAHs, PCBs and organochlorine pesticides in the atmosphere of Eastern Mediterranean: Investigation of their occurrence, sources and gas-particle partitioning in relation to air mass transport pathways, Atmos. Environ., 244, 117931, https://doi.org/10.1016/j.atmosenv.2020.117931, 2021.

IARC (International Agency for Research on Cancer): Polynuclear aromatic compounds. Part 1. Chemical, environmental and experimental data. IARC monographs on the evaluation of carcinogenic risk of chemicals to humans, IARC, Vol. 32, Lyon, France, 1983.

IARC (International Agency for Research on Cancer): Diesel and gasoline exhausts and some nitroarenes, IARC monographs on the evaluation of carcinogenic risk of chemicals to humans, IARC, Vol. 105, Lyon, France, 1989.

IARC (International Agency for Research on Cancer): Agents classified by the IARC monographs, Vol. 1–123, http://monographs.iarc.fr/ENG/Classification/ClassificationsAlphaOrder.pdf, last access: 04 January 2022, 2018.

Jang, M. and McDow, S. R.: Products of benz[a]anthracene photodegradation in the presence of known organic constituents of atmospheric aerosols, Environ. Sci. Technol., 31, 1046–1053, https://doi.org/10.1021/es960559s, 1997.

Jariyasopit, N., Harner, T., Shin, C., and Park, R.: The effects of plume episodes on PAC profiles in the athabasca oil sands region, Environ. Pollut., 282, 1–9. https://doi.org/10.1016/j.envpol.2021.117014, 2021.

Jaward, F. M., Barber, J. L., Booij, K., and Jones, K. C.: Spatial distribution of atmospheric PAHs and PCNs along a north–south Atlantic transect, Environ. Pollut., 132, 173-181, https://doi.org/10.1016/j.envpol.2004.03.029, 2004.

Johansson, L., Jalkanen, J.-P., and Kukkonen, J.: Global assessment of shipping emissions in 2015 on a high spatial and temporal resolution, Atmos. Environ., 167, 403–415, https://doi.org/10.1016/j.atmosenv.2017.08.042, 2017.

Kamens, R. M., Zhi-Hua, F., Yao, Y., Chen, D., Chen, S., and Vartianen, M.: A methodology for modeling the formation and decay of nitro-PAH in the atmosphere, Chemosphere, 28, 1623-1632, https://doi.org/10.1016/0045-6535(94)90421-9, 1994.

Kautzman, K. E., Surratt, J. D., Chan, M. N., Chan, A. W. H., S. P., Chhabra, P. S., Dalleska, N. F., Wennberg, P. O., Flagan, R. C., and Seinfeld, J.H.: Chemical composition of gas- and aerosol-phase products from the photooxidation of naphthalene, J. Phys. Chem. A, 114, 913, https://doi.org/10.1021/jp908530s, 2010.

Keith, L. H.: The source of U.S. EPA's sixteen PAH priority pollutants, Polycycl. Aromat. Compd., 35, 147–160, https://doi.org/10.1080/10406638.2014.892886, 2015.

Kelly, J. M., Ivatt, P. D., Evans, M. J., Kroll, J. H., Hrdina, A. I. H., Kohale, I. N., White, F.M., Engelward, B.P., and Selin, N.E.: Global cancer risk from unregulated polycyclic aromatic hydrocarbons. GeoHealth, 5, e2021GH000401, https://doi.org/10.1029/2021GH000401, 2021.

Keyte, I.J., Harrison, R.M., and Lammel, G.: Chemical reactivity and long-range transport potential of polycyclic aromatic hydrocarbons – a review, Chem. Soc. Rev., 42, 9333-9391, https://doi.org/10.1039/C3CS60147A, 2013.

Kitanovski, Z., Shahpoury, P., Samara, C., Voliotis, A., and Lammel, G.: Composition and mass size distribution of nitrated and oxygenated aromatic compounds in ambient particulate matter from southern and central Europe – implications for the origin, Atmos. Chem. Phys., 20, 2471–2487, https://doi.org/10.5194/acp-20-2471-2020, 2020.

Lammel G.: Polycyclic aromatic compounds in the atmosphere – a review identifying research needs, Polycycl. Aromat. Compd., 35, 316-329, https://doi.org/10.1080/10406638.2014.931870, 2015.

Lammel, G., Meixner, F. X., Vrana, B., Efstathiou, C. I., Kohoutek, J., Kukučka, P., Mulder, M. D., Přibylová, P., Prokeš, R., Rusina, T. P., Song, G.-Z., and Tsapakis, M.: Bidirectional air–sea exchange and accumulation of POPs (PAHs, PCBs, OCPs and PBDEs) in the nocturnal marine boundary layer, Atmos. Chem. Phys., 16, 6381–6393, https://doi.org/10.5194/acp-16-6381-2016, 2016.

Lammel, G., Mulder, M. D., Shahpoury, P., Kukučka, P., Lišková, H., Přibylová, P., Prokeš, R., and Wotawa, G.: Nitro-polycyclic aromatic hydrocarbons – gas–particle partitioning, mass size distribution, and formation along transport in

marine and continental background air, Atmos. Chem. Phys., 17, 6257–6270, https://doi.org/10.5194/acp-17-6257-2017, 2017.
Lammel, G., Kitanovski, Z., Kukučka, P., Novák, J., Arangio, A. M., Codling, G. P., Filippi, A., Hovorka, J., Kuta, J., Leoni, C., Přibylová, P., Prokeš, R., Sáňka, O., Shahpoury, P., Tong, H. J., and Wietzoreck, M.: Oxygenated and nitrated polycyclic aromatic hydrocarbons in ambient air levels, phase partitioning, mass size distributions, and inhalation bioaccessibility, Environ. Sci. Technol., 54, 2615–2625, https://doi.org/10.1021/acs.est.9b06820, 2020.
Lee, J. Y. and Lane, D. A.: Formation of oxidized products from the reaction of gaseous phenanthrene with the OH radical in a reaction chamber, Atmos. Environ., 44, 2469-2477, https://doi.org/10.1016/j.atmosenv.2010.03.008, 2010.
Lee, S., Hong, S., Liu, X., Kim, C., Jung, D., Yim, U. H., Shim, W. J., Khim, J. S., Giesy, J. P., and Choi, K.: Endocrine disrupting potential of PAHs and their alkylated analogues associated with oil spills, Environ. Sci.: Processes Impacts, 19, 1117, https://doi.org/10.1039/C7EM00125H, 2017.
Lee, W., Stevens, P. S., and Hites, R. A.: Rate constants for the gas-phase reactions of methylphenanthrenes with OH as a function of temperature, J. Phys. Chem. A, 107, 6603-6608, https://doi.org/10.1021/jp034159k, 2003.
Lelieveld, J., Berresheim, H., Borrmann, S., Crutzen, P. J., Dentener, F. J., Fischer, H., Feichter, J., Flatau, P. J., Heland, J., Holzinger, R., Korrmann, R., Lawrence, M. G., Levin, Z., Markowicz, K. M., Mihalopoulos, N., Minikin, A., Ramanathan, V., de Reus, M., Roelofs, G. J., Scheeren, H. A., Sciare, J., Schlager, H., Schultz, M., Siegmund, P., Steil, B., Stephanou, E. G., Stier, P., Traub, M., Warneke, C., Williams, J., and Ziereis, H.: Global air pollution crossroads over the Mediterranean, Science, 298, 794–799, https://doi.org/10.1126/science.1075457, 2002.
Lelieveld, J., Hoor, P., Jöckel, P., Pozzer, A., Hadjinicolaou, P., Cammas, J.-P., and Beirle, S.: Severe ozone air pollution in the Persian Gulf region, Atmos. Chem. Phys., 9, 1393–1406, https://doi.org/10.5194/acp-9-1393-2009, 2009.
Lelieveld, J., Evans, J. S., Fnais, M., Giannadaki, D., and Pozzer, A.: The contribution of outdoor air pollution sources to premature mortality on a global scale, Nature, 525, 367–371, https://doi.org/10.1038/nature15371, 2015.
Lelieveld, J., Klingmuller, K., Pozzer, A., Poschl, U., Fnais, M., Daiber, A., and Munzel, T.: Cardiovascular disease burden from ambient air pollution in Europe reassessed using novel hazard ratio functions, Eur. Heart J. 40, 1590–1596, https://doi.org/10.1093/eurheartj/ehz135, 2019.
Li, W., Wang, C., Shen, H., Su, S., Shen, G., Huang, Y., Zhang, Y., Chen, Y., Chen, H., Lin, N., Zhuo, S., Zhong, Q., Wang, X., Liu, J., Li, B., Liu, W., and Tao, S.: Concentrations and origins of nitro-polycyclic aromatic hydrocarbons and oxy-polycyclic aromatic hydrocarbons in ambient air in urban and rural areas in northern China, Environ. Pollut. 197, 156–164, https://doi.org/10.1016/j.envpol.2014.12.019, 2015.
Lin, Y., Ma, Y., Qiu, X., Li, R., Fang, Y., Wang, J., Zhu, Y., and Hu, D.: Sources, transformation, and health implications of PAHs and their nitrated, hydroxylated, and oxygenated derivatives in $PM_{2.5}$ in Beijing, J. Geophys. Res., 120, 7219–7228, http://dx.doi.org/10.1002/2015JD023628, 2015.
Liu, P., Ju, Y., Li, Y., Wang, Z., Mao, X., Cao, H., Jia, C., Huang, T., Gao, H., and Ma, J.: Spatiotemporal variation of atmospheric nitrated polycyclic aromatic hydrocarbons in semi-arid and petrochemical industrialized Lanzhou City, Northwest China, Environ. Sci. Pollut. Res., 26, 1857–1870, https://doi.org/10.1007/s11356-018-3633-3, 2019.
Lyu, Y., Guo, H., Cheng, T., and Li, X.: Particle size distributions of oxidative potential of lung-deposited particles: Assessing contributions from quinones and water-soluble metals, Environ. Sci. Technol., 52, 6592–6600, https://doi.org/10.1021/acs.est.7b06686, 2018.
Mandalakis, M., Tsapakis, M., Tsoga, A., and Stephanou, E. G.: Gas–particle concentrations and distribution of aliphatic hydrocarbons, PAHs, PCBs and PCDD/Fs in the atmosphere of Athens (Greece), Atmos. Environ., 36, 4023-4035, https://doi.org/10.1016/S1352-2310(02)00362-X, 2002.
Marino, F., Cecinato, A., and Siskos, P. A.: Nitro-PAH in ambient particulate matter in the atmosphere of Athens, Chemosphere, 40, 533–537, https://doi.org/10.1016/S0045-6535(99)00308-2, 2000.
Martinez, M., Harder, H., Kubistin, D., Rudolf, M., Bozem, H., Eerdekens, G., Fischer, H., Klüpfel, T., Gurk, C., Königstedt, R., Parchatka, U., Schiller, C. L., Stickler, A., Williams, J., and Lelieveld, J.: Hydroxyl radicals in the tropical troposphere over the Suriname rainforest: airborne measurements, Atmos. Chem. Phys., 10, 3759–3773, https://doi.org/10.5194/acp-10-3759-2010, 2010.
Meusel, H., Kuhn, U., Reiffs, A., Mallik, C., Harder, H., Martinez, M., Schuladen, J., Bohn, B., Parchatka, U., Crowley, J. N., Fischer, H., Tomsche, L., Novelli, A., Hoffmann, T., Janssen, R. H. H., Hartogensis, O., Pikridas, M., Vrekoussis, M., Bourtsoukidis, E., Weber, B., Lelieveld, J., Williams, J., Pöschl, U., Cheng, Y., and Su, H.: Daytime formation of

nitrous acid at a coastal remote site in Cyprus indicating a common ground source of atmospheric HONO and NO, Atmos. Chem. Phys., 16, 14475–14493, https://doi.org/10.5194/acp-16-14475-2016, 2016.

Minero, C., Maurino, V., Borghesi, D., Pelizzetti, E., and Vione, D.: An overview of possible processes able to account for the occurrence of nitro-PAHs in the Antarctic particulate matter, Microchem. J., 96, 213–216, https://doi.org/10.1016/j.microc.2009.07.013, 2010.

Nassar, H.F., Tang, N., Kameda, T., Toriba, A., Khoder, M. I., and Hayakawa, K.,: Atmospheric concentrations of polycyclic aromatic hydrocarbons and selected nitrated derivatives in Greater Cairo, Egypt, Atmos. Environ., 45, 7352-7359, https://doi.org/10.1016/j.atmosenv.2011.07.043, 2011.

Nežiková, B., Degrendele, C., Bandowe, B. A. M., Šmejkalová, A. H., Kukučka, P., Martiník, J., Mayer, L., Prokeš, R., Přibylová, P., Klánová, J., and Lammel, G.: Three years of atmospheric concentrations of nitrated and oxygenated polycyclic aromatic hydrocarbons and oxygen heterocycles at a central European background site, Chemosphere, 269, 128738, https://doi.org/10.1016/j.chemosphere.2020.128738, 2021.

Novelli, A., Hens, K., Tatum Ernest, C., Kubistin, D., Regelin, E., Elste, T., Plass-Dülmer, C., Martinez, M., Lelieveld, J., and Harder, H.: Characterisation of an inlet pre-injector laser-induced fluorescence instrument for the measurement of atmospheric hydroxyl radicals, Atmos. Meas. Tech., 7, 3413–3430, https://doi.org/10.5194/amt-7-3413-2014, 2014.

OEHHA (California Office of Environmental Health Hazard Assessment): Chemicals, https://oehha.ca.gov/chemicals/, last access: 02 December 2021.

Perraudin, E., Budzinski, H., and Villenave, E.: Identification and quantification of primary ozonation products of phenanthrene and anthracene adsorbed on silica particles, Atmos. Environ., 41, 6005–6017, https://doi.org/10.1016/j.atmosenv.2007.03.010, 2007.

Pfannerstill, E. Y., Wang, N., Edtbauer, A., Bourtsoukidis, E., Crowley, J. N., Dienhart, D., Eger, P. G., Ernle, L., Fischer, H., Hottmann, B., Paris, J.-D., Stönner, C., Tadic, I., Walter, D., Lelieveld, J., and Williams, J.: Shipborne measurements of total OH reactivity around the Arabian Peninsula and its role in ozone chemistry, Atmos. Chem. Phys., 19, 11501–11523, https://doi.org/10.5194/acp-19-11501-2019, 2019.

Polissar, A. V., Hopke, P. K., Paatero, P., Malm, W. C., and Sisler, J. F.: Atmospheric aerosol over Alaska: 2. Elemental composition and sources, J. Geophys. Res. 103, 19045–19057, https://doi.org/10.1029/98JD01212, 1998.

Ravindra, K., Sokhi, R., and Van Grieken, R.: Atmospheric polycyclic aromatic hydrocarbons: source attribution, emission factors and regulation, Atmos. Environ., 42, 2895-2921., https://doi.org/10.1016/j.atmosenv.2007.12.010, 2008.

Reisen, F. and Arey, J.: Atmospheric reactions influence seasonal PAH and nitro-PAH concentrations in the Los Angeles basin, Environ. Sci. Technol., 39, 64–73. https://doi.org/10.1021/es035454l, 2005.

Ringuet, J., Albinet, A., Leoz-Garziandia, E., Budzinski, H., and Villenave, E.: Reactivity of polycyclic aromatic compounds (PAHs, NPAHs and OPAHs) adsorbed on natural aerosol particles exposed to atmospheric oxidants, Atmos. Environ., 61, 15–22. http://dx.doi.org/10.1016/j.atmosenv.2012.07.025, 2012a.

Ringuet, J., Leoz-Garziandia, E., Budzinski, H., Villenave, E., and Albinet, A.: Particle size distribution of nitrated and oxygenated polycyclic aromatic hydrocarbons (NPAHs and OPAHs) on traffic and suburban sites of a European megacity: Paris (France), Atmos. Chem. Phys., 12, 8877–8887, https://doi.org/10.5194/acp-12-8877-2012, 2012b.

Rosu, A., Rosu, B., Constantin, D. E., Arseni, M., Voiculescu, M., Georgescu, L. P., and Popa, I. Overview of tropospheric NO_2 using the ozone monitoring observations instrument and human perception about air quality for the most polluting countries accross the world, Carpathian J. Earth Environ. Sci., 14, 423–430, https://doi.org/10.26471/cjees/2019/014/091, 2019.

Schaub, D., Brunner, D., Boersma, K. F., Keller, J., Folini, D., Buchmann, B., Berresheim, H., and Staehelin, J.: SCIAMACHY tropospheric NO_2 over Switzerland: estimates of NO_x lifetimes and impact of the complex Alpine topography on the retrieval, Atmos. Chem. Phys., 7, 5971–5987, https://doi.org/10.5194/acp-7-5971-2007, 2007.

Scipioni, C., Villanueva, F., Pozo, K., and Mabilia, R.: Preliminary characterization of polycyclic aromatic hydrocarbons, nitrated polycyclic aromatic hydrocarbons and polychlorinated dibenzo-p-dioxins and furans in atmospheric PM_{10} of an urban and a remote area of Chile, Environ. Technol., 33, 809–820, https://doi.org/10.1080/09593330.2011.597433, 2012.

Seibert, P. and Frank, A.: Source-receptor matrix calculation with a Lagrangian particle dispersion model in backward mode, Atmos. Chem. Phys., 4, 51–63, https://doi.org/10.5194/acp-4-51-2004, 2004.

Shah, V., Jacob, D. J., Li, K., Silvern, R. F., Zhai, S., Liu, M., Lin, J., and Zhang, Q.: Effect of changing NO_x lifetime on the seasonality and long-term trends of satellite-observed tropospheric NO_2 columns over China, Atmos. Chem. Phys., 20, 1483–1495, https://doi.org/10.5194/acp-20-1483-2020, 2020.

Shen, J., Zhang, S., Lian, J., Kong, L., and Chen, J.: Benz[a]anthracene heterogeneous photochemical reaction on the surface of TiO_2 particles, Acta Phys. Chim. Sin., 23, 1531–1536, https://doi.org/10.1016/S1872-1508(07)60078-3, 2007.

Shiraiwa, M., Garland, R. M., and Pöschl, U.: Kinetic double-layer model of aerosol surface chemistry and gas-particle interactions (K2-SURF): Degradation of polycyclic aromatic hydrocarbons exposed to O_3, NO_2, H_2O, OH and NO_3, Atmos. Chem. Phys., 9, 9571–9586, https://doi.org/10.5194/acp-9-9571-2009, 2009.

Shiraiwa, M., Ueda, K., Pozzer, A., Lammel, G., Kampf, C. J., Fushimi, A., Enami, S., Arangio, A. M., Fröhlich-Nowoisky, J., Fujitani, Y., Furuyama, A., Lakey, P. S. J., Lelieveld, J., Lucas, K., Morino, Y., Pöschl, U., Takahama, S., Takami, A., Tong, H., Weber, B., Yoshino, A., and Sato, K.: Aerosol health effects from molecular to global scales, Environ. Sci. Technol., 51, 1354513567, https://doi.org/10.1021/acs.est.7b04417, 2017.

Stohl, A., Forster, C., Frank, A., Seibert, P., and Wotawa, G.: Technical note: The Lagrangian particle dispersion model FLEXPART version 6.2, Atmos. Chem. Phys., 5, 2461–2474, https://doi.org/10.5194/acp-5-2461-2005, 2005.

Streibel, T., Schnelle-Kreis, J., Czech, H., Harndorf, H., Jakobi, G., Jokiniemi, J., Karg, E., Lintelmann, J., Matuschek, G., Michalke, B., Müller, L., Orasche, J., Passig, J.,Radischat, C., Rabe, R., Reda, A., Rüger, C., Schwemer, T., Sippula, O., Stengel, B.,Sklorz, M., Torvela, T., Weggler, B., and Zimmermann, R.: Aerosol emissions of a ship diesel engine operated with diesel fuel or heavy fuel oil, Environ. Sci. Pollut. Res., 24, 10976–10991, https://doi.org/10.1007/s11356-016-6724-z, 2017.

Sverdrup, L. E., Ekelund, F., Krogh, P. H., Nielsen, T., and Johnsen, K.: Soil microbial toxicity of eight polycyclic aromatic compounds: effects on nitrification, the genetic diversity of bacteria, and the total number of protozoans, Environ. Toxicol. Chem., 21, 1644-1650, https://doi.org/10.1002/etc.5620210815, 2002a.

Sverdrup, L. E., Krogh, P. H., Nielsen, T., and Stenersen, J.: Relative sensitivity of three terrestrial invertebrate tests to polycyclic aromatic compounds, Environ. Toxicol. Chem., 21, 1927-1933, https://doi.org/10.1002/etc.5620210921, 2002b.

Tadic, I., Crowley, J. N., Dienhart, D., Eger, P., Harder, H., Hottmann, B., Martinez, M., Parchatka, U., Paris, J.-D., Pozzer, A., Rohloff, R., Schuladen, J., Shenolikar, J., Tauer, S., Lelieveld, J., and Fischer, H.: Net ozone production and its relationship to nitrogen oxides and volatile organic compounds in the marine boundary layer around the Arabian Peninsula, Atmos. Chem. Phys., 20, 6769–6787, https://doi.org/10.5194/acp-20-6769-2020, 2020.

Tang, N., Sato, K., Tokuda, T., Tatematsu, M., Hama, H., Suematsu, C., Kameda, T., Toriba, A., and Hayakawa, K.: Factors affecting atmospheric 1-, 2-nitropyrenes and 2-nitrofluoranthene in winter at Noto Peninsula, a remote background site, Japan, Chemosphere, 107, 324–330, https://doi.org/10.1016/j.chemosphere.2013.12.077, 2014.

Tobiszewski, M. and Namieśnik, J.: PAH diagnostic ratios for the identification of pollution emission sources, Environ. Pollut., 162, 110-119, https://doi.org/10.1016/j.envpol.2011.10.025, 2012.

Tomaz, S., Shahpoury, P., Jaffrezo, J. L., Lammel, G., Perraudin, E., Villenave, E., and Albinet, A.: One-year study of polycyclic aromatic compounds at an urban site in Grenoble (France): seasonal variations, gas/particle partitioning and cancer risk estimation, Sci. Total Environ., 565, 1071–1083, http://dx.doi.org/10.1016/j.scitotenv.2016.05.137, 2016.

Tomaz, S., Jaffrezo, J.-L., Favez, O., Perraudin, E., Villenave, E., and Albinet, A.: Sources and atmospheric chemistry of oxy- and nitro-PAHs in the ambient air of Grenoble (France), Atmos. Environ., 161, 144–154, https://doi.org/10.1016/j.atmosenv.2017.04.042, 2017.

Tsapakis, M. and Stephanou, E. G.: Occurrence of gaseous and particulate polycyclic aromatic hydrocarbons in the urban atmosphere: study of sources and ambient temperature effect on the gas/particle concentration and distribution, Environ. Pollut., 133, 147-156, https://doi.org/10.1016/j.envpol.2004.05.012, 2005.

Tsapakis, M. and Stephanou, E. G.: Diurnal cycle of PAHs, nitro-PAHs, and oxy-PAHs in a high oxidation capacity marine background atmosphere, Environ. Sci. Technol., 41, 8011–8017, https://doi.org/10.1021/es071160e, 2007.

Turcotte, D., Akhtar, P., Bowerman, M., Kiparissis, Y., Brown, R. S., and Hodson, P. V.: Measuring the toxicity of alkyl-phenanthrenes to early life stages of medaka (Oryzias latipes) using partition controlled delivery, Environ. Toxicol. Chem., 30, 487–495, https://doi.org/10.1002/etc.404, 2011.

USEPA (United States Environmental Protection Agency): Estimation Programs Interface Suite™ for Microsoft® Windows, v 4.11, 2019.

Valavanidis, A., Vlachogianni, T., Triantafyllaki, S., Dassenakis, M., Androutsos, F., and Scoullos, M.: Polycyclic aromatic hydrocarbons in surface seawater and in indigenous mussels (Mytilus galloprovincialis) from coastal areas of the Saronikos Gulf (Greece), Estuar. Coast. Shelf Sci., 79, 733-739, https://doi.org/10.1016/j.ecss.2008.06.018, 2008.

Verma, V., Wang, Y., El-Afifi, R., Fang, T., Rowland, J., Russell, A. G., and Weber, R. J.: Fractionating ambient humic-like substances (HULIS) for their reactive oxygen species activity − Assessing the importance of quinones and atmospheric aging, Atmos. Environ., 120, 351–359, https://doi.org/10.1016/j.atmosenv.2015.09.010, 2015.

Vincenti, M., Maurino, V., Minero, C., and Pelizzetti, E.: Detection of nitro-substituted polycyclic aromatic hydrocarbons in the Antarctic airborne particulate, Int. J. Environ. Anal. Chem., 79, 257–272, https://doi.org/10.1080/03067310108044388, 2001.

Walgraeve, C., Demeestere, K., Dewulf, J., Zimmermann, R., and Van Langenhove, H.: Oxygenated polycyclic aromatic hydrocarbons in atmospheric particulate matter: molecular characterization and occurrence, Atmos. Environ., 44, 1831–1846, https://doi.org/10.1016/j.atmosenv.2009.12.004, 2010.

Wang, L., Atkinson, R., and Arey, J.: Formation of 9,10-phenanthrenequinone by atmospheric gas-phase reactions of phenanthrene, Atmos. Environ., 41, 2025–35, https://doi.org/10.1016/j.atmosenv.2006.11.008, 2007.

Wang, N., Edtbauer, A., Stönner, C., Pozzer, A., Bourtsoukidis, E., Ernle, L., Dienhart, D., Hottmann, B., Fischer, H., Schuladen, J., Crowley, J. N., Paris, J.-D., Lelieveld, J., and Williams, J.: Measurements of carbonyl compounds around the Arabian Peninsula: overview and model comparison, Atmos. Chem. Phys., 20, 10807–10829, https://doi.org/10.5194/acp-20-108072020, 2020.

Wassenaar, P. N. H. and Verbruggen, E. M. J.: Persistence, bioaccumulation and toxicity-assessment of petroleum UVCBs: A case study on alkylated three-ring PAHs, Chemosphere 276, 130113, https://doi.org/10.1016/j.chemosphere.2021.130113, 2021.

Wei, C., Han, Y. M., Bandowe, B. A. M., Cao, J. J., Huang, R. J., Ni, H. Y., Tian, J., and Wilcke, W.: Occurrence, gas/particle partitioning and carcinogenic risk of polycyclic aromatic hydrocarbons and their oxygen and nitrogen containing derivatives in Xi'an, central China, Sci. Total Environ., 505, 814–822, http://dx.doi.org/10.1016/j.scitotenv.2014.10.054, 2015.

Wilson, J., Octaviani, M., Bandowe, B. A. M., Wietzoreck, M., Zetzsch, C., and Pöschl, U.: Modeling the formation, degradation, and spatiotemporal distribution of 2-nitrofluoranthene in the global atmosphere, Environ. Sci. Technol., 54, 14224–14234, https://doi.org/10.1021/acs.est.0c04319, 2020.

Xiong, Q., Yu, H., Wang, R., Wei, J., and Verma, V.: Rethinking dithiothreitol-based particulate matter oxidative potential: measuring dithiothreitol consumption versus reactive oxygen species generation, Environ. Sci. Technol., 51, 6507–6514, https://doi.org/10.1021/acs.est.7b01272, 2017.

Zhang, J., Yang, L., Mellouki, A., Chen, J., Chen, X., Gao, Y., Jiang, P., Li, Y., Yu, H., and Wang, W: Atmospheric PAHs, NPAHs, and OPAHs at an urban, mountainous, and marine sites in Northern China: Molecular composition, sources, and ageing, Atmos. Environ., 173, 256–264, https://doi.org/10.1016/j.atmosenv.2017.11.002, 2018.

Zhao, J., Zhang, Y., Wang, T., Sun, L., Yang, Z., Lin, Y., Chen, Y., and Mao, H.: Characterization of $PM_{2.5}$-bound polycyclic aromatic hydrocarbons and their derivatives (nitro-and oxy-PAHs) emissions from two ship engines under different operating conditions, Chemosphere, 225, 43–52, https://doi.org/10.1016/j.chemosphere.2019.03.022, 2019.

Zhao, J., Zhang, Y., Chang, J., Peng, S., Hong, N., Hu, J., Ly, J., Wang, T., and Mao, H.: Emission characteristics and temporal variation of PAHs and their derivatives from an ocean-going cargo vessel, Chemosphere, 249, 126194, https://doi.org/10.1016/j.chemosphere.2020.126194, 2020.

Zhao, Y., Cao, L., Zhou, Q., Que, Q., and Hong, B.: Effects of oil pipeline explosion on ambient particulate matter and their associated polycyclic aromatic hydrocarbons, Environ. Pollut., 196, 440–449, https://doi.org/10.1016/j.envpol.2014.11.012, 2015.

Zhuo, S., Du, W., Shen, G., Li, B., Liu, J., Cheng, H., Xing, B., and Tao, S.: Estimating relative contributions of primary and secondary sources of ambient nitrated and oxygenated polycyclic aromatic hydrocarbons, Atmos. Environ., 159, 126–134, http://dx.doi.org/10.1016/j.atmosenv.2017.04.003, 2017.

Zimmermann, K., Atkinson, R., Arey, J., Kojima, Y., and Inazu, K.: Isomer distributions of molecular weight 247 and 273 nitro-PAHs in ambient samples, NIST Diesel SRM, and from radical-initiated chamber reactions, Atmos. Environ, 55, 431−439, https://doi.org/10.1016/j.atmosenv.2012.03.016, 2012.

Supplement of

Polycyclic aromatic hydrocarbons (PAHs) and their alkylated-, nitro- and oxy-derivatives in the atmosphere over the Mediterranean and Middle East seas

Marco Wietzoreck et al.

Correspondence to: Prof. Dr. Gerhard Lammel (g.lammel@mpic.de)

Content

1 Methods

1.1 Sampling

a)

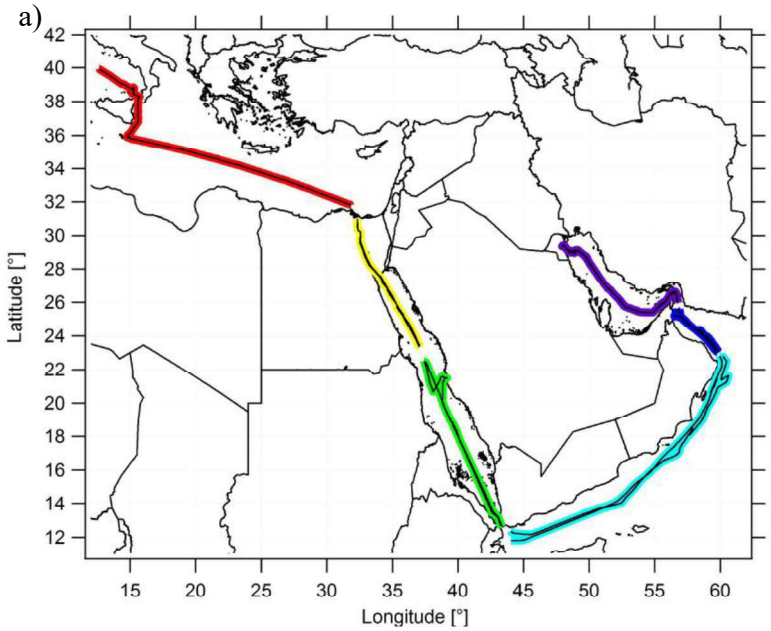

b)

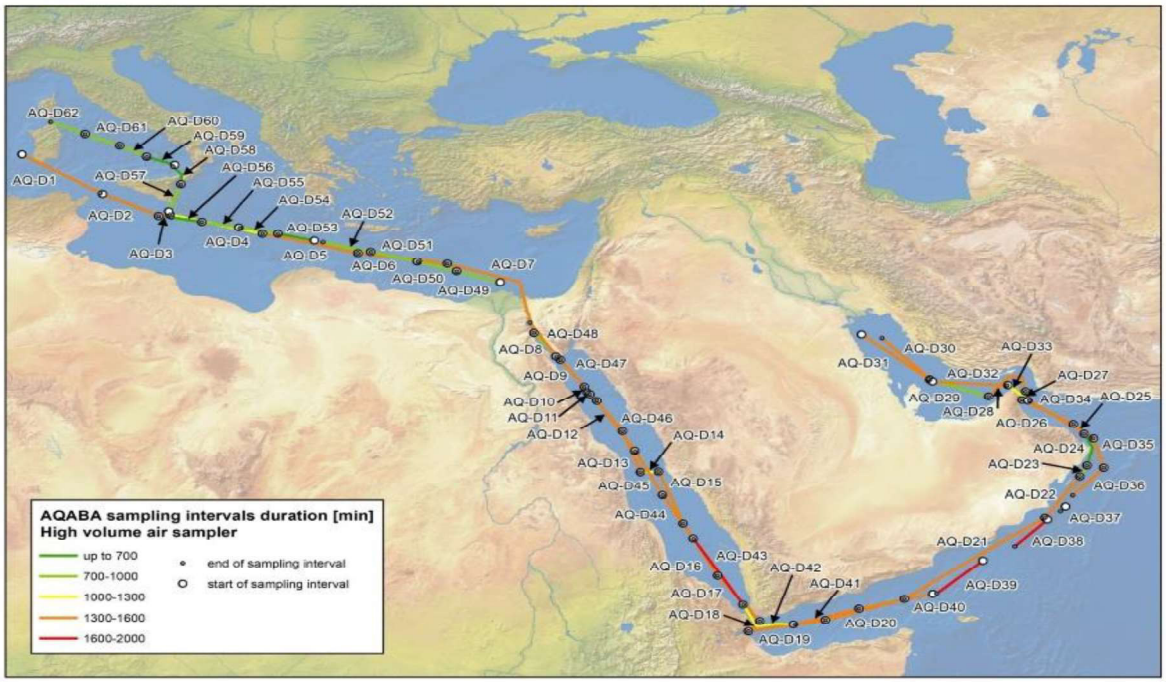

c)

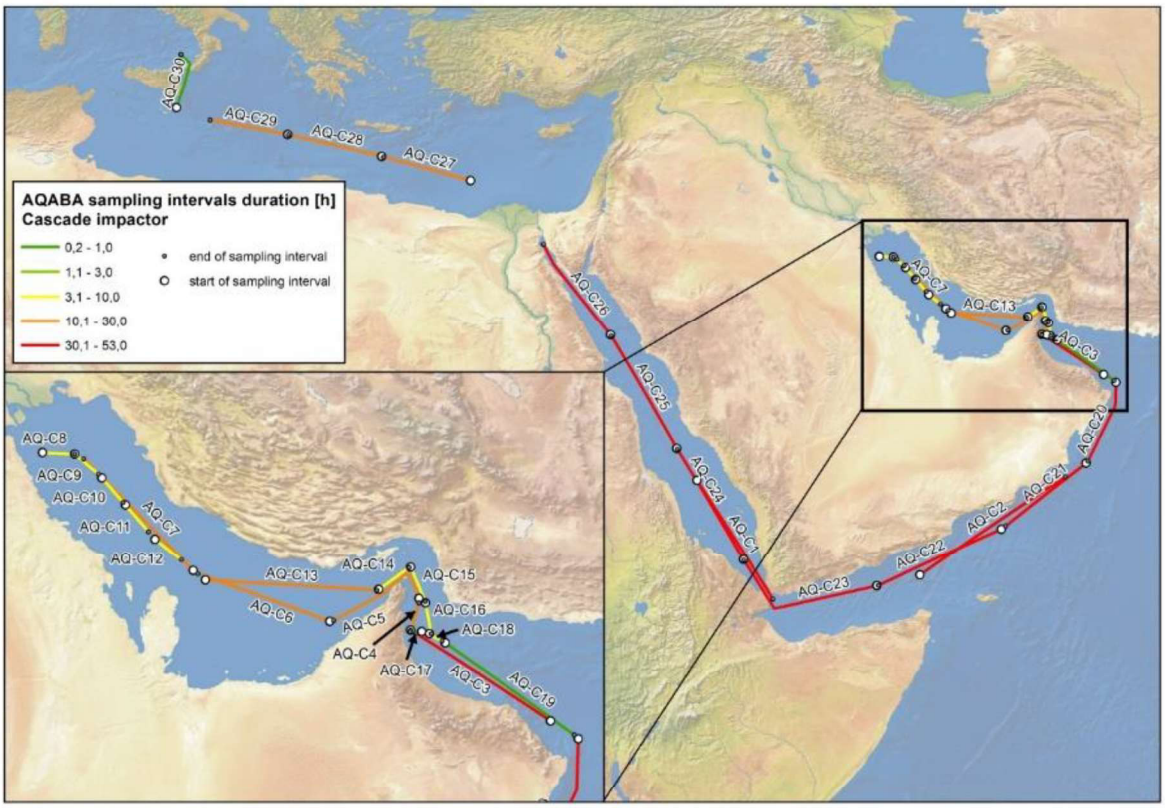

Figure S1. Overview of samples and sampling regions: (a) The ship cruise during both legs divided into six regions i.e. Mediterranean Sea (red), northern Red Sea (yellow), southern Red Sea (green), Arabian Sea (turquoise blue), Oman Gulf (blue) and Arabian Gulf (purple), taken from Tadic et al. (2020); (b) Digitel high volume air samples and (c) cascade impactor samples.

Table S1. Information about a) Digitel high-volume air samples, b) cascade impactor air samples and c) GMWL high volume air samples (MS: Mediterranean Sea; NRS: Northern Red Sea; SRS: Southern Red Sea; AS: Arabian Sea; OG: Gulf of Oman; AG: Arabian Gulf).

a)

Sample	Leg	Date (from)	Time (from) [CEST]	Date (to)	Time (to) [CEST]	GPS (from) N	E	GPS (to) N	E	Measured volume V_M [m³]	Sampling time [min]	Sampling distance [km]	Loca-tion
D1	1.	25.6.	20:00	26.6.	20:00	39.4110	7.8441	37.1900	11.6460	784	1440	436	MS
D2		26.6.	20:03	27.6.	20:03	37.1443	11.7618	35.8793	14.5000	795	1440	295	
D3		27.6.	20:05	28.6.	20:05	35.8793	14.5000	35.9497	15.0443	794	1440	52	
D4		28.6.	23:02	29.6.	20:04	35.9497	15.0443	34.8415	19.5523	695	1260	445	
D5		29.6.	20:06	30.6.	20:06	34.8415	19.5523	33.7255	24.1933	791	1440	458	
D6		30.6.	20:08	1.7.	20:08	33.7255	24.1933	33.1043	28.5567	812	1440	420	
D7		1.7.	20:10	2.7.	20:10	33.1043	28.5567	29.0867	32.7673	817	1440	596	
D8		4.7.	6:57	4.7.	18:57	29.0867	32.7673	27.5277	34.0502	402	720	210	NRS
D9		4.7.	18:59	5.7.	18:59	27.5277	34.0502	25.9717	35.2202	801	1440	204	
D10		5.7.	19:23	6.7.	18:53	25.9717	35.2202	25.6453	35.3770	784	1409	39	
D11		6.7.	18:55	7.7.	18:55	25.6453	35.3770	25.5470	35.4954	790	1440	16	
D12		7.7.	18:58	8.7.	18:58	25.5470	35.4954	23.3869	37.0715	794	1440	281	
D13		8.7.	19:00	9.7.	19:00	23.3869	37.0715	21.0164	37.9455	794	1440	274	
D14		9.7.	19:05	10.7.	12:05	21.0164	37.9455	21.0367	38.8356	568	1020	85	
D15		13.7.	18:39	14.7.	18:09	21.0367	38.8356	18.0332	40.0246	779	1410	349	SRS
D16		14.7.	18:13	15.7.	18:13	18.0332	40.0246	15.0308	41.7014	808	1440	367	
D17		15.7.	18:15	16.7.	18:15	15.0308	41.7014	12.3720	43.7483	803	1440	351	
D18		16.7.	18:18	17.7.	17:18	12.3720	43.7483	11.7775	43.2027	774	1380	83	AS
D19		17.7.	17:20	18.7.	17:20	11.7775	43.2027	12.4396	46.9400	796	1440	362	
D20		18.7.	17:22	19.7.	17:22	12.4396	46.9400	13.6648	50.7978	797	1440	390	

Sample	Leg	Date (from)	Time (from) [CEST]	Date (to)	Time (to) [CEST]	GPS (from) N	E	GPS (to) N	E	Measured volume V_M [m³]	Sampling time [min]	Sampling distance [km]	Loca-tion
D21		19.7.	17:26	20.7.	16:57	13.6648	50.7978	18.3700	57.6239	775	1410	830	
D22		21.7.	16:46	22.7.	16:46	18.3700	57.6239	20.7557	59.3353	809	1440	309	
D23		22.7.	16:57	23.7.	5:33	20.7557	59.3353	21.3861	59.6827	415	756	77	
D24		23.7.	5:37	23.7.	15:42	21.3861	59.6827	23.2304	59.5282	332	607	203	OG
D25		24.7.	16:10	25.7.	16:10	23.2304	59.5282	23.8155	59.0073	799	1440	81	
D26		25.7.	16:18	26.7.	16:18	23.8155	59.0073	25.2141	56.5100	805	1440	283	
D27		26.7.	16:32	27.7.	16:50	25.2141	56.5100	25.7168	56.6810	787	1413	58	
D28		27.7.	16:52	28.7.	16:52	25.7168	56.6810	25.4281	54.8918	817	1440	173	OG+AG
D29		28.7.	16:54	29.7.	17:01	25.4281	54.8918	26.3865	52.0304	499	864	292	AG
D30		29.7.	17:23	30.7.	17:23	26.3865	52.0304	28.7900	49.7010	825	1440	345	
D31		3.8.	17:10	4.8.	17:10	28.9927	48.6996	26.4322	51.9517	812	1441	418	
D32		4.8.	17:21	5.8.	17:20	26.2731	52.1573	26.0567	55.7913	807	1440	346	
D33		5.8.	17:40	6.8.	17:40	26.0756	55.8329	25.1666	56.8767	644	1155	141	AG+OG
D34		6.8.	17:42	7.8.	17:10	25.1700	56.8000	22.9889	59.9747	779	1408	385	OG
D35		7.8.	17:12	8.8.	16:12	22.9634	60.0008	21.2597	60.4880	742	1380	193	OG+AS
D36		8.8.	16:13	9.8.	16:13	21.2587	60.4874	19.6600	58.9770	789	1440	227	AS
D37		10.8.	10:08	10.8.	19:10	19.0221	58.6283	18.7540	58.3900	287	542	37	
D38	2.	11.8.	10:57	12.8.	20:01	18.2657	57.7522	16.7120	56.1640	1095	1984	228	
D39		13.8.	9:15	14.8.	15:55	15.8960	54.6114	14.0040	52.3650	1002	1840	298	
D40		14.8.	16:58	15.8.	16:58	13.9619	52.1715	13.0980	48.5870	793	1440	354	
D41		15.8.	16:59	16.8.	14:59	13.0980	48.5870	12.1754	45.4446	729	1321	315	
D42		16.8.	15:01	17.8.	8:26	12.1785	45.3979	13.3355	42.9452	577	1046	265	AS+SRS
D43		17.8.	8:59	18.8.	15:59	13.3344	42.9399	17.1423	40.5228	1036	1860	478	SRS
D44		18.8.	16:07	19.8.	16:47	17.1647	40.5099	19.6559	39.0315	822	1480	308	
D45		19.8.	16:51	20.8.	17:11	19.6672	39.0248	22.2321	37.6864	805	1460	309	SRS+NRS

Sample	Leg	Date (from)	Time (from) [CEST]	Date (to)	Time (to) [CEST]	GPS (from) N	E	GPS (to) N	E	Measured volume V_M [m³]	Sampling time [min]	Sampling distance [km]	Loca-tion
D46		20.8.	17:19	21.8.	17:39	22.2577	37.6721	25.1606	35.8253	807	1460	364	NRS
D47		21.8.	17:45	22.8.	17:45	25.1640	35.8230	27.7194	33.8617	788	1440	337	
D48		22.8.	17:49	23.8.	17:49	27.7194	33.8402	29.6664	32.5684	766	1390	246	
D49		25.8.	6:16	25.8.	17:56	32.0212	31.1175	32.6587	29.0216	382	700	211	MS
D50		25.8.	18:00	26.8.	5:49	32.6676	28.9995	33.2112	27.1166	387	710	189	
D51		26.8.	6:04	26.8.	17:54	33.2220	27.0848	33.7990	24.8300	388	710	223	
D52		26.8.	17:55	27.8.	5:58	33.7990	24.8260	34.3590	22.5030	390	720	229	
D53		27.8.	6:08	27.8.	18:08	34.4510	22.0770	34.8360	20.3220	327	600	172	
D54		27.8.	18:10	28.8.	5:50	34.8380	20.3110	35.2140	18.4550	380	700	181	
D55		28.8.	6:05	28.8.	18:05	35.2220	18.4070	35.5460	16.6030	395	720	175	
D56		28.8.	18:07	29.8.	5:07	35.5470	16.6000	35.7990	15.1150	364	660	144	
D57		29.8.	18:26	30.8.	6:26	36.1310	14.9850	37.6930	15.5790	393	720	181	
D58		30.8.	6:30	30.8.	17:48	37.7020	15.5790	38.7350	15.1990	370	679	119	
D59		30.8.	20:26	31.8.	6:27	38.8210	15.2770	39.2720	13.9380	327	600	137	
D60		31.8.	6:41	31.8.	18:41	39.2870	13.9100	39.9290	12.6160	391	720	142	
D61		31.8.	18:42	1.9.	6:42	39.9290	12.6160	40.6140	10.9285	393	720	177	
D62		1.9.	6:47	1.9.	18:47	40.6140	10.9285	41.2990	9.2410	397	720	177	

b)

Sample	Leg	Date (from)	Time (from) [CEST]	Date (to)	Time (to) [CEST]	GPS (from) N	E	GPS (to) N	E	Measured volume V_M [m³]	Sampling time [min]	Sampling distance [km]	Loca-tion
C1	1.	14.7.	16:57	16.7.	16:57	18.195	39.955	12.457	43.594	3265	720	2880	SRS
C2		19.7.	16:43	21.7.	16:43	13.618	50.646	18.364	57.617	3264	843	2880	AS
C3		24.7.	16:33	26.7.	16:33	23.2817	59.477	25.214	56.51	3265	353	2880	OG
C4		26.7.	17:24	27.7.	17:24	25.2140	56.5100	25.788	56.683	1634	65	1440	
C5		27.7.	18:07	28.7.	17:07	25.8859	56.6830	25.414	54.875	1565	179	1380	OG+AG
C6		28.7.	17:42	29.7.	17:42	25.3974	54.7936	26.411	51.995	1633	288	1440	AG
C7		29.7.	18:25	30.7.	18:25	26.4764	51.8983	28.861	49.571	1633	343	1440	
C8	2.	3.8.	17:15	3.8.	21:15	28.9927	48.6996	28.9646	49.3836	272	65	240	
C9		3.8.	21:35	4.8.	01:35	28.9646	49.3836	28.5397	49.8889	272	67	240	
C10		4.8.	01:50	4.8.	05:50	28.4588	49.9619	27.9373	50.4113	274	72	240	
C11		4.8.	06:21	4.8.	10:21	27.8865	50.456	27.3166	50.9476	272	78	240	
C12		4.8.	10:50	4.8.	14:50	27.1521	51.0884	26.7096	51.6455	272	72	240	
C13		4.8.	17:20	5.8.	17:20	26.2731	52.1573	26.0567	55.7913	1639	346	1440	
C14		5.8.	18:00	5.8.	22:00	26.0756	55.8329	26.5434	56.473	272	80	240	
C15		5.8.	22:55	6.8.	02:55	26.5498	56.5062	25.821	56.8161	280	85	240	OG
C16		6.8.	03:20	6.8.	07:20	25.7857	56.826	25.1382	56.9413	273	72	240	
C17		6.8.	07:40	6.8.	11:38	25.1349	56.9046	25.174	56.4922	272	39	240	
C18		6.8.	16:20	6.8.	20:20	25.1797	56.7423	24.9866	57.1796	273	47	240	
C19		6.8.	21:15	7.8.	17:17	24.942	57.2383	22.9889	59.9747	1369	337	1202	
C20		7.8.	17:40	9.8.	19:44	22.906	60.0624	19.1271	58.7116	3264	435	3004	AS
C21		10.8.	10:20	13.8.	07:27	19.0221	58.6283	16.006	54.765	3264	495	4147	
C22		13.8.	09:35	15.8.	15:35	15.852	54.5538	13.1192	48.6622	3604	635	3240	
C23		15.8.	16:50	17.8.	16:50	13.101	48.598	14.324	42.2126	3265	621	2880	AS+SRS
C24		17.8.	17:13	19.8.	17:13	14.3559	42.1942	19.6937	39.0091	3265	661	2880	SRS
C25		19.8.	17:33	21.8.	17:33	19.7215	38.9907	25.152	35.832	3264	668	2880	NRS

Sample	Leg	Date (from)	Time (from) [CEST]	Date (to)	Time (to) [CEST]	GPS (from) N	E	GPS (to) N	E	Measured volume V_M [m³]	Sampling time [min]	Sampling distance [km]	Loca-tion
C26		21.8.	17:57	23.8.	15:57	25.19	35.805	29.569	32.587	3128	571	2760	
C27		25.8.	17:34	26.8.	17:34	32.6345	29.0929	33.7758	24.9187	1632	416	1440	MS
C28		26.8.	17:52	27.8.	17:52	33.797	24.836	34.8299	20.355	1632	441	1440	
C29		27.8.	18:07	28.8.	18:07	34.836	20.319	35.547	16.599	1633	362	1440	
C30		29.8.	18:25	30.8.	17:48	36.131	14.985	38.735	15.199	1589	287	1403	

c)

Sample	Leg	Date (from)	Time (from) [CEST]	Date (to)	Time (to) [CEST]	GPS (from) N	E	GPS (to) N	E	Measured volume V_M [m^3]	Sampling time [min]	Location
G1	1	25.06.2017	08:21	26.06.2017	06:52	No data	No data	38.225	9.401	709	1351	MS
G2		26.06.2017	08:14	27.06.2017	06:48	38.105	9.654	36.452	13.553	700	1354	MS
G3		27.06.2017	07:30	28.06.2017	06:44	36.406	13.675	35.879	14.501	720	1394	MS
G4		28.06.2017	07:29	29.06.2017	07:00	35.879	14.501	35.532	16.675	700	1411	MS
G5		29.06.2017	07:42	30.06.2017	06:54	35.497	16.824	34.363	21.593	733	1392	MS
G6		30.06.2017	07:29	01.07.2017	06:46	34.334	21.709	33.198	26.263	704	1397	MS
G7		01.07.2017	07:21	02.07.2017	06:56	33.167	26.383	32.319	30.378	725	1415	MS
G8		02.07.2017	07:34	03.07.2017	07:05	32.280	30.484	30.373	32.357	710	1411	NRS
G9		04.07.2017	07:43	05.07.2017	06:03	29.005	32.802	26.229	35.022	687	1340	NRS
G10		07.07.2017	11:17	08.07.2017	06:26	25.199	35.847	24.927	36.080	574	1152	NRS
G11		08.07.2017	06:56	09.07.2017	05:52	24.876	36.131	22.025	37.610	688	1377	NRS
G12		09.07.2017	06:19	10.07.2017	05:32	21.971	37.625	21.182	38.493	694	1391	NRS/SRS
G13		14.07.2017	05:34	15.07.2017	05:19	19.527	39.109	16.636	40.786	685	1429	SRS
G14		15.07.2017	05:49	16.07.2017	05:28	16.573	40.822	13.634	42.500	687	1424	SRS
G15		16.07.2017	07:47	17.07.2017	07:50	13.394	42.738	11.678	43.154	663	1326	SRS/AS
G16		19.07.2017	06:02	21.07.2017	04:57	13.086	48.956	17.085	56.037	1326	2817	AS
G17		21.07.2017	05:26	22.07.2017	04:59	17.135	56.104	20.012	59.022	714	1416	AS
G18		22.07.2017	05:24	22.07.2017	21:35	20.082	59.068	20.696	59.309	459	926	AS
G19		23.07.2017	04:03	23.07.2017	15:47	21.445	59.700	20.966	59.534	318	713	AS
G20		25.07.2017	09:29	26.07.2017	04:33	24.223	58.598	24.843	57.436	581	1151	OG
G21		26.07.2017	04:55	27.07.2017	05:35	24.878	57.390	25.224	56.499	691	1387	OG
G22		27.07.2017	05:56	28.07.2017	04:36	25.224	56.499	26.433	56.144	681	1363	OG
G23		29.07.2017	06:46	30.07.2017	04:24	25.648	53.110	27.354	50.895	652	1304	AG
G24		30.07.2017	04:50	31.07.2017	08:10	27.397	50.865	29.407	48.081	698	1395	AG

Sample	Leg	Date (from)	Time (from) [CEST]	Date (to)	Time (to) [CEST]	GPS (from) N	E	GPS (to) N	E	Measured volume V_M [m³]	Sampling time [min]	Location
G25		05.08.2017	05:15	06.08.2017	05:15	25.459	53.705	25.446	56.916	485	1012	AG
G26		06.08.2017	06:04	07.08.2017	05:15	25.312	56.949	24.170	58.495	450	931	OG
G27		07.08.2017	06:28	08.08.2017	05:03	24.082	58.683	21.606	60.115	664	1350	OG
G28		09.08.2017	05:32	10.08.2017	10:25	20.350	59.489	19.014	58.612	863	1726	AS
G29		10.08.2017	10:50	11.08.2017	08:38	19.041	58.636	18.103	57.658	677	1310	AS
G30		11.08.2017	11:02	13.08.2017	09:44	18.238	57.736	15.832	54.529	1428	2787	AS
G31		13.08.2017	10:22	14.08.2017	17:02	15.779	54.471	13.974	52.223	945	1830	AS
G32		14.08.2017	17:15	15.08.2017	09:12	13.968	52.195	13.429	49.657	490	957	AS
G33		16.08.2017	12:19	17.08.2017	06:48	12.228	45.788	13.029	43.163	557	1105	AS
G34	2	17.08.2017	07:47	18.08.2017	04:47	13.165	43.099	15.904	41.271	638	1266	SRS
G35		19.08.2017	06:12	20.08.2017	05:05	18.531	39.683	20.974	38.354	672	1367	SRS
G36		20.08.2017	05:26	21.08.2017	05:00	21.011	38.332	23.737	36.817	698	1407	NRS
G37		21.08.2017	05:39	22.08.2017	05:10	23.819	36.760	26.427	34.929	679	1404	NRS
G38		22.08.2017	05:50	23.08.2017	05:18	26.492	34.877	28.700	33.009	713	1403	NRS
G39		23.08.2017	05:52	23.08.2017	17:30	28.749	32.985	29.700	32.564	357	702	NRS
G40		25.08.2017	05:55	26.08.2017	05:15	32.007	31.164	33.177	27.224	732	1394	MS
G41		26.08.2017	05:49	27.08.2017	05:50	33.206	27.134	34.353	22.528	742	1436	MS
G42		27.08.2017	06:25	28.08.2017	05:53	34.381	22.413	35.215	18.447	725	1403	MS
G43		28.08.2017	06:30	29.08.2017	05:45	35.233	18.349	35.813	15.044	723	1389	MS

1.2 Chemicals and physico-chemical properties

Table S2. Physico-chemical properties of a) PAHs, b) OPAHs c) NPAHs taken from EPI-Suite (USEPA 2019); MW = Molecular weight, n.d. = not determined.

a)

Compound	Acro-nym	CAS #	MW [g mol^{-1}]	# of rings	log K_{ow}	Water solubility [mg L^{-1}]	Vapor pressure [Pa]	Subcooled liquid vapour pressure (P_L)[Pa]	Octanol–air partition coeffi-cient (K_{OA})	OH rate constant [cm^3 $molec^{-1}$ sec^{-1}]	Half-life (based on OH rate con-stant) [h]	Ozone rate constant [cm^3 $molec^{-1}$ sec^{-1}]
Naphthalene	NAP	91-20-3	128.18	2	3.94	16.1	8.91E-01	4.14E+00	6.27	75.5 E-12	1.7	25.2 E-17
Acenaphthylene	ACY	208-96-8	152.20	3	3.92	3.9	2.87E-01	1.36E+00	6.31	66.9 E-12	1.92	
Acenaphthene	ACE	83-32-9	154.20	3	4.18	1.69	8.00E-02	6.18E-01	6.79	8.9 E-12	14.501	
Fluorene	FLN	86-73-7	166.23	3	4.46	1.15	1.61E-02	8.74E-02	7.57	13.0 E-12	9.873	
Phenanthrene	PHE	85-01-8	178.24	3	4.45	0.0434	8.71E-04	6.59E-02	7.55	40.0 E-12	3.209	
Anthracene	ANT	120-12-7	178.24	3	5.16	0.26	1.23E-03	8.10E-03	8.88	29.2 E-12	4.392	
Fluoranthene	FLT	206-44-0	202.26	4	4.88	0.135	6.00E-04	1.06E-02	8.80	50.0 E-12	2.567	
Pyrene	PYR	129-00-0	202.26	4	6.35	0.00848	0.000352	1.94E-03	8.70	41.7 E-12	3.078	
Retene	RET	483-65-8	234.34	3	5.77	0.03303	7.33E-06	5.18E-04	9.57	46.6 E-12	2.755	
Benzo(b)fluorene	BBN	243-17-4	216.28	4	5.52	0.04769	2.29E-05	4.66E-04	9.78	62.1 E-12	2.068	
Benzo(ghi)fluoranthene	BGF	203-12-3	226.28	5	5.70	0.03352	6.10E-05	1.06E-03	10.15	100.6 E-12	1.091	25.2 E-17
Cyclopenta(cd)pyrene	CCP	27208-37-3	226.28	5	5.70	0.03352	6.1E-005	0.00106	10.151	100.6 E-12	1.091	25.2 E-17
Benzo(a)anthracene	BAA	56-55-3	228.30	4	5.76	0.0094	2.80E-05	1.07E-04	9.07	50.0 E-12	2.567	
Triphenylene	TPH	217-59-4	228.30	4	5.49	0.0411	2.80E-06	1.47E-04	10.69	50.0 E-12	2.567	
Chrysene	CHR	218-01-9	228.30	4	5.81	0.002	8.31E-07	1.68E-04	9.48	50.0 E-12	2.567	
Benzo(b)fluoranthene	BBF	205-99-2	252.32	5	5.78	0.0015	6.67E-05	1.73E-03	10.35	18.6 E-12	6.918	
Benzo(j)fluoranthene	BJF	205-82-3	252.32	5	6.11	0.0025	3.50E-06	9.91E-05	10.59	53.6 E-12	2.394	
Benzo(k)fluoranthene	BKF	207-08-9	252.32	5	6.11	0.0008	1.29E-07	1.02E-05	10.73	53.6 E-12	2.394	
Benzo(e)pyrene	BEP	192-97-2	252.32	5	6.44	0.0063	7.60E-07	2.45E-05	11.35	50.0 E-12	2.567	
Benzo(a)pyrene	BAP	50-32-8	252.32	5	6.13	0.00162	7.32E-07	2.31E-05	10.86	50.0 E-12	2.567	
Perylene	PER	198-55-0	252.32	5	6.25	0.0004	7.00E-07	2.03E-04	10.08	50.0 E-12	2.567	

Compound	Acro-nym	CAS #	MW [g mol^{-1}]	# of rings	log K_{ow}	Water solubility [mg L^{-1}]	Vapor pressure [Pa]	Subcooled liquid vapour pressure (P_L)[Pa]	Octanol–air partition coeffi-cient (K_{OA})	OH rate constant [cm^3 $molec^{-1}$ sec^{-1}]	Half-life (based on OH rate con-stant) [h]	Ozone rate constant [cm^3 $molec^{-1}$ sec^{-1}]
Indeno(123-cd)pyrene	INP	193-39-5	276.34	6	6.7	0.001176	4.24E-08	3.66E-06	12.37	50.0 E-12	2.567	
Dibenz(ah)anthracene	DBA	53-70-3	278.36	5	6.54	0.00103	1.27E-07	3.33E-05	11.78	50.0 E-12	2.567	
Dibenz(ac)anthracene	DCA	215-58-7	278.36	5	6.41	0.0016	1.33E-08	8.22E-07	11.11	50.0 E-12	2.567	
Benzo(ghi)perylene	BPE	191-24-2	276.34	6	6.63	0.00026	1.33E-08	4.24E-06	11.50	86.9 E-12	1.478	
Anthanthrene	ATT	191-26-4	276.34	6	7.04	0.001269	1.17E-07	8.11E-06	12.31	50.0 E-12	2.567	
Coronene	COR	191-07-1	300.36	7	7.64	0.00014	2.89E-10	3.46E-06	13.70	50.0 E-12	2.567	
Benzonaphtho-thiophene	BNT	239-35-0	234.32	4	5.34	0.06146	4.65E-05	8.42E-04	9.29	50.0 E-12	2.567	

b)

Compound	Acronym	CAS #	MW [g mol^{-1}]	# of rings	log K_{ow}	Water solubility	Vapour pressure [Pa]	Sub-cooled liquid vapour pressure (P_L)[Pa]	Octanol–air partition coefficient (K_{OA})	OH rate constant [cm^3 $molec^{-1}$ sec^{-1}]	Half-life (based on OH rate constant) [h]	Ozone rate constant [cm^3 $molec^{-1}$ sec^{-1}]
1,4-Naphthoquinone	1,4-O_2NAP	130-15-4	158.16	2	1.71 a	2417	2.25E-02	0.244	8.804	3.01E-12	42.71	1.75E-18
Naphthalene-1-aldehyde	1-(CHO)NAP	66-77-3	156.19	2	2.89	244.2	3.33E-01	0.397	7.161	2.78E-11	4.611	
9-Fluorenone	9-OFLN	486-25-9	180.21	3	3.58 [a]	3.74	7.63E-03	2.80E-02	8.138	6.18E-12	20.783	
9,10-Anthraquinone	9,10-O_2ANT	84-65-1	208.22	3	3.39 [a]	1.35 [b]	1.55E-05	5.90E-03	9.407	1.50E-12	85.659	
1,4-Anthraquinone	1,4-O_2ANT	635-12-1	208.22	3	2.84	150.0	3.21E-04	3.95E-03	10.945	1.06E-11	12.160	1.75E-18
9,10-Phenanthroquinone	9,10-O_2PHE	84-11-7	208.22	3	2.52 [a]	7.5 [b]	1.14E-04	1.02E-02	9.477	6.18E-12	20.783	
11H-Benzo(a)fluoren-11-one	11-OBaFLN	479-79-8	230.27	4	4.73	0.22	5.16E-05	9.28E-04	10.298	1.80E-11	7.129	
11H-Benzo(b)fluoren-11-one	11-OBbFLN	3074-03-1	230.27	4	4.73	0.22	5.16E-05	9.28E-04	10.298	1.80E-11	7.129	
Benzanthrone (also called 7H-Benz(de) anthracene-7-one)	BAN	82-05-3	230.27	4	4.81 [a]	0.18	2.95E-05	9.28E-04	10.378	1.80E-11	7.129	
Benz(a)anthracene-7,12-dione	7,12-O_2BAA	2498-66-0	258.27	4	4.61	0.03	5.17E-06	1.59E-04	12.297	9.05E-12	14.185	
5,12-Naphthacenequinone	5,12-O_2NAC	1090-13-7	258.27	4	4.52	0.03	4.67E-06	1.59E-04	12.417	9.05E-12	14.185	

c)

Compound	Acronym	CAS #	MW [g mol^{-1}]	# of rings	log K_{ow}	Water solu-bility	Vapour pressure [Pa]	Sub-cooled liquid vapour pressure (P_L)[Pa]	Octanol–air partition coeffi-cient (K_{OA})	OH rate constant [cm^3 molec^{-1} sec^{-1}]	Half-life (based on OH rate constant) [h]	Ozone rate constant [cm^3 molec^{-1} sec^{-1}]
1-Nitronaphthalene	1-NNAP	86-57-7	173.17	2	3.19[a]	9.18[b]	6.40E-02	1.45E-01	7.31	2.70E-12	47.545	
2-Nitronaphthalene	2-NNAP	581-89-5	173.17	2	3.24[a]	9.24[b]	3.77E-02	1.23E-01	7.31	2.70E-12	47.545	
3-Nitroacenaphthene	3-NACE	3807-77-0	199.21	3	3.97	0.57	3.53E-03	2.97E-02	8.313	8.30E-12	15.457	
5-Nitroacenaphthene	5-NACE	602-87-9	199.21	3	3.85[a]	0.72	5.45E-03	2.97E-02	8.193	8.30E-12	15.457	1.07E-16
2-Nitrofluorene	2-NFLN	607-57-8	211.22	3	3.37	1.60	5.91E-04	1.32E-02	7.939	4.16E-12	30.828	1.45E-16
9-Nitroanthracene	9-NANT	602-60-8	223.23	3	4.78[a]	0.114[b]	1.60E-04	2.71E-03	9.861	5.00E-12	25.675	
9-Nitrophenanthrene	9-NPHE	954-46-1	223.23	3	4.16	0.29	1.80E-04	2.71E-03	9.241	1.62E-12	78.998	
3-Nitrophenanthrene	3-NPHE	17024-19-0	223.23	3	4.16	0.29	1.80E-04	2.71E-03	9.241	1.62E-12	78.998	
2-Nitrofluoranthene	2-NFLT	13177-29-2	247.26	4	4.29	2.12	3.93E-04	5.35E-03	8.517	2.13E-10	0.602	6.66E-16
1-Nitropyrene	1-NPYR	5522-43-0	247.26	4	5.06[a]	0.0118[b]	1.11E-05	2.35E-04	10.934	6.25E-12	20.54	
2-Nitropyrene	2-NPYR	789-07-1	247.26	4	4.75	0.07	7.36E-06	2.35E-04	10.624	6.25E-12	20.54	
7-Nitro-benzo(a)anthracene	7-NBAA	20268-51-3	273.29	4	5.34	0.02	1.01E-06	4.96E-05	11.432	6.25E-12	20.54	
6-Nitrochrysene	6-NCHR	7496-02-8	273.29	4	5.34	0.02	1.01E-06	4.96E-05	11.432	6.25E-12	20.54	
1,3-Dinitropyrene	1,3-N2PYR	75321-20-9	292.25	4	4.57	0.05	1.21E-07	9.70E-06	12.848	5.46E-13	470.136	
1,6-Dinitropyrene	1,6-N2PYR	42397-64-8	292.25	4	4.57	0.05	1.21E-07	9.70E-06	12.848	5.46E-13	470.136	
1,8-Dinitropyrene	1,8-N2PYR	42397-65-9	292.25	4	4.57	0.05	1.21E-07	9.70E-06	12.848	5.46E-13	470.136	
6-Nitro-benzo(a)pyrene	6-NBAP	63041-90-7	297.32	5	5.93	0.003	4.13E-08	4.01E-06	12.813	6.25E-12	20.54	

1.3 Analysis

Table S3. Gas chromatography mass spectrometry (GC-MS) parameters including retention times and mass-to-charge ratios (m/z) of a) PAHs analysis, b) NPAHs and OPAHs analysis and c) RPAHs analysis. SIM: Single ion monitoring; MRM: Multiple Reaction Monitoring

a)

Substance	Acronym	Quantifier SIM [m/z]	Qualifier SIM 1 [m/z]	Qualifier SIM 2 [m/z]	Retention time [min]
Naphthalene	NAP	128.0	129	126	9.167
Acenaphthylene	ACY	152.0	153	150	12.207
Acenaphthene	ACE	154.0	153	155	12.613
Fluorene	FLN	166.0	167	164	13.952
Phenanthrene	PHE	178.0	179	176	16.987
Anthracene	ANT	178.0	179	176	17.170
Fluoranthene	FLT	202.0	203	200	21.628
Pyrene	PYR	202.0	203	200	22.574
Retene	RET	219.0	234	205	23.950
Benzo(b)fluorene	BBN	216.0	215	217	24.369
Benzo(ghi)fluoranthene	BGF	226.0	235	232	27.047
Benzonaphthothiophene	BNT	234.0	227	224	27.222
Cyclopenta(cd)pyrene	CCP	228.0	227	224	27.953
Benzo(a)anthracene	BAA	226.0	229	226	28.056
Triphenylene	TPH	228.0	229	226	28.056
Chrysene	CHR	228.0	229	226	28.105
Benzo(b)fluoranthene	BBF	252.0	253	250	32.634
Benzo(j)fluoranthene	BJF	252.0	253	250	32.674
Benzo(k)fluoranthene	BKF	252.0	253	250	32.742
Benzo(e)pyrene	BEP	252.0	253	250	33.733
Benzo(a)pyrene	BAP	252.0	253	250	33.931
Perylene	PER	252.0	253	250	34.265
Indeno(123-cd)pyrene	INP	276.0	277	274	38.602
Dibenz(ah)anthracene	DBA	278.0	279	276	38.710
Dibenz(ac)anthracene	DCA	278.0	279	276	38.710
Benzo(ghi)perylene	BPE	276.0	277	274	39.848
Anthanthrene	ATT	276.0	277	274	40.510
Coronene	COR	300.0	301	298	49.473

b)

Substance	Acronym	Group	Quantifier SRM transition [m/z]	Qualifier SRM transition [m/z]	Retention time [min]
1,4-Naphthoquinone	1,4-O_2NAP	OPAH	158 > 102	159 > 103	4.06
Naphthalene-1-aldehyde	1-(CHO)NAP	OPAH	156 > 128	157 > 128	5.33
1-Nitronaphthalene	1-NNAP	NPAH	174 > 127	173 > 145	6.01
2-Nitronaphthalene	2-NNAP	NPAH	173 > 127	174 > 127	6.37
9-Fluorenone	9-OFLN	OPAH	180 > 152	181 > 153	7.25
3-Nitroacenaphthene	3-NACE	NPAH	199 > 152	200 > 153	9.81
9,10-Anthraquinone	9,10-O_2ANT	OPAH	208 > 152	209 > 153	9.9
9,10-Phenanthrenequinone	9,10-O_2PHE	OPAH	180 > 152	209 > 153	10.01
5-Nitroacenaphthene	5-NACE	NPAH	199 > 169	199 > 152	10.34
1,4-Anthraquinone	1,4-O_2ANT	OPAH	208 > 152	209 > 153	10.83
2-Nitrofluorene	2-NFLN	NPAH	211 > 164	212 > 195	11.69
9-Nitroanthracene	9-NANT	NPAH	223 > 193	223 > 178	12.06
9-Nitrophenanthrene	9-NPHE	NPAH	223 > 167	223 > 178	13.11
3-Nitrophenanthrene	3-NPHE	NPAH	223 > 176	223 > 193	13.82
Benzo(a)fluoren-11-one	11-OBaFLN	OPAH	230 > 202	231 > 203	15.19
Benzo(b)fluoren-11-one	11-OBbFLN	OPAH	230 > 202	231 > 203	16.09
Benzanthrone	BAN	OPAH	230 > 202	231 > 203	17.28
2-Nitrofluoranthene	2-NFLT	NPAH	247 > 201	248 > 202	18.18
Benz(a)anthracene-7,12-dione	7,12-O_2BAA	OPAH	258 > 202	259 > 203	18.6
1-Nitropyrene	1-NPYR	NPAH	247 > 217	247 > 201	18.77
2-Nitropyrene	2-NPYR	NPAH	247 > 201	248 > 202	19.07
5,12-Naphthacenequinone	5,12-O_2NAC	OPAH	258 > 202	259 > 203	19.77
7-Nitrobenzo(a)anthracene	7-NBAA	NPAH	273 > 215	274 > 257	21.44
6-Nitrochrysene	6-NCHR	NPAH	273 > 215	274 > 226	22.65
1.3-Dinitropyrene	1,3-N_2PYR	NPAH	292 > 188	292 > 176	23.65
1.6-Dinitropyrene	1,6-N_2PYR	NPAH	292 > 176	292 > 232	24.4
1.8-Dinitropyrene	1,8-N_2PYR	NPAH	292 > 176	292 > 232	24.93
6-Nitrobenzo(a)pyrene	6-NBAP	NPAH	297 > 239	297 > 224	26.81

c)

Substance	Acronym	Quantifier SIM (m/z)	Confirmation SIM (m/z)	Retention time [min]
Phenanthrene	PHE	178 $[M]^+$	176 $[M-2H]^+$	12.82
1-Methylphenanthrene	1-MPHE	192 $[M]^+$	189 $[M-3H]^+$	14.77
2-Methylphenanthrene	2-MPHE	192 $[M]^+$	189 $[M-3H]^+$	14.87
3-Methylphenanthrene	3-MPHE	192 $[M]^+$	189 $[M-3H]^+$	15.18
4-Methylphenanthrene	4-MPHE	192 $[M]^+$	189 $[M-3H]^+$	15.28
3,6-Dimethylphenanthrene	3,6-M_2PHE	206 $[M]^+$	202 $[M-4H]^+$	16.37
2,6-Dimethylphenanthrene	2,6-M_2PHE	206 $[M]^+$	202 $[M-4H]^+$	16.71
2,7-Dimethylphenanthrene	2,7-M_2PHE	206 $[M]^+$	202 $[M-4H]^+$	16.83
1,3-/2,10-/3,9-/3,10-Dimethylphenanthrene	1,3-/2,10-/3,9-/1,10-M_2PHE	206 $[M]^+$	202 $[M-4H]^+$	16.92
1,6-/2,9-Dimethylphenanthrene	1,6-/2,9-M_2PHE	206 $[M]^+$	202 $[M-4H]^+$	17.13
1,7-Dimethylphenanthrene	1,7-M_2PHE	206 $[M]^+$	202 $[M-4H]^+$	17.26
2,3-Dimethylphenanthrene	2,3-M_2PHE	206 $[M]^+$	202 $[M-4H]^+$	17.36
1,9-/4,9-Dimethylphenanthrene	1,9-/4,9-M_2PHE	206 $[M]^+$	202 $[M-4H]^+$	17.50
1,8-Dimethylphenanthrene	1,8-M_2PHE	206 $[M]^+$	202 $[M-4H]^+$	18.06

1.4 Measurement of other supporting parameters

1.4.1 Meteorological data

The meteorological data such as GPS position and speed of the ship, wind direction and speed, temperature, humidity etc. was measured by a commercial weather station with GPS (STERELA METEO Neptune). The actinic flux was measured by a CCD spectral radiometer (Metcon 85237).

1.4.2 PM_{10} mass concentration

For PM concentration, QFFs were weighed before and after sampling using a laboratory balance following accommodation to a constant humidity and temperature.

1.4.3 Metals

- The content of transition metals (Ti, V, Cr, Mn, Fe, Co, Ni, Cu, Zn, Mo, Cd) and Pb on baked QFFs was determined after microwave digestion (MWS 3+ Berghof, Eningen, Germany) of samples with concentrated nitric acid (4 mL, p.a., Merck, Darmstadt, Germany) and hydrogen peroxide (2 mL, p.a., Merck, Darmstadt, Germany) followed by inductively coupled plasma mass spectrometry (Agilent 7700x ICP-MS, Santa Clara, USA). The method was validated by analysis of samples spiked with known amount of analytes. Median recoveries for spiked samples were within the range 90–110 %. Relative standard deviations for replicate analyses of spiked samples were within single percentage points.

1.4.4 Elemental and organic carbon (EC/OC)

PM total elemental and organic carbon fraction concentrations were determined from punches of baked QFFs. C fractions were thermally desorbed from the filter medium under a He atmosphere followed by an oxidizing atmosphere using a OC-EC Aerosol Analyzer (Sunset Laboratory, Tigard, USA) with flame ionization detection (FID) measuring the CO_2 concentration. For heating ramps, the EUSAAR-2 protocol (Cavalli and Putaud, 2008) was followed.

1.5 Quality control

1.5.1 Filtering against contamination by the own ship exhaust

A stack contamination filter is available, which was based on wind direction and speed, particle number concentration (measured by condensation particle counter (CPC) and fast mobility particle sizer (FMPS)) and black carbon concentration (Aethalometer), WNC for short using measurement of the ship and from Celik et al (2020). The advantage of that contamination filter compared to the filter applied by other studies of the campaign (Eger et al., 2019; Tadic et al, 2020) was that all of our samples are within the time period the filter can be applied. Moreover, the sampling inlet of the instrument for the parameters, which are crucial for the decision if there was a stack

contamination or not, was closer to our air sampler than the inlets for the NO, O_3 and SO_2 measurement instruments used for the other stack contamination filter.

Nevertheless, it has to be considered that none of the instruments for the decision if there was a contamination by the own ship stack was exactly at the same location and same height as our air samplers. Thus, there is a chance that our sample is contaminated although it should not be the case according to the data of the stack contamination filter and vice versa. However, our approach, which will be discussed in the following, is rather rejecting false positive (samples treated as contaminated but are not) than false negative (samples are contaminated but treated as not contaminated). The difficulty in deciding for stack contamination of a sample is the fact that our instruments sampled on average for 12-24 hours. Since during this time period, the wind and the direction of the ship changed, another criterion was needed to decide if the total sample was contaminated by the ship stack or not. The first criterion was the usage of the percentage of the contaminated time from the total sampling time. Thus, the first criterion for rejecting a sample as "contaminated" was if more than 10 % of the total sampling time was classified as possibly contaminated based on the WNC filter.

However, since it does not only depend on the time of possible contamination but also on the intensity of contamination, we used another criterion. The photoelectric PAH sensor (EcoChem PAS2000, Ansyco, Karlsruhe, Germany) measured photoelectrons from PAHs on the surface of sub-micrometre particles (Niessner and Wilbring, 1989) with a time resolution of 10 s. Whenever the average PAH signal of sampling time marked as "possibly contaminated" by the WNC filter was more than 10 % higher than the PAH signal of the sampling time marked as "not contaminated", the sample was rejected. Based on this stack filtering process, we rejected 20 out of 62 Digitel high volume samples and 6 out of 30 impactor samples, especially from the first leg (see Table S4).

Table S4. Filtering for contamination from own stack of a) Digitel high-volume samples, b) cascade impactor samples and c) GMWL high volume samples.

a)

Sample	Possible contamination in % of sampling time	Percentage difference of average surface PAH of "possibly contaminated" and "not contaminated" sampling time [%]	Reject due to possible contamination?
D1	0.0	0.0	no
D2	4.9	21.4	yes
D3	21.2	1.4	yes
D4	0.0	0.0	no
D5	3.2	3.8	no
D6	4.6	8.2	no
D7	1.3	0.8	no
D8	53.2	1543	yes
D9	11.0	70.8	yes
D10	28.9	0.0	yes
D11	20.7	12.8	yes
D12	7.8	2.6	no
D13	0.0	0.0	no
D14	6.5	0.7	no
D15	7.2	0.2	no
D16	22.7	184	yes
D17	21.2	419	yes
D18	7.8	923	yes
D19	9.4	37.3	yes
D20	43.4	701	yes
D21	2.7	19.4	yes
D22	70.4	3797	yes
D23	51.8	3191	yes
D24	0.0	0.0	no
D25	6.8	0.1	no
D26	9.2	29.0	yes
D27	22.8	28.1	yes
D28	16.2	492	yes
D29	0.5	0.6	no
D30	0.0	0.0	no
D31	0.5	1.0	no
D32	0.2	1.0	no

Sample	Possible contamination in % of sampling time	Percentage difference of average surface PAH of "possibly contaminated" and "not contaminated" sampling time [%]	Reject due to possible contamination?
D33	0.8	0.3	no
D34	0.0	0.0	no
D35	1.4	0.3	no
D36	0.0	0.0	no
D37	26.6	340	yes
D38	12.5	325	yes
D39	0.0	0.0	no
D40	0.0	0.0	no
D41	0.0	0.0	no
D42	0.0	0.0	no
D43	0.0	0.0	no
D44	0.0	0.0	no
D45	0.0	0.0	no
D46	0.0	0.0	no
D47	0.0	0.0	no
D48	0.0	0.0	no
D49	2.6	0.1	no
D50	3.0	0.5	no
D51	0.0	0.0	no
D52	0.0	0.0	no
D53	0.0	0.0	no
D54	0.0	0.0	no
D55	0.0	0.0	no
D56	0.0	0.0	no
D57	0.0	0.0	no
D58	0.0	0.0	no
D59	1.1	1.7	no
D60	0.5	0.0	no
D61	8.5	0.0	no
D62	0.0	0.0	no

b)

Sample	Possible contamination in % of sampling time	Percentage difference of average surface PAH concentration of "possibly contaminated" and "not contaminated" sampling time [%]	Reject due to possible contamination?
C1	21.9	108	yes
C2	46.2	1774	yes
C3	7.9	15.1	yes
C4	22.4	28.1	yes
C5	17.0	507	yes
C6	0.3	0.6	no
C7	0.0	0.0	no
C8	0.0	0.0	no
C9	0.0	0.0	no
C10	0.0	0.0	no
C11	0.0	0.0	no
C12	0.0	0.0	no
C13	0.2	1.0	no
C14	0.0	0.0	no
C15	0.0	0.0	no
C16	0.0	0.0	no
C17	0.0	0.0	no
C18	0.0	0.0	no
C19	0.0	0.0	no
C20	0.6	0.1	no
C21	13.6	213	yes
C22	0.0	0.0	no
C23	0.0	0.0	no
C24	0.0	0.0	no
C25	0.0	0.0	no
C26	0.0	0.0	no
C27	1.5	0.3	no
C28	0.0	0.0	no
C29	0.0	0.0	no
C30	0.0	0.0	no

c)

Sample	Possible contamination in % of sampling time	Percentage difference of average surface PAH concentration of "possibly contaminated" and "not contaminated" sampling time [%]	Reject due to possible contamination?
G1	0.00	0.0	no
G2	0.00	0.0	no
G3	15.46	5.1	yes
G4	11.98	18.7	yes
G5	0.00	0.0	no
G6	3.97	4.7	no
G7	5.27	7.3	no
G8	3.37	24.1	yes
G9	35.93	931.9	yes
G10	0.17	0.8	no
G11	7.99	2.2	no
G12	4.74	0.4	no
G13	2.06	168.3	yes
G14	23.04	0.6	yes*
G15	24.73	1114.4	yes
G16	8.49	2191.5	yes
G17	83.00	2751.8	yes
G18	210.24	1210.5	yes
G19	0.00	0.0	no*[2]
G20	0.00	0.0	no
G21	17.23	40.5	yes
G22	33.02	453.9	yes
G23	0.00	0.0	no
G24	0.00	0.1	no
G25	0.00	0.0	no
G26	0.97	0.3	no
G27	0.00	0.0	no
G28	2.84	103.4	yes
G29	3.28	135.1	yes
G30	8.74	231.9	yes
G31	0.00	0.0	no
G32	0.00	0.0	no
G33	0.00	0.0	no
G34	0.00	0.0	no
G35	0.00	0.0	no
G36	0.00	0.0	no
G37	0.00	0.0	no
G38	0.00	0.0	no
G39	0.00	0.0	no
G40	22.27	0.2	no*

24

Sample	Possible contamination in % of sampling time	Percentage difference of average surface PAH concentration of "possibly contaminated" and "not contaminated" sampling time [%]	Reject due to possible contamination?
G41	0.00	0.0	no
G42	0.00	0.0	no
G43	0.00	0.0	no

1.5.2 Chemical analysis – quality control

Quantification of compounds was based on the calculation of relative response factors (RRF) to an internal standard (p-terphenyl for PAHs and PCB 121 for NPAHs and OPAHs). Each compound was identified by comparing retention time and the ion ratio between quantification and confirmation ion with reference standard mixtures.

1.5.2.1 Recoveries and blank correction

The recoveries for PAHs and NPAHs and OPAHs for gaseous (PUF) samples, as determined based on deuterated standards, ranged 66-94 % (disregarded NAP) and 41-74 %, respectively. For particulate samples (QFF, Digitel high-volume), the recoveries ranged 58-106 % and 46-114 %, respectively, and for size-segregated particulate (QFF, cascade impactor) samples, 52-93 % and 32-161 %, respectively. All results of this study were blank corrected (i.e., subtraction of the mean of 3 field blank values), but not recovery corrected.

The detection frequencies of substances from samples of the Digitel high volume are illustrated in Fig. S1. For calculating average values, values <LOQ of substances in one phase were replaced by blank corrected LOQ/2 if the substance specific detection frequency in one phase was >30 %. In case of a lower detection frequency of the substance in all samples was <30 %, the value 0 was used for further calculations. The same was done for the impactor samples. The detection frequency of each impactor stage was used individually. The results are shown in Table S5.

Recoveries of PAHs and RPAHs from the second high volume sampler ranged 75 – 119%. Blank sample media (3 QFFs, 3 PUFs) were analysed for the presence of target compounds. Blank concentrations ranged 0.03 – 2.7% of the target compounds. The samples were blank but not recovery corrected.

a)

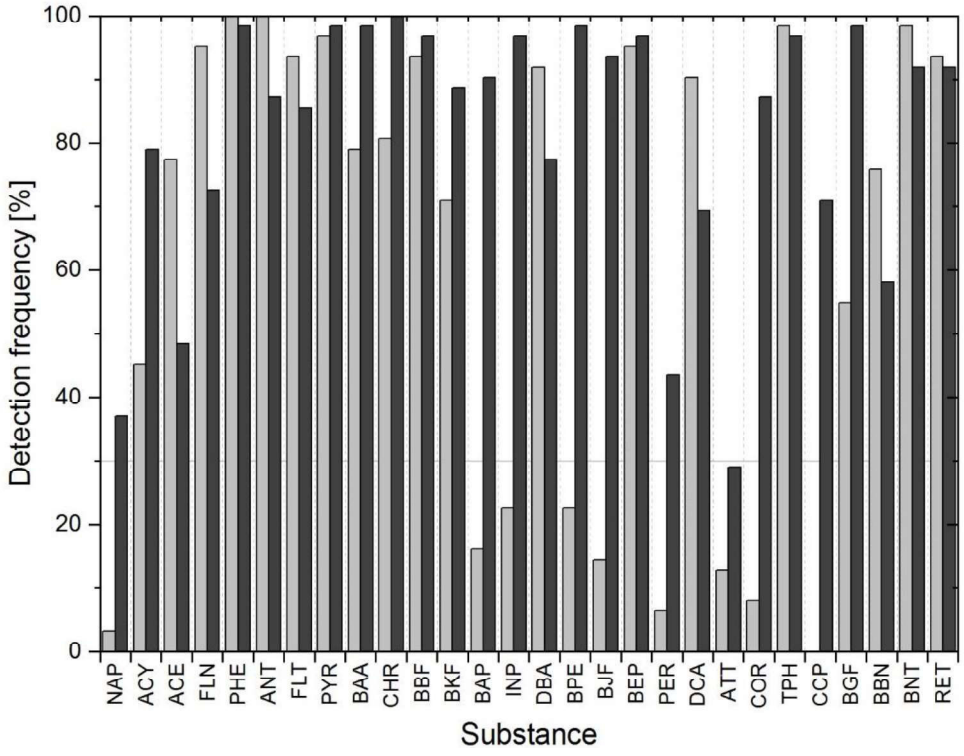
Detection frequency [%]
100
80
60
40
20
0
NAP
ACY
ACE
FLN
PHE
ANT
FLT
PYR
BAA
CHR
BBF
BKF
BAP
INP
DBA
BPE
BJF
BEP
PER
DCA
ATT
COR
TPH
CCP
BGF
BBN
BNT
RET
Substance

b)

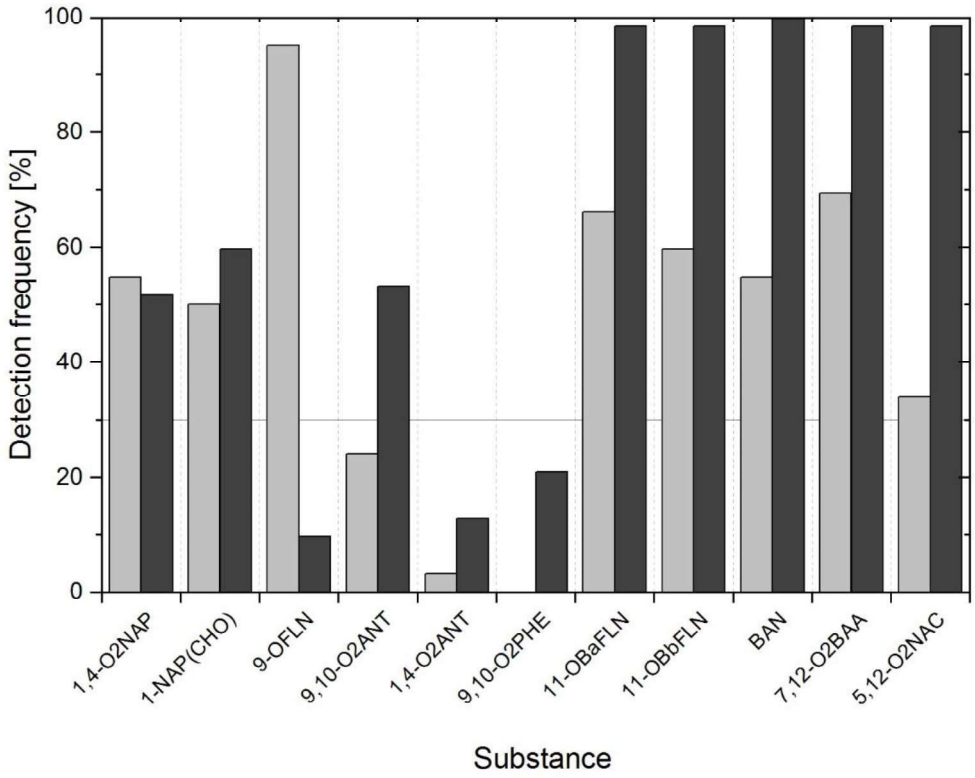
Detection frequency [%]
100
80
60
40
20
0
1,4-O2NAP
1-NAP(CHO)
9-OFLN
9,10-O2ANT
1,4-O2ANT
9,10-O2PHE
11-OBaFLN
11-OBbFLN
BAN
7,12-O2BAA
5,12-O2NAC
Substance

c)

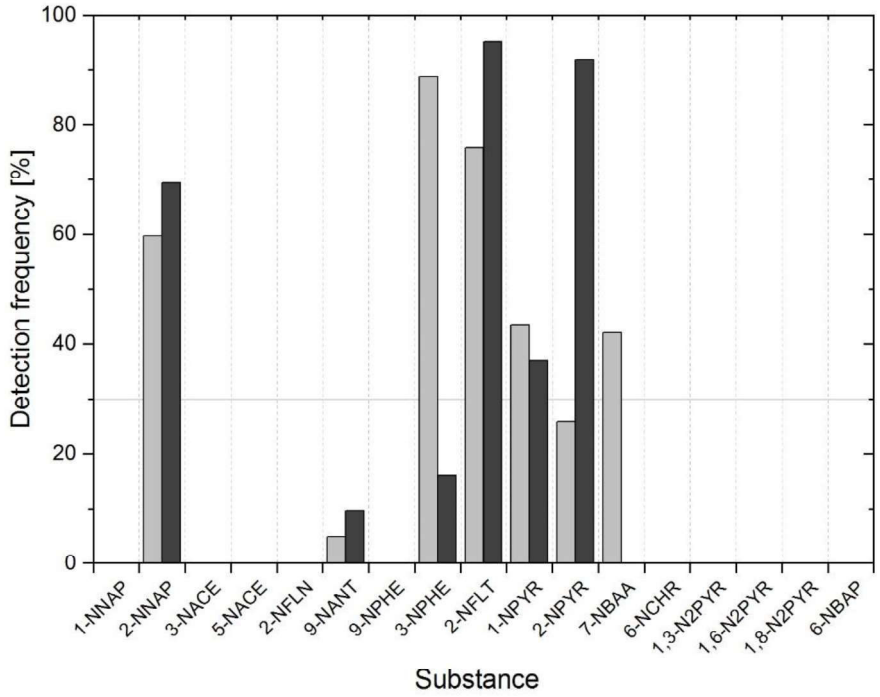

Figure S1. Detection frequency of a) PAHs, b) OPAHs and c) NPAHs in Digitel high volume samples (considering all samples) using the sum of the average of blanks and 3 × standard deviation of blanks as LOQ; Grey: Gas phase; Black: Particulate phase.

Table S5. Detection frequencies (in %) from impactor samples of a) PAHs, b) OPAHs and c) NPAHs.

a)

Substance	All stages	Stage A PM_{7-10}	Stage B PM_{3-7}	Stage C $PM_{1.5-3}$	Stage D $PM_{0.95-1.5}$	Stage E $PM_{0.49-0.95}$	Stage F $PM_{<0.49}$
NAP	**32**	33	43	37	23	33	23
ACY	**0**	0	0	0	0	0	0
ACE	**0**	0	0	0	0	0	0
FLN	**0**	0	0	0	0	0	0
PHE	**56**	57	60	53	63	60	40
ANT	**1**	0	0	0	0	0	7
FLT	**52**	20	37	47	53	60	93
PYR	**48**	20	33	50	53	57	73
BAA	**69**	53	63	63	67	90	80
CHR	**67**	30	57	63	67	83	100
BBF	**79**	47	60	73	93	100	100
BKF	**53**	13	33	47	63	73	87
BAP	**52**	20	50	47	63	70	63
INP	**65**	27	50	63	77	90	83
DBA	**22**	7	27	13	23	30	30
BPE	**77**	43	63	70	90	97	100
BJF	**61**	17	43	57	70	83	97
BEP	**71**	33	53	63	80	93	100
PER	**21**	3	13	7	23	27	53
DCA	**22**	10	27	13	20	27	33
ATT	**42**	30	43	33	50	53	40
COR	**45**	13	30	30	47	67	83
TPH	**52**	17	33	43	57	63	97
CCP	**5**	0	0	0	3	17	10
BGF	**59**	20	43	53	67	77	93
BBN	**13**	0	3	3	17	27	27
BNT	**61**	33	57	60	80	77	57
RET	**19**	0	3	3	3	3	100

b)

Substance	All stages	Stage A PM_{7-10}	Stage B PM_{3-7}	Stage C $PM_{1.5-3}$	Stage D $PM_{0.95-1.5}$	Stage E $PM_{0.49-0.95}$	Stage F $PM_{<0.49}$
1,4-O_2NAP	**1**	3	0	0	0	0	0
1-(CHO)NAP	**67**	67	67	67	67	67	67
9-OFLN	**17**	0	0	0	0	0	100
9,10-O_2ANT	**17**	0	0	0	0	0	100
1,4-O_2ANT	**0**	0	0	0	0	0	0
9,10-O_2PHE	**0**	0	0	0	0	0	0
11-OBaFLN	**44**	7	23	37	43	63	93
11-OBbFLN	**44**	7	20	33	43	63	100
BAN	**35**	7	7	10	33	53	100
7,12-O_2BAA	**63**	20	40	50	73	97	100
5,12-O_2NAC	**76**	37	53	70	100	100	97

c)

Substance	All stages	Stage A PM_{7-10}	Stage B PM_{3-7}	Stage C $PM_{1.5-3}$	Stage D $PM_{0.95-1.5}$	Stage E $PM_{0.49-0.95}$	Stage F $PM_{<0.49}$
1-NNAP	**1**	0	3	0	0	0	0
2-NNAP	**9**	0	0	0	0	0	53
3-NACE	**1**	0	0	0	0	0	7
5-NACE	**7**	0	0	0	3	0	40
2-NFLN	**0**	0	0	0	0	0	0
9-NANT	**1**	0	0	0	0	0	7
9-NPHE	**1**	3	0	0	0	0	0
3-NPHE	**4**	0	3	3	7	10	3
2-NFLT	**51**	10	27	40	53	83	93
1-NPYR	**45**	20	37	37	53	70	53
2-NPYR	**26**	3	7	17	23	40	63
7-NBAA	**17**	3	10	20	23	40	7
6-NCHR	**0**	0	0	0	0	0	0
1,3-N_2PYR	**0**	0	0	0	0	0	0
1,6-N_2PYR	**0**	0	0	0	0	0	0
1,8-N_2PYR	**0**	0	0	0	0	0	0
6-NBAP	**6**	0	3	3	10	10	10

1.5.2.2 Limits of quantification

For the evaluation, we used the maximum of two limits of quantification (LOQs). First, the instrumental LOQ (iLOQ), which is based on the limits in the analysis by the GC-MS and second the LOQ from field blanks (fbLOQ) including possible contamination during storage and transport of the samples and from the complete analytical method (extraction, clean-up and measurement). The fbLOQ was calculated from the average concentration of three field blanks (individual for different sampling media) plus 3 times the standard deviation of the concentration of these three field blank.

The iLOQ of NPAHs and OPAHs was calculated based on the signal to noise ratio (S/N) for a specific compound and specific sample as the concentration which corresponds to S/N = 10:1. For PAHs, the iLOQ is calculated by extrapolation of S/N = 10:1 to the corresponding concentration, based on calibration standards. The LOQs can be found in Table S6 and S8 for the samples of the Digitel high volume sampler and Table S7 for the samples of the impactor sampler. The LOQ for all RPAHs was 0.05 pg m^{-3}.

Table S6. Limits of quantification (LOQ) including instrumental LOQs (iLOQs) and LOQs from field blanks (fbLOQs) from a) PAHs, b) OPAHs and c) NPAHs in ng sample^{-1} from the Digitel high-volume sampler.

a)

Substance	Acronym	iLOQ both phases	fbLOQ gas phase	fbLOQ particulate phase
Naphthalene	NAP	0.17	222.57	7.86
Acenaphthylene	ACY	0.12	5.22	0.24
Acenaphthene	ACE	0.14	17.23	0.20
Fluorene	FLN	0.10	30.21	1.70
Phenantrene	PHE	0.13	54.64	5.29
Anthracene	ANT	0.15	1.73	0.23
Fluoranthene	FLT	0.14	36.74	3.75
Pyrene	PYR	0.15	23.36	0.85
Benz(a)anthracene	BAA	0.15	1.79	0.15
Chrysene	CHR	0.14	4.78	0.28
Benzo(b)fluoranthene	BBF	0.33	1.17	0.33
Benzo(k)fluoranthene	BKF	0.39	0.39	0.39
Benzo(a)pyrene	BAP	0.53	0.53	0.53
Indeno(123-cd)pyrene	INP	0.31	0.31	0.31
Dibenz(ah)anthracene	DBA	0.25	3.29	0.25
Benzo(ghi)perylene	BPE	0.25	0.25	0.25
Benzo(j)fluoranthene	BJF	0.34	1.92	0.34
Benzo(e)pyrene	BEP	0.35	0.35	0.35
Perylene	PER	0.45	0.45	0.45
Dibenzo(ac)anthracene	DCA	0.25	3.06	0.25
Anthanthrene	ATT	0.29	1.14	0.29
Coronene	COR	0.42	0.42	0.42
Triphenylene	TPH	0.12	2.08	0.25
Cyclopenta(cd)pyrene	CCP	0.15	0.15	0.15
Benzo(ghi)fluoranthene	BGF	0.10	4.15	0.16
Benzo(b)fluorene	BBN	0.40	2.96	0.40
Retene	RET	0.34	4.49	0.34
Benzonaphtho-thiophene	BNT	0.12	0.35	0.12

b)

Substance	Average iLOQ gas phase	Standard deviation iLOQ gas phase	Average iLOQ particulate phase	Standard deviation iLOQ particulate phase	fbLOQ gas phase	fbLOQ particulate phase
1,4-O_2NAP	0.89	1.44	0.321	0.703	44.24	6.72
1-(CHO)NAP	1.96	4.14	0.423	0.384	16.25	1.80
9-OFLN	0.51	0.71	0.106	0.141	21.55	11.69
9,10-O_2ANT	0.80	1.52	0.143	0.209	72.76	10.33
1,4-O_2ANT	1.85	3.50	0.330	0.482	0.00	0
9,10-O_2PHE	5723	1317	54.7	144	0.00	2.76
11-OBaFLN	0.85	1.91	0.475	1.441	5.96	0.58
11-OBbFLN	0.68	1.54	0.384	1.163	4.90	0.49
BAN	0.49	1.10	0.274	0.831	5.54	0.71
7,12-O_2BAA	0.34	1.15	0.320	0.802	2.96	0.32
5,12-O_2NAC	0.20	0.66	0.185	0.463	0.21	0.04

c)

Substance	Average iLOQ gas phase	Standard deviation iLOQ gas phase	Average iLOQ particulate phase	Standard deviation iLOQ particulate phase	fbLOQ gas phase	fbLOQ particulate phase
1-NNAP	2.45	4.17	0.445	0.211	0	0
2-NNAP	0.18	0.20	0.028	0.028	0.92	0.05
3-NACE	8.33	9.11	2.764	3.203	0	0
5-NACE	0.95	1.06	0.141	0.167	0	0
2-NFLN	0.07	0.18	0.009	0.010	0	0
9-NANT	5.69	8.96	0.208	0.317	2.67	0.04
9-NPHE	3.24	4.33	0.836	1.515	0	0
3-NPHE	0.54	0.83	0.085	0.136	0.15	0
2-NFLT	0.03	0.06	0.028	0.086	0.19	0.02
1-NPYR	0.62	2.17	0.075	0.294	0.19	0.33
2-NPYR	0.02	0.04	0.019	0.058	0.02	0.004
7-NBAA	0.12	0.17	0.492	1.673	0.07	0
6-NCHR	0.07	0.11	0.298	1.013	0	0
1,3-N_2PYR	0.13	0.05	0.049	0.041	0	0
1,6-N_2PYR	0.29	0.23	0.284	0.330	0	0
1,8-N_2PYR	0.12	0.09	0.119	0.138	0	0
6-NBAP	0.27	0.23	0.339	0.688	0	0

32

Table S7. Limits of quantification (LOQ) including instrumental LOQs (iLOQs) and LOQ from field blanks (fbLOQs) from a) PAHs, b) OPAHs and c) NPAHs in ng sample^{-1} from the impactor sampler.

a)

Substance	Acronym	iLOQ	fbLOQ stages A-E ($PM_{0.49\text{-}10\ \mu m}$)	fbLOQ stage F ($PM_{<0.49\ \mu m}$)
Naphthalene	NAP	0.17	3.92	4.63
Acenaphthylene	ACY	0.12	0.94	1.73
Acenaphthene	ACE	0.14	2.59	10.22
Fluorene	FLN	0.10	2.93	4.46
Phenantrene	PHE	0.13	2.72	5.56
Anthracene	ANT	0.15	2.06	0.15
Fluoranthene	FLT	0.14	2.49	1.92
Pyrene	PYR	0.15	1.97	1.71
Benz(a)anthracene	BAA	0.15	0	0.44
Chrysene	CHR	0.14	0.57	0.55
Benzo(b)fluoranthene	BBF	0.33	0	0
Benzo(k)fluoranthene	BKF	0.39	0	0
Benzo(a)pyrene	BAP	0.53	0	0
Indeno(123cd)pyrene	INP	0.31	0	0
Dibenz(ah)anthracene	DBA	0.25	0	0
Benzo(ghi)perylene	BPE	0.25	0	0
Benzo(j)fluoranthene	BJF	0.34	0	0
Benzo(e)pyrene	BEP	0.35	0	0
Perylene	PER	0.45	0	0
Dibenzo(ac)anthracene	DCA	0.25	0	0
Anthanthrene	ATT	0.29	0	0
Coronene	COR	0.42	0	0
Triphenylene	TPH	0.12	0.45	0.42
Cyclopenta(cd)pyrene	CCP	0.15	0	0
Benzo(ghi)fluoranthene	BGF	0.10	0.34	0.42
Benzo(b)fluorene	BBN	0.40	0	0
Retene	RET	0.34	1.64	0.34
Benzonaphtho-thiophene	BNT	0.12	0	0

b)

Substance	Average iLOQ	Standard deviation iLOQ	fbLOQ stages A-E ($PM_{0.49\text{-}10\ \mu m}$)	fbLOQ stage F ($PM_{<0.49\ \mu m}$)
1,4-O_2NAP	0.23	0.29	0	0
1-(CHO)NAP	0.16	0.20	0	0
9-OFLN	0.04	0.06	16.59	5.50
9,10-O_2ANT	0.16	0.66	36.10	3.43
1,4-O_2ANT	0.27	1.10	0	0
9,10-O_2PHE	688	3074	241	36.4
11-OBaFLN	0.22	1.32	0.40	0.32
11-OBbFLN	0.20	1.20	0.63	0.47
BAN	0.15	0.88	1.44	0.45
7,12-O_2BAA	0.11	0.46	0.39	0.23
5,12-O_2NAC	0.07	0.29	0.04	0.03

c)

Substance	Average iLOQ	Standard deviation iLOQ	fbLOQ stages A-E ($PM_{0.49\text{-}10\ \mu m}$)	fbLOQ stage F ($PM_{<0.49\ \mu m}$)
1-NNAP	0.09	0.08	0	0
2-NNAP	0.03	0.04	0.38	0.08
3-NACE	1.67	2.64	4.10	0.09
5-NACE	0.17	0.35	0.80	0.02
2-NFLN	0.01	0.02	0.02	0.00
9-NANT	0.16	0.43	1.45	0.04
9-NPHE	0.52	1.62	0.09	0.01
3-NPHE	0.08	0.17	0.05	0.00
2-NFLT	0.05	0.31	0.13	0.07
1-NPYR	0.33	1.50	0.15	0.07
2-NPYR	0.04	0.27	0.02	0.01
7-NBAA	0.69	3.27	0.04	0.04
6-NCHR	1.54	7.25	0	0
1,3-N_2PYR	5.15	7.34	3.70	0.00
1,6-N_2PYR	30.60	66.93	11.05	3.84
1,8-N_2PYR	36.68	80.24	13.39	3.01
6-NBAP	1.14	4.49	0.11	0.04

Table S8. Blank subtracted total LOQ (maximum of iLOQ and fbLOQ) of individual samples of a) 16 USEPA-prioritized PAHs, b) other PAHs, c) OPAHs and d) NPAHs in ng m^{-3}.

a)

Sample	NAP	ACY	ACE	FLN	PHE	ANT	FLT	PYR	BAA	CHR	BBF	BKF	BAP	INP	DBA	BPE
D1	6.7E-02	3.2E-03	1.0E-02	1.7E-02	2.5E-02	1.0E-03	2.7E-02	1.8E-02	1.4E-03	3.3E-03	8.7E-04	9.9E-04	1.4E-03	7.8E-04	1.6E-03	6.5E-04
D2	6.6E-02	3.2E-03	1.0E-02	1.7E-02	2.5E-02	9.9E-04	2.7E-02	1.8E-02	1.4E-03	3.3E-03	8.6E-04	9.8E-04	1.3E-03	7.7E-04	1.6E-03	6.4E-04
D3	6.6E-02	3.2E-03	1.0E-02	1.7E-02	2.5E-02	1.0E-03	2.7E-02	1.8E-02	1.4E-03	3.3E-03	8.6E-04	9.8E-04	1.3E-03	7.7E-04	1.6E-03	6.4E-04
D4	7.6E-02	3.6E-03	1.2E-02	1.9E-02	2.8E-02	1.1E-03	3.1E-02	2.0E-02	1.6E-03	3.8E-03	9.8E-04	1.1E-03	1.5E-03	8.8E-04	1.8E-03	7.3E-04
D5	6.6E-02	3.2E-03	1.0E-02	1.7E-02	2.5E-02	1.0E-03	2.7E-02	1.8E-02	1.4E-03	3.3E-03	8.6E-04	9.8E-04	1.3E-03	7.7E-04	1.6E-03	6.4E-04
D6	6.5E-02	3.1E-03	1.0E-02	1.6E-02	2.4E-02	9.7E-04	2.6E-02	1.7E-02	1.4E-03	3.2E-03	8.4E-04	9.6E-04	1.3E-03	7.5E-04	1.5E-03	6.2E-04
D7	6.4E-02	3.1E-03	1.0E-02	1.6E-02	2.4E-02	9.7E-04	2.6E-02	1.7E-02	1.4E-03	3.2E-03	8.4E-04	9.5E-04	1.3E-03	7.5E-04	1.5E-03	6.2E-04
D8	1.3E-01	6.3E-03	2.0E-02	3.3E-02	4.9E-02	2.0E-03	5.3E-02	3.5E-02	2.8E-03	6.5E-03	1.7E-03	1.9E-03	2.7E-03	1.5E-03	3.1E-03	1.3E-03
D9	6.5E-02	3.2E-03	1.0E-02	1.7E-02	2.4E-02	9.9E-04	2.7E-02	1.8E-02	1.4E-03	3.3E-03	8.5E-04	9.7E-04	1.3E-03	7.6E-04	1.5E-03	6.3E-04
D10	6.7E-02	3.2E-03	1.0E-02	1.7E-02	2.5E-02	1.0E-03	2.7E-02	1.8E-02	1.4E-03	3.3E-03	8.7E-04	9.9E-04	1.4E-03	7.8E-04	1.6E-03	6.5E-04
D11	6.6E-02	3.2E-03	1.0E-02	1.7E-02	2.5E-02	1.0E-03	2.7E-02	1.8E-02	1.4E-03	3.3E-03	8.6E-04	9.8E-04	1.3E-03	7.7E-04	1.6E-03	6.4E-04
D12	6.6E-02	3.2E-03	1.0E-02	1.7E-02	2.5E-02	1.0E-03	2.7E-02	1.8E-02	1.4E-03	3.3E-03	8.6E-04	9.8E-04	1.3E-03	7.7E-04	1.6E-03	6.4E-04
D13	6.6E-02	3.2E-03	1.0E-02	1.7E-02	2.5E-02	1.0E-03	2.7E-02	1.8E-02	1.4E-03	3.3E-03	8.6E-04	9.8E-04	1.3E-03	7.7E-04	1.6E-03	6.4E-04
D14	9.2E-02	4.4E-03	1.4E-02	2.3E-02	3.4E-02	1.4E-03	3.8E-02	2.5E-02	2.0E-03	4.6E-03	1.2E-03	1.4E-03	1.9E-03	1.1E-03	2.2E-03	8.9E-04
D15	6.7E-02	3.2E-03	1.1E-02	1.7E-02	2.5E-02	1.0E-03	2.7E-02	1.8E-02	1.4E-03	3.3E-03	8.8E-04	1.0E-03	1.4E-03	7.8E-04	1.6E-03	6.5E-04
D16	6.5E-02	3.1E-03	1.0E-02	1.6E-02	2.4E-02	9.8E-04	2.6E-02	1.7E-02	1.4E-03	3.2E-03	8.5E-04	9.6E-04	1.3E-03	7.6E-04	1.5E-03	6.3E-04
D17	6.5E-02	3.1E-03	1.0E-02	1.7E-02	2.4E-02	9.9E-04	2.7E-02	1.7E-02	1.4E-03	3.2E-03	8.5E-04	9.7E-04	1.3E-03	7.6E-04	1.5E-03	6.3E-04
D18	6.8E-02	3.3E-03	1.1E-02	1.7E-02	2.5E-02	1.0E-03	2.8E-02	1.8E-02	1.4E-03	3.4E-03	8.8E-04	1.0E-03	1.4E-03	7.9E-04	1.6E-03	6.5E-04
D19	6.6E-02	3.2E-03	1.0E-02	1.7E-02	2.5E-02	9.9E-04	2.7E-02	1.8E-02	1.4E-03	3.3E-03	8.6E-04	9.7E-04	1.3E-03	7.7E-04	1.6E-03	6.4E-04
D20	6.6E-02	3.2E-03	1.0E-02	1.7E-02	2.5E-02	9.9E-04	2.7E-02	1.8E-02	1.4E-03	3.3E-03	8.6E-04	9.7E-04	1.3E-03	7.6E-04	1.6E-03	6.3E-04
D21	6.8E-02	3.3E-03	1.1E-02	1.7E-02	2.5E-02	1.0E-03	2.8E-02	1.8E-02	1.4E-03	3.4E-03	8.8E-04	1.0E-03	1.4E-03	7.9E-04	1.6E-03	6.5E-04
D22	6.5E-02	3.1E-03	1.0E-02	1.6E-02	2.4E-02	9.8E-04	2.6E-02	1.7E-02	1.4E-03	3.2E-03	8.4E-04	9.6E-04	1.3E-03	7.5E-04	1.5E-03	6.3E-04
D23	1.3E-01	6.1E-03	2.0E-02	3.2E-02	4.7E-02	1.9E-03	5.1E-02	3.4E-02	2.7E-03	6.3E-03	1.6E-03	1.9E-03	2.6E-03	1.5E-03	3.0E-03	1.2E-03
D24	1.6E-01	7.6E-03	2.5E-02	4.0E-02	5.9E-02	2.4E-03	6.4E-02	4.2E-02	3.4E-03	7.9E-03	2.1E-03	2.3E-03	3.2E-03	1.8E-03	3.7E-03	1.5E-03
D25	6.6E-02	3.2E-03	1.0E-02	1.7E-02	2.4E-02	9.9E-04	2.7E-02	1.8E-02	1.4E-03	3.3E-03	8.5E-04	9.7E-04	1.3E-03	7.6E-04	1.5E-03	6.3E-04
D26	6.5E-02	3.1E-03	1.0E-02	1.6E-02	2.4E-02	9.8E-04	2.6E-02	1.7E-02	1.4E-03	3.2E-03	8.5E-04	9.6E-04	1.3E-03	7.6E-04	1.5E-03	6.3E-04
D27	6.7E-02	3.2E-03	1.0E-02	1.7E-02	2.5E-02	1.0E-03	2.7E-02	1.8E-02	1.4E-03	3.3E-03	8.7E-04	9.9E-04	1.4E-03	7.7E-04	1.6E-03	6.4E-04

Sample	NAP	ACY	ACE	FLN	PHE	ANT	FLT	PYR	BAA	CHR	BBF	BKF	BAP	INP	DBA	BPE
D28	6.4E-02	3.1E-03	1.0E-02	1.6E-02	2.4E-02	9.7E-04	2.6E-02	1.7E-02	1.4E-03	3.2E-03	8.4E-04	9.5E-04	1.3E-03	7.5E-04	1.5E-03	6.2E-04
D29	1.1E-01	5.1E-03	1.6E-02	2.7E-02	3.9E-02	1.6E-03	4.3E-02	2.8E-02	2.2E-03	5.2E-03	1.4E-03	1.6E-03	2.1E-03	1.2E-03	2.5E-03	1.0E-03
D30	6.4E-02	3.1E-03	1.0E-02	1.6E-02	2.4E-02	9.6E-04	2.6E-02	1.7E-02	1.4E-03	3.2E-03	8.3E-04	9.4E-04	1.3E-03	7.4E-04	1.5E-03	6.1E-04
D31	6.5E-02	3.1E-03	1.0E-02	1.6E-02	2.4E-02	9.7E-04	2.6E-02	1.7E-02	1.4E-03	3.2E-03	8.4E-04	9.6E-04	1.3E-03	7.5E-04	1.5E-03	6.2E-04
D32	6.5E-02	3.1E-03	1.0E-02	1.6E-02	2.4E-02	9.8E-04	2.6E-02	1.7E-02	1.4E-03	3.2E-03	8.5E-04	9.6E-04	1.3E-03	7.6E-04	1.5E-03	6.3E-04
D33	8.2E-02	3.9E-03	1.3E-02	2.1E-02	3.0E-02	1.2E-03	3.3E-02	2.2E-02	1.7E-03	4.1E-03	1.1E-03	1.2E-03	1.7E-03	9.5E-04	1.9E-03	7.9E-04
D34	6.7E-02	3.2E-03	1.1E-02	1.7E-02	2.5E-02	1.0E-03	2.7E-02	1.8E-02	1.4E-03	3.3E-03	8.8E-04	1.0E-03	1.4E-03	7.8E-04	1.6E-03	6.5E-04
D35	7.1E-02	3.4E-03	1.1E-02	1.8E-02	2.6E-02	1.1E-03	2.9E-02	1.9E-02	1.5E-03	3.5E-03	9.2E-04	1.0E-03	1.4E-03	8.2E-04	1.7E-03	6.8E-04
D36	6.6E-02	3.2E-03	1.0E-02	1.7E-02	2.5E-02	1.0E-03	2.7E-02	1.8E-02	1.4E-03	3.3E-03	8.7E-04	9.8E-04	1.4E-03	7.7E-04	1.6E-03	6.4E-04
D37	1.8E-01	8.8E-03	2.9E-02	4.6E-02	6.8E-02	2.8E-03	7.4E-02	4.9E-02	3.9E-03	9.1E-03	2.4E-03	2.7E-03	3.7E-03	2.1E-03	4.3E-03	1.8E-03
D38	4.8E-02	2.3E-03	7.5E-03	1.2E-02	1.8E-02	7.2E-04	1.9E-02	1.3E-02	1.0E-03	2.4E-03	6.2E-04	7.1E-04	9.7E-04	5.6E-04	1.1E-03	4.6E-04
D39	5.2E-02	2.5E-03	8.2E-03	1.3E-02	2.0E-02	7.9E-04	2.1E-02	1.4E-02	1.1E-03	2.6E-03	6.8E-04	7.7E-04	1.1E-03	6.1E-04	1.2E-03	5.1E-04
D40	6.6E-02	3.2E-03	1.0E-02	1.7E-02	2.5E-02	1.0E-03	2.7E-02	1.8E-02	1.4E-03	3.3E-03	8.6E-04	9.8E-04	1.3E-03	7.7E-04	1.6E-03	6.4E-04
D41	7.2E-02	3.5E-03	1.1E-02	1.8E-02	2.7E-02	1.1E-03	2.9E-02	1.9E-02	1.5E-03	3.6E-03	9.4E-04	1.1E-03	1.5E-03	8.4E-04	1.7E-03	6.9E-04
D42	9.1E-02	4.4E-03	1.4E-02	2.3E-02	3.4E-02	1.4E-03	3.7E-02	2.4E-02	1.9E-03	4.5E-03	1.2E-03	1.3E-03	1.8E-03	1.1E-03	2.1E-03	8.8E-04
D43	5.1E-02	2.4E-03	7.9E-03	1.3E-02	1.9E-02	7.6E-04	2.1E-02	1.4E-02	1.1E-03	2.5E-03	6.6E-04	7.5E-04	1.0E-03	5.9E-04	1.2E-03	4.9E-04
D44	6.4E-02	3.1E-03	1.0E-02	1.6E-02	2.4E-02	9.6E-04	2.6E-02	1.7E-02	1.4E-03	3.2E-03	8.3E-04	9.4E-04	1.3E-03	7.4E-04	1.5E-03	6.2E-04
D45	6.5E-02	3.1E-03	1.0E-02	1.6E-02	2.4E-02	9.8E-04	2.6E-02	1.7E-02	1.4E-03	3.2E-03	8.5E-04	9.6E-04	1.3E-03	7.6E-04	1.5E-03	6.3E-04
D46	6.5E-02	3.1E-03	1.0E-02	1.6E-02	2.4E-02	9.8E-04	2.6E-02	1.7E-02	1.4E-03	3.2E-03	8.5E-04	9.6E-04	1.3E-03	7.6E-04	1.5E-03	6.3E-04
D47	6.7E-02	3.2E-03	1.0E-02	1.7E-02	2.5E-02	1.0E-03	2.7E-02	1.8E-02	1.4E-03	3.3E-03	8.7E-04	9.8E-04	1.4E-03	7.7E-04	1.6E-03	6.4E-04
D48	6.8E-02	3.3E-03	1.1E-02	1.7E-02	2.6E-02	1.0E-03	2.8E-02	1.8E-02	1.5E-03	3.4E-03	8.9E-04	1.0E-03	1.4E-03	8.0E-04	1.6E-03	6.6E-04
D49	1.4E-01	6.6E-03	2.1E-02	3.5E-02	5.1E-02	2.1E-03	5.6E-02	3.7E-02	2.9E-03	6.8E-03	1.8E-03	2.0E-03	2.8E-03	1.6E-03	3.2E-03	1.3E-03
D50	1.4E-01	6.5E-03	2.1E-02	3.4E-02	5.1E-02	2.0E-03	5.5E-02	3.6E-02	2.9E-03	6.7E-03	1.8E-03	2.0E-03	2.8E-03	1.6E-03	3.2E-03	1.3E-03
D51	1.4E-01	6.5E-03	2.1E-02	3.4E-02	5.0E-02	2.0E-03	5.5E-02	3.6E-02	2.9E-03	6.7E-03	1.8E-03	2.0E-03	2.7E-03	1.6E-03	3.2E-03	1.3E-03
D52	1.3E-01	6.5E-03	2.1E-02	3.4E-02	5.0E-02	2.0E-03	5.5E-02	3.6E-02	2.9E-03	6.7E-03	1.8E-03	2.0E-03	2.7E-03	1.6E-03	3.2E-03	1.3E-03
D53	1.6E-01	7.7E-03	2.5E-02	4.0E-02	6.0E-02	2.4E-03	6.5E-02	4.3E-02	3.4E-03	8.0E-03	2.1E-03	2.4E-03	3.3E-03	1.9E-03	3.8E-03	1.5E-03
D54	1.4E-01	6.6E-03	2.2E-02	3.5E-02	5.1E-02	2.1E-03	5.6E-02	3.7E-02	2.9E-03	6.9E-03	1.8E-03	2.0E-03	2.8E-03	1.6E-03	3.3E-03	1.3E-03
D55	1.3E-01	6.4E-03	2.1E-02	3.4E-02	5.0E-02	2.0E-03	5.4E-02	3.6E-02	2.8E-03	6.6E-03	1.7E-03	2.0E-03	2.7E-03	1.5E-03	3.1E-03	1.3E-03
D56	1.4E-01	6.9E-03	2.3E-02	3.6E-02	5.4E-02	2.2E-03	5.9E-02	3.9E-02	3.1E-03	7.2E-03	1.9E-03	2.1E-03	2.9E-03	1.7E-03	3.4E-03	1.4E-03
D57	1.3E-01	6.4E-03	2.1E-02	3.4E-02	5.0E-02	2.0E-03	5.4E-02	3.6E-02	2.8E-03	6.6E-03	1.7E-03	2.0E-03	2.7E-03	1.6E-03	3.2E-03	1.3E-03
D58	1.4E-01	6.8E-03	2.2E-02	3.6E-02	5.3E-02	2.1E-03	5.8E-02	3.8E-02	3.0E-03	7.0E-03	1.8E-03	2.1E-03	2.9E-03	1.6E-03	3.3E-03	1.4E-03

Sample	NAP	ACY	ACE	FLN	PHE	ANT	FLT	PYR	BAA	CHR	BBF	BKF	BAP	INP	DBA	BPE
D59	1.6E-01	7.7E-03	2.5E-02	4.1E-02	6.0E-02	2.4E-03	6.5E-02	4.3E-02	3.4E-03	8.0E-03	2.1E-03	2.4E-03	3.3E-03	1.9E-03	3.8E-03	1.5E-03
D60	1.3E-01	6.5E-03	2.1E-02	3.4E-02	5.0E-02	2.0E-03	5.5E-02	3.6E-02	2.9E-03	6.7E-03	1.7E-03	2.0E-03	2.7E-03	1.6E-03	3.2E-03	1.3E-03
D61	1.3E-01	6.4E-03	2.1E-02	3.4E-02	5.0E-02	2.0E-03	5.4E-02	3.6E-02	2.8E-03	6.6E-03	1.7E-03	2.0E-03	2.7E-03	1.6E-03	3.1E-03	1.3E-03
D62	1.3E-01	6.4E-03	2.1E-02	3.3E-02	4.9E-02	2.0E-03	5.4E-02	3.5E-02	2.8E-03	6.6E-03	1.7E-03	2.0E-03	2.7E-03	1.5E-03	3.1E-03	1.3E-03

b)

Sample	BJF	BEP	PER	DCA	ATT	COR	TPH	CCP	BGF	BBN	BNT	RET
D1	2.3E-03	8.8E-04	1.1E-03	1.6E-03	1.0E-03	1.1E-03	1.2E-03	3.8E-04	3.1E-03	2.7E-03	3.1E-04	3.1E-03
D2	2.2E-03	8.7E-04	1.1E-03	1.6E-03	1.0E-03	1.1E-03	1.1E-03	3.8E-04	3.0E-03	2.7E-03	3.1E-04	3.1E-03
D3	2.2E-03	8.7E-04	1.1E-03	1.6E-03	1.0E-03	1.1E-03	1.1E-03	3.8E-04	3.0E-03	2.7E-03	3.1E-04	3.1E-03
D4	2.6E-03	9.9E-04	1.3E-03	1.8E-03	1.2E-03	1.2E-03	1.3E-03	4.3E-04	3.4E-03	3.1E-03	3.5E-04	3.6E-03
D5	2.2E-03	8.7E-04	1.1E-03	1.6E-03	1.0E-03	1.1E-03	1.2E-03	3.8E-04	3.0E-03	2.7E-03	3.1E-04	3.1E-03
D6	2.2E-03	8.5E-04	1.1E-03	1.6E-03	1.0E-03	1.0E-03	1.1E-03	3.7E-04	3.0E-03	2.6E-03	3.0E-04	3.0E-03
D7	2.2E-03	8.4E-04	1.1E-03	1.6E-03	9.9E-04	1.0E-03	1.1E-03	3.7E-04	2.9E-03	2.6E-03	3.0E-04	3.0E-03
D8	4.4E-03	1.7E-03	2.2E-03	3.2E-03	2.0E-03	2.1E-03	2.3E-03	7.5E-04	6.0E-03	5.3E-03	6.1E-04	6.1E-03
D9	2.2E-03	8.6E-04	1.1E-03	1.6E-03	1.0E-03	1.1E-03	1.1E-03	3.7E-04	3.0E-03	2.7E-03	3.0E-04	3.1E-03
D10	2.3E-03	8.8E-04	1.1E-03	1.6E-03	1.0E-03	1.1E-03	1.2E-03	3.8E-04	3.1E-03	2.7E-03	3.1E-04	3.1E-03
D11	2.2E-03	8.7E-04	1.1E-03	1.6E-03	1.0E-03	1.1E-03	1.2E-03	3.8E-04	3.0E-03	2.7E-03	3.1E-04	3.1E-03
D12	2.2E-03	8.7E-04	1.1E-03	1.6E-03	1.0E-03	1.1E-03	1.1E-03	3.8E-04	3.0E-03	2.7E-03	3.1E-04	3.1E-03
D13	2.2E-03	8.7E-04	1.1E-03	1.6E-03	1.0E-03	1.1E-03	1.1E-03	3.8E-04	3.0E-03	2.7E-03	3.1E-04	3.1E-03
D14	3.1E-03	1.2E-03	1.6E-03	2.2E-03	1.4E-03	1.5E-03	1.6E-03	5.3E-04	4.2E-03	3.7E-03	4.3E-04	4.3E-03
D15	2.3E-03	8.9E-04	1.2E-03	1.6E-03	1.0E-03	1.1E-03	1.2E-03	3.8E-04	3.1E-03	2.7E-03	3.1E-04	3.2E-03
D16	2.2E-03	8.5E-04	1.1E-03	1.6E-03	1.0E-03	1.0E-03	1.1E-03	3.7E-04	3.0E-03	2.6E-03	3.0E-04	3.1E-03
D17	2.2E-03	8.6E-04	1.1E-03	1.6E-03	1.0E-03	1.0E-03	1.1E-03	3.7E-04	3.0E-03	2.6E-03	3.0E-04	3.1E-03
D18	2.3E-03	8.9E-04	1.2E-03	1.6E-03	1.0E-03	1.1E-03	1.2E-03	3.9E-04	3.1E-03	2.7E-03	3.1E-04	3.2E-03

Sample	BJF	BEP	PER	DCA	ATT	COR	TPH	CCP	BGF	BBN	BNT	RET
D19	2.2E-03	8.7E-04	1.1E-03	1.6E-03	1.0E-03	1.1E-03	1.1E-03	3.8E-04	3.0E-03	2.7E-03	3.1E-04	3.1E-03
D20	2.2E-03	8.7E-04	1.1E-03	1.6E-03	1.0E-03	1.1E-03	1.1E-03	3.8E-04	3.0E-03	2.7E-03	3.1E-04	3.1E-03
D21	2.3E-03	8.9E-04	1.2E-03	1.6E-03	1.0E-03	1.1E-03	1.2E-03	3.9E-04	3.1E-03	2.7E-03	3.1E-04	3.2E-03
D22	2.2E-03	8.5E-04	1.1E-03	1.6E-03	1.0E-03	1.0E-03	1.1E-03	3.7E-04	3.0E-03	2.6E-03	3.0E-04	3.1E-03
D23	4.3E-03	1.7E-03	2.2E-03	3.1E-03	2.0E-03	2.0E-03	2.2E-03	7.2E-04	5.8E-03	5.1E-03	5.9E-04	6.0E-03
D24	5.3E-03	2.1E-03	2.7E-03	3.8E-03	2.4E-03	2.5E-03	2.7E-03	9.0E-04	7.2E-03	6.4E-03	7.3E-04	7.4E-03
D25	2.2E-03	8.6E-04	1.1E-03	1.6E-03	1.0E-03	1.1E-03	1.1E-03	3.8E-04	3.0E-03	2.7E-03	3.0E-04	3.1E-03
D26	2.2E-03	8.6E-04	1.1E-03	1.6E-03	1.0E-03	1.0E-03	1.1E-03	3.7E-04	3.0E-03	2.6E-03	3.0E-04	3.1E-03
D27	2.3E-03	8.8E-04	1.1E-03	1.6E-03	1.0E-03	1.1E-03	1.2E-03	3.8E-04	3.0E-03	2.7E-03	3.1E-04	3.1E-03
D28	2.2E-03	8.4E-04	1.1E-03	1.6E-03	9.9E-04	1.0E-03	1.1E-03	3.7E-04	2.9E-03	2.6E-03	3.0E-04	3.0E-03
D29	3.6E-03	1.4E-03	1.8E-03	2.5E-03	1.6E-03	1.7E-03	1.8E-03	6.0E-04	4.8E-03	4.3E-03	4.9E-04	4.9E-03
D30	2.2E-03	8.4E-04	1.1E-03	1.5E-03	9.8E-04	1.0E-03	1.1E-03	3.6E-04	2.9E-03	2.6E-03	2.9E-04	3.0E-03
D31	2.2E-03	8.5E-04	1.1E-03	1.6E-03	1.0E-03	1.0E-03	1.1E-03	3.7E-04	2.9E-03	2.6E-03	3.0E-04	3.0E-03
D32	2.2E-03	8.5E-04	1.1E-03	1.6E-03	1.0E-03	1.0E-03	1.1E-03	3.7E-04	3.0E-03	2.6E-03	3.0E-04	3.1E-03
D33	2.8E-03	1.1E-03	1.4E-03	2.0E-03	1.3E-03	1.3E-03	1.4E-03	4.7E-04	3.7E-03	3.3E-03	3.8E-04	3.8E-03
D34	2.3E-03	8.9E-04	1.2E-03	1.6E-03	1.0E-03	1.1E-03	1.2E-03	3.8E-04	3.1E-03	2.7E-03	3.1E-04	3.2E-03
D35	2.4E-03	9.3E-04	1.2E-03	1.7E-03	1.1E-03	1.1E-03	1.2E-03	4.0E-04	3.2E-03	2.9E-03	3.3E-04	3.3E-03
D36	2.2E-03	8.7E-04	1.1E-03	1.6E-03	1.0E-03	1.1E-03	1.2E-03	3.8E-04	3.0E-03	2.7E-03	3.1E-04	3.1E-03
D37	6.2E-03	2.4E-03	3.1E-03	4.4E-03	2.8E-03	2.9E-03	3.2E-03	1.0E-03	8.3E-03	7.4E-03	8.5E-04	8.6E-03
D38	1.6E-03	6.3E-04	8.2E-04	1.2E-03	7.4E-04	7.7E-04	8.3E-04	2.7E-04	2.2E-03	1.9E-03	2.2E-04	2.3E-03
D39	1.8E-03	6.9E-04	9.0E-04	1.3E-03	8.1E-04	8.4E-04	9.1E-04	3.0E-04	2.4E-03	2.1E-03	2.4E-04	2.5E-03
D40	2.2E-03	8.7E-04	1.1E-03	1.6E-03	1.0E-03	1.1E-03	1.1E-03	3.8E-04	3.0E-03	2.7E-03	3.1E-04	3.1E-03
D41	2.4E-03	9.5E-04	1.2E-03	1.7E-03	1.1E-03	1.2E-03	1.2E-03	4.1E-04	3.3E-03	2.9E-03	3.3E-04	3.4E-03
D42	3.1E-03	1.2E-03	1.6E-03	2.2E-03	1.4E-03	1.5E-03	1.6E-03	5.2E-04	4.2E-03	3.7E-03	4.2E-04	4.3E-03
D43	1.7E-03	6.7E-04	8.7E-04	1.2E-03	7.8E-04	8.1E-04	8.8E-04	2.9E-04	2.3E-03	2.0E-03	2.3E-04	2.4E-03

Sample	BJF	BEP	PER	DCA	ATT	COR	TPH	CCP	BGF	BBN	BNT	RET
D44	2.2E-03	8.4E-04	1.1E-03	1.5E-03	9.9E-04	1.0E-03	1.1E-03	3.7E-04	2.9E-03	2.6E-03	3.0E-04	3.0E-03
D45	2.2E-03	8.6E-04	1.1E-03	1.6E-03	1.0E-03	1.0E-03	1.1E-03	3.7E-04	3.0E-03	2.6E-03	3.0E-04	3.1E-03
D46	2.2E-03	8.5E-04	1.1E-03	1.6E-03	1.0E-03	1.0E-03	1.1E-03	3.7E-04	3.0E-03	2.6E-03	3.0E-04	3.1E-03
D47	2.3E-03	8.8E-04	1.1E-03	1.6E-03	1.0E-03	1.1E-03	1.2E-03	3.8E-04	3.0E-03	2.7E-03	3.1E-04	3.1E-03
D48	2.3E-03	9.0E-04	1.2E-03	1.7E-03	1.1E-03	1.1E-03	1.2E-03	3.9E-04	3.1E-03	2.8E-03	3.2E-04	3.2E-03
D49	4.6E-03	1.8E-03	2.4E-03	3.3E-03	2.1E-03	2.2E-03	2.4E-03	7.9E-04	6.3E-03	5.6E-03	6.4E-04	6.5E-03
D50	4.6E-03	1.8E-03	2.3E-03	3.3E-03	2.1E-03	2.2E-03	2.4E-03	7.8E-04	6.2E-03	5.5E-03	6.3E-04	6.4E-03
D51	4.6E-03	1.8E-03	2.3E-03	3.3E-03	2.1E-03	2.2E-03	2.3E-03	7.7E-04	6.2E-03	5.5E-03	6.3E-04	6.4E-03
D52	4.5E-03	1.8E-03	2.3E-03	3.2E-03	2.1E-03	2.2E-03	2.3E-03	7.7E-04	6.1E-03	5.4E-03	6.2E-04	6.3E-03
D53	5.4E-03	2.1E-03	2.7E-03	3.9E-03	2.5E-03	2.6E-03	2.8E-03	9.2E-04	7.3E-03	6.5E-03	7.4E-04	7.5E-03
D54	4.7E-03	1.8E-03	2.4E-03	3.3E-03	2.1E-03	2.2E-03	2.4E-03	7.9E-04	6.3E-03	5.6E-03	6.4E-04	6.5E-03
D55	4.5E-03	1.7E-03	2.3E-03	3.2E-03	2.1E-03	2.1E-03	2.3E-03	7.6E-04	6.1E-03	5.4E-03	6.2E-04	6.3E-03
D56	4.9E-03	1.9E-03	2.5E-03	3.5E-03	2.2E-03	2.3E-03	2.5E-03	8.2E-04	6.6E-03	5.8E-03	6.7E-04	6.8E-03
D57	4.5E-03	1.8E-03	2.3E-03	3.2E-03	2.1E-03	2.1E-03	2.3E-03	7.6E-04	6.1E-03	5.4E-03	6.2E-04	6.3E-03
D58	4.8E-03	1.9E-03	2.4E-03	3.4E-03	2.2E-03	2.3E-03	2.5E-03	8.1E-04	6.5E-03	5.7E-03	6.6E-04	6.7E-03
D59	5.4E-03	2.1E-03	2.7E-03	3.9E-03	2.5E-03	2.6E-03	2.8E-03	9.2E-04	7.3E-03	6.5E-03	7.5E-04	7.6E-03
D60	4.5E-03	1.8E-03	2.3E-03	3.2E-03	2.1E-03	2.2E-03	2.3E-03	7.7E-04	6.1E-03	5.4E-03	6.2E-04	6.3E-03
D61	4.5E-03	1.8E-03	2.3E-03	3.2E-03	2.1E-03	2.1E-03	2.3E-03	7.6E-04	6.1E-03	5.4E-03	6.2E-04	6.3E-03
D62	4.5E-03	1.7E-03	2.3E-03	3.2E-03	2.0E-03	2.1E-03	2.3E-03	7.6E-04	6.0E-03	5.3E-03	6.1E-04	6.2E-03

c)

Sample	1,4-O_2NAP	1-(CHO)NAP	9-OFLN	9,10-O_2ANT	1,4-O_2ANT	9,10-O_2PHE	11-OBaFLN	11-OBbFLN	BAN	7,12-O_2BAA	5,12-O_2NAC
D1	2.2E-02	1.2E-02	1.2E-02	5.9E-02	2.0E-03	1.9E-01	4.3E-03	3.2E-03	3.5E-03	3.1E-03	1.4E-03
D2	2.1E-02	1.1E-02	1.2E-02	5.9E-02	1.0E-03	3.8E-01	4.3E-03	3.2E-03	3.4E-03	3.1E-03	1.3E-03

Sample	1,4-O_2NAP	1-(CHO)NAP	9-OFLN	9,10-O_2ANT	1,4-O_2ANT	9,10-O_2PHE	11-OBaFLN	11-OBbFLN	BAN	7,12-O_2BAA	5,12-O_2NAC
D3	2.1E-02	1.1E-02	1.2E-02	5.9E-02	3.6E-03	1.2E+00	4.3E-03	3.2E-03	3.4E-03	3.1E-03	1.4E-03
D4	2.4E-02	1.3E-02	1.4E-02	6.7E-02	6.7E-04	1.2E-01	4.9E-03	3.6E-03	3.9E-03	3.5E-03	1.5E-03
D5	2.1E-02	1.1E-02	1.2E-02	5.9E-02	8.1E-04	1.3E-01	4.3E-03	3.2E-03	3.4E-03	3.1E-03	1.3E-03
D6	2.1E-02	1.1E-02	1.2E-02	5.7E-02	1.9E-03	1.2E-01	4.2E-03	3.1E-03	3.4E-03	3.0E-03	1.3E-03
D7	2.1E-02	1.1E-02	1.2E-02	5.7E-02	1.3E-03	2.0E-01	4.2E-03	3.1E-03	3.3E-03	3.0E-03	1.3E-03
D8	4.2E-02	2.2E-02	2.4E-02	1.2E-01	1.0E-02	5.4E+00	8.5E-03	6.3E-03	6.8E-03	6.1E-03	6.0E-03
D9	2.1E-02	1.1E-02	1.2E-02	5.8E-02	3.7E-03	5.1E-01	4.2E-03	3.2E-03	3.4E-03	3.1E-03	1.3E-03
D10	2.2E-02	1.2E-02	1.3E-02	5.9E-02	1.2E-03	2.7E-01	4.3E-03	3.2E-03	3.5E-03	3.1E-03	1.4E-03
D11	2.1E-02	1.1E-02	1.2E-02	5.9E-02	1.9E-03	1.7E-01	4.3E-03	3.2E-03	3.4E-03	3.1E-03	1.3E-03
D12	2.1E-02	1.1E-02	1.2E-02	5.9E-02	2.5E-03	2.9E-01	4.3E-03	3.2E-03	3.4E-03	3.1E-03	1.3E-03
D13	2.1E-02	1.1E-02	1.2E-02	5.9E-02	9.3E-04	1.9E-01	4.3E-03	3.2E-03	3.4E-03	3.1E-03	1.3E-03
D14	3.0E-02	1.6E-02	1.7E-02	8.2E-02	1.3E-03	2.0E-01	6.0E-03	4.4E-03	4.8E-03	4.3E-03	1.9E-03
D15	2.2E-02	1.2E-02	1.3E-02	6.0E-02	2.4E-03	1.8E-01	4.4E-03	3.2E-03	3.5E-03	3.2E-03	1.4E-03
D16	2.1E-02	1.1E-02	1.2E-02	5.8E-02	1.9E-03	1.0E+00	4.2E-03	3.1E-03	3.4E-03	3.0E-03	1.3E-03
D17	2.1E-02	1.1E-02	1.2E-02	5.8E-02	1.6E-03	4.6E-01	4.2E-03	3.1E-03	3.4E-03	3.1E-03	1.3E-03
D18	2.2E-02	1.2E-02	1.3E-02	6.0E-02	6.1E-03	4.6E+00	4.4E-03	3.3E-03	3.5E-03	3.2E-03	1.5E-03
D19	2.1E-02	1.1E-02	1.2E-02	5.9E-02	8.9E-04	6.6E-01	4.3E-03	3.2E-03	3.4E-03	3.1E-03	1.7E-03
D20	2.1E-02	1.1E-02	1.2E-02	5.8E-02	5.6E-03	1.0E+00	4.3E-03	3.2E-03	3.4E-03	3.1E-03	1.4E-03
D21	2.2E-02	1.2E-02	1.3E-02	6.0E-02	9.4E-04	1.6E-01	4.4E-03	3.3E-03	3.5E-03	3.2E-03	1.4E-03
D22	2.1E-02	1.1E-02	1.2E-02	5.8E-02	1.4E-02	6.7E+00	1.0E-02	7.8E-03	4.2E-03	3.0E-03	2.5E-03
D23	4.1E-02	5.2E-02	2.4E-02	1.1E-01	2.8E-02	1.9E+01	1.3E-02	9.9E-03	6.6E-03	1.9E-02	1.4E-02
D24	5.1E-02	2.7E-02	3.0E-02	1.4E-01	1.9E-03	5.3E-01	1.0E-02	7.6E-03	8.2E-03	7.4E-03	3.2E-03
D25	2.1E-02	1.1E-02	1.2E-02	5.8E-02	1.3E-03	2.6E+00	4.3E-03	3.2E-03	3.4E-03	3.1E-03	1.3E-03
D26	2.1E-02	1.1E-02	1.2E-02	5.8E-02	1.9E-03	1.5E+00	4.2E-03	3.1E-03	3.4E-03	3.1E-03	1.3E-03
D27	2.2E-02	1.1E-02	1.2E-02	5.9E-02	2.4E-03	9.2E-01	4.3E-03	3.2E-03	3.5E-03	3.1E-03	1.3E-03
D28	2.1E-02	1.1E-02	1.2E-02	5.7E-02	2.9E-02	2.2E+00	4.2E-03	3.1E-03	3.3E-03	3.0E-03	1.4E-03
D29	3.4E-02	1.8E-02	2.0E-02	9.3E-02	2.1E-03	1.5E-01	6.8E-03	5.1E-03	5.5E-03	4.9E-03	2.1E-03

Sample	1,4-O_2NAP	1-(CHO)NAP	9-OFLN	9,10-O_2ANT	1,4-O_2ANT	9,10-O_2PHE	11-OBaFLN	11-OBbFLN	BAN	7,12-O_2BAA	5,12-O_2NAC
D30	2.1E-02	1.1E-02	1.2E-02	5.6E-02	3.2E-03	1.4E-01	4.1E-03	3.1E-03	3.3E-03	3.0E-03	1.5E-03
D31	2.1E-02	1.1E-02	1.2E-02	5.7E-02	1.1E-03	3.6E-01	4.2E-03	3.1E-03	3.4E-03	3.0E-03	1.3E-03
D32	2.1E-02	1.1E-02	1.2E-02	5.8E-02	2.7E-03	3.6E-01	4.2E-03	3.1E-03	3.4E-03	3.0E-03	1.3E-03
D33	2.6E-02	1.4E-02	1.5E-02	7.2E-02	1.7E-03	3.2E-01	5.3E-03	3.9E-03	4.2E-03	3.8E-03	1.6E-03
D34	2.2E-02	1.2E-02	1.3E-02	6.0E-02	7.3E-04	1.1E-01	4.4E-03	3.2E-03	3.5E-03	3.2E-03	1.4E-03
D35	2.3E-02	1.2E-02	1.3E-02	6.3E-02	6.8E-04	9.5E-02	4.6E-03	3.4E-03	3.7E-03	3.3E-03	1.4E-03
D36	2.1E-02	1.1E-02	1.2E-02	5.9E-02	5.7E-04	7.6E-02	4.3E-03	3.2E-03	3.5E-03	3.1E-03	1.3E-03
D37	5.9E-02	3.1E-02	3.4E-02	1.6E-01	2.7E-03	4.1E-01	1.2E-02	8.8E-03	9.5E-03	8.6E-03	3.7E-03
D38	1.5E-02	8.3E-03	8.9E-03	4.3E-02	1.5E-03	3.1E-01	3.1E-03	2.3E-03	2.5E-03	2.2E-03	9.7E-04
D39	1.7E-02	9.0E-03	9.8E-03	4.6E-02	6.4E-04	8.4E-02	3.4E-03	2.5E-03	2.7E-03	2.5E-03	1.1E-03
D40	2.1E-02	1.1E-02	1.2E-02	5.9E-02	6.1E-04	6.5E-02	4.3E-03	3.2E-03	3.4E-03	3.1E-03	1.3E-03
D41	2.3E-02	1.2E-02	1.3E-02	6.4E-02	7.7E-04	9.2E-02	4.7E-03	3.5E-03	3.7E-03	3.4E-03	1.5E-03
D42	2.9E-02	1.6E-02	1.7E-02	8.1E-02	5.4E-04	9.0E-02	5.9E-03	4.4E-03	4.7E-03	4.3E-03	1.8E-03
D43	1.6E-02	8.7E-03	9.5E-03	4.5E-02	7.5E-04	1.0E-01	3.3E-03	2.4E-03	2.6E-03	2.4E-03	1.0E-03
D44	2.1E-02	1.1E-02	1.2E-02	5.7E-02	6.1E-04	1.3E-01	4.1E-03	3.1E-03	3.3E-03	3.0E-03	1.3E-03
D45	2.1E-02	1.1E-02	1.2E-02	5.8E-02	8.0E-04	6.5E-02	4.2E-03	3.1E-03	3.4E-03	3.1E-03	1.3E-03
D46	2.1E-02	1.1E-02	1.2E-02	5.8E-02	9.5E-04	1.8E-01	4.2E-03	3.1E-03	3.4E-03	3.0E-03	1.3E-03
D47	2.2E-02	1.1E-02	1.2E-02	5.9E-02	1.7E-03	2.1E-01	4.3E-03	3.2E-03	3.5E-03	3.1E-03	1.3E-03
D48	2.2E-02	1.2E-02	1.3E-02	6.1E-02	1.5E-03	1.6E-01	4.4E-03	3.3E-03	3.6E-03	3.2E-03	1.4E-03
D49	4.4E-02	2.4E-02	2.6E-02	1.2E-01	1.6E-03	2.7E-01	8.9E-03	6.6E-03	7.1E-03	6.4E-03	2.8E-03
D50	4.4E-02	2.3E-02	2.5E-02	1.2E-01	2.3E-03	2.1E-01	8.8E-03	6.5E-03	7.0E-03	6.4E-03	2.7E-03
D51	4.4E-02	2.3E-02	2.5E-02	1.2E-01	1.2E-03	1.0E-01	8.7E-03	6.5E-03	7.0E-03	6.3E-03	2.7E-03
D52	4.3E-02	2.3E-02	2.5E-02	1.2E-01	1.3E-03	1.9E-01	8.7E-03	6.5E-03	7.0E-03	6.3E-03	2.7E-03
D53	5.2E-02	2.8E-02	3.0E-02	1.4E-01	1.5E-03	6.1E-01	1.0E-02	7.7E-03	8.3E-03	7.5E-03	3.2E-03
D54	4.5E-02	2.4E-02	2.6E-02	1.2E-01	6.2E-03	5.7E-01	8.9E-03	6.6E-03	7.2E-03	6.5E-03	2.8E-03
D55	4.3E-02	2.3E-02	2.5E-02	1.2E-01	2.6E-03	2.5E-01	8.6E-03	6.4E-03	6.9E-03	6.2E-03	2.7E-03
D56	4.7E-02	2.5E-02	2.7E-02	1.3E-01	4.2E-03	2.3E-01	9.3E-03	6.9E-03	7.5E-03	6.8E-03	2.9E-03

Sample	1,4-O_2NAP	1-(CHO)NAP	9-OFLN	9,10-O_2ANT	1,4-O_2ANT	9,10-O_2PHE	11-OBaFLN	11-OBbFLN	BAN	7,12-O_2BAA	5,12-O_2NAC
D57	4.3E-02	2.3E-02	2.5E-02	1.2E-01	3.6E-03	6.4E-01	8.7E-03	6.4E-03	6.9E-03	6.3E-03	2.7E-03
D58	4.6E-02	2.4E-02	2.6E-02	1.3E-01	9.5E-03	4.2E-01	9.2E-03	6.8E-03	7.4E-03	6.6E-03	2.9E-03
D59	5.2E-02	2.8E-02	3.0E-02	1.4E-01	3.7E-03	3.9E-01	1.0E-02	7.7E-03	8.3E-03	7.5E-03	3.3E-03
D60	4.3E-02	2.3E-02	2.5E-02	1.2E-01	1.9E-03	3.3E-01	8.7E-03	6.5E-03	7.0E-03	6.3E-03	2.7E-03
D61	4.3E-02	2.3E-02	2.5E-02	1.2E-01	1.5E-03	3.9E-01	8.7E-03	6.4E-03	6.9E-03	6.3E-03	2.9E-03
D62	4.3E-02	2.3E-02	2.5E-02	1.2E-01	1.5E-03	4.0E+00	8.6E-03	6.4E-03	6.9E-03	6.2E-03	2.7E-03

d)

Sample	1-NNAP	2-NNAP	3-NACE	5-NACE	2-NFLN	9-NANT	9-NPHE	3-NPHE	2-NFLT	1-NPYR	2-NPYR	7-NBAA	6-NCHR	1,3-N_2PYR	1,6-N_2PYR	1,8-N_2PYR	6-NBAP
D1	2.4E-03	6.5E-04	1.0E-02	6.2E-04	4.8E-05	2.3E-03	1.9E-03	4.4E-04	5.6E-05	3.6E-04	1.9E-05	1.1E-04	8.3E-05	2.8E-04	6.4E-04	2.7E-04	5.8E-04
D2	4.5E-03	6.4E-04	1.1E-02	1.5E-03	6.1E-05	7.8E-03	4.4E-03	7.2E-04	5.5E-05	4.3E-04	1.8E-05	1.5E-04	1.2E-04	2.5E-04	6.4E-04	2.7E-04	4.8E-04
D3	4.9E-03	6.4E-04	2.7E-02	2.8E-03	1.2E-04	2.4E-02	1.7E-02	2.0E-03	5.5E-05	2.4E-03	5.9E-05	2.5E-04	1.8E-04	2.3E-04	7.2E-04	3.0E-04	6.1E-04
D4	2.2E-03	7.3E-04	8.4E-03	1.8E-03	3.1E-05	2.6E-03	2.4E-03	1.6E-04	6.3E-05	4.1E-04	2.1E-05	1.3E-04	7.8E-05	2.0E-04	4.7E-04	2.0E-04	4.0E-04
D5	2.5E-03	6.4E-04	9.5E-03	1.0E-03	3.7E-05	2.3E-03	2.4E-03	3.0E-04	5.5E-05	3.6E-04	1.3E-04	3.2E-04	2.3E-04	1.7E-04	4.7E-04	2.0E-04	3.9E-04
D6	1.6E-03	6.2E-04	7.5E-03	7.7E-04	3.8E-05	2.3E-03	1.4E-03	1.9E-04	5.4E-05	3.5E-04	1.8E-05	1.1E-04	7.6E-05	1.7E-04	5.2E-04	2.2E-04	3.4E-04
D7	1.8E-03	6.2E-04	8.9E-03	6.6E-04	3.6E-05	2.2E-03	2.2E-03	2.9E-04	5.4E-05	3.4E-04	1.8E-05	1.1E-04	7.5E-05	2.0E-04	4.7E-04	2.0E-04	5.1E-04
D8	6.4E-03	1.3E-03	4.9E-02	5.8E-03	3.2E-04	5.4E-02	2.4E-02	3.4E-03	1.8E-04	7.1E-03	3.6E-04	9.2E-04	6.2E-04	5.6E-04	1.7E-03	7.1E-04	1.4E-03
D9	3.1E-03	6.3E-04	1.7E-02	1.2E-03	5.8E-05	2.4E-03	2.7E-03	4.7E-04	5.5E-05	3.5E-04	1.8E-05	1.1E-04	8.5E-05	2.0E-04	5.0E-04	2.1E-04	1.1E-03
D10	2.9E-03	6.5E-04	1.2E-02	1.3E-03	5.4E-05	3.9E-03	2.5E-03	5.0E-04	5.6E-05	3.6E-04	1.9E-05	1.2E-04	1.0E-04	2.4E-04	5.7E-04	2.4E-04	7.0E-04
D11	2.2E-03	6.4E-04	9.9E-03	6.7E-04	4.0E-05	2.3E-03	2.9E-03	2.9E-04	5.5E-05	3.6E-04	1.9E-05	1.1E-04	8.7E-05	2.7E-04	6.3E-04	2.6E-04	9.8E-04
D12	4.7E-03	6.4E-04	1.2E-02	1.8E-03	5.5E-05	9.7E-03	9.8E-03	6.8E-04	5.5E-05	3.5E-04	1.8E-05	1.3E-04	1.1E-04	2.4E-04	6.6E-04	2.8E-04	5.7E-04
D13	1.6E-03	6.4E-04	1.2E-02	1.7E-03	6.6E-05	4.8E-03	4.6E-03	5.3E-04	5.5E-05	3.5E-04	1.8E-05	1.1E-04	8.1E-05	2.6E-04	5.9E-04	2.5E-04	4.5E-04
D14	2.0E-03	8.9E-04	1.0E-02	9.8E-04	5.5E-05	3.2E-03	2.6E-03	2.6E-04	7.7E-05	5.0E-04	2.6E-05	1.5E-04	9.6E-05	1.9E-04	5.6E-04	2.4E-04	4.4E-04
D15	1.5E-03	6.5E-04	1.0E-02	9.6E-04	4.5E-05	3.7E-03	2.8E-03	4.7E-04	5.6E-05	3.6E-04	1.9E-05	1.1E-04	6.9E-05	1.4E-04	4.7E-04	2.0E-04	4.0E-04
D16	2.0E-03	6.3E-04	2.7E-02	3.0E-03	1.2E-04	1.8E-02	1.1E-02	1.6E-03	5.4E-05	9.5E-04	1.8E-05	3.5E-04	2.4E-04	2.0E-04	5.1E-04	2.1E-04	5.5E-04
D17	2.9E-03	6.3E-04	2.7E-02	2.3E-03	1.1E-04	1.0E-02	6.3E-03	9.6E-04	5.5E-05	5.3E-04	1.8E-05	1.1E-04	9.8E-05	1.2E-04	5.0E-04	2.1E-04	4.1E-04

Sample	1-NNAP	2-NNAP	3-NACE	5-NACE	2-NFLN	9-NANT	9-NPHE	3-NPHE	2-NFLT	1-NPYR	2-NPYR	7-NBAA	6-NCHR	1,3-N_2PYR	1,6-N_2PYR	1,8-N_2PYR	6-NBAP
D18	4.1E-03	6.5E-04	2.6E-02	2.2E-03	2.0E-04	2.9E-02	1.8E-02	1.9E-03	5.7E-05	1.7E-03	1.9E-05	3.0E-04	2.1E-04	1.8E-04	6.7E-04	2.8E-04	5.5E-04
D19	1.7E-03	6.4E-04	1.0E-02	1.3E-03	4.4E-05	7.1E-03	3.4E-03	5.2E-04	5.5E-05	3.9E-04	1.8E-05	1.3E-04	1.1E-04	1.8E-04	4.3E-04	1.8E-04	4.4E-04
D20	7.1E-03	6.3E-04	1.6E-02	2.2E-03	1.5E-04	1.8E-02	1.2E-02	1.2E-03	5.5E-05	1.6E-03	1.8E-05	4.6E-04	3.1E-04	2.1E-04	5.5E-04	2.3E-04	5.2E-04
D21	2.2E-03	6.5E-04	6.2E-03	6.0E-04	2.9E-05	2.4E-03	1.7E-03	1.5E-04	5.6E-05	3.6E-04	1.9E-05	1.1E-04	6.6E-05	1.2E-04	3.9E-04	1.6E-04	3.1E-04
D22	3.6E-02	1.3E-03	5.6E-02	6.2E-03	1.2E-03	4.1E-02	2.0E-02	4.2E-03	5.4E-05	8.4E-03	1.1E-04	7.8E-04	5.0E-04	2.3E-04	1.1E-03	4.6E-04	1.0E-03
D23	4.7E-02	1.2E-03	1.3E-01	1.5E-02	2.5E-03	1.2E-01	5.0E-02	1.3E-02	5.4E-04	3.8E-02	5.9E-04	2.9E-03	1.8E-03	1.0E-03	4.8E-03	2.0E-03	4.4E-03
D24	3.2E-03	1.5E-03	1.8E-02	2.7E-03	9.0E-05	8.6E-03	7.1E-03	8.3E-04	1.3E-04	8.6E-04	4.4E-05	2.6E-04	1.8E-04	3.5E-04	1.1E-03	4.4E-04	9.1E-04
D25	3.2E-03	6.3E-04	1.3E-02	1.3E-03	6.3E-05	5.1E-03	4.0E-03	6.8E-04	5.5E-05	4.5E-04	1.8E-05	1.2E-04	1.0E-04	1.4E-04	4.3E-04	1.8E-04	3.7E-04
D26	2.4E-03	6.3E-04	1.9E-02	2.2E-03	1.2E-04	9.9E-03	1.1E-02	7.4E-04	5.4E-05	5.8E-04	5.6E-05	1.7E-04	1.3E-04	2.0E-04	5.5E-04	2.3E-04	5.3E-04
D27	2.1E-03	6.4E-04	2.6E-02	2.4E-03	2.2E-04	1.8E-02	9.6E-03	1.5E-03	5.6E-05	7.1E-04	1.9E-05	3.1E-04	2.2E-04	2.7E-04	7.1E-04	3.0E-04	7.9E-04
D28	4.6E-03	6.2E-04	3.0E-02	2.5E-03	2.0E-04	2.3E-02	1.2E-02	2.0E-03	5.4E-05	3.9E-03	5.2E-05	5.2E-04	3.5E-04	1.9E-04	6.4E-04	2.7E-04	5.6E-04
D29	2.0E-03	1.0E-03	9.7E-03	7.6E-04	4.9E-05	3.7E-03	1.8E-03	2.3E-04	8.8E-05	5.6E-04	2.9E-05	1.8E-04	9.6E-05	2.4E-04	6.5E-04	2.7E-04	6.2E-04
D30	2.5E-03	6.1E-04	1.4E-02	7.6E-04	4.4E-05	2.2E-03	2.2E-03	4.7E-04	5.3E-05	3.4E-04	1.8E-05	1.1E-04	7.6E-05	1.7E-04	5.6E-04	2.4E-04	3.8E-04
D31	1.6E-03	6.2E-04	2.2E-02	1.6E-03	8.7E-05	6.0E-03	9.3E-03	1.4E-03	5.4E-05	3.5E-04	1.8E-05	1.1E-04	8.9E-05	2.1E-04	6.3E-04	2.6E-04	4.8E-04
D32	4.0E-03	6.3E-04	1.5E-02	1.6E-03	5.5E-05	5.2E-03	3.3E-03	5.1E-04	5.4E-05	3.5E-04	1.8E-05	1.1E-04	8.0E-05	1.4E-04	5.1E-04	2.1E-04	3.1E-04
D33	5.0E-03	7.9E-04	1.4E-02	1.9E-03	5.3E-05	3.9E-03	4.2E-03	4.3E-04	6.8E-05	4.4E-04	2.3E-05	1.4E-04	1.0E-04	1.8E-04	5.7E-04	2.4E-04	5.6E-04
D34	2.0E-03	6.5E-04	7.4E-03	5.1E-04	3.1E-05	2.4E-03	1.4E-03	2.1E-04	5.6E-05	3.6E-04	1.9E-05	1.1E-04	8.9E-05	1.8E-04	4.4E-04	1.8E-04	5.0E-04
D35	3.3E-03	6.8E-04	7.1E-03	1.1E-03	3.2E-05	2.5E-03	2.1E-03	9.2E-04	5.9E-05	3.8E-04	2.0E-05	1.2E-04	7.2E-05	1.6E-04	4.4E-04	1.8E-04	4.5E-04
D36	1.6E-03	6.4E-04	5.9E-03	4.1E-04	2.4E-05	2.3E-03	8.0E-04	1.4E-04	5.5E-05	3.6E-04	1.9E-05	1.1E-04	6.6E-05	1.6E-04	4.5E-04	1.9E-04	4.1E-04
D37	5.3E-03	1.8E-03	2.2E-02	3.6E-03	9.5E-05	8.0E-03	7.0E-03	4.7E-04	1.5E-04	9.8E-04	5.1E-05	3.0E-04	1.8E-04	4.1E-04	1.1E-03	4.7E-04	1.1E-03
D38	4.1E-03	4.6E-04	1.1E-02	2.1E-03	1.0E-04	1.2E-02	5.6E-03	5.6E-04	4.0E-05	5.9E-04	1.3E-05	1.8E-04	1.3E-04	1.0E-04	3.8E-04	1.6E-04	5.5E-04
D39	1.8E-03	5.1E-04	5.2E-03	4.4E-04	2.0E-05	1.8E-03	8.4E-04	1.2E-04	4.4E-05	2.8E-04	1.5E-05	8.7E-05	5.6E-05	1.3E-04	3.3E-04	1.4E-04	3.0E-04
D40	2.3E-03	6.4E-04	7.0E-03	4.1E-04	2.8E-05	2.3E-03	7.6E-04	1.4E-04	5.5E-05	3.6E-04	1.8E-05	1.1E-04	7.5E-05	1.6E-04	4.8E-04	2.0E-04	3.2E-04
D41	2.3E-03	6.9E-04	7.2E-03	5.9E-04	3.0E-05	2.5E-03	1.4E-03	1.6E-04	6.0E-05	3.9E-04	2.0E-05	1.2E-04	7.4E-05	1.6E-04	4.5E-04	1.9E-04	4.5E-04
D42	1.8E-03	8.8E-04	6.9E-03	3.8E-04	2.8E-05	3.2E-03	6.9E-04	2.0E-04	7.6E-05	4.9E-04	2.5E-05	1.5E-04	9.4E-05	1.7E-04	4.9E-04	2.0E-04	3.7E-04
D43	1.8E-03	4.9E-04	6.7E-03	5.8E-04	2.9E-05	1.8E-03	6.7E-03	2.3E-04	4.2E-05	2.7E-04	1.4E-05	8.4E-05	6.1E-05	1.5E-04	3.6E-04	1.5E-04	3.2E-04
D44	1.4E-03	6.2E-04	5.9E-03	4.8E-04	3.1E-05	2.2E-03	8.2E-04	1.4E-04	5.3E-05	3.4E-04	1.8E-05	1.1E-04	7.1E-05	1.7E-04	4.5E-04	1.9E-04	5.1E-04

Sample	1-NNAP	2-NNAP	3-NACE	5-NACE	2-NFLN	9-NANT	9-NPHE	3-NPHE	2-NFLT	1-NPYR	2-NPYR	7-NBAA	6-NCHR	1,3-N_2PYR	1,6-N_2PYR	1,8-N_2PYR	6-NBAP
D45	1.3E-03	6.3E-04	5.8E-03	3.5E-04	2.8E-05	2.3E-03	6.4E-04	1.4E-04	5.4E-05	3.5E-04	1.8E-05	1.1E-04	6.2E-05	2.3E-04	4.8E-04	2.0E-04	4.6E-04
D46	2.1E-03	6.3E-04	6.4E-03	4.5E-04	2.7E-05	2.3E-03	8.0E-04	1.4E-04	5.4E-05	3.5E-04	1.8E-05	1.5E-04	1.2E-04	2.3E-04	6.0E-04	2.5E-04	1.0E-03
D47	2.6E-03	6.4E-04	7.8E-03	6.1E-04	4.2E-05	2.3E-03	1.3E-03	2.3E-04	5.6E-05	3.6E-04	1.9E-05	1.1E-04	7.9E-05	2.4E-04	5.9E-04	2.5E-04	4.6E-04
D48	3.7E-03	6.6E-04	1.1E-02	8.7E-04	9.7E-05	2.4E-03	1.6E-03	2.2E-04	5.7E-05	3.7E-04	1.9E-05	1.1E-04	8.1E-05	2.5E-04	6.5E-04	2.7E-04	4.9E-04
D49	3.9E-03	1.3E-03	1.3E-02	1.2E-03	5.4E-05	4.8E-03	3.5E-03	3.1E-04	1.1E-04	7.4E-04	3.8E-05	2.3E-04	1.4E-04	3.0E-04	8.9E-04	3.7E-04	6.5E-04
D50	5.6E-03	1.3E-03	1.3E-02	1.2E-03	5.0E-05	4.7E-03	2.4E-03	2.9E-04	1.1E-04	7.3E-04	3.8E-05	2.3E-04	1.8E-04	3.7E-04	1.1E-03	4.4E-04	7.1E-04
D51	3.1E-03	1.3E-03	1.0E-02	8.1E-04	5.7E-05	4.7E-03	1.7E-03	2.9E-04	1.1E-04	7.3E-04	3.8E-05	2.2E-04	1.8E-04	3.8E-04	1.1E-03	4.5E-04	7.2E-04
D52	4.8E-03	1.3E-03	1.0E-02	9.7E-04	4.6E-05	4.7E-03	1.7E-03	2.9E-04	1.1E-04	7.2E-04	3.8E-05	2.2E-04	1.8E-04	2.4E-04	7.1E-04	3.0E-04	6.7E-04
D53	3.9E-03	1.5E-03	1.1E-02	7.7E-04	5.0E-05	5.6E-03	1.6E-03	3.5E-04	1.3E-04	8.6E-04	4.5E-05	2.7E-04	2.1E-04	3.3E-04	1.0E-03	4.3E-04	8.1E-04
D54	6.1E-03	1.3E-03	1.4E-02	1.2E-03	5.2E-05	4.8E-03	2.1E-03	3.0E-04	1.2E-04	7.4E-04	4.8E-05	2.3E-04	1.6E-04	3.3E-04	1.1E-03	4.4E-04	8.5E-04
D55	9.4E-03	1.3E-03	1.7E-02	1.3E-03	6.3E-05	4.6E-03	2.6E-03	3.9E-04	1.1E-04	7.1E-04	3.7E-05	2.2E-04	1.8E-04	3.7E-04	9.9E-04	4.1E-04	9.1E-04
D56	3.3E-03	1.4E-03	1.2E-02	7.9E-04	7.5E-05	5.0E-03	1.7E-03	3.1E-04	1.2E-04	7.7E-04	4.0E-05	2.4E-04	1.4E-04	3.0E-04	9.1E-04	3.8E-04	7.4E-04
D57	3.7E-03	1.3E-03	1.5E-02	9.3E-04	6.3E-05	4.7E-03	1.8E-03	2.9E-04	1.1E-04	7.2E-04	3.7E-05	3.1E-04	2.5E-04	6.8E-04	1.3E-03	5.6E-04	1.1E-03
D58	6.6E-03	1.4E-03	2.3E-02	1.8E-03	1.2E-04	5.0E-03	2.8E-03	3.1E-04	1.2E-04	7.6E-04	4.0E-05	2.4E-04	1.7E-04	4.5E-04	1.1E-03	4.7E-04	7.8E-04
D59	5.8E-03	1.5E-03	1.9E-02	1.8E-03	7.2E-05	5.6E-03	3.2E-03	3.5E-04	1.3E-04	8.6E-04	4.5E-05	3.1E-04	2.6E-04	4.6E-04	1.1E-03	4.7E-04	9.6E-04
D60	4.7E-03	1.3E-03	1.1E-02	9.9E-04	6.4E-05	4.7E-03	1.7E-03	2.9E-04	1.1E-04	7.2E-04	3.7E-05	2.2E-04	1.5E-04	2.6E-04	7.7E-04	3.2E-04	6.1E-04
D61	5.5E-03	1.3E-03	1.6E-02	2.1E-03	9.0E-05	4.7E-03	3.4E-03	2.9E-04	1.1E-04	7.2E-04	3.7E-05	2.2E-04	1.3E-04	2.4E-04	7.0E-04	2.9E-04	6.4E-04
D62	4.8E-03	1.3E-03	1.4E-02	8.5E-04	5.0E-05	4.6E-03	1.7E-03	2.9E-04	1.1E-04	7.1E-04	3.7E-05	2.2E-04	1.2E-04	2.9E-04	8.9E-04	3.7E-04	6.6E-04

1.5.3 Aerosol source apportionment

Table S9. Summary of PMF diagnostics as values of objective function Q (USEPA, 2004), results of analysis methods displacement (DISP) and bootstrap (BS). PMF diagnostics are for a) modelled group 1 including sum of individual classes of organic pollutants as PCBs, HCHs, DDX, drins, PAHs, NPAHs and OPAHs – PMF results presented in SI and b) modelled group 2 including selected PAHs, OPAHs and NPAHs – PMF results presented in the main text.

a)

Diagnostic	Ship PM_{10}
$Q_{expected/theoretical}$	690
Q_{true}	714
Q_{robust}	714
Species $Q/Q_{expected}$ >2	–
DISP	0
BS mapping	67 - 100

b)

Diagnostic	Ship PM_{10}
$Q_{expected/theoretical}$	815
Qtrue	825
Qrobust	825
Species Q/Qexpected >2	Mn
DISP	0
BS mapping	94 - 100

2 Results

2.1 Concentrations

Table S10. Concentration of 16 USEPA-prioritized PAHs in high-volume samples (sum of gas and particulate phase) in ng m^{-3}. For calculation of the mean, values <LOQ were replaced by LOQ/2 if the detection frequency in all samples exceeded 30 %, else by 0. LOQ values given in Table S6. STD: Standard deviation.

a) in the Mediterranean Sea

Sam-ple	Leg	NAP	ACY	ACE	FLN	PHE	ANT	FLT	PYR	BAA	CHR	BBF	BKF	BAP	INP	DBA	BPE	Σ_{16}PAHs
D1	1	<6.7E-02	1.7E-03	3.7E-02	9.0E-02	8.0E-01	6.0E-02	1.2E-01	8.2E-02	3.3E-03	2.6E-02	9.9E-03	2.2E-03	2.6E-03	3.6E-03	1.5E-02	3.9E-03	1.3E+00
D4		<7.6E-02	7.7E-03	2.2E-01	5.8E-01	1.3E+00	5.4E-02	4.2E-02	3.4E-02	1.2E-03	2.8E-03	2.5E-03	9.9E-04	1.4E-03	2.1E-03	1.4E-02	3.4E-03	2.3E+00
D5		<6.6E-02	2.6E-02	2.4E-01	4.7E-01	1.5E+00	1.0E-01	1.7E-01	1.5E-01	2.5E-03	1.4E-02	5.4E-03	1.2E-03	3.4E-04	9.2E-04	5.5E-03	1.2E-03	2.6E+00
D6		<6.5E-02	9.9E-03	2.0E-01	3.5E-01	1.1E+00	1.0E-01	1.4E-01	9.4E-02	2.4E-03	7.2E-03	5.6E-03	1.8E-03	2.2E-03	3.9E-03	1.8E-02	3.8E-03	2.0E+00
D7		<6.4E-02	1.7E-03	4.0E-02	2.7E-01	1.6E+00	1.7E-01	2.3E-01	1.9E-01	3.5E-03	1.3E-02	1.0E-02	3.3E-03	5.1E-03	6.8E-03	2.0E-02	7.0E-03	2.5E+00
D49	2	<1.4E-01	1.2E-02	6.0E-01	1.3E+00	2.2E+00	2.6E-01	2.3E-01	1.8E-01	7.7E-03	1.7E-02	2.0E-02	7.1E-03	1.1E-02	1.5E-02	2.1E-02	1.4E-02	4.7E+00
D50		<1.4E-01	2.1E-02	2.0E+00	4.0E+00	4.2E+00	4.9E-01	3.3E-01	1.9E-01	9.0E-03	1.7E-02	1.8E-02	6.8E-03	1.0E-02	1.2E-02	2.1E-02	1.1E-02	1.1E+01
D51		<1.4E-01	<6.5E-03	1.4E-01	2.8E-01	6.4E-01	8.2E-02	8.8E-02	8.2E-02	8.1E-03	1.4E-02	1.6E-02	5.8E-03	9.7E-03	1.1E-02	6.7E-03	1.1E-02	1.4E+00
D52		<1.3E-01	1.2E-02	1.4E+00	2.9E+00	2.5E+00	2.5E-01	1.8E-01	1.2E-01	5.3E-03	1.2E-02	1.3E-02	4.5E-03	7.4E-03	9.0E-03	4.2E-02	9.0E-03	7.5E+00
D53		<1.6E-01	4.0E-03	7.6E-02	3.4E-01	6.4E-01	8.1E-02	7.9E-02	8.5E-02	5.5E-03	8.7E-03	1.3E-02	4.7E-03	7.5E-03	9.1E-03	1.8E-02	8.9E-03	1.4E+00
D54		<1.4E-01	2.3E-02	3.2E+00	6.4E+00	6.0E+00	9.2E-01	4.6E-01	2.7E-01	3.5E-03	9.7E-03	1.1E-02	3.9E-03	5.5E-03	7.7E-03	1.5E-02	6.9E-03	1.7E+01
D55		<1.3E-01	<6.4E-03	8.1E-02	4.8E-01	2.4E+00	3.3E-01	2.4E-01	1.8E-01	3.4E-03	8.3E-03	1.2E-02	4.4E-03	6.8E-03	9.1E-03	2.3E-02	8.5E-03	3.8E+00
D56		<1.4E-01	<6.9E-03	<2.3E-02	4.9E-02	1.7E-01	1.1E-02	3.3E-02	2.4E-02	3.1E-03	7.4E-03	8.8E-03	3.3E-03	3.6E-03	7.1E-03	1.9E-02	6.3E-03	3.6E-01
D57		3.6E-03	3.6E-03	2.5E-01	1.4E+00	1.3E+00	1.5E-01	1.8E-01	1.2E-01	8.5E-03	1.9E-02	2.9E-02	1.1E-02	1.6E-02	1.9E-02	5.6E-02	1.8E-02	3.5E+00
D58		<1.4E-01	4.1E-03	3.2E-01	7.0E-01	2.3E+00	2.1E-01	4.4E-01	2.8E-01	2.8E-02	5.5E-02	7.0E-02	2.4E-02	4.8E-02	6.4E-02	1.8E-02	6.0E-02	4.6E+00
D59		<1.6E-01	4.2E-03	2.6E-01	1.4E+00	1.3E+00	1.2E-01	1.2E-01	1.1E-01	3.4E-03	9.4E-03	1.1E-02	3.9E-03	5.0E-03	7.6E-03	9.0E-03	7.3E-03	3.4E+00
D60		3.2E-03	3.5E-03	7.2E-01	7.7E-01	7.8E-01	9.9E-02	7.3E-02	5.2E-02	2.9E-03	8.3E-03	8.4E-03	3.5E-03	4.1E-03	6.3E-03	2.0E-03	5.9E-03	2.5E+00
D61		<1.3E-01	1.4E-02	7.6E-01	2.7E+00	3.8E+00	5.6E-01	3.9E-01	3.0E-01	1.1E-02	2.1E-02	1.4E-02	4.4E-03	4.4E-03	7.1E-03	1.7E-02	8.5E-03	8.6E+00
D62		3.4E-03	3.5E-03	5.8E-02	1.3E-01	4.2E-01	4.5E-02	1.0E-01	7.2E-02	5.0E-03	2.1E-02	2.8E-02	1.0E-02	1.1E-02	1.4E-02	1.7E-02	1.2E-02	9.6E-01
Mean		**1.6E-03**	**8.5E-03**	**5.6E-01**	**1.3E+00**	**1.8E+00**	**2.2E-01**	**1.9E-01**	**1.4E-01**	**6.2E-03**	**1.5E-02**	**1.6E-02**	**5.6E-03**	**8.5E-03**	**1.1E-02**	**1.9E-02**	**1.1E-02**	**4.3E+00**

Sam-ple	Leg	NAP	ACY	ACE	FLN	PHE	ANT	FLT	PYR	BAA	CHR	BBF	BKF	BAP	INP	DBA	BPE	Σ_{16}PAHs
STD		8.7E-04	7.6E-03	8.1E-01	1.6E+00	1.5E+00	2.3E-01	1.3E-01	8.3E-02	5.9E-03	1.1E-02	1.5E-02	5.1E-03	1.0E-02	1.3E-02	1.2E-02	1.2E-02	4.2E+00
Median		1.5E-03	4.1E-03	2.4E-01	5.8E-01	1.3E+00	1.2E-01	1.7E-01	1.2E-01	3.5E-03	1.3E-02	1.2E-02	4.4E-03	5.5E-03	7.7E-03	1.8E-02	8.5E-03	2.6E+00

b) in the Northern Red Sea

Sample	Leg	NAP	ACY	ACE	FLN	PHE	ANT	FLT	PYR	BAA	CHR	BBF	BKF	BAP	INP	DBA	BPE	Σ_{16}PAHs
D12	1	7.3E-04	3.7E-02	4.7E-01	9.7E-01	4.1E+00	2.2E-01	3.9E-01	3.0E-01	7.0E-03	2.2E-02	1.7E-02	6.0E-03	1.0E-02	1.3E-02	2.1E-02	1.4E-02	6.6E+00
D13		7.3E-04	2.6E-02	4.5E-01	1.1E+00	4.2E+00	3.8E-01	4.3E-01	3.5E-01	6.6E-03	2.3E-02	1.8E-02	5.8E-03	9.2E-03	1.3E-02	1.2E-02	1.3E-02	7.0E+00
D14		1.0E-03	2.4E-03	2.6E-02	1.1E-01	1.5E+00	1.2E-01	1.4E-01	1.3E-01	5.7E-03	1.6E-02	1.6E-02	5.1E-03	6.5E-03	1.0E-02	1.4E-02	9.5E-03	2.2E+00
D45	2	2.2E-03	1.7E-03	5.1E-03	1.9E-02	1.6E-01	1.9E-02	5.4E-02	4.7E-02	3.7E-03	7.9E-03	1.2E-02	4.1E-03	7.9E-03	1.0E-02	2.5E-02	1.0E-02	3.9E-01
D46		3.1E-03	1.8E-03	2.7E-02	5.5E-02	2.5E-01	1.7E-02	5.6E-02	5.0E-02	5.2E-03	1.5E-02	1.4E-02	4.0E-03	7.6E-03	1.0E-02	2.1E-02	1.0E-02	5.4E-01
D47		7.4E-04	4.5E-03	2.6E-02	6.6E-02	3.6E-01	2.3E-02	5.5E-02	5.8E-02	5.5E-03	1.6E-02	1.0E-02	3.2E-03	4.9E-03	7.5E-03	2.4E-02	7.4E-03	6.8E-01
D48		7.6E-04	1.9E-03	5.4E-03	5.9E-02	3.5E-01	1.1E-02	6.3E-02	5.6E-02	6.3E-03	2.0E-02	1.5E-02	4.7E-03	3.5E-04	1.2E-02	3.3E-02	1.2E-02	6.5E-01
Mean		**1.3E-03**	**1.1E-02**	**1.4E-01**	**3.4E-01**	**1.6E+00**	**1.1E-01**	**1.7E-01**	**1.4E-01**	**5.7E-03**	**1.7E-02**	**1.4E-02**	**4.7E-03**	**6.7E-03**	**1.1E-02**	**2.2E-02**	**1.1E-02**	**2.6E+00**
STD		9.6E-04	1.5E-02	2.2E-01	4.8E-01	1.8E+00	1.4E-01	1.7E-01	1.3E-01	1.1E-03	5.0E-03	2.8E-03	1.0E-03	3.3E-03	2.0E-03	7.0E-03	2.3E-03	3.0E+00
Median		7.6E-04	2.4E-03	2.6E-02	6.6E-02	3.6E-01	2.3E-02	6.3E-02	5.8E-02	5.7E-03	1.6E-02	1.5E-02	4.7E-03	7.6E-03	1.0E-02	2.1E-02	1.0E-02	6.8E-01

c) in the Southern Red Sea

Sample	Leg	NAP	ACY	ACE	FLN	PHE	ANT	FLT	PYR	BAA	CHR	BBF	BKF	BAP	INP	DBA	BPE	Σ_{16}PAHs
D15	1	7.5E-04	1.7E-03	1.5E-02	6.3E-02	2.2E+00	1.1E-01	3.0E-01	2.3E-01	5.8E-03	2.0E-02	1.3E-02	3.7E-03	5.5E-03	8.5E-03	2.8E-02	8.3E-03	3.0E+00
D42	2	3.0E-03	1.3E-02	7.2E-03	1.2E-02	6.0E-02	3.7E-03	1.8E-02	1.2E-02	9.7E-04	2.5E-03	5.9E-04	6.7E-04	4.6E-04	2.6E-04	2.1E-03	2.2E-04	1.4E-01
D43		2.5E-03	1.3E-03	4.0E-03	1.7E-02	2.9E-01	1.8E-02	6.7E-02	6.4E-02	3.1E-03	6.8E-03	5.8E-03	2.3E-03	3.0E-03	4.6E-03	1.5E-02	4.7E-03	5.1E-01
D44		2.9E-03	1.7E-03	5.1E-03	8.9E-03	1.4E-01	1.5E-02	5.1E-02	4.9E-02	4.6E-03	1.3E-02	1.6E-02	5.3E-03	1.1E-02	1.4E-02	2.1E-02	1.3E-02	3.7E-01
D45		2.2E-03	1.7E-03	5.1E-03	1.9E-02	1.6E-01	1.9E-02	5.4E-02	4.7E-02	3.7E-03	7.9E-03	1.2E-02	4.1E-03	7.9E-03	1.0E-02	2.5E-02	1.0E-02	3.9E-01
Mean		**2.3E-03**	**3.9E-03**	**7.3E-03**	**2.4E-02**	**5.7E-01**	**3.2E-02**	**9.7E-02**	**8.1E-02**	**3.6E-03**	**1.0E-02**	**9.4E-03**	**3.2E-03**	**5.5E-03**	**7.5E-03**	**1.8E-02**	**7.3E-03**	**8.9E-01**
STD		9.1E-04	5.1E-03	4.6E-03	2.2E-02	9.2E-01	4.1E-02	1.1E-01	8.6E-02	1.8E-03	6.9E-03	6.2E-03	1.8E-03	4.0E-03	5.2E-03	1.0E-02	5.0E-03	1.2E+00
Median		2.5E-03	1.7E-03	5.1E-03	1.7E-02	1.6E-01	1.8E-02	5.4E-02	4.9E-02	3.7E-03	7.9E-03	1.2E-02	3.7E-03	5.5E-03	8.5E-03	2.1E-02	8.3E-03	3.9E-01

d) in the Arabian Sea

Sample	Leg	NAP	ACY	ACE	FLN	PHE	ANT	FLT	PYR	BAA	CHR	BBF	BKF	BAP	INP	DBA	BPE	Σ_{16}PAHs
D35	2	7.8E-04	1.7E-03	1.3E-01	1.9E-01	6.5E-01	7.3E-02	1.0E-01	1.5E-01	3.4E-03	5.2E-03	2.3E-03	5.2E-04	8.4E-04	1.3E-03	3.9E-03	1.5E-03	1.3E+00
D36		7.4E-04	1.6E-03	2.1E-02	1.7E-02	1.1E-01	1.4E-02	1.5E-02	2.3E-02	1.6E-03	2.5E-03	1.6E-03	4.9E-04	1.0E-03	1.5E-03	1.7E-03	1.7E-03	2.1E-01
D39		5.8E-04	1.3E-03	3.9E-02	3.6E-02	1.2E-01	1.4E-02	1.2E-02	2.9E-02	3.3E-03	5.5E-03	2.6E-03	5.8E-04	8.1E-04	1.2E-03	3.2E-03	1.4E-03	2.7E-01
D40		3.0E-03	1.7E-03	5.3E-03	3.1E-02	5.2E-01	1.1E-01	9.1E-02	7.4E-02	5.4E-03	8.9E-03	4.9E-03	1.6E-03	1.5E-03	2.4E-03	8.2E-03	2.5E-03	8.7E-01
D41		2.8E-03	1.7E-03	5.6E-03	2.6E-02	3.9E-01	3.2E-02	5.5E-02	5.9E-02	3.2E-03	8.2E-03	3.6E-03	1.2E-03	1.3E-03	2.1E-03	7.4E-03	2.3E-03	6.1E-01
D42		3.0E-03	1.3E-02	7.2E-03	1.2E-02	6.0E-02	3.7E-03	1.8E-02	1.2E-02	9.7E-04	2.5E-03	5.9E-04	6.7E-04	4.6E-04	2.6E-04	2.1E-03	2.2E-04	1.4E-01
Mean		**1.8E-03**	**3.5E-03**	**3.5E-02**	**5.2E-02**	**3.1E-01**	**4.1E-02**	**4.9E-02**	**5.9E-02**	**3.0E-03**	**5.5E-03**	**2.6E-03**	**8.5E-04**	**9.9E-04**	**1.5E-03**	**4.4E-03**	**1.6E-03**	**5.7E-01**
STD		1.2E-03	4.7E-03	5.0E-02	6.9E-02	2.5E-01	4.1E-02	4.1E-02	5.2E-02	1.6E-03	2.7E-03	1.5E-03	4.5E-04	3.7E-04	7.4E-04	2.8E-03	8.2E-04	4.6E-01
Median		1.8E-03	1.7E-03	1.4E-02	2.8E-02	2.6E-01	2.3E-02	3.6E-02	4.4E-02	3.3E-03	5.4E-03	2.4E-03	6.3E-04	9.2E-04	1.4E-03	3.5E-03	1.6E-03	4.4E-01

e) in the Gulf of Oman

Sample	Leg	NAP	ACY	ACE	FLN	PHE	ANT	FLT	PYR	BAA	CHR	BBF	BKF	BAP	INP	DBA	BPE	Σ_{16}PAHs
D24	1	4.6E-03	3.8E-03	1.2E-02	2.0E-02	6.4E-01	5.6E-02	2.5E-01	5.5E-01	5.4E-02	7.5E-02	6.4E-03	2.8E-03	2.6E-03	2.8E-03	1.9E-03	3.4E-03	1.7E+00
D25		1.8E-03	1.7E-03	7.2E-02	7.2E-02	1.1E+00	8.0E-02	2.4E-01	3.6E-01	2.8E-02	5.7E-02	5.6E-03	1.7E-03	8.3E-04	1.4E-03	1.0E-02	1.5E-03	2.0E+00
D33	2	3.2E-03	4.3E-03	7.7E-02	9.0E-01	1.8E+00	1.6E-01	2.8E-01	3.4E-01	1.3E-02	2.6E-02	1.7E-02	4.7E-03	3.8E-03	1.0E-02	1.4E-02	1.1E-02	3.7E+00
D34		2.4E-03	1.8E-03	1.5E-01	9.4E-02	3.1E-01	3.2E-02	4.9E-02	5.8E-02	5.8E-03	1.3E-02	4.4E-03	9.4E-04	3.4E-04	6.1E-04	5.8E-03	7.2E-04	7.3E-01
D35		7.8E-04	1.7E-03	1.3E-01	1.9E-01	6.5E-01	7.3E-02	1.0E-01	1.5E-01	3.4E-03	5.2E-03	2.3E-03	5.2E-04	8.4E-04	1.3E-03	3.9E-03	1.5E-03	1.3E+00
Mean		**2.5E-03**	**2.6E-03**	**9.0E-02**	**2.6E-01**	**9.0E-01**	**8.0E-02**	**1.9E-01**	**2.9E-01**	**2.1E-02**	**3.5E-02**	**7.1E-03**	**2.1E-03**	**1.7E-03**	**3.3E-03**	**7.2E-03**	**3.6E-03**	**1.9E+00**
STD		1.5E-03	1.3E-03	5.6E-02	3.6E-01	5.9E-01	4.8E-02	1.0E-01	1.9E-01	2.1E-02	3.0E-02	5.7E-03	1.7E-03	1.5E-03	4.0E-03	4.9E-03	4.2E-03	1.1E+00
Median		2.4E-03	1.8E-03	7.7E-02	9.4E-02	6.5E-01	7.3E-02	2.4E-01	3.4E-01	1.3E-02	2.6E-02	5.6E-03	1.7E-03	8.4E-04	1.4E-03	5.8E-03	1.5E-03	1.7E+00

181

f) in the Arabian Gulf

Sample	Leg	NAP	ACY	ACE	FLN	PHE	ANT	FLT	PYR	BAA	CHR	BBF	BKF	BAP	INP	DBA	BPE	Σ_{16}PAHs
D29	1	3.5E-03	2.8E-03	8.2E-03	4.0E-02	9.6E-01	6.0E-02	1.6E-01	1.7E-01	5.8E-03	1.9E-02	1.6E-02	5.2E-03	5.7E-03	1.1E-02	5.3E-02	9.7E-03	1.5E+00
D30		2.8E-03	2.0E-03	2.5E-02	5.5E-02	7.2E-01	6.6E-02	2.4E-01	1.9E-01	1.3E-02	2.9E-02	5.1E-02	1.5E-02	3.1E-02	4.6E-02	4.3E-02	4.4E-02	1.6E+00
D31	2	2.3E-03	1.8E-03	1.1E-01	2.8E-01	1.7E+00	1.9E-01	3.9E-01	3.4E-01	6.3E-03	2.4E-02	1.6E-02	5.2E-03	6.2E-03	1.2E-02	3.1E-02	1.1E-02	3.2E+00
D32		2.2E-03	1.7E-03	4.8E-02	1.3E-01	2.1E+00	2.9E-01	4.6E-01	3.5E-01	6.9E-03	1.8E-02	1.0E-02	2.8E-03	3.0E-03	5.2E-03	1.9E-03	5.8E-03	3.4E+00
D33		3.2E-03	4.3E-03	7.7E-02	9.0E-01	1.8E+00	1.6E-01	2.8E-01	3.4E-01	1.3E-02	2.6E-02	1.7E-02	4.7E-03	3.8E-03	1.0E-02	1.4E-02	1.1E-02	3.7E+00
Mean		**2.8E-03**	**2.5E-03**	**5.4E-02**	**2.8E-01**	**1.5E+00**	**1.5E-01**	**3.1E-01**	**2.8E-01**	**9.0E-03**	**2.3E-02**	**2.2E-02**	**6.5E-03**	**9.9E-03**	**1.7E-02**	**2.9E-02**	**1.6E-02**	**2.7E+00**
STD		5.4E-04	1.1E-03	4.2E-02	3.6E-01	6.0E-01	9.4E-02	1.2E-01	9.0E-02	3.6E-03	4.4E-03	1.7E-02	4.8E-03	1.2E-02	1.7E-02	2.1E-02	1.6E-02	1.0E+00
Median		2.8E-03	2.0E-03	4.8E-02	1.3E-01	1.7E+00	1.6E-01	2.8E-01	3.4E-01	6.9E-03	2.4E-02	1.6E-02	5.2E-03	5.7E-03	1.1E-02	3.1E-02	1.1E-02	3.2E+00

Table S11. Concentration of PAHs, additional to the 16 USEPA-prioritized PAHs, including one S-heterocycle in high-volume samples (sum of gas and particulate phase) in ng m³. For calculation of the mean, values <LOQ were replaced by LOQ/2 if the detection frequency in all samples exceeded 30 %, else by 0. LOQ values given in Table S6. STD: Standard deviation.

a) in the Mediterranean Sea

Sample	Leg	BJF	BEP	PER	DCA	ATT	COR	TPH	CCP	BGF	BBN	BNT	Σ_{26}PAHs + BNT
D1	1	1.92E-03	4.73E-03	2.86E-04	1.09E-02	<LOQ	1.81E-03	1.78E-02	7.27E-04	8.25E-03	5.74E-03	6.88E-03	1.3E+00
D4		1.24E-03	2.18E-03	3.23E-04	8.77E-03	<LOQ	1.07E-03	2.11E-03	4.75E-04	2.17E-03	1.53E-03	1.45E-03	2.3E+00
D5		1.06E-03	1.92E-03	2.84E-04	4.71E-03	<LOQ	2.66E-04	9.74E-03	3.28E-04	6.00E-03	6.30E-03	6.91E-03	2.7E+00
D6		2.19E-03	3.76E-03	2.77E-04	1.33E-02	<LOQ	1.83E-03	3.97E-03	5.23E-04	2.46E-03	4.26E-03	3.81E-03	2.0E+00
D7		3.66E-03	6.88E-03	6.33E-04	1.68E-02	<LOQ	2.99E-03	7.90E-03	1.03E-03	6.01E-03	7.17E-03	6.28E-03	2.6E+00
D49	2	7.93E-03	1.20E-02	5.88E-04	2.07E-02	<LOQ	4.77E-03	1.04E-02	2.05E-03	8.72E-03	3.88E-03	7.63E-03	4.9E+00
D50		7.02E-03	1.13E-02	5.81E-04	1.59E-02	<LOQ	3.61E-03	7.27E-03	2.15E-03	7.84E-03	6.50E-03	5.78E-03	1.1E+01
D51		4.46E-03	1.04E-02	2.18E-03	2.13E-03	<LOQ	2.45E-03	6.83E-03	1.22E-03	6.70E-03	3.39E-03	4.91E-03	1.4E+00
D52		3.40E-03	8.21E-03	2.14E-03	2.99E-02	<LOQ	1.81E-03	8.64E-03	9.38E-04	5.54E-03	2.72E-03	5.74E-03	7.6E+00
D53		2.87E-03	8.84E-03	2.61E-03	1.41E-02	1.80E-03	1.45E-03	5.13E-03	7.59E-04	5.62E-03	3.24E-03	5.37E-03	1.4E+00
D54		5.31E-03	8.73E-03	5.90E-04	1.28E-02	<LOQ	2.15E-03	6.23E-03	8.96E-04	5.92E-03	6.81E-03	6.16E-03	1.7E+01
D55		4.10E-03	8.04E-03	0.00E+00	2.23E-02	1.37E-03	2.06E-03	7.43E-03	1.05E-03	5.65E-03	2.69E-03	7.13E-03	3.8E+00
D56		2.90E-03	6.20E-03	6.17E-04	2.09E-02	1.82E-03	1.51E-03	5.24E-03	6.15E-04	5.43E-03	2.92E-03	3.61E-03	4.1E-01
D57		1.12E-02	1.94E-02	2.57E-03	3.57E-02	1.11E-03	4.48E-03	1.33E-02	2.50E-03	8.14E-03	4.44E-03	9.61E-03	3.7E+00
D58		3.15E-02	4.50E-02	6.72E-03	1.23E-02	8.17E-03	2.32E-02	2.77E-02	1.72E-02	3.60E-02	1.90E-02	2.35E-02	4.9E+00
D59		5.03E-03	7.59E-03	6.87E-04	9.33E-03	<LOQ	1.66E-03	6.06E-03	5.77E-04	5.74E-03	3.25E-03	5.17E-03	3.4E+00
D60		3.85E-03	6.71E-03	5.74E-04	1.62E-03	<LOQ	1.48E-03	4.53E-03	5.86E-04	4.78E-03	2.72E-03	3.43E-03	2.6E+00
D61		4.52E-03	9.81E-03	5.72E-04	1.12E-02	<LOQ	2.06E-03	1.03E-02	7.01E-04	1.31E-02	1.42E-02	7.68E-03	8.7E+00
D62		1.08E-02	1.68E-02	5.65E-04	1.05E-02	<LOQ	2.65E-03	9.18E-03	8.11E-04	5.71E-03	5.48E-03	9.32E-03	1.0E+00
Mean		**6.1E-03**	**1.0E-02**	**1.2E-03**	**1.4E-02**	**7.5E-04**	**3.3E-03**	**8.9E-03**	**1.9E-03**	**7.9E-03**	**5.6E-03**	**6.9E-03**	**4.4E+00**
STD		6.8E-03	9.4E-03	1.6E-03	8.7E-03	1.9E-03	4.9E-03	5.8E-03	3.8E-03	7.2E-03	4.3E-03	4.5E-03	4.2E+00
Median		4.1E-03	8.2E-03	5.9E-04	1.3E-02	<LOQ	2.1E-03	7.4E-03	8.1E-04	5.9E-03	4.3E-03	6.2E-03	2.7E+00

b) in the Northern Red Sea

Sample	Leg	BJF	BEP	PER	DCA	ATT	COR	TPH	CCP	BGF	BBN	BNT	Σ_{26}PAHs + BNT
D12	1	6.86E-03	1.28E-02	1.05E-03	1.63E-02	1.23E-03	6.42E-03	1.16E-02	1.93E-03	8.66E-03	1.12E-02	1.11E-02	6.7E+00
D13		7.29E-03	1.22E-02	9.55E-04	1.23E-02	8.53E-04	5.80E-03	1.37E-02	1.16E-03	9.84E-03	1.22E-02	1.19E-02	7.1E+00
D14		5.18E-03	1.04E-02	3.95E-04	1.23E-02	<LOQ	4.22E-03	9.02E-03	7.58E-04	5.10E-03	6.83E-03	7.44E-03	2.2E+00
D45	2	4.55E-03	8.60E-03	1.06E-03	1.68E-02	1.29E-03	3.69E-03	4.02E-03	8.84E-04	4.24E-03	1.95E-03	3.47E-03	4.4E-01
D46		4.82E-03	9.13E-03	1.09E-03	1.84E-02	1.25E-03	3.90E-03	1.07E-02	1.06E-03	4.46E-03	4.75E-03	1.01E-02	6.1E-01
D47		3.41E-03	7.09E-03	8.15E-04	1.45E-02	7.43E-04	3.58E-03	8.95E-03	8.28E-04	5.45E-03	5.05E-03	1.23E-02	7.4E-01
D48		5.48E-03	1.07E-02	2.93E-04	2.65E-02	<LOQ	6.28E-03	1.37E-02	6.18E-04	6.81E-03	5.32E-03	1.74E-02	7.4E-01
Mean		**5.4E-03**	**1.0E-02**	**8.1E-04**	**1.7E-02**	**7.7E-04**	**4.8E-03**	**1.0E-02**	**1.0E-03**	**6.4E-03**	**6.8E-03**	**1.1E-02**	**2.7E+00**
STD		1.3E-03	2.0E-03	3.3E-04	4.9E-03	5.6E-04	1.3E-03	3.4E-03	4.3E-04	2.2E-03	3.7E-03	4.3E-03	3.0E+00
Median		5.2E-03	1.0E-02	9.5E-04	1.6E-02	8.5E-04	4.2E-03	1.1E-02	8.8E-04	5.4E-03	5.3E-03	1.1E-02	7.4E-01

184

c) in the Southern Red Sea

Sample	Leg	BJF	BEP	PER	DCA	ATT	COR	TPH	CCP	BGF	BBN	BNT	Σ_{26}PAHs + BNT
D15	1	4.12E-03	8.11E-03	6.19E-04	2.69E-02	6.14E-04	3.89E-03	1.33E-02	8.19E-04	1.00E-02	8.36E-03	1.18E-02	3.1E+00
D42	2	2.96E-04	5.98E-04	3.89E-04	3.00E-03	1.56E-03	3.65E-04	7.89E-04	1.30E-04	2.19E-03	1.84E-03	2.11E-04	1.5E-01
D43		1.93E-03	4.38E-03	5.11E-04	1.23E-02	1.41E-03	2.91E-03	4.19E-03	3.63E-04	2.70E-03	2.26E-03	3.33E-03	5.4E-01
D44		6.13E-03	1.11E-02	1.33E-03	1.27E-02	5.40E-03	5.19E-03	5.43E-03	1.18E-03	5.32E-03	2.18E-03	4.59E-03	4.3E-01
D45		4.55E-03	8.60E-03	1.06E-03	1.68E-02	1.29E-03	3.69E-03	4.02E-03	8.84E-04	4.24E-03	1.95E-03	3.47E-03	4.4E-01
Mean		**3.4E-03**	**6.6E-03**	**7.8E-04**	**1.4E-02**	**2.1E-03**	**3.2E-03**	**5.5E-03**	**6.7E-04**	**4.9E-03**	**3.3E-03**	**4.7E-03**	**9.4E-01**
STD		2.3E-03	4.1E-03	4.0E-04	8.7E-03	1.9E-03	1.8E-03	4.7E-03	4.2E-04	3.1E-03	2.8E-03	4.3E-03	1.2E+00
Median		4.1E-03	8.1E-03	6.2E-04	1.3E-02	1.4E-03	3.7E-03	4.2E-03	8.2E-04	4.2E-03	2.2E-03	3.5E-03	4.4E-01

d) in the Arabian Sea

Sample	Leg	BJF	BEP	PER	DCA	ATT	COR	TPH	CCP	BGF	BBN	BNT	Σ_{26}PAHs + BNT
D35	2	5.37E-04	1.56E-03	3.03E-04	2.70E-03	<LOQ	2.84E-04	3.98E-03	2.41E-04	3.72E-03	5.49E-03	3.37E-03	1.4E+00
D36		5.75E-04	1.44E-03	2.85E-04	1.89E-03	<LOQ	2.67E-04	2.70E-03	9.51E-05	2.07E-03	1.35E-03	1.92E-03	2.3E-01
D39		5.17E-04	1.92E-03	2.24E-04	3.36E-03	7.61E-04	9.18E-04	3.68E-03	7.49E-05	1.63E-03	2.75E-03	4.19E-03	2.9E-01
D40		2.77E-03	3.01E-03	6.07E-04	6.48E-03	<LOQ	6.72E-04	4.53E-03	9.46E-05	2.29E-03	4.37E-03	4.54E-03	9.0E-01
D41		2.54E-03	2.41E-03	3.08E-04	5.25E-03	<LOQ	7.40E-04	7.06E-03	1.03E-04	2.27E-03	3.35E-03	6.32E-03	6.4E-01
D42		2.96E-04	5.98E-04	3.89E-04	3.00E-03	1.56E-03	3.65E-04	7.89E-04	1.30E-04	2.19E-03	1.84E-03	2.11E-04	1.5E-01
Mean		**1.2E-03**	**1.8E-03**	**3.5E-04**	**3.8E-03**	**3.9E-04**	**5.4E-04**	**3.8E-03**	**1.2E-04**	**2.4E-03**	**3.2E-03**	**3.4E-03**	**5.9E-01**
STD		1.1E-03	8.4E-04	1.4E-04	1.7E-03	6.5E-04	2.7E-04	2.1E-03	6.0E-05	7.1E-04	1.6E-03	2.1E-03	4.7E-01
Median		5.6E-04	1.7E-03	3.1E-04	3.2E-03	<LOQ	5.2E-04	3.8E-03	9.9E-05	2.2E-03	3.0E-03	3.8E-03	4.6E-01

e) in the Gulf of Oman

Sample	Leg	BJF	BEP	PER	DCA	ATT	COR	TPH	CCP	BGF	BBN	BNT	Σ_{26}PAHs + BNT
D24	1	5.15E-04	3.58E-03	6.77E-04	1.91E-03	<LOQ	6.34E-04	5.70E-02	2.26E-04	5.62E-02	7.51E-02	3.81E-02	1.9E+00
D25		1.08E-03	2.94E-03	2.81E-04	6.21E-03	<LOQ	6.63E-04	4.20E-02	9.38E-05	2.90E-02	3.52E-02	2.72E-02	2.1E+00
D33	2	4.87E-03	1.13E-02	3.49E-04	7.30E-03	<LOQ	5.08E-03	2.08E-02	6.44E-04	1.53E-02	1.96E-02	1.44E-02	3.8E+00
D34		2.19E-04	2.98E-03	2.88E-04	4.22E-03	<LOQ	2.70E-04	9.80E-03	9.62E-05	1.60E-03	5.91E-03	1.10E-02	7.6E-01
D35		5.37E-04	1.56E-03	3.03E-04	2.70E-03	<LOQ	2.84E-04	3.98E-03	2.41E-04	3.72E-03	5.49E-03	3.37E-03	1.4E+00
Mean		**1.4E-03**	**4.5E-03**	**3.8E-04**	**4.5E-03**	**<LOQ**	**1.4E-03**	**2.7E-02**	**2.6E-04**	**2.1E-02**	**2.8E-02**	**1.9E-02**	**2.0E+00**
STD		1.9E-03	3.9E-03	1.7E-04	2.3E-03	<LOQ	2.1E-03	2.2E-02	2.3E-04	2.2E-02	2.9E-02	1.4E-02	1.1E+00
Median		5.4E-04	3.0E-03	3.0E-04	4.2E-03	<LOQ	6.3E-04	2.1E-02	2.3E-04	1.5E-02	2.0E-02	1.4E-02	1.9E+00

185

f) in the Arabian Gulf

Sample	Leg	BJF	BEP	PER	DCA	ATT	COR	TPH	CCP	BGF	BBN	BNT	Σ_{26}PAHs + BNT
D29	1	5.85E-03	1.05E-02	4.50E-04	3.85E-02	1.50E-03	4.24E-03	1.05E-02	1.50E-04	5.77E-03	7.04E-03	1.23E-02	1.6E+00
D30		2.04E-02	3.53E-02	3.51E-03	2.60E-02	5.57E-03	2.20E-02	1.58E-02	5.64E-03	1.15E-02	4.86E-03	2.36E-02	1.7E+00
D31	2	6.10E-03	1.06E-02	2.76E-04	2.53E-02	<LOQ	5.74E-03	2.00E-02	6.17E-04	1.24E-02	1.07E-02	2.57E-02	3.3E+00
D32		2.72E-03	5.92E-03	2.78E-04	1.69E-03	<LOQ	2.39E-03	1.37E-02	4.95E-04	8.86E-03	1.19E-02	1.40E-02	3.5E+00
D33		4.87E-03	1.13E-02	0.00E+00	7.11E-03	<LOQ	5.08E-03	2.08E-02	6.44E-04	1.53E-02	1.96E-02	1.44E-02	3.8E+00
Mean		**8.0E-03**	**1.5E-02**	**9.0E-04**	**2.0E-02**	**1.4E-03**	**7.9E-03**	**1.6E-02**	**1.5E-03**	**1.1E-02**	**1.1E-02**	**1.8E-02**	**2.8E+00**
STD		7.1E-03	1.2E-02	1.5E-03	1.5E-02	2.4E-03	8.0E-03	4.3E-03	2.3E-03	3.6E-03	5.7E-03	6.2E-03	1.0E+00
Median		5.8E-03	1.1E-02	2.8E-04	2.5E-02	<LOQ	5.1E-03	1.6E-02	6.2E-04	1.1E-02	1.1E-02	1.4E-02	3.3E+00

Table S12. Concentration of OPAHs in high volume samples (sum of gas and particulate phase) in ng m³. For calculation of the mean, values <LOQ were replaced by LOQ/2 if the detection frequency in all samples exceeded 30 %, else by 0. LOQ values given in Table S6. STD: Standard deviation.

a) in the Mediterranean Sea

Sample	Leg	1,4-O_2NAP	1-(CHO)NAP	9-OFLN	9,10-O_2ANT	1,4-O_2ANT	9,10-O_2PHE	11-OBaFLN	11-OBbFLN	BAN	7,12-O_2BAA	5,12-O_2NAC	Σ_{11}OPAHs
D1	1	8.46E-02	3.85E-02	3.10E-02	6.92E-02	<LOQ	<LOQ	4.57E-02	4.73E-02	2.52E-02	3.98E-02	3.46E-03	3.8E-01
D4		<LOQ	2.61E-02	1.38E-02	<LOQ	<LOQ	<LOQ	3.32E-03	6.10E-03	6.75E-03	1.09E-02	1.68E-03	8.5E-02
D5		<LOQ	<LOQ	2.49E-02	9.21E-03	<LOQ	<LOQ	1.49E-02	1.33E-02	1.01E-02	1.47E-02	1.83E-03	1.1E-01
D6		<LOQ	1.90E-02	1.69E-02	1.02E-02	<LOQ	8.66E-03	9.57E-03	9.00E-03	1.12E-02	1.13E-02	1.36E-03	1.1E-01
D7		<LOQ	2.03E-02	2.66E-02	3.45E-03	<LOQ	<LOQ	1.28E-02	1.05E-02	1.09E-02	1.67E-02	1.78E-03	1.1E-01
D49	2	<LOQ	1.18E-02	2.23E-02	2.09E-02	<LOQ	<LOQ	8.23E-03	9.83E-03	1.37E-02	4.67E-03	1.46E-03	1.2E-01
D50		2.70E-02	2.70E-02	2.68E-02	4.07E-02	<LOQ	<LOQ	9.80E-03	1.12E-02	1.55E-02	5.35E-03	2.04E-03	1.7E-01
D51		4.17E-02	<LOQ	3.34E-02	1.88E-02	<LOQ	<LOQ	7.53E-03	8.23E-03	1.17E-02	4.15E-03	1.36E-03	1.4E-01
D52		<LOQ	<LOQ	1.87E-02	5.51E-02	<LOQ	<LOQ	7.54E-03	7.38E-03	1.05E-02	4.68E-03	1.26E-03	1.4E-01
D53		1.51E-01	1.58E-02	2.26E-02	2.54E-02	<LOQ	<LOQ	7.78E-03	8.28E-03	9.52E-03	4.77E-03	1.07E-03	2.5E-01
D54		2.34E-01	1.30E-02	4.70E-02	2.56E-01	<LOQ	<LOQ	8.32E-03	1.02E-02	1.16E-02	4.92E-03	1.41E-03	5.9E-01
D55		1.62E-01	1.31E-02	4.47E-02	1.47E-01	<LOQ	<LOQ	6.87E-03	1.04E-02	1.05E-02	7.02E-03	1.48E-03	4.0E-01
D56		1.24E-01	<LOQ	2.89E-02	1.31E-01	<LOQ	<LOQ	6.29E-03	6.64E-03	9.91E-03	3.98E-03	9.61E-04	3.2E-01
D57		4.30E-01	3.68E-02	9.66E-02	2.75E-01	<LOQ	<LOQ	1.57E-02	2.50E-02	2.43E-02	1.01E-02	4.25E-03	9.2E-01
D58		6.84E-01	1.38E-01	1.00E-01	3.08E-01	<LOQ	<LOQ	3.61E-02	5.18E-02	6.67E-02	2.28E-02	1.39E-02	1.4E+00
D59		1.79E-01	<LOQ	4.64E-02	1.62E-01	<LOQ	<LOQ	8.09E-03	8.79E-03	1.27E-02	5.32E-03	1.91E-03	4.4E-01
D60		1.75E-01	<LOQ	2.70E-02	1.23E-01	<LOQ	<LOQ	6.98E-03	7.57E-03	9.81E-03	4.09E-03	1.37E-03	3.7E-01
D61		4.59E-02	9.56E-02	2.65E-02	<LOQ	<LOQ	<LOQ	1.62E-02	1.36E-02	2.50E-02	6.73E-03	2.70E-03	2.4E-01
D62		2.14E-01	1.23E-02	3.29E-02	1.46E-01	<LOQ	<LOQ	1.93E-02	2.40E-02	2.13E-02	1.06E-02	3.90E-03	4.8E-01
Mean		**1.4E-01**	**2.8E-02**	**3.6E-02**	**9.5E-02**	<LOQ	**4.6E-04**	**1.3E-02**	**1.5E-02**	**1.7E-02**	**1.0E-02**	**2.6E-03**	**3.6E-01**
STD		1.7E-01	3.3E-02	2.4E-02	9.9E-02		2.0E-03	1.1E-02	1.3E-02	1.3E-02	8.8E-03	2.9E-03	3.3E-01
Median		8.5E-02	1.4E-02	2.7E-02	5.5E-02	<LOQ	<LOQ	8.3E-03	1.0E-02	1.2E-02	6.7E-03	1.7E-03	2.5E-01

b) in the Northern Red Sea

Sample	Leg	1,4-O_2NAP	1-(CHO)NAP	9-OFLN	9,10-O_2ANT	1,4-O_2ANT	9,10-O_2PHE	11-OBaFLN	11-OBbFLN	BAN	7,12-O_2BAA	5,12-O_2NAC	Σ_{11}OPAHs
D12	1	<LOQ	5.15E-02	5.36E-02	1.09E-02	<LOQ	9.48E-03	2.21E-02	1.36E-02	1.50E-02	1.56E-02	1.64E-03	2.0E-01
D13		<LOQ	3.46E-02	4.44E-02	<LOQ	<LOQ	1.37E-02	1.88E-02	1.06E-02	1.45E-02	1.34E-02	1.36E-03	1.7E-01
D14		3.01E-02	2.12E-02	1.75E-02	1.09E-02	2.45E-03	<LOQ	1.29E-02	9.97E-03	7.79E-03	8.00E-03	1.33E-03	1.2E-01
D45	2	3.85E-02	6.49E-03	6.72E-03	<LOQ	<LOQ	<LOQ	5.33E-03	4.73E-03	6.59E-03	4.34E-03	1.25E-03	7.7E-02
D46		7.41E-02	7.14E-03	1.18E-02	7.05E-02	<LOQ	<LOQ	8.51E-03	5.33E-03	1.06E-02	9.98E-03	1.76E-03	2.0E-01
D47		1.11E-01	3.73E-02	1.94E-02	7.75E-02	3.36E-04	<LOQ	1.09E-02	8.57E-03	1.38E-02	8.62E-03	1.89E-03	2.9E-01
D48		1.85E-01	6.72E-03	2.27E-02	7.22E-02	<LOQ	<LOQ	1.45E-02	1.23E-02	1.27E-02	1.09E-02	2.54E-03	3.4E-01
Mean		**6.6E-02**	**2.4E-02**	**2.5E-02**	**3.6E-02**	**4.0E-04**	**3.3E-03**	**1.3E-02**	**9.3E-03**	**1.2E-02**	**1.0E-02**	**1.7E-03**	**2.0E-01**
STD		6.4E-02	1.8E-02	1.7E-02	3.6E-02	9.1E-04	5.8E-03	5.8E-03	3.3E-03	3.3E-03	3.7E-03	4.5E-04	9.1E-02
Median		3.8E-02	2.1E-02	1.9E-02	1.1E-02	<LOQ	<LOQ	1.3E-02	1.0E-02	1.3E-02	1.0E-02	1.6E-03	2.0E-01

c) in the Southern Red Sea

Sample	Leg	1,4-O_2NAP	1-(CHO)NAP	9-OFLN	9,10-O_2ANT	1,4-O_2ANT	9,10-O_2PHE	11-OBaFLN	11-OBbFLN	BAN	7,12-O_2BAA	5,12-O_2NAC	Σ_{11}OPAHs
D15	1	<LOQ	<LOQ	3.36E-02	<LOQ	<LOQ	<LOQ	1.41E-02	9.99E-03	8.92E-03	1.38E-02	1.02E-03	1.0E-01
D42	2	<LOQ	<LOQ	<LOQ	<LOQ	<LOQ	<LOQ	<LOQ	<LOQ	2.84E-03	<LOQ	1.16E-04	3.9E-02
D43		2.64E-02	5.44E-03	1.71E-02	5.46E-02	<LOQ	<LOQ	4.77E-03	2.98E-03	4.85E-03	4.29E-03	6.33E-04	1.2E-01
D44		4.92E-02	7.37E-03	9.49E-03	<LOQ	<LOQ	<LOQ	6.38E-03	6.75E-03	1.15E-02	6.58E-03	1.76E-03	1.0E-01
D45		3.85E-02	6.49E-03	6.72E-03	<LOQ	<LOQ	<LOQ	5.33E-03	4.73E-03	6.59E-03	4.34E-03	1.25E-03	7.7E-02
Mean		**2.8E-02**	**6.6E-03**	**1.4E-02**	**1.4E-02**	<LOQ	<LOQ	**6.7E-03**	**5.3E-03**	**6.9E-03**	**6.0E-03**	**9.6E-04**	**8.8E-02**
STD		1.6E-02	1.0E-03	1.2E-02	2.3E-02			4.3E-03	3.1E-03	3.4E-03	4.8E-03	6.2E-04	3.2E-02
Median		2.6E-02	6.5E-03	9.5E-03	3.6E-03	<LOQ	<LOQ	5.3E-03	4.7E-03	6.6E-03	4.3E-03	1.0E-03	1.0E-01

d) in the Arabian Sea

Sample	Leg	1,4-O_2NAP	1-(CHO)NAP	9-OFLN	9,10-O_2ANT	1,4-O_2ANT	9,10-O_2PHE	11-OBaFLN	11-OBbFLN	BAN	7,12-O_2BAA	5,12-O_2NAC	Σ_{11}OPAHs
D35	2	1.27E-02	1.48E-02	1.03E-02	<LOQ	<LOQ	<LOQ	3.06E-03	3.16E-03	3.53E-03	1.66E-03	2.68E-04	5.3E-02
D36		1.51E-02	7.48E-03	<LOQ	<LOQ	<LOQ	<LOQ	3.12E-03	2.88E-03	3.09E-03	1.21E-03	3.11E-04	3.9E-02
D39		1.18E-02	5.27E-03	<LOQ	<LOQ	<LOQ	<LOQ	2.55E-03	2.36E-03	5.22E-03	3.17E-03	4.94E-04	3.5E-02
D40		1.51E-02	7.12E-03	1.03E-02	<LOQ	<LOQ	<LOQ	3.12E-03	2.92E-03	3.66E-03	4.32E-03	3.98E-04	5.0E-02
D41		3.35E-02	7.93E-03	7.99E-03	<LOQ	<LOQ	<LOQ	3.04E-03	3.50E-03	4.73E-03	4.84E-03	7.66E-04	7.0E-02
D42		<LOQ	<LOQ	<LOQ	<LOQ	<LOQ	<LOQ	<LOQ	<LOQ	2.84E-03	<LOQ	1.16E-04	3.9E-02
Mean		**1.7E-02**	**8.4E-03**	**5.8E-03**	**3.7E-03**	<LOQ	<LOQ	**3.0E-03**	**2.8E-03**	**3.8E-03**	**2.7E-03**	**3.9E-04**	**4.8E-02**
STD		8.1E-03	3.3E-03	4.2E-03	6.7E-04			2.2E-04	4.9E-04	9.4E-04	1.7E-03	2.2E-04	1.3E-02
Median		1.5E-02	7.7E-03	5.3E-03	3.7E-03	<LOQ	<LOQ	3.0E-03	2.9E-03	3.6E-03	2.4E-03	3.5E-04	4.5E-02

e) in the Gulf of Oman

Sample	Leg	1,4-O_2NAP	1-(CHO)NAP	9-OFLN	9,10-O_2ANT	1,4-O_2ANT	9,10-O_2PHE	11-OBaFLN	11-OBbFLN	BAN	7,12-O_2BAA	5,12-O_2NAC	Σ_{11}OPAHs
D24	1	<LOQ	1.47E-02	1.33E-02	<LOQ	<LOQ	1.20E-01	7.24E-02	4.80E-02	4.73E-02	9.79E-03	1.65E-03	3.6E-01
D25		<LOQ	7.04E-03	1.92E-02	1.05E-02	<LOQ	3.51E-02	4.15E-02	3.32E-02	3.41E-02	1.68E-02	1.58E-03	2.1E-01
D33	2	1.46E-02	1.51E-02	2.32E-02	<LOQ	<LOQ	<LOQ	1.38E-02	1.63E-02	2.33E-02	1.15E-02	2.42E-03	1.2E-01
D34		1.40E-02	7.10E-03	4.29E-03	<LOQ	<LOQ	<LOQ	6.04E-03	4.78E-03	6.86E-03	7.18E-03	8.00E-04	5.5E-02
D35		1.27E-02	1.48E-02	1.03E-02	<LOQ	<LOQ	<LOQ	3.06E-03	3.16E-03	3.53E-03	1.66E-03	2.68E-04	5.3E-02
Mean		**1.5E-02**	**1.2E-02**	**1.4E-02**	**6.2E-03**	<LOQ	**3.1E-02**	**2.7E-02**	**2.1E-02**	**2.3E-02**	**9.4E-03**	**1.3E-03**	**1.6E-01**
STD		5.8E-03	4.3E-03	7.4E-03	3.1E-03		5.2E-02	2.9E-02	1.9E-02	1.8E-02	5.6E-03	8.3E-04	1.3E-01
Median		1.4E-02	1.5E-02	1.3E-02	4.4E-03	<LOQ	<LOQ	1.4E-02	1.6E-02	2.3E-02	9.8E-03	1.6E-03	1.2E-01

189

f) in the Arabian Gulf

Sample	Leg	1,4-O_2NAP	1-(CHO)NAP	9-OFLN	9,10-O_2ANT	1,4-O_2ANT	9,10-O_2PHE	11-OBaFLN	11-OBbFLN	BAN	7,12-O_2BAA	5,12-O_2NAC	Σ_{11}OPAHs
D29	1	7.84E-02	9.05E-03	1.34E-02	<LOQ	<LOQ	<LOQ	9.52E-03	6.38E-03	1.05E-02	5.35E-03	8.91E-04	1.4E-01
D30		1.59E-01	6.81E-03	3.35E-02	8.77E-02	<LOQ	1.11E-02	1.52E-02	1.01E-02	1.81E-02	1.98E-02	3.00E-03	3.6E-01
D31	2	1.41E-02	1.31E-02	3.71E-02	8.21E-03	<LOQ	<LOQ	2.04E-02	1.28E-02	1.21E-02	1.06E-02	9.56E-04	1.3E-01
D32		5.40E-02	6.16E-03	3.74E-02	1.03E-02	<LOQ	<LOQ	1.35E-02	8.70E-03	8.38E-03	9.26E-03	9.68E-04	1.5E-01
D33		2.63E-03	1.46E-02	2.32E-02	<LOQ	<LOQ	<LOQ	1.38E-02	1.63E-02	2.33E-02	1.15E-02	2.37E-03	1.1E-01
Mean		**6.2E-02**	**1.0E-02**	**2.9E-02**	**2.2E-02**	<LOQ	**2.2E-03**	**1.4E-02**	**1.1E-02**	**1.4E-02**	**1.1E-02**	**1.6E-03**	**1.8E-01**
STD		6.2E-02	3.8E-03	1.0E-02	3.7E-02		5.0E-03	3.9E-03	3.8E-03	6.1E-03	5.3E-03	9.8E-04	1.1E-01
Median		5.4E-02	9.1E-03	3.3E-02	8.2E-03	<LOQ	<LOQ	1.4E-02	1.0E-02	1.2E-02	1.1E-02	9.7E-04	1.4E-01

Table S13. Concentration of NPAHs in high volume samples (sum of gas and particulate phase) in ng m³. For calculation of the mean, values <LOQ were replaced by LOQ/2 if the detection frequency in all samples exceeded 30 %, else by 0. LOQ values given in Table S6. STD: Standard deviation.

a) in the Mediterranean Sea

Sample	Leg	2-NNAP	9-NANT	3-NPHE	2-NFLT	1-NPYR	2-NPYR	7-NBAA	Σ_{17}NPAHs
D1	1	3.58E-03	3.50E-03	1.43E-03	7.68E-03	5.19E-04	1.86E-04	5.57E-05	1.7E-02
D4		9.98E-04	<LOQ	2.05E-04	3.41E-04	<LOQ	5.47E-05	<LOQ	1.8E-03
D5		<LOQ	<LOQ	7.09E-04	8.82E-04	<LOQ	1.73E-05	<LOQ	2.2E-03
D6		7.48E-04	<LOQ	2.89E-04	5.17E-04	5.30E-04	5.67E-05	5.01E-05	2.2E-03
D7		1.09E-03	<LOQ	5.68E-04	2.29E-04	2.41E-04	5.99E-05	6.93E-05	2.3E-03
D49	2	7.07E-04	<LOQ	6.25E-04	4.32E-04	7.4E-04	4.89E-05	<LOQ	2.2E-03
D50		7.09E-04	<LOQ	2.24E-04	2.16E-04	<LOQ	3.02E-05	<LOQ	1.6E-03
D51		<LOQ	<LOQ	1.38E-04	2.24E-04	<LOQ	<LOQ	<LOQ	1.4E-03
D52		6.90E-04	<LOQ	1.79E-04	3.13E-04	<LOQ	<LOQ	<LOQ	1.6E-03
D53		8.41E-04	<LOQ	<LOQ	2.09E-04	<LOQ	2.65E-05	<LOQ	1.6E-03
D54		7.16E-04	7.21E-04	<LOQ	2.71E-04	4.92E-04	3.33E-05	<LOQ	2.3E-03
D55		1.27E-03	<LOQ	2.73E-04	6.36E-04	5.25E-04	2.96E-05	<LOQ	2.8E-03
D56		7.20E-04	<LOQ	2.33E-04	3.43E-04	<LOQ	1.83E-05	<LOQ	1.8E-03
D57		1.46E-03	3.39E-04	4.04E-04	1.40E-03	9.38E-04	<LOQ	<LOQ	4.7E-03
D58		2.99E-02	1.33E-03	1.14E-02	2.97E-03	<LOQ	5.51E-04	<LOQ	4.7E-02
D59		<LOQ	<LOQ	6.57E-04	6.18E-04	<LOQ	2.96E-05	<LOQ	2.6E-03
D60		6.78E-04	<LOQ	3.11E-04	7.26E-05	<LOQ	1.71E-05	<LOQ	1.5E-03
D61		<LOQ	<LOQ	3.84E-04	9.00E-05	4.74E-04	<LOQ	<LOQ	1.7E-03
D62		6.88E-04	<LOQ	3.64E-04	1.67E-04	<LOQ	4.20E-05	<LOQ	1.7E-03
Mean		**2.5E-03**	**3.1E-04**	**9.7E-04**	**9.3E-04**	**4.2E-04**	**6.9E-05**	**5.6E-05**	**5.2E-03**
STD		6.7E-03	8.4E-04	2.5E-03	1.8E-03	1.6E-04	1.2E-04	2.2E-05	1.1E-02
Median		7.2E-04	<LOQ	3.1E-04	3.4E-04	<LOQ	3.0E-05	<LOQ	2.2E-03

b) in the Northern Red Sea

Sample	Leg	2-NNAP	9-NANT	3-NPHE	2-NFLT	1-NPYR	2-NPYR	7-NBAA	Σ_{17}NPAHs
D12	1	1.82E-03	<LOQ	9.22E-04	9.11E-04	3.31E-04	1.22E-04	<LOQ	4.1E-03
D13		1.41E-03	<LOQ	6.61E-04	2.38E-04	<LOQ	5.12E-05	6.88E-05	2.6E-03
D14		1.77E-03	<LOQ	2.60E-04	5.26E-04	<LOQ	7.74E-05	<LOQ	2.9E-03
D45	2	3.34E-04	<LOQ	<LOQ	1.81E-04	<LOQ	2.07E-05	<LOQ	8.4E-04
D46		1.31E-03	4.65E-03	2.63E-04	3.84E-04	<LOQ	2.81E-05	3.22E-04	7.1E-03
D47		2.64E-03	<LOQ	<LOQ	3.18E-04	3.07E-04	2.75E-05	1.39E-04	3.8E-03
D48		5.48E-03	2.29E-03	7.06E-04	9.13E-04	4.93E-04	6.88E-05	2.92E-04	1.0E-02
Mean		**2.1E-03**	**9.9E-04**	**4.6E-04**	**5.0E-04**	**2.7E-04**	**5.7E-05**	**1.3E-04**	**4.5E-03**
STD		1.6E-03	1.8E-03	3.0E-04	3.0E-04	1.2E-04	3.6E-05	1.3E-04	3.2E-03
Median		1.8E-03	0.0E+00	3.3E-04	3.8E-04	<LOQ	5.1E-05	6.9E-05	3.8E-03

c) in the Southern Red Sea

Sample	Leg	2-NNAP	9-NANT	3-NPHE	2-NFLT	1-NPYR	2-NPYR	7-NBAA	Σ_{17}NPAHs
D15	1	2.31E-03	<LOQ	9.95E-04	9.66E-04	<LOQ	3.04E-05	5.47E-05	4.5E-03
D42	2	<LOQ	<LOQ	<LOQ	4.91E-05	<LOQ	4.62E-06	<LOQ	8.1E-04
D43		6.88E-04	<LOQ	1.91E-04	1.68E-04	<LOQ	1.61E-05	<LOQ	1.2E-03
D44		3.62E-04	<LOQ	1.77E-04	2.52E-04	<LOQ	3.12E-05	<LOQ	1.0E-03
D45		3.34E-04	<LOQ	1.05E-04	1.81E-04	<LOQ	2.07E-05	<LOQ	8.4E-04
Mean		**8.3E-04**	<LOQ	**3.0E-04**	**3.2E-04**	**1.8E-04**	**2.1E-05**	**2.9E-05**	**1.7E-03**
STD		8.4E-04		3.9E-04	3.7E-04	3.9E-05	1.1E-05	1.5E-05	1.6E-03
Median		4.4E-04	<LOQ	1.8E-04	1.8E-04	<LOQ	2.1E-05	<LOQ	1.0E-03

d) in the Arabian Sea

Sample	Leg	2-NNAP	9-NANT	3-NPHE	2-NFLT	1-NPYR	2-NPYR	7-NBAA	Σ_{17}NPAHs
D35	2	3.60E-04	<LOQ	<LOQ	7.62E-05	2.98E-04	3.60E-06	<LOQ	1.2E-03
D36		3.32E-04	<LOQ	8.32E-05	7.14E-05	<LOQ	8.45E-06	<LOQ	7.0E-04
D39		2.92E-04	<LOQ	1.28E-04	1.11E-04	<LOQ	7.65E-06	9.25E-05	7.7E-04
D40		3.87E-04	<LOQ	3.29E-05	3.95E-05	3.95E-04	3.36E-06	5.76E-05	9.2E-04
D41		4.03E-04	<LOQ	1.13E-04	1.29E-04	3.09E-04	3.66E-06	<LOQ	9.8E-04
D42		<LOQ	<LOQ	<LOQ	4.91E-05	<LOQ	4.62E-06	<LOQ	8.1E-04
Mean		**3.7E-04**	<LOQ	**1.4E-04**	**7.9E-05**	**2.6E-04**	**5.2E-06**	**4.2E-05**	**8.9E-04**
STD		5.2E-05		1.4E-04	3.5E-05	9.3E-05	2.2E-06	2.8E-05	1.7E-04
Median		3.7E-04	<LOQ	9.8E-05	7.4E-05	2.7E-04	4.1E-06	<LOQ	8.6E-04

e) in the Gulf of Oman

Sample	Leg	2-NNAP	9-NANT	3-NPHE	2-NFLT	1-NPYR	2-NPYR	7-NBAA	Σ_{17}NPAHs
D24	1	<LOQ	<LOQ	1.98E-03	1.13E-04	<LOQ	2.01E-05	5.39E-05	3.4E-03
D25		2.12E-03	<LOQ	1.83E-03	3.14E-04	9.05E-04	7.38E-05	2.74E-05	5.3E-03
D33	2	3.63E-03	<LOQ	1.87E-03	5.34E-04	4.23E-03	6.32E-05	2.06E-04	1.1E-02
D34		<LOQ	<LOQ	3.36E-04	1.58E-04	4.15E-04	5.99E-06	2.54E-04	1.5E-03
D35		3.60E-04	<LOQ	<LOQ	7.62E-05	2.98E-04	3.60E-06	<LOQ	1.2E-03
Mean		**1.4E-03**	<LOQ	**1.3E-03**	**2.4E-04**	**1.3E-03**	**3.3E-05**	**1.1E-04**	**4.4E-03**
STD		1.4E-03		8.3E-04	1.9E-04	1.7E-03	3.3E-05	1.1E-04	3.8E-03
Median		7.6E-04	<LOQ	1.8E-03	1.6E-04	4.3E-04	2.0E-05	5.4E-05	3.4E-03

f) in the Arabian Gulf

Sample	Leg	2-NNAP	9-NANT	3-NPHE	2-NFLT	1-NPYR	2-NPYR	7-NBAA	Σ_{17}NPAHs
D29	1	6.29E-04	<LOQ	2.36E-04	1.33E-04	2.82E-04	3.14E-05	<LOQ	1.3E-03
D30		5.92E-03	<LOQ	1.24E-03	2.15E-03	8.48E-04	1.61E-04	<LOQ	1.0E-02
D31	2	1.86E-03	<LOQ	1.57E-03	4.79E-04	2.09E-03	3.53E-05	<LOQ	6.1E-03
D32		1.94E-03	<LOQ	8.02E-04	1.10E-03	9.89E-04	4.05E-05	9.75E-05	5.0E-03
D33		3.63E-03	<LOQ	1.87E-03	5.34E-04	4.23E-03	6.32E-05	2.06E-04	1.1E-02
Mean		**2.8E-03**	<LOQ	**1.1E-03**	**8.8E-04**	**1.7E-03**	**6.6E-05**	**7.7E-05**	**6.6E-03**
STD		2.0E-03		6.4E-04	7.9E-04	1.6E-03	5.4E-05	7.9E-05	3.9E-03
Median		1.9E-03	<LOQ	1.2E-03	5.3E-04	9.9E-04	4.0E-05	<LOQ	6.1E-03

Table S14. Total concentration (sum of gas and particulate phase) of RPAHs and PHE in high volume samples (sum of gas and particulate phase) in ng m³ (only samples filtered for stack contamination). STD: Standard deviation.

Sample	1-MPHE	2-MPHE	3-MPHE	4-MPHE	3,6-M_2PHE	2,6-M_2PHE	2,7-M_2PHE	1,3-/2,10-/3,9-/1,10-M_2PHE	1,6-/2,9-M_2PHE	1,7-M_2PHE	2,3-M_2PHE	1,9-/4,9-M_2PHE	1,8-M_2PHE	PHE	ΣMPHE/PHE	1,7-M_2PHE/(1,7-M_2PHE+2,6-M_2PHE)
G1	0.111	0.178	0.092	0.101	0.006	0.023	0.029	0.026	0.072	0.039	0.035	0.026	0.006	0.751	0.64	0.62
G2	0.09	0.114	0.057	0.053	0.005	0.019	0.025	0.017	0.045	0.023	0.017	0.017	0.003	0.437	0.72	0.54
G5	0.066	0.088	0.044	0.042	0.003	0.007	0.016	0.011	0.032	0.017	0.015	0.012	0.003	0.389	0.61	0.70
G6	0.214	0.254	0.169	0.133	0.012	0.028	0.053	0.035	0.124	0.06	0.046	0.041	0.009	0.768	1.00	0.68
G7	0.493	0.688	0.37	0.371	0.044	0.14	0.203	0.146	0.442	0.215	0.143	0.131	0.025	1.113	1.73	0.61
G10	0.075	0.105	0.054	0.05	0.004	0.013	0.02	0.01	0.039	0.02	0.015	0.013	0.003	0.469	0.61	0.61
G11	0.475	0.614	0.403	0.336	0.035	0.09	0.169	0.107	0.409	0.189	0.127	0.134	0.028	0.544	3.36	0.68
G20	0.179	0.245	0.144	0.129	0.013	0.033	0.059	0.038	0.126	0.064	0.044	0.042	0.009	0.59	1.18	0.66
G24	0.192	0.264	0.163	0.154	0.013	0.029	0.051	0.036	0.132	0.069	0.056	0.044	0.009	0.573	1.35	0.70
G25	0.134	0.209	0.119	0.113	0.012	0.033	0.044	0.035	0.1	0.058	0.051	0.044	0.009	0.47	1.22	0.64
G27	0.074	0.098	0.052	0.047	0.004	0.01	0.019	0.014	0.043	0.024	0.018	0.017	0.003	0.267	1.02	0.71
G32	0.048	0.065	0.036	0.034	0.003	0.011	0.015	0.011	0.032	0.017	0.012	0.01	0.002	0.231	0.79	0.61
G33	0.145	0.205	0.098	0.099	0.009	0.028	0.043	0.035	0.082	0.045	0.041	0.031	0.007	0.568	0.96	0.62
G34	0.073	0.105	0.053	0.054	0.006	0.012	0.019	0.014	0.043	0.023	0.021	0.015	0.004	0.249	1.14	0.65
G35	0.077	0.133	0.058	0.073	0.009	0.023	0.031	0.025	0.061	0.038	0.037	0.028	0.004	0.237	1.44	0.62
G36	0.084	0.123	0.057	0.059	0.007	0.023	0.032	0.025	0.059	0.031	0.025	0.022	0.005	0.245	1.32	0.57
G37	0.055	0.081	0.037	0.04	0.004	0.013	0.019	0.016	0.037	0.022	0.019	0.017	0.003	0.221	0.96	0.62
G40	0.036	0.045	0.028	0.025	0.002	0.004	0.008	0.006	0.021	0.019	0.009	0.012	0.001	0.205	0.65	0.81

Sample	1-MPHE	2-MPHE	3-MPHE	4-MPHE	3,6-M_2PHE	2,6-M_2PHE	2,7-M_2PHE	1,3-/2,10-/3,9-/1,10-M_2PHE	1,6-/2,9-M_2PHE	1,7-M_2PHE	2,3-M_2PHE	1,9-/4,9-M_2PHE	1,8-M_2PHE	PHE	ΣMPHE/PHE	1,7-M_2PHE/(1,7-M_2PHE+2,6-M_2PHE)
G41	0.037	0.059	0.025	0.026	0.003	0.009	0.014	0.012	0.024	0.012	0.011	0.01	0.002	0.055	2.65	0.58
G42	0.026	0.05	0.019	0.022	0.002	0.006	0.009	0.008	0.018	0.01	0.009	0.007	0.001	0.147	0.79	0.61
G43	0.047	0.066	0.031	0.031	0.003	0.006	0.011	0.008	0.023	0.012	0.011	0.009	0.002	0.267	0.65	0.65
Mean	**0.130**	**0.180**	**0.100**	**0.095**	**0.009**	**0.027**	**0.042**	**0.030**	**0.094**	**0.048**	**0.036**	**0.032**	**0.007**	**0.419**	**1.18**	**0.64**
STD	0.129	0.171	0.105	0.095	0.011	0.032	0.050	0.034	0.116	0.054	0.036	0.035	0.007	0.253	0.67	0.057
Median	0.077	0.114	0.057	0.054	0.006	0.019	0.025	0.017	0.045	0.024	0.021	0.017	0.004	0.389	1.00	0.62

Table S15. Particulate mass (PM), elemental carbon (EC) and organic carbon (OC) concentration in Digitel high volume samples.

Sample	PM [µg m^{-3}]	EC [µg m^{-3}]	OC [µg m^{-3}]
D1	13.07	0.18	1.27
D4	24.04	0.12	1.09
D5	16.38	0.16	0.90
D6	30.80	0.21	1.17
D7	30.95	0.19	1.59
D12	34.93	0.45	2.11
D13	25.88	0.37	1.22
D14	16.10	0.30	0.87
D15	85.19	0.34	1.77
D24	62.38	<LOQ	1.27
D25	101.21	1.92	0.94
D29	80.84	1.13	0.93
D30	77.60	1.55	2.35
D31	79.37	1.00	1.25
D32	89.02	0.81	1.44
D33	58.65	0.72	1.64
D34	70.82	<LOQ	1.36
D35	19.48	<LOQ	0.71
D36	52.22	0.12	1.90
D39	43.22	<LOQ	1.71
D40	55.44	<LOQ	1.66
D41	37.36	<LOQ	1.22
D42	18.02	<LOQ	<LOQ
D43	73.55	0.33	0.84
D44	60.31	0.36	0.99

Sample	PM [µg m^{-3}]	EC [µg m^{-3}]	OC [µg m^{-3}]
D45	39.61	0.38	1.37
D46	37.66	0.38	1.42
D47	32.54	0.30	1.30
D48	124.37	0.24	2.39
D49	42.53	0.21	1.85
D50	53.66	0.17	1.75
D51	36.94	<LOQ	1.71
D52	25.89	<LOQ	1.23
D53	42.48	0.20	2.30
D54	33.53	0.33	3.46
D55	50.43	0.24	2.49
D56	19.23	0.35	1.82
D57	11.59	0.24	3.50
D58	54.59	0.51	3.76
D59	25.72	0.25	3.19
D60	29.56	0.25	2.36
D61	63.53	0.32	2.31
D62	9.57	<LOQ	0.60

2.2 Back trajectories

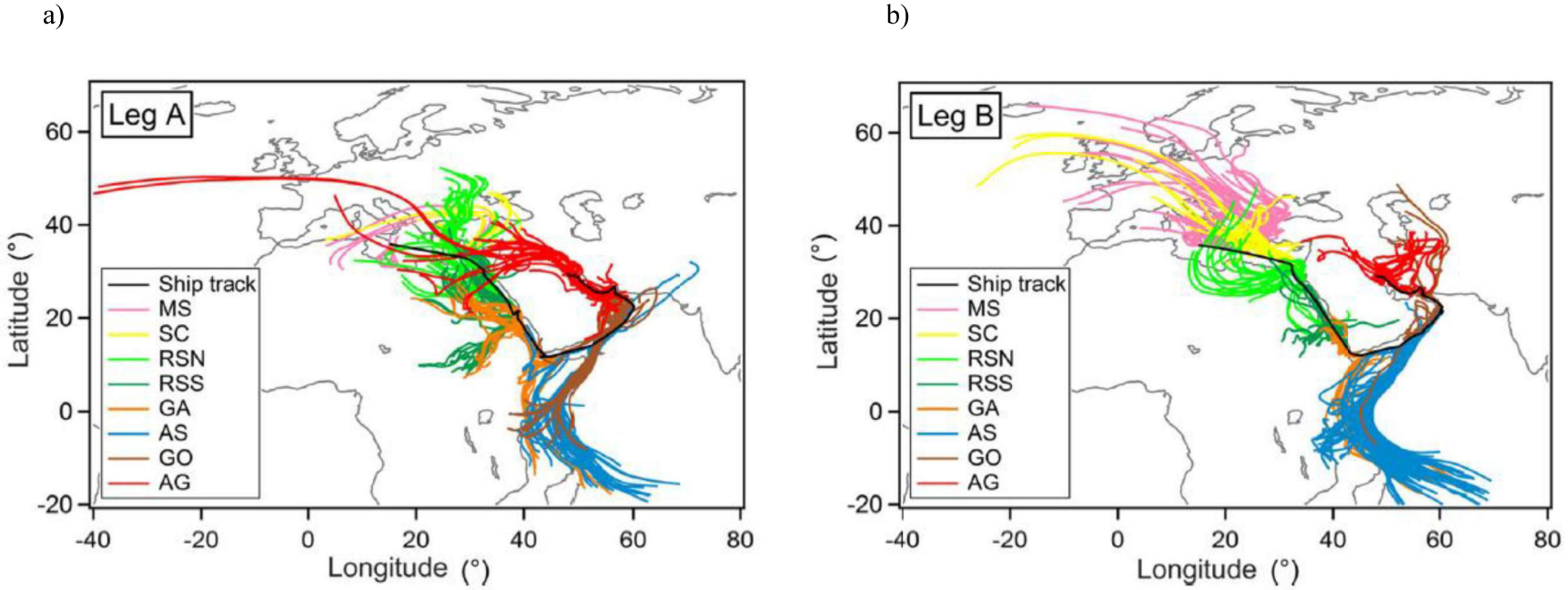

Figure S2. Summary of air mass back trajectories (4 days on an hourly time grid, HYSPLIT model, NOAA) during the AQABA ship campaign, taken from Bourtsoukidis et al. (2019), a) 1. leg; b) 2. leg (MS: Mediterranean Sea; SC: Suez canal; RSN: Northern Red Sea; RSS: Southern Red Sea; GA: Gulf of Aden; AS: Arabian Sea; OG: Gulf of Oman; AG: Arabian Gulf).

Residence time distributions of air mass histories:

a) Mediterranean Sea:

1. Leg:

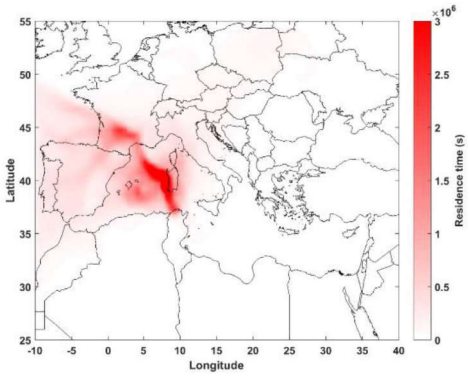

25.-26.06. (D1)

2. Leg:

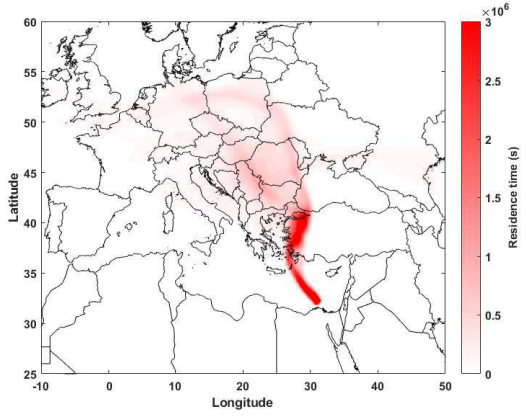

25.08. (D49)

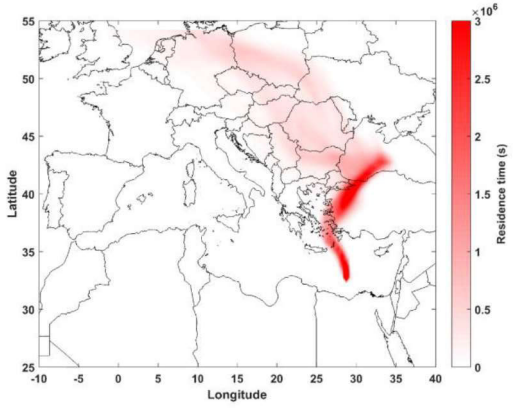

25.-26.08. (D49-51, C27)

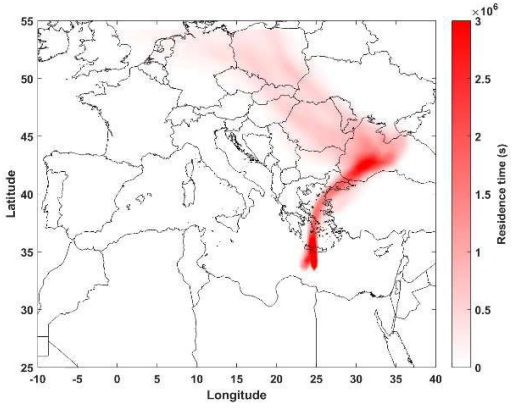

26.-27.08. (D52-53; C28)

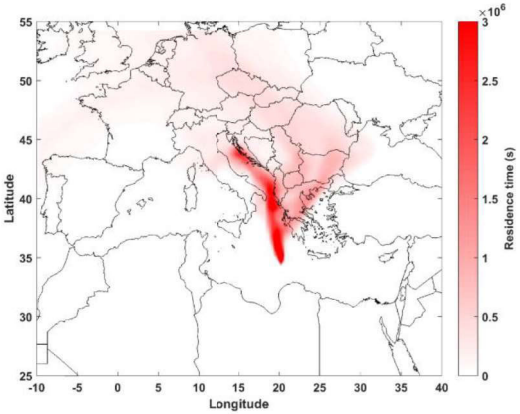

27.-28.08. (D54-55, C29)

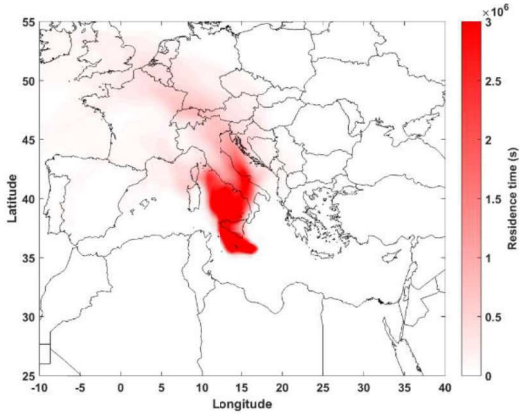

28.-29.08. (D56)

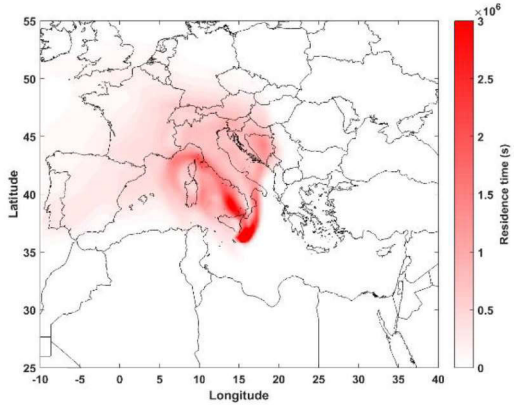

29.-30.08. (D55-58; C30)

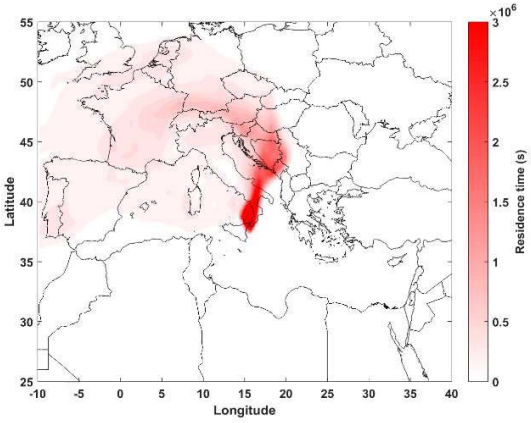

30.-31.08. (D59-60)

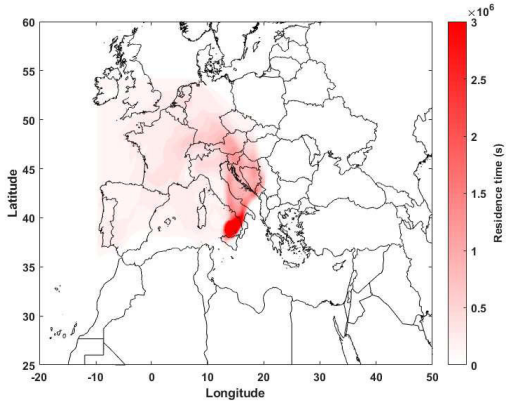

31.08. (D60)

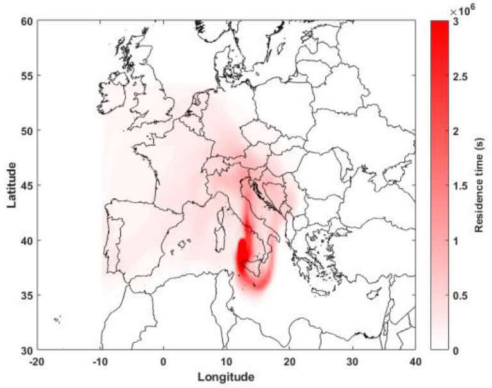

31.08.-01.09. (D61)

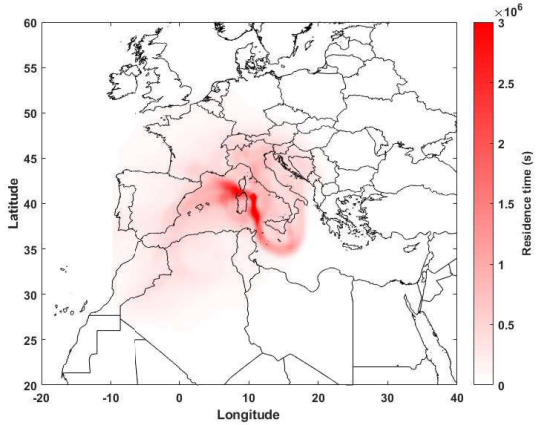

01.09. (D62)

b) Northern Red Sea:

1. Leg:

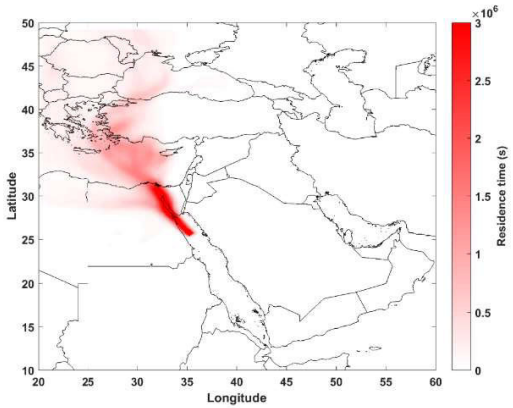

07.-08.07. (D12)

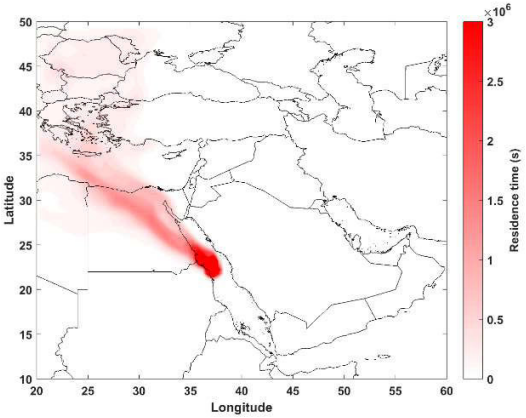

08.-09.07. (D13)

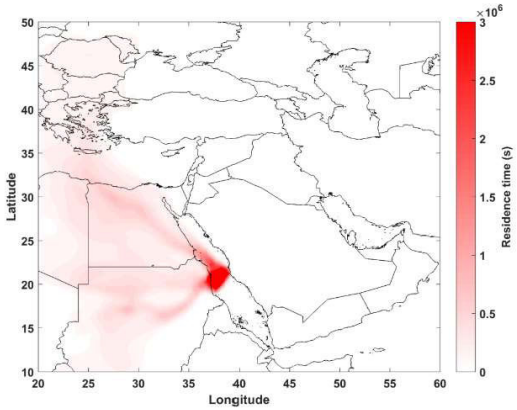

09.-10.07. (D14)

2. Leg:

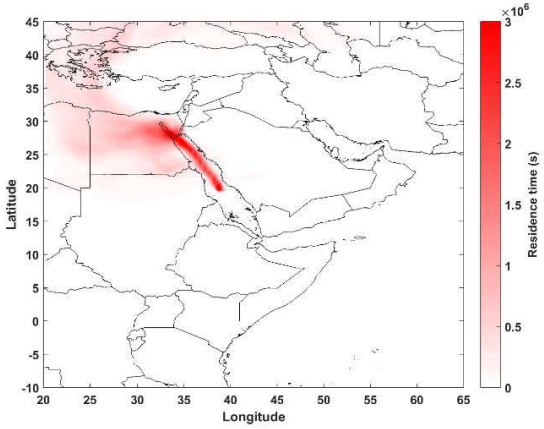

19.-20.08. (D45, C25)

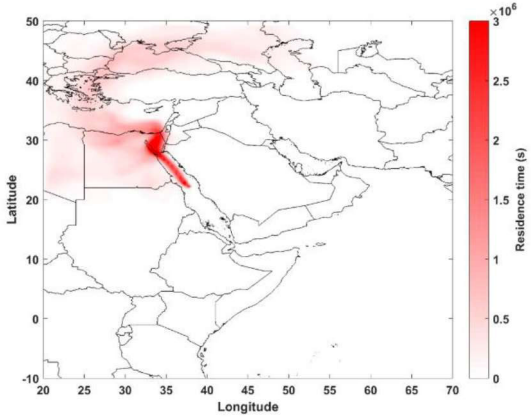

20.-21.08. (D46, C25)

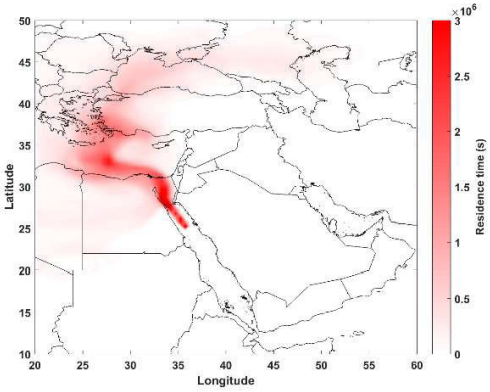

21.-22.08. (D47; C26)

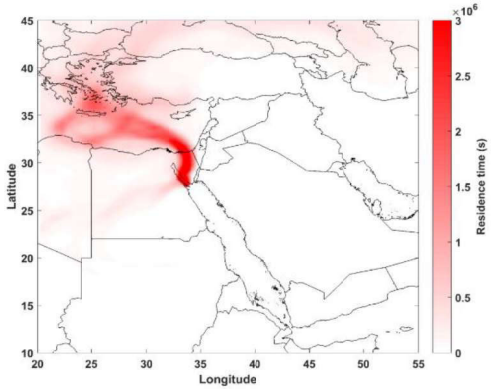

22.-23.08. (D48, C26)

c) Southern Red Sea

1. Leg:

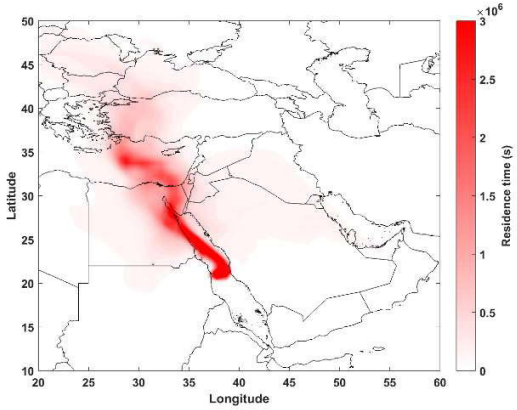

13.-14.07. (D15)

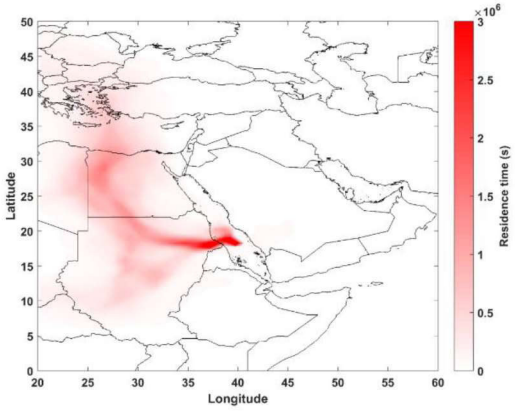

14.-15.07. (D16; C1)

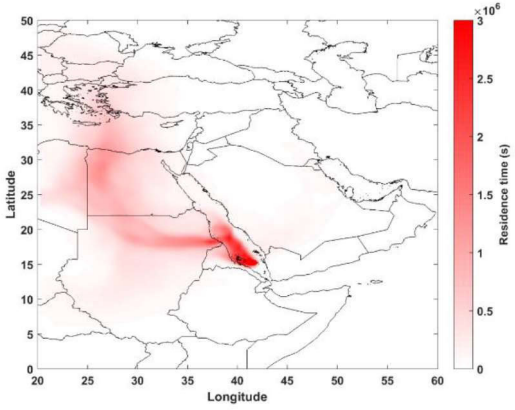

15.-16.07. (D17; C1)

2.Leg:

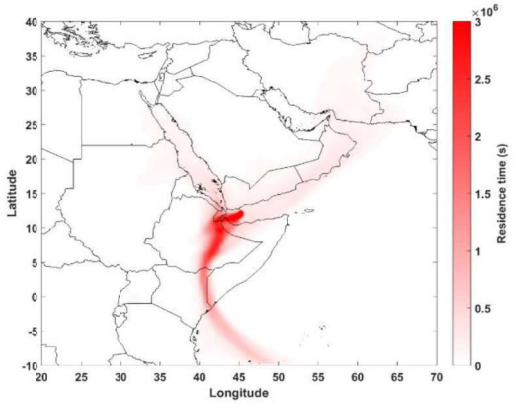

16.-17.08. (D42, C23)

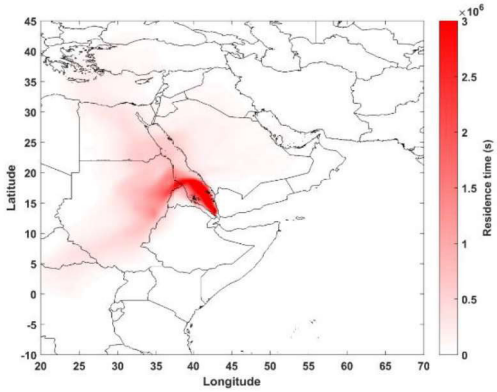

17.-18.08. (D43, C24)

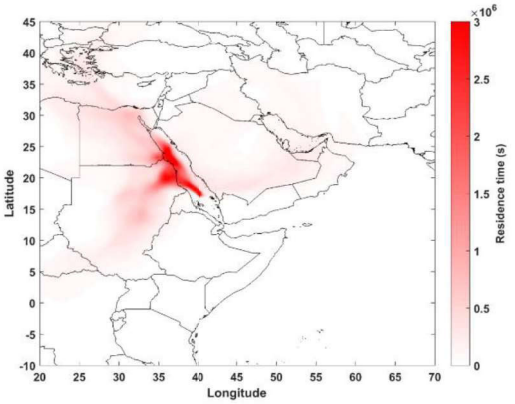

18.-19.08. (D44; C24)

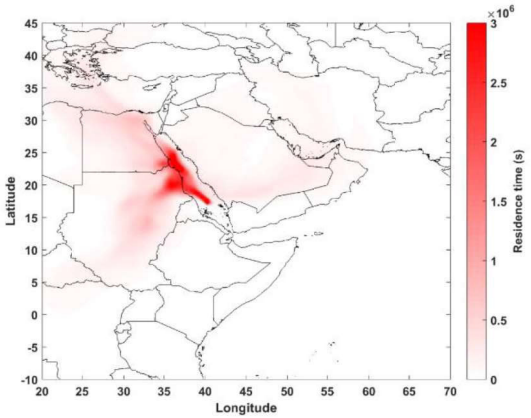

18.-19.08. (D44, C24)

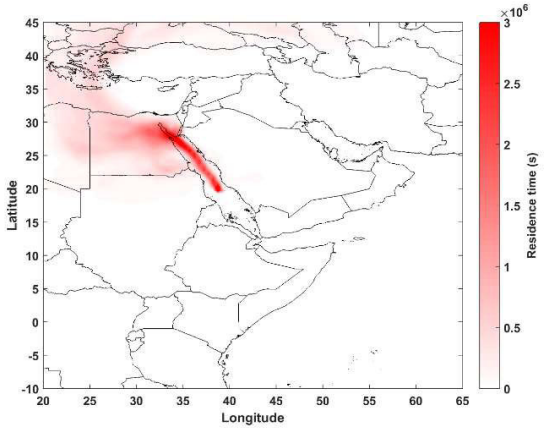

19.-20.08. (D45, C25)

d) Arabian Sea

1. Leg:

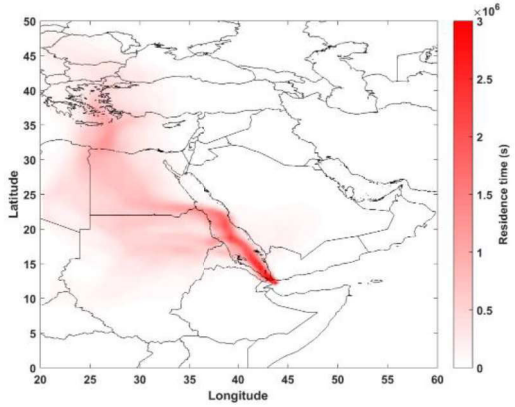

16.-17.07. (D18)

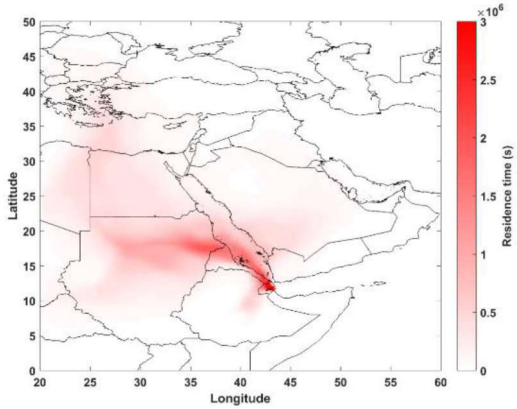

17.-18.07. (D19)

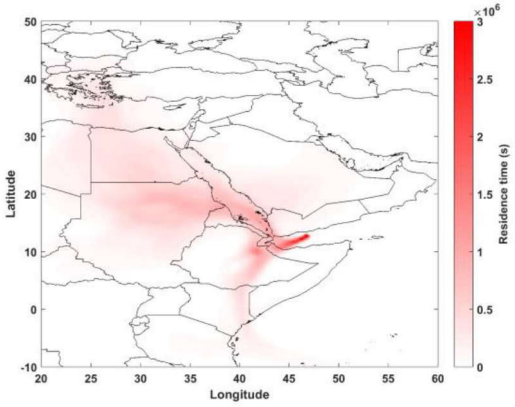

18.-19.07. (D20)

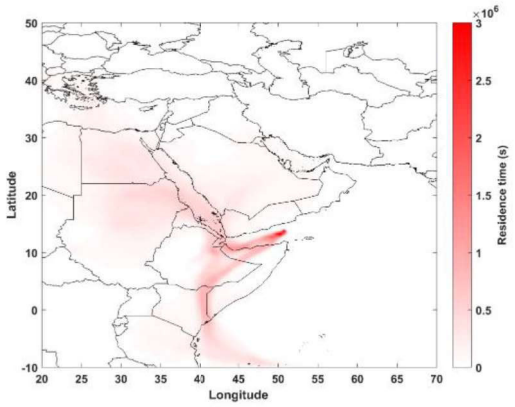

19.-20.07. (D21, C2)

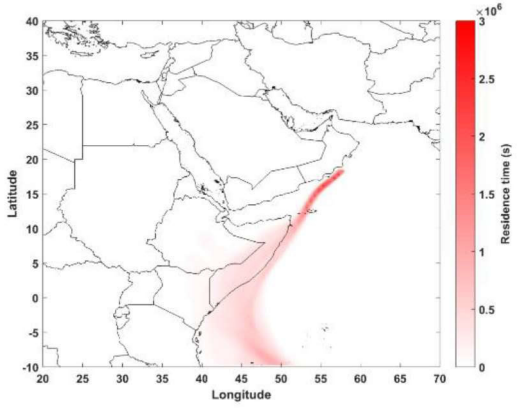

21.-22.07. (D22)

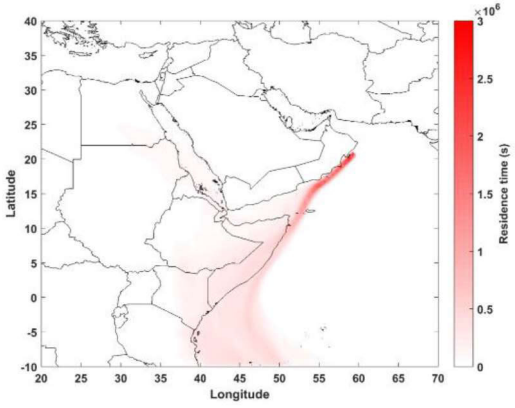

22.-23.07. (D23; D24)

2.Leg:

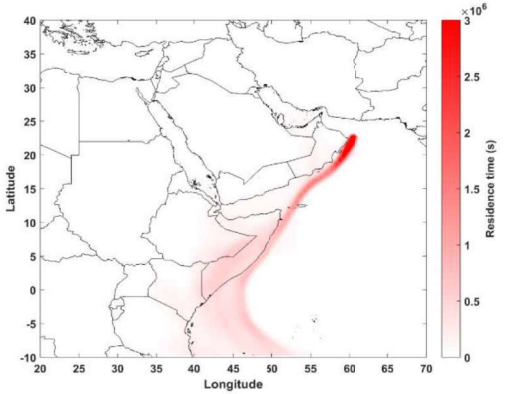

07.-08.08. (D35; C20)

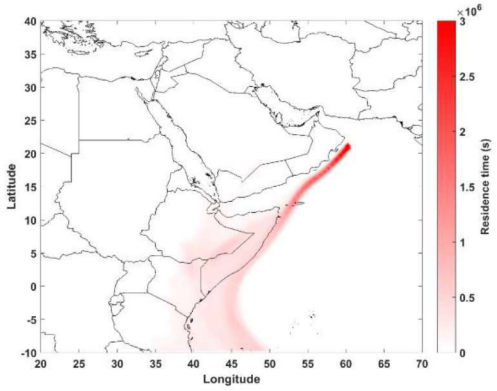

08.-09.08. (D36, C20)

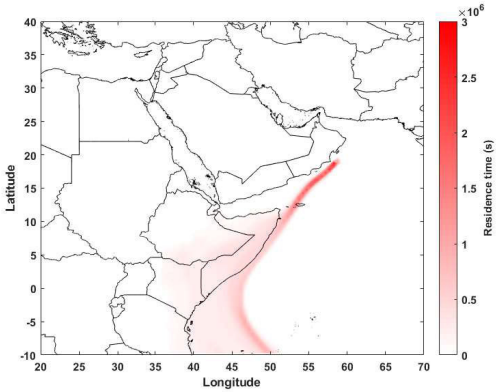

10.08. (D37)

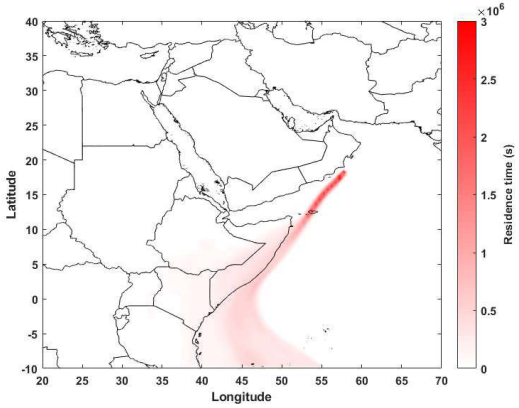

11.-12.08. (D38; C21)

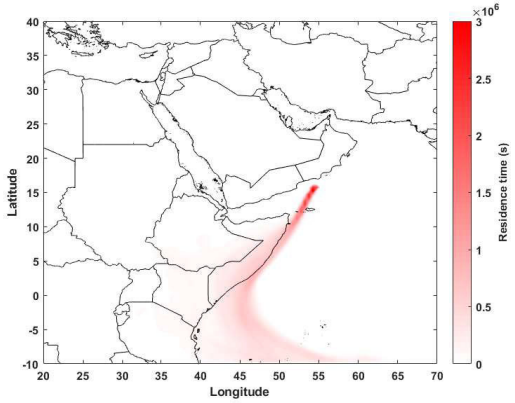

13.-14.08. (D39, C22)

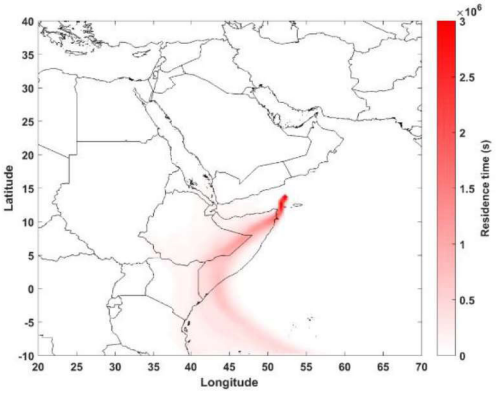

14.-15.08. (D40)

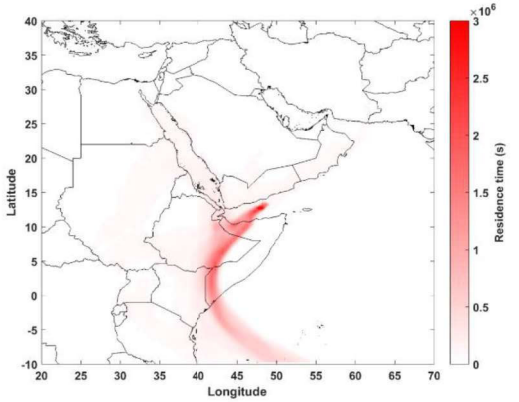

15.-16.08. (D41; C23)

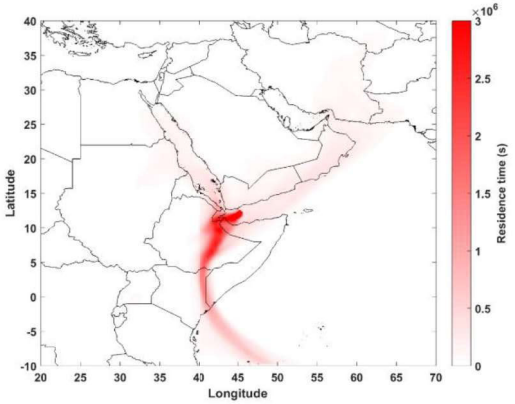

16.-17.08. (D42, C23)

e) Gulf of Oman

1. Leg:

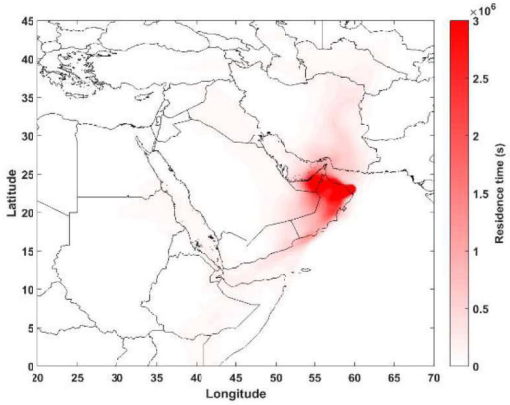

24-25.07. (D25, C3)

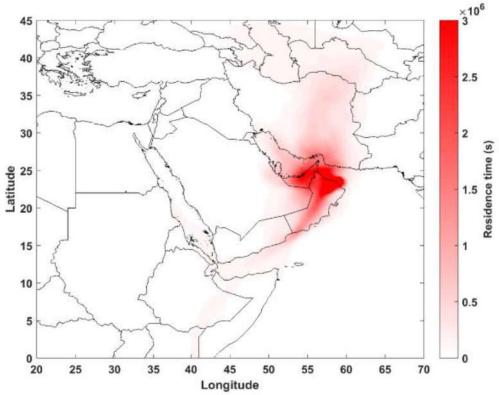

25.-26.07. (D26, C3)

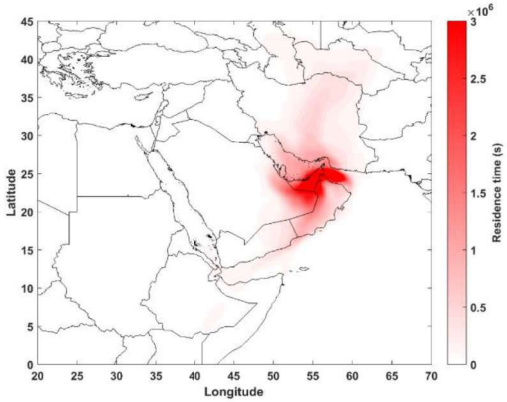

26.-27.07. (D27; C4)

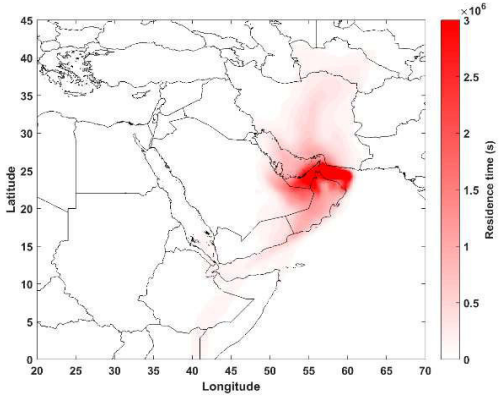

27-28.07. (D28, C5)

2. Leg:

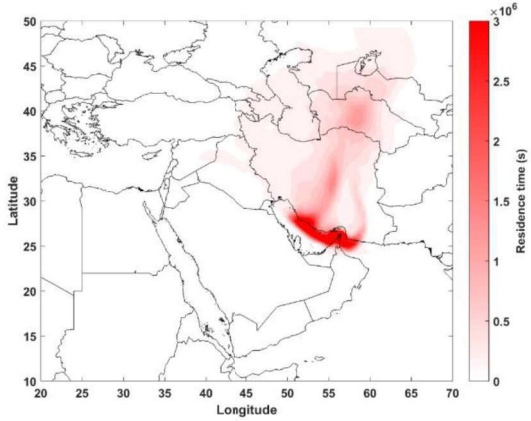

05.-06.08. (D33; C14-17)

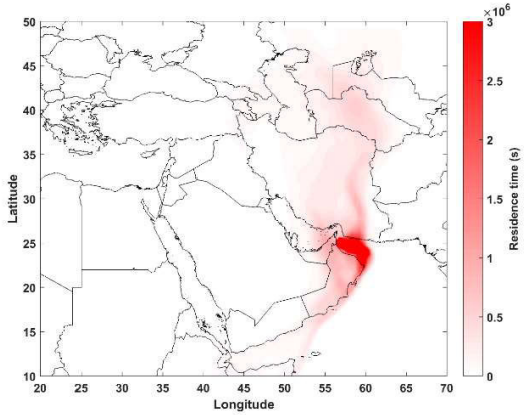

06.-07.08. (D34, C18-19)

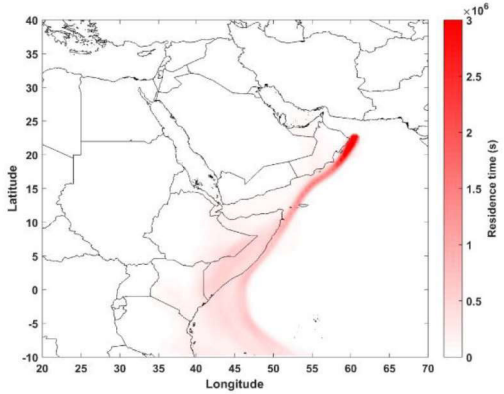

07.-08.08. (D35; C20)

f) Arabian Gulf

1. Leg:

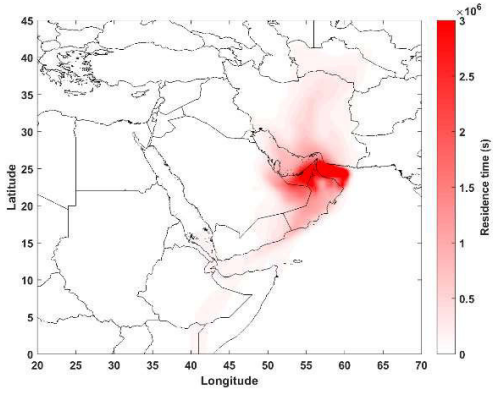

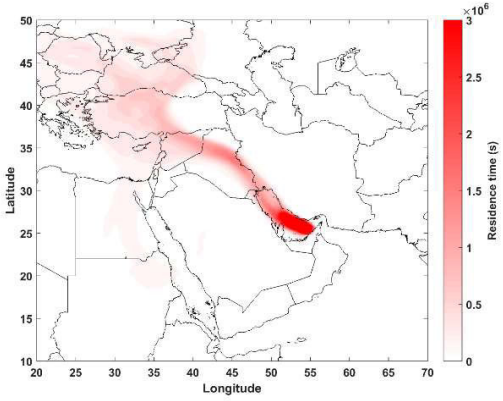

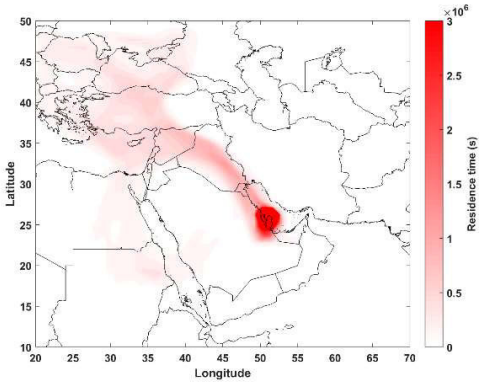

27-28.07. (D28, C5) 28.-29.07. (D29, C6) 29.-30.07. (D30; C7)

2. Leg:

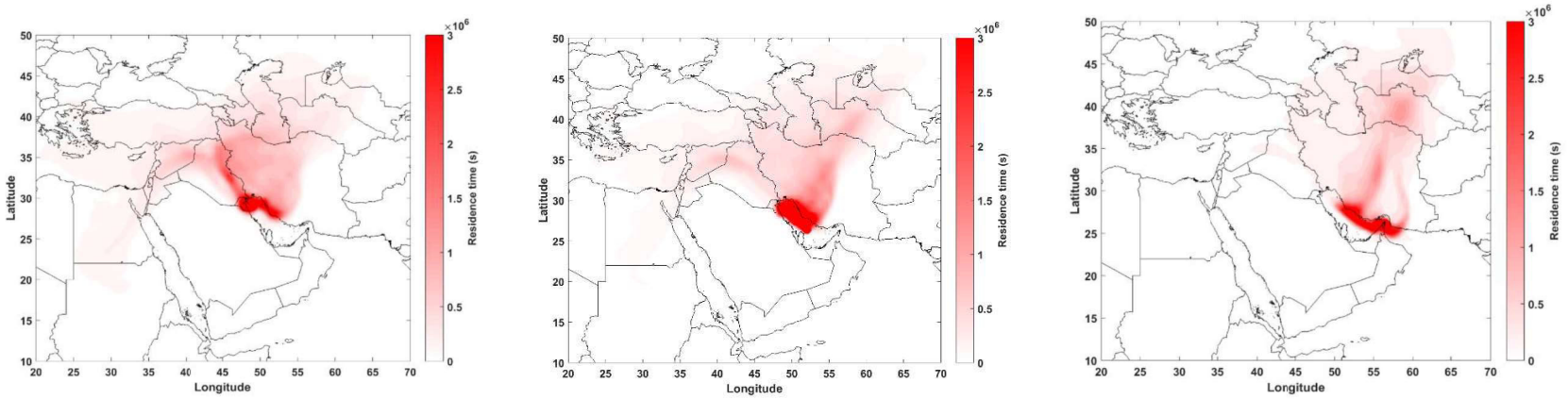

03.-04.08. (D31, C8-C12) 04.-05.08. (D32, C13) 05.-06.08. (D33; C14-17)

Figure S3. Distribution of residence times of air masses received at specified dates using FLEXPART Lagrangian particle dispersion model, with ECMWF meteorological data ordered by sea regions and legs: a) Mediterranean Sea, b) Northern Red Sea, c) Southern Red Sea, d) Arabian Sea, e) Gulf of Oman, f) Arabian Gulf. All particles were followed for 10 days backward in time.

2.3 Composition pattern

Table S16. Relative contribution (in %) of individual compounds to the sum of the concentration of all compounds from the same class, a) PAHs, b) OPAHs, c) NPAHs

a)

Sample	NAP	ACY	ACE	FLN	PHE	ANT	FLT	PYR	BAA	CHR	BBF	BKF	BAP	INP	DBA	BPE
D1	0.1	0.1	2.9	7.0	62.2	4.7	9.4	6.4	0.3	2.0	0.8	0.2	0.2	0.3	1.1	0.3
D4	0.0	0.3	9.3	25.1	58.1	2.3	1.8	1.5	0.0	0.1	0.1	0.0	0.1	0.1	0.6	0.1
D5	0.0	1.0	9.0	17.6	54.4	3.8	6.5	5.6	0.1	0.5	0.2	0.0	0.0	0.0	0.2	0.0
D6	0.0	0.5	9.9	17.5	53.0	4.9	6.8	4.7	0.1	0.4	0.3	0.1	0.1	0.2	0.9	0.2
D7	0.0	0.1	1.6	10.6	61.6	6.5	9.2	7.4	0.1	0.5	0.4	0.1	0.2	0.3	0.8	0.3
D12	0.0	0.6	7.2	14.7	62.4	3.3	5.9	4.6	0.1	0.3	0.3	0.1	0.2	0.2	0.3	0.2
D13	0.0	0.4	6.4	15.6	59.8	5.4	6.2	5.0	0.1	0.3	0.3	0.1	0.1	0.2	0.2	0.2
D14	0.0	0.1	1.2	4.9	72.1	5.6	6.7	6.2	0.3	0.8	0.8	0.2	0.3	0.5	0.7	0.4
D15	0.0	0.1	0.5	2.1	72.7	3.4	9.8	7.6	0.2	0.7	0.4	0.1	0.2	0.3	0.9	0.3
D24	0.2	0.2	0.7	1.1	33.8	2.9	13.1	29.0	2.8	4.0	0.3	0.1	0.1	0.1	0.1	0.2
D25	0.1	0.1	3.4	3.4	50.2	3.8	11.4	16.7	1.3	2.7	0.3	0.1	0.0	0.1	0.5	0.1
D29	0.2	0.2	0.5	2.6	62.0	3.8	10.5	11.1	0.4	1.2	1.0	0.3	0.4	0.7	3.4	0.6
D30	0.2	0.1	1.7	3.8	49.7	4.5	16.6	12.8	0.9	2.0	3.5	1.0	2.1	3.2	3.0	3.1
D31	0.1	0.1	3.5	8.7	54.6	5.8	12.4	10.7	0.2	0.7	0.5	0.2	0.2	0.4	1.0	0.3
D32	0.1	0.1	1.4	3.6	60.9	8.4	13.4	10.2	0.2	0.5	0.3	0.1	0.1	0.2	0.1	0.2
D33	0.1	0.1	2.1	24.0	49.2	4.3	7.6	9.1	0.3	0.7	0.5	0.1	0.1	0.3	0.4	0.3
D34	0.3	0.2	20.4	12.4	40.6	4.2	6.4	7.7	0.8	1.8	0.6	0.1	0.0	0.1	0.8	0.1
D35	0.1	0.1	10.0	14.3	48.8	5.4	7.7	11.5	0.3	0.4	0.2	0.0	0.1	0.1	0.3	0.1
D36	0.4	0.8	10.3	8.3	52.6	6.6	7.1	11.3	0.8	1.2	0.8	0.2	0.5	0.7	0.8	0.8
D39	0.2	0.5	14.1	13.2	42.9	5.3	4.3	10.6	1.2	2.0	0.9	0.2	0.3	0.5	1.2	0.5
D40	0.3	0.2	0.6	3.5	59.6	12.5	10.5	8.5	0.6	1.0	0.6	0.2	0.2	0.3	0.9	0.3
D41	0.5	0.3	0.9	4.2	64.7	5.2	8.9	9.6	0.5	1.4	0.6	0.2	0.2	0.3	1.2	0.4

Sample	NAP	ACY	ACE	FLN	PHE	ANT	FLT	PYR	BAA	CHR	BBF	BKF	BAP	INP	DBA	BPE
D42	2.2	9.5	5.3	8.9	43.6	2.7	13.5	9.1	0.7	1.8	0.4	0.5	0.3	0.2	1.5	0.2
D43	0.5	0.3	0.8	3.3	57.5	3.6	13.3	12.8	0.6	1.4	1.2	0.5	0.6	0.9	3.1	0.9
D44	0.9	0.5	1.6	2.8	43.8	4.5	15.8	15.4	1.4	4.0	5.1	1.7	3.3	4.3	6.5	4.1
D45	0.6	0.5	1.4	5.3	44.6	5.4	15.0	13.1	1.0	2.2	3.3	1.1	2.2	2.9	7.0	2.8
D46	0.6	0.3	5.1	10.4	46.8	3.2	10.7	9.5	1.0	2.9	2.6	0.8	1.4	1.9	4.0	1.9
D47	0.1	0.7	3.8	9.7	53.5	3.5	8.1	8.6	0.8	2.4	1.5	0.5	0.7	1.1	3.6	1.1
D48	0.1	0.3	0.8	9.2	53.7	1.7	9.8	8.7	1.0	3.1	2.3	0.7	0.1	1.9	5.1	1.9
D49	0.0	0.2	12.5	26.1	45.6	5.4	4.9	3.8	0.2	0.4	0.4	0.1	0.2	0.3	0.4	0.3
D50	0.0	0.2	17.7	35.6	37.0	4.4	2.9	1.7	0.1	0.2	0.2	0.1	0.1	0.1	0.2	0.1
D51	0.1	0.2	10.2	20.1	47.1	6.0	6.5	6.0	0.6	1.0	1.2	0.4	0.7	0.8	0.5	0.8
D52	0.0	0.2	18.5	39.3	33.1	3.4	2.4	1.6	0.1	0.2	0.2	0.1	0.1	0.1	0.6	0.1
D53	0.1	0.3	5.6	25.1	46.7	5.9	5.7	6.2	0.4	0.6	0.9	0.3	0.5	0.7	1.3	0.6
D54	0.0	0.1	18.3	36.9	34.9	5.3	2.7	1.6	0.0	0.1	0.1	0.0	0.0	0.0	0.1	0.0
D55	0.0	0.1	2.1	12.9	63.0	8.9	6.3	4.8	0.1	0.2	0.3	0.1	0.2	0.2	0.6	0.2
D56	0.4	1.0	3.1	13.4	46.3	3.0	9.0	6.7	0.9	2.0	2.4	0.9	1.0	2.0	5.3	1.7
D57	0.1	0.1	7.2	39.1	37.1	4.2	5.1	3.5	0.2	0.5	0.8	0.3	0.5	0.5	1.6	0.5
D58	0.0	0.1	7.2	15.5	51.2	4.8	9.8	6.3	0.6	1.2	1.6	0.5	1.1	1.4	0.4	1.3
D59	0.1	0.1	7.7	40.7	39.9	3.6	3.6	3.3	0.1	0.3	0.3	0.1	0.1	0.2	0.3	0.2
D60	0.1	0.1	28.6	30.8	30.9	3.9	2.9	2.1	0.1	0.3	0.3	0.1	0.2	0.2	0.1	0.2
D61	0.0	0.2	8.8	31.1	44.5	6.5	4.5	3.5	0.1	0.2	0.2	0.1	0.1	0.1	0.2	0.1
D62	0.4	0.4	6.9	15.6	50.1	5.3	12.2	8.5	0.6	2.5	3.3	1.2	1.3	1.7	2.0	1.4

Sample	BJF	BEP	PER	DCA	ATT	COR	TPH	CCP	BGF	BBN	BNT
D1	0.15	0.37	0.02	0.85	0.00	0.14	1.39	0.06	0.64	0.45	0.54
D4	0.05	0.09	0.01	0.38	0.00	0.05	0.09	0.02	0.09	0.07	0.06
D5	0.04	0.07	0.01	0.18	0.00	0.01	0.36	0.01	0.22	0.24	0.26
D6	0.11	0.19	0.01	0.66	0.00	0.09	0.20	0.03	0.12	0.21	0.19
D7	0.14	0.27	0.02	0.66	0.00	0.12	0.31	0.04	0.23	0.28	0.25
D12	0.10	0.19	0.02	0.25	0.02	0.10	0.18	0.03	0.13	0.17	0.17
D13	0.10	0.17	0.01	0.18	0.01	0.08	0.20	0.02	0.14	0.17	0.17
D14	0.24	0.49	0.02	0.58	0.00	0.20	0.42	0.04	0.24	0.32	0.35
D15	0.13	0.27	0.02	0.88	0.02	0.13	0.43	0.03	0.33	0.27	0.39
D24	0.03	0.19	0.04	0.10	0.00	0.03	3.01	0.01	2.97	3.97	2.02
D25	0.05	0.14	0.01	0.29	0.00	0.03	1.97	0.00	1.36	1.66	1.28
D29	0.38	0.67	0.03	2.48	0.10	0.27	0.68	0.01	0.37	0.45	0.79
D30	1.40	2.43	0.24	1.79	0.38	1.51	1.09	0.39	0.79	0.33	1.62
D31	0.19	0.33	0.01	0.80	0.00	0.18	0.63	0.02	0.39	0.34	0.81
D32	0.08	0.17	0.01	0.05	0.00	0.07	0.40	0.01	0.26	0.35	0.41
D33	0.13	0.30	0.01	0.20	0.00	0.14	0.56	0.02	0.41	0.53	0.39
D34	0.03	0.39	0.04	0.56	0.00	0.04	1.30	0.01	0.21	0.78	1.46
D35	0.04	0.12	0.02	0.20	0.00	0.02	0.30	0.02	0.28	0.41	0.25
D35	0.04	0.12	0.02	0.20	0.00	0.02	0.30	0.02	0.28	0.41	0.25
D36	0.28	0.69	0.14	0.91	0.00	0.13	1.31	0.05	1.00	0.65	0.93
D39	0.19	0.70	0.08	1.23	0.28	0.34	1.35	0.03	0.60	1.01	1.53
D40	0.32	0.35	0.07	0.75	0.00	0.08	0.52	0.01	0.26	0.50	0.52
D41	0.42	0.39	0.05	0.86	0.00	0.12	1.16	0.02	0.37	0.55	1.04
D42	0.22	0.44	0.28	2.19	1.14	0.27	0.58	0.09	1.60	1.34	0.15
D43	0.39	0.88	0.10	2.46	0.28	0.58	0.84	0.07	0.54	0.45	0.67
D44	1.91	3.47	0.41	3.96	1.68	1.62	1.69	0.37	1.66	0.68	1.43
D45	1.27	2.39	0.30	4.67	0.36	1.03	1.12	0.25	1.18	0.54	0.97
D46	0.92	1.74	0.21	3.50	0.24	0.74	2.03	0.20	0.85	0.90	1.92

Sample	BJF	BEP	PER	DCA	ATT	COR	TPH	CCP	BGF	BBN	BNT
D47	0.50	1.04	0.12	2.13	0.11	0.53	1.32	0.12	0.80	0.74	1.82
D48	0.85	1.66	0.05	4.12	0.00	0.98	2.13	0.10	1.06	0.83	2.70
D49	0.16	0.25	0.01	0.43	0.00	0.10	0.22	0.04	0.18	0.08	0.16
D50	0.06	0.10	0.01	0.14	0.00	0.03	0.06	0.02	0.07	0.06	0.05
D51	0.33	0.76	0.16	0.16	0.00	0.18	0.50	0.09	0.49	0.25	0.36
D52	0.05	0.11	0.03	0.40	0.00	0.02	0.12	0.01	0.07	0.04	0.08
D53	0.21	0.64	0.19	1.03	0.13	0.11	0.37	0.06	0.41	0.24	0.39
D54	0.03	0.05	0.00	0.07	0.00	0.01	0.04	0.01	0.03	0.04	0.04
D55	0.11	0.21	0.00	0.59	0.04	0.05	0.20	0.03	0.15	0.07	0.19
D56	0.80	1.71	0.17	5.77	0.50	0.42	1.45	0.17	1.50	0.80	1.00
D57	0.32	0.56	0.07	1.02	0.03	0.13	0.38	0.07	0.23	0.13	0.27
D58	0.70	1.00	0.15	0.27	0.18	0.52	0.62	0.38	0.80	0.42	0.52
D59	0.15	0.23	0.02	0.28	0.00	0.05	0.18	0.02	0.17	0.10	0.15
D60	0.15	0.27	0.02	0.06	0.00	0.06	0.18	0.02	0.19	0.11	0.14
D61	0.05	0.11	0.01	0.13	0.00	0.02	0.12	0.01	0.15	0.16	0.09
D62	1.28	1.99	0.07	1.24	0.00	0.31	1.09	0.10	0.68	0.65	1.10

b)

Sample	1,4-O_2NAP	1-(CHO)NAP	9-OFLN	9,10-O_2ANT	1,4-O_2ANT	9,10-O_2PHE	11-OBaFLN	11-OBbFLN	BAN	7,12-O_2BAA	5,12-O_2NAC
D1	22.0	10.0	8.0	18.0	0	0	11.9	12.3	6.5	10.3	0.9
D4	14.4	30.8	16.3	4.8	0	0	3.9	7.2	8.0	12.8	2.0
D5	10.2	5.4	23.6	8.7	0	0	14.1	12.6	9.6	13.9	1.7
D6	9.7	17.6	15.7	9.5	0	8.0	8.9	8.4	10.4	10.5	1.3
D7	9.1	17.9	23.4	3.0	0	0	11.3	9.2	9.6	14.7	1.6
D12	5.2	25.3	26.2	5.3	0	4.6	10.8	6.7	7.4	7.6	0.8
D13	6.5	20.9	26.8	2.1	0	8.3	11.4	6.4	8.8	8.1	0.8
D14	24.7	17.3	14.3	8.9	2.0	0	10.5	8.2	6.4	6.5	1.1
D15	10.7	5.7	33.0	3.6	0	0	13.9	9.8	8.8	13.6	1.0
D24	7.1	4.1	3.7	2.3	0	33.3	20.0	13.3	13.1	2.7	0.5
D25	5.1	3.4	9.2	5.0	0	16.7	19.8	15.8	16.3	8.0	0.8
D29	56.3	6.5	9.6	4.1	0	0	6.8	4.6	7.6	3.8	0.6
D30	43.6	1.9	9.2	24.1	0	3.1	4.2	2.8	5.0	5.4	0.8
D31	10.9	10.2	28.7	6.4	0	0	15.7	9.9	9.3	8.2	0.7
D32	36.3	4.1	25.1	6.9	0	0	9.1	5.9	5.6	6.2	0.7
D33	11.7	12.1	18.6	3.5	0	0	11.1	13.1	18.7	9.2	1.9
D34	25.6	13.0	7.8	6.6	0	0	11.0	8.7	12.5	13.1	1.5
D35	23.9	27.7	19.4	7.1	0	0	5.7	5.9	6.6	3.1	0.5
D36	39.0	19.4	4.8	9.3	0	0	8.1	7.5	8.0	3.1	0.8
D39	33.6	15.0	4.2	8.0	0	0	7.2	6.7	14.9	9.0	1.4
D40	29.8	14.1	20.4	7.0	0	0	6.2	5.8	7.2	8.6	0.8
D41	47.8	11.3	11.4	5.5	0	0	4.3	5.0	6.7	6.9	1.1
D42	37.7	20.1	6.6	12.5	0	0	7.6	5.6	7.3	2.3	0.3
D43	21.8	4.5	14.1	45.1	0	0	3.9	2.5	4.0	3.5	0.5
D44	48.0	7.2	9.3	3.3	0	0	6.2	6.6	11.3	6.4	1.7

Sample	1,4-O_2NAP	1-(CHO)NAP	9-OFLN	9,10-O_2ANT	1,4-O_2ANT	9,10-O_2PHE	11-OBaFLN	11-OBbFLN	BAN	7,12-O_2BAA	5,12-O_2NAC
D45	49.7	8.4	8.7	4.5	0	0	6.9	6.1	8.5	5.6	1.6
D46	37.1	3.6	5.9	35.3	0	0	4.3	2.7	5.3	5.0	0.9
D47	38.4	12.9	6.7	26.8	0.1	0	3.8	3.0	4.8	3.0	0.7
D48	54.6	2.0	6.7	21.2	0	0	4.3	3.6	3.7	3.2	0.7
D49	19.3	10.3	19.4	18.1	0	0	7.1	8.5	11.9	4.1	1.3
D50	16.3	16.3	16.2	24.6	0	0	5.9	6.7	9.4	3.2	1.2
D51	30.1	8.4	24.1	13.6	0	0	5.4	5.9	8.5	3.0	1.0
D52	15.7	8.4	13.5	39.8	0	0	5.4	5.3	7.6	3.4	0.9
D53	61.3	6.4	9.2	10.3	0	0	3.2	3.4	3.9	1.9	0.4
D54	39.9	2.2	8.0	43.6	0	0	1.4	1.7	2.0	0.8	0.2
D55	40.2	3.3	11.1	36.5	0	0	1.7	2.6	2.6	1.7	0.4
D56	38.3	3.8	8.9	40.4	0	0	1.9	2.0	3.1	1.2	0.3
D57	46.9	4.0	10.5	30.0	0	0	1.7	2.7	2.7	1.1	0.5
D58	48.1	9.7	7.0	21.7	0	0	2.5	3.6	4.7	1.6	1.0
D59	40.9	3.2	10.6	37.0	0	0	1.8	2.0	2.9	1.2	0.4
D60	47.7	3.2	7.4	33.6	0	0	1.9	2.1	2.7	1.1	0.4
D61	19.2	39.9	11.1	3.0	0	0	6.8	5.7	10.5	2.8	1.1
D62	44.1	2.5	6.8	30.2	0	0	4.0	5.0	4.4	2.2	0.8

c)

Sample	Region & leg	2-NNAP	9-NANT	3-NPHE	2-NFLT	1-NPYR	2-NPYR	7-NBAA
D1	MS1	**21.1**	**20.6**	**8.4**	**45.3**	**3.1**	**1.1**	**0.3**
D4	MS1	**54.6**	**0.0**	**11.2**	**18.7**	**11.1**	**3.0**	**1.4**
D5	MS1	**14.3**	**0.0**	**31.7**	**39.4**	**8.0**	**0.8**	**5.8**
D6	MS1	**34.1**	**0.0**	**13.2**	**23.6**	**24.2**	**2.6**	**2.3**
D7	MS1	**48.2**	**0.0**	**25.2**	**10.1**	**10.7**	**2.7**	**3.1**
D12	NRS1	**44.0**	**0.0**	**22.3**	**22.0**	**8.0**	**2.9**	**0.8**
D13	NRS1	**54.1**	**0.0**	**25.4**	**9.1**	**6.8**	**2.0**	**2.6**
D14	NRS1	**60.7**	**0.0**	**8.9**	**18.1**	**8.5**	**2.7**	**1.1**
D15	SRS1	**51.0**	**0.0**	**21.9**	**21.3**	**4.0**	**0.7**	**1.2**
D24	OG1	**22.7**	**0.0**	**58.9**	**3.4**	**12.8**	**0.6**	**1.6**
D25	OG1	**40.2**	**0.0**	**34.7**	**6.0**	**17.2**	**1.4**	**0.5**
D29	AG1	**46.7**	**0.0**	**17.5**	**9.9**	**21.0**	**2.3**	**2.7**
D30	AG1	**57.3**	**0.0**	**12.0**	**20.7**	**8.2**	**1.6**	**0.2**
D31	AG2	**30.7**	**0.0**	**25.9**	**7.9**	**34.5**	**0.6**	**0.4**
D32	AG2	**39.0**	**0.0**	**16.2**	**22.1**	**19.9**	**0.8**	**2.0**
D33	AG2, OG2	**34.5**	**0.0**	**17.7**	**5.1**	**40.2**	**0.6**	**2.0**
D34	OG2	**21.8**	**0.0**	**22.5**	**10.6**	**27.8**	**0.4**	**17.0**
D35	OG2, AS2	**30.6**	**0.0**	**35.3**	**6.5**	**25.3**	**0.3**	**2.0**
D36	AS2	**47.7**	**0.0**	**11.9**	**10.3**	**25.6**	**1.2**	**3.3**
D39	AS2	**37.8**	**0.0**	**16.6**	**14.4**	**18.2**	**1.0**	**12.0**
D40	AS2	**42.3**	**0.0**	**3.6**	**4.3**	**43.1**	**0.4**	**6.3**
D41	AS2	**41.0**	**0.0**	**11.5**	**13.1**	**31.4**	**0.4**	**2.5**
D42	AS2, SRS2	**54.0**	**0.0**	**5.6**	**6.0**	**30.0**	**0.6**	**3.8**
D43	SRS2	**56.6**	**0.0**	**15.7**	**13.8**	**11.2**	**1.3**	**1.4**
D44	SRS2	**35.6**	**0.0**	**17.5**	**24.8**	**16.9**	**3.1**	**2.1**

Sample	Region & leg	2-NNAP	9-NANT	3-NPHE	2-NFLT	1-NPYR	2-NPYR	7-NBAA
D45	SRS2, NRS2	**39.9**	**0.0**	**12.5**	**21.6**	**20.9**	**2.5**	**2.7**
D46	NRS2	**18.3**	**65.2**	**3.7**	**5.4**	**2.4**	**0.4**	**4.5**
D47	NRS2	**70.1**	**0.0**	**8.8**	**8.5**	**8.2**	**0.7**	**3.7**
D48	NRS2	**53.5**	**22.4**	**6.9**	**8.9**	**4.8**	**0.7**	**2.9**
D49	MS2	**31.7**	**0.0**	**28.0**	**19.4**	**16.6**	**2.2**	**2.1**
D50	MS2	**44.6**	**0.0**	**14.1**	**13.6**	**22.9**	**1.9**	**2.9**
D51	MS2	**45.4**	**0.0**	**9.6**	**15.6**	**25.3**	**0.8**	**3.2**
D52	MS2	**43.2**	**0.0**	**11.2**	**19.6**	**22.6**	**0.5**	**2.9**
D53	MS2	**51.2**	**0.0**	**4.9**	**12.8**	**26.2**	**1.6**	**3.3**
D54	MS2	**30.5**	**30.7**	**2.9**	**11.5**	**21.0**	**1.4**	**2.0**
D55	MS2	**45.8**	**0.0**	**9.8**	**22.9**	**18.9**	**1.1**	**1.6**
D56	MS2	**41.1**	**0.0**	**13.3**	**19.6**	**22.1**	**1.0**	**2.8**
D57	MS2	**31.0**	**7.2**	**8.6**	**29.7**	**20.0**	**1.5**	**1.9**
D58	MS2	**64.2**	**2.9**	**24.4**	**6.4**	**0.8**	**1.2**	**0.1**
D59	MS2	**29.9**	**0.0**	**25.4**	**23.9**	**16.7**	**1.1**	**2.9**
D60	MS2	**45.7**	**0.0**	**21.0**	**4.9**	**24.3**	**1.1**	**3.1**
D61	MS2	**39.0**	**0.0**	**23.2**	**5.4**	**28.7**	**0.9**	**2.8**
D62	MS2	**41.4**	**0.0**	**21.9**	**10.1**	**21.4**	**2.5**	**2.7**

2.4 Source apportionment

2.4.1 Positive matrix factorization

Five factors of predominated anthropogenic sources with 61 % and 74% contribution to PM_{10} were identified based on two subsets of species (groups 1 and 2, respectively; Figs. 4, S4). The first factor, *desert dust*, was associated with high concentration of the Earth's crust elements (Ti, Mn, Fe, Co, Cr) and endosulfan sulfate (Figs. 4 and S4) a banned insecticide's metabolite still used in many countries despite the high toxicity to humans and its persistence in the environment (US EPA, 2002; Tuduri et al., 2006). The factor contributed to PM_{10} by 39 % and 36 % in the first and the second subset of species input, respectively (Fig. S4).

The second factor assigned as *aged ship emissions* contained primarily BC, Zn, Pb, Cd (Isakson et al., 2001; Viana et al., 2014) and also PAHs and their nitrated and oxygenated derivatives (Zhao et al., 2019, 2020). Diesel PM emitted by ship engines is a mixture of different kinds of particles with size spanning from few nanometers to several microns (di Natale and Carotenuto, 2015). The factor shows moderate to strong correlation with SO_2, CH_4, CO and O_3 (Pearson correlation coefficient r = 0.74/54, 0.64/65, 0.63/60 and 0.56/59) and a contribution of 26% and 35% to PM_{10} in PMF group 1 and 2, respectively.

The third factor (the forth factor in PMF group 2) was ascribed to *continental pollution*, which is characterized by a strong contribution of OC, Ni, PAHs, OPAHs, PCBs and several pesticide/insecticides (HCH, DDX and drins). Several studies showed that these substances can come from continental pollution (Menichini et al., 2007), The factor contributed by 18 and 10% to PM_{10}. The air masses of continental origin represent the second most important source of PAHs and OPAHs (Gevao et al., 2006; Romagnoli et al., 2016, 2019; Merico et al., 2017; Rhusdi et al., 2017; Javed et al., 2019).

The fourth factor (the third factor in PMF group 2), *fresh ship emissions*, dominated by EC, OC, PAHS, OPAHs and NPAHs (Yu et al., 2004; Gregoris et al., 2016; Merico et al., 2017; Zhao et al., 2019, 2020) and contributed by 15 % and 17% to PM_{10}. Fresh ship emissions represent the main source of PAHs as well as their nitrated and oxygenated derivatives in this campaign. The peaks in the factor time series correspond primarily to the stock emissions of the research vessel. The factor shows strong correlation with NO and SO_2 (Pearson correlation coefficient r = 0.85/80 and 0.69/56), gases heavily emitted from ship engines (Agrawal et al., 2008a, b) since around

15% of global anthropogenic NO_x and 5 – 8 % of global SO_x emissions are attributable to oceangoing ships (Eyring et al., 2005; Corbett et al., 2007).

The last factor, *residual oil combustion*, was represented by V, Ni and Mo i.e., markers for fuel oil/pet-coke combustion, petrochemical sources, or industrial emissions (Querol et al., 2002; Alleman et al., 2010). However, the calculated Ni/V ratio of 0.4 corresponds to the petro-chemical industry, mainly at the coasts (Alleman et al., 2010). The factor residual oil combustion moderately correlates with NO_2, SO_2 and CO (Pearson correlation coefficients r = 0.54/67; 0.50; 0.47). The factor contributed by 2% to PM_{10} (Fig. S4).

a) b)

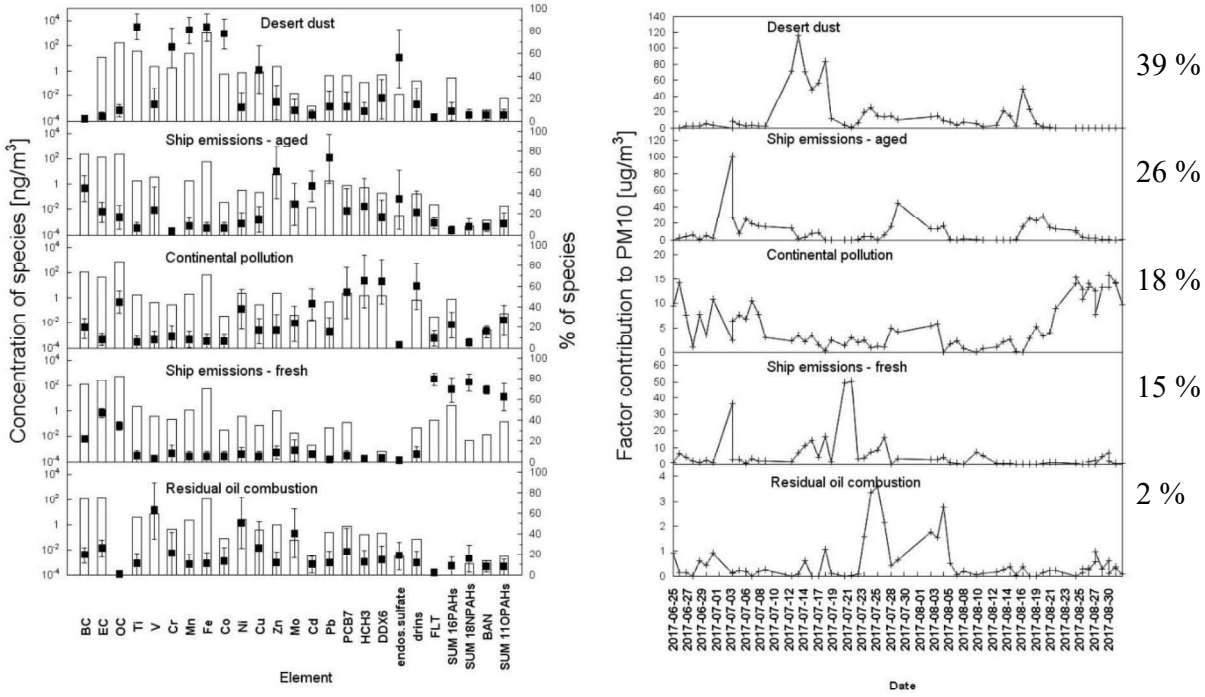

Figure S4. PMF group 1: a) Factor profiles (Bars: Concentration of the species, black squares: Percentage of the species explained, box: Displacement (DISP) average, whiskers: DISP max and DISP min) and b) time series of factor contributions to sample composition with their relative contributions.

Table S17. Relative concentration of target compounds in samples strongly influenced by own ship emissions (see Table S4 and Fig. S4) compared to average concentration of samples not influences by own ship emissions in the same region for a) PAHs, b) OPAHs and c) NPAHs.

a)

Substance	D16;17 compared to average of Southern Red Sea	D20;22;23;37;38 compared to average of Arabian Sea	D28 compared to average of Oman and Arabian Gulf
NAP	44.1	2.1	0.9
ACY	56.7	16.1	4.6
ACE	59.4	2.4	1.7
FLN	37.8	22.0	1.4
PHE	7.4	30.8	3.4
ANT	10.4	20.2	3.2
FLT	5.9	23.0	3.2
PYR	9.9	38.7	4.6
BAA	10.8	69.8	7.4
CHR	5.7	42.8	4.8
BBF	2.1	52.5	3.4
BKF	1.8	48.6	3.0
BAP	1.5	54.9	1.2
INP	1.5	58.4	2.2
DBA	0.4	2.0	0.8
BPE	1.9	84.1	3.5
Σ_{16}PAHs	9.3	27.7	3.3
BJF	2.5	48.7	4.3
BEP	2.2	55.4	3.9
PER	1.2	25.5	1.3
DCA	0.4	2.0	1.0
ATT	0.3	0.0	0.0
COR	1.5	42.3	2.7
TPH	7.7	45.7	4.8
CCP	0.5	1.1	0.1
BGF	4.7	61.2	4.8
BBN	17.4	63.7	5.5
BNT	7.7	30.5	3.5
Σ_{26}PAHs+BNT	9.0	28.2	3.3
RET	9.1	19.0	3.9

b)

Substance	D16;17 compared to average of Southern Red Sea	D20;22;23;37;38 compared to average of Arabian Sea	D28 compared to average of Oman and Arabian Gulf
1,4-O_2NAP	2.3	31.9	1.6
1-(CHO)NAP	21.2	46.7	4.5
9-OFLN	5.3	28.9	3.7
9,10-O_2ANT	3.1	8.1	1.3
1,4-O_2ANT	a	a	a
9,10-O_2PHE	a	a	6.2
11-OBaFLN	9.1	66.2	4.5
11-OBbFLN	7.4	42.0	4.9
BAN	7.9	31.2	4.8
7,12-O_2BAA	5.2	16.0	5.4
5,12-O_2NAC	12.1	25.7	12.3
Σ_{11}OPAHs	6.5	34.4	3.8

a: Quantified in contaminated samples but not possible to calculate ratio because <LOQ in stack filtered regional averages

c)

Substance	D16;17 compared to average of Southern Red Sea	D20;22;23;37;38 compared to average of Arabian Sea	D28 compared to average of Oman and Arabian Gulf
2-NNAP	4.0	27.9	2.6
3-NPHE	6.5	23.0	2.7
2-NFLT	1.0	5.6	0.9
1-NPYR	17.7	53.4	3.1
2-NPYR	11.5	64.9	7.8
7-NBAA	4.8	12.2	2.4
Σ_{17}NPAHs	5.5	32.1	2.6

2.4.2 Source attribution additional data

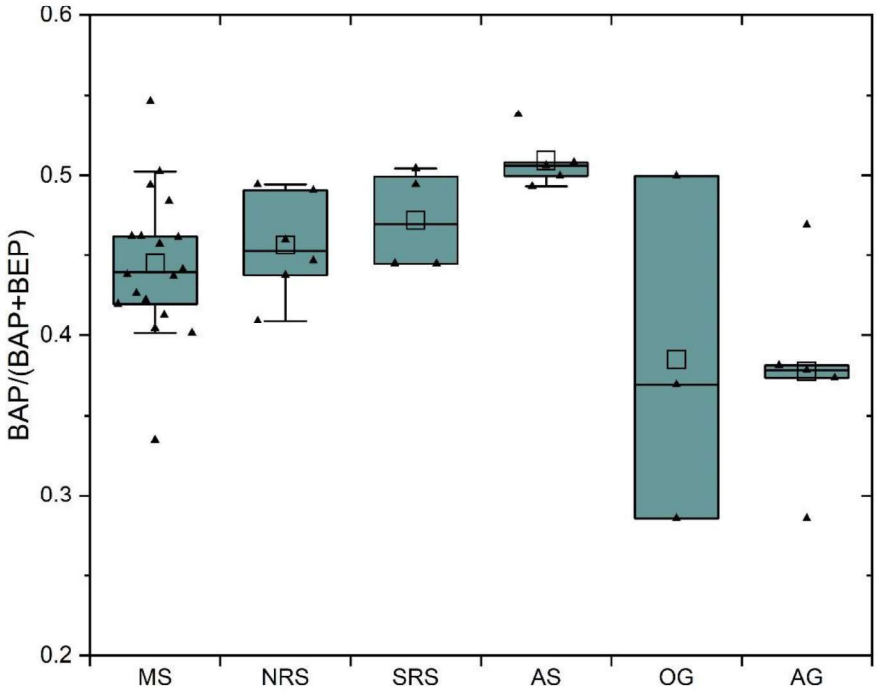

Figure S5. Box-Whisker plot of the ratios of the particulate concentrations of BAP/(BAP+BEP) across sea regions (without samples with BAP or BEP <LOQ; MS: Mediterranean Sea; NRS: Northern Red Sea; SRS: Southern Red Sea; AS: Arabian Sea; OG: Gulf of Oman; AG: Arabian Gulf; Empty square: Mean value; Filled, grey triangles: Measurement points; Box with additional borders: Interquartile range (IQR) bound by the 75th and 25th percentile and range of 1.5 IQR; Horizontal line: Median).

Table S18. Number of bypassing ships (n) influencing a) Digitel and b) impactor samples, based on ship counts based on same analysis as done in Celik et al. (2020).

a)

Sample	Amount of ship plumes	Sample	Amount of ship plumes	Sample	Amount of ship plumes
D1	0	**D22**	1	**D43**	9
D2	0	**D23**	1	**D44**	8
D3	0	**D24**	0	**D45**	2
D4	0	**D25**	41	**D46**	24
D5	0	**D26**	26	**D47**	24
D6	6	**D27**	0	**D48**	25
D7	31	**D28**	37	**D49**	2
D8	1	**D29**	28	**D50**	2
D9	3	**D30**	14	**D51**	1
D10	9	**D31**	4	**D52**	3
D11	8	**D32**	41	**D53**	6
D12	17	**D33**	35	**D54**	15
D13	28	**D34**	34	**D55**	4
D14	9	**D35**	11	**D56**	2
D15	19	**D36**	4	**D57**	10
D16	4	**D37**	0	**D58**	4
D17	25	**D38**	12	**D59**	1
D18	16	**D39**	21	**D60**	3
D19	0	**D40**	0	**D61**	0
D20	12	**D41**	21	**D62**	6
D21	18	**D42**	24		

b)

Sample	Amount of ship plumes	Sample	Amount of ship plumes
C1	29	**C16**	5
C2	19	**C17**	2
C3	67	**C18**	7
C4	0	**C19**	30
C5	37	**C20**	14
C6	29	**C21**	18
C7	10	**C22**	31
C8	0	**C23**	52
C9	0	**C24**	4
C10	0	**C25**	26
C11	0	**C26**	41
C12	1	**C27**	3
C13	41	**C28**	8
C14	1	**C29**	19
C15	4	**C30**	14

2.5 Mass size distributions

Substances	Sample C8 (03.08.), mostly fresh aerosol	Sample C7 (29.-30.07.), mostly aged aerosol
$\sum_{27}$PAHs	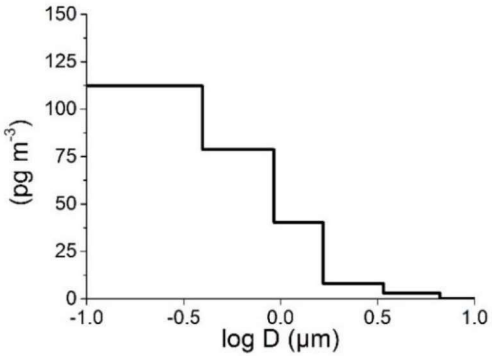	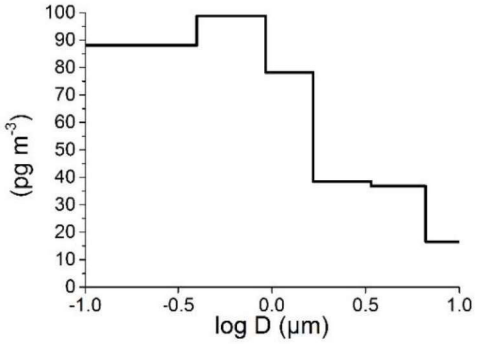
$\sum_{11}$OPAHs	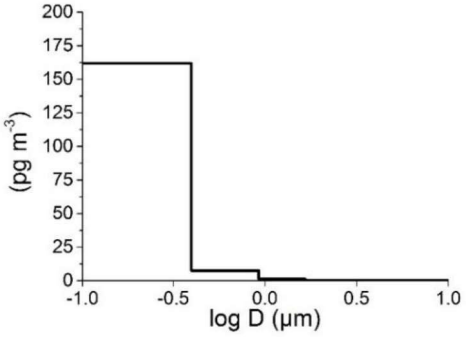	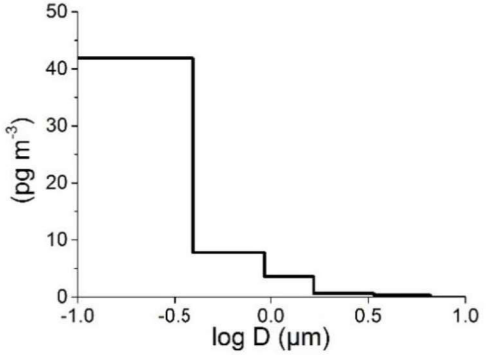

Substances	Sample C8 (03.08.), mostly fresh aerosol	Sample C7 (29.-30.07.), mostly aged aerosol
$\sum_{17}$NPAHs	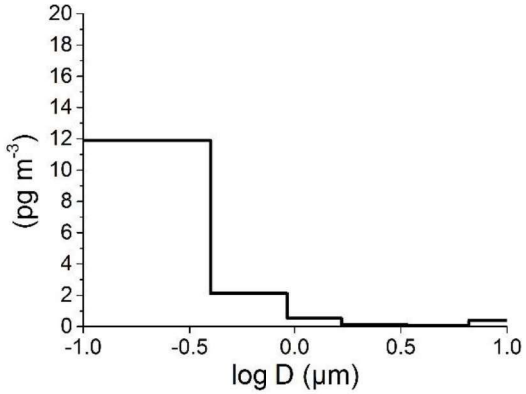	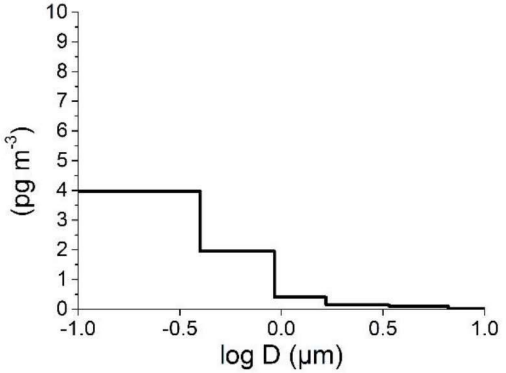

Fig. S6: Exemplary mass size distributions for fresh (1st column) and aged (2nd column) aerosols, respectively.

227

Table S19. Campaign average mass median diameter (MMD) (calculated from campaign average concentrations) of a) PAHs, b) OPAHs and c) NPAHs. (n.d.: not determined since not detected in particulate phase)

a)

Substance	MMD average (from average concentrations)	Detection frequency all stages (only filtered) [%]
NAP	1.87	24
ACY	n.d.	0
ACE	n.d.	0
FLN	n.d.	0
PHE	0.55	48
ANT	0.02	1
FLT	0.60	49
PYR	0.48	44
BAA	0.32	65
CHR	0.29	62
BBF	0.19	75
BKF	0.27	49
BAP	0.38	48
DBA	0.26	60
INP	0.43	15
BPE	0.26	74
BJF	0.23	58
BEP	0.22	66
PER	0.08	20
DCA	0.12	14
ATT	1.00	33
COR	0.18	38
TPH	0.25	46
CCP	0.12	6
BGF	0.27	54
BBN	0.12	10
BNT	0.47	56
RET	0.02	19

b)

Substance	MMD average (from average concentrations)	Detection frequency all stages (only filtered) [%]
1,4-O2NAP	8.49	1
1-(CHO)NAP	0.42	63
9-OFLN	0.02	17
9,10-O2ANT	0.02	17
1,4-O2ANT	n.d.	0
9,10-O2PHE	n.d.	0
11-OBaFLN	0.13	37
11-OBbFLN	0.07	36
BAN	0.07	27
7,12-O2BAA	0.07	57
5,12-O2NAC	0.08	72

c)

Substance	MMD average (from average concentrations)	Detection frequency all stages (only filtered) [%]
1-NNAP	4.65	1
2-NNAP	0.02	8
3-NACE	0.02	1
5-NACE	0.02	8
2-NFLN	n.d.	0
9-NANT	0.02	1
9-NPHE	n.d.	0
3-NPHE	0.06	3
2-NFLT	0.08	47
1-NPYR	0.04	35
2-NPYR	0.05	17
7-NBAA	0.05	10
6-NCHR	n.d.	0
1,3-N2PYR	n.d.	0
1,6-N2PYR	n.d.	0
1,8-N2PYR	n.d.	0
6-NBAP	0.03	3

3 References

Agrawal, H., Malloy, Q. G. J., Welch, W. A., Miller, J. W., and Cocker, D. R.: In-use gaseous and particulate matter emissions from a modern ocean going container vessel, Atmos. Environ., 42, 5504–5510, https://doi.org/10.1016/j.atmosenv.2008.02.053, 2008a.

Agrawal, H., Welch, W. A., Miller, J. W., and Cocker, D. R.: Emission measurements from a crude oil tanker at sea, Environ. Sci. Technol., 42, 7098–7103, https://doi.org/10.1021/es703102y, 2008b.

Alleman, L. Y., Lamaison, L., Perdrix, E., Robache, A., and Galloo, J.-C.: PM_{10} metal concentrations and source identification using positive matrix factorization and wind sectoring in a French industrial zone, Atmos. Res., 96, 612–625, https://doi.org/10.1016/j.atmosres.2010.02.008, 2010.

Bourtsoukidis, E., Ernle, L., Crowley, J. N., Lelieveld, J., Paris, J.-D., Pozzer, A., Walter, D., and Williams, J.: Nonmethane hydrocarbon (C2–C8) sources and sinks around the Arabian Peninsula, Atmos. Chem. Phys., 19, 7209–7232, https://doi.org/10.5194/acp-19-7209-2019, 2019.

Cavalli, F. and Putaud, J. P.: Toward a standardized thermal-optical protocol for measuring atmospheric organic and elemental carbon: The EUSAAR protocol, Report #EUR 23441 EN, Office for Official Publications of the European Communities, Luxembourg, 2008.

Celik, S., Drewnick, F., Fachinger, F., Brooks, J., Darbyshire, E., Coe, H., Paris, J.-D., Eger, P. G., Schuladen, J., Tadic, I., Friedrich, N., Dienhart, D., Hottmann, B., Fischer, H., Crowley, J. N., Harder, H., and Borrmann, S.: Influence of vessel characteristics and atmospheric processes on the gas and particle phase of ship emission plumes: in situ measurements in the Mediterranean Sea and around the Arabian Peninsula, Atmos. Chem. Phys., 20, 4713–4734, https://doi.org/10.5194/acp-20-4713-2020, 2020.

Corbett, J. J., Winebrake, J. J., Green, E. H., Kasibhatla, P., Eyring, V., and Lauer, A.: Mortality from ship emissions: a global assessment, Environ. Sci. Technol., 41, 8512–8518, https://doi.org/10.1021/es071686z, 2007.

Di Natale, F. and Carotenuto, C.: Particulate matter in marine diesel engines exhausts: Emissions and control strategies, Transp. Res. D Transp. Environ., 40, 166–191, https://doi.org/10.1016/j.trd.2015.08.011, 2015.

Eger, P. G., Friedrich, N., Schuladen, J., Shenolikar, J., Fischer, H., Tadic, I., Harder, H., Martinez, M., Rohloff, R., Tauer, S., Drewnick, F., Fachinger, F., Brooks, J., Darbyshire, E., Sciare, J., Pikridas, M., Lelieveld, J., and Crowley, J. N.: Shipborne measurements of $ClNO_2$ in the Mediterranean Sea and around the Arabian Peninsula during summer, Atmos. Chem. Phys., 19, 12121–12140, https://doi.org/10.5194/acp-19-12121-2019, 2019.

Eyring, V., Köhler, H. W., van Aardenne, J., and Lauer, A.: Emissions from International Shipping: 1. The last 50 Years, J. Geo-phys. Res., 110, D17305, https://doi.org/10.1029/2004JD005619, 2005.

Gevao, B., Al-Bahloul, M., Al-Ghadban, A. N., Ali, L., Al-Omair, A., Helaleh, M., Al-Matrouk, K., and Zafar, J.: Passive sampler-derived air concentrations for polybrominated diphenyl ethers and polycyclic aromatic hydrocarbons in Kuwait, Environ. Toxicol. Chem., 25, 1496–502, https://doi.org/10.1897/05-442R.1, 2006.

Gregoris, E., Barbaro, E., Morabito, E., Toscano, G., Donateo, A., Cesari, D., Contini, D., and Gambaro, A.: Impact of maritime traffic on polycyclic aromatic hydrocarbons, metals and particulate matter in Venice air, Environ. Sci. Pollut. Res., 23, 6951–6959, https://doi.org/10.1007/s11356-015-5811-x, 2016.

Isakson, J., Persson, T. A., and Lindgren, S.: Identification and assessment of ship emissions and their effect in the harbour of Göteborg, Sweden, Atmos. Environ., 35, 3659–3666, https://doi.org/10.1016/S1352-2310(00)00528-8, 2001.
Javed, W., Iakovides, M., Stephanou, E. G., Wolfson, J. M., Koutrakis, P., and Guo, B.: Concentrations of aliphatic and polycyclic aromatic hydrocarbons in ambient $PM_{2.5}$ and PM_{10} particulates in Doha, Qatar, J. Air Waste Manag. Assoc., 69, 2, 162–177, https://doi.org/10.1080/10962247.2018.1520754, 2019.
Menichini, E., Iacovella, N., Monfredini, F., and Turrio-Baldassarri, L.: Atmospheric pollution by PAHs, PCDD/Fs and PCBs simultaneously collected at a regional background site in central Italy and at an urban site in Rome, Chemosphere, 69, 422–434, https://doi.org/10.1016/j.chemosphere.2007.04.078, 2007.
Merico, E., Gambaro, A., Argiriou, A., Alebic-Juretic, A., Barbaro, E., Cesari, D., Chasapidis, L., Dimopoulos, S., Dinoi, A., Donateo, A., Giannaros, C., Gregoris, E., Karagiannidis, A., Konstandopoulos, A. G., Ivošević, T., Liora, N., Melas, D., Mifka, B., Orlić, I., Poupkou, A., Sarovic, K., Tsakis, A., Giua, R., Pastore, T., Nocioni, A., and Contini, D.: Atmospheric impact of ship traffic in four Adriatic-Ionian port-cities: Comparison and harmonization of different approaches, Transport. Res. D, 50, 431–445, https://doi.org/10.1016/j.trd.2016.11.016, 2017.
Niessner, R. and Wilbring, P.: Ultrafine particles as trace catchers for polycyclic aromatic hydrocarbons: the photoelectric aerosol sensor as a tool for in situ sorption and desorption studies, Anal. Chem., 61, 708–714, https://doi.org/10.1021/ac00182a014, 1989.
Querol, X., Alastuey, A., Rosa, J. d. l., Sánchez, A., Plana, F., and Ruiz, C. R.: Source apportionment analysis of atmospheric particulates in an industrialized urban site in southwestern Spain, Atmos. Environ., 36, 3113–3125, https://doi.org/10.1016/S1352-2310(02)00257-1, 2002.
Romagnoli, P., Balducci, C., Perilli, M., Perreca, E., and Cecinato, A.: Particulate PAHs and n-alkanes in the air over Southern and Eastern Mediterranean Sea, Chemosphere 159, 516–525, https://doi.org/10.1016/j.chemosphere.2016.06.024, 2016.
Romagnoli, P., Balducci, C., Perilli, M., Perreca, E., and Cecinato, A.: Organic molecular markers in marine aerosols over the Western Mediterranean Sea, Environ. Pollut., 248, 145–158, https://doi.org/10.1016/j.envpol.2019.02.020, 2019.
Rushdi, A. I., El-Mubarak, A. H., Lijotra, L., Al-Otaibi, M. T., Qurban, M. A., Al-Mutlaq, K. F., and Simoneit, B. R. T.: Characteristics of organic compounds in aerosol particulate matter from Dhahran city, Saudi Arabia, Arab. J. Chem., 10, S3532–S3547, https://doi.org/10.1016/j.arabjc.2014.03.001, 2017.
Tadic, I., Crowley, J. N., Dienhart, D., Eger, P., Harder, H., Hottmann, B., Martinez, M., Parchatka, U., Paris, J.-D., Pozzer, A., Rohloff, R., Schuladen, J., Shenolikar, J., Tauer, S., Lelieveld, J., and Fischer, H.: Net ozone production and its relationship to nitrogen oxides and volatile organic compounds in the marine boundary layer around the Arabian Peninsula, Atmos. Chem. Phys., 20, 6769–6787, https://doi.org/10.5194/acp-20-6769-2020, 2020.
Tuduri, L., Harner, T., Blanchard, P., Li, Y.-F., Poissant, L., Waite, D. T., Murphy, C., and Belzer, W. : A review of currently used pesticides (CUPs) in Canadian air and precipitation: Part 1: Lindane and endosulfans, Atmos. Environ., 40, 1563–78, https://doi.org/10.1016/j.atmosenv.2005.11.034, 2006.

USEPA (United States Environmental Protection Agency): Reregistration eligibility decision for Endosulfan, EPA 738-R-02-013, Prevention, Pesticides and Toxic Substances (7508C), 2002.
USEPA (United States Environmental Protection Agency): EPA Positive Matrix Factorization (PMF) 5.0 Fundamentals and User Guide, EPA/600/R-14/108, 2004.
USEPA (United States Environmental Protection Agency): Estimation Programs Interface Suite™ for Microsoft® Windows, v 4.11, 2019.
Viana, M., Hammingh, P., Colette, A., Querol, X., Degraeuwe, B., de Vlieger, I., and van Aardenne, J.: Impact of maritime transport emissions on coastal air quality in Europe, Atmos. Environ., 90, 96–105, https://doi.org/10.1016/j.atmosenv.2014.03.046, 2014.
Yu, J. Z., Tung, J. W. T., Wu, A. W. M., Lau, A. K. H., Louie, P. K. K., and Fung, J. C. H.: Abundance and seasonal characteristics of elemental and organic carbon in Hong Kong PM_{10}, Atmos. Environ., 38, 1511–1521, https://doi.org/10.1016/j.atmosenv.2003.11.035, 2004.
Zhao, J., Zhang, Y., Wang, T., Sun, L., Yang, Z., Lin, Y., Chen, Y., and Mao, H.: Characterization of $PM_{2.5}$-bound polycyclic aromatic hydrocarbons and their derivatives (nitro-and oxy-PAHs) emissions from two ship engines under different operating conditions, Chemosphere, 225, 43–52, https://doi.org/10.1016/j.chemosphere.2019.03.022, 2019.
Zhao, J., Zhang, Y., Chang, J., Peng, S., Hong, N., Hu, J., Ly, J., Wang, T., and Mao, H.: Emission characteristics and temporal variation of PAHs and their derivatives from an ocean-going cargo vessel, Chemosphere, 249, 126194, https://doi.org/10.1016/j.chemosphere.2020.126194, 2020.

2.3 Oxidative potential of PACs

This chapter represents the almost final state of a manuscript in preparation for submission as a research article to the peer reviewed scientific journal *Environmental Science & Technology*. As the first author of this manuscript, I was significantly involved in the design of the study. I planned the experiments and evaluated most of the data. Furthermore, I was mainly responsible for the processing, analysis, and visualization of the data. I wrote the first draft of the manuscript, organized the contributions from the coauthors and edited the manuscript based on feedback and exchange with the coauthors.

To be submitted to Environ. Sci. Tech. (2022)

Oxidative potential of polycyclic aromatic compounds (PACs) in particulate matter: measurement and prediction by chemical structure and reduction potential

M. Wietzoreck[1], A. Filippi[1], S. Hildmann[1], B. Mashtakov[1], P. Shahpoury[1,2], J. Wilson[1], T. Berkemeier[1], U. Pöschl[1], H. Tong[1,3], G. Lammel[1], B. A. M. Bandowe[1]

[1]Department of Multiphase Chemistry, Max Planck Institute for Chemistry, Mainz, 55128, Germany

[2]Air Quality Research Division, Environment and Climate Change Canada, Toronto, M3H 5T4, Canada

[3]Department of Civil and Environmental Engineering, The Hong Kong Polytechnic University, Hong Kong, China

Oxidative potential of polycyclic aromatic compounds (PACs) in particulate matter: measurement and prediction by chemical structure and reduction potential

Marco Wietzoreck[1], Alexander Filippi[1], Jake Wilson[1], Stefanie Hildmann[1], Boris Mashtakov[1], Pourya Shahpoury[1,2], Thomas Berkemeier[1], Haijie Tong[1,3], Ulrich Pöschl[1], Gerhard Lammel[1], Benjamin A. Musa Bandowe[1]

[1]Department of Multiphase Chemistry, Max Planck Institute for Chemistry, Mainz, 55128, Germany

[2]Air Quality Research Division, Environment and Climate Change Canada, Toronto, M3H 5T4, Canada

[3]Department of Civil and Environmental Engineering, The Hong Kong Polytechnic University, Hong Kong, China

Abstract

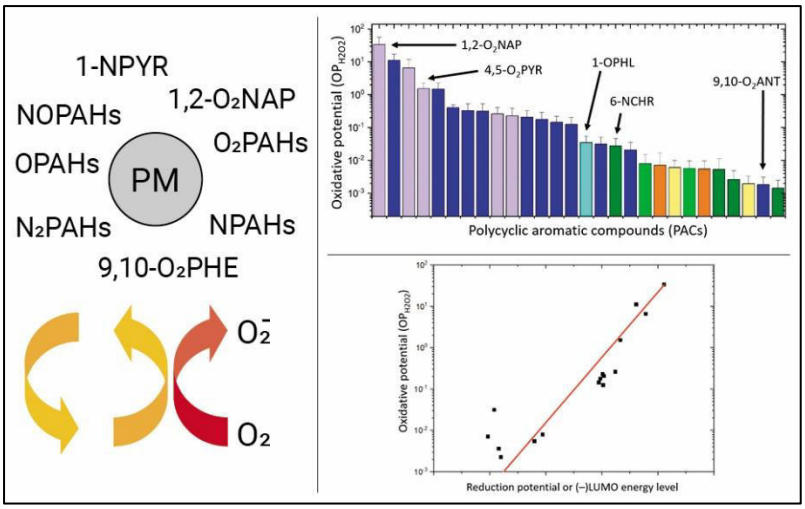

The oxidative potential (OP) of aerosols particles and their individual chemical components is an important metric for estimating their adverse health effects due to inhalation. Certain polycyclic aromatic compounds (PACs) cause oxidative stress via the generation of reactive oxygen species (ROS: H_2O_2, $^{\cdot}OH$, $O_2^{\cdot-}$). However, existing studies focus mostly on a limited set of low molecular weight quinones. In this work, we determine the OP of the largest ever reported dataset of atmospherically relevant oxygenated and nitrated polycyclic aromatic hydrocarbons (OPAHs and NPAHs) using two acellular methods, the dithiothreitol (DTT) depletion assay and the H_2O_2 formation assay. We confirm the importance of 1,2-naphthoquinone, 1,4-naphthoquinone and 9,10-phenanthrenequinone on the OP of particulate matter (PM) through a high OP in both assays. Additionally, we demonstrate for the first time that 4- and 5-ring quinones can play a significant role, too. Although we observe that several NPAHs produce ROS, they do not contribute significantly to the overall OP of all 39 analyzed PACs. Utilizing the large dataset, we demonstrate predictability of the OP by the molecular structure, the one-electron reduction potential and the energy level of the lowest unoccupied molecular orbital (LUMO). The gained knowledge could be used e.g. for structure activity relationship for classification of newly detected pollutants or in models calculating the ROS formation of aerosols.

Keywords: Oxidative potential, polycyclic aromatic compounds, ambient particulate matter, air pollution health effects, predictability, reactive oxygen species, quinones.

Synopsis: This work provides a large dataset of the oxidative potential of polycyclic aromatic compounds and an approach for its predictability by the molecular structure and physico-chemical properties such as reduction potential and LUMO energy level.

1. Introduction

Air pollution is a major contributor to the global burden of diseases such as chronic obstructive pulmonary diseases (COPD), respiratory diseases and cancer.[1-5] The adverse effects on human health have been linked to the concentration of fine particulate matter (PM), as well as specific chemicals, such as polycyclic aromatic compounds (PACs). PACs, which include polycyclic aromatic hydrocarbons (PAHs), oxygenated PAHs (OPAHs), nitrated PAHs (NPAHs) and nitrated ketones (NOPAHs) among others, are products of combustion processes, with some OPAHs and NPAHs additionally formed from post-emission photochemical conversion of PAHs.[6-8] Several PACs are known to be mutagenic and are classified as human carcinogens.[9,10] One proposed mechanism by which OPAHs, NPAHs and NOPAHs are believed to instigate adverse health effects is via the production of excess reactive oxygen species (ROS).[11-14] ROS oxidize cells, tissues and biological molecules, such as DNA, resulting in mutation and injury to cells.[15,16] Hence, the ability of PACs to produce ROS should be considered an important criterion by which to judge their toxicity and their adverse effects on human health. Oxidative potential (OP) is an umbrella term used to describe the ability of chemicals including PACs to produce ROS.[17,18] Several tests (cellular and acellular) have been developed to measure the OP of PACs.[18,19] For instance, the dithiothreitol (DTT) assay measures the ability of a compound to oxidize a thiol group,[20,21] thus mimicking reactions that may take place with physiologically relevant antioxidants such as glutathione[22] or cellular reducing agents such as nicotinamide adenine dinucleotide phosphate (NADPH).[20] Another acellular OP assay measures the ability of a compound to produce H_2O_2 after oxidizing ascorbic acid.[23] To produce ROS, PACs such as

quinones are reduced by antioxidants to form a radical. Subsequently, the reduced PAC will be oxidized back to the PAC by molecular oxygen, while the oxygen is reduced to the superoxide anion ($O_2^{\cdot-}$), which can further react to hydrogen peroxide (H_2O_2) and OH radicals.[11,16,24,25]

Acellular assays have suggested that 1,2-naphthoquinone (1,2-O_2NAP), 1,4-naphthoquinone (1,4-O_2NAP) and 9,10-phenanthrenequinone (9,10-O_2PHE) have the highest OP among quinones.[23,26] Other studies noted a relatively high OP for 5-hydroxy-1,4-naphthoquinone.[27-30] To the best of our knowledge, apart from quinones, no other PAH derivatives have been measured in an acellular assay yet. However, studies using cellular assays have identified NPAHs and other non-quinone OPAHs as having ROS producing abilities.[12-14,31-33]

OPAHs and NPAHs with diverse molecular size and structure have already been measured in air samples,[6,8] many of which have not been considered in OP studies to this date. However, it remains unclear whether these compounds may produce ROS and contribute to oxidative stress. Currently, there is no complete understanding of the properties that determine the ROS producing abilities of these compounds.

The (bio-)chemical reactions that result in the production of ROS and the reactions that lead to adverse health effects of PACs are redox reactions in which PACs can serve as one electron donors and acceptors.[11,34-36] Hence, it is conceivable that the energy level of the lowest unoccupied molecular orbital (LUMO) and the standard reduction potential could be used to predict ROS production abilities.[35,37-39] In a recent study, Shahpoury et al. (2021)[40] used the empirical reduction potential to characterize the OP of $PM_{2.5}$ containing redox-active species. The ability of PACs to produce ROS is potentially influenced by its chemical structure, such as number of aromatic rings, presence of electron-withdrawing or -donating substituents, and their ability to stabilize the formed intermediate radical.[41-43] To the best of our knowledge, there has

not been a study that systematically connects the structural or physico-chemical properties of OPAHs and NPAHs identified in ambient air to their OP.

Therefore, in this study, we have selected 39 PACs including OPAHs (quinones and ketones), NPAHs, and nitrated ketones (NOPAHs) plus 1,4-benzoquinone (1,4-BQ) that have already been quantified in air samples.[6,8,44-49] We evaluated the OP of these chemicals using the DTT depletion and H_2O_2 formation assay, targeting the PACs' ability to oxidize antioxidants, and to form ROS, respectively.

We aimed to evaluate how the PACs' structural and physico-chemical properties can be used to predict the compounds' OP. Specifically, we aimed to answer the following questions: [a] what is the OP of ambient PACs using the DTT and H_2O_2 assays? [b] Are the reduction potential and the LUMO energy level good predictors for OP? [c] What are the effects of molecular size, structure of the carbon chain and the presence and position of functional groups on the OP? [d] Which PACs contribute the most to the overall additive OP of all 39 targeted PACs in a model PM sample?

2. Materials and Methods

All target substances are shown in Table S1 in the Supporting Information (SI).

2.1. H_2O_2 formation assay

The ability to form the ROS species H_2O_2 in a simulated epithelial lung fluid (SELF) was examined by the fluorescence-based hydrogen peroxide assay (MAK165, Sigma Aldrich, Germany). The assay itself was performed similarly to Tong et al. (2018).[50] Briefly: the SELF was prepared based on the instructions from Boisa et al. (2014)[51] (composition shown in Table S2) but modified as explained in Section S1.2 in the SI to ensure a homogeneous and non-

inflammatory fluid. The antioxidants were freshly prepared on a daily basis and added prior to the start of the experiment to prevent oxidation prior to the experiment. For that purpose, stock solutions of the antioxidants (uric acid, Sigma Aldrich, Germany) (3.2 g L^{-1}) in 0.05 M NaOH (Sigma Aldrich, Germany) and ascorbic acid (Sigma Aldrich, Germany) (1.8 g L^{-1}) in ultra-pure water) were prepared in Nalgene HDPE bottles (Fisher Scientific, Germany) to prevent contamination by transitions metals from glass surfaces.

All target compounds were dissolved in dimethyl sulfoxide (DMSO) (for analysis, Fisher Scientific, Germany) (0.1 mg mL^{-1}) in order to ensure the solubility of all analytes. Each analyte stock solution was spiked into the SELF solution to obtain solutions of the analyte in SELF with concentrations of 1 and 7.5 µg mL^{-1}. The amount of formed H_2O_2 from 1,2-naphthoquinone, 1,4-naphthoquinone and 9,10-phenanthrenequinone exceeded the H_2O_2 calibration curve at the before mentioned concentrations. Hence, the samples were diluted before measuring the H_2O_2 concentration (end concentration of 10 and 25 ng mL^{-1}). After adding the antioxidants (1:100 of the total volume), the samples were incubated for 20 min at room temperature without shaking. Subsequently, three aliquots of 50 µL from each sample were transferred to a 96 well plate and 50 µL of the detection reagent was added. After the incubation time of 15 min, the fluorescence intensity (l_{ex} = 540 nm; l_{em} = 590 nm) was measured using a fluorescence plate reader (Synergy Neo, BioTek, Winooski, United States). The amount of formed H_2O_2 was calculated based on a seven-point H_2O_2 calibration curve. An exemplary calibration curve is shown in Figure S1A in the SI. Each sample was measured in triplicate and the average value was blank corrected by a triplicate measurement of a SELF solution without any analyte. All compounds were measured at least in duplicate and the average of all values was calculated.

2.2. DTT depletion assay

The measurement of the activity of the investigated analytes in a DTT assay was performed as outlined in Tong et al. (2018).[50] Briefly summarized: We dissolved the respective substances at 0.1 mg mL^{-1} in acetonitrile and then diluted them in phosphate buffer (0.05 M potassium monobasic-sodium hydroxide with 1 mM ethylenediaminetetraacetic acid (EDTA) to prevent contamination from transition metals) to an analyte-specific level, which allowed us to reliably observe its activity over at least one hour. A DTT solution of 1 mM was prepared in phosphate buffer and mixed with the analyte solution to obtain a final concentration of 100 µM of DTT. Following this step, immediately the first aliquot of the sample in triplicate was withdrawn from each mixture in order to measure the remaining DTT: The aliquot was quenched into an excess solution (1 mM in phosphate buffer) of Ellman's reagent (5,5′-dithiobis-(2-nitrobenzoic acid) or DTNB) in a 96-well plate. The samples were immediately analyzed in a plate reader (Synergy Neo, BioTek, Winooski, United States) at 412 nm wavelength. After distinct time intervals (15 min to several hours depending on the analyte), additional aliquots were withdrawn and the remaining DTT was measured. Following these measurements, the DTT activity was obtained by regression analysis of the decaying response of the DTT-DTNB adduct. The DTT concentration was calculated by comparison with a six-point calibration of a DTT concentration between 0 and 120 µM. An exemplary calibration curve is shown in Figure S1B in the SI. After normalization of this decay by the concentration of the analyte in the solution, a substance-specific DTT-depletion rate is obtained.

2.3. Reduction potential and LUMO energy level values

Reduction potential and LUMO energy level values were collected from literature. Only for a few PACs the published literature reports standard reduction potentials in aqueous solution.[39,52,53]

Several studies reported the reduction potential in organic solvents.[35,43,54] Nevertheless, the reduction potential values of PACs in aqueous solution can be estimated from the ones measured in organic solvents due to a linear relationship with high correlation.[53,55] For that purpose, we plotted the reduction potential values of PACs in aqueous solution with the same compounds measured in another solvent. Based in the linear fit, we estimated the reduction potential of PACs in aqueous phase which were not available. Similarly, LUMO energy level values reported in the literature are not based on the same methods and input parameters. Most LUMO energy level values in the literature are calculated by the density functional theory (DFT) but using different DFT levels (basis sets) and the solvent effect of different solvents.[56-58] However, the literature values calculated using different DFT levels and with different solvents have a high correlation and hence can be converted to one common method. More details about the reduction potential and LUMO energy level values can be found in the Sections S2.3 and S2.5 in the SI, respectively.

3. Results and Discussion

3.1. H_2O_2 formation assay

As shown in Figure 1A, 26 out of the 40 target compounds produce H_2O_2 in this assay. The exact values including the standard deviations are shown in Table S3 in the SI. The H_2O_2 formation of the compounds ranges from 33.7 $\mu M_{H2O2}\ \mu M_{PAC}^{-1}$ to $1.4x10^{-3}$ $\mu M_{H2O2}\ \mu M_{PAC}^{-1}$. The highest H_2O_2 formation potentials are shown by 1,2-O_2NAP, 1,4-O_2NAP and 9,10-O_2PHE (33.7 $\mu M_{H2O2}\ \mu M_{PAC}^{-1}$, 11.1 $\mu M_{H2O2}\ \mu M_{PAC}^{-1}$ and 6.5 $\mu M_{H2O2}\ \mu M_{PAC}^{-1}$, respectively) similar to previous reports.[23,26,28] All of these earlier studies observed a high H_2O_2 formation by 1,2-O_2NAP, 1,4-O_2NAP, 9,10-O_2PHE and 5-OH-1,4-O_2NAP. Charrier et al. (2014) reported 44 $\mu M_{H2O2}\ \mu M_{PAC}^{-1}$, 1.3 $\mu M_{H2O2}\ \mu M_{PAC}^{-1}$ and 2.6 $\mu M_{H2O2}\ \mu M_{PAC}^{-1}$ for 1,2-O_2NAP, 1,4-O_2NAP,

9,10-O_2PHE, respectively.[23] Such small differences between the studies are attributable to differences in reaction time, reductant and method of evaluation.[23,26,28]

Our results also demonstrate for the first time that other PAH derivatives (besides the above four quinones) are active H_2O_2 producers despite an up to four orders of magnitude lower OP than 1,4-O_2NAP (Figure 1A). Many of the compounds that have shown to be active in our current study have never been previously tested with an H_2O_2 formation assay or were reported not to be active (1,4-chrysenequinone (1,4-O_2CHR), 9,10-anthraquinone (9,10-O_2ANT) and 5,12-naphthacene-quinone (5,12-O_2NAC)).[26] As shown in Figure 1, 2-OH-1,4-O_2NAP, 2-methyl-1,4-naphthoquinone (2-M-1,4-O_2NAP) and 1,4-phenanthrene-quinone (1,4-O_2PHE), which are isomers and derivatives of the four previously reported H_2O_2 producers, are relevant H_2O_2 producers, too. The H_2O_2 formation of 2-M-1,4-O_2NAP is 0.21 μM_{H2O2} μM_{PAC}^{-1}, almost 2 orders of magnitude lower than the one of 1,4-O_2NAP. In addition, 4- and 5-ring quinones (4,5-pyrenequinone (4,5-O_2PYR), 1,4-O_2CHR, 5,6-O_2CHR, 5,12-O_2NAC, and different benzo[a]pyrene quinones (O_2BAPs), i.e. 4,5-O_2BAP, 1,6-O_2BAP, and 1,6-O_2BAP) have a high OP_{H2O2} as well. The OP_{H2O2} of 5,6-O_2CHR (0.26 μM_{H2O2} μM_{PAC}^{-1}) is only one order of magnitude lower than of 1,2-O_2NAP. This study also shows that besides quinones, other compound groups such as ketones (1-phenalenone (1-OPHL)), heterocyclic aromatic compounds and anhydrides (6H-benzo[c]chromen-6-one, 1,8-naphthalic anhydride), NPAHs and NOPAHs show measurable ROS formation in an acellular assay. 1-OPHL has, with 0.03 μM H_2O_2 μM^{-1}, the highest OP_{H2O2} among all non-quinone target compounds. It is an efficient singlet oxygen sensitizer and used as reference compound for this purpose.[59,60] Until now, ROS formation of NPAHs (6-nitrochrysene (6-NCHR), 1-nitropyrene (1-NPYR), 3-nitrofluoranthene (3-NFLT) and 9-nitroanthracene (9-NANT)), NOPAHs (3-nitrobenzanthrone (3-NBAN)) and ketones (9-fluorenone (9-OFLN)) has only been detected in cellular assays.[12-14,31-33]

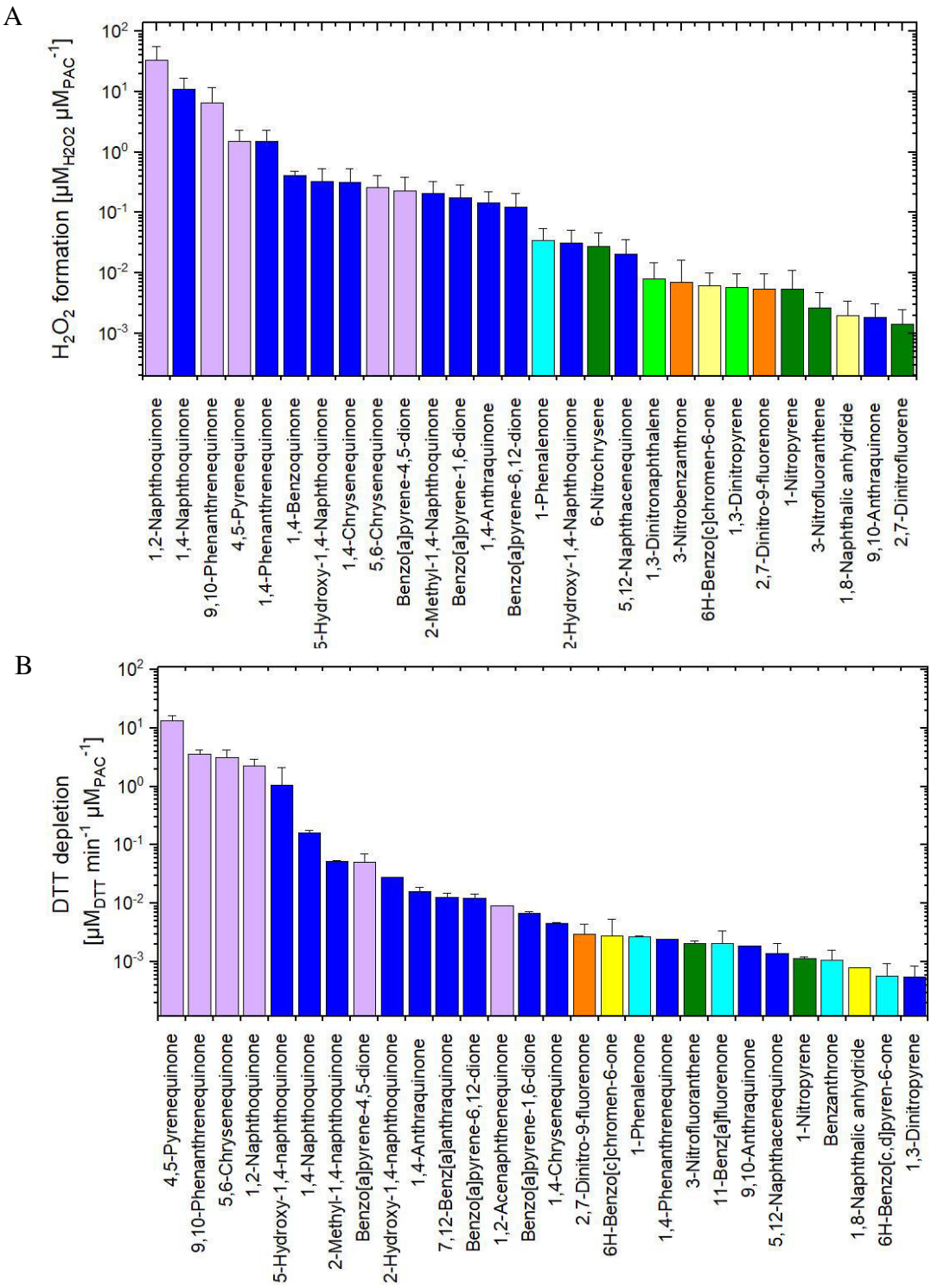

Figure 1. [A] H_2O_2 formation of target compounds in SELF. H_2O_2 formation was measured after 20 min reaction time and 15 min assay incubation time. Error bars represent the standard deviation of all repeated measurements. [B] DTT depletion rate of target compounds in phosphate buffer. Error bars represent the standard deviation of all repeated measurements. All values shown in Table S3 in the SI. Color code depending on substance class: Purple: ortho-quinones (O_2PAHs); blue: other O_2PAHs; cyan blue: OPAHs; orange: NOPAHs; olive green: NPAHs, bright green: N_2PAHs; yellow: O-heterocycles.

3.2. DTT depletion assay

As shown in Figure 1B, 28 of the 40 compounds tested with the DTT assay were found to substantially deplete DTT (Table S3). Similar to the results of the H_2O_2 assay, the OP_{DTT} varies across several orders of magnitude, from $6*10^{-4}$ μM_{DTT} min^{-1} μM_{PAC}^{-1} to 13.4 μM_{DTT} min^{-1} μM_{PAC}^{-1}. We found the two 4-ring quinones 4,5-O_2PYR and 5,6-O_2CHR showing the highest and the third-highest OP_{DTT} of all examined PACs. This result is similar to a recent study from Okubo et al. (2021).[61] They revealed an almost similar DTT depletion rate as in our study as well as the same order of their targeted compounds. Prior to our study, the most extensive dataset of OP_{DTT} of PACs in the literature were reported by Verma et al. (2015)[27] and Lyu et al. (2018)[29] but these studies did not include 4,5-O_2PYR and 5,6-O_2CHR. When considering the same set of PACs as previous studies, our results (Figure 1B) are largely similar in order and magnitude compared to most of the other studies.[27,29,62] 9,10-O_2PHE, which has the highest OP_{DTT} (4 μM_{DTT} min^{-1} μM_{PAC}^{-1}) in our study is slightly lower than values in the literature, which range between 6.9 and 19 μM_{DTT} min^{-1} μM_{PAC}^{-1}.[27,29,62,63]

Our results show that some NPAHs can deplete DTT but only at a rate of up to 0.0021 μM_{DTT} min^{-1} μM_{PAC}^{-1}, which is between 3 and 4 orders of magnitude lower than the quinones with the highest OP_{DTT}. Nevertheless, their OP is comparable to the OP of several quinones or other OPAHs, such as 9,10-O_2ANT and 11-benz[a]fluorenone, with 0.0019 μM_{DTT} min^{-1} μM_{PAC}^{-1} and 0.0021 μM_{DTT} min^{-1} μM_{PAC}^{-1}, respectively. We found that several OPAHs (9-OFLN, 9,10-O_2ANT and benzanthrone (BAN)), which are often very abundant in atmospheric PM, are not or only slightly active in both assays.

Furthermore, we could observe that most compounds with a high OP_{DTT} are quinones with the second carbonyl in the ortho-position. A few studies using enzymes or cellular assays already

reported that ortho-quinones of 4- and 5-ring OPAHs have significant OP.[64-66] Motoyama et al. (2009) found that 5,6-O_2CHR and benzo[c]phenanthrene-5,6-quinone produce high amounts of H_2O_2 (in A549 cells using the FOX assay).[64] Studies by Jabarak et al. also showed that 5,6-O_2CHR, 5,6-benz[a]anthracenequinone, 4,5-O_2BAP, and 7,8-O_2BAP undergo redox cycling, which can cause the formation of H_2O_2.[65,66]

3.3. Correlation of DTT depletion with H_2O_2 formation

Both assays have different endpoints but are interchangeably applied as a measure of the OP of individual compounds and PM. As shown in Figure 2, the OP_{DTT} and OP_{H2O2} of the 39 studied compounds are linearly correlated ($r = 0.78$, $p < 0.05$). Xiong et al. (2017) also found that the DTT depletion strongly correlates with the H_2O_2 formation ($r = 0.91$) but not with the OH radical formation ($r = -0.04$).[28] Tong et al. (2018) found a good correlation between the DTT depletion rate and the H_2O_2 yield of secondary organic aerosols (SOA) in simulated lung fluid.[50]

The similarity of the results can be explained by the similar underlying processes of the reduction of the PACs in both assays. The recycling of the reduced PAC, while forming superoxide, is directly captured in the H_2O_2 assay, since H_2O_2 is formed from further reactions including $O_2^{\cdot-}$. The process is also captured indirectly by the DTT assay since recycled PACs can oxidize another DTT molecule again. For the evaluation of the correlation, we converted the DTT depletion rate to an absolute DTT depletion after 20 min in order to compare it to the H_2O_2 formation after 20 min of reaction time.

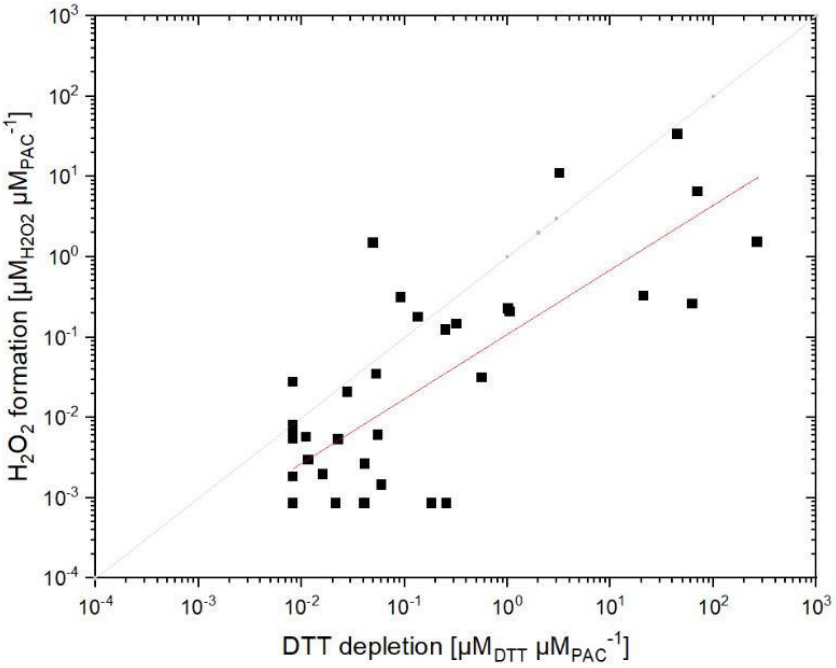

Figure 2. H_2O_2 formation in dependence of DTT depletion using a reaction time of 20 min for both assays. Regression line with Pearson R = 0.78 in red; 1:1 line in grey.

The DTT assay measures the ability of a compound, in our case a PAC, to oxidize the thiol group of DTT.[20] The similar process, the reduction of PACs by reaction with ascorbic acid and uric acid is the basis of the H_2O_2 assay. It quantifies the additional step of the formation of H_2O_2. One step is the oxidation of the reduced PAC, while oxygen is reduced to superoxide. Subsequently, the recycled PAC can undergo the same reaction again, while the formed superoxide can further react to hydrogen peroxide. The recycling of the PAC is also indirectly captured by the DTT test, since recycled PACs can oxidize another DTT molecule again.

However, the OP values are not the same because of different reasons. First, the difference could be due to the additional steps regarding the formation and destruction of H_2O_2. Second, the quinones with high reduction potentials can undergo side reactions such as the Michael reaction with thiol groups in the DTT assay.[53,64] Third, the variations could be caused by the different reduction potentials of the reductants (as shown in Table S4).

3.4. Predictability

Reduction potential

Data on experimentally determined and theoretically calculated reduction potentials of PACs have been previously reported in the literature.[43,52,67] We examined the relationship between the OP determined by the two assays and electrochemical one-electron reduction potentials (in or converted to aqueous solution, neutral pH, measured using normal hydrogen electrode (NHE), Section 2.3 in the SI and Table S5).

The relationship between the reduction potentials and OPs (as the logarithm) can be fitted by a sigmoidal curve (Figure 3). We observed an insensitive and a sensitive area of the OP to the reduction potential. In the H_2O_2 assay, the sensitive window is starting at around -400 mV (in aqueous phase against NHE). The sensitive window of the OP_{DTT} starts at around -250 mV. PACs with an OP lower than -400 mV (in the H_2O_2 assay) and –250 mV (in the DTT assay) do not show a significant signal in the respective assay because these compounds cannot oxidize ascorbic acid and uric acid (in the H_2O_2 assay) or DTT (in the DTT assay).

In the sensitive window of the reduction potential, we observed an increasing OP with increasing reduction potential reaching a maximum at around -90 mV and -165 mV for the OP_{H2O2} and the OP_{DTT}, respectively. The increasing OP can be explained by a faster reduction of the PAC with increasing reduction potential (leading to higher consumption of DTT in the DTT assay and results in higher formation of H_2O_2). With higher reduction potential of the PAC, the equilibrium of the reaction between PAC and the reductant to form a reduced PAC and an oxidized antioxidant will be shifted to the product side. The reaction rate constant, calculated by the Nernst equation, increases with increasing reduction potential of the PAC. The OP increases exponentially since the reduced PACs react back to form an oxidized PAC with molecular

oxygen and the recycled PAC can undergo the same process again. This redox cycling is already known for several quinones.[11]

However, the OP values reach an upper limit with increasing reduction potential since the rate of the back reaction (oxidation of the reduced PAC) will decrease if the electron affinity of the PAC is too high. This was already shown by Song and Buettner (2010).[53] In the study, they collected the rate constants for the reactions of different semiquinones with dioxygen. The rate constants of the reactions decrease with increasing reduction potential of the quinone. In addition, Song and Buettner (2010) showed that quinones with a high reduction potential can undergo different side reactions, which might decrease or stop their ability for redox cycling.[53]

1,4-BQ, 1,4-O_2PHE in both plots in Figure 3 and 5-OH-1,4-O_2NAP only in the plot of the log OP_{H2O2} as a function of the reduction potential (Figure 3A) had a reduction potential already above the maximum. The same was already shown for 1,4-BQ and other quinones with high reduction potential in the study from Roginsky et al. (1999).[55] They also found that the relationship between reduction potentials and the formation of ROS by quinones (via ascorbate oxidation and oxygen reduction) can be fitted by a sigmoidal curve with a linear relationship in the range of –250 mV to 0 mV.

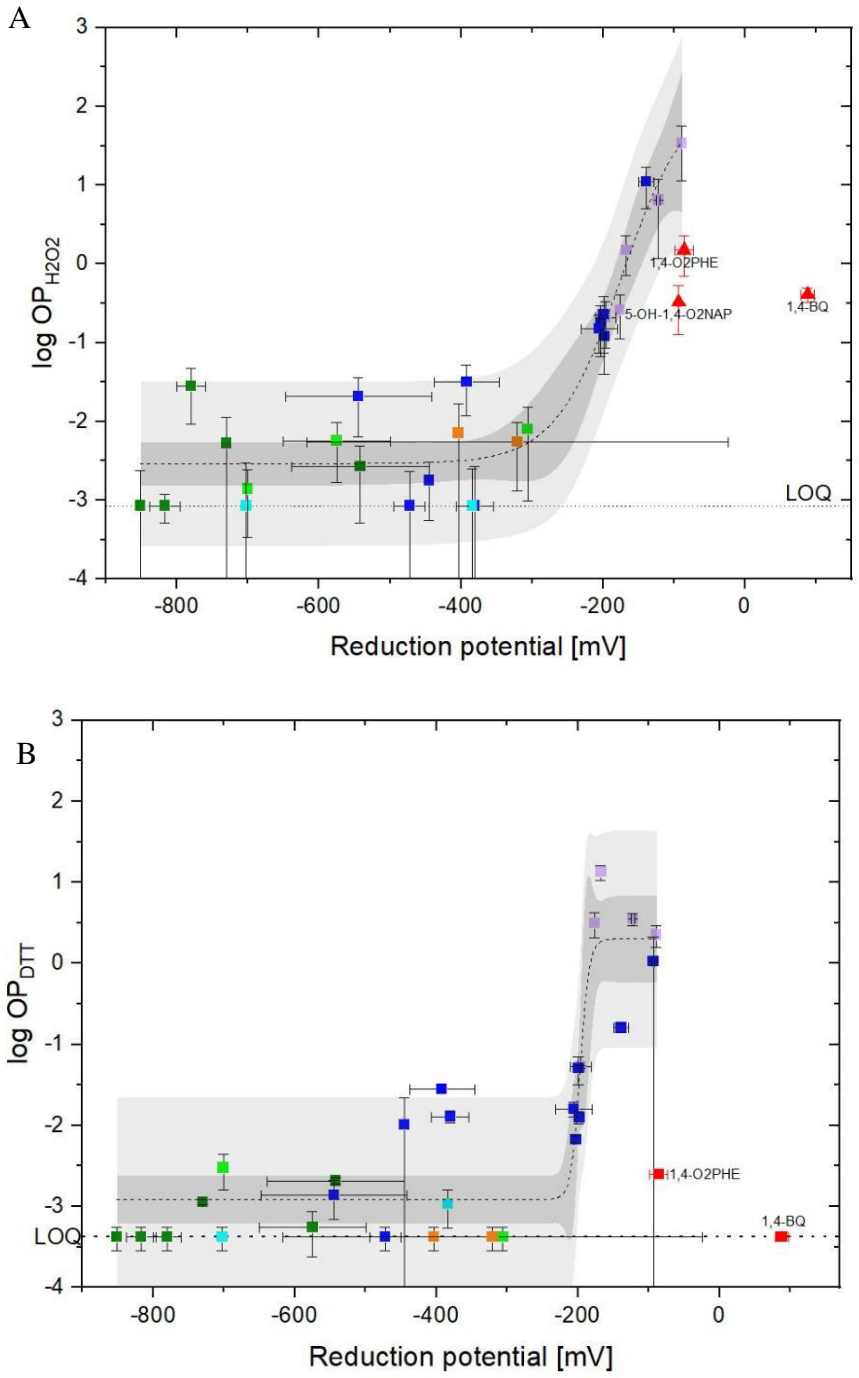

Figure 3. (A) log OP_{H2O2} (OP in μM_{H2O2} μM_{PAC}^{-1}) and (B) log OP_{DTT} (OP in μM_{DTT} min^{-1} μM_{PAC}^{-1}) as a function of the reduction potential with sigmoidal regression curve (dashed line) including the 95 % confidence intervals (grey) and 95 % prediction band (light grey). Compounds marked as red triangles not considered for the regression curve. The dotted horizontal line represents the LOQ. Reduction potential values against normal hydrogen electrode (NHE) in aqueous phase. Reduction potential values shown in Table S5. Error bars represent standard deviations. Color code depending on substance class: Purple: ortho-quinones (O_2PAHs); blue: other O_2PAHs; cyan blue: OPAHs; orange: NOPAHs; olive green: NPAHs, bright green: N_2PAHs.

When plotting only the part of increasing OP_{H2O2} with increasing reduction potential, i.e. between -400 and -90 mV, we found an exponential (log-linear) relationship. It is shown in Figure 4. Since the increase of the OP_{DTT} with increasing reduction potential is relatively steep in comparison to the OP_{H2O2} (as visible in Figure 3), the fit using the OP_{DTT} only includes seven compounds. It is shown in Figure S3B in the SI. The equation of the exponential (log-linear) fitted curve using OP_{H2O2} is shown in Equation 1, with $E(PAC/PAC^{\cdot-})$ as the one-reduction potential of the PACs.

$$OP_{H2O2} = 849 \pm 311 * (1.037 \pm 0.004)^{E(PAC/PAC.-)} \quad \text{Equation 1}$$

The slope of the fitted curve when plotting the logarithm of the OP (m=0.011; shown in Figure S3A) is comparable to the slope observed by Roginsky et al. (1999) (m=0.014).[55] It can be used the predict the OP_{H2O2} of compounds only from their reduction potential, which is an easily accessible physico-chemical parameter. We hypothesize that compounds with reduction potential lower than -400 mV have a negligible OP. For compounds with a reduction potential higher than -90 mV, a prediction is still difficult. If the reduction potential is far higher than -90 mV, we hypothesize a negligible OP, too. However, more research is needed to predict the OP for ccompounds with a reduction potential in this range.

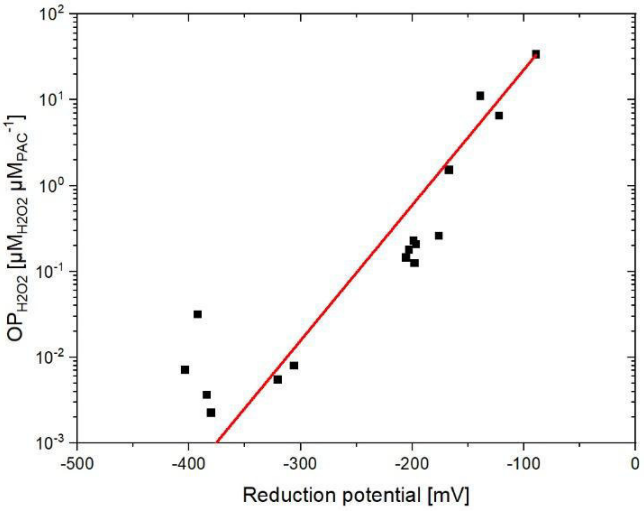

Figure 4. Exponential fit (in red) for part of increasing OP_{H2O2} with increasing reduction potential.

LUMO energy level

The electron affinity is indicated in molecular orbital theory by the energy of the LUMO level. The LUMO energy is the energy that is needed to add an electron to a molecule and can be calculated theoretically or from experimental data.[68] Thus, it could be a predictor for OP. Several studies found high correlations between experimental reduction potentials and theoretically calculated LUMO values.[69-71] The conversion of LUMO values to one common condition (density functional theory (DFT) at the B3LYP + 6-311+G(d,p) level with 1,2-dimethoxymethane (DME) as solvent) is given in Section 2.5 in the SI. The used LUMO energy values are given in Table S6.

As a result, we found a relation between the LUMO energy level values and both OPs, the H_2O_2 formation and the DTT depletion rate (Figure 5A and B). The plots look very similar to the relation between the reduction potential and the OP with an inverse relation, since higher reduction potentials mean more negative LUMO energy levels. Accordingly, the OP increases with decreasing LUMO energy level of the compound in a sigmoidal curve, reaching a maximum at around -3.4 eV. The equation of the log-linear fit for the part of increasing OP_{H2O2} with decreasing LUMO energy level (shown in Figure S5A), including the high correlation coefficients, is given in Equation 2. As illustrated in Figure S5B, the scattering of the values around the log-linear fit of the DTT results as a function of the LUMO energy level was higher than for the H_2O_2 assay results.

$\log (OP_{H2O2}) = -10.85 * LUMO - 35.92$ with Pearson R = -0.96 Equation 2

The OPs of the NPAHs depending on the LUMO energies measured by semi-empirical methods are shown in Figures S6 and S7 in the SI. Except for two outliers, namely 6-NCHR and 2,7-dinitrofluorene, the OP_{H2O2} is increasing with decreasing LUMO but reaching a maximum.

Reaching this maximum value could either be due to the possible irreversible two-electron reduction of the nitro group by losing water to form a nitroso group or because of the instability of the nitroaryl radical, which is formed by the one-electron reduction of the NPAH.[36] In the DTT assay, the trend of increasing OP with decreasing LUMO energy levels is not that clearly visible, since the OP_{DTT} of most NPAHs is <LOQ (Figure S7).

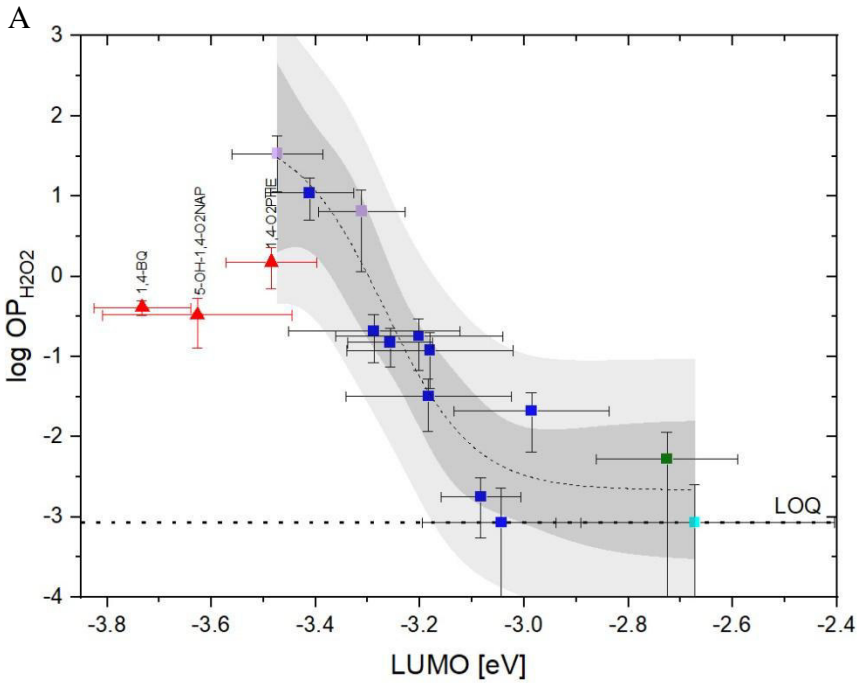

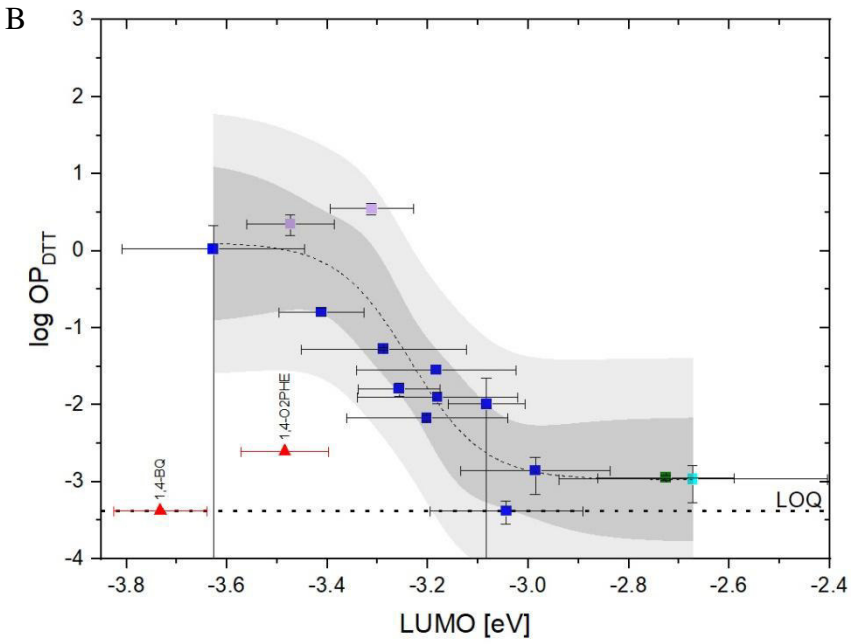

Figure 5. (A) log OP_{H2O2} (OP in μM_{H2O2} μM_{PAC}^{-1}) and (B) log OP_{DTT} (OP in μM_{DTT} min^{-1} μM_{PAC}^{-1}) as a function of the LUMO energy level with sigmoidal regression curve (dashed line) including the 95 % confidence intervals (grey) and 95 % prediction band (light grey). The dotted horizontal line represents the LOQ. LUMO energy levels from density functional theory (DFT) at the B3LYP + 6-311+G(d,p) level with 1,2-DME as solvent. LUMO energy level values shown in Table S6. Error bars represent standard deviations. Color code depending on substance class: Purple: ortho-quinones (O_2PAHs); blue: other O_2PAHs; cyan blue: OPAHs; olive green: NPAHs.

Structure

We evaluated the influence of molecular structure on OP (Figure 6). We found that functional groups with an electron-donating effect, such as methyl groups as well as an additional aromatic ring, reduce the OP (shown as blue boxes in Figure 6), while electron-withdrawing groups, such as nitro- and carbonyl groups, increase the OP (illustrated as red boxed in Figure 6). Hydroxyl groups have an electron-withdrawing, i.e. negative inductive (-I-) effect but a positive mesomeric (+M) effect. Thus, the influence on the OP depends on the position of the functional group and the structure of the compound. Furthermore, we found that quinones with the second carbonyl

group at the ortho-position obtain a higher OP than quinones with the group at any other position. This was also shown in other studies in the literature.[64-66] Similar influences of functional groups were already found and can be similarly applied to the reduction potential. However, these predictions are only valid for the OP if the OP of the precursor and the modified PAC are not in the range of high reduction potentials leading to decreasing OP values. A more detailed explanation of the influence of the molecular structure with examples and exceptions is given in Section S2.7 in the SI.

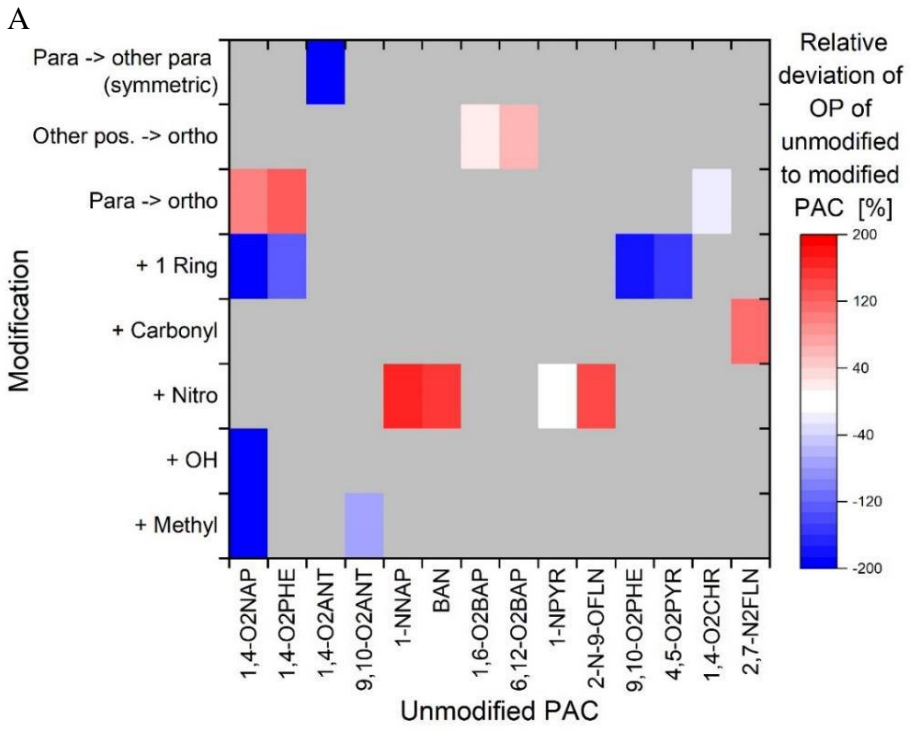

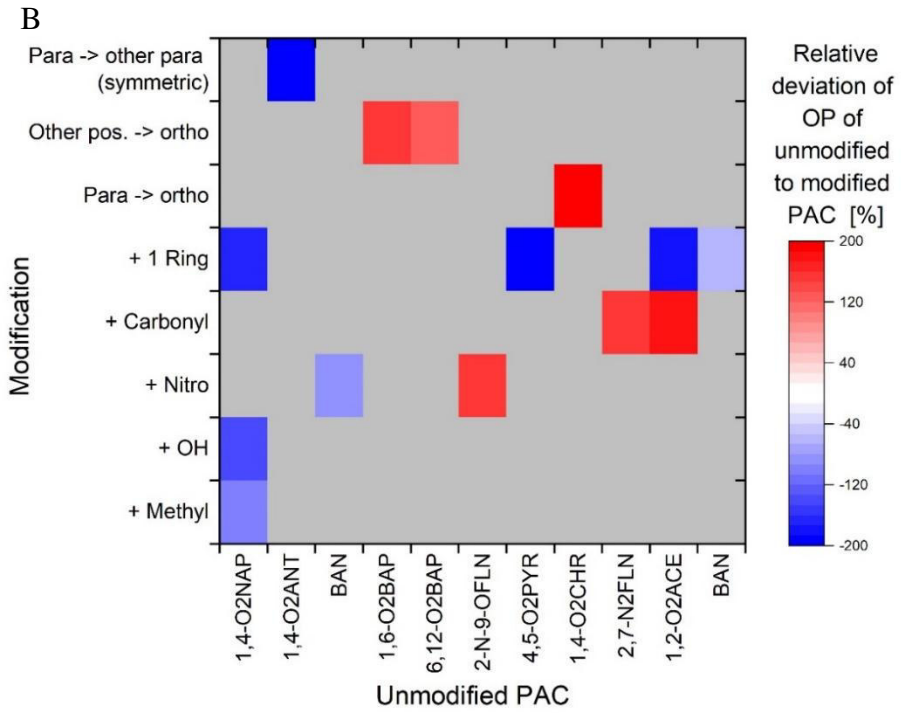

Figure 6. Influence of structural modifications of PAC compounds on OP_{H2O2} (A) and OP_{DTT} (B). On the x-axis, the unmodified PAC is given. The figure shows, how the OP changes when the structure is modified according to the y-axis. A red box represents a higher OP of the modified PAC compared to the unmodified one, a blue box illustrates that the modification has decreased the OP of the resulting compound. Difference given as relative deviation [%] to average of modified substance compared to unmodified PAC.

3.5. Relative importance of studied PACs

To demonstrate the relative contribution of each target compound to the overall OP in a typical real PM sample, we chose the standard reference material (SRM) 1649b (urban dust). We calculated the expected OP from the average of their reported concentrations in the SRM PM (summarized in Table S7)[44-49,72] and their experimental OP (OP_{H2O2} and OP_{DTT}) measured in this study (in total 32 compounds included since for seven compounds there is no concentration data in SRM dust 1649b available in the literature). The results for the expected OP_{H2O2} and the OP_{DTT} are shown in Figure 7. The total theoretically expected mass normalized OP_{H2O2} from the 32 investigated PACs is 0.021 $nmol_{H2O2}$ μg_{PM}^{-1}, while the OP_{DTT} is 0.016 $nmol_{DTT}$ min^{-1} μg_{PM}^{-1}. In addition, we calculated the percentage contribution of individual PACs to the OP of all 32 included PACs. It should be considered that this calculation as well as the total theoretically

expected OP are based on the assumption of additivity of OP values, which has been previously applied in other studies.[27,29,63] Using the H_2O_2 formation data, three quinones, namely 9,10-O_2PHE, 1,4-O_2NAP and 1,2-O_2NAP contribute approximately 93 % to the sum of OP from all investigated PAH derivatives in the urban dust. This is in accordance with the current knowledge in literature.[23,27,63] For this reason, the three compounds were exclusively included in kinetics models designed to assess the OP of PM.[24,73] However, in the DTT assay, these three substances only explain around 28 % of the total OP of all 32 considered PACs. The highest contribution of approximately 70 % was from 4,5-O_2PYR (also visible in Figure 7), since it showed the highest OP_{DTT} and has a relatively high concentration in SRM urban dust and ambient air.[49,74] The concentration of 4,5-O_2PYR was previously reported to be 857 ng g^{-1} in the SRM urban dust (1649b).[49] In conclusion, we suggest including 4,5-O_2PYR in future studies measuring or predicting the OP of atmospheric aerosols.

In contrast, we found that NPAHs are insignificant contributors to OP of PM because of relatively low concentration and low inherent OP. Furthermore, all other OPAHs targeted in this study, except the mentioned quinones, may be neglected as they only have a minor contribution (≤2 %) to OP. Even several oxygenated PAHs, which are most abundant in ambient PM,[6,47,48] do not contribute significantly to the overall OP of aerosols due to a low (or below LOQ) OP in both OP assays. Only 5,6-O_2CHR contributed to ~1 % to OP (using OP_{DTT}) in this study. McWhinney et al. (2013)[75] showed that 5-OH-1,4-O_2NAP was responsible for a significant part of the OP (using the DTT assay) in naphthalene secondary organic aerosols (SOA). We could not quantify the contribution of 2-OH-1,4-O_2NAP and 5-OH-1,4-O_2NAP, which have a high OP in our study and other reports because their concentrations have not been reported in SRM urban dust (1649b).[27,29] However, when assuming comparable concentrations of 5-OH-1,4-O_2NAP in SRM

dust as reported in ambient PM by Wnorowsky and Charland (2007),[72] 5-OH-1,4-O_2NAP may have a significant contribution to the OP of the considered PACs.

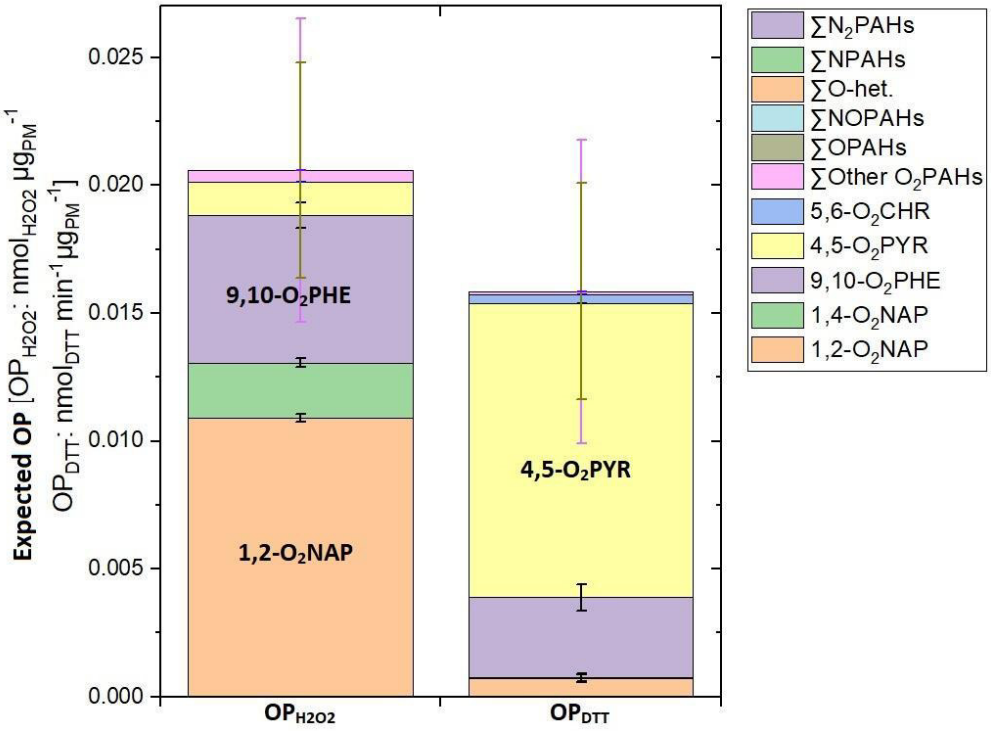

Figure 7. Expected OP of PACs in SRM urban dust 1649b calculated from experimentally determined OP (OP_{H2O2} and OP_{DTT}) of individual compounds and their respective ambient concentrations in SRM dust (see Table S7; as shown in the Table, seven compounds are not included since no concentration data in SRM dust 1649b available).

3.6. Implications

The predictability of the OP would be a significant advantage, since the measurement of OPs is not standardized. Different cellular and acellular assays measure different endpoints and use different concentrations, reductants and reaction times. In addition, the measurement of the OP is time-consuming and can be expensive. The easiest way to predict the OP would be to estimate it just by the molecular structure. Based on known OP values of PACs with one core structure, it could be possible to estimate the OP of another compound due to the known effects of different additional functional groups. Another way would be the prediction of the OP by other physico-chemical or quantum mechanical substance properties, which are either already available in

literature, measured with easy, cheap and standardized methods, or calculated theoretically. We found that the one-electron reduction potential and the LUMO energy level fulfill at least one of the requirements and are good predictors of the OP. Another advantage of the predictability of the OP is the possibility to decide which substances are worth to study in more detail, either for determining their OP, their air concentrations or their bioaccessibility. Furthermore, the reduction potential or the LUMO energy level can be included as a physico-chemical parameter into models that predict the oxidative stress without the necessity of having kinetic measurement data of all compounds.

Supporting Information:

The Supporting Information is available.

Acknowledgements

This work was supported by the Max Planck Society. We thank Karsten Baumann and Matteo Krüger for discussion and Anna Lena Leifke for support in the laboratory.

References

(1) Shiraiwa, M.; Selzle, K.; Pöschl, U. Hazardous components and health effects of atmospheric aerosol particles: reactive oxygen species, soot, polycyclic aromatic compounds and allergenic proteins. Free Radical Res. 2012, 46, 927-939.

(2) Shiraiwa, M.; Ueda, K.; Pozzer, A.; Lammel, G.; Kampf, C. J.; Fushimi, A.; Enami, S.; Arangio, A. M.; Fröhlich-Nowoisky, J.; Fujitani, Y.; Furuyama, A.; Lakey, P. S. J.; Lelieveld, J.; Lucas, K.; Morino, Y.; Pöschl, U.; Takahama, S.; Takami, A.; Tong, H.; Weber, B.; Yoshino, A.; Sato, K. Aerosol health effects from molecular to global scales. Environ. Sci. Technol. 2017, 51, 13545−13567.

(3) Lelieveld, J.; Evans, J. S.; Fnais, M.; Giannadaki, D.; Pozzer, A. The contribution of outdoor air pollution sources to premature mortality on a global scale. Nature 2015, 525, 367-371.

(4) Lelieveld, J.; Klingmüller, K.; Pozzer, A.; Pöschl, U.; Fnais, M.; Daiber, A.; Münzel, T. Cardiovascular disease burden from ambient air pollution in Europe reassessed using novel hazard ratio functions. Eur. Heart J. 2019, 40, 1590−1596.

(5) Burnett, R.; Chen, H.; Szyszkowicz, M.; Fann, N.; Hubbell, B.; Pope, C. A.; Apte, J. S.; Brauer, M.; Cohen, A.; Weichenthal, S.; Coggins, J.; Di, Q.; Brunekreef, B.; Frostad, J.; Lim, S. S.; Kan, H. D.; Walker, K. D.; Thurston, G. D.; Hayes, R. B.; Lim, C. C.; Turner, M. C.; Jerrett, M.; Krewski, D.; Gapstur, S. M.; Diver, W. R.; Ostro, B.; Goldberg, D.; Crouse, D. L.; Martin, R. V.; Peters, P.; Pinault, L.; Tjepkema, M.; van

Donkelaar, A.; Villeneuve, P. J.; Miller, A. B.; Yin, P.; Zhou, M. G.; Wang, L. J.; Janssen, N. A. H.; Marra, M.; Atkinson, R. W.; Tsang, H.; Quoc Thach, T.; Cannon, J. B.; Allen, R. T.; Hart, J. E.; Laden, F.; Cesaroni, G.; Forastiere, F.; Weinmayr, G.; Jaensch, A.; Nagel, G.; Concin, H.; Spadaro, J. V. Global estimates of mortality associated with long-term exposure to outdoor fine particulate matter. Proc. Natl. Acad. Sci. U. S. A. 2018, 115 (38), 9592−9597.

(6) Walgraeve, C.; Demesstere, K.; Dewulf, J.; Zimmermann, R.; van Langenhove, H. Oxygenated polycyclic aromatic hydrocarbons in atmospheric particulate matter: Molecular characterization and occurrence. Atmos. Environ. 2010, 44, 1831−1846.

(7) Keyte, I. J.; Harrison, R. M.; Lammel, G. Chemical reactivity and long-range transport potential of polycyclic aromatic hydrocarbons-a review. Chem. Soc. Rev. 2013, 42, 9333-9391.

(8) Bandowe, B. A. M.; Meusel, H. Nitrated polycyclic aromatic hydrocarbons (nitro-PAHs) in the environment -A review. Sci. Total Environ. 2017, 581-582, 237-257.

(9) IARC (International Agency for Research on Cancer). Some non-heterocyclic polycyclic aromatic hydrocarbons and some related exposures. IARC Monogr. Eval. Carcinog. Risks Hum. 2010, 92, 1−853.

(10) IARC (International Agency for Research on Cancer). Diesel and gasoline engine exhausts and some nitroarenes. IARC Monogr. Eval. Carcinog. Risks Hum. 2013, 105, 1−714.

(11) Bolton, J. L.; Trush, M. A.; Penning, T. M.; Dryhurst, G.; Monks, T. J. Role of quinones in toxicology. Chem. Res. Toxicol. 2000, 13, 135−160.

(12) Hansen, T.; Seidel, A.; Borlak, J. The environmental carcinogen 3-nitrobenzanthrone and its main metabolite 3-aminobenzanthrone enhance formation of reactive oxygen intermediates in human A549 lung epithelial cells. Toxicol. Appl. Pharmacol. 2007, 221, 222-234.

(13) Andersson, H.; Piras, E.; Demma, J.; Hellman, B.; Brittebo, E. Low levels of the air pollutant 1-nitropyrene induce DNA damage, increased levels of reactive oxygen species and endoplasmic reticulum stress in human endothelial cells. Toxicology 2009, 262, 57−64.

(14) Zhao, L.; Zhang, L.; Chen, M.; Dong, C.; Li, R.; Cai, Z. Effects of ambient atmospheric $PM_{2.5}$, 1-nitropyrene and 9-nitroanthracene on DNA damage and oxidative stress in hearts of rats. Cardiovasc. Toxicol. 2019, 19, 178–190.

(15) Penning, T. M. Human aldo-keto reductases and the metabolic activation of polycyclic aromatic hydrocarbons. Chem. Res. Toxicol. 2014, 27, 1901−1917.

(16) Penning, T. M. Genotoxicity of ortho-quinones: reactive oxygen species versus covalent modification. Toxicol. Res. 2017, 6, 740−754.

(17) Ayres, J. G.; Borm, P.; Cassee, F. R.; Castranova, V.; Donaldson, K.; Ghio, A.; Harrison, R. M.; Hider, R.; Kelly, F.; Kooter, I. M.; Marano, F.; Maynard, R. L.; Mudway, I.; Nel, A.; Sioutas, C.; Smith, S.; Baeza-Squiban, A.; Cho, A.; Duggan, S.; Froines, J. Evaluating the toxicity of airborne particulate matter and nanoparticles by measuring oxidative stress potential—a workshop report and consensus statement. Inhalation Toxicol. 2008, 20, 75-99.

(18) Bates, J. T.; Fang, T.; Verma, V.; Zeng, L.; Weber, R. J.; Tolbert, P. E.; Abrams, J. Y.; Sarnat, S. E.; Klein, M.; Mulholland, J. A.; Russell, A. G. Review of acellular assays of ambient particulate matter oxidative potential: methods and relationships with composition, sources, and health effects. Environ. Sci. Technol. 2019, 53, 4003− 4019.

(19) Jiang, H.; Ahmed, C.; Canchola, A.; Chen, J. Y.; Lin, Y.-H. Use of dithiothreitol assay to evaluate the oxidative potential of atmospheric aerosols. Atmosphere 2019, 10, 571.
(20) Kumagai, Y.; Koide, S.; Taguchi, K.; Endo, A.; Nakai, Y.; Yoshikawa, T.; Shimojo, N. Oxidation of proximal protein sulfhydryls by phenanthraquinone, a component of diesel exhaust particles. Chem. Res. Toxicol. 2002, 15 (4), 483−489.
(21) Kishikawa, N.; Ohkubo, N.; Ohyama, K.; Nakashima, K.; Kuroda, N. Chemiluminescence assay for quinones based on generation of reactive oxygen species through the redox cycle of quinone. Anal. Bioanal. Chem. 2009, 393 (4), 1337−1343.
(22) Gao, D.; Godri Pollitt, K. J.; Mulholland, J. A.; Russell, A. G.; Weber, R. J. Characterization and comparison of $PM_{2.5}$ oxidative potential assessed by two acellular assays. Atmos. Chem. Phys. 2020, 20, 5197−5210.
(23) Charrier, J. G.; McFall, A. S.; Richards-Henderson, N. K.; Anastasio, C. Hydrogen peroxide formation in a surrogate lung fluid by transition metals and quinones present in particulate patter. Environ. Sci. Technol. 2014, 48, 7010-7017.
(24) Lakey, P. S. J.; Berkemeier, T.; Tong, H.; Arangio, A. M.; Lucas, K.; Pöschl, U.; Shiraiwa, M. Chemical exposure-response relationship between air pollutants and reactive oxygen species in the human respiratory tract. Sci. Rep. 2016, 6, 32916.
(25) Sies, H.; Berndt, C.; Jones, D. P. Oxidative stress. Annu. Rev. Biochem. 2017, 86 (1), 715−748.
(26) Chung, M. Y.; Lazaro, R. A.; Lim, D.; Jackson, J.; Lyon, J.; Rendulic, D.; Hasson, A. S. Aerosol-borne quinones and reactive oxygen species generation by particulate matter extracts. Environ. Sci. Technol. 2006, 40, 4880−4886.
(27) Verma, V.; Wang, Y.; El-Afifi, R.; Fang, T.; Rowland, J.; Russell, A. G.; Weber, R. J. Fractionating ambient humic-like substances (HULIS) for their reactive oxygen species activity − Assessing the importance of quinones and atmospheric aging. Atmos. Environ. 2015, 120, 351−359.
(28) Xiong, Q.; Yu, H.; Wang, R.; Wei, J.; Verma, V. Rethinking dithiothreitol-based particulate matter oxidative potential: measuring dithiothreitol consumption versus reactive oxygen species generation. Environ. Sci. Technol. 2017, 51, 6507−6514.
(29) Lyu, Y.; Guo, H.; Cheng, T.; Li, X. Particle size distributions of oxidative potential of lung-deposited particles: assessing contributions from quinones and water-soluble metals. Environ. Sci. Technol. 2018, 52, 6592−6600.
(30) Yu, H. R.; Wei, J. L.; Cheng, Y. L.; Subedi, K.; Verma, V. Synergistic and antagonistic interactions among the particulate matter components in generating reactive oxygen species based on the dithiothreitol assay. Environ. Sci. Technol. 2018, 52, 2261− 2270.
(31) Park, E. J.; Park, K. Induction of pro-inflammatory signals by 1-nitropyrene in cultured BEAS-2B cells. Toxicol. Lett. 2009, 184, 126−133.
(32) Shang, Y.; Zhou, Q.; Wang, T.; Jiang, Y.; Zhong, Y.; Qian, G.; Zhu, T.; Qiu, X.; An, J. Airborne nitro-PAHs induce Nrf2/ARE defense system against oxidative stress and promote inflammatory process by activating PI3K/Akt pathway in A549 cells. Toxicol. In Vitro 2017, 44, 66−73.
(33) Tuet, W. Y.; Liu, F.; de Oliveira Alves, N.; Fok, S.; Artaxo, P.; Vasconcellos, P.; Champion, J. A.; Ng, N. L. Chemical oxidative potential and cellular oxidative stress from open biomass burning aerosol. Environ. Sci. Technol. Lett. 2019, 6, 126−132.
(34) Debnath, A. K.; Lopez de Compadre, R. L.; Debnath, G.; Shusterman, A. J.; Hansch, C. Structure-activity relationship of mutagenic aromatic and heteroatomic nitro compounds. Correlation with molecular orbital energies and hydrophobicity. J. Med. Chem. 1991, 34, 786-797.

(35) Fukuhara, K.; Hara, Y.; Miyata, N. Electron transfer from quinone and nitroarene anion radicals to molecular oxygen studied by the potential-step chronocoulometry method, J. Chem. Soc., Chem. Commun., 1994, 955–956.
(36) Uchimiya, M.; Gorb, L.; Isayev, O.; Qasim, M. M.; Leszczynski, J. One electron standard reduction potentials of nitroaromatic and cyclic nitramine explosives. Environ. Pollut. 2010, 158, 3048-3053.
(37) Klopman, G.; Tonucci, D. A.; Holloway, M.; Rosenkranz, H. S. Relationship between polarographic reduction potential and mutagenicity of nitroarenes. Mutat. Res. 1984, 126, 139-144.
(38) Fu, P. P.; Heflich, R. H.; Unruh, L. E.; Shaikh, A. V.; Wu, Y.-S.; Lai, C.-C.; Lai, J. S. Relationships among direct-acting mutagenicity, nitro group orientation and polarographic reduction potential of 6-nitrobenzo[a]pyrene, 7-nitrobenz[a]anthracene and their derivatives. Mutat. Res. 1988, 209, 115-122.
(39) O'Brien, P. J. Molecular mechanisms of quinone cytotoxicity. Chem.-Biol. Interact. 1991, 80, 1-14.
(40) Shahpoury, P.; Zhang, Z. W.; Arangio, A.; Celo, V.; Dabek-Zlotorzynska, E.; Harner, T.; Nenes, A. The influence of chemical composition, aerosol acidity, and metal dissolution on the oxidative potential of fine particulate matter and redox potential of the lung lining fluid. Environ. Int. 2021, 148, 106343
(41) Kitchin, R. M.; Bechtold, W. E.; Brooks, A. L. The structure-function relationships of nitrofluorenes and nitrofluorenones in the Salmonella mutagenicity and CHO sisterchromatid exchange assays. Mutat. Res. 1988, 206, 367-377.
(42) Jung, H.; Heflich, R. H.; Fu, P. P.; Shaikh, A. U.; Hartman, P. Nitro group orientation, reduction potential, and direct-acting mutagenicity of nitro-polycyclic aromatic hydrocarbons. Environ. Mol. Mutagen. 1991, 17, 169−180.
(43) Huynh, M. T.; Anson, C. W.; Cavell, A. C.; Stahl, S. S.; Hammes-Schiffer, S. Quinone 1 e^- and $2e^-/2H^+$ reduction potentials: identification and analysis of deviations from systematic scaling relationships. J. Am. Chem. Soc. 2016, 138, 15903−15910.
(44) Layshock, J. A.; Wilson, G.; Anderson, K. A. Ketone and quinone substituted polycyclic aromatic hydrocarbons in mussel tissue, sediment, urban dust, and diesel particulate matrices. Environ. Toxicol. Chem. 2010, 29, 2450−2460.
(45) Delgado-Saborit, J. M.; Alam, M. S.; Pollitt, K. J.G.; Stark, C.; Harrison, R. M. Analysis of atmospheric concentrations of quinones and polycyclic aromatic hydrocarbons in vapour and particulate phase. Atmos. Environ. 2013, 77, 974−982.
(46) Nocun, M. S.; Schantz, M. M. Determination of selected oxygenated polycyclic aromatic hydrocarbons (oxy-PAHs) in diesel and air particulate matter standard reference materials (SRMs). Anal. Bioanal. Chem. 2013, 405, 5583−5593.
(47) Albinet, A.; Nalin, F.; Tomaz, S.; Beaumont, J.; Lestremau, F. A simple QuECHERS-like extraction approach for molecular chemical characterization of organic aerosols: application to nitrated and oxygenated PAH derivatives (NPAHs and OPAHs) quantified by GC-NCIMS. Anal. Bioanal. Chem. 2014, 406, 3131-3148.
(48) Tomaz, S.; Shahpoury, P.; Jaffrezo, J.-L.; Lammel, G.; Perraudin, E.; Villenave, E.; Albinet, A. One-year study of polycyclic aromatic compounds at an urban site in Grenoble (France): Seasonal variations, gas/particle partitioning and cancer risk estimation. Sci. Total Environ. 2016, 565, 1071−1083.
(49) Toriba, A.; Homma, C.; Kita, M.; Uozaki, W.; Boongla, Y.; Orakij, W.; Hayakawa, K. Simultaneous determination of polycyclic aromatic hydrocarbon quinones by gas

chromatography-tandem mass spectrometry, following a one-pot reductive trimethylsilyl derivatization. J. Chromatogr. A 2016, 1459, 89–100.
(50) Tong, H.; Lakey, P. S.; Arangio, A. M.; Socorro, J.; Shen, F.; Lucas, K.; Brune, W. H.; Pöschl, U.; Shiraiwa, M. Reactive oxygen species formed by secondary organic aerosols in water and surrogate lung fluid. Environ. Sci. Technol. 2018, 52, 11642−11651.
(51) Boisa, N.; Elom, N.; Dean, J. R.; Deary, M. E.; Bird, G.; Entwistle, J. A. Development and application of an inhalation bioaccessibility method (IBM) for lead in the PM_{10} size fraction of soil. Environ. Int. 2014, 70, 132−142.
(52) Wardman, P. Reduction potentials of one-electron couples involving free radicals in aqueous solution. J. Phys. Chem. Ref. Data 1989, 18, 1637-1755.
(53) Song, Y.; Buettner, G. R. Thermodynamic and kinetic considerations for the reaction of semiquinone radicals to form superoxide and hydrogen peroxide. Free Radical Biol. Med. 2010, 49 (6), 919−962.
(54) Wardman, P. Bioreductive activation of quinones: redox properties and thiol reactivity, Free Radic. Res. Commun. 1990, 8, 219-229.
(55) Roginsky, V. A.; Barsukova, T. K.; Stengmann, H. B. Kinetics of redox interaction between substituted quinones and ascorbate under aerobic conditions. Chem. Biol. Interact. 1999, 121, 177-197.
(56) Namazian, M.; Almodarresieh, H. A.; Noorbala, M. R.; Zare, H. R. DFT calculation of electrode potentials for substituted quinones in aqueous solution. Chem. Phys. Lett. 2004, 396, 424-428.
(57) Ding, Y.; Li, Y.; Yu, G. Exploring bio-inspired quinone-based organic redox flow batteries: a combined experimental and computational study. Chem. 2016, 1, 790−801.
(58) Miao, L.; Liu, L.; Shang, Z.; Li, Y.; Lu, Y.; Cheng, F.; Chen, J. The structure–electrochemical property relationship of quinone electrodes for lithium-ion batteries. Phys. Chem. Chem. Phys. 2018, 20, 13478−13484.
(59) Oliveros, E.; Murasecco, P. S.; Saghafi, T. A.; Braun, A. M.; Hansen, H. J. 1H-Phenalen-1-one: photophysical properties and singlet-oxygen production, HelV. Chim. Acta 1991, 74, 79-90.
(60) Schmidt, R.; Tanielian, C.; Dunsbach, R.; Wolff, C. Phenalenone, a universal reference compound for the determination of quantum yields of singlet oxygen O_2 ($^1\Delta_g$) sensitization. J. Photochem. Photobiol. A: Chem. 1994, 79, 11-17.
(61) Okubo, R.; Kameda, T.; Tohno, S. Evaluation of oxidative potential of pyrenequinone isomers by the dithiothreitol (DTT) assay. Polycycl. Aromat. Compd. 2021, DOI: 10.1080/10406638.2021.1925711.
(62) Visentin, M.; Pagnoni, A.; Sarti, E.; Pietrogrande, M. C. Urban $PM_{2.5}$ oxidative potential: Importance of chemical species and comparison of two spectrophotometric cell-free assays. Environ. Pollut. 2016, 219 (Supplement C), 72−79.
(63) Charrier, J. G.; Anastasio, C. Impacts of antioxidants on hydroxyl radical production from individual and mixed transition metals in a surrogate lung fluid. Atmos. Environ. 2011, 45, 7555−7562.
(64) Motoyama, Y.; Bekki, K.; Chung, S.; Tang, N.; Kameda, T.; Toriba, A.; Taguchi, K.; Hayakawa, K. Oxidative stress more strongly induced by ortho-than para-quinoid polycyclic aromatic hydrocarbons in A549 cells. J. Health Sci. 2009, 55, 845−850.
(65) Jabarak, R.; Harvey, R. G.; Jarabak, J. Redox cycling of polycyclic aromatic hydrocarbon o-quinones: reversal of superoxide dismutase inhibition by ascorbate. Arch. Biochem. Biophys. 1997, 339, 92–98.

(66) Jarabak, R.; Harvey, R. G.; Jarabak, J. Redox cycling of polycyclic aromatic hydrocarbon o-quinones: metal ion-catalyzed oxidation of catechols bypasses inhibition by superoxide dismutase. Chem.-Biol. Int. 1998, 115, 201-213.
(67) Er, S.; Suh, C.; Marshak, M. P.; Aspuru-Guzik, A. Computational design of molecules for an all-quinone redox flow battery. Chem. Sci. 2015, 6, 885-893.
(68) Leonat, L. N.; Sbarcea, G.; Branzoi, I. V. Cyclic voltammetry for energy levels estimation of organic materials. UPB Sci. Bull. Ser. B 2013, 75, 111−118.
(69) Krygowski, T. M.; Stencel, M.; Galus, Z. J. Polarographic and voltammetric study of mono-nitro derivatives of benzenoid hydrocarbons in DMF-interpretation within hammett-streitwieser equation and HMO-theory. Electroanal. Chem. 1972, 39, 395-405.
(70) Iwata, N.; Fukuhara, K.; Suzuki, K.; Miyata, N.; Takahashi, A. Reduction properties of nitrated naphthalenes: relationship between electrochemical reduction potential and the enzymatic reduction by microsomes or cytosol from rat liver. Chem.-Biol. Interact. 1992, 85, 187-197.
(71) Méndez-Hernández, D. D.; Tarakeshwar, P.; Gust, D.; Moore, T. A.; Moore, A. L.; Mujica, V. Simple and accurate correlation of experimental redox potentials and DFT-calculated HOMO/LUMO energies of polycyclic aromatic hydrocarbons. J. Mol. Model. 2013, 19, 2845−2848.
(72) Wnorowski, A.; Charland, J.-P. Profiling quinones in ambient air samples collected from the Athabasca region (Canada). Chemosphere 2017, 189, 55−66.
(73) Lelieveld, S.; Wilson, J.; Dovrou, E.; Mishra, A.; Lakey, P. S. J.; Shiraiwa, M.; Pöschl, U.; Berkemeier, T. Hydroxyl radical production by air pollutants in epithelial lining fluid governed by interconversion and scavenging of reactive oxygen species. Environ. Sci. Technol. 2021, 55, 14069−14079.
(74) Delhomme, O.; Millet, M.; Herckes, P. Determination of oxygenated polycyclic aromatic hydrocarbons in atmospheric aerosol samples by liquid chromatography–tandem mass spectrometry. Talanta 2008, 74, 703-710.
(75) McWhinney, R. D.; Zhou, S.; Abbatt, J. P. D. Naphthalene SOA: redox activity and naphthoquinone gas–particle partitioning. Atmos. Chem. Phys. 2013, 13, 9731-9744.

Supporting Information

Oxidative potential of polycyclic aromatic compounds (PACs) in particulate matter: measurement and prediction by chemical structure and reduction potential

Marco Wietzoreck[1], Alexander Filippi[1], Stefanie Hildmann[1], Boris Mashtakov[1], Pourya Shahpoury[1,2], Jake Wilson[1], Thomas Berkemeier[1], Haijie Tong[1,3], Ulrich Pöschl[1], Gerhard Lammel[1], Benjamin A. Musa Bandowe[1]

[1]Department of Multiphase Chemistry, Max Planck Institute for Chemistry, Mainz, 55128, Germany

[2]Air Quality Research Division, Environment and Climate Change Canada, Toronto, M3H 5T4, Canada

[3]Department of Civil and Environmental Engineering, The Hong Kong Polytechnic University, Hong Kong, China

Content

1 Materials and methods

1.1 Chemicals

Table S 1. List of target substances, their abbreviations, CAS number, molecular weight and number of rings.

Substance class	Substance name	Acronym	CAS Number	Molecular weight [g mol^{-1}]	Number of rings
NPAHs	1-Nitronaphthalene	1-NNAP	86-57-7	173	2
	9-Nitrophenanthrene	9-NPHE	954-46-1	223	3
	1-Nitropyrene	1-NPYR	5522-43-0	247	4
	3-Nitrofluoranthene	3-NFLT	892-21-7	247	4
	6-Nitrochrysene	6-NCHR	7496-02-8	273	4
N_2PAHs	1,3-Dinitronaphthalene	1,3-N_2NAP	606-37-1	218	2
	2,7-Dinitrofluorene	2,7-N_2FLN	5405-53-8	256	3
	1,3-Dinitropyrene	1,3-N_2PYR	75321-20-9	292	4
O_2PAHs	1,2-Naphthoquinone	1,2-O_2NAP	524-42-5	158	2
	1,4-Naphthoquinone	1,4-O_2NAP	130-15-4	158	2
	2-Methyl-1,4-naphthoquinone (Menadione)	2-M-1,4-O_2NAP	58-27-5	172	2
	2-Hydroxy-1,4-naphthoquinone	2-OH-1,4-O_2NAP	83-72-7	174	2
	5-Hydroxy-1,4-naphthoquinone	5-OH-1,4-O_2NAP	481-39-0	174	2
	1,2-Acenaphthenequinone	1,2-O_2ACE	82-86-0	182	3
	1,4-Anthraquinone	1,4-O_2ANT	635-12-1	208	3
	1,4-Phenanthrenequinone	1,4-O_2PHE	569-15-3	208	3

Substance class	Substance name	Acronym	CAS Number	Molecular weight [g mol^{-1}]	Number of rings
	9,10-Anthraquinone	9,10-O_2ANT	84-65-1	208	3
	9,10-Phenanthrenequinone	9,10-O_2PHE	84-11-7	208	3
	2-Methyl-9,10-anthraquinone	2-M-9,10-O_2ANT	84-54-8	222	3
	1,2-Aceanthrenequinone	1,2-O_2AAN	6373-11-1	232	4
	4,5-Pyrenequinone	4,5-O_2PYR	6217-22-7	232	4
	1,4-Chrysenequinone	1,4-O_2CHR	100900-16-1	258	4
	5,6-Chrysenequinone	5.6-O_2CHR	2051-10-7	258	4
	5,12-Naphthacenequinone	5,12-O_2NAC	1090-13-7	258	4
	Benz[a]anthracene-7,12-dione	7,12-O_2BAN	2498-66-0	258	4
	Benzo[a]pyrene-1,6-dione	1,6-O_2BAP	3067-13-8	282	5
	Benzo[a]pyrene-4,5-dione	4,5-O_2BAP	42286-46-4	282	5
	Benzo[a]pyrene-6,12-dione	6,12-O_2BAP	3067-12-7	282	5
OPAHs	1-Acenaphthenone	1-OACE	2235-15-6	168	3
	9-Fluorenone	9-OFLN	486-25-9	180	3
	1-Phenalenone (Perinaphthenone)	1-OPHL	548-39-0	180	3
	Benzanthrone (7H-Benz[de]anthracene-7-one)	BAN	82-05-3	230	4
	Benzo[a]fluoren-11-one	11-OBaFLN	479-79-8	230	4
	6H-Benzo[c,d]pyren-6-one	6-OBPYR	3074-00-8	254	5
NOPAHs	2-Nitro-9-fluorenone	2-N-9-OFLN	3096-52-4	225	3
	2,7-Dinitro-9-fluorenone	2,7-N_2-9-OFLN	31551-45-8	270	3
	3-Nitrobenzanthrone	3-NBAN	17117-34-9	275	4
O-heterocycle	1,8-Naphthalic anhydride	1,8-NAA	81-84-5	198	3
	6H-Benzo[c]chromen-6-one (Dibenzo[b,d]pyran-6-one)	6-OBCC	2005-10-9	196	3

Substance class	Substance name	Acronym	CAS Number	Molecular weight [g mol^{-1}]	Number of rings
Monoaromatic hydrocarbon	1,4-Benzoquinone	1,4-BQ	106-51-4	108	1

Table S 2. Composition of simulated epithelial lung fluids (SELF) based on the modified Gamble's solution from Boisa et al. (2014). pH adjusted to 7.4. All compounds from Sigma Aldrich, Germany.

Compound	Concentration [mg L^{-1}]
NaCl	6020
$CaCl_2$ * 2 H_2O	256
Na_2HPO_4	150
$NaHCO_3$	2600
KCl	298
$MgCl_2$	93.7
Na_2SO_4	72
Bovine Serum Albumin	260
Dipalmitoylphosphatidylcholine (DPPC)	100
Glycine	376

268

1.2 Modification of simulated lung fluid

In order to ensure a homogeneous, non-inflammatory SELF solution, the procedure of preparing the lung fluid from Boisa et al. (2014) was slightly changed. Mucin was omitted since mucin from porcine stomach was leading to inflammation in cell tests. In addition, glutathione, as well as cysteine, were omitted since thiol groups disturb the H_2O_2 assay (Li & Imlay, 2019; Wang et al., 2017; Votyakova & Reynolds, 2004). The SELF solution was sterile filtrated and an antibiotic, antimycotic solution (10,000 units penicillin, 10 mg streptomycin and 25 µg amphotericin B per mL, Sigma Aldrich, Germany) was added since the assay preparation could not be done under sterile conditions. Furthermore, dipalmitoylphosphatidylcholine (DPPC) (Sigma Aldrich, Germany) was solubilized by using an ultrasonic homogenizer 700 W (Fisher, Germany) and added after sterile filtration.

1.3 Calibration curves of OP assays

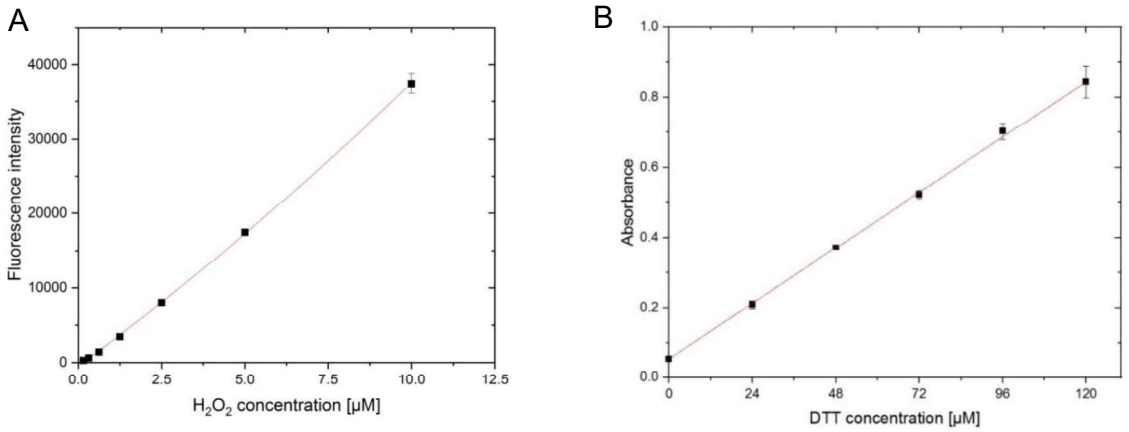

Figure S 1. (A) Exemplary 7-point H_2O_2 calibration plot with polynomial regression curve ($y = 49.4 x^2 + 3308 x - 499$ with $R^2 = 0.9998$). Each calibration point is measured in triplicate. Error bars represent standard deviation of triplicate measurements. (B) Exemplary 6-point DTT calibration plot with linear fit ($0.0066 x + 0.055$ with Pearson $R = 0.99$). Each calibration point is measured in triplicate. Error bars represent standard deviation of triplicate measurements.

2 Results and discussion

2.1 Oxidative potential of PACs

Table S 3. OP_{H2O2} and OP_{DTT} of PACs including the standard deviation.

Substance class	Substance	H_2O_2 formation [µM (H_2O_2) $µM^{-1}$]	Standard deviation [µM (H_2O_2) $µM^{-1}$]	DTT depletion rate [µM (DTT) min^{-1} $µM^{-1}$]	Standard deviation [µM (DTT) min^{-1} $µM^{-1}$]
NPAHs	1-NNAP	<8.5E-04	3.34E-04	<4.2E-04	1.36E-04
	9-NPHE	<8.5E-04	1.51E-03	<4.2E-04	1.36E-04
	1-NPYR	5.30E-03	5.93E-03	1.13E-03	8.20E-05
	3-NFLT	2.70E-03	2.18E-03	2.07E-03	1.86E-04
	6-NCHR	2.80E-02	1.88E-02	<4.2E-04	1.36E-04
N_2PAHs	1,3-N_2NAP	8.00E-03	7.02E-03	<4.2E-04	1.36E-04
	2,7-N_2FLN	1.40E-03	1.06E-03	3.00E-03	1.38E-03
	1,3-N_2PYR	5.70E-03	4.02E-03	5.55E-04	3.13E-04
O_2PAHs	1,2-O_2NAP	3.40E+01	2.26E+01	2.25E+00	6.56E-01
	1,4-O_2NAP	1.10E+01	5.92E+00	1.61E-01	2.05E-02
	2-M-1,4-O_2NAP	2.10E-01	1.25E-01	5.30E-02	1.78E-03
	2-OH-1,4-O_2NAP	3.20E-02	2.03E-02	2.82E-02	a
	5-OH-1,4-O_2NAP	3.30E-01	2.03E-01	1.06E+00	1.08E+00
	1,2-O_2ACE	<8.5E-04	1.63E-03	9.14E-03	8.49E-05
	1,4-O_2ANT	1.5E-01	7.6E-02	1.60E-02	3.19E-03
	1,4-O_2PHE	1.5E+00	8.1E-01	2.49E-03	a
	9,10-O_2ANT	1.80E-03	1.25E-03	1.02E-02	1.19E-02
	9,10-O_2PHE	6.50E+00	5.34E+00	3.53E+00	6.06E-01
	2-M-9,10-O_2ANT	<8.5E-04	1.46E-03	<4.2E-04	1.36E-04
	1,2-O_2AAN	<8.5E-04	8.83E-04	<4.2E-04	1.36E-04
	4,5-O_2PYR	1.50E+00	7.86E-01	1.34E+01	2.83E+00
	1,4-O_2CHR	3.20E-01	2.14E-01	4.64E-03	1.34E-04
	5.6-O_2CHR	2.60E-01	1.48E-01	3.12E+00	1.08E+00
	5,12-O_2NAC	2.10E-02	1.46E-02	1.39E-03	7.01E-04
	7,12-O_2BAN	<8.5E-04	1.85E-03	1.28E-02	2.02E-03
	1,6-O_2BAP	1.80E-01	1.13E-01	6.73E-03	6.24E-04
	4,5-O_2BAP	2.30E-01	1.57E-01	5.07E-02	1.92E-02

Substance class	Substance	H_2O_2 formation [µM (H_2O_2) $µM^{-1}$]	Standard deviation [µM (H_2O_2) $µM^{-1}$]	DTT depletion rate [µM (DTT) min^{-1} $µM^{-1}$]	Standard deviation [µM (DTT) min^{-1} $µM^{-1}$]
	6,12-O_2BAP	1.20E-01	8.02E-02	1.25E-02	2.10E-03
OPAHs	1-OACE	<8.5E-04	2.03E-03	<4.2E-04	1.36E-04
	9-OFLN	<8.5E-04	2.14E-03	<4.2E-04	1.36E-04
	1-OPHL	3.50E-02	1.97E-02	2.67E-03	1.47E-04
	BAN	<8.5E-04	1.68E-03	1.08E-03	5.39E-04
	11-OBaFLN	<8.5E-04	9.47E-04	2.05E-03	1.33E-03
	6-OBPYR	<8.5E-04	9.35E-04	5.84E-04	3.68E-04
NOPAHs	2-N-9-OFLN	<8.5E-04	1.00E-03	<4.2E-04	1.36E-04
	2,7-N_2-9-OFLN	5.50E-03	4.19E-03	<4.2E-04	1.36E-04
	3-NBAN	7.10E-03	9.57E-03	<4.2E-04	1.36E-04
O-heterocycle	1,8-NAA	1.90E-03	1.46E-03	8.04E-04	a
	6-OBCC	6.10E-03	3.87E-03	2.77E-03	2.69E-03
Monoarom.	1,4-BQ	4.10E-01	8.37E-02	<4.2E-04	1.36E-04

[a]No standard deviation since only one measurement above LOQ

2.2 Reduction potential of reductants

Under physiological conditions, AA is to 99.9 % in the form of the ascorbate (AscH-) (Asard et al. 2004). When it is oxidized, it normally loses one electron, and one proton since the neutral ascorbate radical is highly acidic (Warren and Mayer, 2010).The ascorbate radical (Asc^{-}) / ascorbate ($AscH^{-}$) has a reduction potential of 282 mV at pH 7 (Williams et al., 1982). Merkhofer et al. (2006) reported the reduction potential of that couple at biologically relevant conditions (pH and steady-state concentrations) as 105 mV which is the value adopted in the study of Charrier et al. (2014). The real value in the lung fluid can be even different since the value reported by Merkofer and colleagues is only an estimation for the $AscH^{-}/Asc^{-}$ ratio at steady-state conditions in cells.

Table S 4. Reduction potential of antioxidants. Reaction conditions: In aqueous phase at pH 7.

Reductant	Reduction potential [mV]	Reference
DTT: RSH/ $RS^{\cdot}$	-330	Cleland, 1963
Ascorbic acid: Ascorbate ($AscH^{-}$)/ascorbate radical ($Asc^{\cdot -}$)	282	Williams et al., 1982
Uric acid: UH^{2-}/$^{\cdot}UH^{-}$	590	Simic & Jovanovic, 1989

2.3 Reduction potential of PACs

The reduction potential values of the target compounds used in this paper are shown in Table S4. An overview about the reduction potential values used in this paper is shown in Table S4. Published literature report standard reduction potentials (determined in aqueous solution) for only a few PACs probably due to the low aqueous solubility of some PACs (O'Brien et al., 1991; Wardman et al., 1989; Song & Buettner, 2010). According to Wardman (1990), the reduction potentials in organic solvents are not the same as reduction potentials determined in water since the semiquinones are more stable in aprotic solvents such as dimethylformamide (DMF). However, the reduction potential of PACs in aqueous solution can be estimated from the values measured in organic solvents. This is because the reduction potentials of PACs determined in organic solvents are highly correlated with reduction potentials determined in aqueous phase (Song & Buettner, 2010; Roginsky et al., 1999). For example the reduction potential of quinones in aqueous phase ($E(Q/Q^{\cdot -})_{aq}$) was calculated from the values in acetonitrile ($E(Q/Q^{\cdot -})_{ACN}$) using the correlation in Equation 1 (Roginsky et al., 1999).

$$E(Q/Q^{\cdot -})_{aq} = 600 + 1.1E(Q/Q^{\cdot -})_{ACN} \quad \text{Equation 1}$$

The equations for the conversion of reduction potential values in an organic solvent using different electrodes to the reduction potential values in aqueous phase against the normal hydrogen electrode (NHE) are shown in the correlation plots in Figure S2. The correlations were performed with compounds with known values at both conditions. The resulting equations were used to convert the compounds with reduction potentials in organic phase to the reduction potential values in aqueous phase, which were not known before.

For some of the OPAHs, measured reduction potential values are not available in the literature (neither in aqueous solution nor in an organic solvent). For some of such compounds, their theoretically calculated reduction potentials were adopted (Er et al., 2015).

There are uncertainties in the adopted reduction potentials due to differences in the methods of determination and the estimations of the reduction potential in aqueous solution based on experimental values in an organic phase. The uncertainties in the measured reduction potentials were not available for some compounds. Roginsky et al. (1999) concluded that most of the values will reliably be better than +/- 10 mV for values experimentally determined. The error of the calculated values based on correlations will be even higher.

Table S 5. Reduction potential of PACs in aqueous phase against normal hydrogen electrode (NHE) at pH 7. "/" when not found in the literature.

Substance	Reduction potential [mV]	Standard deviation [mV]	Conver-ted*	Literature source
1-NNAP	-817	21	yes	Tachibana et al., 1967; Klopman et al., 1984; Jung et al., 1991
9-NPHE	-851	a	yes	Fukuhara et al., 1994
1-NPYR	-730	a	no	Kovacic et al., 1990
3-NFLT	-542	97	yes	Fukuhara et al., 1994; Lopes et al., 2005
6-NCHR	-780	20	yes	Fu et al., 1988; Jung et al., 1991; Lopes et al., 2005
1,3-N_2NAP	-306	a	yes	Fukuhara et al., 1994
2,7-N_2FLN	-701	a	yes	Klopman et al., 1984
1,3-N_2PYR	-575	76	yes	Klopman et al., 1984; Jung et al., 1991
1,2-O_2NAP	-89	0	no	Butler and Hoey, 1986; Roginsky et al., 1999; Huynh et al., 2016
1,4-O_2NAP	-139	10	no	Butler and Hoey ,1986; Wardman, 1989; Öllinger et al., 1990; Bironaite et al., 1991; Čénas et al., 1994; Roginsky et al., 1999; Anusevičius et al., 2002; Huynh et al., 2016
2-M-1,4-O_2NAP	-196	15	no	Ilan et al., 1976; Trumpower et al., 1982; Butler and Hoey , 1986; Mukherjee, 1987; Wilson et al., 1986; Wardman, 1989; Öllinger et al., 1990; Bironaite et al., 1991; Čénas et al., 1994; Roginsky et al., 1999; Anusevičius et al., 2002; Huynh et al., 2016
2-OH-1,4-O_2NAP	-392	46	no	Wardman, 1989; Öllinger et al., 1990; Čénas et al., 1994; Roginsky et al., 1999; Anusevičius et al., 2002
5-OH-1,4-O_2NAP	-93	2	no	Wardman 1989; Öllinger et al., 1990; Čénas et al., 1994; Roginsky et al., 1999; Anusevičius et al., 2002
1,2-O_2ACE	/	/		
1,4-O_2ANT	-205	26	yes	Josien et al., 1953; Moriconi et al., 1962; Yamaji et al., 2002
1,4-O_2PHE	-86	13	yes	Josien et al., 1953
9,10-O_2ANT	-445	a	no	Pal et al., 1994; Roginsky et al., 1999; Huynh et al., 2016
9,10-O_2PHE	-122	2	no	Butler and Hoey, 1986; Wardman 1989; Bironaite et al., 1991; Čénas et al., 1994; Roginsky et al., 1999; Anusevičius et al., 2002
2-M-9,10-O_2ANT	-472	22	yes	Conant and Fieser, 1924; Er et al., 2015

Substance	Reduction potential [mV]	Standard deviation [mV]	Conver-ted*	Literature source
1,2-O_2AAN	/	/		
4,5-O_2PYR	-167		yes	Moriconi et al., 1962
1,4-O_2CHR	/	/		
5.6-O_2CHR	-176	a	yes	Fieser and Dietz, 1931
5,12-O_2NAC	-545	103	yes	Kano and Uno, 1993; Fukuhara et al., 1994; Yamaji et al., 2002
7,12-O_2BAN	-380	26	yes	Badger and McKenzie, 1953; Josien et al., 1953
1,6-O_2BAP	-203	a	yes	Moriconi et al., 1962
4,5-O_2BAP	-199	a	yes	Moriconi et al., 1962
6,12-O_2BAP	-198	a	yes	Moriconi et al., 1962
1-OACE	/	/		
9-OFLN	-702	a	yes	Kuder et al., 1978
1-OPHL	/	/		
BAN	-384	a	yes	Onchoke and Trevino, 2019
11-OBaFLN	/	/		
6-OBPYR	/	/		
2-N-9-OFLN	/	/		
2,7-N_2-9-OFLN	-320	297	yes	Kuder et al., 1978; Klopman et al., 1984
3-NBAN	-404	a	yes	Takamura-Enya et al., 2006
1,8-NAA	/	/		
6-OBCC	/	/		
1,4-BQ	88	10	no	Rich and Bendall, 1980; Trumpower et al., 1982; Wardman, 1989; Bironaite et al., 1991; Čénas et al., 1994; Roginsky et al., 1999; Anusevičius et al., 2002; Cape et al., 2006; Huynh et al., 2016

[a]No standard deviation since value from only one study.

2.3.1 Plots for conversion to common conditions

a)

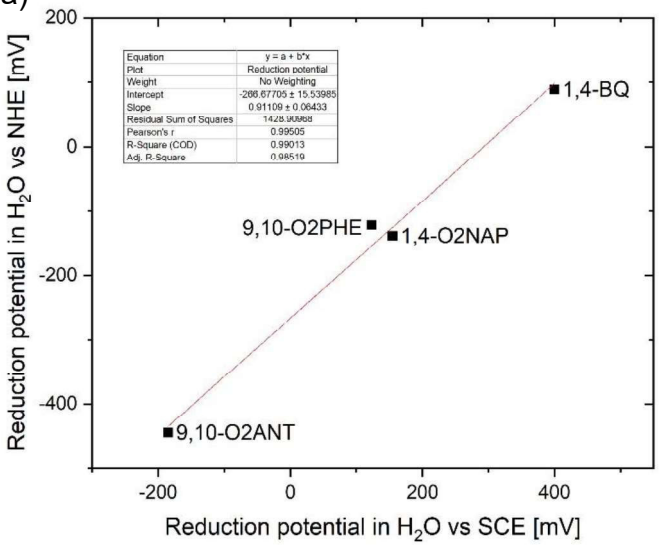

b)

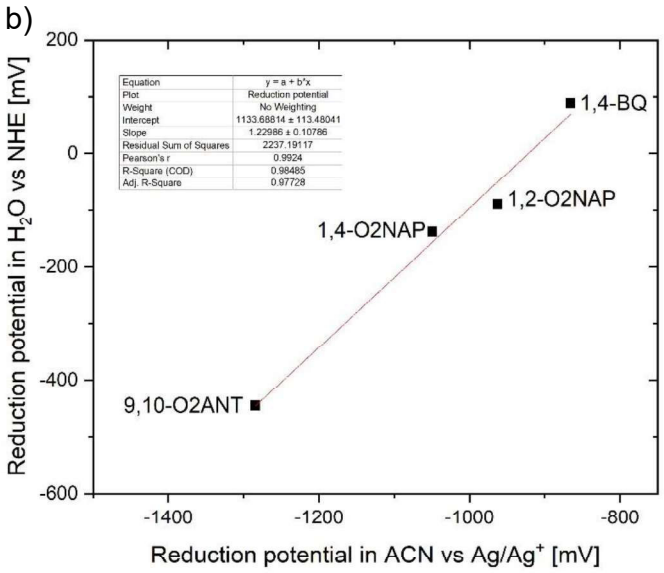

c)

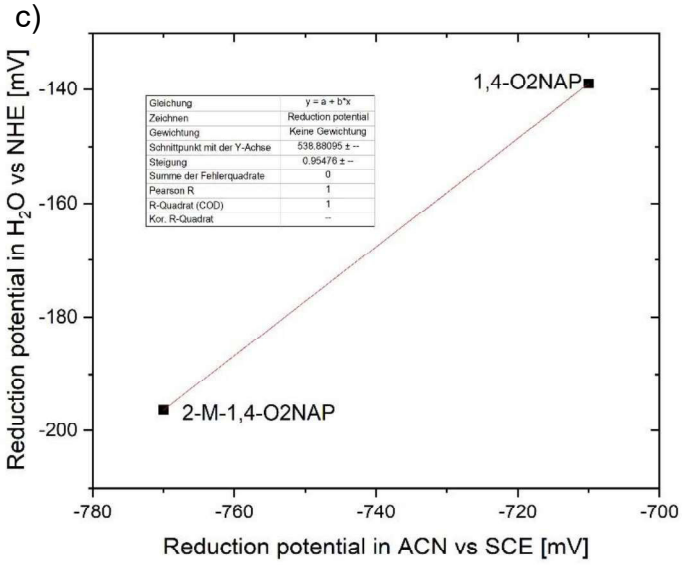
Gleichung y = a + b*x
Zeichnen Reduction potential
Gewichtung Keine Gewichtung
Schnittpunkt mit der Y-Achse 538.88095 ± --
Steigung 0.95476 ± --
Summe der Fehlerquadrate 0
Pearson R 1
R-Quadrat (COD) 1
Kor. R-Quadrat --
1,4-O2NAP
2-M-1,4-O2NAP
-140
-160
-180
-200
-780
-760
-740
-720
-700
Reduction potential in H2O vs NHE [mV]
Reduction potential in ACN vs SCE [mV]

d)

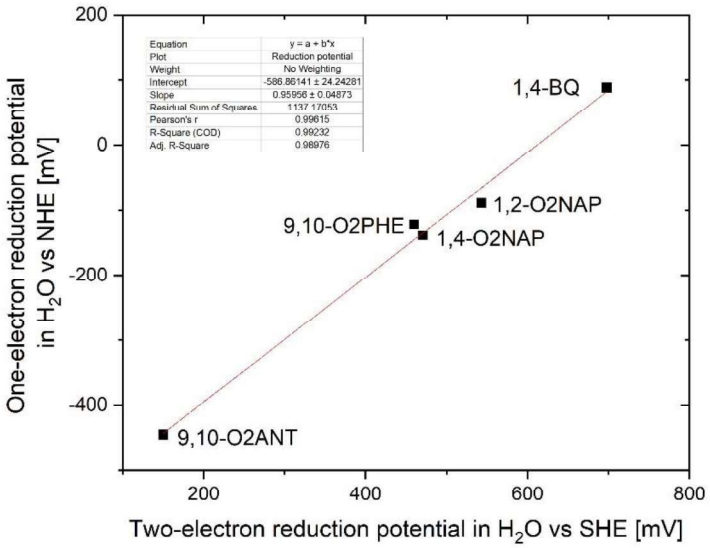
Equation y = a + b*x
Plot Reduction potential
Weight No Weighting
Intercept -586.86141 ± 24.24281
Slope 0.95956 ± 0.04873
Residual Sum of Squares 1137.17053
Pearson's r 0.99615
R-Square (COD) 0.99232
Adj. R-Square 0.98976
1,4-BQ
1,2-O2NAP
9,10-O2PHE
1,4-O2NAP
9,10-O2ANT
200
0
-200
-400
200
400
600
800
One-electron reduction potential in H2O vs NHE [mV]
Two-electron reduction potential in H2O vs SHE [mV]

e)

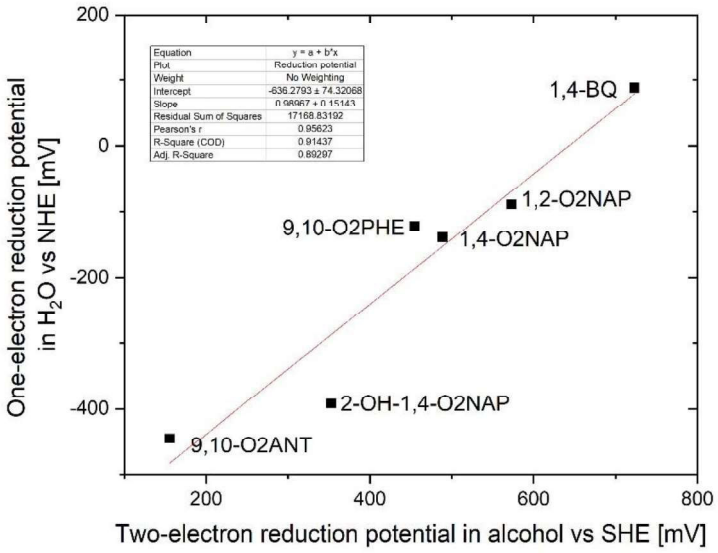
Equation y = a + b*x
Plot Reduction potential
Weight No Weighting
Intercept -636.2793 ± 74.32068
Slope 0.98667 ± 0.15143
Residual Sum of Squares 17168.83192
Pearson's r 0.95623
R-Square (COD) 0.91437
Adj. R-Square 0.89297
1,4-BQ
1,2-O2NAP
9,10-O2PHE
1,4-O2NAP
2-OH-1,4-O2NAP
9,10-O2ANT
One-electron reduction potential in H2O vs NHE [mV]
Two-electron reduction potential in alcohol vs SHE [mV]
200
0
-200
-400
200
400
600
800

f)

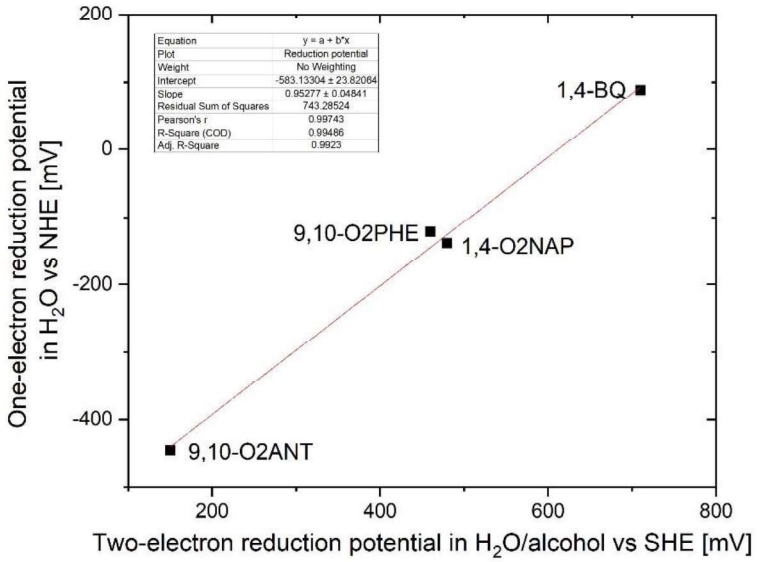
Equation y = a + b*x
Plot Reduction potential
Weight No Weighting
Intercept -583.13304 ± 23.82064
Slope 0.95277 ± 0.04841
Residual Sum of Squares 743.28524
Pearson's r 0.99743
R-Square (COD) 0.99486
Adj. R-Square 0.9923
1,4-BQ
9,10-O2PHE
1,4-O2NAP
9,10-O2ANT
One-electron reduction potential in H2O vs NHE [mV]
Two-electron reduction potential in H2O/alcohol vs SHE [mV]
200
0
-200
-400
200
400
600
800

15

g)

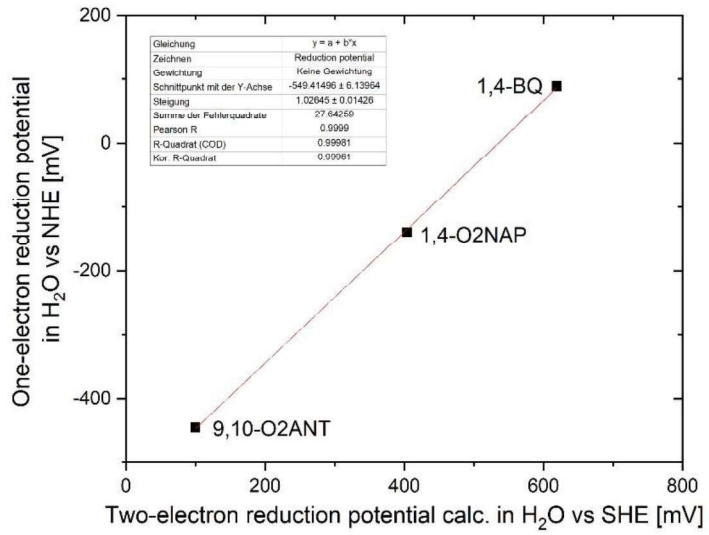

Figure S 2. Correlation plot of reduction potential values with different experimental conditions including the linear fit in order to convert values measured with other experimental conditions to one common method (in H_2O vs NHE). One-electron reduction potential in H_2O vs NHE against a) one-electron reduction potential in H_2O vs standard calomel electrode (SCE) (Kano & Uno, 1993), b) one-electron reduction potential in acetonitrile (ACN) vs Ag/Ag+ electrode (Huynh et al., 2016; Onchoke & Trevino, 2019), c) one-electron reduction potential in ACN vs SCE (Kuder et al., 1978; Yamaji et al., 2002; Takamura-Enya et al., 2006), d) two-electron reduction potential in H_2O vs standard hydrogen electrode (SHE) (Conant & Fieser, 1922; 1924; Josien et al., 1953), e) two-electron reduction potential in alcohol vs SHE (Conant & Fieser, 1922; 1924; Fieser and Dietz, 1931; Badger and McKenzie, 1953; Moriconi et al., 1962), f) two-electron reduction potential in H_2O/alcohol vs SHE (Josien et al., 1953) and g) theoretically calculated two-electron reduction potential in H_2O vs SHE (Er et al., 2015).

2.4 Predictability of OP by reduction potential

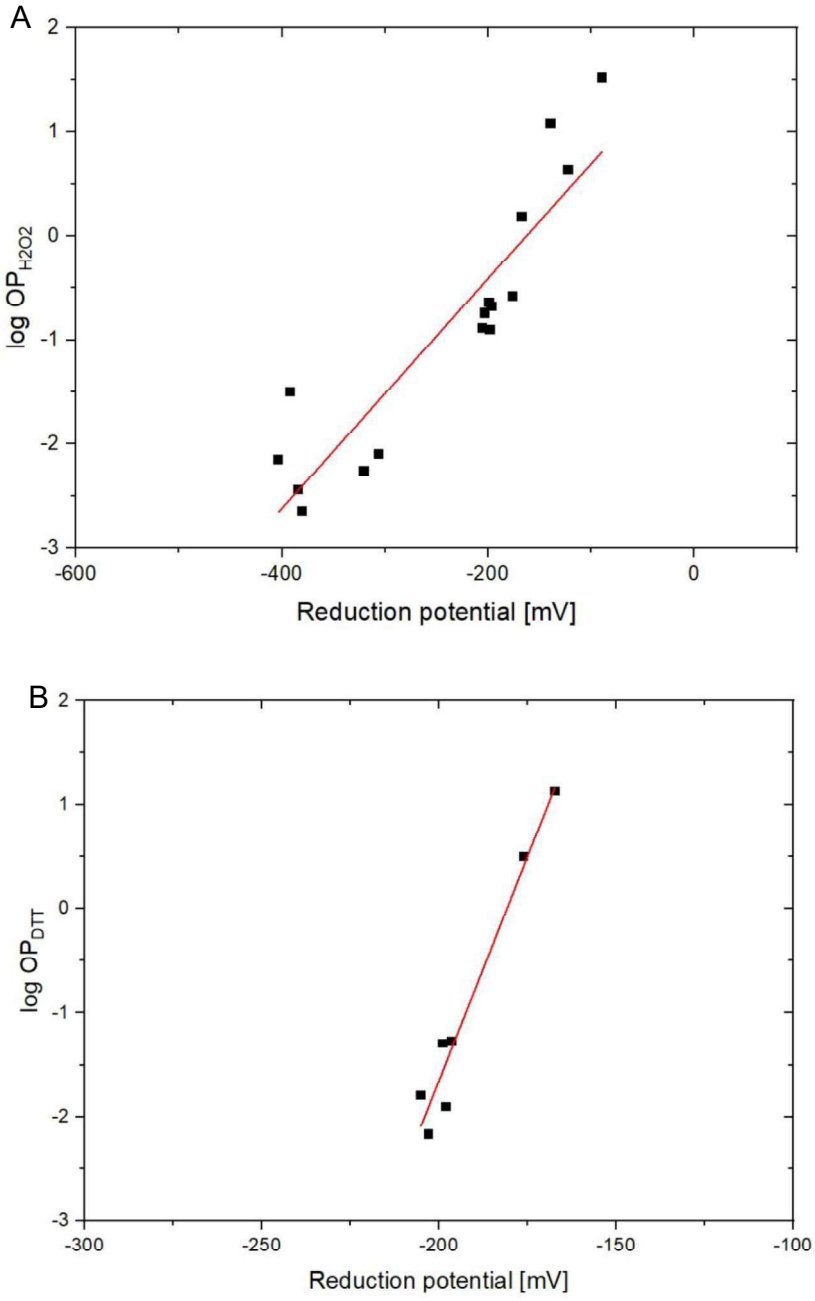

Figure S 3. Log-linear fit (in red) for part of increasing log OP (A: OP_{H2O2}; B: log OP_{DTT}) with increasing reduction potential (A: $\log(OP_{H2O2}) = 0.011\ E(PAC/PAC^{-}) + 1.75$ with Pearson R = 0.91; B: $\log(OP_{DTT}) = 0.086\ E(PAC/PAC^{-}) + 15.55$ with Pearson R = 0.98).

2.5 LUMO energy level of PACs

Most LUMO energy level values of OPAHs in the literature are calculated by the density functional theory (DFT) (Namazian et al., 2004; Ding et al., 2016; Miao et al., 2018). In contrast, most LUMO values of the NPAHs are calculated by semi-empirical methods, namely the Austin Model 1 (AM1) method and the Modified Neglect of Diatomic Overlap (MNDO) method (Debnath et al., 1991; Lopez de Compadre et al., 1990).

The values reported in the literature by each method do not encompass the complete set of target compounds in our study. The most advanced method would be to calculate the LUMO energies of all targeted PACs by using a theoretical quantum mechanical model with the same level and input parameters. Though, this is beyond the scope of this paper. Hence, one ends up with having to collect LUMO energy level data calculated with different methods, with its inherent internal inconsistencies. However, the literature values calculated by different DFT levels and with different solvents have a high correlation (Figure S4 with R^2 = 0.96-0.9999) and hence can be converted to one common method. However, this is only possible for the OPAHs since the NPAHs values are almost completely measured by semi-empirical methods. Consequently, for our particular study, the relationships between our measured OP and LUMO energy level could, in each case, only be derived from a subset of compounds.

As visible in Figure S4, the correlations between different methods were performed with compounds with known values at both conditions. The resulting equations were used to convert the compounds with LUMO energy level calculated by another basis set to the LUMO energy level using DFT at the B3LYP + 6-311+G(d,p) level with 1,2-dimethoxymethane (DME) as solvent, which were not known before (Table S6).

The amount of literature reporting LUMO energy values of PACs is much lower than studies reporting reduction potential values. Due to that, we did not have several values from one compound calculated with the same method to derive a standard deviation. In addition, the values in the literature are frequently reported without standard deviation. For that reason, we hypothesized a standard deviation of 2.5 % for the values calculated by the method, which is finally used for our plots. All values converted from another method based on correlation are reported with a standard deviation of 5 %. BAN, which is converted by a correlation of values with the same method but from another paper is reported with a standard deviation of 10 %.

Table S 6. LUMO energy level values a) (DFT at the B3LYP + 6-311+G(d,p) level with 1,2-dimethoxymethane (DME) as solvent) of PACs, b) MNDO method, c) AM1 method, d) STO-3G and Hückel method. "/" when not found in the literature.

a)

Substance	LUMO energy level [eV]	Standard deviation [eV]	Source	Method
1-NNAP	/	/		
9-NPHE	/	/		
1-NPYR	-2.726	-0.136	Xia et al., 2013	DFT B3LYP + 6-31G(d) in methanol
3-NFLT	/	/		
6-NCHR	/	/		
1,3-N_2NAP	/	/		
2,7-N_2FLN	/	/		
1,3-N_2PYR	/	/		
1,2-O_2NAP	-3.474	-0.087	Miao et al., 2018	same as final
1,4-O_2NAP	-3.412	-0.085	Miao et al., 2018	same as final
2-M-1,4-O_2NAP	-3.289	-0.164	El-Hout et al., 2017	DFT B3LYP + 6-31G(d,p)
2-OH-1,4-O_2NAP	-3.183	-0.159	Wang et al., 2011	DFT PBE0 + 6-31G(d)
5-OH-1,4-O_2NAP	-3.627	-0.181	Wang et al., 2011	DFT PBE0 + 6-31G(d)
1,2-O_2ACE				
1,4-O_2ANT	-3.257	-0.081	Miao et al., 2018	same as final
1,4-O_2PHE	-3.485	-0.087	Miao et al., 2018	same as final
9,10-O_2ANT	-3.083	-0.077	Miao et al., 2018	same as final
9,10-O_2PHE	-3.312	-0.083	Miao et al., 2018	same as final

Substance	LUMO energy level [eV]	Standard deviation [eV]	Source	Method
2-M-9,10-O_2ANT	-3.044	-0.152	Uno et al., 1985; Namazian et al., 2003	PPP-SCF-MO, DFT B3LYP + 6-31G(d,p) in acetonitrile
1,2-O_2AAN	/	/		
4,5-O_2PYR	/	/		
1,4-O_2CHR	/	/		
5.6-O_2CHR	/	/		
5,12-O_2NAC	-2.986	-0.149	Uno et al., 1985; Ding et al., 2016	PPP-SCF-MO; DFT B3LYP + 6-31G(d,p) in dimethylacetamide
7,12-O_2BAN	/	/		
1,6-O_2BAP	-3.202	-0.160	Zhao et al., 2011	DFT B3LYP + 6-31G(d) in methanol
4,5-O_2BAP	/	/		
6,12-O_2BAP	-3.181	-0.159	Zhao et al., 2011	DFT B3LYP + 6-31G(d) in methanol
1-OACE	/	/		
9-OFLN	/	/		
1-OPHL	/	/		
BAN	-2.673	-0.267	Onchoke et al., 2011	DFT B3LYP + 6-311+G(d,p)
11-OBaFLN	/	/		
6-OBPYR	/	/		
2-N-9-OFLN	/	/		
2,7-N_2-9-OFLN	/	/		
3-NBAN	/	/		
1,8-NAA	/	/		
6-OBCC	/	/		
1,4-BQ	-3.733	-0.093	Miao et al., 2018	same as final

b)

Substance	LUMO value [eV]	Source
1-NNAP	-1.267	Lopez de Compadre, 1990
1-NPYR	-1.67	Lopez de Compadre, 1990
3-NFLT	-1.634	Lopez de Compadre, 1990
6-NCHR	-1.621	Lopez de Compadre, 1990
1,3-N_2NAP	-2.025	Lopez de Compadre, 1990
2,7-N_2FLN	-2.229	Lopez de Compadre, 1990
2,7-N_2-9-OFLN	-2.312	Lopez de Compadre, 1990

20

c)

Substance	LUMO value [eV]	Source
1-NNAP	-1.266	Debnath et al. 1991
9-NPHE	-1.254	Debnath et al. 1991
1-NPYR	-1.698	Debnath et al. 1991
3-NFLT	-1.676	Debnath et al. 1991
6-NCHR	-1.61	Debnath et al. 1991
1,3-N_2NAP	-1.952	Debnath et al. 1991
2,7-N_2FLN	-2.155	Debnath et al. 1991
2,7-N_2-9-OFLN	-2.338	Debnath et al. 1991
3-NBAN	-2.099	Takamura-Enya (2006)

d)

Substance	LUMO value [a.u.]	LUMO value [ß]	Source
1-NNAP	0.16769	-0.309	Maynard et al., 1986
2-NFLN	0.16155	-0.348	Maynard et al., 1986
3-NFLT	0.13248	-0.219	Maynard et al., 1986
1-NPYR	0.13838	-0.263	Maynard et al., 1986
2,7-N_2FLN	0.13026	-0.289	Maynard et al., 1986
1,3-N_2PYR	0.11448	-0.217	Maynard et al., 1986
2,7-N_2-9-OFLN	0.11694	-0.088	Maynard et al., 1986

2.5.1 Plots for conversion to common DFT method

a)

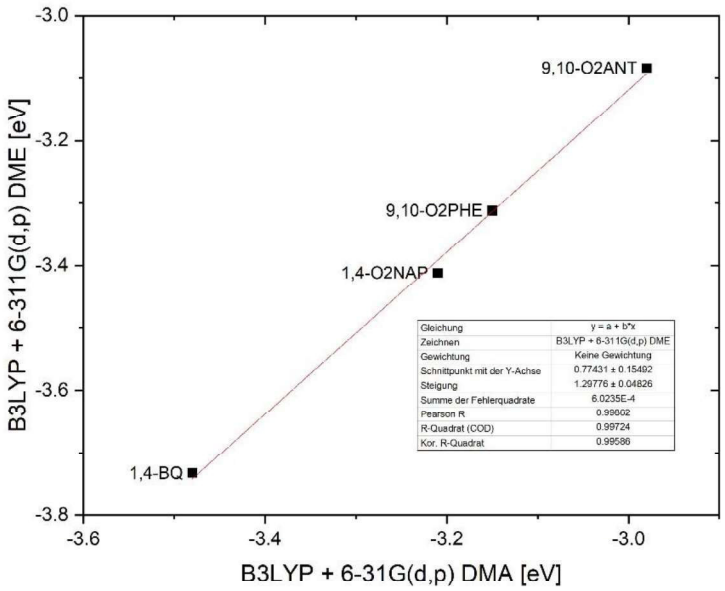

b)

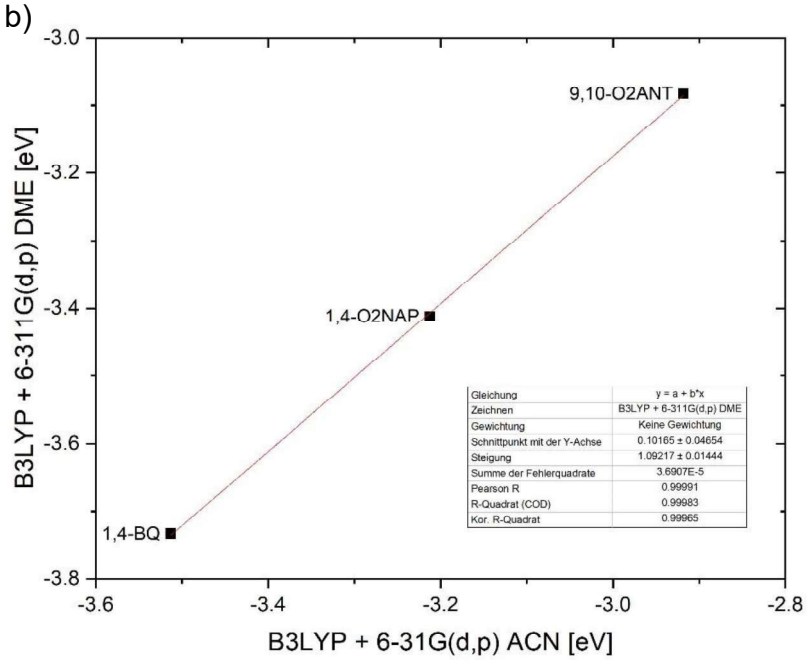

c)

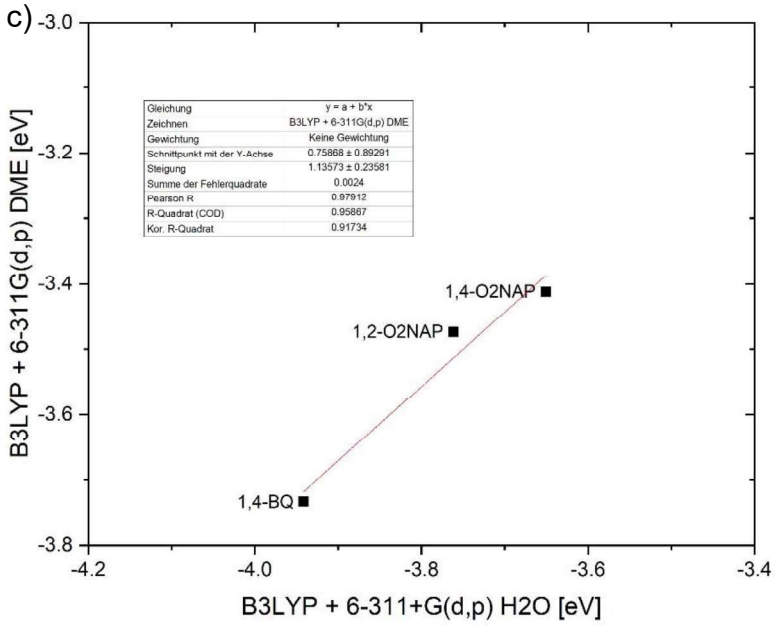
Gleichung y = a + b*x
Zeichnen B3LYP + 6-311G(d,p) DME
Gewichtung Keine Gewichtung
Schnittpunkt mit der Y-Achse 0.75868 ± 0.89291
Steigung 1.13573 ± 0.23581
Summe der Fehlerquadrate 0.0024
Pearson R 0.97912
R-Quadrat (COD) 0.95867
Kor. R-Quadrat 0.91734
1,4-O2NAP
1,2-O2NAP
1,4-BQ
-3.0
-3.2
-3.4
-3.6
-3.8
-4.2
-4.0
-3.8
-3.6
-3.4
B3LYP + 6-311G(d,p) DME [eV]
B3LYP + 6-311+G(d,p) H2O [eV]

d)

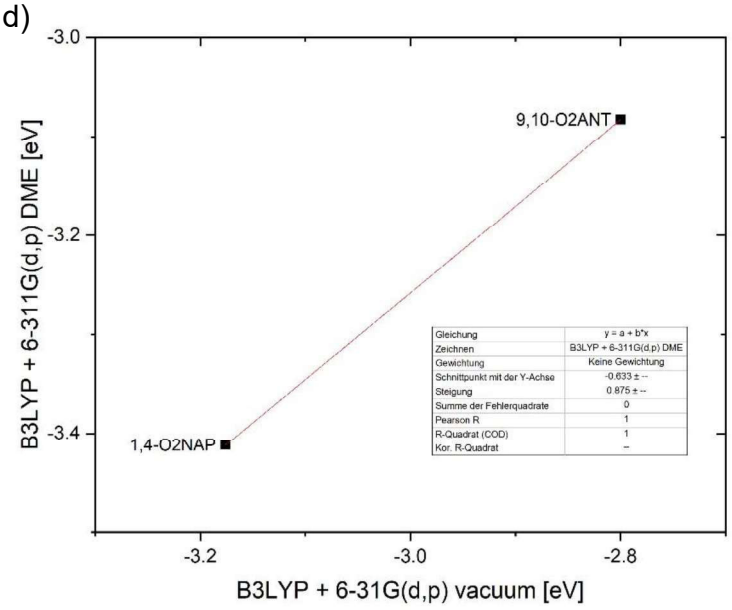
9,10-O2ANT
1,4-O2NAP
Gleichung y = a + b*x
Zeichnen B3LYP + 6-311G(d,p) DME
Gewichtung Keine Gewichtung
Schnittpunkt mit der Y-Achse -0.633 ± --
Steigung 0.875 ± --
Summe der Fehlerquadrate 0
Pearson R 1
R-Quadrat (COD) 1
Kor. R-Quadrat --
-3.0
-3.2
-3.4
-3.2
-3.0
-2.8
B3LYP + 6-311G(d,p) DME [eV]
B3LYP + 6-31G(d,p) vacuum [eV]

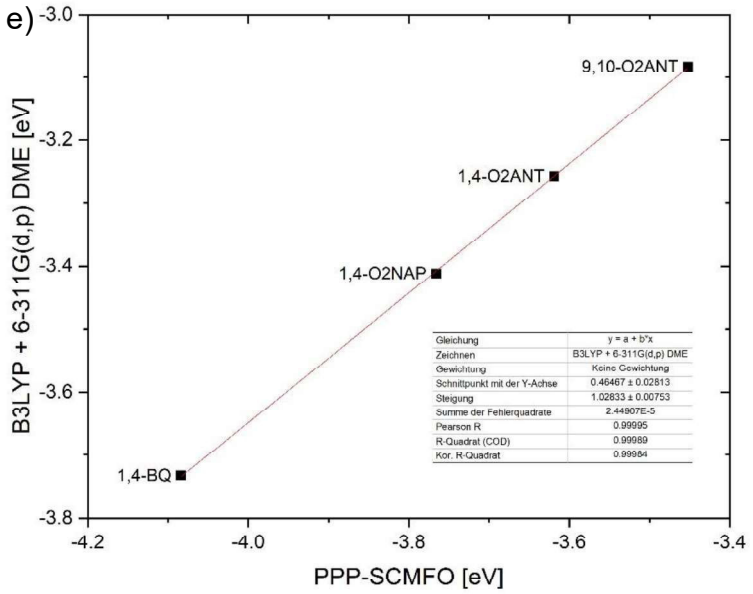

Figure S 4. Correlation plot of LUMO values: DFT B3LYP + 6-311G(d,p) with solvent DME a) vs DFT B3LYP + 6-31G(d,p) with solvent DMA with regression line: y = 1.30 x + 0.77 with Pearson R = 0.9986; b) vs DFT B3LYP + 6-31G(d,p) with solvent acetonitrile (ACN) with regression line: y = 1.09 x + 0.10 with Pearson R = 0.9999; c) vs B3LYP + 6-311+G(d,p) with solvent H2O with regression line: y = 1.14 x + 0.76 with Pearson R = 0.9791; d) vs B3LYP + 6-31G(d,p) in vacuum with regression line: y = 0.88 x - 0.63 with Pearson R = 1 (only 2 values) and e) vs PPP-SCMFO with regression line: y = 1.03 x + 0.46 with R^2 = 0.99995.

2.6 Predictability of OP by LUMO energy level

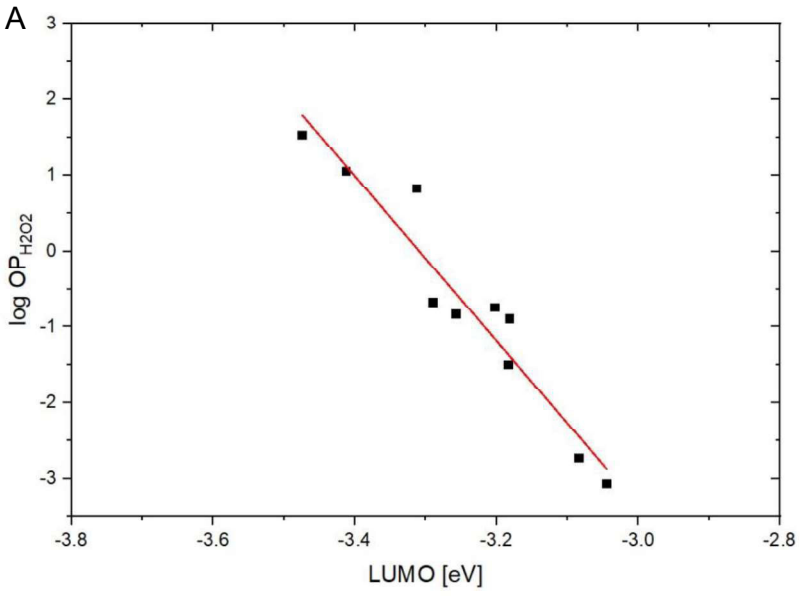

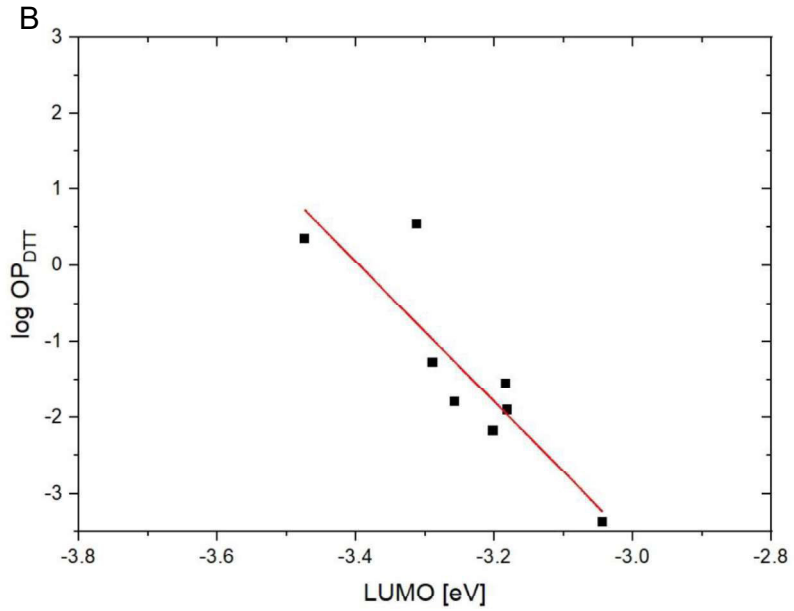

Figure S 5. Log-linear fit (in red) for part of increasing OP A: OP_{H2O2}; B: log OP_{DTT}) with decreasing LUMO energy level (A: log (OP_{H2O2}) = -10.85 * LUMO - 35.92 with Pearson R = -0.96; B: log (OP_{DTT}) = -9.2 * LUMO – 31.26 with Pearson R = -0.88).

2.6.1 OP vs LUMO energy levels – NPAHs

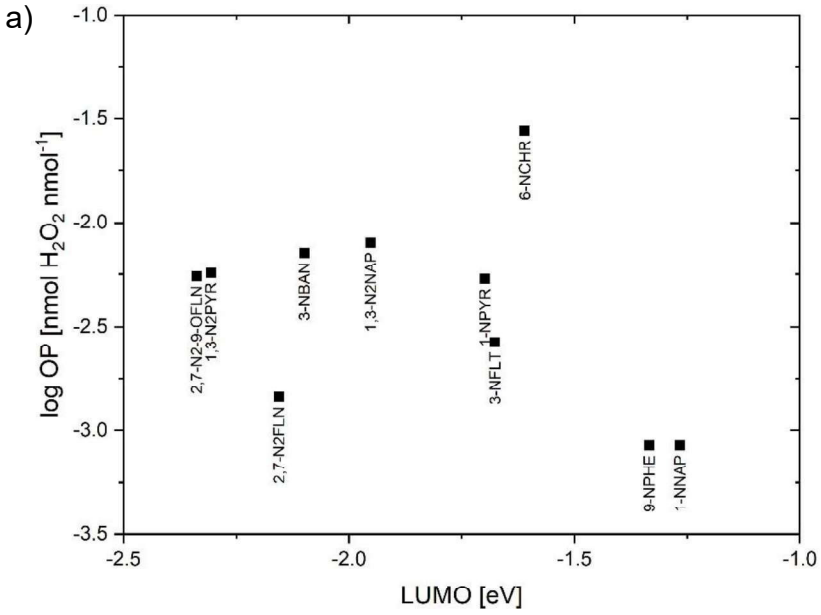

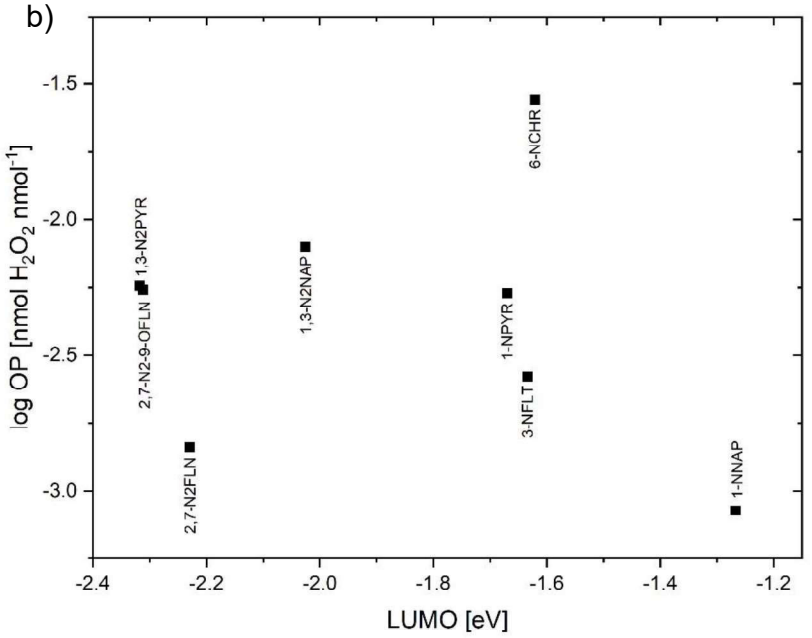
b)
log OP [nmol H_2O_2 $nmol^{-1}$]
-1.5
-2.0
-2.5
-3.0
-2.4
-2.2
-2.0
-1.8
-1.6
-1.4
-1.2
LUMO [eV]
1,3-N2PYR
2,7-N2-9-OFLN
2,7-N2FLN
1,3-N2NAP
6-NCHR
1-NPYR
3-NFLT
1-NNAP

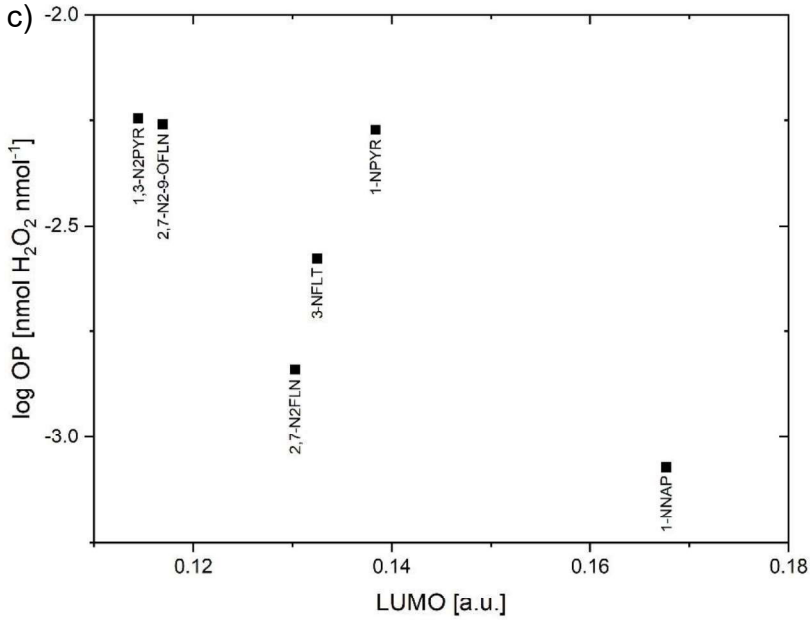
c)
log OP [nmol H_2O_2 $nmol^{-1}$]
-2.0
-2.5
-3.0
0.12
0.14
0.16
0.18
LUMO [a.u.]
1,3-N2PYR
2,7-N2-9-OFLN
3-NFLT
1-NPYR
2,7-N2FLN
1-NNAP

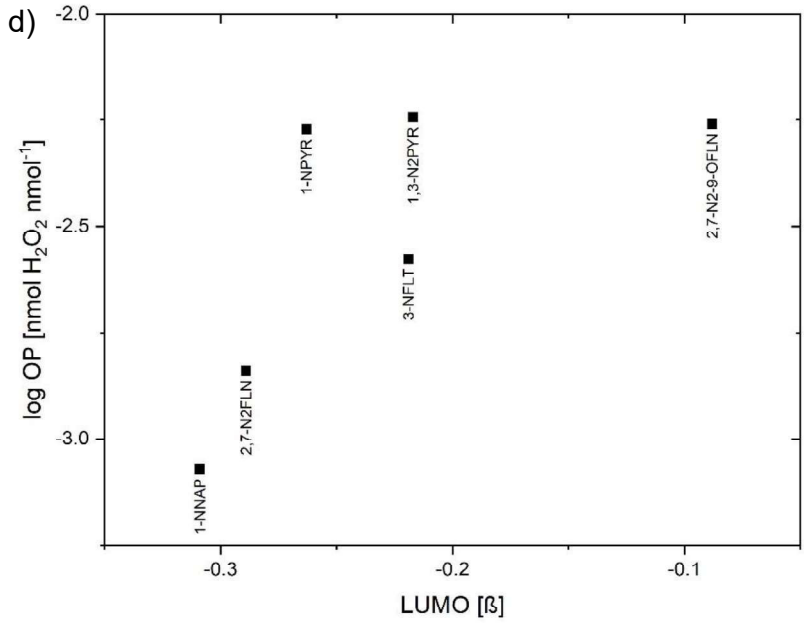

Figure S 6. Logarithm of the OP_{H2O2} in dependence of the LUMO energy level a) from the semiempirical Austin Model 1 (AM1) method (Debnath et al., 1991; Takamura-Enya et al., 2006, b) from the Modified Neglect of Diatomic Overlap (MNDO) method (Lopez de Compadre et al., 1990), c) from the STO-3G method (Maynard et al., 1986) and d) from the Hückel method (inversed order) (Maynard et al., 1986).

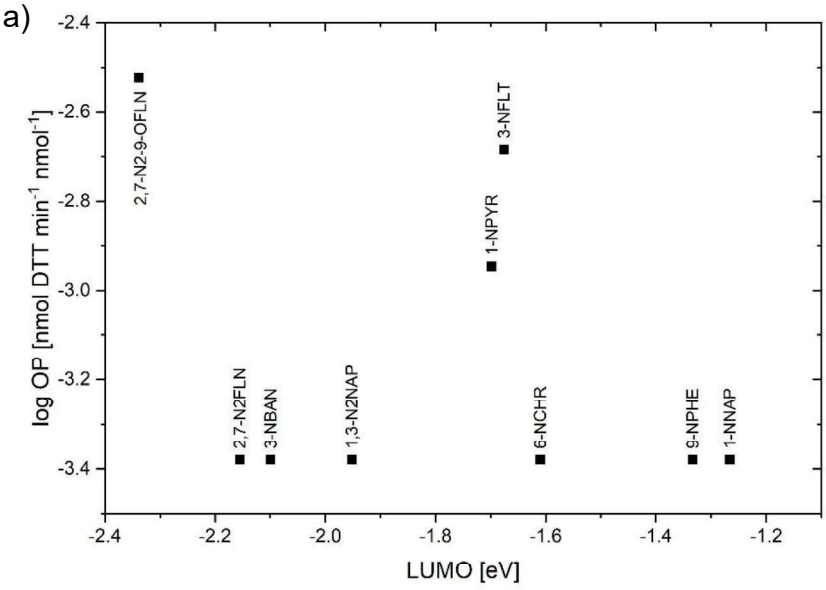

b)

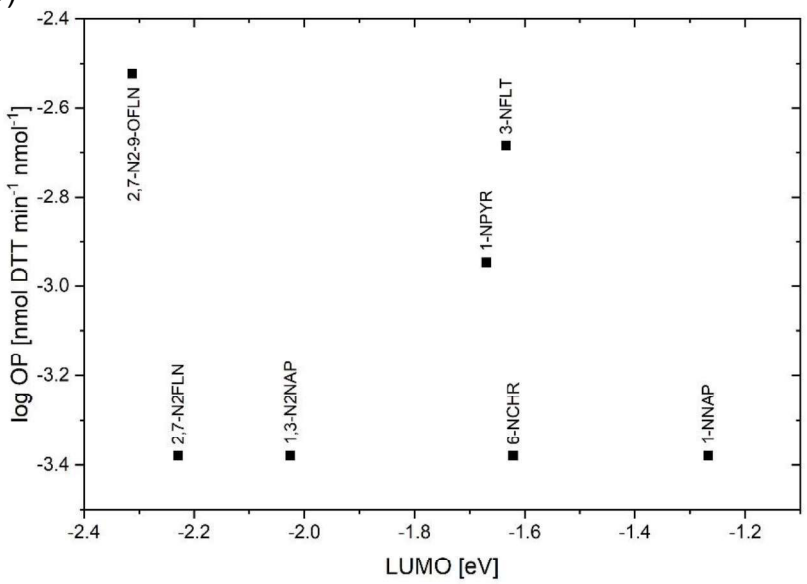
log OP [nmol DTT min-1 nmol-1]
LUMO [eV]
2,7-N2-9-OFLN
2,7-N2FLN
1,3-N2NAP
1-NPYR
3-NFLT
6-NCHR
1-NNAP

c)

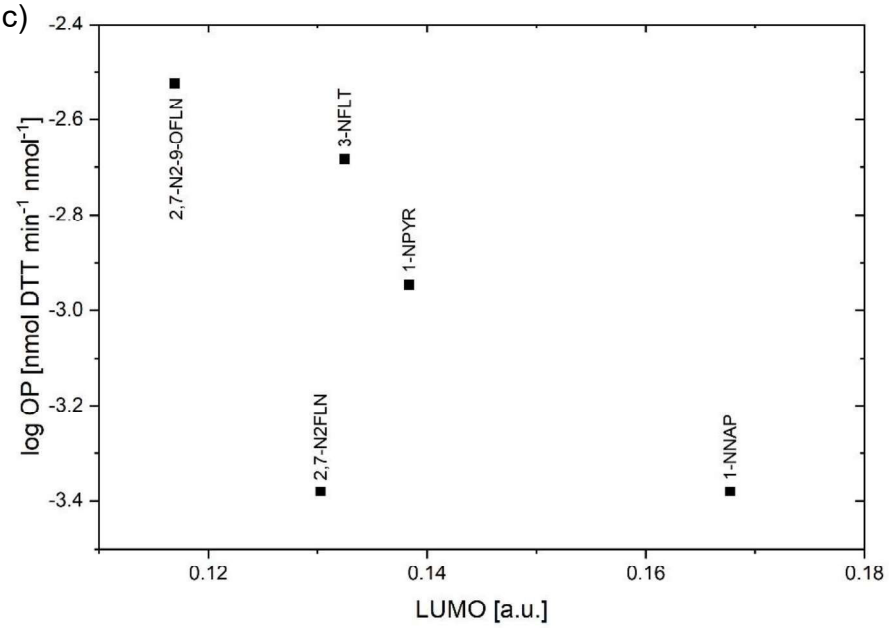
log OP [nmol DTT min-1 nmol-1]
LUMO [a.u.]
2,7-N2-9-OFLN
3-NFLT
1-NPYR
2,7-N2FLN
1-NNAP

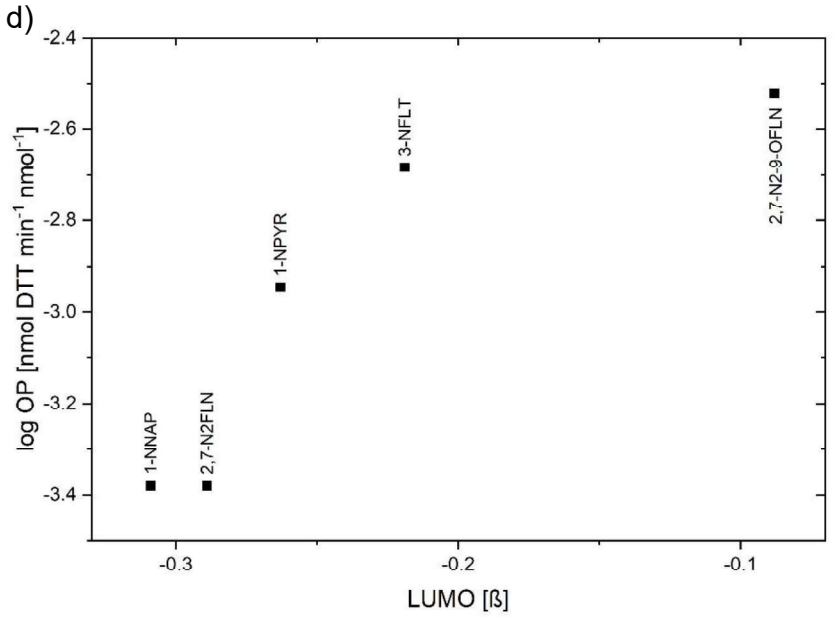

Figure S 7. Logarithm of the OP_{DTT} in dependence of the LUMO energy level a) from the semiempirical Austin Model 1 (AM1) method (Debnath et al., 1991; Takamura-Enya et al., 2006, b) from the Modified Neglect of Diatomic Overlap (MNDO) method (Lopez de Compadre et al., 1990;), c) from the STO-3G method (Maynard et al., 1986) and d) from the Hückel method (inversed order) (Maynard et al., 1986).

2.7 Predictability of OP by structural indicators

The substitution of a methyl group decreases the OP of the parent compound (Figure 6). For example in our results, 2-M-1,4-O_2NAP and 2-M-9,10-O_2ANT, have a lower OP than the 1,4-O_2NAP and 9,10-O_2ANT, respectively. This is due to the positive inductive (+I-) effect of methyl groups, which increases the electron density in the ring, and thus diminishes their ability to be reduced by antioxidants or DTT (Roginsky et al., 1999). It has also been shown that the reduction potential of compounds decreases with the number methyl groups on a compound, which related to the increases of electron density (Josien et al., 1953; Uno et al., 1985; Čénas et al., 1994; Song & Buettner, 2010; Er et al., 2015). Bachman et al. (2014) also obtained a linear decrease in the reduction potential with an increasing number of methyl groups.

As expected, the impact of the substitution of electron-withdrawing groups (nitro and carbonyl groups) was opposite to that of the methyl group (Figure 6 in main text). Since the nitro group has a negative inductive (-I-) as well as negative mesomeric (-M-) effect, the addition of a nitro group increases the OP. This could be shown for 1,3-N_2NAP vs. 1-NNAP, 3-NBAN vs BAN and 1,3-N_2PYR vs. 1-NPYR for the H_2O_2 formation potential. The influence of the nitro group on the OP is also visible in the DTT assay when comparing 9-OFLN to 2-N-9-OFLN and 2,7-N_2-9-OFLN. The OP_{DTT} was higher than the LOQ for the twice-nitrated fluorenone, while it was lower for 9-OFLN and 2-N-9-OFLN. In the H_2O_2 assay, we could observe the similar trend. The effect of an additional nitro group can also be seen from the comparison of all active NPAHs vs their non-active parent PAHs. PAHs are known not to produce ROS and they need to be oxidized to derivatives to be producers of ROS (Cho et al., 2005). Er et al. (2015) revealed from the theoretical calculation of the reduction potential that the nitro group is one of the functional groups, which increases the reduction potential the most for different naphthoquinones, benzoquinones and anthraquinones.

A **carbonyl group** also increases the OP since it has a –M-effect and a small -I-effect. This could be shown for the example 1,2-O_2ACE vs. 1-OACE and 2,7-N_2-9-OFLN vs 2,7-N_2-FLN in the DTT test. In the H_2O_2 assay, 1,2-O_2ACE and also 1-OACE did not show any effect, but the influence of the carbonyl group could be shown for 2,7-N_2-9-OFLN vs 2,7-N_2-FLN. Furthermore, the influence on the OP becomes apparent when comparing the OPAHs with their parent PAHs, which are, as stated above, not producing ROS in acellular OP assays. Also for the carbonyl group, Er et al. (2015) showed an increasing reduction potential in their theoretical calculations.

The **hydroxyl group** has an electron-withdrawing -I-effect and a +M-effect, being able to push an electron pair into the ring. In this case, it depends on the position of the hydroxyl group and the mesomeric structures if the OP of the compound is higher or lower than the unsubstituted compound. Similar results were also examined by Roginsky et al. (1999) and in the review paper from O'Brien (1991). Using the DTT assay, 5-OH-1,4-O_2NAP had a higher OP than 1,4-O_2NAP, but 2-OH-1,4-O_2NAP had a lower DTT depletion rate. The same was found in the study by Lyu et al. (2018). Roginsky et al. (1999) also found a higher reaction rate coefficient for the catalysis of the ascorbate oxidation by 5-OH-1,4-O_2NAP compared to 1,4-O_2NAP and a lower value for 2-OH-1,4-O_2NAP.

The reason for this difference could be that the 2-OH-1,4-O_2NAP pushes the electron pair (+M-effect) into the ring with the carbonyl groups, while the electron pair of the 5-OH-1,4-O_2NAP is mainly distributed in the ring without the carbonyl groups. In the case of 5-OH-1,4-O_2NAP, it seems that the -I-effect of the hydroxyl group has a higher impact on the ability to form a semiquinone and produce ROS than the +M-effect. Interestingly, this difference is not that pronounced in the H_2O_2 assay. Even though the 5-OH-isomer has a higher H_2O_2 formation potential than the 2-OH-isomer, both are less active than the unsubstituted quinone. Conant & Fieser (1924) also found that the influence of hydroxyl groups on the reduction potential depends on the position, whether the hydroxyl group is on the quinoid moiety or at the aromatic nucleus. They found a lowering effect of the addition of a hydroxyl group for all of their examples. However, they did not include 5-OH-1,4-O_2NAP. Looking at the experimental reduction potentials of 2- and 5-OH-1,4-O_2NAP, the same trend as for the DTT depletion rate can be found. The reduction potential of 5-OH-1,4-O_2NAP is higher than the unsubstituted quinone, while 2-OH-1,4-O_2NAP has a lower reduction potential (Čénas et al., 1994). This could be an explanation, why 5-OH-

1,4-O_2NAP has a lower OP in the H_2O_2 assay. The reduction potential of 5-OH-1,4-O_2NAP is already higher than the reduction potential, which leads to the highest OP.

Structural isomers also showed differences in OP. In general, it could be observed that the quinones with a vicinal position of the carbonyl groups have a significantly higher OP in both assays than their isomers in the para or at any other position. The same was found in several studies (e.g. by Motoyama et al., 2009). For the reduction potential, this was confirmed by Miao et al. (2018) in theoretical calculations. The studies from Tabor et al. (2019) and Er et al. (2015) mostly support this too.

As the last structural feature, it was also possible to study the influence of the **number of aromatic rings**. Since aromatic rings have a weak +M-effect, the OP is decreasing with increasing ring size. This could be shown on several examples like 1,4-O_2NAP vs. 1,4-O_2ANT, 1,2-O_2ACE vs. 1,2-O_2ACEANT (only in DTT assay since both are lower than the LOQ in the H_2O_2 assay), BAN vs 6-OBPYR (only in DTT assay since both are lower than the LOQ in the H_2O_2 assay), 9,10-O_2PHE vs 5,6-O_2CHR, 1,4-O_2PHE vs. 1,4-O_2CHR (only in H_2O_2 assay) and 4,5-O_2PYR vs 4,5-O_2BAP. The decreasing reduction potential with increasing ring number is also clearly shown by Uno et al. (1985).

However, there are a few exceptions to the rule. We hypothesize that this can be explained by two reasons. First, the reduction potential of one of the compounds is already higher than the maximal limit of increasing OP with increasing reduction potential. This is the case for 1,4-O_2PHE in the DTT assay. The same is true for 1,4-BQ vs 1,4-O_2NAP in both OP assays.

The second reason might be that the additional ring is not added in the way that the ring structure is prolonged linearly (as for 1,4-O_2ANT compared to 1,4-O_2NAP) but in the way to form a bay region (as for 1,4-O_2PHE compared to 1,4-O_2NAP and 11-OBaFLN

compared to 9-OFLN). The bigger quinones with the formed bay region have a higher reduction potential (1,4-O_2PHE vs 1,4-O_2NAP (Conant & Fieser, 1924; Josien et al., 1953; Moriconi et al., 1962; Miao et al., 2018) and 7,12-O_2BAA vs 9,10-O_2ANT (Josien et al., 1953; Trumpower, 1982)).

Furthermore, quinones with the same number of rings and the same position of the carbonyl groups can also differ in their OP depending on the **position of the rings**. The OP changes with varying linearity and symmetry. The linear quinone 1,4-O_2ANT obtains a lower reduction potential (Moriconi et al. 1962; Miao et al., 2018) and a lower OP than the non-linear isomer 1,4-O_2PHE in the H_2O_2 assay since the non-linearly arranged rings of 1,4-O_2PHE have a lower total +M-effect, which leads to higher OP. In addition, 1,4-O_2PHE has a structure with a bay region which is more reactive than other quinone structures.

The influence of other **functional groups** was not investigated in this paper. However, based on the theoretical considerations about the influence of negative and positive I- as well as M-effects, the influence of other functional groups can be predicted. Within the already mentioned limitations of the upper limit of the increasing OP, it can be stated that electron-withdrawing groups increase the OP, while electron-donating groups decrease the OP. An overview of the properties of different functional groups and their influence on the reduction potential can be found in Huynh et al. (2016). Er et al. (2015) also showed the influence of several functional groups on the reduction potential. Roginsky et al. (1999) showed experimental results of the influence of several functional groups on the catalytic effects of quinones on the ascorbate oxidation. The study also shows that additional electron-withdrawing groups, such as halogens, can decrease the catalytic effect in case

that the parent compound is already closely before or even after the maximum (such as 1,4-BQ).

2.8 PAC concentrations in SRM urban dust

Table S 7. Concentrations of target PACs in SRM urban dust 1649b from different studies (Layshock et al., 2010; Delgado-Saborit et al., 2013; Nocun and Schantz, 2013; Albinet et al., 2014; Toriba et al., 2016; Wnorowski and Charland, 2017). "/" when not found in the literature.

Substance	Average concentration [ng g^{-1}]	Standard deviation [ng g^{-1}]
1-NNAP	10.6	a
9-NPHE	11.4	a
1-NPYR	104.1	a
3-NFLT	4.35	a
6-NCHR	11.6	a
1,3-N_2NAP	/	a
2,7-N_2FLN	/	a
1,3-N_2PYR	<LOQ	a
1,2-O_2NAP	321	134
1,4-O_2NAP	197	170
2-M-1,4-O_2NAP	329	25
2-OH-1,4-O_2NAP	/	/
5-OH-1,4-O_2NAP	/	/
1,2-O_2ACE	1511	1646
1,4-O_2ANT	166	58
1,4-O_2PHE	30.0	a
9,10-O_2ANT	2112	497
9,10-O_2PHE	887	506
2-M-9,10-O_2ANT	610	204
1,2-O_2AAN	680	1118
4,5-O_2PYR	857	a
1,4-O_2CHR	113	97
5.6-O_2CHR	109	a
5,12-O_2NAC	2013	1003
7,12-O_2BAN	3690	1122
1,6-O_2BAP	787	55
4,5-O_2BAP	93.5	a
6,12-O_2BAP	425	109
1-OACE	93.2	a
9-OFLN	1112	293
1-OPHL	/	/
BAN	4813	2181

Substance	Average concentration [ng g^{-1}]	Standard deviation [ng g^{-1}]
11-OBaFLN	2227	832
6-OBPYR	3070	919
2-N-9-OFLN	21.0	a
2,7-N_2-9-OFLN	/	/
3-NBAN	/	/
1,8-NAA	165	a
6-OBCC	772	a

[a]No standard deviation since value from only one study.

3 References

Albinet, A.; Nalin, F.; Tomaz, S.; Beaumont, J.; Lestremau, F. A simple QuECHERS-like extraction approach for molecular chemical characterization of organic aerosols: application to nitrated and oxygenated PAH derivatives (NPAHs and OPAHs) quantified by GC-NCIMS. Anal. Bioanal. Chem. 2014, 406, 3131-3148.

Anusevičius, Ž.; Šarlauskas, J.; Čénas, N. Two-electron reduction of quinones by rat liver NAD(P)H: quinone oxidoreductase: quantitative structure-activity relationships. Arch. Biochem. Biophys. 2002, 404, 254–262.

Asard, H.; May, J.; Smirnoff, N. Vitamin C: Its functions and biochemistry in animals and plants. BIOS Scientific Publishers 2004, London and New York, 173-185.

Badger, G. M.; McKenzie, A. Bond-orders in aromatic compounds. 1953 Nature, 172, 458-459.

Bironaite, D. A.; Čénas, N. K.; Kulys, J. J. The rotenone-insensitive reduction of quinones and nitrocompounds by mitochondrial NADH:ubiquinone reductase. Biochim. Biophys. Acta 1991, 1060, 203–209.

Boisa, N.; Elom, N.; Dean, J. R.; Deary, M. E.; Bird, G.; Entwistle, J. A. Development and application of an inhalation bioaccessibility method (IBM) for lead in the PM_{10} size fraction of soil. Environ. Int. 2014, 70, 132–142.

Butler, J.; Hoey, B. M. The apparent inhibition of superoxide dismutase activity by quinones. J. Free Radic. Biol. Med. 1986, 2, 77–81.

Čénas, N.; Anusevičius, Ž.; Bironaité, D.; Bachmanova, G. I.; Archakov, A. I.; Öllinger, K. The electron-transfer reactions of NADPH-cytochrome P450 reductase with nonphysiological oxidants. Arch. Biochem. Biophys. 1994, 315, 400-406.

Charrier, J. G.; McFall, A. S.; Richards-Henderson, N. K.; Anastasio, C. Hydrogen peroxide formation in a surrogate lung fluid by transition metals and quinones present in particulate matter. Environ. Sci. Technol. 2014, 48, 7010-7017.

Cho, A. K.; Sioutas, C.; Miguel, A. H.; Kumagai, Y.; Schmitz, D. A.; Singh, M.; Eiguren-Fernandez, A.; Froines, J. R. Redox activity of airborne particulate matter at different sites in the Los Angeles Basin. Environ. Res. 2005, 99, 40-47.

Chung, M. Y.; Lazaro, R. A.; Lim, D.; Jackson, J.; Lyon, J.; Rendulic, D.; Hasson, A. S. Aerosol-borne quinones and reactive oxygen species generation by particulate matter extracts. Environ. Sci. Technol. 2006, 40, 4880–4886.

Cleland, W. W. Dithiothreitol, a new protective reagent for SH groups. Biochemistry 1964, 3, 480-482.
Conant, J.; Fieser, L. Free and total energy changes in the reduction of quinones. J. Am. Chem. Soc. 1922, 44, 2480−2493.
Conant, J. B.; Fieser, L. F. Reduction potentials of quinones. II. The potentials of certain derivatives of benzoquinone, naphthoquinone and anthraquinone. J. Am. Chem. Soc. 1924, 46, 1858−1881.
Debnath, A. K.; de Compadre, R. L. L.; Debnath, G.; Shusterman, A.; Hansch, C. Structure-activity relationship of mutagenic aromatic and heteroaromatic nitro compounds. correlation with molecular orbital energies and hydrophobicity. J. Med. Chem. 1991, 34, 786-797.
Delgado-Saborit, J. M.; Alam, M. S.; Pollitt, K. J.G.; Stark, C.; Harrison, R. M. Analysis of atmospheric concentrations of quinones and polycyclic aromatic hydrocarbons in vapour and particulate phase. Atmos. Environ. 2013, 77, 974−982.
Ding, Y.; Li, Y.; Yu, G. Exploring bio-inspired quinone-based organic redox flow batteries: a combined experimental and computational study. Chem. 2016, 1, 790−801.
El-Hout, S. I.; Suzuki, H.; El-Sheikh, S. M.; Hassan, H. M. A.; Harraz, F. A.; Ibrahim, I. A.; El-Sharkawy, E. A.; Tsujimura, S.; Holzinger; Nishina, M. Y. Tuning the redox potential of vitamin K_3 derivatives by oxidative functionalization using a Ag(I)/GO catalyst. Chem. Commun. 2017, 53, 8890−8893.
Er, S.; Suh, C.; Marshak, M. P.; Aspuru-Guzik, A. Computational design of molecules for an all-quinone redox flow battery. Chem. Sci. 2015, 6, 885-893.
Fieser, L. F.; Dietz, E. M. The reduction potentials of some higher benzologues of the quinones. J. Amer. Chem. Soc. 1931, 53, 1128-1133.
Fu, P. P.; Heflich, R. H.; Unruh, L. E.; Shaikh, A. V.; Wu, Y.-S.; Lai, C.-C.; Lai, J. S. Relationships among direct-acting mutagenicity, nitro group orientation and polarographic reduction potential of 6-nitrobenzo[a]pyrene, 7-nitrobenz[a]anthracene and their derivatives. Mutat. Res. 1988, 209, 115-122.
Fukuhara, K.; Hara, Y.; Miyata, N. Electron transfer from quinone and nitroarene anion radicals to molecular oxygen studied by the potential-step chronocoulometry method, J. Chem. Soc., Chem. Commun., 1994, 955–956
Huynh, M. T.; Anson, C. W.; Cavell, A. C.; Stahl, S. S.; Hammes-Schiffer, S. Quinone 1 e^- and $2e^-/2H^+$ reduction potentials: identification and analysis of deviations from systematic scaling relationships. J. Am. Chem. Soc. 2016, 138, 15903−15910.
Ilan, Y. A.; Czapski, G.; Meisel, D. The one-electron transfer redox potentials of free radicals. I. The oxygen/superoxide system. Biochim. Biophys. Acta 1976, 430, 209-224.
Josien, M.-L.; Fuson, N.; Lebas, J.-M.; Gregory, T. M. An infrared spectroscopic study of the carbonyl stretching frequency in a group of ortho and para quinones. J. Chem. Phys. 1953, 21, 331-340.
Jung, H.; Heflich, R. H.; Fu, P. P.; Shaikh, A. U.; Hartman, P. Nitro group orientation, reduction potential, and direct-acting mutagenicity of nitro-polycyclic aromatic hydrocarbons. Environ. Mol. Mutagen. 1991, 17, 169−180.
Kano, K.; Uno, B. Surface-redox reaction mechanism of quinones adsorbed on basal-plane pyrolytic graphite electrodes. Anal. Chem. 1993, 65, 1088-1093.

Klopman, G.; Tonucci, D. A.; Holloway, M.; Rosenkranz, H. S. Relationship between polarographic reduction potential and mutagenicity of nitroarenes. Mutat. Res. 1984, 126, 139-144.

Kovacic, P.; Kassel, M. A.; Feinbery, B. A.; Corbett, M. D.; McCleilland, R. A. Reduction potentials in relation to physiological activities of benzenoid and heterocyclic nitroso compounds. Comparison with nitroso precursors. Biorg. Chem. 1990, 18, 265–275.

Kuder, J. K.; Pochan, J. M.; Turner, S. R.; Hinman, D. F. Fluorenone derivatives as electron transport materials: The relationship of electron affinity and electrochemistry with photoelectric behavior. J. Electrochem. Soc. 1978, 125, 1750-1758.

Layshock, J. A.; Wilson, G.; Anderson, K. A. Ketone and quinone substituted polycyclic aromatic hydrocarbons in mussel tissue, sediment, urban dust, and diesel particulate matrices. Environ. Toxicol. Chem. 2010, 29, 2450−2460.

Li, X.; Imlay, J.A. Improved measurements of scant hydrogen peroxide enable experiments that define its threshold of toxicity for *Escherichia coli*. Free Radic. Biol. Med. 2019, 120, 217–227.

Lopes, W. A.; Pereira, P. A. de P.; Viertler, H.; de Andrade, J. B. Electrochemical reduction potentials of 1-nitropyrene, 9-nitroanthracene, 6-nitrochrysene and 3-nitrofluoranthene and their correlation with direct-acting mutagenicities. J. Braz. Chem. Soc. 2005, 16, 1099-1103.

Lopez de Compadre, R. L.; Debnath, A. K.; Shusterman, A. J.; Hansch, C. LUMO Energies and hydrophobicity as determinants of mutagenicity by nitroaromatic compounds in *Salmonella typhimurium*. Environ. Mol. Mutagen. 1990, 15, 44-55.

Lyu, Y.; Guo, H.; Cheng, T.; Li, X. Particle Size Distributions of oxidative potential of lung-deposited particles: assessing contributions from quinones and water-soluble metals. Environ. Sci. Technol. 2018, 52, 6592−6600.

Maynard, A. T.; Pedersen, L. G.; Posner, H. S.; Mckinney, J. D. An Ab initio study of the relationship between nitroarene mutagenicity and electron affinity. Mol. Pharmacol. 1986, 29, 629-636.

Merkofer, M.; Kissner, R.; Hider, R. C.; Brunk, U. T.; Koppenol, W. H. Fenton chemistry and iron chelation under physiologically relevant conditions: electrochemistry and kinetics. Chem. Res. Toxicol. 2006, 19, 1263−1269.

Miao, L.; Liu, L.; Shang, Z.; Li, Y.; Lu, Y.; Cheng, F.; Chen, J. The structure–electrochemical property relationship of quinone electrodes for lithium-ion batteries. Phys. Chem. Chem. Phys. 2018, 20, 13478−13484.

Moriconi, E. J.; Rakoczy, B.; O'Connor, W. F. Oxidation-reduction potentials and absorption spectra of polycyclic aromatic quinones. J. Org. Chem. 1962, 27, 2772-2776.

Motoyama, Y.; Bekki, K.; Chung, S.; Tang, N.; Kameda, T.; Toriba, A.; Taguchi, K.; Hayakawa, K. Oxidative stress more strongly induced by ortho-than para-quinoid polycyclic aromatic hydrocarbons in A549 cells. J. Health Sci. 2009, 55, 845−850.

Mukherjee, T. One-electron reduction of juglone (5-hydroxy-1,4naphthoquinone): a pulse radiolysis study. Radiat. Phys. Chem. 1987, 29, 455–462.

Namazian, M. Density functional theory response to the calculation of electrode potentials of quinones in non-aqueous solution of acetonitrile. THEOCHEM 2003, 273, 664–665.

Namazian, M.; Almodarresieh, H. A.; Noorbala, M. R.; Zare, H. R. DFT calculation of electrode potentials for substituted quinones in aqueous solution. Chem. Phys. Lett. 2004, 396, 424-428.
Nocun, M. S.; Schantz, M. M. Determination of selected oxygenated polycyclic aromatic hydrocarbons (oxy-PAHs) in diesel and air particulate matter standard reference materials (SRMs). Anal. Bioanal. Chem. 2013, 405, 5583−5593.
O'Brien, P. J. Molecular mechanisms of quinone cytotoxicity. Chem.-Biol. Interact. 1991, 80, 1-14.
Öllinger, K.; Buffinton, G. D.; Ernster, L.; Cadenas, E. Effect of superoxide dismutase on the autoxidation of substituted hydro- and semi-naphthoquinones. Chem.-Biol. Interact. 1990, 73, 53-76.
Onchoke, K. K. DFT/TD-DFT investigation of optical absorption spectra, electron affinities, and ionization potentials of mono-nitrated benzanthrones. Comput. Theor. Chem. 2011, 963, 40−50.
Onchoke, K. K.; Trevino, A. D. Electrochemical characteristics of benzanthrone studied via cyclic voltammetry: charge transfer redox processes. Anal. Chem. Lett. 2019, 9, 128 -142.
Pal, H.; Mukherjee, T.; Mittal, J. P. Pulse radiolytic one-electron reduction of 2-hydroxy- and 2,6-dihydroxy-9,10-anthraquinones. J. Chem. Soc., Faraday Trans. 1994, 90, 711−716.
Rich, P. R.; Bendall, D. S. The kinetics and thermodynamics of the reduction of cytochrome c by substituted p-benzoquinols in solution. Biochim. Biophys. Acta 1980, 592, 506-518.
Roginsky, V. A.; Barsukova, T. K.; Stengmann, H. B. Kinetics of redox interaction between substituted quinones and ascorbate under aerobic conditions. Chem. Biol. Interact. 1999, 121, 177-197.
Simic, M. G.; Jovanovic, S. V. Antioxidation mechanisms of uric acid. J. Am. Chem. Soc. 1989, 111, 5778-5782.
Song, Y.; Buettner, G. R. Thermodynamic and kinetic considerations for the reaction of semiquinone radicals to form superoxide and hydrogen peroxide. Free Radical Biol. Med. 2010, 49, 919−962.
Tabor, D. P.; Gomez-Bombarelli, R.; Tong, L.; Gordon, R. G.; Aziz, M. J.; Aspuru-Guzik, A. Mapping the frontiers of quinone stability in aqueous media: implications for organic aqueous redox flow batteries. J. Mater. Chem. A 2019, 7, 12833−12841.
Tachibana, M.; Sawaki, S.; Kawazoe, Y. Studies on chemical carcinogens. III. polarographic reduction potentials of nitroquinoline derivatives. Chem. Pharm Bull. 1967, 15, 1112.
Takamura-Enya, T.; Suzuki, H.; Hisamatsu, Y. Mutagenic activities and physicochemical properties of selected nitrobenzanthrones. Mutagenesis 2006, 21, 399–404.
Toriba, A.; Homma, C.; Kita, M.; Uozaki, W.; Boongla, Y.; Orakij, W.; Hayakawa, K. Simultaneous determination of polycyclic aromatic hydrocarbon quinones by gas chromatography-tandem mass spectrometry, following a one-pot reductive trimethylsilyl derivatization. . J. Chromatogr. A 2016, 1459, 89–100.
Trumpower, B. L., Ed. Functions of quinones in energy conserving systems; Academic Press: New York, 1982.

Uno, B.; Kano, K.; Konse, T.; Kubota, T.; Matsuzaki, S.; Kuboyama, Origin of the negative shift of half-wave reduction potentials of aromatic polynuclear p-quinones with increasing conjugation. A. Chem. Pharm. Bull. 1985, 33, 5155–5166.

Votyakova, T. V.; Reynolds, I. J. Detection of hydrogen peroxide with Amplex Red: interference by NADH and reduced glutathione auto-oxidation. Arch. Biochem. Biophys. 2004, 431, 138− 144.

Wang, L.; Su R.; Qi, S.; Gong, W.; Cheng, T. DFT Study of substituted effect on absorption and emission spectra of naphthoquinone derivatives. Adv. Mater. 2011, 233-235, 1878-1883.

Wang, N.; Miller, C. J.; Wang, P.; Waite, T. D. Quantitative determination of trace hydrogen peroxide in the presence of sulfide using the Amplex Red/horseradish peroxidase assay. Anal. Chim. Acta 2017, 963, 61−67.

Wardman, P. Reduction Potentials of one-electron couples involving free radicals in aqueous solution. J. Phys. Chem. Ref. Data 1989, 18, 1637-1755.

Wardman, P. Bioreductive activation of quinones: redox properties and thiol reactivity, Free Radic. Res. Commun. 1990, 8, 219-229.

Warren, J. J.; Mayer, J. M. Tuning of the thermochemical and kinetic properties of ascorbate by its local environment: solution chemistry and biochemical implications. J.Am.Chem.Soc. 2010, 132, 7784-7793.

Williams, N. H.; Yandell, J. K. Outer-sphere electron-transfer reactions of ascorbate anions. Aust. J. Chem. 1982, 35, 1133-1144.

Wilson, I.; Wardman, P.; Lin, T. S.; Sartorelli, A. C. One-electron reduction of 2-and 6-methyl-1,4-naphthoquinone bioreductive alkylating agents. J. Med. Chem. 1986, 29, 1381–1384.

Wnorowski, A.; Charland, J.-P. Profiling quinones in ambient air samples collected from the Athabasca region (Canada). Chemosphere 2017, 189, 55−66.

Xia, Q.; Yin, J. J.; Zhao, Y.; Wu, Y. S.; Wang, Y. Q.; Ma, L.; Chen, S.; Sun, X.; Fu, P. P.; Yu, H. UVA photoirradiation of nitro-polycyclic aromatic hydrocarbons—induction of reactive oxygen species and formation of lipid peroxides. Int. J. Environ. Res. Public Health 2013, 10, 1062−1084.

Xiong, Q.; Yu, H.; Wang, R.; Wei, J.; Verma, V. Rethinking dithiothreitol-based particulate matter oxidative potential: measuring dithiothreitol consumption versus reactive oxygen species generation. Environ. Sci. Technol. 2017, 51, 6507−6514.

Yamaji, M.; Itoh, T.; Tobita, S. Photochemical properties of the triplet π, π* state, anion and ketyl radicals of 5,12-naphthacenequinone in solution studied by laser flash photolysis: electron transfer and phenolic H-atom transfer. Photochem. Phobiol. Sci. 2002, 1, 869-876.

Zhao, Y.; Xia, Q; Yin, J. J.; Yu, H.; Fu, P. Photoirradiation of polycyclic aromatic hydrocarbon diones by UVA light leading to lipid peroxidation. Chemosphere 2011, 85, 83−91.

2.4 Other related studies

Along the three main studies, this PhD thesis contributed to 15 additional studies which are already published or will be submitted to international peer-review journals (see Appendix A, underlined in the text). All of these studies either deal with the occurrence, cycling and fate of semivolatile pollutants in the atmospheric environment or with the uptake and health effects of PACs. Several studies even connect these two topics. My contributions to each individual publication are summarized in Table 1.

The gas-particle partitioning of PACs in the marine environment during the AQABA campaign will be discussed in a separate, short communication paper (Wietzoreck et al., 2022c, in preparation). Because of the high temperatures and relatively low levels of air pollution in some maritime regions, the particulate mass fractions of the targeted semivolatile pollutants were lower than reported elsewhere. Furthermore, we could show that the particulate mass fraction strongly depends on the aerosol composition, which will be compared to the predicted particulate mass fraction based on a model using polyparameter linear free energy relationships (ppLFER) from Shahpoury et al. (2016).

Apart from PACs, there are also other pollutants, such as organohalogen pesticides, polychlorinated biphenyls (PCBs), novel flame retardants and polybrominated diphenyl ethers (PBDEs), which are long-lived and can be long-range transported and potentially harmful for biota and human health (Safe, 1994, McDonald, 2002; Sjödin et al., 2003; Srogi, 2008; Letcher et al., 2010). Several of these air pollutants were also measured during the AQABA campaign in the marine atmosphere above the Mediterranean Sea and the seas around the Arabian Peninsula in order to determine the occurrence, levels, sources, cycling and fate of these compounds (Kyprianou et al., 2022, in preparation). Similarly, these compounds as well as PAH derivatives were measured on two ship-borne campaigns in the Equatorial Atlantic Ocean. Simultaneous to the collection of air samples, the compounds were collected from the surface water of the ocean by a passive sampler (Vrana et al., 2018). I collected the air and surface water samples during one of the Meteor ship-borne campaigns (M157). Based on the data, we derive air-sea exchange data, which is still lacking in the literature for many targeted compounds. In addition, we sampled air at the coast of Barbados and French Guiana simultaneously to the measurements onboard the ship, ideally in order to collect the same air which was transported from the western African coast over the Atlantic Ocean (Lagrangian field experiment; Kim et al., 2022, in preparation).

Since field measurements cannot describe large-scale 3-dimensional pollutant distributions, models are in use. Wilson et al. (2020) published a global chemical transport model, including two NPAHs, which are formed in the atmosphere. The study considers the formation and degradation processes of these two compounds and compares the results to data from observations.

Apart from the measurement of air samples, the measurement of soil samples, as done in the study in Chapter 2.1, was part of this PhD project. By measuring the pollutant concentrations in both environmental compartments simultaneously, we could derive air-soil fugacities of PAHs and PAH derivatives. The fugacity ratios showed that the soil at receptor sites in central and northern Europe can be a source for some of these semivolatile pollutants due to revolatilization from the surface soil (Nežiková et al., 2022, in preparation).

The topic of the study of Lammel et al. (2020) is on the interface between studies about the occurrence of PACs in the environment and the uptake. First, the concentrations of NPAHs and OPAHs at one background and two urban sites were reported. Second, the bioaccessibility of the pollutants from PM was investigated, showing a low bioaccessibility of <2 % for NPAHs and ≈5 % for OPAHs. Similarly, the study by Besis et al. (2022, in preparation) links the measurement of air pollutants in the ambient air with one pathway for adverse health effects. The OP of the aqueous extract and the bioaccessibility of NPAHs and OPAHs from PM on filters were determined to link the health effects to the specific compounds. By analyzing air samples from a polluted site in southern Europe and a background site in central Europe, two different site characteristics could be compared.

Similarly, the OP of PM was determined the study by Lelieveld et al. (2022, in preparation). The DTT depletion, the H_2O_2 formation assay and the amount of radicals by electron paramagnetic resonance (EPR) spectroscopy was measured in the samples from the AQABA campaign. The driving forces of the OP of aerosols over the sea regions of the Mediterranean Sea and around the Arabian Peninsula are investigated by comparing the OP results to the concentrations of heavy metals and several OPAHs.

In the literature, there are several different assays to measure the ROS producing abilities of compounds. In the study from Shahpoury et al. (2022, in preparation), eleven different acellular assays indicating the OP by using the standard reference material urban dust are compared. The assays showed first order kinetics only at low PM concentrations. The OP indicators were rarely proportional to the PM concentrations and showed different sensitivities to PM.

Based on the results of the study in Chapter 2.3, we also found high OP values for different monoaromatic quinones. These compounds were mostly not considered in the determination of the contribution of different pollutants on the OP, although they have a high concentration in urban dust (Toriba et al., 2016). We could demonstrate their importance for the OP compared to other quinones (Wietzoreck et al., 2022d, in preparation). This can also be supported by the reduction potential of these monoaromatic quinones, which can be used to estimate the OP. In order to quickly access reduction potential values, e.g. for predicting the OP, Krüger et al. (2022, in preparation) developed a model applying convolutional neural networks.

The OPs of individual OPAHs were not only determined in the study in Chapter 2.3 but also in a study by Baumann et al. (2022, in preparation). However, the paper focuses on the uptake of PACs in the human lung. We tried to mimic the processes of the uptake of these compounds associated with ultrafine particles in simulated epithelial lung fluid (SELF), in the lung spread out over a very large interfacial area. SELF samples could be loaded with PAH derivatives attached to particles dispersed in air and from the gas phase using a scrubber. These samples showed a higher OP than samples prepared at the same concentration by bulk mixing.

In another study (Lammel et al., 2022, in preparation), the importance of the PACs in the gaseous phase for the uptake by inhalation of polluted air, exemplary on the PAHs, is shown. Even for PAHs with high particulate fractions, the total dose of PAHs taken up into the body is dominated by the compounds from the gas phase.

The resulting toxicity of PAHs and their derivatives after the uptake into the human body was explored in cellular assays by Nováková et al. (2020). The study revealed significant biological effects (various human cell models) of compounds in gas and particulate phase on different endpoints, showing endocrine disrupting potencies. The bioaccessibility by simulated lung fluids was tested and the contributions of targeted PACs (PAHs, NPAHs and OPAHs) to the toxicity were examined by reconstructed mixtures.

Apart from sources of air pollutants outdoors, indoor sources receive increasing importance. Sheu et al. (under review in Environ. Sci. Atmos.) studied thirdhand smoke emissions from deposited PM and lung lining fluid exposed to smoke. From these reservoirs, different volatile and semivolatile pollutants can be re-emitted, including PAH derivatives.

Table 1: My contributions to published articles and articles in preparation (listed in Appendix A). "(X)" means that the experimental work was mainly done by a student assistant but following my instructions or that contribution to data evaluation and discussion was limited to discussion of one topic, e.g. the experimental data set provided.

Number of article	Article	Sampling	Sample preparation	GC-MS analysis	OP assay	Data evaluation	Discussion
4	Lammel et al., 2020		(X)				(X)
5	Nováková et al., 2020		(X)				(X)
6	Wilson et al., 2020						(X)
7	Shahpoury et al., 2022, in preparation		(X)		(X)	(X)	(X)
8	Sheu et al., under review					(X)	(X)
9	Lammel et al., 2022, in preparation		(X)				(X)
10	Besis et al., 2022, in preparation		(X)			(X)	(X)
11	Lelieveld et al., 2022, in preparation					X	(X)
12	Baumann et al., 2022, in preparation		(X)	X	(X)	X	X
13	Kim et al., 2022, in preparation	X					(X)
14	Kyprianou et al., 2022, in preparation						(X)
15	Krüger et al., 2022, in preparation						(X)
16	Nežiková et al., 2022, in preparation		X			X	X
17	Wietzoreck et al., 2022c, in preparation					X	X
18	Wietzoreck et al., 2022d, in preparation		(X)		(X)	X	X

3 Summary and conclusion

Occurrence of nitro- and oxy-PAHs in soil

The occurrence of nitrated and oxygenated polycyclic aromatic hydrocarbons (nitro-PAHs: NPAHs and oxy-PAHs: OPAHs) in soil is only rarely studied. The published study is the first paper reporting a long-term measurement of PAH derivatives in soil. The concentrations of NPAHs and OPAHs in archived grassland soil samples from four locations at one background site and one semi-urban site in the Czech Republic were determined. The soil from the semi-urban site Mokrá was more polluted than the background site Košetice, which showed concentrations among the lowest ever reported in soil. At both sites, 1-nitropyrene and less so 6-nitrobenzo[a]pyrene were the most abundant NPAHs among the five detected of 17 targeted NPAHs. From the more equally distributed OPAHs, 9-fluorenone, 11-benzo[a]fluorenone and 11-benzo[b]fluorenone contributed the most to the total OPAH burden. The concentration of the polycyclic aromatic compounds (PACs) suggests long-range transported aerosols deposited in the analyzed soil samples at the background site Košetice. In addition, a dependence of the high-molecular weight compounds on the total organic carbon content in soil could be determined. The temporal variation of the PACs in soil seemed to be influenced by several factors, such as the gas-particle partitioning in air. However, more research is needed to understand long-term variations of the PAH derivatives in detail.

Occurrence of nitro- and oxy-PAHs in the marine atmosphere

The occurrence of parent PAHs, their nitrated and oxygenated derivatives as well as alkylated PAHs was determined in the marine boundary layer in the Mediterranean Sea and the seas around the Arabian Peninsula in a comprehensive ship-borne campaign, which took place in summer 2017. In several regions, this was the first time that these air pollutants were measured offshore. Pronounced regional differences in the concentrations and composition patterns of the PAHs and their derivatives were found. Apart from very clean areas in the Arabian Sea, the research vessel traveled through polluted regions with some plumes from shipping (Suez Canal, Strait of Hormuz) and continental emissions as well as from the petrochemical industry in the Arabian Gulf. The major sources of the PACs in this region according to positive matrix factorization were shipping emissions, continental pollution and residual oil combustion. By means of several auxiliary

parameters that have been measured simultaneously on the ship, it could be shown that 2-nitrofluoranthene, 2-nitropyrene, benz[a]anthracene-7,12-dione, 2-nitronaphthalene, 1,4-naphthoquinone and 9-fluorenone had significant photochemical sources.

In order to enhance the knowledge of the cycling of the PACs in the marine environment, the mass size distributions were investigated. Except for a few samples with a higher mass median diameter because of the redistribution during long-range transport, the PACs showed the highest concentrations in the sub-micrometer fraction of PM.

Oxidative potential (OP) of polycyclic aromatic compounds (PACs)

The OP of 39 PACs was determined by using two acellular OP assays, namely the H_2O_2 formation assay and the widely used DTT depletion assay. This was the first acellular OP measurement of NPAHs and several OPAHs. The importance of 1,2-naphthoquinone, 1,4-naphthoquinone and 9,10-phenanthrenequinone, known from the literature, could be confirmed. However, several 4-5 ring quinones showed a high OP in both assays, too. 4,5-Pyrenequinone even showed the highest DTT depletion rate of all targeted PACs. It could be shown that the OP can be estimated by structural indicators, the reduction potential and the energy level of the lowest unoccupied molecular orbital (LUMO). Up to an assay-specific maximum value, the OP is increasing with increasing reduction potential. A similar behavior could also be found for the relation between OP and the LUMO energy level. Since the reduction potential and the LUMO energy level are measured by well-established, widely used methods or can be calculated theoretically, these physico-chemical properties can be used to estimate the OP of compounds found in the environment or can also help to select new target compounds with high adverse health effects.

Overall conclusion and outlook

Within this PhD project, the occurrence of NPAHs and OPAHs in different environmental compartments, the cycling and fate in the environment, as well as the uptake and one pathway for adverse health effects, were investigated.

We published the first long-term measurement of PAH derivatives in soil. It could be shown that the concentration of PACs at the semi-urban site was higher than at the background site. However, the concentrations were obviously influenced by various parameters, such as the total organic carbon content in soil and the differences in the gas-particle partitioning in air due to changes in temperature, and possibly by other unidentified parameters. By comparing concentrations in air

and soil at the same location, we could observe differences in the composition patterns of PAH derivatives at the background site. But in order to understand the long-term trends of NPAHs and OPAHs in soil, more research is still needed to determine the kinetic data of formation and degradation of PAH derivatives in air and soil, leaching to lower soil horizons and the deposition from air to soil. In addition, more long-term measurements of air and soil at sites with various type of soil are necessary.

Furthermore, we could show the occurrence, levels, sources and multiphase cycling of PACs in the marine environment over the Mediterranean Sea and the seas around the Arabian Peninsula. Since we sampled air at very diverse marine regions such as source regions with dense ship traffic and emissions from the petrochemical industry as well as background regions, such as the Arabian Sea, we could enhance the knowledge about PACs in the marine atmosphere. This knowledge can be used, e.g. for the development and the evaluation of global models. Nevertheless, the exact rates of deposition, formation and degradation in the marine atmosphere are still unknown and should be investigated in the future.

Apart from the occurrence of PACs, we also determined the potential adverse health effects of these air pollutants. Several PACs were measured for the first time in an acellular OP assay. We could confirm the importance of 1,2- and 1,4-naphthoquinone and 9,10-phenanthrenequinone on the OP of PM. Moreover, we could demonstrate for the first time that some 4-5 ring quinones play a significant role, too. This should be considered in future research on the occurrence and the OP of atmospheric PM. At least 4,5-pyrenequinone, 5,6-chrysenequinone, but also 2- and 5-hydroxy-1,4-naphthoquinone should be quantified in the atmosphere in future studies. Based on a very large dataset, we were able to predict the OP of PACs by their molecular structure, the reduction potential and the LUMO energy level. First, this knowledge could be used in models predicting the OP of aerosols. Second, it could be used to decide, which compounds could be worth to measure in the air based on the predicted OP.

In conclusion, this PhD thesis enhanced the knowledge about the PACs in the environment and the possible adverse health effects but it also showed that there is still a lot more research needed to understand all underlying processes which determine the concentrations, the exposure and the health effects of these compounds.

4 Bibliography

Abdel-Shafy, H. I. and Mansour, M. S. M.: A review on polycyclic aromatic hydrocarbons: Source, environmental impact, effect on human health and remediation, Egypt. J. Pet., 25, 107-123, 2016.

Albinet, A., Leoz-Garziandia, E., Budzinski, H., and Villenave, E.: Polycyclic aromatic hydrocarbons (PAHs), nitrated PAHs and oxygenated PAHs in ambient air of the Marseilles area (South of France): concentrations and sources. Sci. Total Environ., 384, 280-292, 2007.

Albinet, A., Leoz-Garziandia, E., Budzinski, H., Villenave, E., and Jaffrezo, J. L.: Nitrated and oxygenated derivatives of polycyclic aromatic hydrocarbons in the ambient air of two French alpine valleys. Part 1: concentrations, sources and gas/particle partitioning, Atmos. Environ., 42, 43-54, 2008.

Alves, C. A., Vicente, A. M. P., Gomes, J., Nunes, T., Duarte, M., and Bandowe, B. A. M.: Polycyclic aromatic hydrocarbons (PAHs) and their derivatives (oxygenated-PAHs, nitrated-PAHs and azaarenes) in size-fractionated particles emitted in an urban road tunnel, Atmos. Res., 180, 128–137, 2016.

Alves, C. A., Vicente, A. M., Custódio, D., Cerqueira, M., Nunes, T., Pio, C., Lucarelli, F., Calzolai, G., Nava, S., Diapouli, E., Eleftheriadis, K., Querol, X., and Bandowe, B. A. M.: Polycyclic aromatic hydrocarbons and their derivatives (nitro-PAHs, oxygenated PAHs, and azaarenes) in $PM_{2.5}$ from southern European cities, Sci. Total Environ., 595, 494–504, 2017.

Andersson, H., Piras, E., Demma, J., Hellman, B., and Brittebo, E.: Low levels of the air pollutant 1-nitropyrene induce DNA damage, increased levels of reactive oxygen species and endoplasmic reticulum stress in human endothelial cells, Toxicology, 262, 57-64, 2009.

Andersson, J. T. and Achten, C.: Time to say goodbye to the 16 EPA PAHs? Toward an up-to-date use of PACs for environmental purposes, Polycyclic Aromat. Compd., 35, 330-354, 2015.

Arp, H. P. H., Lundstedt, S., Josefsson, S., Cornelissen, G., Enell, A., Allard, A.-S., and Kleja, D. B.: Native oxy-PAHs, N-PACs, and PAHs in historically contaminated soils from Sweden, Belgium, and France: Their soil-porewater partitioning behavior, bioaccumulation in Enchytraeus crypticus, and bioavailability, Environ. Sci. Technol., 48, 11187−11195, 2014.

Atkinson, R. and Arey, J.: Atmospheric chemistry of gas-phase polycyclic aromatic hydrocarbons: formation of atmospheric mutagens, Environ. Health Perspect., 102, 117–126, 1994.

Atsumi, T., Ishihara, M., Kadoma, Y., Tonosaki, K., and Fujisawa, S.: Comparative radical production and cytotoxicity induced by camphorquinone and 9-fluorenone against human pulp fibroblasts, J. Oral Rehabil., 31, 1155-1164, 2004.

Baek, S. O., Field, R. A., Goldstone, M. E., Kirk, P. W., Lester, J. N., and Perry, R.: A review of atmospheric polycyclic aromatic hydrocarbons: Sources, fate and behaviour, Water Air Soil Pollut., 60, 279–300, 1991.

Bamford, H. A. and Baker, J. E.: Nitro-polycyclic aromatic hydrocarbon concentrations and sources in urban and suburban atmospheres of the mid-Atlantic region, Atmos. Environ., 37, 2077-2091, 2003.

Bamford, H. A., Bezabeh, D. Z., Schantz, M. M., Wise, S. A., and Baker, J. E.: Determination and comparison of nitrated-polycyclic aromatic hydrocarbons measured in air and diesel particulate reference materials, Chemosphere, 50, 575-587, 2003.

Bandowe, B. A. M., Shukurov, N., Kersten, M., and Wilcke, W.: Polycyclic aromatic hydrocarbons (PAHs) and their oxygen-containing derivatives (OPAHs) in soils from the Angren industrial area, Uzbekistan, Environ. Pollut., 158, 2888–2899, 2010.

Bandowe, B. A. M. and Wilcke, W.: Analysis of polycyclic aromatic hydrocarbons and their oxygen-containing derivatives and metabolites in soils, J. Environ. Qual., 39, 1349–1358, 2010.

Bandowe, B. A. M., Sobocka J., and Wilcke W.: Oxygen-containing polycyclic aromatic hydrocarbons (OPAHs) in urban soils of Bratislava, Slovakia: patterns, relation to PAHs and vertical distribution, Environ. Pol., 159, 539–549, 2011.

Bandowe, B. A. M., Bigalke, M., Boamah, L., Nyarko, E., Saalia, F., and Wilcke, W.: Polycyclic aromatic compounds (PAHs and oxygenated PAHs) and trace metals in fish species from Ghana (West Africa): Bioaccumulation and health risk assessment, Environ. Int., 65, 135–146, 2014a.

Bandowe, B. A. M., Meusel, H., Huang, R.-J., Ho, K., Cao, J., Hoffmann, T., and Wilcke, W.: $PM_{2.5}$-bound oxygenated PAHs, nitro-PAHs and parent-PAHs from the atmosphere of a Chinese megacity: seasonal variation, sources and cancer risk assessment, Sci. Total Environ., 473–474, 77–87, 2014b.

Bandowe, B. A. M. and Meusel, H.: Nitrated polycyclic aromatic hydrocarbons (nitro-PAHs) in the environment – A review, Sci. Total Environ., 581–582, 237–257, 2017.

Bandowe, B. A. M., Wei, C., Han, Y. M., Cao, J. J., Zhan, C., and Wilcke, W.: Polycyclic aromatic compounds (PAHs, oxygenated PAHs, nitrated PAHs and azaarenes) in soils from China and their relationship with geographic location, land use and soil carbon fractions, Sci. Total Environ., 690, 1268–1276, 2019.

Bates, J. T., Fang, T., Verma, V., Zeng, L., Weber, R. J., Tolbert, P. E., Abrams, J. Y., Sarnat, S. E., Klein, M., Mulholland, J. A., and Russell, A. G.: Review of acellular assays of ambient particulate matter oxidative potential: methods and relationships with composition, sources, and health effects, Environ. Sci. Technol., 53, 4003–4019, 2019.

Bausinger, T., Bonnaire, E., and J. Preuß: Exposure assessment of a burning ground for chemical ammunition on the Great War battlefields of Verdun, Sci. Total Environ., 382, 259–271, 2007.

Bezabeh, D. Z., Bamford, H. A., Schantz, M. M., and Wise, S. A.: Determination of nitrated polycyclic aromatic hydrocarbons in diesel particulate-related standard reference materials by using gas chromatography/mass spectrometry with negative ion chemical ionization, Anal. Bioanal. Chem., 375, 381–388, 2003.

Bodzek, D., Tyrpien, K., and Warzecha, L.: Identification of oxygen derivatives of polycyclic aromatic hydrocarbons in airborne particulate matter of Upper Silesia (Poland), Int. J. Environ. Anal. Chem., 52 75– 85, 1993.

Bolton, J. L., Trush, M. A., Penning, T. M., Dryhurst, G., and Monks, T. J.: Role of quinones in toxicology, Chem. Res. Toxicol., 13, 135–160, 2000.

Borm, P. J. A., Kelly, F., Künzli, N., Schins, R. P. F., and Donaldson, K.: Oxidant generation by particulate matter: from biologically effective dose to a promising, novel metric, Occup. Environ. Med., 64, 73–74, 2007.

Bozlaker, A., Muezzinoglu, A., and Odabasi, M.: Atmospheric concentrations, dry deposition and air–soil exchange of polycyclic aromatic hydrocarbons (PAHs) in an industrial region in Turkey, J. Hazard. Mater., 153, 1093–1102, 2008.

Brorström-Lundén, E., Remberger, M., Kaj, L., Hansson, K., Palm Cousins, A., Andersson, H., Haglund, P., Ghebremeskel, M., and Schlabach, M.: Results From the Swedish National Screening Programme 2008: Screening of unintentionally produced organic contaminants, Swedish Environmental Research Institute (IVL) report B1944, Göteborg, Sweden, 2010.

Cai, C. Y., Li, J. Y., Wu, D., Wang, X. L., Tsang, D. C. W., Li, X. D., Sun, J. T., Zhu, L. Z., Shen, H. Z., Tao, S., and Liu, W. X.: Spatial distribution, emission source and health risk of parent

PAHs and derivatives in surface soils from the Yangtze River Delta, Eastern China, Chemosphere, 178, 301–308, 2017.

Calas, A., Uzu, G., Kelly, F. J., Houdier, S., Martins, J. M. F., Thomas, F., Molton, F., Charron, A., Dunster, C., Oliete, A., Jacob, V., Besombes, J.-L., Chevrier, F., and Jaffrezo, J.-L.: Comparison between five acellular oxidative potential measurement assays performed with detailed chemistry on PM_{10} samples from the city of Chamonix (France), Atmos. Chem. Phys., 18, 7863-7875, 2017a.

Calas, A., Uzu, G., Martins, J. M. F., Voisin, D., Spadini, L., Lacroix, T. and Jaffrezo, J.: The importance of simulated lung fluid (SLF) extractions for a more relevant evaluation of the oxidative potential of particulate matter, Sci. Reports, 7, 11617, 2017b.

CARB (California Air Resources Board): Benzo[a]pyrene as a Toxic Air Contaminant, Report to the air resources board on benzo[a]pyrene, 1994

Castells, P., Santos, F.J., and Gaiceran, M.T.: Development of a sequential supercritical fluid extraction method for the analysis of nitrated and oxygenated derivatives of polycyclic aromatic hydrocarbons in urban aerosols, J. Chromatogr. A, 1010, 141-151, 2003.

Cave, M. R., Wragg, J., Beriro, D. J., Vane, C., Thomas, R., Riding, M., and Taylor, C.: An overview of research and development themes in the measurement and occurrences of polyaromatic hydrocarbons in dusts and particulates, J. Hazard Mater., 360, 373-390, 2018.

Charrier, J. G. and Anastasio, C.: On dithiothreitol (DTT) as a measure of oxidative potential for ambient particles: evidence for the importance of soluble transition metals, Atmos. Chem. Phys., 12, 9321–9333, 2012.

Charrier, J. G., McFall, A. S., Richards-Henderson, N. K., and Anastasio, C.: Hydrogen peroxide formation in a surrogate lung fluid by transition metals and quinones present in particulate matter, Environ. Sci. Technol., 48, 7010–7017, 2014.

Cho, A. K., Di Stefano, E., You, Y., Rodriguez, C. E., Schmitz, D. A., Kumagai, Y., Miguel, A. H., Eiguren-Fernandez, A., Kobayashi, T., Avol, E., and Froines, J. R.: Determination of four quinones in diesel exhaust particles, SRM 1649a, an atmospheric $PM_{2.5}$, Aerosol Sci. Technol., 38, 68–81, 2004.

Cho, A. K., Sioutas, C., Miguel, A. H., Kumagai, Y., Schmitz, D. A., Singh, M., Eiguren-Fernandez, A., and Froines, J. R.: Redox activity of airborne particulate matter at different sites in the Los Angeles Basin, Environ. Res., 99, 40–47, 2005.

Chung, M. Y., Lazaro, R. A., Lim, D., Jackson, J., Lyon, J., Rendulic, D., and Hasson, A. S.: Aerosol-borne quinones and reactive oxygen species generation by particulate matter extracts, Environ. Sci. Technol., 40, 4880–4886, 2006.

Chung, S. W., Chung, H. Y., Toriba, A., Kameda, T., Tang, N., Kizu, R., and Hayakawa, K.: An environmental quinoid polycyclic aromatic hydrocarbon, acenaphthenequinone, modulates cyclooxygenase-2 expression through reactive oxygen species generation and nuclear factor kappa B activation in A549 cells, Toxicol. Sci., 95, 348-355, 2007.

Cerniglia, C. E.: Biodegradation of polycyclic aromatic hydrocarbons, Biodegradation 3, 351-368, 1992.

Clergé, A., Le Goff, J., Lopez, C., Ledauphin, J., and Delépée, R.: Oxy-PAHs: Occurrence in the environment and potential genotoxic/mutagenic risk assessment for human health, Crit. Rev. Toxicol., 49, 302–328, 2019.

Cochran, R. E., Dongari, N., Jeong, H., Beranek, J., Haddadi, S., Shipp, J., and Kubatova, A.: Determination of polycyclic aromatic hydrocarbons and their oxy-, nitro- and hydroxyl-oxidation products, Anal. Chim. Acta, 740, 93–103, 2012.

Collins, J. F., Brown, J. P., Alexeeff, G. V., and Salmon, A. G.: Potency equivalency factors for some polycyclic aromatic hydrocarbons and polycyclic aromatic hydrocarbon derivatives, Regul. Toxicol. Pharm., 28, 45–54, 1998.

Cousins, I. T., Beck, A. J., and Jones, K. C.: A review of the processes involved in the exchange of semi-volatile organic compounds (SVOC) across the air–soil interface, Sci. Total Environ., 228, 5–24, 1999.

Daellenbach, K. R., Uzu, G., Jiang, J., Cassagnes, L.-E., Leni, Z., Vlachou, A., Stefenelli, G., Canonaco, F., Weber, S., Segers, A., Kuenen, J. J. P., Schaap, M., Favez, O., Albinet, A., Aksoyoglu, S., Dommen, J., Baltensperger, U., Geiser, M., El Haddad, I., Jaffrezo, J.-L., and Prévôt, A. S. H.: Sources of particulate-matter air pollution and its oxidative potential in Europe, Nature, 587, 414–419, 2020.

Degrendele, C., Kanduč, T., Kocman, D., Lammel, G., Cambelová, A., Dos Santos, S. G., Horvat, M., Kukučka, P., Holubová Šmejkalová, A., Mikeš, O., Nuñez-Corcuera, B., Přibylová, P., Prokeš, R., Saňka, O., Maggos, T., Sarigiannis, D., and Klánová, J.: NPAHs and OPAHs in the atmosphere of two central european cities: seasonality, urban-to-background gradients, cancer risks and gas-to-particle partitioning, Sci. Total Environ., 793, 148528, 2021.

de Jesus, R. M., Mosca, A. C., Guarieiro, A. L. N., Rocha, G. O. D., and Andrade, J. B. D.: In vitro evaluation of oxidative stress caused by fine particles ($PM_{2.5}$) exhausted from heavy-duty vehicles using diesel/biodiesel blends under real world conditions. J. Braz. Chem. Soc., 29, 1268-1277, 2018.

de Oliveira Galvão, M. F., de Oliveira Alves, N., Ferreira, P. A., Caumo, S., de Castro Vasconcellos, P., Artaxo, P., de Souza Hacon, S., Roubicek, D.A., de Medeiros, S. R. B.: Biomass burning particles in the Brazilian Amazon region: mutagenic effects of nitro and oxy-PAHs and assessment of health risks, Environ. Pollut., 233, 960–970, 2018.

Degrendele, C., Audy, O., Hofman, J., Kučerik, J., Kukučka, P., Mulder, M. D., Přibylová, P., Prokeš, R., Sáňka, M., Schaumann, G. E., and Lammel, G.: Diurnal variations of air-soil exchange of semivolatile organic compounds (PAHs, PCBs, OCPs, and PBDEs) in a central European receptor area, Environ. Sci. Technol., 50, 4278–4288, 2016.

Delgado-Saborit, J. M., Alam, M.S ., Pollitt, K. J. G., Stark, C., and Harrison, R. M.: Analysis of atmospheric concentrations of quinones and polycyclic aromatic hydrocarbons in vapour and particulate phases, Atmos. Environ., 77, 974–982, 2013.

Durant, J. L., Busby Jr., W. F., Lafleur, A. L., Penman, B. W., and Crespi, C. L.: Human cell mutagenicity of oxygenated, nitrated and unsubstituted polycyclic aromatic hydrocarbons associated with urban aerosols, Mutat. Res., 371, 123–157, 1996.

Eiguren-Fernandez, A., Miguel, A. H., Lu, R., Purvis, K., Grant, B., Mayo, P., Di Stefano, E., Cho, A. K., and Froines, J.: Atmospheric formation of 9,10-phenanthraquinone in the Los Angeles air basin, Atmos. Environ., 42, 2312–2319, 2008

El Alawi, Y. S., McConkey, B. J., Dixon, D. G., and Greenberg, B. M.: Measurement of short and long-term toxicity of polycyclic aromatic hydrocarbons using luminescent bacteria, Ecotoxicol. Environ. Saf., 51, 12–21, 2002.

Fan, Z. H., Kamens, R. M., Hu, J. X., Zhang, J. B., and McDow, S.: Photostability of nitro polycyclic aromatic hydrocarbons on combustion soot particles in sunlight, Environ. Sci. Technol., 30, 1358–1364, 1996.

Fang, T., Verma, V., Bates, J. T., Abrams, J., Klein, M., Strickland, M. J., Sarnat, S. E., Chang, H. H., Mulholland, J. A., Tolbert, P. E., Russell, A. G., and Weber, R. J.: Oxidative potential of ambient water-soluble $PM_{2.5}$ in the southeastern United States: contrasts in sources and health associations between ascorbic acid (AA) and dithiothreitol (DTT) assays, Atmos. Chem. Phys., 16, 3865–3879, 2016.

Fang, T., Lakey, P. S. J., Weber, R. J., and Shiraiwa, M.: Oxidative potential of particulate matter and generation of reactive oxygen species in epithelial lining fluid, Environ. Sci. Technol., 53, 12784–12792, 2019.

Feilberg, A., Kamens, R. M., Strommen, M. R., and Nielsen, T.: Modeling the formation, decay, and partitioning of semivolatile nitro-polycyclic aromatic hydrocarbons (nitronaphthalenes) in the atmosphere, Atmos. Environ., 33, 1231-1243, 1999.

Feilberg, A., Poulsen, M. W. B., Nielsen, T., and Skov, H.: Occurrence and sources of particulate nitro-polycyclic aromatic hydrocarbons in ambient air in Denmark, Atmos. Environ., 35, 353–366, 2001.

Finlayson-Pitts, B. and Pitts, J. N.: Chemistry of the upper and lower atmosphere: theory, experiments, application, Academic Press, San Diego, USA, 2000.

Fujiwara, F., Guiñez, M., Cerutti, S., and Smichowski, P.: UHPLC(+)APCI-MS/MS determination of oxygenated and nitrated polycyclic aromatic hydrocarbons in airborne particulate matter and tree barks collected in Buenos Aires city, Microchem. J., 116, 118–124, 2014.

Galarneau, E., Makar, P. A., Zheng, Q., Narayan, J., Zhang, J., Moran, M. D., Bari, M. A., Pathela, S., Chen, A., and Chlumsky, R.: PAH concentrations simulated with the AURAMS-PAH chemical transport model over Canada and the USA, Atmos. Chem. Phys., 14, 4065–4077, 2014.

Galmiche, M., Delhomme, O., François, Y., and Millet, M.: Environmental analysis of polar and non-polar polycyclic aromatic compounds in airborne particulate matter, settled dust and soot: Part I: sampling and sample preparation, Trends Anal. Chem., 134, 116099, 2021a.

Galmiche, M., Delhomme, O., François, Y., and Millet, M.: Environmental analysis of polar and non-polar polycyclic aromatic compounds in airborne particulate matter, settled dust and soot: Part I: Sampling and sample preparation, Trends Anal. Chem., 134, 116099, 2021b.

Gao, D., Ripley, S., Weichenthal, S., and Godri Pollitt, K. J.: Ambient particulate matter oxidative potential: Chemical determinants, associated health effects, and strategies for risk management, Free Radical Bio. Med., 151, 7–25, 2020.

Garcia-Alonso, S., Barrado-Olmedo, A. I., and Perez-Pastor, R. M.: An analytical method to determine selected nitro-PAHs in soil samples by HPLC with fluorescence detection, Polycycl. Aromat. Compd., 32, 669–682, 2012.

González-Gaya, B., Fernandez-Pinos, M.-C., Morales, L., Mejanelle, L., Abad, E., Pina, B., Duarte, C. M., Jimenez, B., and Dachs, J.: High atmosphere-ocean exchange of semivolatile aromatic hydrocarbons, Nat. Geosci., 9, 438–442, 2016.

Hansen, T., Seidel, A., and Borlak, J.: The environmental carcinogen 3-nitrobenzanthrone and its main metabolite 3-aminobenzanthrone enhance formation of reactive oxygen intermediates in human A549 lung epithelial cells, Toxicol. Appl. Pharmacol., 221, 222–234, 2007.

Haritash, A. K., and Kaushik, C. P.: Biodegradation aspects of polycyclic aromatic hydrocarbons (PAHs): A review, J. Hazard. Mater., 169, 1–15, 2009.

Hedayat, F., Stevanovic, S., Miljevic, B., Bottle, S., and Ristovski, Z.: Review-evaluating the molecular assays for measuring the oxidative potential of particulate matter, Chem. Ind. Chem. Eng. Q., 21, 201–210, 2014.

Hellack, B., Nickel, C., Albrecht, C., Kuhlbusch, T. A. J., Boland, S., Baeza-Squiban, A., Wohlleben, W., and Schins, R. P. F.: Analytical methods to assess the oxidative potential of nanoparticles: A review, Environ. Sci. Nano, 4, 1920–1934, 2017.

Holoubek, I., Klanova, J., Jarkovsky, J., and Kohoutek, J.: Trends in background levels of persistent organic pollutants at Kosetice observatory, Czech Republic, Part I: Ambient air and wet deposition 1996–2005, J. Environ. Monit., 9, 557–563, 2007.

Horstmann, M. and McLachlan, M. S.: Forests as filters of airborne organic pollutants: A model, Environ. Sci. Technol., 32, 413-420, 1998.
Huang, W., Huang, B., Bi, X., Lin, Q., Liu, M., Ren, Z., Zhang, G., Wang, X., Sheng, G., and Fu, J.: Emission of PAHs, NPAHs and OPAHs from residential honeycomb coal briquette combustion, Energ. Fuel., 28, 636–642, 2014.
IARC (International Agency for Research on Cancer): Polynuclear aromatic compounds. Part 1. Chemical, environmental and experimental data, IARC Monogr. Eval. Carcinog. Risk Chem. Hum., 32, 1-453, 1983.
IARC (International Agency for Research on Cancer): Diesel and gasoline exhausts and some nitroarenes, IARC Monogr. Eval. Carcinog. Risk Chem. Hum., 46, 375, 1989.
IARC (International Agency for Research on Cancer): Agents Classified by the IARC Monographs. Available in: List of classifications by alphabetical order, 1-123, http://monographs.iarc.fr/ENG/Classification/ClassificationsAlphaOrder.pdf, 2012.
Idowu, O., Carbery, M., O'Connor, W., and Thavamani, P.: Speciation and source apportionment of polycyclic aromatic compounds (PACs) in sediments of the largest salt water lake of Australia, Chemosphere, 246, 125779, 2020.
Jariyasopit, N., McIntosh, M., Zimmermann, K., Arey, J., Atkinson, R., Cheong, P. H.-Y., Carter, R. G., Yu, T.-W., Dashwood, R. H., and Massey Simonich, S. L.: Novel Nitro-PAH Formation from Heterogeneous Reactions of PAHs with NO2, NO3/N2O5, and OH Radicals: Prediction, Laboratory Studies, and Mutagenicity, Environ. Sci. Technol., 48, 412–419, 2014.
Jariyasopit, N., Harner, T., Wu, D., Williams, A., Halappanavar, S., and Su, K.: Mapping indicators of toxicity for polycyclic aromatic compounds in the atmosphere of the Athabasca oil sands region, Environ. Sci. Technol., 50, 11282–11291, 2016.
Jiang, H., Ahmed, C. M. S., Canchola, A., Chen, J. Y., and Lin, Y.-H.: Use of dithiothreitol assay to evaluate the oxidative potential of atmospheric aerosols, Atmosphere, 10, 571, 2019.
Keith, L. H.: The source of U.S. EPA's sixteen PAH priority pollutants, Polycycl. Aromat. Compd., 35, 147–160, 2015.
Kelly, J. M., Ivatt, P. D., Evans, M. J., Kroll, J. H., Hrdina, A. I. H., Kohale, I. N., White, F. M., Engelward, B. P., and Selin, N. E.: Global cancer risk from unregulated polycyclic aromatic hydrocarbons, Geohealth, 5, e2021GH000401, 2021.
Keyte, I.J., Harrison, R.M., and Lammel, G.: Chemical reactivity and long-range transport potential of polycyclic aromatic hydrocarbons – a review, Chem. Soc. Rev., 42, 9333-9391, 2013.
Kojima, Y., Inazu, K., Hisamatsu, Y., Okochi, H., Baba, T., and Nagoya, T.: Influence of secondary formation on atmospheric occurrences of oxygenated polycyclic aromatic hydrocarbons in airborne particles, Atmos. Environ., 44, 2873–2880, 2010.
Kumagai, Y., Koide, S., Taguchi, K., Endo, A., Nakai, Y., Yoshikawa, T., and Shimojo, N.: Oxidation of proximal protein sulfhydryls by phenanthraquinone, a component of diesel exhaust particles, Chem. Res. Toxicol., 15, 483–489, 2002.
Kurihara, R., Shiraishi, F., Tanaka, N., and Hashimoto, S.: Presence and estrogenicity of anthracene derivatives in coastal Japanese waters, Environ. Toxicol. Chem., 24, 1984–1993, 2005
Lakey, P. S. J., Berkemeier, T., Tong, H., Arangio, A. M., Lucas, K., Pöschl, U., and Shiraiwa, M.: Chemical exposure response relationship between air pollutants and reactive oxygen species in the human respiratory tract, Sci. Rep., 6, 32916, 2016.
Lammel, G., Sehili, A. M., Bond, T. C., Feichter, J., and Grassl, H.: Gas/particle partitioning and global distribution of polycyclic aromatic hydrocarbons – A modelling approach, Chemosphere, 76, 98–106, 2009.

Lammel, G.: Polycyclic aromatic compounds in the atmosphere a review identifying research needs, Polycyclic Aromat. Comp., 35, 316–329, 2015.

Lammel, G., Degrendele, C., Gunthe, S. S., Mu, Q., Muthalagu, A., Audy, O., Biju, C. V., Kukučka, P., Mulder, M. D., Octaviani, M., Příbylová, P., Shahpoury, P., Stemmler, I., and Valsan, A. E.: Revolatilisation of soil-accumulated pollutants triggered by the summer monsoon in India, Atmos. Chem. Phys., 18, 11031–11040, 2018.

Lampi, M. A., Gurska, J., McDonald, K. I. C., Xie, F. L., Huang, X. D., Dixon, D. G., and Greenberg, B. M.: Photoinduced toxicity of polycyclic aromatic hydrocarbons to Daphnia magna: ultraviolet-mediated effects and the toxicity of polycyclic aromatic hydrocarbon photoproducts, Environ. Toxicol. Chem., 25, 1079-1087, 2006.

Lao, J.-Y., Xie, S.-Y., Wu, C.-C., Bao, L.-J., Tao, S., and Zeng, E. Y.: Importance of dermal absorption of polycyclic aromatic hydrocarbons derived from barbecue fumes, Environ. Sci. Technol., 52, 8330–8338, 2018.

Layshock, J. A., Wilson, G., and Anderson, K. A.: Ketone and quinone-substituted polycyclic aromatic hydrocarbons in mussel tissue, sediment, urban dust, and diesel particulate matrices, Environ. Toxicol. Chem., 29, 2450-2460, 2010.

Letzel, T., Rosenberg, E., Wissiack, R., Grasserbauer, M., and Niessner, R.: Separation and identification of polar degradation products of benzo[a]pyrene with ozone by atmospheric pressure chemical ionization–mass spectrometry after optimized column chromatographic clean-up, R.J. Chrom. A, 855, 501-514, 1999.

Lelieveld, J., Klingmuller, K., Pozzer, A., Poschl, U., Fnais, M., Daiber, A., and Munzel, T.: Cardiovascular disease burden from ambient air pollution in Europe reassessed using novel hazard ratio functions, Eur. Heart J., 40, 1590−1596, 2019.

Lelieveld, J., Pozzer, A., Pöschl, U., Fnais, M., Haines, A., and Münzel, T.: Loss of life expectancy from air pollution compared to other risk factors: a worldwide perspective, Cardiovasc. Res., 116, 1910-1917, 2020.

Lelieveld, S., Wilson, J., Dovrou, E., Mishra, A., Lakey, P. S. J., Shiraiwa, M., Poschl, U., and Berkemeier, T.: Hydroxyl Radical Production by Air Pollutants in Epithelial Lining Fluid Governed by Interconversion and Scavenging of Reactive Oxygen Species, Environ. Sci. Technol., 55, 14069−14079, 2021.

Li, W., Wang, C., Shen, H., Su, S., Shen, G., Huang, Y., Zhang, Y., Chen, Y., Chen, H., Lin, N., Zhuo, S., Zhong, Q., Wang, X., Liu, J., Li, B., Liu, W., and Tao, S.: Concentrations and origins of nitro-polycyclic aromatic hydrocarbons and oxy-polycyclic aromatic hydrocarbons in ambient air in urban and rural areas in northern China, Environ. Pollut., 197, 156–164, 2015.

Li, H., Wang, Y., Wang, Y., Wang, H., Sun, K., and Lu, Z.: Bacterial degradation of anthraquinone dyes, J. Zhejiang Univ.-Sc. B, 20, 528–540, 2019.

Ligocki, M. P., Leuenberger, C., and Pankow, J. F.: Trace organic compounds in rain - II. Gas scavenging of neutral organic compounds, Atmos. Environ., 19, 1609-1617, 1985a.

Ligocki, M. P., Leuenberger, C., and Pankow, J. F.: Trace organic compounds in rain - III. Particle scavenging of neutral organic compounds, Atmos. Environ., 19, 1619-1626, 1985b.

Lin, Y., Ma, Y., Qiu, X., Li, R., Fang, Y., Wang, J., Zhu, Y., and Hu, D.: Sources, transformation, and health implications of PAHs and their nitrated, hydroxylated, and oxygenated derivatives in $PM_{2.5}$ in Beijing, J. Geophys. Res., 120, 7219– 7228, 2015.

Lin, Y., Qiu, X. H,, Ma, Y. Q., Ma, .J, Wang, J. X., Wu, Y. S., Zeng, L. M., Hu, M., Zhu, T., and Zhu, Y. F.: A novel approach for apportionment between primary and secondary sources of airborne nitrated polycyclic aromatic hydrocarbons (NPAHs), Atmos. Environ., 138, 108–113, 2016.

Lohmann, R. and Lammel, G.: Adsorptive and absorptive contributions to the gas-particle partitioning of polycyclic aromatic hydrocarbons: state of knowledge and recommended parametrization for modelling, Environ. Sci. Technol., 38, 3793-3803, 2004.

Lundstedt, S., White, P. A., Lemieux, C. L., Lynes, K. D., Lambert, L. B., Öberg, L., Haglund, P., and Tysklind, M.: Sources, fate, and toxic hazards of oxygenated polycyclic aromatic hydrocarbons (PAHs) at PAH-contaminated sites, Ambio, 36, 475–485, 2007.

Lyu, Y., Guo, H., Cheng, T., and Li, X.: Particle Size Distributions of Oxidative Potential of Lung-Deposited Particles: Assessing Contributions from Quinones and Water-Soluble Metals, Environ. Sci. Technol., 52, 6592–6600, 2018.

Ma, Y., Cheng, Y., Qiu, X., Lin, Y., Cao, J., and Hu, D.: A quantitative assessment of source contributions to fine particulate matter ($PM_{2.5}$)-bound polycyclic aromatic hydrocarbons (PAHs) and their nitrated and hydroxylated derivatives in Hong Kong, Environ. Pollut., 219, 742–749, 2016.

McWhinney, R. D., Zhou, S., and Abbatt, J. P. D.: Naphthalene SOA: redox activity and naphthoquinone gas–particle partitioning, Atmos. Chem. Phys., 13, 9731–9744, 2013.

Miet, K., Le Menach, K., Flaud, P.-M., Budzinski, H. and Villenave, E.: Heterogeneous reactivity of pyrene and 1–nitropyrene withNO_2: Kinetics, product yields and mechanism, Atmos. Environ., 43, 837–843, 2009.

Minero, C., Maurino, V., Borghesi, D., Pelizzetti, E., and Vione, D.: An overview of possible processes able to account for the occurrence of nitro-PAHs in the Antarctic particulate matter, Microchem. J., 96, 213–216, 2010.

Mirivel, G., Riffault, V., and Galloo, J.-C.: Simultaneous determination by ultra-performance liquid chromatography-atmospheric pressure chemical ionization time-of flight mass spectrometry of nitrated and oxygenated PAHs found in air and soot particles, Anal. Bioanal. Chem., 397, 243–256, 2010.

Misaki, K., Takamura-Enya, T., Ogawa, H., Takamori, K., and Yanagida, M.: Tumour-promoting activity of polycyclic aromatic hydrocarbons and their oxygenated or nitrated derivatives, Mutagenesis, 31, 205−213, 2016.

Mitra, S., and Ray, B.: Patterns and sources of Polycyclic Aromatic Hydrocarbons and their derivatives in indoor air, Atmos. Environ., 29, 3345, 1995.

Mudway, I. S., Stenfors, N., Duggan, S. T., Roxborough, H., Zielinski, H., Marklund, S. L., Blomberg, A., Frew, A. J., Sandstrom, T., and Kelly, F. J.: An in vitro and in vivo investigation of the effects of diesel exhaust on human airway lining fluid antioxidants, Arch. Biochem. Biophys., 423, 200–212, 2004.

Murahashi, T., Ito, M., Kizu, R., and Hayakawa, K.: Determination of nitroarenes in precipitation collected in Kanazawa, Japan, Water Res., 35, 3367–3372, 2001.

Nalin, F., Golly, B., Besombes, J.-L., Pelletier, C., Aujay, R., Verlhac, S., Dermigny, A., Fievet, A., Karoski, N., Dubois, P., Collet, S., Favez, O., and Albinet, A.: Fast oxidation processes from 90 emission to ambient air introduction of aerosol emitted by residential log wood stoves, Atmos. Environ., 143, 15–26, 2016.

Nawrot, T. S., Kuenzli, N., Sunyer, J., Shi, T. M., Moreno, T., Viana, M., Heinrich, J., Forsberg, B., Kelly, F. J., Sughis, M., Nemery, B., and Borm, P.: Oxidative properties of ambient $PM_{2.5}$ and elemental composition: Heterogeneous associations in 19 European cities, Atmos. Environ., 43, 4595–4602, 2009.

Nel, A.: Air pollution-related illness: effects of particles, Science, 308, 804–806, 2005.

Nežiková, B., Degrendele, C., Bandowe, B. A. M., Šmejkalová, A. H., Kukučka, P., Martiník, J., Mayer, L., Prokeš, R., Přibylová, P., Klánová, J., and Lammel, G.: Three years of atmospheric concentrations of nitrated and oxygenated polycyclic aromatic hydrocarbons

and oxygen heterocycles at a central European background site, Chemosphere, 269, 128738, 2021.
Nováková, Z., Novák, J., Kitanovski, Z., Kukučka, P., Smutá, M., Wietzoreck, M., Lammel, G., and Hilscherová, K.: Toxic potentials of particulate and gaseous air pollutant mixtures and the role of PAHs and their derivatives, Environ. Int., 139, 105634, 2020.
Nyiri, Z., Novák, M., Bodai, Z., Szabó, B. S., Ekea, Z., Zárayc, G., and Szigeti, T.: Determination of particulate phase polycyclic aromatic hydrocarbons and their nitrated and oxygenated derivatives using gas chromatography–mass spectrometry and liquid chromatography–tandem mass spectrometry, J. Chromatogr. A, 1472, 88–98, 2016.
Octaviani, M., Tost, H., and Lammel, G.: Global simulation of semivolatile organic compounds – development and evaluation of the MESSy submodel SVOC (v1.0), Geosci. Model Dev., 12, 3585–3607, 2019.
Odabasi, M., Sofuoglu, A., Vardar, N., Tasdemir, Y., and Holsen, T. M.: Measurement of dry deposition and air-water exchange of polycyclic aromatic hydrocarbons with the water surface sampler, Environ. Sci. Technol., 33, 426–434, 1999.
Park, E. J. and Park. K.: Induction of pro-inflammatory signals by 1-nitropyrene in cultured BEAS-2B cells, Toxicol. Lett. ,184, 126-133, 2009.
Pham, C.T., Tang, N., and Toriba, A.: Polycyclic aromatic hydrocarbons and nitropolycyclic aromatic hydrocarbons in atmospheric particles and soil at a traffic site in Hanoi, Vietnam. Polycycl. Aromat. Compd., 35, 353-371, 2015.
Phillips, D. H.: Fifty years of benzo(a)pyrene, Nature, 303, 468-472, 1983.
Pietrogrande, M. C., Russo, M., and Zagatti, E.: Review of PM Oxidative Potential Measured with Acellular Assays in Urban and Rural Sites across Italy, Atmosphere, 10, 626, 2019.
Pöhlker C., Baumann K., and Lammel G.: Methods of sampling trace substances in air, in: Foken T. (ed.): Handbook of atmospheric measurements, Springer, Cham, Switzerland, pp. 565-608, 2021.
Priego-Capote, F., Luque-Garcia, U., and de Castro, M. D. L.: Automated fast extraction of nitrated polycyclic aromatic hydrocarbons from soil by focused microwave-assisted soxhlet extraction prior to gas chromatography-electron-capture detection, J. Chromatogr. A, 994, 159–167, 2003.
Ravindra, K., Sokhi, R., and Van Grieken, R.: Atmospheric polycyclic aromatic hydrocarbons: source attribution, emission factors and regulation, Atmos. Environ., 42, 2895-2921, 2008.
Reisen, F. and Arey, J.: Atmospheric reactions influence seasonal PAH and nitro-PAH concentrations in the Los Angeles basin, Environ. Sci. Technol., 39, 64–73, 2005.
Ringuet, J., Albinet, A., Leoz-Garziandia, E., Budzinski, H., and Villenave, E.: Reactivity of polycyclic aromatic compounds (PAHs, NPAHs and OPAHs) adsorbed on natural aerosol particles exposed to atmospheric oxidants, Atmos. Environ., 61, 15–22, 2012.
Ruby, M. V., Lowney, Y. W., Bunge, A. L., Roberts, S. M., Gomez-Eyles, J. L., Ghosh, U. Kissel, J. C., Priscilla Tomlinson, P., and Menzie, C.: Oral bioavailability, bioaccessibility, and dermal absorption of PAHs for soil-state of the science, Environ. Sci. Technol., 50, 2151–2164, 2016.
Saffari, A., Daher, N., Shafer, M. M., Schauer, J. J., and Sioutas, C.: Global perspective on the oxidative potential of airborne particulate matter: a synthesis of research findings, Environ. Sci. Technol., 48, 7576–7583, 2014.
Schaumann, F., Borm, P. J. A., Herbrich, A., Knoch, J., Pitz, M., Schins, R. P. F., Luettig, B., Hohlfeld, J. M., Heinrich, J., and Krug, N.: Metal-rich ambient particles (particulate matter 2.5) cause airway inflammation in healthy subjects, Am. J. Respir. Crit. Care Med., 170, 898–903, 2004.

Scipioni, C., Villanueva, F., Pozo, K., and Mabilia, R.: Preliminary characterization of polycyclic aromatic hydrocarbons, nitrated polycyclic aromatic hydrocarbons and polychlorinated dibenzo-p-dioxins and furans in atmospheric PM_{10} of an urban and a remote area of Chile, Environ. Technol., 33, 809–820, 2012.

Shahpoury, P., Lammel, G., Holubová Šmejkalová, A., Klánová, J., Přibylová, P., and Váňa, M.: Polycyclic aromatic hydrocarbons, polychlorinated biphenyls, and chlorinated pesticides in background air in central Europe – investigating parameters affecting wet scavenging of polycyclic aromatic hydrocarbons, Atmos. Chem. Phys., 15, 1795–1805, 2015.

Shahpoury, P., Lammel, G., Albinet, A., Sofuoglu, A., Dumanoğlu, Y., Sofuoglu, S. C., Wagner, Z., and Zdimal, V.: Evaluation of a conceptual model for gas-particle partitioning of polycyclic aromatic hydrocarbons using polyparameter linear free energy relationships, Environ. Sci. Technol., 50, 12312–12319, 2016.

Shahpoury, P., Kitanovski, Z., and Lammel, G.: Snow scavenging and phase partitioning of nitrated and oxygenated aromatic hydrocarbons in polluted and remote environments in central Europe and the European Arctic, Atmos. Chem. Phys., 18, 13495–13510, 2018.

Shahpoury, P.; Zhang, Z. W.; Arangio, A.; Celo, V.; Dabek-Zlotorzynska, E.; Harner, T.; Nenes, A. The influence of chemical composition, aerosol acidity, and metal dissolution on the oxidative potential of fine particulate matter and redox potential of the lung lining fluid, Environ. Int., 148, 106343, 2021.

Shang, Y., Zhou, Q., Wang, T., Jiang, Y., Zhong, Y., Qian, G., Zhu, T., Qiu, X., and An, J.: Airborne nitro-PAHs induce Nrf2/ARE defense system against oxidative stress and promote inflammatory process by activating PI3K/Akt pathway in A549 cells, Toxicol. In Vitro, 44, 66–73, 2017.

Shannigrahi, A. S., Fukushima, T., and Ozaki, N.: Comparison of different methods for measuring dry deposition fluxes of particulate matter and polycyclic aromatic hydrocarbons (PAHs) in the ambient air, Atmos. Environ., 39, 653–662, 2005.

Shen, H. and Anastasio, C.: Formation of hydroxyl radical from San Joaquin Valley particles extracted in a cell-free surrogate lung fluid, Atmos. Chem. Phys., 11, 9671–9682, 2011.

Shen, G., Tao, S., Wei, S., Chen, Y., Zhang, Y., Shen, H., Huang, Y., Zhu, D., Yuan, C., Wang, H., Wang, Y., Pei, L., Liao, Y., Duan, Y., Wang, B., Wang, R., Lv, Y., Li, W., Wang, X. and Zheng, X.: Field measurement of emission factors of PM, EC, OC, parent, nitro-, and oxy-polycyclic aromatic hydrocarbons for residential briquette, coal cake, and wood in rural Shanxi, China, Environ. Sci. Technol., 47, 2998–3005, 2013.

Sheu, H.-L., Lee, W.-J., Su, C.-C., Chao, H.-R., and Fan, Y.-C.: Dry deposition of polycyclic aromatic hydrocarbons in ambient air, J. Environ. Eng., 122, 1101–1109, 1996.

Shiraiwa, M., Ueda, K., Pozzer, A., Lammel, G., Kampf, C. J., Fushimi, A., Enami, S., Arangio, A. M., Fröhlich-Nowoisky, J., Fujitani, Y., Furuyama, A., Lakey, P. S. J., Lelieveld, J., Lucas, K., Morino, Y., Pöschl, U., Takahama, S., Takami, A., Tong, H., Weber, B., Yoshino, A., and Sato, K.: Aerosol health effects from molecular to global scales, Environ. Sci. Technol., 51, 13545–13567, 2017.

Sies, H., Berndt, C. and Jones, D. P.: Oxidative Stress, Annu. Rev. Biochem., 86, 715–748, 2017.

Sousa, E. T., Cardoso, M. P., Silva, L. A., and de Andrade, J. B.: Direct determination of quinones in fine atmospheric particulate matter by GC–MS, Microchem. J., 118, 26-31, 2015.

Souza, K. F., Carvalho, L. R. F., Allen, A. G., and Cardoso, A. A.: Diurnal and nocturnal measurements of PAH, nitro-PAH, and oxy-PAH compounds in atmospheric particulate matter of a sugar cane burning region, Atmos. Environ., 83, 193–201, 2014.

Sverdrup, L. E., Ekelund, F., Krogh, P. H., Nielsen, T., and Johnsen, K.: Soil microbial toxicity of eight polycyclic aromatic compounds: effects on nitrification, the genetic diversity of

bacteria, and the total number of protozoans, Environ. Toxicol. Chem., 21, 1644-1650, 2002a.

Sverdrup, L. E., Krogh, P. H., Nielsen, T., and Stenersen, J.: Relative sensitivity of three terrestrial invertebrate tests to polycyclic aromatic compounds, Environ. Toxicol. Chem., 21, 1927-1933, 2002b.

Tang, N., Sato, K., Tokuda, T., Tatematsu, M., Hama, H., Suematsu, C., Kameda, T., Toriba, A., and Hayakawa, K.: Factors affecting atmospheric 1-, 2-nitropyrenes and 2-nitrofluoranthene in winter at Noto Peninsula, a remote background site, Japan, Chemosphere, 107, 324–330, 2014.

Terzi, E. and Samara, C.: Dry deposition of polycyclic aromatic hydrocarbons in urban and rural sites of Western Greece, Atmos. Environ., 39, 6261–6270, 2005.

Toledo, M., Lanças, F. M., and Carrilho, E.: Solid-phase extraction of nitro-PAH from aquatic samples and its separation by reverse-phase capillary liquid chromatography, J. Braz. Chem. Soc., 18, 1004–1010, 2007.

Tomaz, S., Shahpoury, P., Jaffrezo, J. L., Lammel, G., Perraudin, E., Villenave, E., and Albinet, A.: One-year study of polycyclic aromatic compounds at an urban site in Grenoble(France): seasonal variations, gas/particle partitioning and cancer risk estimation, Sci. Total Environ., 565, 1071–1083, 2016.

Tong, H., Lakey, P. S., Arangio, A. M., Socorro, J., Shen, F., Lucas, K., Brune, W. H., Pöschl, U., and Shiraiwa, M.: Reactive oxygen species formed by secondary organic aerosols in water and surrogate lung fluid, Environ. Sci. Technol., 52, 11642–11651, 2018.

Toriba, A., Homma, C., Kita, M., Uozaki, W., Boongla, Y., Orakij, W., Tang, N., Kameda, T., and Hayakawa, K.: Simultaneous determination of polycyclic aromatic hydrocarbon quinones by gas chromatography-tandem mass spectrometry, following a one-pot reductive trimethylsilyl derivatisation, J. Chromatogr. A, 1459, 89–100, 2016.

Tsapakis, M., and Stephanou, E. G.: Diurnal cycle of PAHs, nitro-PAHs, and oxy-PAHs in a high oxidation capacity marine background atmosphere, Environ. Sci. Technol., 41, 8011-8017, 2007.

Tuet, W. Y., Fok, S., Verma, V., Tagle Rodriguez, M. S., Grosberg, A., Champion, J. A., and Ng, N. L.: Dose-dependent intracellular reactive oxygen and nitrogen species production from particulate matter exposure: comparison to oxidative potential and chemical composition, Atmos. Environ., 144, 335-344, 2016.

Tuet, W. Y., Liu, F., de Oliveira Alves, N., Fok, S., Artaxo, P., Vasconcellos, P., Champion, J. A., and Ng, N. L.: Chemical oxidative potential and cellular oxidative stress from open biomass burning aerosol, Environ. Sci. Tech. Let., 6, 126–132, 2019.

Verma, V., Ning, Z., Cho, A., Schauer, J., Shafer, M., and Sioutas, C.: Redox activity of urban quasi-ultrafine particles from primary and secondary sources, Atmos. Environ., 43, 6360–6368, 2009.

Verma, V., Pakbin, P., Cheung, K., Cho, A., Schauer, J., Shafer, M., Kleinman, M., and Sioutas, C.: Physicochemical and oxidative characteristics of semi-volatile components of quasi-ultrafine particles in an urban atmosphere, Atmos. Environ., 45, 1025–1033, 2011.

Verma, V., Wang, Y., El-Afifi, R., Fang, T., Rowland, J., Russell, A. G., and Weber, R. J.: Fractionating ambient humic-like substances (HULIS) for their reactive oxygen species activity–Assessing the importance of quinones and atmospheric aging, Atmos. Environ., 120, 351–359, 2015a.

Verma, V., Fang, T., Xu, L., Peltier, R. E., Russell, A. G., Ng, N. L., and Weber, R. J.: Organic Aerosols Associated with the Generation of Reactive Oxygen Species (ROS) by Water-Soluble $PM_{2.5}$, Environ. Sci. Technol., 41, 4646–4656, 2015b.

Vincenti, M., Minero, C., and Pelizzetti, E.: Sub-parts-per-billion determination of nitrosubstituted polynuclear aromatic hydrocarbons in airborne particulate matter and soil by electron capture-tandem mass spectrometry, J. Am. Soc. Mass Spectrom., 7, 1255–1265, 1996.

Vincenti, M., Maurino, V., Minero, C., and Pelizzetti, E.: Detection of nitro-substituted polycyclic aromatic hydrocarbons in the Antarctic airborne particulate, Int. J. Environ. Anal. Chem., 79, 257–272, 2001.

Vione, D., Barra, S., De Gennaro, G., De Rienzo, M., Gilardoni, S., Perrone, M. G., and Pozzoli, L.: Polycyclic aromatic hydrocarbons in the atmosphere: monitoring, sources, sinks and fate. II: sinks and fate, Ann. Chim. (Rome), 94, 257-268, 2004.

Vione, D., Maurino, V., Minero, C., and Pelizzetti, E.: Nitration and photonitration of naphthalene in aqueous systems, Environ. Sci. Technol., 39, 1101-1110, 2005.

Visentin, M., Pagnoni, A., Sarti, E., and Pietrogrande, M. C.: Urban $PM_{2.5}$ oxidative potential: Importance of chemical species and comparison of two spectrophotometric cell-free assays, Environ. Pollut., 219, 72–79, 2016.

Walgraeve, C., Demeestere, K., Dewulf, J., Zimmermann, R., and van Langenhove, H.: Oxygenated polycyclic aromatic hydrocarbons in atmospheric particulate matter: Molecular characterization and occurrence, Atmos. Environ., 44, 1831−1846, 2010.

Wang, S., Ye, J., Soong, R., Wu, B., Yu, L., Simpson, A. J., and Chan, A. W. H.: Relationship between chemical composition and oxidative potential of secondary organic aerosol from polycyclic aromatic hydrocarbons, Atmos. Chem. Phys., 18, 3987–4003, 2018.

Watanabe, T., Ohe, T., and Hirayama, T.: Occurrence and origin of mutagenicity in soil and water environment, Environ. Sci., 12, 325-346, 2005.

Watanabe, M. and Noma, Y.: Influence of combustion temperature on formation of nitro-PAHs and decomposition and removal behaviors in pilot-scale waste incinerator, Environ. Sci. Technol., 43, 2512–2518, 2009.

Wei, S., Huang, B., Liu, M., Bi, X., Ren, Z. F., Sheng, G., and Fu, J.: Characterization of $PM_{2.5}$-bound nitrated and oxygenated PAHs in two industrial sites of South China, Atmos. Res., 109–110, 76–83, 2012.

Wei, C., Bandowe, B. A. M., Han, Y., Cao, J., Zhan, C., and Wilcke, W.: Polycyclic aromatic hydrocarbons (PAHs) and their derivatives (alkyl-PAHs, oxygenated PAHs, nitrated-PAHs and azaarenes) in urban road dusts from Xi'an, Central China, Chemosphere, 134, 512–520, 2015.

Wei, W. J., Bonvallot, N., Gustafsson, Å., Raffy, G., Glorennec, P., Krais, A., Ramalho, O., le Bot, B., and Mandin, C.: Bioaccessibility and bioaccessibility of environmental semi-volatile organic compounds via inhalation: a review of methods and models, Environ. Int., 113, 202–213, 2018.

WHO (World Health Organization): Indoor air quality: organic pollutants, Report on a WHO Meeting, Berlin, 23-27 August 1987. EURO Reports and Studies 111. Copenhagen, World Health Organization Regional Office for Europe, 1989.

WHO (World Health Organization): WHO global air quality guidelines. Particulate matter ($PM_{2.5}$ and PM_{10}), ozone, nitrogen dioxide, sulfur dioxide and carbon monoxide, World Health Organization: Geneva, Switzerland, 2021.

Wilcke, W., Kiesewetter, M., and Bandowe, B. A. M.: Microbial formation and degradation of oxygen-containing polycyclic aromatic hydrocarbons (OPAHs) in soil during short-term incubation, Environ. Pollut., 184, 385-390, 2014a.

Wilcke, W., Bandowe, B. A. M., Gomez Lueso, M., Ruppenthal, M., del Valle, H., and Oelmann, Y.: Polycyclic aromatic hydrocarbons (PAHs) and their polar derivatives (oxygenated PAHs,

azaarenes) in soils along a climosequence in Argentina, Sci. Total Environ., 473–474, 317–325, 2014b.

Xiong, Q., Yu, H., Wang, R., Wei, J., and Verma, V.: Rethinking Dithiothreitol-Based Particulate Matter Oxidative Potential: Measuring Dithiothreitol Consumption versus Reactive Oxygen Species Generation, Environ. Sci. Technol., 51, 6507–6514, 2017.

Yang, A., Wang, M., Eeftens, M., Beelen, R., Dons, E., Leseman, D. L. A. C., Brunekreef, B., Cassee, F. R., Janssen, N. A. H., and Hoek, G.: Spatial Variation and Land Use Regression Modeling of the Oxidative Potential of Fine Particles, Environ. Health Persp., 123, 1187–1192, 2015.

Zhang, Y., Yang, B., Gan, J., Liu, C., Shu, X., and Shu, J.: Nitration of particle-associated PAHs and their derivatives (nitro-, oxy-, and hydroxy-PAHs) with NO_3 radicals, Atmos. Environ., 45, 2515–2521, 2011.

Zhao, L., Zhang, L., Chen, M., Dong, C., Li, R., and Cai, Z.: Effects of ambient atmospheric $PM_{2.5}$, 1-nitropyrene and 9-nitroanthracene on DNA damage and oxidative stress in hearts of rats, Cardiovasc. Toxicol., 19, 178–190, 2019.

Zhao, J., Zhang, Y., Chang, J., Peng, S., Hong, N., Hu, J., Ly, J., Wang, T., and Mao, H.: Emission characteristics and temporal variation of PAHs and their derivatives from an ocean-going cargo vessel, Chemosphere, 249, 126194, 2020.

Zhuo, S., Du, W., Shen, G., Li, B., Liu, J., Cheng, H., Xing, B., and Tao, S.: Estimating relative contributions of primary and secondary sources of ambient nitrated and oxygenated polycyclic aromatic hydrocarbons, Atmos. Environ., 159, 126–134, 2017.

Appendix A: List of publications including articles in preparation

Journal articles, published and in preparation

1) Wietzoreck, M., Bandowe, B. A. M., Hofman, J., Martiník, J., Nežiková, B., Kukučka, P., Přibylová, P., and Lammel, G.: Nitro- and oxy-PAHs in grassland soils from decade-long sampling in central Europe, Environ. Geochem. Health, https://doi.org/10.1007/s10653-021-01066-y, 2021.

2) Wietzoreck, M., Kyprianou, M., Bandowe, B. A. M., Celik, S., Crowley, J. N., Drewnick, F., Eger, P., Friedrich, N., Iakovides, M., Kukučka, P., Kuta, J., Nežiková, B., Pokorná, P., Přibylová, P., Prokeš, R., Rohloff, R., Tadic, I., Tauer, S., Wilson, J., Harder, H., Lelieveld, J., Pöschl, U., Stephanou, E. G., and Lammel, G.: Polycyclic aromatic hydrocarbons (PAHs) and their alkylated-, nitro- and oxy-derivatives in the atmosphere over the Mediterranean and Middle East seas, Atmos. Chem. Phys. Discuss., submitted (2022a).

3) Wietzoreck, M., Filippi, A., Wilson, J., Hildmann, S., Mashtakov, B., Shahpoury, P., Berkemeier, T., Tong, H., Pöschl, U., Lammel, G., and Bandowe, B. A. M.: Oxidative potential of polycyclic aromatic compounds (PACs) in particulate matter: measurement and prediction by chemical structure and reduction potential, in preparation (2022b).

4) Lammel, G., Kitanovski, Z., Kukučka, P., Novak, J., Arangio, A. M., Codling, G. P., Filippi, A., Hovorka, J., Leoni, C., Přibylová, P., Prokeš, R., Sáňka, O., Shahpoury, P., Tong, H. and Wietzoreck, M.: Oxygenated and Nitrated Polycyclic Aromatic Hydrocarbons in Ambient Air—Levels, Phase Partitioning, Mass Size Distributions, and Inhalation Bioaccessibility, Environ. Sci. Technol., 54, 2615-262, 2020.

5) Nováková, Z., Novák, J., Kitanovski, Z., Kukučka, P., Přibylová, P., Prokeš, R., Smutná, M., Wietzoreck, M., Lammel, G., and Hilscherová, K.: Toxic potentials of particulate and gaseous air pollutant mixtures and the role of PAHs and their derivatives, Environ. Int. 139, 105634, 2020.

6) Wilson, J., Octaviani, M., Bandowe, B. A. M., Wietzoreck, M., Zetzsch, C., Pöschl, U., Berkemeier, T., and Lammel, G.: Modeling the formation, degradation and spatiotemporal distribution of 2-nitrofluoranthene and 2-nitropyrene in the global atmosphere, Environ. Sci. Technol., 54, 22, 14224-14234, 2020.

7) Shahpoury, P., Zhang, Z. W., Filippi, A., Hildmann, S., Lelieveld, S., Patel, B. R., Traub, A., Umbrio, D., Wietzoreck, M., Wilson, J., Berkemeier, T., Celo, V., Dabek-Zlotorzynska, E., Evans, G., Harner, T., Kerman, K., Lammel, G., Noroozifar, M., Pöschl, U., and Tong, H.: Inter-comparison of oxidative potential metrics for airborne particles identifies differences between acellular chemical assays, in preparation, 2022.

8) Sheu, R., Hass-Mitchell, T., Ringsdorf, A., Berkemeier, T., Machesky, J., Edtbauer, A., Klüpfel, T., Filippi, A., Bandowe, B. A. M., Wietzoreck, M., Tong, H., Lammel, G., Pöschl, U., Williams, J., and Gentner, D. R.: Deposited particulate matter and human lung lining fluid are prominent reservoirs for off-gassing third hand tobacco smoke emissions, Environ. Sci. Atmos., under review, 2022.

9) Lammel, G., Shahpoury, P., Berkemeier, T., Hilscherová, K., Kitanovski, Z., Kukučka, P., Kyprianou, M., Lucas, K., Novák, J., Pöschl, U., Přibylová, P., Prokeš, R., Sáňka, O., Stephanou, E., and Wietzoreck, M.: Inhalation exposure to PAHs dominated by the gaseous mass fraction even if minute, in preparation, 2022.

10) Besis, A., Bandowe, B. A. M., Degrendele, C., Kim, J. T., Jin, R., Wietzoreck, M., Samara, C., and Lammel, G.: Oxidative potential in ambient PM in polluted and background air in southern and central Europe related to mass size distributions and bioavailability of PAH derivatives", in preparation, 2022.

11) Lelieveld S., Wietzoreck M., Filippi A., Iakovides M., Kukučka P., Kuta J., Prokeš R., Pöschl U., Lammel G., and Tong, H.: Concentrations of EPFR, aqueous ROS, and transition metals in PM of Middle East seas, in preparation, 2022.

12) Baumann, K., Wietzoreck, M., Filippi, A., Hildmann, S., Lelieveld, S., Shahpoury, P., Wilson, J., Berkemeier, T., Tong, H., Pöschl, U., and Lammel, G.: Mimicking the uptake of toxic environmental organic compounds in ultrafine PM in the deep lung and related oxidative potential, in preparation, 2022.

13) Kim, J. T., Degrendele, C., Kohoutek, J., Kretzschmann, L., Kukučka, P., Luttringer, L., Martiník, J., Nežiková, B., Nillius, B., Panechou, K., Přibylová, P., Sobotka, J., Wietzoreck, M., Vrana, B., and Lammel, G.: Atmospheric transport and air-sea exchange of organic pollutants in the Equatorial Atlantic - I. PAHs and derivatives; II. OCP, PCB and PBDE, in preparation, 2022.

14) Kyprianou, M., Jin, R., Vrana, B., Sobotka, J, Wietzoreck, M., Kukučka, P., Přibylová, P., Prokeš, R., Iakovides, M., Harder, H., Crowley, J.N., Lammel, G., and Stephanou, E.: Organohalogen pesticides, PCBs and flame retardants in the atmosphere of Middle East seas, in preparation, 2022.

15) Krüger, M., Wilson, J., Wietzoreck, M., Schmidt, B., Pöschl, U., and Berkemeier, T. et al.: Application of convolutional neural networks for the prediction of reduction potentials of quinones based on their molecular structure, in preparation, 2022.

16) Nežiková B., Wietzoreck, M., Bandowe B.A.M., Degrendele C., Kukučka P., Martiník J., Přibylová P., Halse A.K., Bohlin-Nizzetto P., Kallenborn R., Mwangi J.K., and Lammel G.: Long-range transport and air-soil cycling of nitro- and oxy-PAHs in central and northern Europe, in preparation, 2022.

17) Wietzoreck, M., Bandowe, B. A. M., Iakovides, M., Kukučka, P., Kyprianou, M., Přibylová, P., Prokeš, R., Shahpoury, P., Harder, H., Stephanou, E., Pöschl, U., and Lammel, G.: Gas-particle partitioning of polycyclic aromatic hydrocarbons (PAHs) and their oxygenated derivatives in a hot marine environment determined by PM composition, short commun., in preparation, 2022c.

18) Wietzoreck, M., Bandowe, B. A. M., Hildmann, S., Mashtakov, B. and Lammel, G.: Overlooked importance of the oxidative potential of monoaromatic quinones, in preparation, 2022d.

Oral presentations at national and international scientific conferences and workshops

1. Wietzoreck, M.: Nitro and oxy-aromatic compounds in the atmospheric environment, Doktorandenseminar (DoSe), Johannes Gutenberg University Mainz, Institute for Atmospheric Physics, Mainz, Germany, 20th October 2017.

2. Wietzoreck, M., Bandowe, B. A. M., Degrendele, C., Filippi, A., Iakovides, M., Kukučka, P., Kuta, J., Kyprianou, M., Lelieveld, S., Nitzler, E., Příbylová, P., Prokeš, R., Stephanou, E. G., Tong, H., Harder, H., Lelieveld, J., Pöschl, U., and Lammel, G.: Polycyclic aromatic hydrocarbons (PAHs) and their nitrated and oxygenated derivatives in the Arabian Basin, AQABA Science meeting, Max Planck Institute for Chemistry, Mainz, Germany, 22nd November 2018.

3. Wietzoreck, M., Bandowe, B. A. M.., Iakovides, M., Kukučka, P., Kuta, J., Kyprianou, M., Nežiková, B., Přibylová, P., Prokeš, R., Stephanou, E. G., Harder, H., Lelieveld, J., Pöschl, U., and Lammel, G.: Polycyclic aromatic hydrocarbons (PAHs) and their nitrated and oxygenated derivatives in air of the Arabian Basin, International Conference on Carbonaceous Particles in the Atmosphere, Vienna, Austria, 3rd – 6th April 2019.

4. Wietzoreck, M., Bandowe, B. A. M.., Iakovides, M., Kukučka, P., Kuta, J., Kyprianou, M., Nežiková, B., Přibylová, P., Prokeš, R., Stephanou, E. G., Harder, H., Lelieveld, J., Pöschl, U., and Lammel, G.: Polycyclic aromatic hydrocarbons (PAHs) and their nitrated and oxygenated derivatives in air of the Arabian Basin, General Assembly of the European Geosciences Union, Vienna, Austria, 7th – 12th April 2019.

5. Wietzoreck, M., Baumann, K., Filippi, A., Lelieveld, S., Shahpoury, P., Wilson, J., Tong, H., Pöschl, U., and Lammel, G.: Simulating the Uptake of Toxic Organic Pollutants from Ultrafine Particulate Matter in the Deep Lung and Determining the Related Oxidative Potential, European Aerosol Conference, Gothenburg, Sweden, 25th – 30th August 2019.

6. Wietzoreck, M., Filippi, A., Wilson, J., Hildmann, S., Shahpoury, P., Berkemeier, T., Pöschl, U., Lammel, G.., Tong, H., Bandowe, B. A. M.: Oxidative potentials of oxygenated and nitrated aromatic compounds and their predictability by molecular structure and reduction potential, European Aerosol Conference, virtual, 30th August – 3rd September 2021.

Poster presentations at national and international scientific conferences

1. Wietzoreck, M., Bandowe, B. A. M., Degrendele, C., Filippi, A., Iakovides, M., Kukučka, P., Kuta, J., Kyprianou, M., Lelieveld, S., Přibylová, P., Prokeš, R., Stephanou, E. G., Tong, H., Harder, H., Lelieveld, J., Pöschl, U., and Lammel, G.: Polycyclic aromatic hydrocarbons (PAHs) and their nitrated and oxygenated derivatives in air of the Arabian Basin, Umwelt 2018, Münster, Germany, 2018

2. M., Filippi, A., Hildmann, S., Lelieveld, S., Shahpoury, P., Wilson, J., Berkemeier, T., Tong, H., Pöschl, U., Lammel, G., and Baumann, K.: Simulating the uptake of toxic environmental organic compounds in ultrafine PM in the deep lung and related oxidative potentials, European Aerosol Conference, virtual, 30th August – 3rd September 2021.

Appendix B: Curriculum vitae